frontiers | Research Topics

Novel technologies for enrichment, extraction, and determination of phenolic compounds in foods

volume 1

Edited by
Runqiang Yang, Yu Xiao and Baoru Yang

Published in
Frontiers in Nutrition

ISSN 1664-8714
ISBN 978-2-8325-2771-9
DOI 10.3389/978-2-8325-2771-9

About Frontiers

Frontiers is more than just an open access publisher of scholarly articles: it is a pioneering approach to the world of academia, radically improving the way scholarly research is managed. The grand vision of Frontiers is a world where all people have an equal opportunity to seek, share and generate knowledge. Frontiers provides immediate and permanent online open access to all its publications, but this alone is not enough to realize our grand goals.

Frontiers journal series

The Frontiers journal series is a multi-tier and interdisciplinary set of open-access, online journals, promising a paradigm shift from the current review, selection and dissemination processes in academic publishing. All Frontiers journals are driven by researchers for researchers; therefore, they constitute a service to the scholarly community. At the same time, the *Frontiers journal series* operates on a revolutionary invention, the tiered publishing system, initially addressing specific communities of scholars, and gradually climbing up to broader public understanding, thus serving the interests of the lay society, too.

Dedication to quality

Each Frontiers article is a landmark of the highest quality, thanks to genuinely collaborative interactions between authors and review editors, who include some of the world's best academicians. Research must be certified by peers before entering a stream of knowledge that may eventually reach the public - and shape society; therefore, Frontiers only applies the most rigorous and unbiased reviews. Frontiers revolutionizes research publishing by freely delivering the most outstanding research, evaluated with no bias from both the academic and social point of view. By applying the most advanced information technologies, Frontiers is catapulting scholarly publishing into a new generation.

What are Frontiers Research Topics?

Frontiers Research Topics are very popular trademarks of the *Frontiers journals series*: they are collections of at least ten articles, all centered on a particular subject. With their unique mix of varied contributions from Original Research to Review Articles, Frontiers Research Topics unify the most influential researchers, the latest key findings and historical advances in a hot research area.

Find out more on how to host your own Frontiers Research Topic or contribute to one as an author by contacting the Frontiers editorial office: frontiersin.org/about/contact

Novel technologies for enrichment, extraction, and determination of phenolic compounds in foods - volume 1

Topic editors

Runqiang Yang — Nanjing Agricultural University, China
Yu Xiao — Hunan Agricultural University, China
Baoru Yang — University of Turku, Finland

Citation

Yang, R., Xiao, Y., Yang, B., eds. (2023). *Novel technologies for enrichment, extraction, and determination of phenolic compounds in foods - volume 1*. Lausanne: Frontiers Media SA. doi: 10.3389/978-2-8325-2771-9

Table of contents

frontiers | Frontiers in Nutrition

TYPE Editorial
PUBLISHED 27 June 2023
DOI 10.3389/fnut.2023.1238748

OPEN ACCESS

EDITED AND REVIEWED BY
Elena Ibañez,
Spanish National Research Council (CSIC), Spain

*CORRESPONDENCE
Runqiang Yang
✉ yangrq@njau.edu.cn

RECEIVED 12 June 2023
ACCEPTED 14 June 2023
PUBLISHED 27 June 2023

CITATION
Xiao Y, Yang B and Yang R (2023) Editorial: Novel technologies for enrichment, extraction, and determination of phenolic compounds in foods, volume I. *Front. Nutr.* 10:1238748. doi: 10.3389/fnut.2023.1238748

Editorial: Novel technologies for enrichment, extraction, and determination of phenolic compounds in foods, volume I

Yu Xiao[1], Baoru Yang[2] and Runqiang Yang[3]*

[1]College of Food Science and Technology, Hunan Agricultural University, Changsha, China, [2]Department of Biochemistry and Food Chemistry, University of Turku, Turku, Finland, [3]College of Food Science and Technology, Whole Grain Food Engineering Research Center, Nanjing Agricultural University, Nanjing, Jiangsu, China

KEYWORDS

phenolic compounds, enrichment, extraction, determination, food

Editorial on the Research Topic
Novel technologies for enrichment, extraction, and determination of phenolic compounds in foods, volume I

Phenolic compounds, a class of plant secondary metabolites with high biological activity, are mainly composed of flavonoids, phenolic acids, and anthocyanins (1). Due to the large amount of active phenolic hydroxyl groups in phenolics, they have a strong ability to scavenge free radicals and have various physiological and biochemical functions, including anti-cancer, anti-tumor, anti-aging, and other health-promoting functions (2). However, they cannot be synthesized in the human body and need to be ingested through external sources (3). Therefore, the novel technologies for enrichment, extraction, and determination of phenolic compounds have received widespread attention.

Phenolic compounds are widely distributed in vegetables, fruits and grains (4). The metabolomics approaches based on mass spectrometry can achieve comprehensive extraction and determination of different phenolic compounds. Zhang et al. found that isoflavones, sinapic acid derivatives, catechin and epicatechin, phenolic alcohols, chlorogenic acid, and lignans were the main phenolic compounds in soybean, rapeseed, peanut skin, olive, sunflower seed, sesame and flaxseed, respectively. Liu H.-Y. et al. reported that four phenolic classes with 316 phenolic metabolites were identified in white radish. Liu S. et al. concluded that *Citrus* L. fruit, as a functional fruit, was also rich in health-promoting phytonutrients and bioactive compounds, such as flavonoids, phenolic acids, vitamins, carotenoids, pectins, and fatty acids. A thorough understanding of phenolic components among different species may provide scientific guidance for better enrichment and extraction of specific phenolic compounds and benefit the extension of the value chain of functional foods.

In recent years, it has become a major development trend in enhancing the activity of phenolic compounds through biotic or abiotic stress (5, 6), which is of great significance for the extension of the food industry chain. Villamil-Galindo et al. showed that Ellagitannins and UVA radiation were proved to be efficient in biofortify strawberry agro-industrial by-products, significantly improving the phenolic compounds content and their bioactive properties with adequate bioaccessibility, adding value to the strawberry agro-industrial by-products. Wang M. et al. found that UV-B radiation promoted the accumulation and synthesis of isoflavones

in soybean hypocotyls and cotyledon callus tissues, particularly malonyl isoflavones. Also, a combination of ultrasound and exogenous GABA treatment can be used to produce mung bean sprouts with enriched polyphenols content and enhanced antioxidant activity (Wang L. et al.). Xie et al. investigated that ultrasound-assisted aqueous two-phase (ATP) extraction was used as an effective method to achieve the simultaneous separation and preliminary purification of phenolics from grape pomace. Interestingly, Hong et al. found that ultrasonic washing was an abiotic elicitor to induce the accumulation of phenolics in fruit and vegetables while retaining quality attributes and microbial safety. Besides, fermentation is an effective way to increase the content of endogenous phenolic compounds in plants. Yang J. et al. found that the content of total organic acids, phenols and flavonoids increased in fermented ginkgo biloba kernel juice by *Lactobacillus plantarum* Y2, which effectively improved the nutritional value and safety of ginkgo biloba kernel juice. Wang K. et al. showed that the nutritional value and bioactivity of black beans were enhanced when fermented as tempeh, and the total respective levels of phenolics, flavonoids, and proanthocyanidins released from black bean tempeh were 1.21, 1.40, and 1.55 times higher than those of unfermented black beans following *in vitro* digestion, respectively. Zheng et al. comprehensively investigated three modification methods (shear emulsifying, ball milling, and autoclave treatment) to improve the structure, physicochemical properties, phenolic compounds, and antioxidant capacity of food.

These studies emphasize phenolic-rich foods have become a major trend in the future. The technologies for enrichment, extraction, and determination of phenolic compounds in foods are becoming increasingly abundant, which has an important contribution to improving food nutrition and processing quality, and developing healthy foods.

In general, the article discussed in this editorial analyzes the composition of phenolic compounds in different plants, explores new technologies for enriching and extracting phenolic compounds, and demonstrates the potential of enhancing the activity of phenolic compounds and increasing their production to extend the food industry chain. As our understanding of phenolic compounds and their novel technologies continues to grow, it can provide valuable supplements to existing technologies for enrichment, extraction, and determination of phenolic compounds, and contribute to improving the nutritional value and industrial added value of food.

The articles discussed in this editorial demonstrate the potential of phenolic-rich foods as a promising dietary intervention in fighting against obesity. It would be more and more clear that they may offer a valuable addition to existing weight loss and metabolic health interventions and ultimately contribute to the development of more effective and holistic approaches to obesity prevention and treatment.

Author contributions

YX: writing—original draft and writing—review and editing. BY: writing—review and editing. RY: investigation and writing—review and editing. All authors contributed to the article and approved the submitted version.

Acknowledgments

We deeply thank all the authors and reviewers who have participated in this Research Topic.

Conflict of interest

The authors declare that the research was conducted in the absence of any commercial or financial relationships that could be construed as a potential conflict of interest.

Publisher's note

References

1. Martínez-Silvestre KE, Santiz-Gómez JA, Luján-Hidalgo MC, Ruiz-Lau N, Sánchez-Roque Y, Gutiérrez-Miceli FA. Effect of UV-B radiation on flavonoids and phenols accumulation in tempisque (*Sideroxylon capiri* Pittier) callus. *Plants-Basel.* (2022) 11:473. doi: 10.3390/plants11040473

2. Xiong W, Li Y, Yao Y, Xu Q, Wang L. Antioxidant mechanism of a newly found phenolic compound from adlay (NDPS) in HepG2 cells via Nrf2 signalling. *Food Chem.* (2022) 378:132034. doi: 10.1016/j.foodchem.2021.132034

3. Tyagi A, Shabbir U, Chen X, Chelliah R, Elahi F, Ham HJ, et al. Phytochemical profiling and cellular antioxidant efficacy of different rice varieties in colorectal adenocarcinoma cells exposed to oxidative stress. *PLoS ONE.* (2022) 17:e0269403. doi: 10.1371/journal.pone.0269403

4. Jacobo-Velazquez DA, Moreira-Rodriguez M, Benavides J. UVA and UVB radiation as innovative tools to biofortify horticultural crops with nutraceuticals. *Horticulturae.* (2022) 8:387. doi: 10.3390/horticulturae8050387

5. Mencin M, Abramovič H, Jamnik P, Petkovšek MM, Veberič R, Terpinc P. Abiotic stress combinations improve the phenolics profiles and activities of extractable and bound antioxidants from germinated spelt (*Triticum spelta* L.) seeds. *Food Chemistry.* (2020) 344:128704. doi: 10.1016/j.foodchem.2020.128704

6. Zhang L, Du L, Shi T, Xie M, Liu X, Yu M. Effects of pulsed light on germination and gamma-aminobutyric acid synthesis in brown rice. *J. Food Sci.* (2022) 87:1601–9. doi: 10.1111/1750-3841.16087

frontiers | Frontiers in Nutrition

TYPE Review
PUBLISHED 18 July 2022
DOI 10.3389/fnut.2022.968604

OPEN ACCESS

EDITED BY
Zhaojun Wei,
Hefei University of Technology, China

REVIEWED BY
Siyu Li,
Kunming University of Science and Technology, China
Hongming Su,
University of Minnesota Twin Cities, United States

*CORRESPONDENCE
Qing Gu
guqing@zjsu.edu.cn

†These authors have contributed equally to this work

SPECIALTY SECTION
This article was submitted to Nutrition and Food Science Technology, a section of the journal Frontiers in Nutrition

RECEIVED 14 June 2022
ACCEPTED 28 June 2022
PUBLISHED 18 July 2022

CITATION
Liu S, Lou Y, Li Y, Zhang J, Li P, Yang B and Gu Q (2022) Review of phytochemical and nutritional characteristics and food applications of *Citrus* L. fruits. *Front. Nutr.* 9:968604. doi: 10.3389/fnut.2022.968604

Review of phytochemical and nutritional characteristics and food applications of *Citrus* L. fruits

Shuxun Liu[1†], Ying Lou[1†], Yixian Li[1], Jiaojiao Zhang[2], Ping Li[1], Baoru Yang[1,3] and Qing Gu[1*]

[1]Key Laboratory for Food Microbial Technology of Zhejiang Province, College of Food Science and Biotechnology, Zhejiang Gongshang University, Hangzhou, China, [2]College of Food and Health, Zhejiang Agriculture and Forestry University, Hangzhou, China, [3]Food Sciences, Department of Biochemistry, University of Turku, Turku, Finland

Since the dietary regimen rich in fruits is being widely recognized and encouraged, *Citrus* L. fruits have been growing in popularity worldwide due to their high amounts of health-promoting phytonutrients and bioactive compounds, such as flavonoids, phenolic acids, vitamins, carotenoids, pectins, and fatty acids. The diverse physicochemical properties and multiple utilization of citrus fruits in food industry are associated with their unique chemical compositions. Throughout the world, citrus has been used for producing various value-added and nutritionally enhanced products, including juices, wines, jams, canned citrus, and dried citrus. However, the current studies regarding the phytochemical and nutritional characteristics and food applications of citrus are scattered. This review systematically summarizes the existing bibliography on the chemical characteristics, functional and nutraceutical benefits, processing, and potential applications of citrus. A thorough understanding of this information may provide scientific guidance for better utilizing citrus as a functional fruit and benefit the extension of citrus value chain.

KEYWORDS

citrus, phytochemicals, nutrients, health benefits, food applications

Introduction

Citrus (genus *Citrus* L.), which belongs to the citrus genus of the *Rutaceae* family and *Aurantioidae* subfamily according to the botanical classification, is currently among the most economically important cultivated crops in terms of area and production values around the world. Citrus is believed to have originated in the Himalayan area of southwestern China, northeastern India, and northern Burma, and now has been diffused in more than 140 countries (1). According to statistics from the Food and Agriculture Organization of the United Nations (FAO), the total global production of citrus in 2019 was about 144 million tons, with a planting area of 9.89 million hectares, of which, the output and cultivation area of citrus in China reached 38 million tons and 2.88 million hectares, respectively, ranking first place worldwide. Sweet orange (*Citrus sinensis*), sour

orange (*C. aurantium*), mandarin (*C. reticulata*), grapefruit (*C. paradisi*), pummelo (*C. grandis*), lemon (*C. limon*), citron (*C. medica*), lime (*C. aurantifolia*), kumquat (*C. japonica*), and hybrids are known as the most commercially important citrus species (Figure 1) (2).

Citrus fruits are common foodstuffs for human health thanks to their extremely high contents of health-promoting phytochemical and nutritional substances, such as multivitamins, pectins, carotenoids, fatty acids, and especially polyphenols (3). In recent years, along with the increasing public interest in plant antioxidants, the citrus fruits with high antioxidant ability associated with phytochemicals and nutrients are attracting more attention due to their potential health-promoting functions. The results of numerous epidemiological studies indicated a direct correlation between citrus fruit consumption and low risks of chronic diseases, such as cancer, cardiovascular diseases, and diabetes (4, 5). In addition, some curative components with pharmacological effects have also been found in citrus fruits and citrus by-products. Specifically, some phytochemicals in essential oils extracted from citrus peel have been demonstrated to have high free radical scavenging and anti-fungal activity; anti-pathogenic effects on healing sore throat, cough, earache, and vomiting have been demonstrated relating to citrus pulp and peel; and the extracts prepared using steam-distillation from citrus fruit and fruit/seeds have been used as a sedative and cardiac tonics, respectively (1, 6).

Short harvest time and shelf life are usually the flaws of fresh fruits and limit their availability and the possibility of enjoying the nutritional and functional properties all year round, as only a few days to months are generally the optimal time for fruit picking and consumption. Therefore, although most of the harvested citrus are freshly consumed, processing citrus into value-added products are important ways to extend the citrus industry chain and prolong the shelf life of citrus to several months or years, which is beneficial for the safe transportation of citrus products from the growing region of citrus to all over the world. However, currently, the actual conversion rate is extremely low in comparison with the colossal yield of citrus on the earth. For example, <5% of the total citrus yield in China is exploited annually. Even worse, a portion of the harvested citrus is lost because of the lack of adequate post-harvest management and processing infrastructures, which is a considerable economic loss for orchardists and farmers. Hence, processing of citrus into various products; such as citrus juices, citrus wines, citrus jams, canned citrus, and dried citrus is gaining attention by enriching the diversity of the citrus sector and thus minimizing postharvest losses.

To date, the information about the chemical composition, mainly including phytochemicals and nutrients, and the health-promoting properties and food applications of citrus is scattered. This study summarizes the current knowledge on the phytochemical and nutritional components in citrus. The health benefits of these compounds are discussed as well. Regarding the phytochemicals and nutrients, the composition, structure, and distribution, as well as bioactivities are priorly summarized. Thereafter, the utilization of citrus for the development of citrus products is reviewed. The review facilitates a better understanding of citrus composition and provides important references for future research and innovations to promote the production and utilization of citrus.

Phytochemical profiles of citrus

Flavonoids

As one the most abundant secondary metabolites, natural plant polyphenols have long been the subject of studies since they are essential for the protection of plants and exert functions of defense. To date, hundreds of polyphenols have been detected in citrus with flavonoids being the most important bioactive components with wide variety and distribution, and new polyphenols are being constantly discovered with the advancement in extraction and analytical methods (7–9). Flavonoids are naturally occurring low molecular weight phenolic compounds containing two aromatic rings (A and B) bound by a 3-carbon bridge (C6-C3-C6 structure) (Figure 2). Among the over 250 flavonoids have so far been identified in citrus (10), citrus flavonoids can be further structurally categorized into flavanones, flavones, flavonols, and anthocyanins (only in blood oranges), which are present in the form of aglycones or glycosides. Neohesperidoside and rutinoside are the most significant and common forms of flavonoids in citrus. Besides, hydroxylation and methylation are also frequently involved (11).

Flavonoids affect the quality of fruits in terms of taste, appearance, and bioactivities. For example, neohesperidosides, including naringin, neohesperidin, poncirin, and neoeriocitrin, consist of a flavanone with neohesperidose (rhamnosyl-a-1,2 glucose) and contribute the primary bitterness to citrus (12). Whereas rutinosides, such as hesperidin, narirutin, eriocitrin, and didymin, have a basic flavanone combined with a disaccharide residue of rutinose (ramnosyl-a-1,6 glucose) and are tasteless. Flavanones present in diglycoside form usually confer a typical taste of bitterness to citrus fruit (2). The accumulation of anthocyanins is the fundamental reason of pigmentation of blood oranges (13). With regard to the therapeutic and nutraceutical potentials, these bioactive ingredients help to reduce the risk of many chronic diseases (such as cardiovascular disease), with important nutritional health care functions (14). A large number of studies have demonstrated that citrus flavonoids can regulate the expression of inflammation-related factors, inhibit the adhesion of monocytes to endothelial cells, regulate cell migration

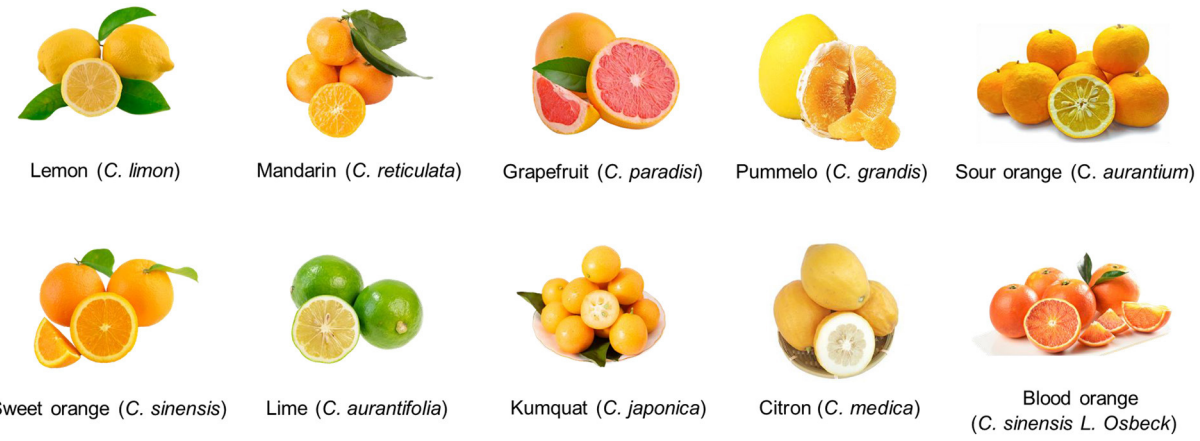

FIGURE 1
Phenotypes and genotypes of main citrus varieties and hybrids.

and possess vascular protection, anti-hypertension, and anti-atherosclerosis effects (Figure 3) (15, 16). Nowadays, the prevalence of diabetes and obesity is rapidly increasing due to unhealthy dietary habits and a lack of daily physical exercise. Some *in vitro* studies have revealed that citrus flavonoids have the robust pharmacological properties of antidiabetic activity and anti-obesity action (17–19). For example, citrus flavonoid narirutin can block the digestive enzymes that hydrolyze polysaccharides into small absorbable fragments to regulate the blood glucose level in people with diabetes. Citrus flavonoids have been associated with reducing adiposity through the inhibitory effect on adipogenesis *via* the downregulation of genes associated with lipid metabolism and adipogenic transcription factors and the upregulation of certain lipolysis enzymes such as hormone-sensitive lipase (HSL) and AMP-activated protein kinase (AMPK).

The level and composition of flavonoids change with the development and maturation of citrus fruits and vary among different citrus species. A study on the flavonoid evolution during navel orange maturation found that the total flavonoid content continuously decreased during maturity, from 538 mg/100 g dry weight (DW) at the young fruit period to 69 mg/100 g DW at commercial maturity (20). Some researchers have evaluated the changes in phenolic profiles of lemon fruits during maturity and found that the total flavonoid content of lemon pulps ranged from 630 to 1460 mg/100 g fresh weight (FW) and the highest total flavonoid content occurred in April (21). A previous study accurately described the flavonoid profile of different citrus fruits using a new UPLC-PDA method, and the results indicated that the flavonoid contents in the fruits varied significantly among different citrus varieties cultivated in the same area, and different cultivated species were characterized by varying predominant flavonoid compounds; for example, naringin, erocitrin, and hesperidin are the most predominant components of pummelo, lemon, mandarin, and sweet orange, respectively (22). A comparative study on the flavonoid level in different citrus varieties reported that the total flavonoid concentrations in navel oranges (mean value: 95.3 mg/100 g FW), common oranges (mean value: 82.6 mg/100 g FW), and satsume oranges (mean value: 75.45 mg/100 g FW) were higher than that in clementine groups (mean value: 35.6 mg/100 g FW), sanguine groups (mean value: 56.9 mg/100 g FW), and hybrid groups (mean value: 56.4 mg/100 g FW) (23).

Flavanones

Flavanones are low in molecular weight, C6-C3-C6 parent nuclear structure consisting of 15 carbon atoms, and often contain multiple hydroxyl groups. Their flavonoid skeletons contain two aromatic rings (A and B rings), connected by an oxygen-containing heterocyclic ring consisting of three carbon atoms (C rings). Flavanones are the major polyphenols in citrus in comparison with other flavonoids and phenolic acids (24). Numerous epidemiological studies have reported the inverse relationships between citrus flavanones intake and the risks of cardiovascular diseases, hypertension, lipid-lowering, insulin-sensitization, atherosclerosis, and inflammation properties (Figure 3) (25, 26).

The compositions and contents of flavanones in citrus vary dramatically between different citrus varieties and fruit parts. For instance, the dominant flavanones in sweet oranges and mandarin both are tasteless hesperidin (15.25 mg/100 g FW) and bitter narirutin (2.33 mg/100 g FW), whereas in sour oranges the predominant flavanones are bitter neohesperidin (11.09 mg/100 g FW) and naringin (18.83 mg/100 g FW) (27). Pummelo is characterized by an abundance of naringin (218.65–783.91 mg/100 g FW), lemon is characterized by eriocitrin (9.46 mg/100 g FW) and hesperidin (15.78 mg/100 g FW) (22, 28).

10.3389/fnut.2022.968604

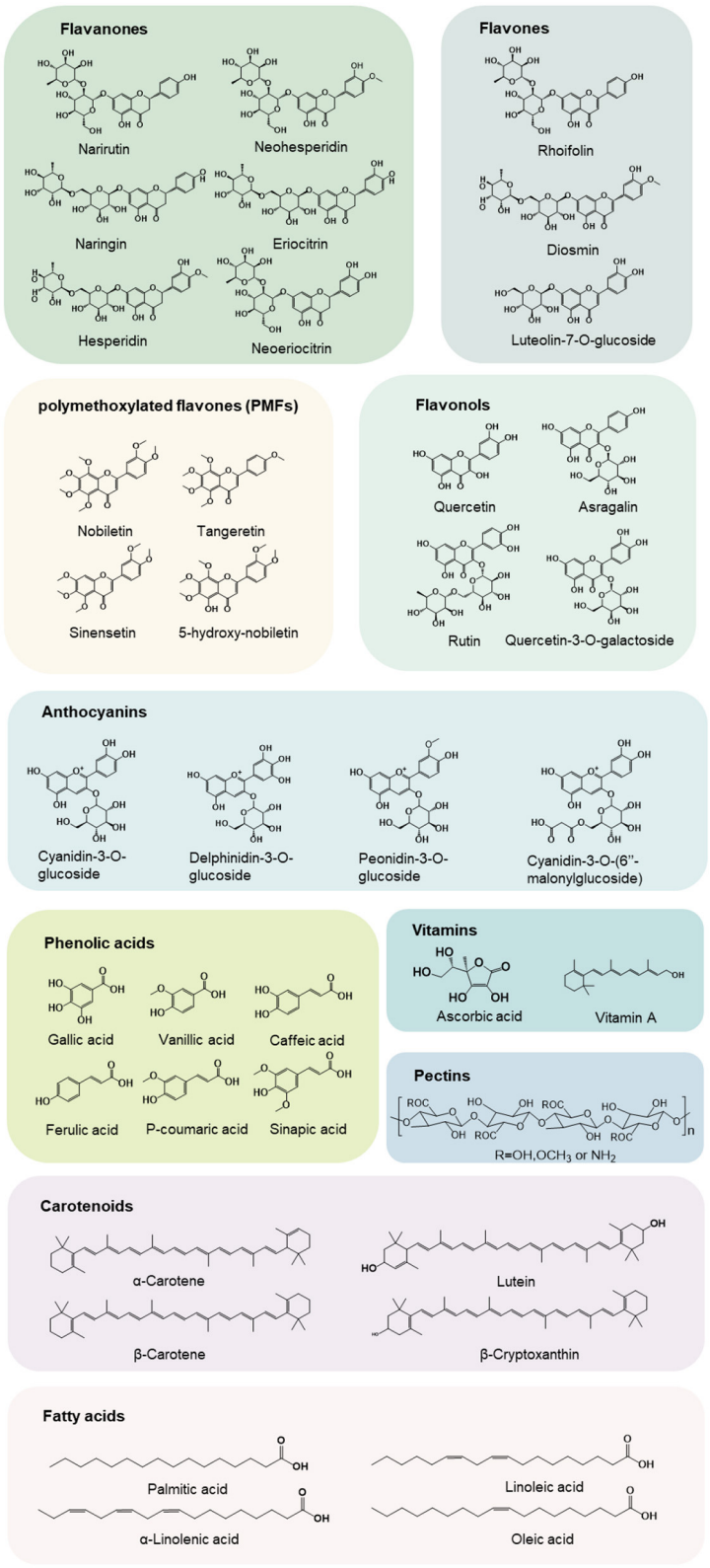

FIGURE 2
Chemical structures of major phytochemicals and nutrients in citrus.

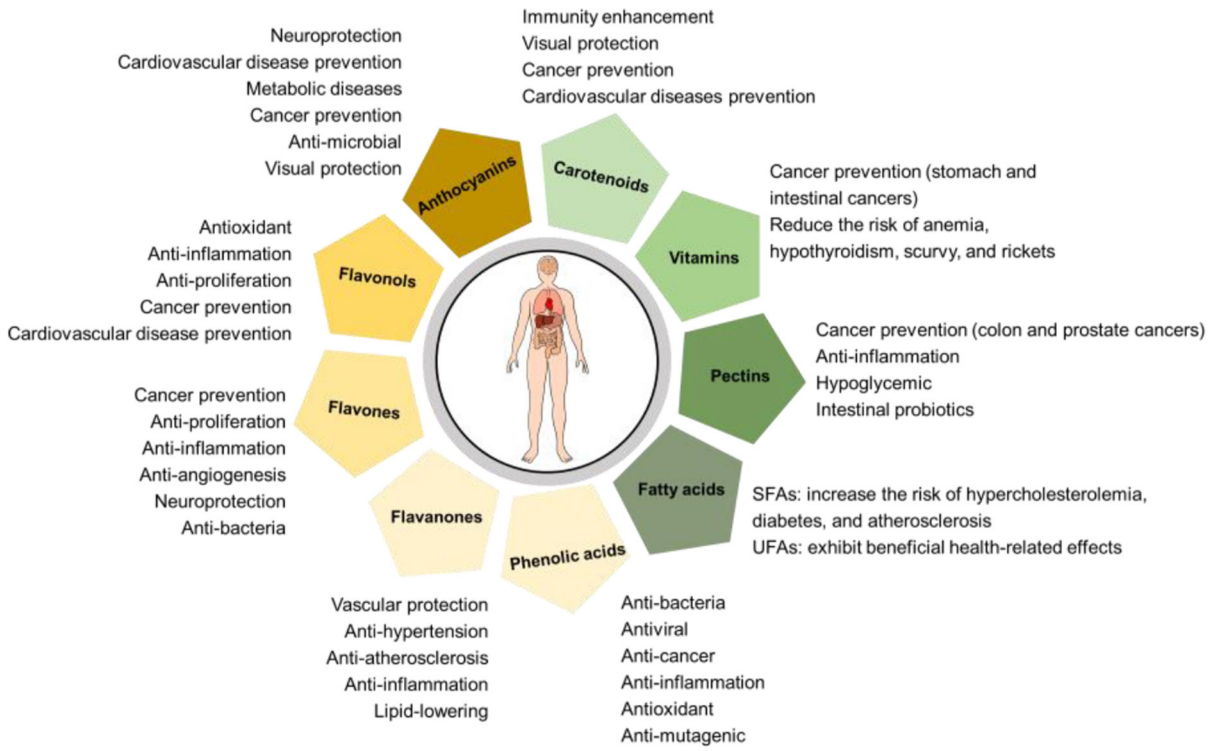

FIGURE 3
Potential health-promoting effects of phytochemical and nutritional compounds in citrus.

The concentration of naringin in grapefruits (654.35–987.17 mg/100 g FW) is comparatively higher than that in others (29, 30). Taking fruit parts into consideration, hesperidin is the dominant flavonoid in the pulps of lemons (74.3–181.6 mg/100 g FW), tangerine (167.5 mg/100 g FW), and sweet oranges (100.1 mg/100 g FW), and in the peels of mandarins (660.26–924.05 mg/100 g FW), sweet oranges (567.62–916.29 mg/100 g FW), and lemons (214.61–406.77 mg/100 g FW) (21, 22). The contents of eriocitrin reached 470.5 and 204.7 mg/100 g FW respectively, in the peel and pulp of lemon, which are much higher than those of the other citrus species (22).

The information regarding the distribution of flavanone in the products made from citrus is also considerable. HPLC-DAD-ESI-MS-MS separation allowed for the identification, for the first time, of narirutin 4'-O-glucoside, hesperidin, and narirutin in blood orange (Sanguinello and Tarocco) juices (31). Six flavanones of narirutin (39.91 mg/L), naringin (2.23 mg/L), hesperidin (171.17 mg/L), neohesperidin (0.95 mg/L), didymin (6.07 mg/L), and apigenin (32.37 mg/L) have been accurately quantified in orange juices made from Turkish cv. Kozan, while yeast fermentation significantly reduced their levels ranging from 42 to 50% (32). Gattuso et al. (33) summarized the flavanone composition in different citrus juices and found that the total flavanone contents in the juices made from *C. sinensis*, *C. reticulata*, *C. clementina*, *C. limon*, *C. aurantifolia*, *C. paradisi*, *C. deliciosa*, and *C. aurantium* are 4.74–73.17, 1.11–58.55, 5.26–86.22, 5.51–80.1, 1.52–2.02, 9.61–83.35, 2.12, and 4.34 mg/100 mL, respectively. Furthermore, hesperidin is

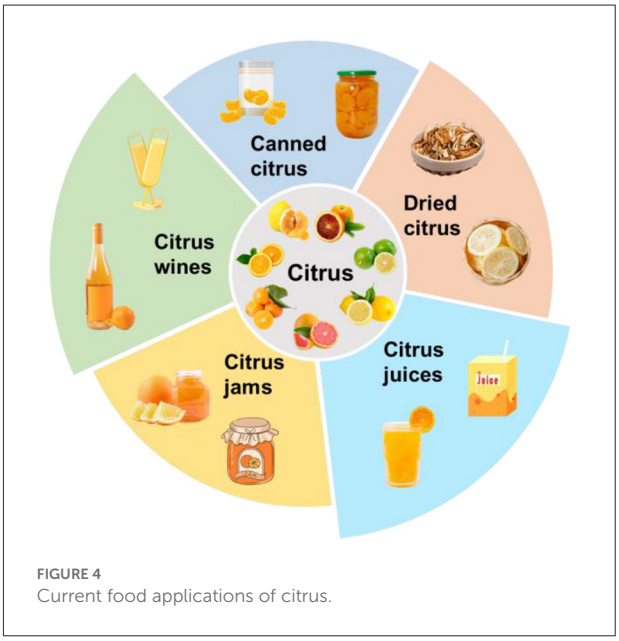

FIGURE 4
Current food applications of citrus.

usually the predominant flavanone in all the juices other than *C. aurantium* juice with this compound being virtually absent.

Flavones

Flavones possess 2-phenyl-1,4-benzopyrone skeletons, with hydroxyl groups usually at the 5- and 7-position, and often also at the 4'- and/or 3'-position. Six major flavone aglycones that are frequently reported include sinensetin, nobiletin, tangeretin, apigenin, luteolin, and diosmetin (Figure 2). The types and substitution positions of flavone glycosides are more diverse than those of flavanones. Glycosides can be substituted at positions 5, 6, 7, and 8 in A ring and 3' and 4' in B ring. The glycosylation may take place in (1) one or more hydroxyl groups of the aglycone bounding to glycoses to form an acid-labile glycosidic O–C bond (namely flavone *C*-glycosides) or (2) direct linkage of the glycoses to the basic nucleus of the aglycone, *via* an acid-resistant C–C bond (namely flavone *O*-glycosides) (11). The types of glycosides include rutinoside, neohesperidoside, glucoside, rhamnoside, arabinoside, and xyloside.

A previous study has reported, for the first time, the presence of five *C*-glycosyl flavones (lucenin-2, vicenin-2, stellarin-2, lucenin-2 4'-methyl ether, and scoparin) and a flavone *O*-glycosides (chrysoeriol 7-*O*-neoesperidoside) in blood orange juices (34). Abad-García et al. (35) have developed a method using HPLC-DAD coupled to ESI and triple quadrupole mass spectrometry to isolate different varieties of flavones from a series of citrus juices. The distinct flavones in the juices made from sweet orange, tangerine, lemon, and grapefruit are apigenin-7-*O*-rutinoside-4′-*O*-glucoside, luteolin-7-*O*-neohesperidoside-4′-*O*-glucoside, luteolin-6-*C*-glucoside, 6,8-di-*C*-acylhexosides of chrysoeriol and diosmetin, 6-*C*-and 8-*C*-glucoside-*O*-pentoside of apigenin, apigenin-6-*C*-hexoside-*O*-hexoside, and apigenin-8-*C*-hexoside-*O*-acylrhamnoside. Although the variety of flavones in citrus is diversified, the content of flavones only accounts for from trace to approximately 10% of total flavonoids (6, 14), which could be explained by the predisposed conversion from flavones into polymethoxylated flavones (PMFs) rather than being glycosylated (36, 37). Preclinical studies have demonstrated the promising physiological and pharmacological effects of citrus flavones, such as prevention and treatment of inflammation through the inhibition of regulatory enzymes or transcription factors that control mediators involved in inflammation (38), the antimicrobial effect on some Gram-negative and positive bacteria and *Saccharomyces cerevisiae* (39), and the anticancer activity *via* the suppression of cell growth and the promotion of cell death by regulating key molecular pathways related to cancer cell proliferation and immune cell function (Figure 3) (40, 41).

PMFs are unique constituents that almost exist exclusively in citrus and can thereby be used as biomarkers for citrus classification. PMFs exist in large amounts in the waxy constituents separated from the cold-pressed orange peel oil after long-term freezing treatment, while only a small amount is present in the fruit juice and pulp (42). PMFs, naturally occurring as free aglycones with at least two methoxy groups, have been reported in high concentrations in the peels of sweet, bitter, and mandarin oranges (29). Among the different citrus species, mandarins have the highest levels of PMFs, followed by sweet oranges, lemons, and pummelos (43). On the basis of the ESI-MS^n characteristics of PMFs and the results of EIC-MS/MS experiment, 32 PMFs have been screened from the complex extract of the peels of "Shatangju" mandarin (44). Nobiletin and tangeretin are common PMFs in citrus fruits, and supercritical carbon dioxide extraction using aqueous ethanol as co-solvent is considered the most environmentally friendly method for the extraction of these two PMFs from *C. depressa* Hayata peel (45). Many *in vitro* and *in vivo* studies have demonstrated anti-cancer, anti-proliferative, anti-inflammatory, anti-angiogenic, and neuroprotective properties of nobiletin and tangeretin (Figure 3) (46). However, these two PMFs are scarcely used as functional foods due to their low water solubility. Some studies have used debranched waxy maize starch *via* encapsulation to enhance the storage stability of tangeretin (47). Meanwhile, Sun et al. (48) have developed a method to encapsulate nobiletin using the cinnamaldehyde-modified whey protein stabilized microcapsules. The study indicated that the presence of cinnamaldehyde maintained or increased the bioaccessibility of nobiletin, regardless of emulsions or microcapsules.

Flavonols

Flavonols, the ancient and widespread class of polyphenolics, exhibit great antioxidant potential and are considered effective UV filters, thereby performing important functional roles during plant evolution (49). Flavonols represent the main fraction of bioactive compounds in plants with antioxidant, anti-inflammatory, and anti-proliferative capacities, having great health-promoting effects such as protection against cancer and cardiovascular disease (Figure 3) (50). Compared with flavone and flavanone aglycones, the main feature of flavonol aglycone is the existence of a hydroxyl group at C3 in the C-ring. Flavonol glycosides, especially *O*-glycoside, have the sugar moieties attached at position C7 of A-ring and position C3 of C-ring.

Kaempferol, quercetin, limocitrin, and isorhamnetin are the four main flavonols in citrus. The contents of flavonol in citrus juice generally are low in the range of 0.74–3.4 mg/100 mL (36). A comparative study suggested that the distribution of flavonols in citrus usually is variety dependent as the percentages of flavonols in the total polyphenol content are 1.0–3.5% in sweet orange juices, 0.3–9.5% in tangerine juices, 3.4–6.0% in lemon juices, and 0.1–0.2% in grapefruit juices (24). The accumulation of flavonols is divergent in citrus organs, as they are preferentially accumulated in leaves of most citrus varieties,

while only a very small amount of flavonols is found in fruit tissues of a limited number of varieties such as lemon and lime (51).

Anthocyanins

Anthocyanins are water-soluble flavylium cation derivatives belonging to the flavonoid family involved in nature in several aspects of plant development and defense (52). Their unique structures in C rings are different from that of other flavonoids. In general, anthocyanin aglycones (namely anthocyanidins) are rarely found in nature due to their poor stability, while usually exist in the form connected with glycosides. According to the difference in the patterns of hydroxylation and methylations on the different positions of B ring of aglycones, approximately 25 anthocyanidins have been identified in nature. However, only six of them, including pelargonidin, cyanidin, delphinidin, peonidin, petunidin, and malvidin, linking with different glycoses, such as glucose, rhamnose, galactose, arabinose, xylose, and rutinose, are commonly found in plant-based food, accounting for about 95% of all anthocyanins (53). Apart from the chromogenic properties, anthocyanins are also important components of the human diet and, thanks to their radical-scavenging properties, therapeutic agents (54). The biological and pharmacological studies on these molecules have demonstrated their counteractive effects on oxidative stress and onset and progression of several non-communicable diseases (e.g., neurodegenerative, cardiovascular, metabolic diseases, and cancer), antimicrobial ability, and visual protective function (Figure 3) (55, 56).

Blood oranges, such as Tarocco, Moro, and Sanguinello, are typical varieties colored by anthocyanins that are present in both the rind and fruit juice vesicles. The content and composition of anthocyanins in blood oranges vary tremendously depending on variety, maturity, region of cultivation, and many other environmental factors. Cebadera-Miranda et al. (57) identified ten different anthocyanins, including seven cyanidin derivatives and three delphinidin derivatives, in blood oranges, and reported that cyanidin 3-(6"-malonylglucoside) and cyanidin 3-glucoside are the most abundant anthocyanins in both Sanguinello and Tarocco varieties. These two anthocyanins have also been dominantly found in Moro oranges (58). The total anthocyanin concentrations in Tarocco Ippolito (8.67–25.26 μg/100 g DW) and Sanguinelli (10.53–22.70 μg/100 g DW) generally are higher than that in Tarocco Rosso (6.95–12.12 μg/100 g DW) (57). Lo Piero (54) found that pigmentation levels varied significantly with cultivars of pigmented sweet oranges growing under even the same conditions. Specifically, the pigmentation level in OTA9 is highest, followed by Moro (high pigmentation), Tarocco (low to medium pigmentation), and Navelina (no pigmentation), in decreasing order. With regard to the environmental factor, cold treatment has been documented to extend Tarocco's shelf life and increase anthocyanin levels (59, 60). The anthocyanin accumulation in blood oranges during storage at low temperatures could be explained by the activation of enzymes involved in phenylpropanoid metabolism (61).

The accumulation of anthocyanins during plant development suggests that anthocyanin evolution is controlled and induced in favor of plants (54). Some studies have demonstrated that the accumulation of anthocyanins in blood oranges is closely correlated with fruit maturity. Cotroneo et al. (62) reported that the total anthocyanins of Moro orange are undetectable in the first two ripening stages (mid-to-late October to the beginning of November). However, their levels rise from the third and fourth stages (end of November to mid-December), remaining below 2 mg/100 g FW, and show a sharp increase starting from the sixth and reaching 22.2 mg/100 g FW in the seventh stage. The direct correlation between the accumulation of pigments and transcript levels for genes encoding chalcone synthase (CHS), anthocyanidin synthase (ANS), and UDP-glucose-flavonoid 3-*O*-glucosyltransferase (UFGT) was confirmed using quantitative real-time reverse transcriptase-PCR.

Phenolic acids

Phenolic acids are phenols containing one carboxylic acid and can be structurally divided into hydroxycinnamic acids, which are characterized by C6–C3 structures, and hydroxybenzoic acids, which possess common C6–C1 structures. Phenolic acids are often combined with other substances (organic acids, flavones, cellulose, flavones, proteins, lignin, monosaccharides, etc.) in the form of ester bond, glycoside bond, ether bond, and rarely exist in a free state (63).

Although a fraction of phenolic acids can be produced through the metabolism of other kinds of polyphenols by microflora in colon of humans and animals, the majority of phenolic acids are supplemented by dietary sources (63). The dietary phenolic acids exist ubiquitously in plants, as citrus is one of the most important sources of these antioxidants. The health-promoting effects of phenolic acids have been well acknowledged. For example, phenolic acids possess much higher *in vitro* antioxidant activity than the well-known antioxidant vitamins and have various biological activities of antibacterial, antiviral, anticarcinogenic, anti-inflammatory, anti-mutagenic, and vasodilatory actions (Figure 3) (63, 64). These functions emphasize the potential utilization of phenolic acids in citrus in pharmaceutical industries.

Phenolic acid composition and content are different in diverse citrus fruits, which are mainly related to fruit variety, part, and ripeness. For example, some studies have found that the content of phenolic acid in citrus peel is much higher than that in citrus flesh, particularly in semi-mature stage (20). Hydroxycinnamic acids, such as ferulic acid, *p*-coumaric acid, caffeic acid, sinapic acid, and chlorogenic acid, are mainly found in various parts of citrus fruits, while hydroxybenzoic acids, such as vanillic acid, *p*-hydroxybenzoic acid, and gallic

acid, are found in a small amount in citrus peels (65). Seven phenolic acids, including four hydroxycinnamic acids (caffeic, *p*-coumaric, sinapic, and ferulic acids) and three hydroxybenzoic acids (protocatechuic, *p*-hydroxybenzoic, and vanillic acids), have been determined by HPLC-PDA in the peels of *C. reticulata* (66). A similar profile of phenolic acids has also been detected in calamansi peel (67). *p*-Coumaric (24.68%) and ferulic (23.79%) acids are the most abundant phenolic acids in the peel extract of bitter orange (68), and gallic acid is the most abundant in the peels of several pomelo varieties (45). However, the major phenolic acid in Persian lime is *p*-coumaric acid (37). Ferulic acid was found as the predominant phenolic acid in the range of 31.6–63.7 mg/L in blood orange juices (6). An accordant result (37.7 mg/L) has been detected in juices made from Valencia late (69).

The remarkable effect of maturation on the evolution of phenolic acids in citrus has been well demonstrated. For example, Hou et al. (20) suggested that the concentrations of most phenolic acids in navel orange decreased during fruit maturation with exception of free fractions of sinapic acid and bound fractions of ferulic and caffeic acids. A study assessed the evolution of phenolic compounds in Eureka lemon fruits during ripening and found that *p*-coumaric acid and ferulic acid are among the major phenolic acids, and the maximum levels of phenolic acids are accumulated in the pulps of April fruits (26.94 mg/100 g FW) but in the peels of June fruits (76.93 mg/100 g FW) (21). A previous study evaluated the content of *p*-coumaric acid in Persian Lime over time and found that the concentration of this acid increased significantly from week 1 (0.98 mg/100 g FW) to week 5 (3.04 mg/100 g FW), then decreased drastically till week 7 (0.155 mg/100 g FW), and keep constant in the subsequent weeks (37).

Carotenoids

Citrus carotenoids are a class of C40 isoprenoids, categorized into carotenes (hydrocarbonated carotenoids) and xanthophylls containing one or more oxygens. Carotenoids have special relevance to human nutrition and health-related aspects of immunity enhancement, eyes protection, and cancer and cardiovascular disease prevention (Figure 3) (10). As an important source of natural carotenoids, citrus carotenoids not only contribute nutritional value to citrus fruits, but also are responsible for the attractive color of yellow, orange, and red (10, 70). Carotenoids are naturally occurring fat-soluble pigments with antioxidant functions and some of them (provitamin A carotenoids, including α-carotene, β-carotene, and β-cryptoxanthin) can be converted into vitamin A (retinol) (71), thus make citrus become a valuable source to fulfill the recommended daily ingestion specifications.

Approximately 115 carotenoids have been detected in citrus species, including both carotene (α-carotene, β-carotene, and lycopene) and xanthophyll (β-cryptoxanthin, lutein, zeaxanthin, and violaxanthin) (71). The total content of carotenoids in citrus is located in the ranges of 2.5–50.1 mg/100 g FW (72). The content and composition of carotenoids in citrus are closely correlated with the types of citrus variety, maturity, and environmental conditions of cultivation and storage. A comparative study evaluating the carotenoid contents in different citrus food matrices (pulp and fresh juice) and their content in bioaccessible fraction and relative bioaccessibility of bioactive carotenoids in different varieties of two citrus species that are highly consumed worldwide, sweet orange and mandarins, suggested that the pulp of citrus fruits contains a similar or higher content of soluble bioactive carotenoids compared to fresh juice. Consequently, potential nutritional and health benefits are obtained by the consumption of pulp with respect to fresh juice (73). During ripening, due to the gradual conversion of chloroplasts to chromoplasts, the carotenoid contents in citrus fruits keep increasing with the degradation of chlorophyll (74). Besides, the genotype and environment conditions also impact the content of carotenoids significantly. A large number of studies on different cultivated citrus species have agreed on the accumulation of violaxanthin and β-cryptoxanthin can only be noted in mandarins and oranges in comparison with lemon, pummelo, and grapefruit (75–77). Moreover, the carotenoid composition of mandarins, oranges, and their hybrids could be distinguished by the concentration of β-cryptoxanthin (78). The study of Dhuique-Mayer (79) revealed the significant differences in carotenoid contents of citrus juices produced from fruits grown in Mediterranean, subtropical, and tropical countries. Furthermore, during juice processing, the applications of thermal or other stabilization treatments and the acidic condition stimulate the formation of carotenoid isomers and rearrangements of epoxy groups (73). With the aim to improve nutritional and functional values of citrus fruits in terms of carotenoid accumulation, storage at 12°C has been suggested as the feasible postharvest strategy (80).

Bioavailability, including absorption, metabolism, tissue distribution, and bioactivity, is a necessary prerequisite for assessing the role of a bioactive compound on human health and is strongly dependent on bioaccessibility. Due to the disturbance of poor solubility and chemical stability, and easy combination with food components, carotenoids are usually poor in human digestion. Some studies carried out using *in vitro* digestion models reported that the bioaccessibility of carotenoids could be improved by the presence of other dietary constituents, such as flavanones and pectin (3, 81).

Nutritional compounds in citrus

Vitamins

Vitamins are a general term for a series of organic micronutrients that are required by organisms for proper

functioning. The deficiency of vitamins is a major public health issue worldwide and is closely related to numerous serious health problems, such as anemia, hypothyroidism, scurvy, and rickets. According to statistics, more than two billion people are suffering from vitamin deficiency and most of them belong to developing countries (82). Vitamins generally cannot be synthesized by organisms, and need to be obtained through diet and other means, making it possible to consume citrus, the source of abundant vitamins, as an important dietary vitamin uptake.

The vitamins in citrus can be divided into two main categories, namely fat-soluble vitamins (vitamin A and vitamin E, etc.,) and water-soluble vitamins (vitamin C and B-complex vitamins, such as vitamin B1, vitamin B2, and folate, etc.,). Among them, vitamin E and vitamin C are the most representative components in these two categories in citrus, respectively. In citrus fruits, vitamin A is the only fat-soluble vitamin that exists in an adequate quantity in the form of provitamin A carotenoids, with the carotenes and β-cryptoxanthin as the major vitamin A precursors (83). Vitamin C is widely considered the most important water-soluble antioxidant in citrus. This vitamin can prevent digestive tract cancers such as stomach and intestinal cancers, inhibit the formation of harmful substances such as free radicals and lipid peroxide in the body, and protect intra- and extra-cellular compounds (Figure 3) (84). Citrus juices are excellent sources of vitamin C and are widely available and commonly consumed beverages worldwide. The study of Rampersaud and Valim (85) has suggested that citrus juices, especially orange and pink grapefruit juices, were more vitamin C-dense than other commonly consumed juices.

Many factors affect vitamin content of citrus, including variety, maturity, breeding and storage conditions, and rootstocks. Cardeñosa et al. (86) assessed the effect of the citrus rootstocks on vitamin content and antioxidant activity of citrus fruits and found that the differences in antioxidant activity and related vitamin compounds are mainly dependent on the citrus rootstock, despite ripening stage had also some particular effects. However, in comparison with variety, harvesting season presented more remarkable impacts on vitamin contents and antioxidant activity of sweet oranges, as the highest values were found in the oranges harvested in January.

Pectins

Pectins are complex polysaccharide polymer compounds widely found in fruits, roots, stems, and leaves of plants, with a chain-like molecular structure. The majority of pectins generally coexist with hemicellulose, lignin, cellulose, and other components, with the highest content being in fruit cell wall (87). The binding unit of pectins is D-galacturonic acid linked by 1,4-bonds to long chains, which usually exists in the methyl esterified state, and also includes L-arabinose, D-galactose, D-sorbose, L-rhamnose and other sugars in its main chain (88). According to the difference in structure, pectins can be divided into homogalacturonans, rhamnogalacturonan I, rhamnogalacturonan II, xylogalacturonan, apiogalacturonan, galactogalacturonan, galacturonogalacturonan, and arabinogalacturonan (89). Additionally, pectins can also be classified into high methoxy pectins and low methoxy pectins based on methoxylation degree (88).

Pectins are mostly extracted from fruit processing by-products, with the characteristics of low cost, simple operation, and avoidance of resource waste. Among them, citrus pectins are among the main source of commercial pectins. Citrus pectin is mainly found in the primary cell walls of citrus peels with the content accounting for 18–25% of the dry weight of peel (90). Citrus pectins have been used as good stabilizers and thickeners to improve the texture and quality of foods such as fruit and vegetable juices, jams, and jellies because of their outstanding thickening, stabilizing, gelling, and emulsifying properties (91). In order to meet people's wide extensive demand for healthy food, citrus pectins have been used as ideal fat alternatives in food processing, such as baked goods, salad dressings, ice creams, and other foods with high-fat levels (89). In addition, citrus pectins can act as degradable environmental protection films being used as substitutes for synthetic macromolecular polymers in food preservation, which can not only prolong the fresh-keeping period of foods but also is environmentally friendly (92).

Citrus pectins have been demonstrated important physiological functions and biological activities for human health, to name a few, including the prevention of colon and prostate cancers, anti-inflammation, hypoglycemic effects, and promotes the growth of beneficial bacteria in the gut (Figure 3) (45, 89). Citrus pectins are known to influence carotenoid bioaccessibility and absorption in humans. The structure of pectins, more specifically regarding their degree of methoxylation, favors carotenoid bioaccessibility but impairs the intestinal absorption of carotenoids from citrus concentrates (3).

Fatty acids

Fatty acids are organic compounds formed by an aliphatic chain and a carboxylic group normally bounded with glycerol-forming acylglycerides (93). They are generally derived from triglycerides and phospholipids, and are important nutritional substances and metabolites in living organisms (94). In citrus fruits, fatty acids constitute the largest citrus lipid components and vary in saturation and configuration being grouped into saturated fatty acids (SFAs) and unsaturated fatty acids (UFAs), while the latter can be further divided into monounsaturated fatty acids and polyunsaturated fatty acids. Epidemiological studies have reported that SFAs increase the risk of hypercholesterolemia, diabetes, and atherosclerosis,

whereas UFAs such as linolenic and linoleic acids, exhibit beneficial health-related effects (Figure 3) (94). In general, UFAs predominate over the SFAs in citrus and represent approximately 70% of total fatty acid content (TFA) (95). Data from USDA Food Data Central indicated that the total SFA in tangerines, oranges, limes, and grapefruits are 39, 15, 22, and 14 mg/100 g FW, respectively, while the total UFA are 125, 48, 74, and 37 mg/100 g FW, respectively. Matsuo et al.(96) found that the major fatty acids present in three cultivars of citrus natsudaidai peel are linoleic acid ($C_{18:2}$, *cis*-9, 12, 42.8–48.5% of TFA), followed by palmitic acid ($C_{16:0}$, 20.2–20.8% of TFA), α-linolenic acid ($C_{18:3}$, *cis*-9, 12, 15, 12.1–14.6% of TFA) and oleic acid ($C_{18:1}$, *cis*-9, 8.60–10.1% of TFA). An accordant result has been reported in the study comparing the fatty acid profiles of six citrus species breeding in South Korea (93). Eighteen fatty acids have been identified in five citrus juices (blood orange, sweet orange, lemon, bergamot, and bitter orange) and the mean concentration of fatty acids varies from 311.8 mg/L in blood orange juice to 678 mg/L in bitter orange juice (95).

Food applications of citrus

Nowadays, the flaws of short harvest time and shelf life of fresh citrus limit their supply and availability. Moreover, some popular cultivated citrus growing areas are being expanded for economic benefits, thus causing an oversupply of citrus in the market. Hence, further preservation and processing of citrus are vital approaches to maintain the majority of nutritional and phytochemical values of citrus, and to make the best use of citrus resources. In this section, various applications on how to better utilize the citrus are provided to facilitate its food industrial application and thus extend its industrial chain. The food applications include citrus juices, citrus wines, citrus jams, canned fruits, and dried citrus (Figure 4).

Citrus juices

Citrus juice is the most popular fruit juice with the largest trade volume worldwide, accounting for about 2/3 of the global juice market. However, the undesirable bitterness of citrus juice has always been the main problem faced by the citrus juice industry, which makes the product unacceptable. Studies have shown that the bitter taste of citrus after juicing is caused by two aspects, one is the bitter taste derived from the flavonoids and their derivatives in citrus fruit, and the other is the bitterness caused by the conversion of non-bitter precursors into bitter substances. For example, limonin A-ring lactone (LARL) can convert into limonoids by the enzymolysis of limonin D-ring lactone hydrolase (LDRLase) (97). Therefore, in recent years, researchers are focusing on debittering citrus juices to elevate their flavor and thus increase consumer acceptability. At present, an array of debitterness techniques, including physical, chemical, and biotechnology methods, have been developed. The mechanisms of bitterness reduction mainly include (1) removal of citrus parts that are rich in bitter components (such as peels segment membranes and seeds); (2) removal of bitter compounds in citrus (such as resins adsorption and ultrafiltration membrane filtration); (3) addition of bitter compound scavengers (such as cyclodextrin, neodiosmin, and neohesperidin dihydrochalcone); (4) enzymatic conversion of bitter compounds (such as naringinase, transeliminase, Acetyl-lyase, and limonoate dehydrogenase); (5) use of genetic engineering method to regulate the synthesis pathway of bitter compounds (98, 99).

Among the multifarious citrus juices on the market, the novel products using probiotics, such as *Lactobacillus fermentium*, *L. casei*, *L. plantarum*, and *L. pentosus*, for fermentation have received widespread attention (100–102). This kind of citrus juice makes it possible to integrate the characteristics and properties of citrus and fermentation strain, showing unique nutritional and functional values, such as anti-pathogenic bacteria, immune regulation, cancer prevention, and cardiovascular disease prevention, to name a few.

Citrus wines

The development of citrus wine not only makes full use of citrus resources but also greatly increases the added-value of citrus, which is of great significance to promote the development of the citrus industry. Compared to wines, citrus wines are usually characterized by lower alcohol and mellow body. Moreover, citrus wine retains to a large extent the original flavor and functional components of citrus, including a variety of vitamins, polyphenols, pectins, carotenoids, and fatty acids. These nutrients and bioactive substances endow citrus wine with unique flavor and biological functions, such as antiaging, health care, nourishment, moistening the lung, nourishing the liver, and relieving tension (103).

In recent years, the research of citrus wine has attracted extensive interest, and numerous excellent results have been achieved at present. The flavor features of citrus wine are mainly determined by the substances derived from citrus fruit and that are produced by microbes during fermentation. Therefore, citrus varieties, fermentation technology, and microbial metabolism are the factors that have been placed more attention by researchers and fermentation practitioners for making citrus wine with premium quality. Nowadays, like citrus juice, citrus wine is also disturbed by strong bitterness. The debittering practices of citrus wine mainly include the selection of citrus varieties with low acidity, low content of bitter compounds, and high sugar content, the pretreatment of citrus juice in the early stage of fermentation, like that have been aforementioned

in the section "Citrus Juices," and optimization of final citrus wine, such as aging and fining (104). In addition, blended citrus wines fermented with citrus and other fruits or vegetables, such as apple, pineapple, carrot, and Chinese jujube are gaining ground in recent years (105, 106). The blended products could provide the advantages of multi-variety, multi-type, and multi-function that citrus single fermented wine lacks. Various indicators have demonstrated that the quality of wines made by multi-fruit blending has been significantly improved, which may provide a reference for the development of novel citrus wines.

Canned citrus

Canned citrus is among the largest variety of canned foods in the world and plays an important role in the international canned trade (107). In recent years, canned citrus caters to modern and fast consumption mode and is welcomed by consumers. Thermal treatment is one of the main processes during the production of canned food. However, in the process of canning, sealing, and sterilization, high temperature will not only change the physical properties such as pulp chroma, hardness, and brittleness, but also accelerate the oxidation, decomposition, and loss of vitamins, carotenoids, flavonoids, reducing sugar and aroma substances, which will affect the color, flavor, and nutritional quality of canned citrus (108). Therefore, some new thermal methods, such as microwave, ohmic heating, and infrared radiation, and non-thermal protocols, such as pulsed electric fields, high-pressure processing, high-pressure carbon dioxide, sonication, and ultraviolet have been extensively applied in the development of canned citrus products. Compared to the conventional thermal treatments, these novel methods showed better preservation of the nutritional values and flavor of canned citrus (109).

The citrus canning processing water from the production of canned citrus is an important resource of pectin and sugar (110, 111). The wastewater mainly comes from scalding citrus, peeling and splitting, fruit sac transportation, acid-base treatment, classification, inspection and selection, sterilization, and so on. The citrus canning processing wastewater without treatment is detrimental to the water ecological environment, the growth and propagation of organisms, and even human life. Therefore, some methods, including physical method, chemical method, and biological method have been exploited to better utilize the citrus resource (110, 111).

Citrus jams

Jam, made from fresh fruit with the addition of sugar, thickeners, and other excipients, is a kind of fruit processed product, which mainly aims to extend the preservation of fruits. Bright color, delicate taste, rich in nutrition, and unique flavor maintaining of fruits are the principal characteristics of jam. With the rise of fast-food culture, jam plays an important role in daily diet. Nowadays, citrus jams, such as orange jam and grapefruit jam, are widely consumed at breakfast and in dairy products, bakery products, and confectionery. Normally, in order to obtain better texture and retention, the sugar content of the traditional citrus jam is mostly between 50 and 70%, which results in a sweet and greasy taste. The existence of high sugar is harmful to human health, making the traditional citrus jam-making process unable to meet the requirements of contemporary consumers for healthy food. Hence, how to reduce the content of sugar in citrus jam is a topic of significance. The utilization of alternative natural sweeteners with the merits of non-cariogenicity and less glycemia, such as tagatose and isomaltulose, is considered an effective attempt (112). Moreover, to reduce the important losses of beneficial properties of citrus fruits resulting from the application of prolonged heat treatments during jam production, some novel protocols employing microwave heating technique and osmotic dehydration have been used as alternatives to the conventional methods (113, 114).

Dried citrus

With the aim to extend the shelf-life of fruits, dehydration is usually a process that is widely employed for partial removal of water from high moisture fruits. In the case of citrus, both the pulp and peel of fruit, the pomace generated during juice production, and the juice are rich in polyphenols, vitamins, pectins, and other substances and can be dried to dehydrated products. However, undesirable drying protocols may result in dramatic degradations of phytochemicals and nutrients.

Numerous drying methods, such as freeze-drying, hot-air drying, vacuum drying, drum drying, microwave drying, and sun drying, have been applied to the dehydration of citrus and its by-products (107, 115). However, there are discriminations regarding the dehydration methods for different parts of citrus. Taking lemon as an example, the techniques of hot-air drying (45°C) and freeze-drying have been used for the dehydration of lemon fruits (116), hot-air drying (40, 50, and 60°C) and combined osmotic hot-air drying for lemon peels (117), and freeze-drying, hot-air drying (70, 90, and 110°C), and vacuum drying (70, 90, and 110°C) for lemon pomace aqueous extracts (118). Moreover, the applications of different drying techniques significantly impact the chemical composition of raw materials. For example, the flavonol concentration extracted from lemon fruit using hot-air drying is higher than that using freeze-drying, whereas the results of flavanone and flavone contents are contrary (116); freeze-dried lemon powder has a significantly lower phenolic content than the low-vacuum-dried lemon (119).

In addition, drying temperature also influenced the evolution of polyphenols remarkably. For instance, the study of Papoutsis et al. (118) compared the vacuum dying temperatures of 70, 90, and 110°C on the recovery of flavonoids in lemon by-products and found that 70 and 90°C were the optimum rather than 110°C, while Ghanem et al. (120) found that the degradation rates of phenolics and flavonoids increased with increasing air drying temperature.

Drying of citrus juices to free-flowing powders that can be reconstituted with water to drinks of acceptable flavor meets the demand of convenience from consumers. However, citrus juices are much more difficult to dry than other liquid foods such as milk, due mainly to the high content of sugar mixtures. During the drying process, especially with high drying temperatures, citrus juice may become highly viscous, thermoplastic, and sticky masses. The commonly applied methods to overcome this problem are the addition of drying carriers, such as maltodextrins, low dextrose equivalent, β-cyclodextrin, and gum arabic, which acted to increase the glass transition temperature and sticky point of the concentrated juice (107). However, these carriers are usually expensive and undesirable in the composition of the final product. Hence, the application of suitable drying techniques could greatly protect citrus juice flavor, phytochemicals, and nutrients. Nowadays, the primary drying methods used in the dehydration of citrus juices include spray drying, drum drying, vacuum drying, foam mat drying, and freeze-drying (107).

Conclusions and future perspectives

Citrus fruits are consumed in large quantities worldwide due to their attractive aromas and taste. The high abundance of phytochemicals, including flavonoids, phenolic acids, and carotenoids, and nutrients, including vitamins, pectins, and fatty acids, characterize citrus and citrus products' distinct flavor and various therapeutic and nutraceutical potentials, such as antioxidant, anti-inflammatory, antimicrobial, anticancer, neuroprotective effect, and other biological properties. The composition and content of phytochemical and nutritional compounds in citrus vary dramatically among varieties, fruit parts, maturity, region of cultivation, and many other environmental factors. The developments of value-added citrus products, including citrus juices, citrus wines, citrus jams, canned citrus, and dried citrus, can partly overcome the defects of seasonality and short life of fresh citrus, extend the citrus industry chain, and meet the nutritional requirements of novel fruit products from consumers. In conclusion, citrus is a functional and nutritional fruit and can complement other fruit and fruit products for various applications.

However, there are some challenges and issues that should be overcome or addressed in the future study of citrus. Under the premise of accurate profiling of phytochemical and nutritional substances in citrus, and given the tremendous differences in the chemical substances among different citrus varieties, fruit parts, maturity, and cultivation region, targeted utilization of citrus resources should be made in the future. Nowadays, citrus industries are confronted with the dilemma that the phytochemicals and nutrients in citrus are vulnerable when introduced into the food and digestive system, hence more studies on the protection of these bioactive compounds are of great importance for enhancing the commercial value of citrus. Moreover, at present, clinical research on citrus mainly focuses on the structure-activity relationships of specific compounds extracted from citrus, while as a whole, the health-promoting effect of citrus on human health should be paid more attention. To meet the growing demand for high-quality citrus products from the market, we should develop novel cultivation strategies and processing techniques to maximally retain citrus flavor, phytochemical, and nutritional values. The health potentials of these novel citrus products also need to be clarified to facilitate their food application. Furthermore, the food applications of citrus are mainly determined by their flavor profiles, the mapping and correlation between citrus sensory quality and specific flavor compounds should also be systematically revealed. From the perspective of sustainable development, the residues of citrus, such as peels, pomace, seeds, and leaves, have a high rate of waste worldwide and are unfavorable for the environment. These side streams in foods and other industries should be exploited as equally important as citrus flesh to broaden their utilization in the future. And environmentally friendly protocols must be preferentially applied during the valorization of citrus.

Author contributions

SL and YLo reviewed the literature and elaborated the figures. SL, YLo, YLi, and JZ drafted the manuscript. PL and BY: writing—review and editing. QG: writing—review and editing, and funding acquisition. All authors contributed to the article and approved the submitted version.

Funding

This work was supported by the Chinese Academy of Engineering Academy-Locality Cooperation Project (No. 2019-ZJ-JS-02) and the National Key Research and Development Program of China (No. 2017YFE0122300).

Conflict of interest

The authors declare that the research was conducted in the absence of any commercial or financial relationships that could be construed as a potential conflict of interest.

Publisher's note

References

1. Sharma K, Mahato N, Lee YR. Extraction, characterization and biological activity of citrus flavonoids. *Rev Chem Eng.* (2019) 35:265–84. doi: 10.1515/revce-2017-0027

2. Porat R, Deterre S, Giampaoli P, Plotto A. The flavor of citrus fruit. In: *Biotechnology in Flavor Production*. Chichester, UK: John Wiley & Sons, Ltd (2016). p. 1–31 doi: 10.1002/9781118354056.ch1

3. Gence L, Servent A, Poucheret P, Hiol A, Dhuique-Mayer C. Pectin structure and particle size modify carotenoid bioaccessibility and uptake by Caco-2 cells in citrus juices vs. concentrates. *Food Funct.* (2018) 9:3523–31. doi: 10.1039/C8FO00111A

4. Chidambara Murthy KN, Jayaprakasha GK, Safe S, Patil BS. Citrus limonoids induce apoptosis and inhibit the proliferation of pancreatic cancer cells. *Food Funct.* (2021) 12:1111–20. doi: 10.1039/D0FO02740E

5. Wang F, Zhao C, Yang M, Zhang L, Wei R, Meng K, et al. Four citrus flavanones exert atherosclerosis alleviation effects in apoe-/-mice *via* different metabolic and signaling pathways. *J Agric Food Chem.* (2021) 69:5226–37. doi: 10.1021/acs.jafc.1c01463

6. Grosso G, Galvano F, Mistretta A, Marventano S, Nolfo F, Calabrese G, Buscemi S, Drago F, Veronesi U, Scuderi A. Red orange: Experimental models and epidemiological evidence of its benefits on human health. *Oxid Med Cell Longev.* (2013) 2013:1–11. doi: 10.1155/2013/157240

7. Li C, Schluesener H. Health-promoting effects of the citrus flavanone hesperidin. *Crit Rev Food Sci Nutr.* (2017) 57:613–31. doi: 10.1080/10408398.2014.906382

8. Chaves JO, Sanches VL, Viganó J, de Souza Mesquita LM, de Souza MC, da Silva LC, et al. Integration of pressurized liquid extraction and in-line solid-phase extraction to simultaneously extract and concentrate phenolic compounds from lemon peel (Citrus limon L.). *Food Res Int* (2022) 157:111252. doi: 10.1016/j.foodres.2022.111252

9. Yue ZX, Gu YX, Yan TC, Liu FM, Cao J, Ye LH. Phase I and phase II metabolic studies of Citrus flavonoids based on electrochemical simulation and in vitro methods by EC-Q-TOF/MS and HPLC-Q-TOF/MS. *Food Chem.* (2022) 380:132202. doi: 10.1016/j.foodchem.2022.132202

10. Karn A, Zhao C, Yang F, Cui J, Gao Z, Wang M, et al. *In vivo* biotransformation of citrus functional components and their effects on health. *Crit Rev Food Sci Nutr.* (2021) 61:756–76. doi: 10.1080/10408398.2020.1746234

11. Abad-García B, Berrueta LA, Garmón-Lobato S, Gallo B, Vicente F, A. general analytical strategy for the characterization of phenolic compounds in fruit juices by high-performance liquid chromatography with diode array detection coupled to electrospray ionization and triple quadrupole mass spectrometry. *J Chromatogr A.* (2009) 1216:5398–415. doi: 10.1016/j.chroma.2009.05.039

12. Chen J, Li G, Zhang H, Yuan Z, Li W, Peng Z, et al. Primary bitter taste of citrus is linked to a functional allele of the 1,2-rhamnosyltransferase gene originating from citrus grandis. *J Agric Food Chem.* (2021) 69:9869–82. doi: 10.1021/acs.jafc.1c01211

13. Morales J, Bermejo A, Navarro P, Forner-Giner MÁ, Salvador A. Rootstock effect on fruit quality, anthocyanins, sugars, hydroxycinnamic acids and flavanones content during the harvest of blood oranges 'Moro' and 'Tarocco Rosso' grown in Spain. *Food Chem.* (2021) 342:128305. doi: 10.1016/j.foodchem.2020.128305

14. Singh B, Singh JP, Kaur A, Singh N. Phenolic composition, antioxidant potential and health benefits of citrus peel. *Food Res Int.* (2020) 132:109114. doi: 10.1016/j.foodres.2020.109114

15. Bharti S, Rani N, Krishnamurthy B, Arya DS. Preclinical evidence for the pharmacological actions of naringin: a review. *Planta Med.* (2014) 80:437–51. doi: 10.1055/s-0034-1368351

16. Ghanbari-Movahed M, Jackson G, Farzaei MH, Bishayee A. A systematic review of the preventive and therapeutic effects of naringin against human malignancies. *Front Pharmacol.* (2021) 12:250. doi: 10.3389/fphar.2021.639840

17. Jiang H, Zhang W, Xu Y, Chen L, Cao J, Jiang W. An advance on nutritional profile, phytochemical profile, nutraceutical properties, and potential industrial applications of lemon peels: a comprehensive review. *Trends Food Sci Technol.* (2022) 124:219–36. doi: 10.1016/j.tifs.2022.04.019

18. Maugeri A, Cirmi S, Minciullo PL, Gangemi S, Calapai G, Mollace V, et al. Citrus fruits and inflammaging: a systematic review. *Phytochem Rev.* (2019) 18:1025–49. doi: 10.1007/s11101-019-09613-3

19. Mitra S, Lami MS, Uddin TM, Das R, Islam F, Anjum J, et al. Prospective multifunctional roles and pharmacological potential of dietary flavonoid narirutin. *Biomed Pharmacother.* (2022) 150:112932. doi: 10.1016/j.biopha.2022.112932

20. Hou J, Liang L, Su M, Yang T, Mao X, Wang Y. Variations in phenolic acids and antioxidant activity of navel orange at different growth stages. *Food Chem.* (2021) 360:129980. doi: 10.1016/j.foodchem.2021.129980

21. Dong X, Hu Y, Li Y. Zhou Z. The maturity degree, phenolic compounds and antioxidant activity of Eureka lemon [Citrus limon (L) Burm f]: a negative correlation between total phenolic content, antioxidant capacity and soluble solid content. *Sci Hortic.* (2019) 243:281–9. doi: 10.1016/j.scienta.2018.08.036

22. Zhao Z, He S, Hu Y, Yang Y, Jiao B, Fang Q, et al. Fruit flavonoid variation between and within four cultivated Citrus species evaluated by UPLC-PDA system. *Sci Hortic.* (2017) 224:93–101. doi: 10.1016/j.scienta.2017.05.038

23. Cano A, Medina A, Bermejo A. Bioactive compounds in different citrus varieties. *Discrimination among cultivars. J Food Compos Anal.* (2008) 21:377–81. doi: 10.1016/j.jfca.2008.03.005

24. Abad-García B, Garmón-Lobato S, Sánchez-Ilárduya MB, Berrueta LA, Gallo B, Vicente F, et al. Polyphenolic contents in citrus fruit juices: authenticity assessment. *Eur Food Res Technol.* (2014) 238:803–18. doi: 10.1007/s00217-014-2160-9

25. Barreca D, Gattuso G, Bellocco E, Calderaro A, Trombetta D, Smeriglio A, et al. Flavanones: citrus phytochemical with health-promoting properties. *BioFactors.* (2017) 43:495–506. doi: 10.1002/biof.1363

26. Chanet A, Milenkovic D, Manach C, Mazur A, Morand C. Citrus flavanones: what is their role in cardiovascular protection? *J Agric Food Chem.* (2012) 60:8809–22. doi: 10.1021/jf300669s

27. Khan MK. Zill-E-Huma, Dangles O. A comprehensive review on flavanones, the major citrus polyphenols. *J Food Compos Anal.* (2014) 33:85–104. doi: 10.1016/j.jfca.2013.11.004

28. Peterson JJ, Dwyer JT, Beecher GR, Bhagwat SA, Gebhardt SE, Haytowitz DB, et al. Flavanones in oranges, tangerines (mandarins), tangors, and tangelos: a compilation and review of the data from the analytical literature. *J Food Compos Anal.* (2006) 19:66–73. doi: 10.1016/j.jfca.2005.12.006

29. Zhang M, Zhu S, Yang W, Huang Q, Ho CT. The biological fate and bioefficacy of citrus flavonoids: bioavailability, biotransformation, and delivery systems. *Food Funct.* (2021) 12:3307–23. doi: 10.1039/D0FO03403G

30. Erlund I. Review of the flavonoids quercetin, hesperetin, and naringenin. Dietary sources, bioactivities, bioavailability, and epidemiology. *Nutr Res.* (2004) 24:851–74. doi: 10.1016/j.nutres.2004.07.005

31. Barreca D, Gattuso G, Laganà G, Leuzzi U. Bellocco E. C- and O-glycosyl flavonoids in Sanguinello and Tarocco blood orange (*Citrus sinensis* (L) Osbeck) juice: Identification and influence on antioxidant properties and acetylcholinesterase activity. *Food Chem.* (2016) 196:619–27. doi: 10.1016/j.foodchem.2015.09.098

32. Kelebek H, Selli S, Canbas A, Cabaroglu T. HPLC determination of organic acids, sugars, phenolic compositions and antioxidant capacity of orange juice and orange wine made from a Turkish cv. *Kozan Microchem J.* (2009) 91:187–92. doi: 10.1016/j.microc.2008.10.008

33. Gattuso G, Barreca D, Gargiulli C, Leuzzi U, Caristi C. Flavonoid composition of citrus juices. *Molecules.* (2007) 12:1641–73. doi: 10.3390/12081641

34. Barreca D, Bellocco E, Leuzzi U. Gattuso G. First evidence of C- and O-glycosyl flavone in blood orange (Citrus sinensis (L) Osbeck) juice

and their influence on antioxidant properties. *Food Chem.* (2014) 149:244–52. doi: 10.1016/j.foodchem.2013.10.096

35. Abad-García B, Garmón-Lobato S, Berrueta LA, Gallo B, Vicente F. On line characterization of 58 phenolic compounds in Citrus fruit juices from Spanish cultivars by high-performance liquid chromatography with photodiode-array detection coupled to electrospray ionization triple quadrupole mass spectrometry. *Talanta.* (2012) 99:213–24. doi: 10.1016/j.talanta.2012.05.042

36. Wang Y, Liu X-J, Chen J-B, Cao J-P, Li X, Sun C-D. Citrus flavonoids and their antioxidant evaluation. *Crit Rev Food Sci Nutr.* (2021) 62:1–22.

37. Ledesma-Escobar CA, Priego-Capote F, Robles Olvera VJ, Luque De Castro MD. Targeted analysis of the concentration changes of phenolic compounds in Persian Lime (*Citrus latifolia*) during Fruit Growth. *J Agric Food Chem.* (2018) 66:1813–20. doi: 10.1021/acs.jafc.7b05535

38. Sudhakaran M, Doseff AI. The targeted impact of flavones on obesity-induced inflammation and the potential synergistic role in cancer and the gut microbiota. *Molecules.* (2020) 25:1–29. doi: 10.3390/molecules25112477

39. Barreca D, Mandalari G, Calderaro A, Smeriglio A, Trombetta D, Felice MR, et al. Citrus flavones: an update on sources, biological functions, and health promoting properties. *Plants.* (2020) 9:1–23. doi: 10.3390/plants9030288

40. Maggioni D, Garavello W, Rigolio R, Pignataro L, Gaini R, Nicolini G. Apigenin impairs oral squamous cell carcinoma growth in vitro inducing cell cycle arrest and apoptosis. *Int J Oncol.* (2013) 43:1675–82. doi: 10.3892/ijo.2013.2072

41. Sudhakaran M, Sardesai S, Doseff AI. Flavonoids: new frontier for immuno-regulation and breast cancer control. *Antioxidants.* (2019) 8:103. doi: 10.3390/antiox8040103

42. Gao Z, Gao W, Zeng SL Li P, Liu EH. Chemical structures, bioactivities and molecular mechanisms of citrus polymethoxyflavones. *J Funct Foods.* (2018) 40:498–509. doi: 10.1016/j.jff.2017.11.036

43. Wang S, Yang C, Tu H, Zhou J, Liu X, Cheng Y, Luo J, Deng X, Zhang H, Xu J. Characterization and metabolic diversity of flavonoids in Citrus species. *Sci Rep.* (2017) 7:10549. doi: 10.1038/s41598-017-10970-2

44. Zhang JY, Zhang Q, Zhang HX, Ma Q, Lu JQ, Qiao YJ. Characterization of polymethoxylated flavonoids (PMFs) in the peels of "Shatangju" mandarin (Citrus reticulata Blanco) by online high-performance liquid chromatography coupled to photodiode array detection and electrospray tandem mass spectrometry. *J Agric Food Chem.* (2012) 60:9023–34. doi: 10.1021/jf302713c

45. Tocmo R, Pena-Fronteras J, Calumba KF, Mendoza M, Johnson JJ. Valorization of pomelo (Citrus grandis Osbeck) peel: a review of current utilization, phytochemistry, bioactivities, and mechanisms of action. *Compr Rev Food Sci Food Saf.* (2020) 19:1969–2012. doi: 10.1111/1541-4337.12561

46. Onda K, Horike N, Suzuki TI, Hirano T. Polymethoxyflavonoids tangeretin and nobiletin increase glucose uptake in murine adipocytes. *Phyther Res.* (2013) 27:312–6. doi: 10.1002/ptr.4730

47. Wang C, Chen X, Liu S. Encapsulation of tangeretin into debranched-starch inclusion complexes: Structure, properties and stability. *Food Hydrocoll.* (2020) 100:105409. doi: 10.1016/j.foodhyd.2019.105409

48. Sun G, Liu F, Zhao R, Hu Y, Li B, Liu S, et al. Enhanced stability and bioaccessibility of nobiletin in whey protein/cinnamaldehyde-stabilized microcapsules and application in yogurt. *Food Struct.* (2021) 30:100217. doi: 10.1016/j.foostr.2021.100217

49. Pollastri S, Tattini M. Flavonols: old compounds for old roles. *Ann Bot.* (2011) 108:1225–33. doi: 10.1093/aob/mcr234

50. Wang L, Tu YC, Lian TW, Hung JT, Yen JH, Wu MJ. Distinctive antioxidant and antiinflammatory effects of flavonols. *J Agric Food Chem.* (2006) 54:9798–804. doi: 10.1021/jf0620719

51. Liu C, Long J, Zhu K, Liu L, Yang W, Zhang H, et al. Characterization of a Citrus R2R3-MYB transcription factor that regulates the flavonol and hydroxycinnamic acid biosynthesis. *Sci Rep.* (2016) 6:1–16. doi: 10.1038/srep25352

52. Castañeda-Ovando A, Pacheco-Hernández M de L, Páez-Hernández ME, Rodríguez JA, Galán-Vidal CA. Chemical studies of anthocyanins: a review. *Food Chem.* (2009) 113:859–71. doi: 10.1016/j.foodchem.2008.09.001

53. He J, Giusti MM. Anthocyanins: natural colorants with health-promoting properties. *Annu Rev Food Sci Technol.* (2010) 1:163–87. doi: 10.1146/annurev.food.080708.100754

54. Lo Piero AR. The state of the art in biosynthesis of anthocyanins and its regulation in pigmented sweet oranges [(*Citrus sinensis*) L. *Osbeck] J Agric Food Chem.* (2015) 63:4031–41. doi: 10.1021/acs.jafc.5b01123

55. Chen J, Xu B, Sun J, Jiang X, Bai W. Anthocyanin supplement as a dietary strategy in cancer prevention and management: a comprehensive review. *Crit Rev Food Sci Nutr.* (2021) 1–13. doi: 10.1080/10408398.2021.1913092

56. Mattioli R, Francioso A, Mosca L, Silva P. Anthocyanins: a comprehensive review of their chemical properties and health effects on cardiovascular and neurodegenerative diseases. *Molecules* (2020) 25:3809. doi: 10.3390/molecules25173809

57. Cebadera-Miranda L, Domínguez L, Dias MI, Barros L, Ferreira ICFR, Igual M, et al. Cámara M. Sanguinello and Tarocco *(Citrus sinensis [L] Osbeck):* Bioactive compounds and colour appearance of blood oranges. *Food Chem.* (2019) 270:395–402. doi: 10.1016/j.foodchem.2018.07.094

58. Legua P, Modica G, Porras I, Conesa A, Continella A. Bioactive compounds, antioxidant activity and fruit quality evaluation of eleven blood orange cultivars. *J Sci Food Agric.* (2022) 102:2960–71. doi: 10.1002/jsfa.11636

59. Pannitteri C, Continella A, Lo Cicero L, Gentile A, La Malfa S, Sperlinga E, et al. Influence of postharvest treatments on qualitative and chemical parameters of Tarocco blood orange fruits to be used for fresh chilled juice. *Food Chem.* (2017) 230:441–7. doi: 10.1016/j.foodchem.2017.03.041

60. Chen J, Liu F, Ismail BB. wang W, Xu E, Pan H, Ye X, Liu D, Cheng H. Effects of ethephon and low-temperature treatments on blood oranges *(Citrus sinensis L Osbeck):* anthocyanin accumulation and volatile profile changes during storage. *Food Chem.* (2022) 393:133381. doi: 10.1016/j.foodchem.2022.133381

61. Lo Piero AR, Puglisi I, Rapisarda P, Petrone G. Anthocyanins accumulation and related gene expression in red orange fruit induced by low temperature storage. *J Agric Food Chem.* (2005) 53:9083–8. doi: 10.1021/jf051609s

62. Cotroneo PS, Russo MP, Ciuni M, Recupero GR, Lo Piero AR. Quantitative real-time reverse transcriptase-PCR profiling of anthocyanin biosynthetic genes during orange fruit ripening. *J Am Soc Hortic Sci.* (2006) 131:537–43. doi: 10.21273/JASHS.131.4.537

63. Kumar N, Goel N. Phenolic acids: Natural versatile molecules with promising therapeutic applications. *Biotechnol Reports.* (2019) 24:e00370. doi: 10.1016/j.btre.2019.e00370

64. Ghasemzadeh A, Ghasemzadeh N. Flavonoids and phenolic acids: role and biochemical activity in plants and human. *J Med Plant Res.* (2011) 5:6697–703. doi: 10.5897/JMPR11.1404

65. Panwar D, Panesar PS, Chopra HK. Recent trends on the valorization strategies for the management of Citrus by-products. *Food Rev Int.* (2021) 37:91–120. doi: 10.1080/87559129.2019.1695834

66. Xu GH, Chen JC, Liu DH, Zhang YH, Jiang P, Ye XQ. Minerals, phenolic compounds, and antioxidant capacity of citrus peel extract by hot water. *J Food Sci* (2008) 73:C11–C18. doi: 10.1111/j.1750-3841.2007.00546.x

67. Cheong MW, Chong ZS, Liu SQ, Zhou W, Curran P, Yu B. Characterisation of calamansi (*Citrus microcarpa*). Part I: Volatiles, aromatic profiles and phenolic acids in the peel. *Food Chem.* (2012) 134:686–95. doi: 10.1016/j.foodchem.2012.02.162

68. Kurowska EM, Manthey JA. Hypolipidemic effects and absorption of Citrus polymethoxylated flavones in hamsters with diet-induced hypercholesterolemia. *J Agric Food Chem.* (2004) 52:2879–86. doi: 10.1021/jf035354z

69. Rapisarda P, Carollo G, Fallico B, Tomaselli F, Maccarone E. Hydroxycinnamic acids as markers of Italian blood orange juices. *J Agric Food Chem.* (1998) 46:464–70. doi: 10.1021/jf9603700

70. Borredá C, Perez-Roman E, Talon M, Terol J. Comparative transcriptomics of wild and commercial Citrus during early ripening reveals how domestication shaped fruit gene expression. *BMC Plant Biol.* (2022) 22:1–21. doi: 10.1186/s12870-022-03509-9

71. Ikoma Y, Matsumoto H, Kato M. Diversity in the carotenoid profiles and the expression of genes related to carotenoid accumulation among citrus genotypes. *Breed Sci.* (2016) 66:139–47. doi: 10.1270/jsbbs.66.139

72. Yoo KM, Moon BK. Comparative carotenoid compositions during maturation and their antioxidative capacities of three citrus varieties. *Food Chem.* (2016) 196:544–9. doi: 10.1016/j.foodchem.2015.09.079

73. Rodrigo MJ, Cilla A, Barberá R, Zacarías L. Carotenoid bioaccessibility in pulp and fresh juice from carotenoid-rich sweet oranges and mandarins. *Food Funct.* (2015) 6:1950–9. doi: 10.1039/C5FO00258C

74. Lux PE, Carle R, Zacarías L, Rodrigo MJ, Schweiggert RM. Steingass CB. *genuine carotenoid profiles in sweet orange [Citrus sinensis (L)* Osbeck cv Navel] Peel and Pulp at Different Maturity Stages. *J Agric Food Chem.* (2019) 67:13164–75. doi: 10.1021/acs.jafc.9b06098

75. Fanciullino AL, Dhuique-Mayer C, Luro F, Casanova J, Morillon R, Ollitrault P. Carotenoid diversity in cultivated citrus is highly influenced by genetic factors. *J Agric Food Chem.* (2006) 54:4397–406. doi: 10.1021/jf0526644

76. Kato M, Ikoma Y, Matsumoto H, Sugiura M, Hyodo H, Yano M. Accumulation of carotenoids and expression of carotenoid biosynthetic genes during maturation in citrus fruit. *Plant Physiol.* (2004) 134:824–37. doi: 10.1104/pp.103.031104

77. Matsumoto H, Ikoma Y, Kato M, Kuniga T, Nakajima N, Yoshida T. Quantification of carotenoids in citrus fruit by LC-MS and comparison of patterns of seasonal changes for carotenoids among citrus varieties. *J Agric Food Chem.* (2007) 55:2356–68. doi: 10.1021/jf062629c

78. Goodlier KL, Rouseff RL, Hofsommer HJ. Orange, Mandarin, and hybrid classification using multivariate statistics based on carotenoid profiles. *J Agric Food Chem.* (2001) 49:1146–50. doi: 10.1021/jf000866o

79. Dhuique-Mayer C, Fanciullino AL, Dubois C, Ollitrault P. Effect of genotype and environment on citrus juice carotenoid content. *J Agric Food Chem.* (2009) 57:9160–8. doi: 10.1021/jf901668d

80. Carmona L, Zacarías L, Rodrigo MJ. Stimulation of coloration and carotenoid biosynthesis during postharvest storage of 'Navelina' orange fruit at 12°C. *Postharvest Biol Technol.* (2012) 74:108–17. doi: 10.1016/j.postharvbio.2012.06.021

81. Verkempinck SHE, Salvia-Trujillo L, Denis S, Van Loey AM, Hendrickx ME, Grauwet T. Pectin influences the kinetics of in vitro lipid digestion in oil-in-water emulsions. *Food Chem.* (2018) 262:150–61. doi: 10.1016/j.foodchem.2018.04.082

82. Chaudhary R, Chaturvedi S, Sharma R, Tiwari S. Global scenario of vitamin deficiency and human health. In:*Advances in Agri-Food Biotechnology*. Singapore: Springer Singapore (2020). p. 199–220 doi: 10.1007/978-981-15-2874-3_9

83. Liu Y, Heying E, Tanumihardjo SA. History, Global distribution, and nutritional importance of citrus fruits. *Compr Rev Food Sci Food Saf.* (2012) 11:530–45. doi: 10.1111/j.1541-4337.2012.00201.x

84. Byers T, Guerrero N. Epidemiologic evidence for vitamin C and vitamin E in cancer prevention. *Am J Clin Nutr.* (1995) 62:1385S–92S. doi: 10.1093/ajcn/62.6.1385S

85. Rampersaud GC, Valim MF. *100% citrus juice: Nutritional contribution, dietary benefits, and association with anthropometric measures. Crit Rev Food Sci Nutr.* (2017). 129–40 . doi: 10.1080/10408398.2013.862611

86. Cardeñosa V, Barros L, Barreira JCM, Arenas F, Moreno-Rojas JM, Ferreira ICFR. Different Citrus rootstocks present high dissimilarities in their antioxidant activity and vitamins content according to the ripening stage. *J Plant Physiol.* (2015) 174:124–30. doi: 10.1016/j.jplph.2014.10.013

87. Liu N, Li X, Zhao P, Zhang X, Qiao O, Huang L, et al. review of chemical constituents and health-promoting effects of citrus peels. *Food Chem.* (2021) 365:130585. doi: 10.1016/j.foodchem.2021.130585

88. Fracasso AF, Perussello CA, Carpiné D, Petkowicz CL de O, Haminiuk CWI. Chemical modification of citrus pectin: structural, physical and rheologial implications. *Int J Biol Macromol.* (2018) 109:784–92. doi: 10.1016/j.ijbiomac.2017.11.060

89. Wu D, Zheng J, Mao G, Hu W, Ye X, Linhardt RJ, et al. Rethinking the impact of RG-I mainly from fruits and vegetables on dietary health. *Crit Rev Food Sci Nutr.* (2020) 60:2938–60. doi: 10.1080/10408398.2019.1672037

90. Wei R, Zhao S, Zhang L, Feng L, Zhao C, An Q, et al. Upper digestion fate of citrus pectin-stabilized emulsion: an interfacial behavior perspective. *Carbohydr Polym.* (2021) 264:118040. doi: 10.1016/j.carbpol.2021.118040

91. Chen J, Cheng H, Zhi Z, Zhang H, Linhardt RJ, Zhang F, et al. Extraction temperature is a decisive factor for the properties of pectin. *Food Hydrocoll.* (2021) 112:106160. doi: 10.1016/j.foodhyd.2020.106160

92. Nisar T, Wang ZC, Yang X, Tian Y, Iqbal M, Guo Y. Characterization of citrus pectin films integrated with clove bud essential oil: Physical, thermal, barrier, antioxidant and antibacterial properties. *Int J Biol Macromol.* (2018) 106:670–80. doi: 10.1016/j.ijbiomac.2017.08.068

93. Assefa AD, Saini RK, Keum YS. Fatty acids, tocopherols, phenolic and antioxidant properties of six citrus fruit species: a comparative study. *J Food Meas Charact.* (2017) 11:1665–75. doi: 10.1007/s11694-017-9546-x

94. Chen J, Liu H. Nutritional indices for assessing fatty acids: a mini-review. *Int J Mol Sci.* (2020) 21:1–24. doi: 10.3390/ijms21165695

95. Moufida S, Marzouk B. Biochemical characterization of blood orange, sweet orange, lemon, bergamot and bitter orange. *Phytochemistry.* (2003) 62:1283–9. doi: 10.1016/S0031-9422[02]00631-3

96. Matsuo Y, Miura LA, Araki T, Yoshie-Stark Y. Proximate composition and profiles of free amino acids, fatty acids, minerals and aroma compounds in Citrus natsudaidai peel. *Food Chem.* (2019) 279:356–63. doi: 10.1016/j.foodchem.2018.11.146

97. Fabroni S, Amenta M, Timpanaro N, Todaro A, Rapisarda P. Change in taste-altering non-volatile components of blood and common orange fruit during cold storage. *Food Res Int.* (2020) 131:108916. doi: 10.1016/j.foodres.2019.108916

98. Kore VT, Chakraborty I. Efficacy of various techniques on biochemical characteristics and bitterness of pummelo juice. *J Food Sci Technol.* (2015) 52:6073–7. doi: 10.1007/s13197-014-1629-7

99. Purewal SS, Sandhu KS. Debittering of citrus juice by different processing methods: A novel approach for food industry and agro-industrial sector. *Sci Hortic.* (2021) 276:109750. doi: 10.1016/j.scienta.2020.109750

100. Yu Y, Xiao G, Xu Y, Wu J, Fu M, Wen J. Slight Fermentation with *Lactobacillus fermentium* improves the taste (Sugar: Acid Ratio) of Citrus *(Citrus reticulata* cv. *chachiensis). Juice J Food Sci.* (2015) 80:M2543–7. doi: 10.1111/1750-3841.13088

101. Miranda RF, de Paula MM, da Costa GM, Barão CE, da Silva ACR, Raices RSL, et al. Orange juice added with *L. casei:* is there an impact of the probiotic addition methodology on the quality parameters? *LWT.* (2019) 106:186–93. doi: 10.1016/j.lwt.2019.02.047

102. Yuasa M, Shimada A, Matsuzaki A, Eguchi A, Tominaga M. Chemical composition and sensory properties of fermented citrus juice using probiotic lactic acid bacteria. *Food Biosci.* (2021) 39:100810. doi: 10.1016/j.fbio.2020.100810

103. Selli S. Volatile constituents of orange wine obtained from moro oranges (*Citrus sinensis* [L.] osbeck). *J Food Qual.* (2007) 30:330–41. doi: 10.1111/j.1745-4557.2007.00124.x

104. Bi J, Li H, Wang H. Delayed bitterness of citrus wine is removed through the selection of fining agents and fining optimization. *Front Chem.* (2019) 7:185. doi: 10.3389/fchem.2019.00185

105. Archibong EJ, Ezemba CC, Chukwujama IC, Archibong UE. Production of wine from mixed fruits: pineapple (*Ananas comosus*) and Orange (*Citrus sinensis*) using yeast isolated from palm wine. *World J Pharm Pharm Sci.* (2015) 4:126–36.

106. Xu X, Bao Y, Wu B, Lao F, Hu X, Wu J. Chemical analysis and flavor properties of blended orange, carrot, apple and Chinese jujube juice fermented by selenium-enriched probiotics. *Food Chem.* (2019) 289:250–8. doi: 10.1016/j.foodchem.2019.03.068

107. Berk Z. Miscellaneous citrus products. In:*Citrus Fruit Processing*. Amsterdam, The Netherlands: Elsevier Science (2016). p. 235–249. doi: 10.1016/B978-0-12-803133-9.00011-4

108. Tiwari BK. O' Donnell CP, Muthukumarappan K, Cullen PJ. Ascorbic acid degradation kinetics of sonicated orange juice during storage and comparison with thermally pasteurised juice. *LWT - Food Sci Technol.* (2009) 42:700–4. doi: 10.1016/j.lwt.2008.10.009

109. Aghajanzadeh S, Ziaiifar AM, Verkerk R. Effect of thermal and non-thermal treatments on the color of citrus juice: a review. *Food Rev Int.* (2021) 00:1–23. doi: 10.1080/87559129.2021.2012799

110. Li G, Wang F, Wang MM, Tang MT, Zhou T, Gu Q. Physicochemical, structural and rheological properties of pectin isolated from citrus canning processing water. *Int J Biol Macromol.* (2022) 195:12–21. doi: 10.1016/j.ijbiomac.2021.11.203

111. Wang MM, Wang F, Li G, Tang MT, Wang C, Zhou QQ, et al. Antioxidant and hypolipidemic activities of pectin isolated from citrus canning processing water. *LWT.* (2022) 159:113203. doi: 10.1016/j.lwt.2022.113203

112. Rubio-Arraez S, Capella J V, Ortola MD, Castello ML. Effect of replacing sucrose with tagatose and isomaltulose in Mandarin orange marmalade on rheology, colour, antioxidant activity, and sensory properties. *Acta Aliment.* (2016) 45:406–15. doi: 10.1556/066.2016.45.3.12

113. Igual M, Contreras C, Martínez-Navarrete N. Non-conventional techniques to obtain grapefruit jam. *Innov Food Sci Emerg Technol.* (2010) 11:335–41. doi: 10.1016/j.ifset.2010.01.009

114. Igual M, García-Martínez E, Camacho M. del M, Martínez-Navarrete N. Physicochemical and Sensorial Properties of Grapefruit Jams as Affected by Processing. *Food Bioprocess Technol.* (2013) 6:177–85. doi: 10.1007/s11947-011-0696-2

115. Papoutsis K, Vuong Q V, Golding JB, Hasperué JH, Pristijono P, Bowyer MC, et al. Pretreatment of citrus by-products affects polyphenol recovery: a review. *Food Rev Int.* (2018) 34:770–95. doi: 10.1080/87559129.2018.1438471

116. Carlos ALE. Feliciano Priego-Capote, De Castro MDL. Comparative study of the effect of sample pretreatment and extraction on the determination of flavonoids from lemon *(Citrus limon). PLoS ONE.* (2016) 11:1–16. doi: 10.1371/journal.pone.0148056

117. Romdhane NG, Djendoubi N, Bonazzi C, Kechaou N, Mihoubi NB. Effect of combined air-drying-osmotic dehydration on kinetics of techno-functional properties, color and total phenol contents of lemon (*Citrus limon. v lunari) Peels Int J Food Eng.* (2016) 12:515–25. doi: 10.1515/ijfe-2015-0252

118. Papoutsis K, Pristijono P, Golding JB, Stathopoulos CE, Bowyer MC, Scarlett CJ, et al. Effect of vacuum-drying, hot air-drying and freeze-drying on polyphenols and antioxidant capacity of lemon (*Citrus limon*) pomace aqueous extracts. *Int J Food Sci Technol.* (2017) 52:880–7. doi: 10.1111/ijfs.13351

119. García-Salas P, Gómez-Caravaca AM, Arráez-Román D, Segura-Carretero A, Guerra-Hernández E, García-Villanova B, et al. Influence of technological processes on phenolic compounds, organic acids, furanic derivatives, and antioxidant activity of whole-lemon powder. *Food Chem.* (2013) 141:869–78. doi: 10.1016/j.foodchem.2013.02.124

120. Ghanem Romdhane N, Bonazzi C, Kechaou N, Mihoubi NB. Effect of Air-drying temperature on kinetics of quality attributes of lemon (*Citrus limon* cv. *lunari) Peels Dry Technol.* (2015) 33:1581–9. doi: 10.1080/07373937.2015.1012266

frontiers | Frontiers in Nutrition

TYPE Original Research
PUBLISHED 12 October 2022
DOI 10.3389/fnut.2022.1017765

OPEN ACCESS

EDITED BY
Yu Xiao,
Hunan Agricultural University, China

REVIEWED BY
Jie Yang,
Jiangsu Ocean University, China
Er Sheng Gong,
Gannan Medical University, China
Xiaoli Liu,
Jiangsu Academy of Agricultural Sciences (JAAS), China

*CORRESPONDENCE
Feng Zuo
zuofeng-518@126.com
Xiqun Zheng
zhengxiqun@126.com

†These authors have contributed equally to this work

SPECIALTY SECTION
This article was submitted to Nutrition and Food Science Technology, a section of the journal Frontiers in Nutrition

RECEIVED 12 August 2022
ACCEPTED 27 September 2022
PUBLISHED 12 October 2022

CITATION
Wang K, Gao Y, Zhao J, Wu Y, Sun J, Niu G, Zuo F and Zheng X (2022) Effects of *in vitro* digestion on protein degradation, phenolic compound release, and bioactivity of black bean tempeh.
Front. Nutr. 9:1017765.
doi: 10.3389/fnut.2022.1017765

Effects of *in vitro* digestion on protein degradation, phenolic compound release, and bioactivity of black bean tempeh

Kun Wang[1,2†], Yongjiao Gao[1†], Jing Zhao[1], Yue Wu[1], Jingchen Sun[1], Guangcai Niu[1], Feng Zuo[1,3*] and Xiqun Zheng[1,2*]

[1]College of Food Science, Heilongjiang Bayi Agricultural University, Daqing, China, [2]National Coarse Cereals Engineering Research Center, Daqing, China, [3]Engineering Research Center of Processing and Utilization of Grain By-products, Ministry of Education, Daqing, China

The nutritional value and bioactivity of black beans are enhanced when fermented as tempeh, but their bioaccessibility and bioactivity after ingestion remain unclear. In this study, black bean tempeh and unfermented black beans were digested *in vitro* and changes in protein degradation, phenolic compound release, angiotensin I-converting enzyme (ACE)-inhibitory activity, and antioxidant activity between the two groups were compared. We observed that the soluble protein content of digested black bean tempeh was generally significantly higher than that of digested unfermented black beans at the same digestion stage ($P < 0.05$). The degree of protein hydrolysis and the content of <10 kDa peptides were also significantly higher in the digested black bean tempeh than in digested unfermented black beans ($P < 0.05$). SDS-polyacrylamide gel electrophoresis (SDS-PAGE) and reversed-phase high-performance liquid chromatography (RP-HPLC) analysis showed that most macromolecular proteins in tempeh had been degraded during fermentation and more of the small peptides were released from black bean tempeh during digestion, respectively. Compared to that of the unfermented black beans, the level of ACE inhibition of black bean tempeh was lower, but this significantly increased to 82.51% following digestion, closing the gap with unfermented black beans. In addition, the total respective levels of phenolics, flavonoids, and proanthocyanidins released from black bean tempeh were 1.21, 1.40, and 1.55 times those of unfermented black beans following *in vitro* digestion, respectively. Antioxidant activity was also significantly higher in digested black bean tempeh than in digested unfermented black beans and showed a positive correlation with phenolic compound contents ($P < 0.05$). The results of this study proved that, compared to unfermented black beans, black bean tempeh retained protein and phenolic compound bioaccessibility and antioxidant activity and showed an improved ACE-inhibitory activity even after consumption.

KEYWORDS

black bean, tempeh, antioxidant, ACE-inhibitory activity, bioaccessibility

Introduction

Tempeh is a fermented bean-based product original from Indonesia that can be eaten as a staple food. Traditionally, tempeh is pie-shaped with white mycelia on the surface and it is obtained by soaking, peeling, cooking, and acid-adjusting ordinary soybeans, and finally fermenting them using *Rhizopus oligosporus* (1, 2). In recent years, various types of grains and legumes such as oats, barley, wheat, mung bean, broad bean, chickpea, and corn/soybean have also been used in the production of tempeh, further enriching its variety (3). Tempeh is a nutritious food, containing high amounts of dietary fiber, vitamin B12, folic acid, unsaturated fatty acids, isoflavones, and minerals, as well as a high protein content, making it an ideal meat substitute for vegetarians (2, 4, 5). In addition to its high nutritional value, tempeh also has a variety of physiological benefits such as antioxidation, lowering of blood lipid levels and blood pressure, tumor inhibition, prevention of atherosclerosis, and improvement of iron deficiency in anemia (3, 5, 6). Therefore, tempeh has cemented its position as a "superfood" in the modern society, in which the pursuit of high-quality nutrition has become increasingly important.

Besides being rich in high-quality protein, black beans [*Glycine max* (L.) merr.], otherwise known as black soybeans, also contain isoflavones, vitamin E, saponins, carotenoids, anthocyanins, and other active ingredients that grant them anti-inflammatory, antioxidant, anti-tumor, cholesterol-lowering, and analgesic benefits, and making them one of the black-colored foods with the highest nutritional and health care value (7–10). However, currently, the evaluation of the nutrition and health benefits of food is mainly performed through direct chemical analysis without considering the influence of bodily digestion upon human consumption. The conditions of human gastrointestinal digestion and organic extraction can differ greatly, and certain biologically active ingredients can undergo further degradation and metabolism under the action of digestive enzymes during the process of digestion, potentially affecting their biological activity following digestion. Giusti et al. (11) reported that only a fraction of the phenolic compounds from the coat and cotyledons of black beans was bioaccessible after simulated gastrointestinal digestion, and some phenolics were absent after small intestinal digestion due to their pH instability. Sancho et al. (12) investigated the effects of *in vitro* digestion on polyphenols and the antioxidant activity of black bean seed coats and found that the digestion reduced the levels of total phenols and anthocyanins but not the antioxidant activity. Meanwhile, López-Barrios et al. (13) observed that the anti-inflammatory activity of black bean protein isolates was reduced after simulated gastrointestinal digestion. Though the nutritional value and bioactivity of black beans are enhanced when fermented as tempeh (1, 14), it remains unclear whether the active ingredients of black bean tempeh can still retain their biological activity after gastrointestinal digestion *in vitro*.

Based on the previous research, this study simulated the buccal, gastric, and small intestinal digestion of black bean tempeh *in vitro* and investigated the protein degradation, phenolic release, angiotensin I-converting enzyme (ACE)-inhibitory activity, and antioxidant activity of black bean tempeh to assess the effects of digestion on its nutrient release and bioactivity. This study can serve as a theoretical reference for the development of black bean products with high nutritional value and bioactivity.

Materials and methods

Chemicals and materials

Black beans were purchased from Jiansanjiang Farm, Heilongjiang Province, China. Food-grade lactic acid was purchased from Zhengzhou Gaoyan Biotechnology Co., Ltd. (Zhengzhou, China). *R. oligosporus* starter powder was purchased from Nanjing Tianbeiren Fermentation Technology Co., Ltd. (Nanjing, China). Chromatography-grade methanol, trifluoroacetic acid (TFA), and acetonitrile were purchased from Merck (Darmstadt, Germany). Water-soluble vitamin E (Trolox), 1,1-diphenyl-2-picrylhydrazyl (DPPH), pepsin, trypsin, salivary amylase, angiotensin I-converting enzyme (ACE), and 2,2'-azino-bis(3-ethylbenzothiazoline-6-sulfonic acid) (ABTS) were purchased from Sigma-Aldrich Chemical Co., Ltd. (St. Louis, MO, USA). All other chemicals and reagents were of analytical grade and purchased from Sinopharm Chemical Reagents Co., Ltd. (Shanghai, China).

Black bean tempeh production

Black beans were washed with clean water, soaked in a ratio of 1:3 beans to water (m/v) for 24 h at room temperature, peeled, and steamed until soft and without hard cores. After cooling to room temperature, 1.5% (w/w) lactic acid and 0.26% (w/w) *R. oligosporus* starter powder were added and stirred evenly, then placed in an 8 cm × 12 cm fermenting bag with holes (1.25 holes per square centimeter) and incubated at 35 °C for 39 h to obtain the finished product. Unfermented cooked beans served as the experimental control.

In vitro digestion

The preparation of artificial saliva, gastric juice, and small intestinal juice, as well as the procedures for *in vitro* digestion, were performed according to the methods reported by Rui et al. (15) and Xing et al. (16) with a slight modification. Briefly, 10 g of fresh samples were weighed, and 40 ml of distilled water was added to homogenize the initial samples with a miniature

beater. To simulate buccal digestion, 20 ml of 0.2 mg/ml salivary amylase (in 20 mM phosphate buffer at pH 7.0) was added to the initial sample, and the samples were put into a shaking water bath (SWB series; Biobase, Shandong, China) at 55 rpm and 37°C for 3 min. Then, 6 M HCl was used to adjust the pH to 2.0, and 30 ml of 3.2 mg/ml pepsin (in 0.1 M HCl) was added. The simulation of gastric digestion was performed at 55 rpm, 37°C for 1 h. Subsequently, the pH of the reaction was adjusted to 7.0 with 6 M NaOH, and then 20 ml of artificial bile acids (0.4 mg/ml sodium cholate in 10 mM phosphate buffer at pH 7.0) and pancreatic juice (0.4 mg/ml trypsin in 10 mM phosphate buffer at pH 7.0) were added, and the slurry was shaken at 37°C and 150 rpm for 120 min to simulate small intestinal digestion. At the end of each stage, the digestion solution was boiled for 5 min to terminate the enzymatic hydrolysis reaction, then distilled water was added for a constant volume of 130 ml. Next, the solution was centrifuged at 4°C and 12,000 r/min for 15 min, then the supernatant was collected and frozen at −20°C for later use. The samples were labeled according to the digestion stage and substrate; namely, P1 was the initial sample of unfermented black bean control, and P2–P4 were the control samples following the simulated buccal, gastric, and small intestinal digestion. P5 was the initial sample of black bean tempeh and P6–P8 were the tempeh samples following the simulated buccal, gastric, and small intestinal digestion.

Soluble protein analysis

The soluble protein content was determined by the Bradford protein quantification assay using bovine serum albumin as the protein standard (17).

Electrophoresis

SDS-polyacrylamide gel electrophoresis analysis was performed using a DYCZ-24D vertical electrophoresis unit (Baygene Biotech Co., Ltd., Beijing, China) coupled with a DYY-III-5 electric source (Beijing Liuyi Instrument Factory, Beijing, China). The loading volume was 25 μl. Separation gels consisted of a 5% polyacrylamide stacking gel and a 12% polyacrylamide resolving gel, and the voltages used for the gels were 60 and 120 V, respectively. A protein standard (14.4–116.0 kDa) was used as the molecular mass ladder.

Determination of degree of hydrolysis

The *o*-phthaldialdehyde (OPA) spectrophotometric assay was used to determine the number of free amino groups and quantitatively analyze the degree of proteolysis (18). Three milliliters of OPA reagent was added to 400 μl of the solution under test. After mixing, the reaction was accurate for 2 min at room temperature, and the absorbance was measured at 340 nm wavelength using a SPECORD 210 Plus UV/VIS Spectrometer (Analytik Jena AG, Germany). Peptide bonds were quantified using 0.1 mg/ml serine standard solution. The degree of hydrolysis (DH)was calculated according to the formula (1):

$$DH\% = \frac{(W_{serine-NH2} - \beta)}{\alpha \times H_{tot}} \times 100 \quad (1)$$

where

$$W_{serine-NH2} = \frac{A_{sample} - A_{blank}}{A_{std} - A_{blank}} \times \frac{C_{serine-NH2}}{C_{pro}} \quad (2)$$

and $W_{serine-NH2}$ is the millimole number of peptide bonds of the sample protein (mmol/g), A_{sample} is the absorbance of the sample tube, A_{blank} is the absorbance of the blank tube, A_{std} is the absorbance of the serine standard tube, C_{pro} is the concentration of the sample protein (g/L), $C_{serine-NH2}$ is the concentration of the serine standard solution (0.9516 mM), α and β are constants of 0.4 and 1, respectively, and the total peptide bond number (H_{tot} value) of black bean protein was 10.32 mmol/g.

Measurement of peptide contents

Peptide contents were measured as previously reported (19). The solution under test was filtered using a filter membrane with an interception molecular weight of 10,000 Da (Millipore, USA), and then 50 μL of the filtrate was absorbed and reacted with 2 ml of OPA reagent for 2 min at room temperature. The absorbance was measured at a wavelength of 340 nm. A series of casein tryptone solutions at different concentrations were used as the standard for quantification. The results were expressed as casein tryptone equivalents (mg CTE per g fresh sample).

Reversed-phase high-performance liquid chromatography

Reversed-phase high-performance liquid chromatography (RP-HPLC) analysis was performed using a 1260 Infinity II HPLC (Agilent, USA) equipped with a Supersil AQ-C18 reverse-phase column (250 mm × 4.6 mm, 5 μm, Dalian Elite Analytical Instruments, Dalian, China). After filtration using a 0.45-μm filter, 20 μl of sample was applied to the column. The column temperature was 25°C. The mobile phases were composed of solvent A (0.10% TFA in water, v/v) and B (0.10% TFA in acetonitrile, v/v). The elution program started at 5% B, was increased to 17% within 16 min and further to 95% within 2 min, then maintained at 95% for 2 min before being increased to 100% within 1 min and then maintained at 100% for 7 min. The flow rate was 0.80 ml/min and the elution was monitored at 282 nm using a diode-array detector.

Analysis of angiotensin I-converting enzyme-inhibitory activity

An appropriate volume of the solution under test was mixed with 0.1 M boric acid buffer (pH 8.3) in equal volume, and the supernatant was collected by centrifugation at 12,000 rpm, 4°C for 15 min after standing for 1 h. According to a previous method reported by Zhu et al. (20), the determination of the ACE-inhibitory activity of samples was done through monitoring the formation of hippuric acid (HA) from Hippuryl-His-Leu (HHL) as the reaction substrate. Briefly, 10 μl of supernatant was mixed with 50 μl of 2.17 mM HHL and 10 μl of ACE (100 mU/ml). After 30 min of shock reaction at 37°C, the reaction was terminated by adding 85 μl of 1 M HCl. The reaction solution was filtered using a 0.45-μm filter membrane and analyzed using Agilent 1260 Infinity II HPLC. The sample (20 μl) was injected into a Supersil AQ-C18 column (250 mm × 4.60 mm, 5 μm, 25°C, Dalian Elite Analytical Instruments, Dalian, China) and eluted with a 50% methanol solution (v/v) containing 0.1% TFA at a flow rate of 0.50 ml/min. The detection wavelength was 228 nm.

The ACE inhibition rate (IR) of the sample was calculated according to formula (3):

$$IR\ (\%) = \frac{A_1 - A_2}{A_1 - A_3} \times 100 \quad (3)$$

where A_1 is the peak area of the reaction system when boric acid buffer is used instead of sample, A_2 is the peak area of the sample reaction system, and A_3 is the peak area of the reaction system without ACE.

Determination of total phenolic content

The total phenolic content (TPC) was measured using the Folin-Ciocalteu method as described by Tao et al. (21). Folin-Ciocalteu's reagents (0.5 ml) and 2.3 ml of deionized water were added to 200 μl of the solution under test and the mixture was incubated for 1 min. Then, 2 ml of 7.5% (w/v) Na_2CO_3 was added and the mixture was subjected to a dark reaction for 2 h at room temperature. After the reaction was complete, the absorbance at 760 nm was measured with deionized water as the blank control. TPC was expressed as gallic acid equivalents (mg GAE per g fresh sample).

Determination of total flavone content

The total flavone content (TFC) was determined by referring to the method of Sandhu and Punia with a slight modification (22). A 60% ethanol solution (4.4 ml) and a 5% (g/ml) $NaNO_2$ solution (0.3 ml) were added to 0.6 ml of the solution under test, then mixed and left to rest for 6 min. Next, 0.3 ml of 10% $Al(NO_3)_3$ solution was added and the mixture was left to rest for another 6 min. Finally, 4.0 ml of 1 M NaOH solution was added, and the volume was fixed to 10 ml with 60% ethanol solution. The absorbance at 510 nm was measured with deionized water used as the blank control. The TFC was expressed as rutin equivalents (mg RE per g fresh sample).

Determination of proanthocyanidin content (PC)

The proanthocyanidin content (PC) was determined according to the method reported by Saifullah et al. (23). The mixture of 1 ml of the solution under test, 3 ml of 3% (g/ml) vanillin-methanol solution, and 1.5 ml of concentrated hydrochloric acid was placed in a water bath at 30 °C in the dark for 15 min and then the absorbance at 500 nm was measured with methanol as blank control. The PC was expressed as catechin equivalents (mg CE per g fresh sample).

Antioxidant activity analysis

The DPPH radical scavenging activity was determined according to the method described by Tian et al. (24). The $ABTS^+$ radical scavenging ability was determined according to the method of Dong et al. (25). The hydroxyl radical scavenging activity and ferric reducing antioxidant power (FRAP) were determined according to the method of Wang et al. (26). Trolox was used as the positive control and FRAP was expressed as $FeSO_4$ equivalents (μmol $FeSO_4$ equivalents per g fresh sample).

Statistical analysis

All assays were performed in triplicate, and the results are presented as the mean ± standard deviation (SD). Statistical analysis was performed using the SPSS 17.0 software. One-way ANOVA and Duncan's test were used to analyze significant differences in the means at the 0.05 level.

Results and discussion

Soluble protein contents

As shown in **Figure 1**, the average soluble protein contents of black bean tempeh and unfermented black beans were 3.08 and 1.44 mg/g, respectively, indicating that *R. oligosporus* fermentation evidently induced the hydrolysis of black bean proteins. The soluble protein contents of both samples were largely unchanged after buccal digestion. This is because

artificial saliva lacks a protein digestive enzyme system, and salivary amylase mainly acts on soluble starch such as amylose and glycogen; therefore, it has no obvious effect on protein structure. In the subsequent stage of gastric digestion, the presence of pepsin, a strong acid environment, and continuous mechanical shaking causes the disintegration of the protein network and promotes the release of soluble proteins (27). The average soluble protein contents of both black bean tempeh and unfermented black bean samples were significantly increased to 4.44 and 4.15 mg/g, respectively. The soluble protein content of black bean tempeh samples was still significantly higher than that of unfermented black bean samples ($P < 0.05$), which may be because a large degree of degradation of black bean tempeh proteins had occurred during the fermentation stage, causing the spatial structure of the proteins to be relatively relaxed, exposing a large number of digestive enzyme action sites, thus making them more conducive to pepsin digestion. Following small intestinal digestion, the soluble protein content of unfermented black beans was chiefly unchanged, but that of black bean tempeh was significantly lower than that of the tempeh sample in the previous stage of digestion ($P < 0.05$). This likely happened because partial soluble proteins released in the early stage of digestion were further degraded into peptides or free amino acids, which are not detected by Coomassie brilliant blue dye (17). The difference in the outcome of trypsin hydrolysis during small intestinal digestion also suggested that *R. oligosporus* fermentation had a considerable effect on the amino acid composition of black bean protein products after *in vitro* gastrointestinal digestion, imparting a positive effect on digestion.

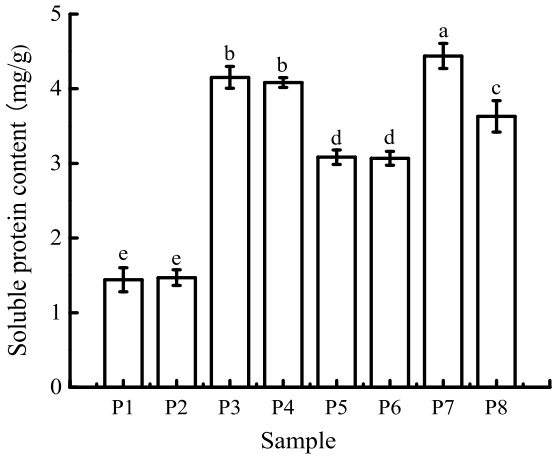

FIGURE 1
Soluble protein contents of samples in different simulated digestion stages. P1 was the initial sample of unfermented black bean control and P2–P4 were the control samples following the simulated buccal, gastric, and small intestinal digestion. P5 was the initial sample of black bean tempeh and P6–P8 were the tempeh samples following the simulated buccal, gastric, and small intestinal digestion, similarly hereinafter. Data with different lowercase letters indicate significant differences ($P < 0.05$).

Electrophoresis

The molecular weight distribution of unfermented black bean and black bean tempeh proteins was investigated by SDS-PAGE during *in vitro* digestion. In **Figure 2** it can be seen that the protein bands of P1 were mainly concentrated between 35 and 45 kDa, and several clear bands also appeared in the >45-kDa region. However, the intensity of the P5 band was lighter and diffusely distributed within the whole lane. These results indicated that *R. oligosporus* fermentation mainly induced the hydrolysis of 35–45-kDa proteins in black beans. The electrophoretic bands of P2 and P6, which represented protein samples at the buccal digestion stage, remained unchanged compared with the samples at the previous stage, indicating that buccal digestion had no obvious effect on the proteins, consistent with the previous results of soluble protein content analysis. The hydrolysis of the sample proteins mainly occurred at the gastric digestion stage. After gastric digestion, the electrophoretic bands of both samples changed significantly. The intensity of the protein bands of P3 within the >35-kDa region, especially the bands between 35 and 45 kDa, became evidently lighter, while the intensity of the protein bands of P3 within the <14.4-kDa region was significantly higher. Meanwhile, the P7 bands migrated further into the <14.4-kDa region. In the final stage of small intestinal digestion, the P4 and P8 bands moved further down, became lighter in intensity, and began to disappear, indicating that the proteins had been further degraded into low molecular fragments that could not be detected by SDS-PAGE (16). Overall, the patterns of electrophoretic protein bands between unfermented black bean samples and black bean tempeh samples during *in vitro* digestion were essentially similar and consequently displayed similar effects of digestion. However, it is worth noting that unlike the macromolecular proteins in the unfermented black bean samples, most of those in black bean tempeh samples had been hydrolyzed to small molecules before digestion, thus reducing the workload of protein digestion.

Degree of hydrolysis and peptide contents

As can be seen in **Figure 3A**, the DH of unfermented black bean and black bean tempeh proteins were 3.60 ± 0.27% and 10.65 ± 0.43%, respectively. Buccal digestion did not affect the proteolysis degree of samples, but the DH of each sample showed a continuous and obvious upward trend in the gastrointestinal digestion stage. This was due to the proteins being successively hydrolyzed by pepsin and trypsin in the

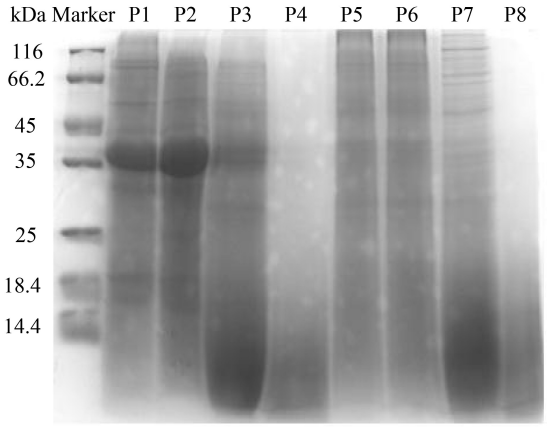

FIGURE 2
SDS-polyacrylamide gel electrophoresis (SDS-PAGE) patterns of samples in different simulated digestion stages.

gastric and small intestinal fluids, leading to the release of a large number of peptides and free amino acids. After digestion, the DH of samples increased to 17.57 ± 0.86% and 22.60 ± 0.8%, respectively. The DH of tempeh proteins was 0.29 times higher than that of unfermented black bean proteins. This fully indicated that the tempeh proteins were hydrolyzed more thoroughly than the unfermented black bean proteins after digestion *in vitro*, making them more conducive to subsequent absorption and utilization. As can be seen in **Figure 3B**, the content of peptides below 10 kDa in the unfermented black bean samples and black bean tempeh samples did not change significantly after buccal digestion, but they progressively increased significantly ($P < 0.05$) after the gastric and small intestinal digestion stages, with the unfermented samples and tempeh samples increasing from 40.03 ± 2.30 mg CTE/g and 102.26 ± 1.29 mg CTE/g to 151.44 ± 1.25 mg CTE/g and 183.95 ± 0.43 mg CTE/g, respectively. At the same digestion stage, the peptide content of tempeh was generally significantly higher than that of unfermented black beans. The production of small peptides (below 10 kDa) may confer better bioactivities such as antioxidation and anti-tumor activities, as well as blood pressure-lowering and anti-inflammation properties to black bean tempeh (17).

Reversed-phase high-performance liquid chromatography (RP-HPLC)

The peptide profiles of unfermented black beans and black bean tempeh were analyzed by RP-HPLC at different stages of digestion. Differences in hydrophobicity can lead to differences in the binding ability of peptides and proteins to the reversed-phase column material, and they can be eluted sequentially under suitable conditions (18). The results are shown in

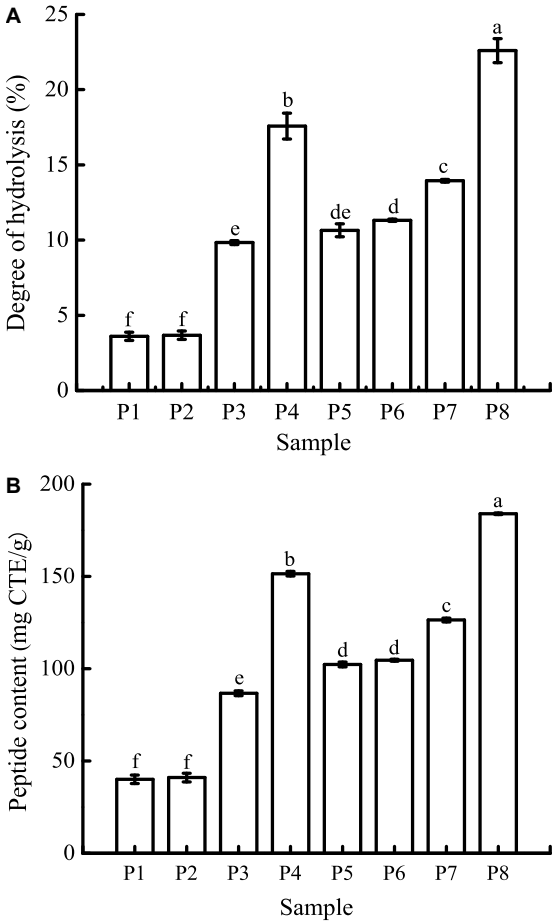

FIGURE 3
Degree of hydrolysis (DH) **(A)** and peptide contents **(B)** of samples in different simulated digestion stages. Data with different lowercase letters indicate significant differences ($P < 0.05$).

Figure 4. Within the retention time from 3.5 to 28 min, the RP-HPLC chromatograms of all the samples with different digestion treatments showed a total of nine chromatographic peaks with larger areas or significant changes, which were successively labeled 1–9 according to their order. There was no significant change in the species and area of main peaks in the buccal digested samples (P2/P6) of unfermented black beans and black bean tempeh compared with the same groups of samples prior to digestion (P1/P5). The stages with a greater influence on peak output were mainly gastric digestion and small intestinal digestion. The respective areas of peaks 8 and 9 of gastric digested samples from unfermented black beans (P3) were 2.34 and 5.20 times those of buccal digested samples from unfermented black beans (P2), while the respective areas of peaks 6, 8, and 9 of gastric digested samples from black bean tempeh (P7) were 1.11, 1.32, and 5.40 times those of buccal digested samples from black bean tempeh (P6). However, the peak areas numbered 1–4 in both samples decreased

significantly after gastric digestion. The eluting components appearing in the early stage should be the peptide segments with very low molecular weight (≤22 kDa) and high hydrophilicity (28), which indicates that gastric digestion mainly promotes the hydrolysis of hydrophilic, small-molecule peptides and the release of more hydrophobic, large-molecule peptides. This is consistent with the result that gastric digestion caused a significant increase in the DH of samples. The areas of peaks 1–3 and 5 in the small intestinal digestion samples (P4/P8) were significantly increased compared with those of the samples in the previous stage. Most notably, the areas of peak 1 from the samples of unfermented black beans and black bean tempeh were 38.82 and 45.13 times those of the gastric digestion samples, respectively. However, the areas of peak 9 in the small intestinal digestion samples were significantly reduced, suggesting that these newly added small peptides may come from the degradation of elution components in the later stage. In addition, the total area of early elution peaks of black bean tempeh samples, both at the initial stage and at the end of digestion, was much higher than those of unfermented black bean samples, and the respective areas of peaks 2–5 of P8 were 1.92, 7.68, 1.03, and 0.30 times higher than those of the peaks of P4. However, the areas of peak 8 and peak 9 were lower than those of unfermented black bean samples. Combined with the previous soluble protein content and DH analysis results, we speculate that this was potentially because the digestion limit of black bean tempeh proteins under these conditions had already been reached, so the small intestinal digestion stage was unable to extract any more peptide segments. In summary, *in vitro* digestion caused the degradation of black bean proteins and the release of polypeptides, and *R. oligosporus* fermentation promoted the release of a higher number of small peptides during the process of digestion, which could improve the absorption and utilization of proteins in black bean tempeh by the human body.

Angiotensin I-converting enzyme-inhibitory activity

Angiotensin I-converting enzyme regulates arterial blood pressure by converting inactive angiotensin I into angiotensin II, which has a strong vasoconstrictor effect and causes a rise in blood pressure (29). Therefore, the use of natural ACE inhibitors can effectively reduce blood pressure to a certain extent and avoid the potential risks caused by synthetic drugs. The ACE-inhibitory activity of unfermented black beans and black bean tempeh in different digestion stages is shown in **Figure 5**. The inhibition rate of ACE in unfermented black bean samples showed no change during buccal digestion but continued to increase after gastrointestinal digestion and ultimately reached 94.67 ± 0.07%. The change in the ACE inhibition rate in black bean tempeh samples was similar to the change observed in unfermented black bean samples during buccal and gastric digestion, but this trend decreased slightly after small intestinal digestion. Overall, the inhibition rate of black bean tempeh samples was also greatly improved, from the original 30.63 ± 0.67% up to 82.51 ± 0.63%. It is worth noting that the initial ACE-inhibitory activity of black bean tempeh was much lower than that of unfermented black beans. At first glance, this observation seemed to be inconsistent with the results above showing that fermentation leads to the increase of DH and peptide release of black bean proteins, especially small peptides, which are believed to have a higher ACE-inhibitory activity (30). However, there is no conclusive study on the influence of fermentation on the ACE-inhibitory activity of food. A study by Wu et al. (18) showed that the ACE-inhibitory activity of oats fermented by *Rhizopus oryzae*, either alone or in conjunction with *Lactobacillus plantarum* B1–6, was higher than that of unfermented oats. Rui et al. (29) also found that lactic acid bacteria fermentation could improve the release of ACE-inhibitory peptides from navy bean milk. However, a previous study by Nielsen et al. (31) showed that 13 lactobacillus strains had different effects on the ACE-inhibitory activity of yogurt. Although most strains contributed to the increase of the inhibitory activity, *Lactobacillus helveticus* fermentation could lead to a decrease in the ACE-inhibitory activity of yogurt (pH 3.5). The ACE-inhibitory activity of peptides is influenced by multiple factors, including molecular weight distribution and structural features such as terminal amino acid residues (30, 32). The differences in microbial restriction sites and the structure of raw proteins may influence the ACE-inhibitory activity of fermented products, which may be the reason for the lower initial ACE-inhibitory activity of black bean tempeh in this study. However, interestingly, *in vitro* digestion significantly increased the ACE-inhibitory activity of black bean tempeh by 1.69 times, greatly closing the gap with unfermented black beans. Jakubczyk et al. (33) fermented pea seeds with *L. plantarum* 299V for different times and at different temperatures and found that none of the fermented samples possessed ACE-inhibitory activity, though *in vitro* digestion subsequently induced the release of ACE-inhibitory peptides. Studies by Vermeirssen et al. (34) showed that *Saccharomyces cerevisiae* fermentation did not influence the ACE-inhibitory activity of whey protein under 28°C. The ACE-inhibitory activity of unfermented whey protein and pea protein *in vitro* digestion solution was even higher than that of the fermented sample. Therefore, they hypothesized that *in vitro* digestion was the predominant factor influencing the ACE-inhibitory activity.

Phenolic compound contents

Bioaccessibility, defined as the potential for compounds to be released from the food matrix and be dissolved in

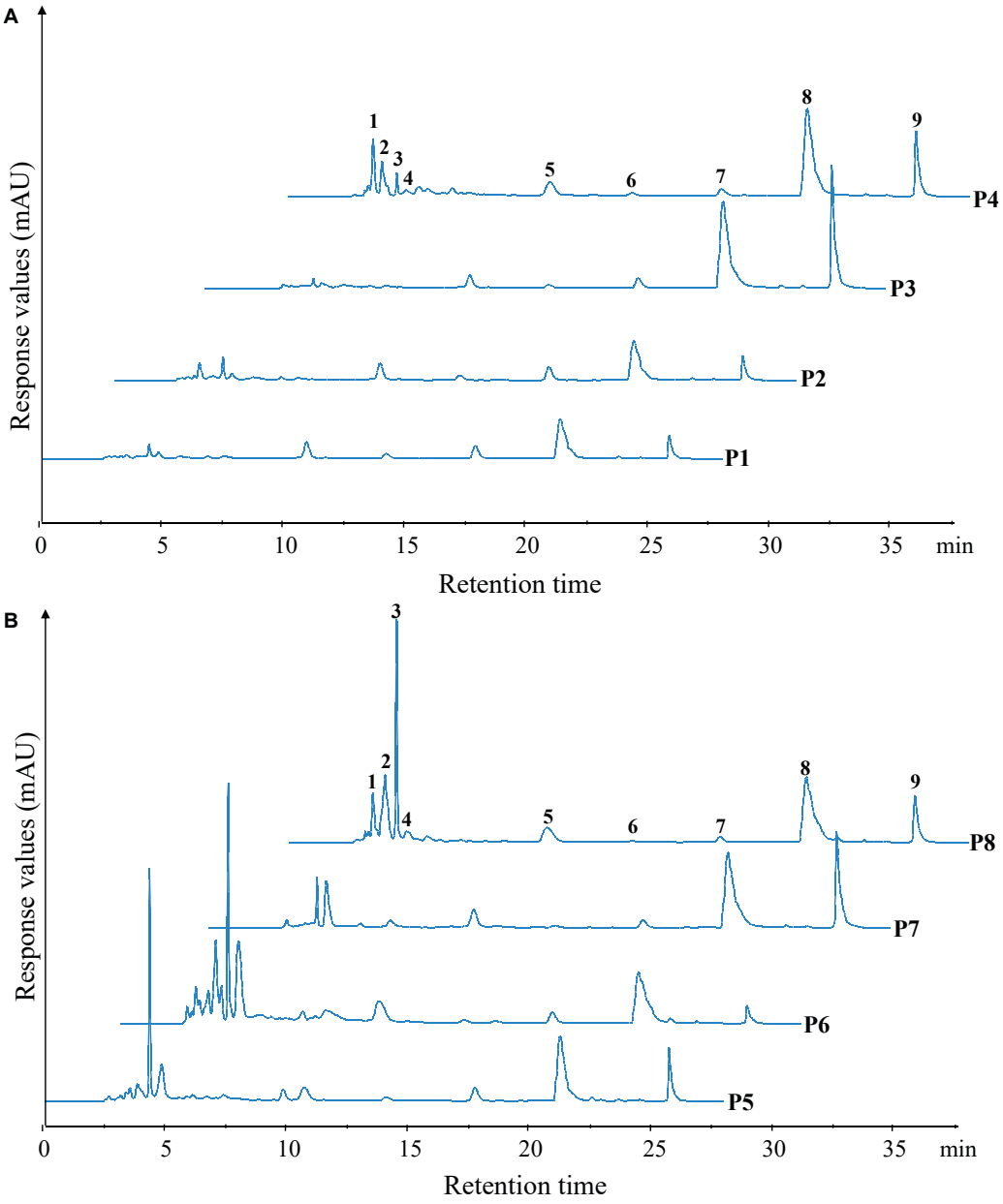

FIGURE 4
Reversed-phase high-performance liquid chromatography (RP-HPLC) patterns of unfermented black bean **(A)** and black bean tempeh **(B)** samples in different simulated digestion stages. Peaks with larger areas or significant changes were successively labeled 1–9 according to their order.

the gastrointestinal tract during digestion, is one of the most important factors that determines the bioavailability of phenolic compounds. *In vitro* digestion models are often used to study the effects of digestion on these compounds to predict their release from the food matrix and assess their bioaccessibility (35).

The TPC at different digestion stages is shown in **Figure 6A**. The initial TPC of unfermented black bean samples and black bean tempeh samples were 0.35 ± 0.01 mg GAE/g and 0.95 ± 0.02 mg GAE/g, respectively. There were no significant changes in the TPC in both types of samples after buccal digestion, which might be due to the short interaction time with the buccal enzyme system. This implies that buccal digestion had little effect on polyphenol availability and was limited to high-carbohydrate foods, which explains why many studies did not carry out this step on phenolic compounds (36, 37). The TPC increased significantly after gastric digestion, most likely because plant polyphenols mainly exist in covalently bound states and thus are not easily released

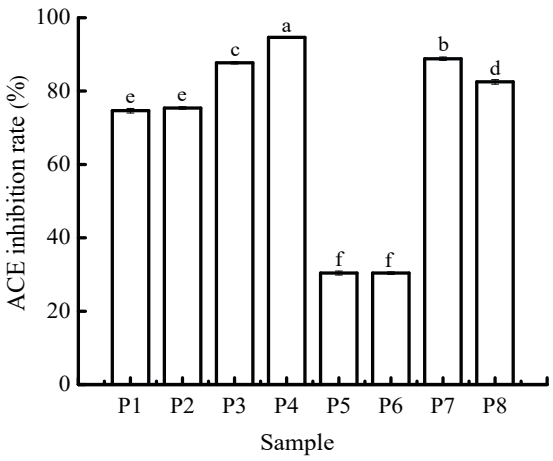

FIGURE 5
Angiotensin I-converting enzyme (ACE)-inhibitory activity of samples in different simulated digestion stages. Data with different lowercase letters indicate significant differences ($P < 0.05$).

by conventional treatment. Extreme pH and the presence of digestive enzymes in the stomach enable them to be released from proteins (38, 39). After intestinal digestion, TPC was further increased and ultimately reached 1.90 ± 0.03 mg GAE/g and 2.29 ± 0.05 mg GAE/g in the unfermented black bean samples and tempeh samples, respectively. Similar results were reported by Scrob et al. (40) in their study, in which the TPC of dried fruits after gastrointestinal digestion was increased compared to the TPC of dried fruits after gastric digestion; according to the researchers, this phenomenon could be explained by the extra extraction time and the influence of intestinal digestive enzymes on the food matrix. However, studies with opposing results also exist in the literature. For example, *in vitro* gastrointestinal digestion was shown to greatly reduce the TPC of brown algae extract (41), and simulated gastric digestion led to a substantial reduction in the phenolic compound content of *Arbutus unedo* (42). The bioaccessibility of polyphenols is influenced by multiple factors, such as their own physicochemical properties, food matrix, interaction with other components, and the presence of cofactors or inhibitors (35). Therefore, we speculate that the composition of phenolic compounds in the food matrix might be the cause of these differences in the results.

As shown in **Figure 6B**, the initial TFC of unfermented black bean samples was 0.011 ± 0.001 mg RE/g, which was not significantly affected by buccal digestion. After gastric digestion, the TFC increased sharply and then remained basically unchanged after small intestinal digestion before finally reaching 0.052 ± 0.002 mg RE/g. The TFC change in the whole digestive process of black bean tempeh was the same as that of unfermented black beans, which increased from 0.028 ± 0.006 mg RE/g to 0.073 ± 0.004 mg RE/g, indicating that

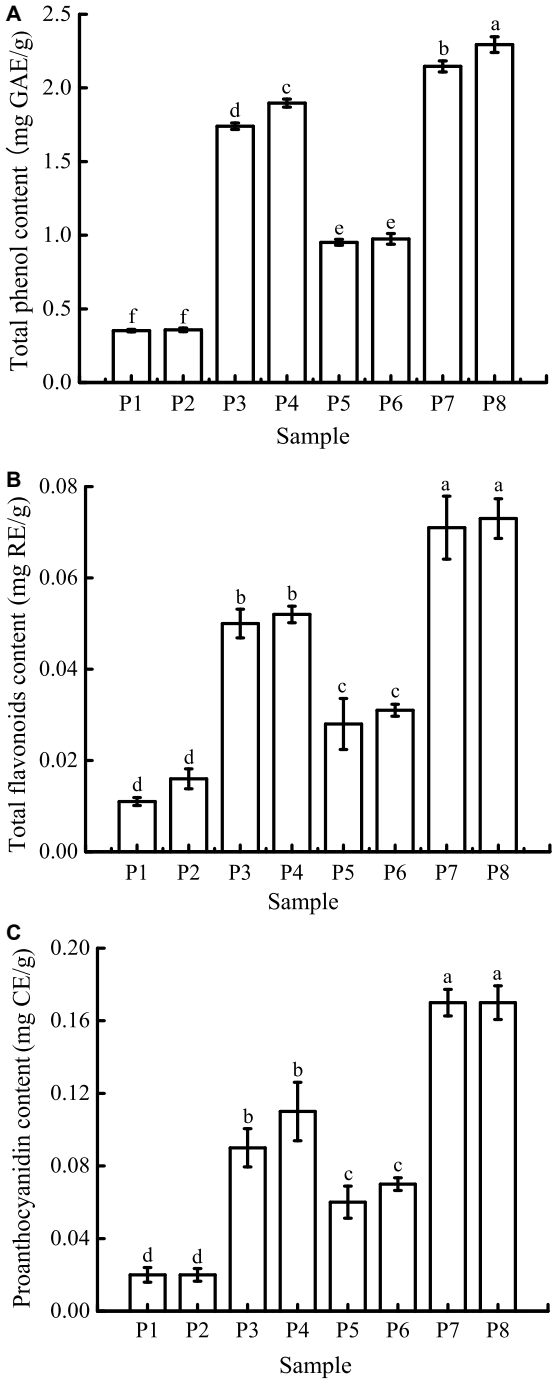

FIGURE 6
Total phenolic content (TPC) **(A)**, total flavone content (TFC) **(B)**, and proanthocyanidin content (PC) **(C)** of samples in different simulated digestion stages. Data with different lowercase letters indicate significant differences ($P < 0.05$).

in vitro digestion promoted the release of flavonoids from black beans. Unlike TPC, small intestinal digestion failed to further improve the TFC of the samples. A similar trend was observed in the *in vitro* digestion of baobab fruit shell, where there was no

significant difference in the TFC between samples undergoing gastric and small intestinal digestion (37). Meanwhile, Gawlik-Dziki et al. (43) found that the TFC of bread without or with the addition of 2.5% tartary buckwheat flavones was increased during *in vitro* digestion, but small intestinal digestion led to a significant decrease in the TFC of bread with the addition of 5% tartary buckwheat flavones. This implies that the food matrix as well as the flavonoid content may have an important effect on the release of flavonoids during *in vitro* digestion.

The trend in the change in PC was similar to that in TFC (**Figure 6C**). Gastric digestion is an important stage for PC increase, which is potentially due to the strong acid environment at this stage, thus promoting the hydrolysis of proanthocyanidins to isoforms such as proanthocyanidin trimers, tetramers, and pentamers (37). The final PC of unfermented black bean samples and black bean tempeh samples reached 0.11 ± 0.02 mg CE/g and 0.17 ± 0.02 mg CE/g, respectively. Ismail et al. (37) also found that the baobab fruit shell PC increased after gastric digestion, and what differed from our findings was that the PC continued to increase significantly after small intestinal digestion. They believed that the release of food matrix-binding proanthocyanidins catalyzed by trypsin or the depolymerization and release of insoluble proanthocyanidins caused by the rise of pH were the possible reasons for this result.

In conclusion, although the content of phenolic compounds in the digestion solution of unfermented black bean samples was also significantly increased during *in vitro* digestion, the release of phenolic compounds from black bean tempeh samples was generally significantly higher than that of unfermented black bean samples at the same digestion stage ($P < 0.05$). These results indicated that fermentation could improve the bioaccessibility of phenolic compounds in black beans. This should be attributed to the rich enzyme system produced by *R. oligosporus* during fermentation, as several studies have confirmed that the release of phenolic compounds from plant raw materials or food is related to the microbial enzyme system (17, 44–47).

Antioxidant activity

Due to the differences in the mechanisms of antioxidant detection methods, it is difficult to objectively measure the actual antioxidant capacity of a sample using just a single evaluation method (48). In this study, four antioxidant evaluation models, including DPPH, $ABTS^+$, hydroxyl radical scavenging ability, and FRAP were used to evaluate the effect of *in vitro* digestion on the antioxidant capacity of the study samples. The results are shown in **Figure 7**.

The scavenging rates of DPPH, $ABTS^+$, and hydroxyl radicals of unfermented black bean samples and black bean tempeh samples were not affected by buccal digestion, but they

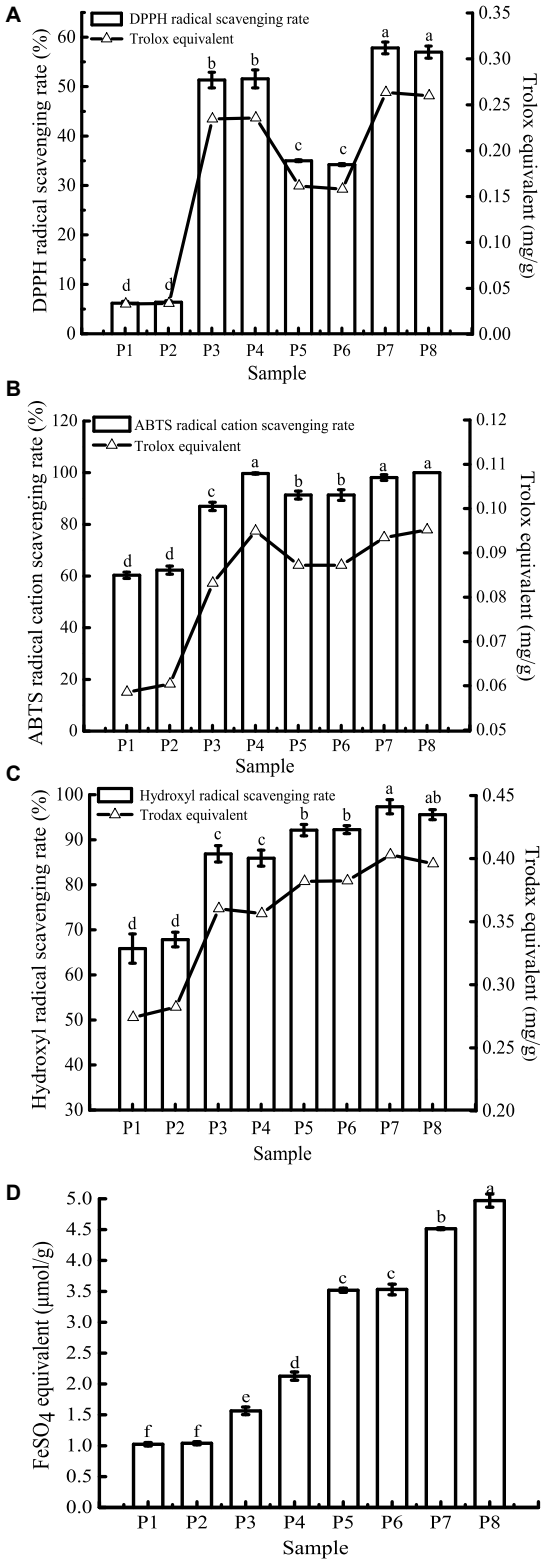

FIGURE 7
1,1-Diphenyl-2-picrylhydrazyl (DPPH) **(A)**, $ABTS^+$ **(B)**, hydroxyl radical scavenging activity **(C)**, and FRAP **(D)** of samples in different simulated digestion stages. Data with different lowercase letters indicate significant differences ($P < 0.05$).

TABLE 1 Pearson's correlation coefficients among total phenolic content (TPC), total flavone content (TFC), proanthocyanidin content (PC), and antioxidant activity.

	DPPH	$ABTS^+$	Hydroxyl radical	FRAP
TPC	0.968**	0.864**	0.779*	0.651
TFC	0.938**	0.830*	0.782*	0.711*
PC	0.912**	0.838*	0.807*	0.793*

*Correlation was significant at the 0.05 level (one-tailed).
**Correlation was significant at the 0.01 level (two-tailed).

were significantly increased after gastric digestion ($P < 0.05$), while small intestinal digestion did not further improve the scavenging rates. The change in FRAP was consistent with the free-radical scavenging rate before small intestinal digestion, but it continued to increase significantly after intestinal digestion ($P < 0.05$). There have been many reports on the effect of *in vitro* digestion on the antioxidant capacity of food. For example, compared with that of cooked rice, the oxygen free radical absorption capacity of brown rice and milled rice after *in vitro* digestion was increased by 185.7 and 293.4%, respectively (49). Additionally, *in vitro* digestion improved the antioxidant activity of common beans and pinto beans (50). There are also contradictory results: for instance, Rodriguez-Roque et al. (51) found that *in vitro* gastric digestion significantly increased the total antioxidant activity of soy milk (76%), while small intestinal digestion caused a significant decrease, and they speculated that this decrease may be due to the fact that some substances with antioxidant activity, such as phenolic compounds, are sensitive to alkaline pH. Therefore, these compounds are transformed into compounds with a structural form that exhibits different chemical properties. The plant matrix has a matrix effect on the retention rate of specific phytochemicals (52), hence the food matrix and the composition of phytochemicals may also be responsible for the differences in antioxidant capacity of different food after *in vitro* digestion. In the present study, after *in vitro* digestion, the DPPH, $ABTS^+$, hydroxyl radical scavenging rates, and FRAP of unfermented black bean samples reached 8.34, 1.65, 1.30, and 2.09 times the initial values, respectively. In contrast, the corresponding values in black bean tempeh samples only increased 0.63, 0.09, 0.04, and 0.41 times compared to the initial values, respectively. However, in terms of absolute values, at the same digestion stage, the DPPH, hydroxyl radical scavenging ability, and FRAP of unfermented black bean samples were significantly lower than those of black bean tempeh samples ($P < 0.05$), and only the free radical scavenging ability of $ABTS^+$ in the unfermented samples was equal to that of tempeh samples after small intestinal digestion, which proved that processing black beans into tempeh could improve their antioxidant activity after consumption.

For DPPH, $ABTS^+$, hydroxyl radical scavenging capacity, and FRAP, consistent with the results of TPC, TFC, and PC analysis, *in vitro* digestion caused a significant increase in the antioxidant capacity of both samples. Although the specific assay mechanisms were different, all antioxidant activity resulted in a similar trend. To further clarify the correlation between the content of phenolic compounds and different antioxidant activities, Pearson's correlation analysis was performed using SPSS 17.0 software. The results are shown in Table 1. DPPH, $ABTS^+$, and hydroxyl radical scavenging rates were positively correlated with TPC, TFC, and PC, either significantly or highly significantly. FRAP was positively correlated with TFC and PC ($P < 0.05$). The significant positive correlation indicated that the antioxidant activity was closely related to the release of phenolic compounds during *in vitro* digestion. This was consistent with the conclusion of Zheng et al. (53) that the oxygen radical absorption capacity (ORAC) and the rapid peroxyl radical scavenging capacity of Chinese hawthorn fruit were significantly positively correlated with the amount of total phenolics or flavonoids released. However, Sancho et al. (12) found that although *in vitro* digestion reduced the TPC in the seed coats of black beans and small red beans, as well as the TFC of black bean seed coats, the antioxidant activity of both groups of samples remained unchanged, and the ORAC in the black bean group even increased significantly. This suggests that other soluble compounds present in the digestive fluid, such as simple carbohydrates or amino acids, may interfere with the antioxidant test or the determination of total phenols and that some non-phenolic compounds, such as carotenoids and tocopherols, may also contribute to the antioxidant activity (38, 43).

Conclusion

The results of this study confirmed that the proteins of unfermented black beans and black bean tempeh were degraded during *in vitro* digestion, the content of hydrolysates such as soluble proteins and small peptides and the DH of proteins were significantly increased, and phenolic compounds were released, the bioactivity of which was also greatly improved. However, compared with unfermented black beans, the black bean tempeh demonstrated higher bioavailability of proteins and phenolic compounds, and its antioxidant activity was stronger as well. Additionally, its ACE-inhibitory activity was greatly improved following *in vitro* digestion, closing the gap with unfermented black beans. These differences between unfermented black beans and black bean tempeh may be attributed to the biochemical reactions caused by the enzymes produced by *R. oligosporus* during fermentation. Although these *in vitro* results cannot be fully and directly extended to *in vivo* conditions, these data provide preliminary evidence that the nutritional values and potential health benefits of black bean tempeh remain higher than those of unfermented black beans even after consumption.

Data availability statement

The original contributions presented in this study are included in the article/supplementary material, further inquiries can be directed to the corresponding authors.

Author contributions

KW and YG designed the research, performed the experiments, and wrote the original draft. JZ, YW, JS, and GN conducted the statistical analysis and the analysis of the results. FZ and XZ designed the experimental scheme, supervised the experiments, and revised the manuscript. All authors contributed to the article and agreed to the published version of the manuscript.

Funding

This work was co-financed by Key Research and Development Project of Heilongjiang Province (Grant No. GA21B011), Natural Science Foundation of Heilongjiang Province (Grant No. YQ2021C029), Dr. Startup Project in Heilongjiang Bayi Agricultural University (No. XYB-2016-06), and was also supported by Heilongjiang Bayi Agricultural University Intramural Cultivation Project (No. XZR2017-08).

Conflict of interest

The authors declare that the research was conducted in the absence of any commercial or financial relationships that could be construed as a potential conflict of interest.

Publisher's note

All claims expressed in this article are solely those of the authors and do not necessarily represent those of their affiliated organizations, or those of the publisher, the editors and the reviewers. Any product that may be evaluated in this article, or claim that may be made by its manufacturer, is not guaranteed or endorsed by the publisher.

References

1. Ahnan-Winarno AD, Cordeiro L, Winarno FG, Gibbons J, Xiao H. Tempeh: A semicentennial review on its health benefits, fermentation, safety, processing, sustainability, and affordability. *Compr Rev Food Sci Food Saf.* (2021) 20:1717–67. doi: 10.1111/1541-4337.12710

2. Huang L, Huang ZH, Zhang YZ, Zhou SD, Hu WX, Dong MS. Impact of tempeh flour on the rheology of wheat flour dough and bread staling. *LWT-Food Sci Technol.* (2019) 111:694–702. doi: 10.1016/j.lwt.2019.04.004

3. Sánchez-Magana LM, Cuevas-Rodríguez EO, Gutiérrez-Dorado R, Ayala-Rodríguez AE, Valdez-Ortiz A, Milán-Carrillo J, et al. Solid-state bioconversion of chickpea (*Cicer arietinum* L.) by *Rhizopus oligosporus* to improve total phenolic content, antioxidant activity and hypoglycemic functionality. *Int J Food Sci Nutr.* (2014) 65:558–64. doi: 10.3109/09637486.2014.893284

4. Borges CWC, Carrão-Panizzi MC, Mandarino JMG, Silva JB, Benedetti S, Ida E. Contents and bioconversion of β-glycoside isoflavones to aglycones in the processing conditions of soybean tempeh. *Pesqui Agropecu Bras.* (2016) 51:271–9. doi: 10.1590/S0100-204X2016000300009

5. Chang CT, Hsu CK, Chou ST, Chen YC, Huang FS, Chung YC. Effect of fermentation time on the antioxidant activities of tempeh prepared from fermented soybean using *Rhizopus oligosporus*. *Int J Food Sci Tech.* (2009) 44:799–806. doi: 10.1111/j.1365-2621.2009.01907.x

6. Nakajima N, Nozaki N, Ishihara K, Ishikawa A, Tsuji H. Analysis of isoflavone content in tempeh, a fermented soybean, and preparation of a new isoflavone-enriched tempeh. *J Biosci Bioeng.* (2005) 100:685–7. doi: 10.1263/jbb.100.685

7. Lee IH, Hung YH, Chou CC. Solid-state fermentation with fungi to enhance the antioxidative activity, total phenolic and anthocyanin contents of black bean. *Int J Food Microbiol.* (2008) 121:150–6. doi: 10.1016/j.ijfoodmicro.2007.09.008

8. Jeong EW, Park SY, Yang YS, Beak YJ, Yun DM, Kim HJ, et al. Black soybean and adzuki bean extracts lower blood pressure by modulating the renin-angiotensin system in spontaneously hypertensive rats. *Foods.* (2021) 10:1571. doi: 10.3390/foods10071571

9. Xu BJ, Chang SKC. Total phenolic content and antioxidant properties of eclipse black beans (*Phaseolus vulgaris* L.) as affected by processing methods. *J Food Sci.* (2008) 73:H19–27. doi: 10.1111/j.1750-3841.2007.00625.x

10. Xu BJ, Yuan SH, Chang SKC. Comparative studies on the antioxidant activities of nine common food legumes against copper-induced human low-density lipoprotein oxidation in vitro. *J Food Sci.* (2007) 72:S522–7. doi: 10.1111/j.1750-3841.2007.00464.x

11. Giusti F, Capuano E, Sagratini G, Pellegrini N. A comprehensive investigation of the behaviour of phenolic compounds in legumes during domestic cooking and in vitro digestion. *Food Chem.* (2019) 285:458–67. doi: 10.1016/j.foodchem.2019.01.148

12. Sancho RAS, Pavan V, Pastore GM. Effect of in vitro digestion on bioactive compounds and antioxidant activity of common bean seed coats. *Food Res Int.* (2015) 76:74–8. doi: 10.1016/j.foodres.2014.11.042

13. López-Barrios L, Antunes-Ricardo M, Gutiérrez-Uribe JA. Changes in antioxidant and antiinflammatory activity of black bean (*Phaseolus vulgaris* L.) protein isolates due to germination and enzymatic digestion. *Food Chem.* (2016) 203:417–24. doi: 10.1016/j.foodchem.2016.02.048

14. Rochín-Medina JJ, Gutiérrez-Dorado R, Sánchez-Magaña LM, Milán-Carrillo J, Cuevas-Rodríguez EO, Mora-Rochín S, et al. Enhancement of nutritional properties, and antioxidant and antihypertensive potential of black common bean seeds by optimizing the solid state bioconversion process. *Int J Food Sci Nutr.* (2015) 66:498–504. doi: 10.3109/09637486.2015.1052377

15. Rui X, Zhang Q, Huang J, Li W, Chen XH, Jiang M, et al. Does lactic fermentation influence soy yogurt protein digestibility: a comparative study between soymilk and soy yogurt at different pH. *J Sci Food Agri.* (2019) 99:861–7. doi: 10.1002/jsfa.9256

16. Xing G, Rui X, Jiang M, Xiao Y, Guan Y, Wang D, et al. In vitro gastrointestinal digestion study of a novel bio-tofu with special emphasis on the impact of microbial transglutaminase. *Peer J.* (2016) 4:e2754. doi: 10.7717/peerj.2754

17. Wang K, Niu M, Song D, Liu Y, Wu Y, Zhao J, et al. Evaluation of biochemical and antioxidant dynamics during the co-fermentation of dehusked barley with *Rhizopus oryzae* and *Lactobacillus plantarum*. *J Food Biochem.* (2020) 44:e13106. doi: 10.1111/jfbc.13106

18. Wu H, Rui X, Li W, Xiao Y, Zhou JZ, Dong MS. Whole-grain oats (avena *sativa* l.) as a carrier of lactic acid bacteria and a supplement rich in angiotensin converting enzyme inhibitory peptides through solid-state fermentation. *Food Funct.* (2018) 9:2270–81. doi: 10.1039/C7FO01578J

19. Rui X, Huang J, Xing G, Zhang Q, Li W, Dong M. Changes in soy protein immunoglobulin E reactivity, protein degradation, and conformation through fermentation with *Lactobacillus plantarum* strains. *LWT-Food Sci Technol.* (2019) 99:156–65. doi: 10.1016/j.lwt.2018.09.034

20. Zhu Z, Qiu N, Yi J. Production and characterization of angiotensin converting enzyme (ACE) inhibitory peptides from apricot (*Prumus armeniaca* L.) kernel protein hydrolysate. *Eur Food Res Technol.* (2010) 231:13–9. doi: 10.1007/s00217-010-1235-5

21. Tao Y, Wu P, Dai Y, Luo X, Manickam S, Li D, et al. Bridge between mass transfer behavior and properties of bubbles under two-stage ultrasound-assisted physisorption of polyphenols using macroporous resin. *Chem Eng J.* (2022) 436:135158. doi: 10.1016/j.cej.2022.135158

22. Sandhu KS, Punia S. Enhancement of bioactive compounds in barley cultivars by solid substrate fermentation. *J Food Meas Charact.* (2017) 11:1355–61. doi: 10.1007/s11694-017-9513-6

23. Saifullah M, Akanbi TO, McCullum R, Vuong QV. Optimization of commercial microwave assisted-extraction conditions for recovery of phenolics from lemon-scented tee tree (*Leptospermum petersonii*) and comparison with other extraction techniques. *Foods.* (2021) 11:50. doi: 10.3390/foods11010050

24. Tian J, Mao Q, Dong M, Wang X, Rui X, Zhang Q, et al. Structural characterization and antioxidant activity of exopolysaccharide from soybean whey fermented by *Lacticaseibacillus plantarum* 70810. *Foods.* (2021) 10:2780. doi: 10.3390/foods10112780

25. Dong Y, Yan W, Zhang YQ. Effects of spray drying and freeze drying on physicochemical properties, antioxidant and ace inhibitory activities of bighead carp (*Aristichthys nobilis*) skin hydrolysates. *Foods.* (2022) 11:2083. doi: 10.3390/foods11142083

26. Wang K, Niu M, Yao D, Zhao J, Wu Y, Lu B, et al. Physicochemical characteristics and in vitro and in vivo antioxidant activity of a cell-bound exopolysaccharide produced by *Lactobacillus fermentum* S1. *Int J Biol Macromol.* (2019) 139:252–61. doi: 10.1016/j.ijbiomac.2019.07.200

27. Rui X, Fu Y, Zhang Q, Li W, Zare F, Chen X, et al. A comparison study of bioaccessibility of soy protein gel induced by magnesiumchloride, glucono-δ-lactone and microbial transglutaminase. *LWT-Food Sci Technol.* (2016) 71:234–42. doi: 10.1016/j.lwt.2016.03.032

28. Rui X, Boye JI, Ribereau S, Simpson BK, Prasher SO. Comparative study of the composition and thermal properties of protein isolates prepared from nine *Phaseolus vulgaris* legume varieties. *Food Res Int.* (2011) 44:2497–504. doi: 10.1016/j.foodres.2011.01.008

29. Rui X, Wen D, Li W, Chen X, Jiang M, Dong MS. Enrichment of ACE inhibitory peptides in navy bean (*Phaseolus vulgaris*) using lactic acid bacteria. *Food Funct.* (2015) 6:622–9. doi: 10.1039/C4FO00730A

30. Rui X, Boye JI, Simpson BK, Prasher SO. Angiotensin I-converting enzyme inhibitory properties of *Phaseolus vulgaris* bean hydrolysates: Effects of different thermal and enzymatic digestion treatments. *Food Res Int.* (2012) 49:739–46. doi: 10.1016/j.foodres.2012.09.025

31. Nielsen MS, Martinussen T, Flambard B, Sørensen KI, Otte J. Peptide profiles and angiotensin-I-converting enzyme inhibitory activity of fermented milk products: Effect of bacterial strain, fermentation pH, and storage time. *Int Dairy J.* (2009) 19:155–65. doi: 10.1016/j.idairyj.2008.10.003

32. Li GH, Le GW, Shi YH, Shrestha S. Angiotensin I-converting enzyme inhibitory peptides derived from food proteins and their physiological and pharmacological effects. *Nutr Res.* (2004) 24:469–86. doi: 10.1016/j.nutres.2003.10.014

33. Jakubczyk A, Karaś M, Baraniak B, Pietrzak M. The impact of fermentation and in vitro digestion on formation angiotensin converting enzyme (ACE) inhibitory peptides from pea proteins. *Food Chem.* (2013) 141:3774–80. doi: 10.1016/j.foodchem.2013.06.095

34. Vermeirssen V, Van Camp J, Decroos K, Verstraete W. The impact of fermentation and in vitro digestion on the formation of angiotensin-I-converting enzyme inhibitory activity from pea and whey protein. *J Dairy Sci.* (2003) 86:429–38. doi: 10.3168/jds.S0022-0302(03)73621-2

35. Wojtunik-Kulesza K, Oniszczuk A, Oniszczuk T, Combrzyński M, Nowakowska D, Matwijczuk A. Influence of in vitro digestion on composition, bioaccessibility and antioxidant activity of food polyphenols—A non-systematic review. *Nutrients.* (2020) 12:1401. doi: 10.3390/nu12051401

36. Hur SJ, Lim BO, Decker EA, McClements J. In vitro human digestion models for food applications. *Food Chem.* (2011) 125:1–12. doi: 10.1016/j.foodchem.2010.08.036

37. Ismail BB, Guo M, Pu Y, Çavuş O, Ayub KA, Watharkar RB. Investigating the effect of in vitro gastrointestinal digestion on the stability, bioaccessibility, and biological activities of baobab (*Adansonia digitata*) fruit polyphenolics. *LWT-Food Sci Technol.* (2021) 145:111348. doi: 10.1016/j.lwt.2021.111348

38. Chandrasekara A, Shahidi F. Bioaccessibility and antioxidant potential of millet grain phenolics as affected by simulated in vitro digestion and microbial fermentation. *J Funct Foods.* (2012) 4:226–37. doi: 10.1016/j.jff.2011.11.001

39. Liyanapathirana C, Shahidi F. Antioxidant activity of wheat extracts as affected by in vitro digestion. *Biofactors.* (2010) 21:325–8. doi: 10.1002/biof.552210163

40. Scrob T, Covaci E, Hosu A, Tanaselia C, Casoni D, Torok A, et al. Effect of in vitro simulated gastrointestinal digestion on some nutritional characteristics of several dried fruits. *Food Chem.* (2022) 385:132713. doi: 10.1016/j.foodchem.2022.132713

41. Corona G, Coman MM, Guo Y, Hotchkiss S, Gill C, Yaqoob P, et al. Effect of simulated gastrointestinal digestion and fermentation on polyphenolic content and bioactivity of brown seaweed phlorotannin-rich extracts. *Mol Nutr Food Res.* (2017) 61:1700223. doi: 10.1002/mnfr.201700223

42. Mosele JI, Macià A, Romero MP, Motilva MJ. Stability and metabolism of *Arbutus unedo* bioactive compounds (phenolics and antioxidants) under in vitro digestion and colonic fermentation. *Food Chem.* (2016) 201:120–30. doi: 10.1016/j.foodchem.2016.01.076

43. Gawlik-Dziki U, Dziki D, Baraniak B, Lin R. The effect of simulated digestion in vitro on bioactivity of wheat bread with tartary buckwheat flavones addition. *LWT-Food Sci Technol.* (2009) 42:137–43. doi: 10.1016/j.lwt.2008.06.009

44. Xiao Y, Wu X, Yao X, Chen Y, Ho CT, He C, et al. Metabolite profiling, antioxidant and α-glucosidase inhibitory activities of buckwheat processed by solid-state fermentation with *Eurotium cristatum* YL-1. *Food Res Int.* (2021) 143:110262. doi: 10.1016/j.foodres.2021.110262

45. Zhang XY, Chen J, Li XL, Yi K, Ye Y, Liu G, et al. Dynamic changes in antioxidant activity and biochemical composition of tartary buckwheat leaves during *Aspergillus niger* fermentation. *J Funct Foods.* (2017) 32:375–81. doi: 10.1016/j.jff.2017.03.022

46. Chen Y, Wang Y, Chen J, Tang H, Wang C, Li Z, et al. Bioprocessing of soybeans (*Glycine max L.*) by solid-state fermentation with *Eurotium cristatum* YL-1 improves total phenolic content, isoflavone aglycones, and antioxidant activity. *RSC Adv.* (2020) 10:16928–41. doi: 10.1039/C9RA10344A

47. Singh HB, Singh BN, Singh SP, Nautiyal CS. Solid-state cultivation of *Trichoderma harzianum* NBRI-1055 for modulating natural antioxidants in soybean seed matrix. *Bioresource Technol.* (2010) 101:6444–53. doi: 10.1016/j.biortech.2010.03.057

48. Xiao Y, Xing G, Rui X, Li W, Chen X, Jiang M, et al. Enhancement of the antioxidant capacity of chickpeas by solid state fermentation with *Cordyceps militaris* SN-18. *J Funct Foods.* (2014) 10:210–22. doi: 10.1016/j.jff.2014.06.008

49. Ti H, Zhang R, Li Q, Wei Z, Zhang M. Effects of cooking and in vitro digestion of rice on phenolic profiles and antioxidant activity. *Food Res Int.* (2015) 76:813–20. doi: 10.1016/j.foodres.2015.07.032

50. Akillioglu HG, Karakaya S. Changes in total phenols, total flavonoids, and antioxidant activities of common beans and pinto beans after soaking, cooking, and in vitro digestion process. *Food Sci Biotechnol.* (2010) 19:633–9. doi: 10.1007/s10068-010-0089-8

51. Rodríguez-Roque MJ, Rojas-Graü MA, Elez-Martínez P, Martín-Belloso O. Soymilk phenolic compounds, isoflavones and antioxidant activity as affected by in vitro gastrointestinal digestion. *Food Chem.* (2013) 136:206–12. doi: 10.1016/j.foodchem.2012.07.115

52. Tungmunnithum D, Drouet S, Lorenzo JM, Hano C. Effect of traditional cooking and in vitro gastrointestinal digestion of the ten most consumed beans from the fabaceae family in Thailand on their phytochemicals, antioxidant and anti-diabetic potentials. *Plants.* (2021) 11:67. doi: 10.3390/plants11010067

53. Zheng G, Deng J, Wen L, You L, Zhao Z, Zhou L. Release of phenolic compounds and antioxidant capacity of Chinese hawthorn "*Crataegus pinnatifida*" during in vitro digestion. *J Funct Foods.* (2018) 40:76–85. doi: 10.1016/j.jff.2017.10.039

frontiers | Frontiers in Nutrition

TYPE Original Research
PUBLISHED 28 October 2022
DOI 10.3389/fnut.2022.1025080

OPEN ACCESS

EDITED BY
Yu Xiao,
Hunan Agricultural University, China

REVIEWED BY
Hongshun Yang,
National University of Singapore, Singapore
Dinh Toi Chu,
Vietnam National University, Hanoi, Vietnam
Jinhua Zhang,
Shanxi University, China

*CORRESPONDENCE
Jing Lu
jinglu@jou.edu.cn

SPECIALTY SECTION
This article was submitted to Nutrition and Food Science Technology, a section of the journal Frontiers in Nutrition

RECEIVED 22 August 2022
ACCEPTED 13 October 2022
PUBLISHED 28 October 2022

CITATION
Yang J, Sun Y, Chen J, Cheng Y, Zhang H, Gao T, Xu F, Pan S, Tao Y and Lu J (2022) Fermentation of ginkgo biloba kernel juice using *Lactobacillus plantarum* Y2 from the ginkgo peel: Fermentation characteristics and evolution of phenolic profiles, antioxidant activities *in vitro*, and volatile flavor compounds. *Front. Nutr.* 9:1025080. doi: 10.3389/fnut.2022.1025080

Fermentation of ginkgo biloba kernel juice using *Lactobacillus plantarum* Y2 from the ginkgo peel: Fermentation characteristics and evolution of phenolic profiles, antioxidant activities *in vitro*, and volatile flavor compounds

Jie Yang[1,2], Yue Sun[1,2], Jinling Chen[1,2], Yu Cheng[1,2], Haoran Zhang[1,2], Tengqi Gao[1,2], Feng Xu[1,2], Saikun Pan[1,2], Yang Tao[3] and Jing Lu[1,2]*

[1]Co-Innovation Center of Jiangsu Marine Bio-industry Technology, Jiangsu Ocean University, Lianyungang, China, [2]Jiangsu Key Laboratory of Marine Bioresources and Environment/Jiangsu Key Laboratory of Marine Biotechnology, Jiangsu Ocean University, Lianyungang, China, [3]College of Food Science and Technology, Nanjing Agricultural University, Nanjing, China

In this study, a strain of *Lactobacillus plantarum* Y2 was isolated from the ginkgo peel, and showed adequate adaptation to the ginkgo biloba kernel juice. After 48 h of fermentation, the number of viable cells in the stable growth phase was remained at 10.0 Log CFU/mL, while the content of total organic acid increased by 5.86%. Phenolic substances were significantly enriched, and the content of total phenolic substances increased by 9.72%, and the content of total flavonoids after fermentation exceeded 55.33 mg/L, which was 3.6 times that of the unfermented ginkgo juice. The total relative content of volatile flavor compounds increased by 125.48%, and 24 new volatile flavor substances were produced. The content of total sugar, total protein, and total free amino acid decreased to 44.85, 67.51, and 6.88%, respectively. Meanwhile, more than 82.25% of 4′-*O*-methylpyridoxine was degraded by lactic acid fermentation, and the final concentration in ginkgo biloba kernel juice was lower than 41.53 mg/L. In addition, the antioxidant and antibacterial activities of fermented ginkgo biloba kernel juice were significantly enhanced. These results showed that LAB fermentation could effectively improve the nutritional value and safety of ginkgo biloba kernel juice.

KEYWORDS

ginkgo biloba kernel juice, lactic acid bacteria fermentation, phenolic substances, free amino acids (FAAs), volatile flavor substances

Introduction

Ginkgo biloba L., one of the oldest living tree species on earth (1), has been reported to have great development potential in the field of functional food (2). Meanwhile, ginkgo biloba kernel juice contains various active ingredients such as ginkgo phenolic acids, flavonoids, and polysaccharides, etc., making it widely used in food, health products, cosmetics, medicine and other fields (3). In particular, the special physiologically active components such as flavonoids and ginkgoid acid contained in it have the functions of anti-oxidation, anti-aging, anti-inflammatory, anti-allergic, and inhibiting nerve cell apoptosis (4). Recent studies on ginkgo have mainly focused on ginkgo leaves and relatively few studies on ginkgo kernels (5). Therefore, it is necessary and meaningful to further develop and utilize ginkgo kernels.

4′-O-methylpyridoxine (MPN) is a vitamin 6 derivative which can cause in pregnancy, radiation sickness, seborrheic dermatitis, and other pathologies. Interestingly, only a threshold concentration of MPN is beneficial to the human body; a higher concentration can lead to toxic reactions in the human body. The MPN content in medicine ranged from 0 to 9.77 μg/mL (6), and in ginkgo kernels ranged from 172.8 to 404.2 μg/g, indicating that excessive consumption of ginkgo kernels was harmful to human health (7). As MPN concentrations severely limit the development and utilization of ginkgo kernels, MPN degradation during the production process of ginkgo is a vital concern that needs to be addressed.

Lactic acid bacteria (LAB) have been widely used in the fermentation of pickles, yogurt, soy sauce and tempeh, owing to their ability to regulate the human intestinal flora, promote the absorption of nutrition substances, kill harmful flora and the toxins, and ameliorate food flavor (8). Moreover, the secondary metabolites in the fermentation process with LAB have several health benefits, such as promoting the activity of antioxidant enzymes in cells, and increasing the content of beneficial substances. For example, Verón found that LAB fermentation could increase the activities of ferulic acid, caffeic acid derivatives and intracellular antioxidant enzymes, and enhance the overall antioxidant capacity of the fermentation broth (9).

Currently, studies on ginkgo mainly focuses on ginkgo leaves, while there are relatively few studies on ginkgo kernels. Ginkgo products mainly include canned ginkgo kernel, ginkgo wine, and beverages (10, 11). However, only a few studies had been conducted on fermented silver almonds. In this study, a LAB strain was selected from ginkgo peel to ferment ginkgo biloba kernel juice. The physiological and biochemical indices of fermented ginkgo biloba kernel juice were analyzed, and the antioxidation activity and bacteriostatic ability were evaluated. The results of this study will enrich the physiological and biochemical studies of LAB-fermented ginkgo biloba kernel, and improve the reference for the development of ginkgo products.

Materials and methods

Screening and identification of lactic acid bacteria strains from the surface of ginkgo peel

Ginkgo was sourced from the campus of Jiangsu Ocean University (Lianyun Gang, Jiangsu province), and the LAB strains were screened from the surface of the ginkgo fruit. The ginkgo fruit was inoculated in MRS culture medium (g: mL, 1:1.5) and cultured at 37°C for 24 h. The fermentation broth was spreaded on MRS plates to obtain single colonies which were underlined on MRS plates and placed in a 37°C incubator for 24 h to obtain single colonies. The obtained single colonies were then grown in MRS medium, with 40% glycerol stocks stored and frozen in a −40°C refrigerator. These LAB strains were identified using 16S-rRNA, physiological and biochemical tests in accordance with conventional methods (12).

Preparation and fermentation of ginkgo biloba kernel juice

The ginkgo fruit was boiled for 5–10 min, and the shell and seed coat were removed. After washing with water, the shelled ginkgo kernels were crushed and broken up in a certain proportion (ginkgo biloba kernels: distilled water = 1:2.2, g:mL), and the starch dissolution rate was required to reach more than 80%.The α-amylase (20 U/g, ginkgo mass) and saccharification enzyme (30 U/g, ginkgo mass) were added, and then ginkgo biloba kernel juice was saccharified at 50°C for 2 h. After the enzymatic hydrolysis the ginkgo biloba kernel juice was completed. It was filtered through a 100-mesh filter, and pasteurized in a water bath at 90°C for 20 min (13). In a 500 mL sealed Erlenmeyer flask, 1% (v/v) inoculum of ginkgo biloba kernel juice was inoculated to ensure an initial viable count of approximately 5.0 Log CFU/mL. The fermentation process was performed in an incubator at 37°C for 48 h. At the end of fermentation, the bacterial cells were removed by centrifugation (10,000 *g*, 10 min, 4°C), and the supernatant was collected for further chemical analysis.

TABLE 1 The pH change and antibacterial activity determination of Ginkgo biloba kernel juice fermented by LAB strains used in this study.

Strain	Species	pH	Diameter of the inhibition zone (mm)		
			E. coli	*S. aureus*	*B. cereus*
Y1	*L. plantarum*	4.13 ± 0.03^{a}	13.10 ± 0.10^{ABab}	10.65 ± 0.35^{Bb}	13.05 ± 0.05^{Ab}
Y2	*L. plantarum*	4.03 ± 0.02^{b}	13.20 ± 0.10^{Ba}	13.05 ± 0.05^{Ba}	15.15 ± 0.15^{Aa}
Y3	*L. plantarum*	4.13 ± 0.03^{a}	10.85 ± 0.15^{Ab}	10.65 ± 0.35^{Aab}	11.95 ± 0.05^{Ab}
Y4	*L. plantarum*	4.15 ± 0.04^{a}	12.30 ± 0.20^{Ab}	12.05 ± 0.05^{Aab}	13.85 ± 0.15^{Ab}
Y5	*L. plantarum*	4.07 ± 0.07^{a}	9.75 ± 0.25^{Ab}	9.70 ± 0.30^{Aab}	11.30 ± 0.30^{Ab}
Y6	*L. plantarum*	4.08 ± 0.06^{a}	11.80 ± 0.20^{Ab}	10.40 ± 0.40^{Aab}	12.70 ± 0.20^{Ab}
Y7	*L. plantarum*	4.12 ± 0.01^{a}	11.80 ± 0.20^{Ab}	10.90 ± 0.10^{Aab}	13.05 ± 0.05^{Ab}
Y8	*L. plantarum*	4.09 ± 0.01^{a}	12.45 ± 0.15^{Ab}	12.10 ± 0.10^{Aab}	11.80 ± 0.20^{Ab}
Y9	*L. plantarum*	4.10 ± 0.01^{a}	9.60 ± 0.20^{Bab}	12.90 ± 0.10^{Cb}	13.05 ± 0.05^{Ab}

The diameter of the inhibition zone is greater than 15 mm as strong; 10–14 mm as medium; less than 10 mm as weak. Capital letters indicate significant differences between samples in the same row ($p < 0.05$). Lowercase letters indicate significant differences between samples in the same column ($p < 0.05$).

Determination of viable cell count, pH and antibacterial activity of fermented ginkgo biloba kernel juice

Viable cell counts were determined using the standard plate method (14). The fermentation broth was first diluted to an appropriate concentration, then the diluted liquid was spread on a plate and the colonies that grew were counted. A precision pH meter (PHS-3C, Shanghai INESA Scientific Instrument Co., Ltd., Shanghai, China) was used to measure the pH value of each sample of ginkgo biloba kernel juice fermentation broth and the bacteriostatic activity was assessed by measuring the diameter of the outward inhibition zone of the Oxford cup using a Vernier caliper (15). The centrifuged supernatant (10 mL) was concentrated in vacuo to 2 ml, and then screening through a 0.22 μm membrane screening. The bacterial pathogens were *Escherichia coli* CICC 10003, *Staphylococcus aureus* CICC 23656, and *Bacillus cereus s* CICC 23828.

Determination of total sugar content and total protein content of fermented ginkgo biloba kernel juice

The total sugar content was determined using the sulfuric acid phenol method (16). The principle of this method was that polysaccharides were hydrolyzed into monosaccharides under the action of sulfuric acid, and then rapidly dehydrated to form uronic derivatives, which were then combined with phenol to form orange-yellow compounds. The absorbance values at 470 nm of the orange-yellow compounds were linearly related to the monosaccharide concentration. A standard curve was established using anhydrous glucose and the results were expressed in μg/mL of glucose equivalents. Protein was detected using the Coomassie brilliant blue method G250 (17). A standard curve was established using a Bovine Serum Albumin (BSA) standard solution, and the total protein equivalent was expressed in mg/mL.

Determination of organic acid and free amino acid content of fermented ginkgo biloba kernel juice

The organic acid spectrum was analyzed using a the Shimadzu LC-2010A system (Shimadzu, Tokyo, Japan), following the method of Luo Ke with some modifications (18). The chromatographic column was an Agilent TC-C18 column (4.6 × 25 mm, 5 μm), the detection wavelength was 210 nm, 0.08 M KH_2PO_4 solution (adjusted to pH 2.5 with phosphoric acid) was used for isocratic elution. The column temperature was 30°C, the flow rate was 0.7 mL/min, and the injection volume was 20 μL. The free amino acids were quantified using Adeyeye's method with slight modifications. The analytical column was 2622PH 4.6 mm I.D. × 60 mm, the flow rate was 0.40 mL/min, the column temperature was 57°C, the reaction temperature was 135°C, and the detection wavelength was 570 nm, and the injection volume was 20 μ L.

Determination of phenolic content of fermented ginkgo biloba kernel juice

The total flavonoids was determined according to the method of Kwaw et al. (19). A calibration curve was constructed with rutin and the results were expressed in μg/mL of rutin equivalents. The total phenolic content of crude polyphenols in fermented or unfermented ginkgo biloba kernel was determined using the Folin-Ciocalteu method.

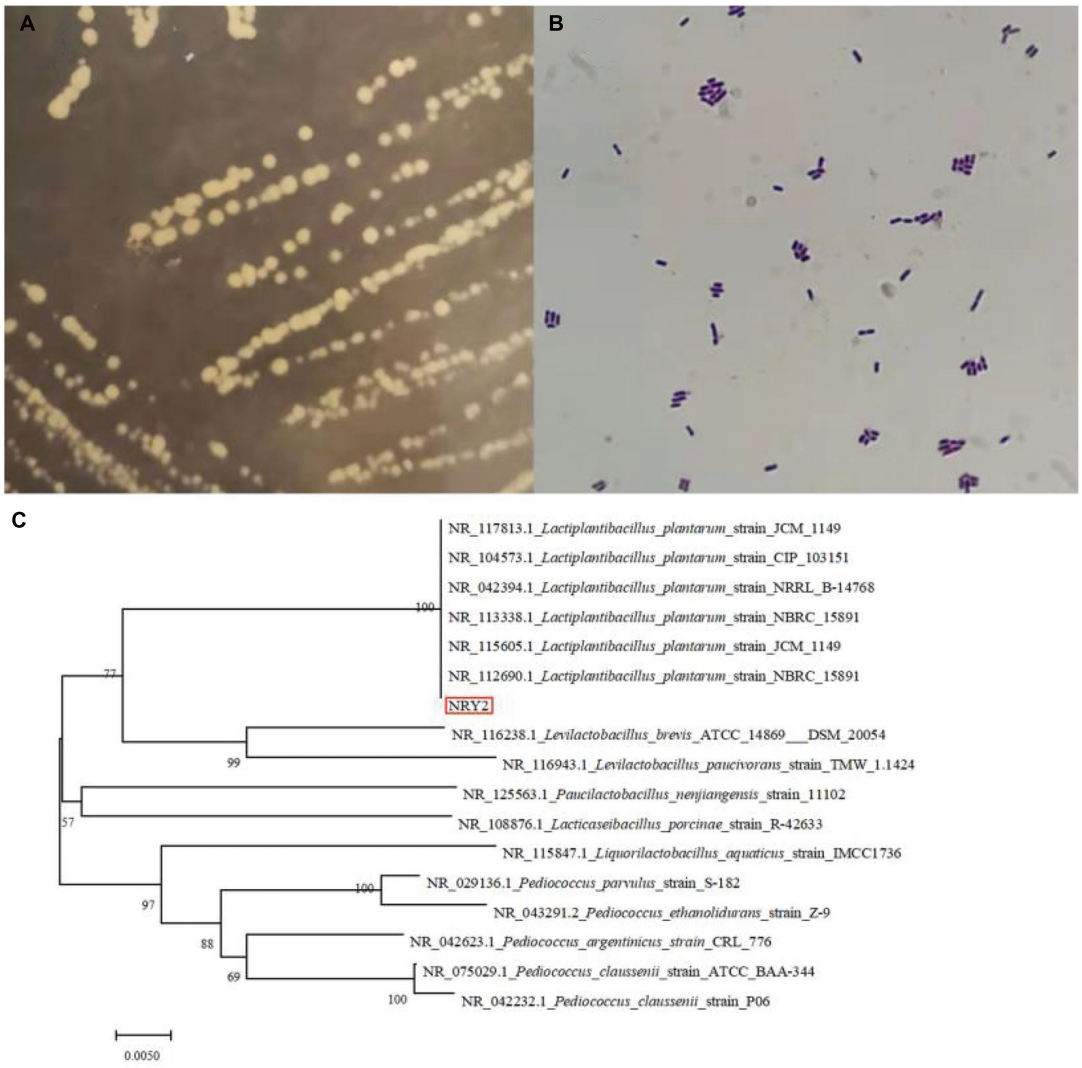

FIGURE 1
The colonial morphology (**A**, MRS plate), gram staining picture **(B)** and colonial morphology the hylogenetic tree **(C)** of *Lactobacillus plantarum* Y2.

A calibration curve constructed using gallic acid and the results were expressed in mg/L of gallic acid equivalents. Phenolic acid and flavonoids content were determined according to the method described by Chiang et al. (20). The column was Inertsil ODS-3 5 μm (4.6 × 250 mm, 5 μm), and the column temperature was 25°C. The mobile phase was composed of solution A (1% acetic acid in water) and the solution B (1% acetic acid in methanol), and the flow rate was 0.6 mL/min. The gradient set was as follows: 0–10 min, 10–26% B; 10–25 min, 26–40% B; 25–45 min, 40–65% B; 45–55 min, 65–95% B; 55–58 min, 95–10% B; 58–65 min, 10% B. The wavelength for determination of phenolic acids and flavonoids was 280 and 350 nm, respectively. The concentration of each phenolic compound was calculated according to the standard calibration curve, and the results were expressed in mg/mL.

Evaluation of antioxidant activity of fermented ginkgo biloba kernel juice

Total antioxidant capacity was measured in the same way as previously described (21). The total antioxidant capacity was calculated as follows: total antioxidant capacity = (Measured OD − Control OD)/0.01/30 × total reaction volume/sampling volume × sample dilution ratio before testing. The $ABTS^{+}$-SA assay was performed using the method described by Tao et al. (21). Trolox was used as the

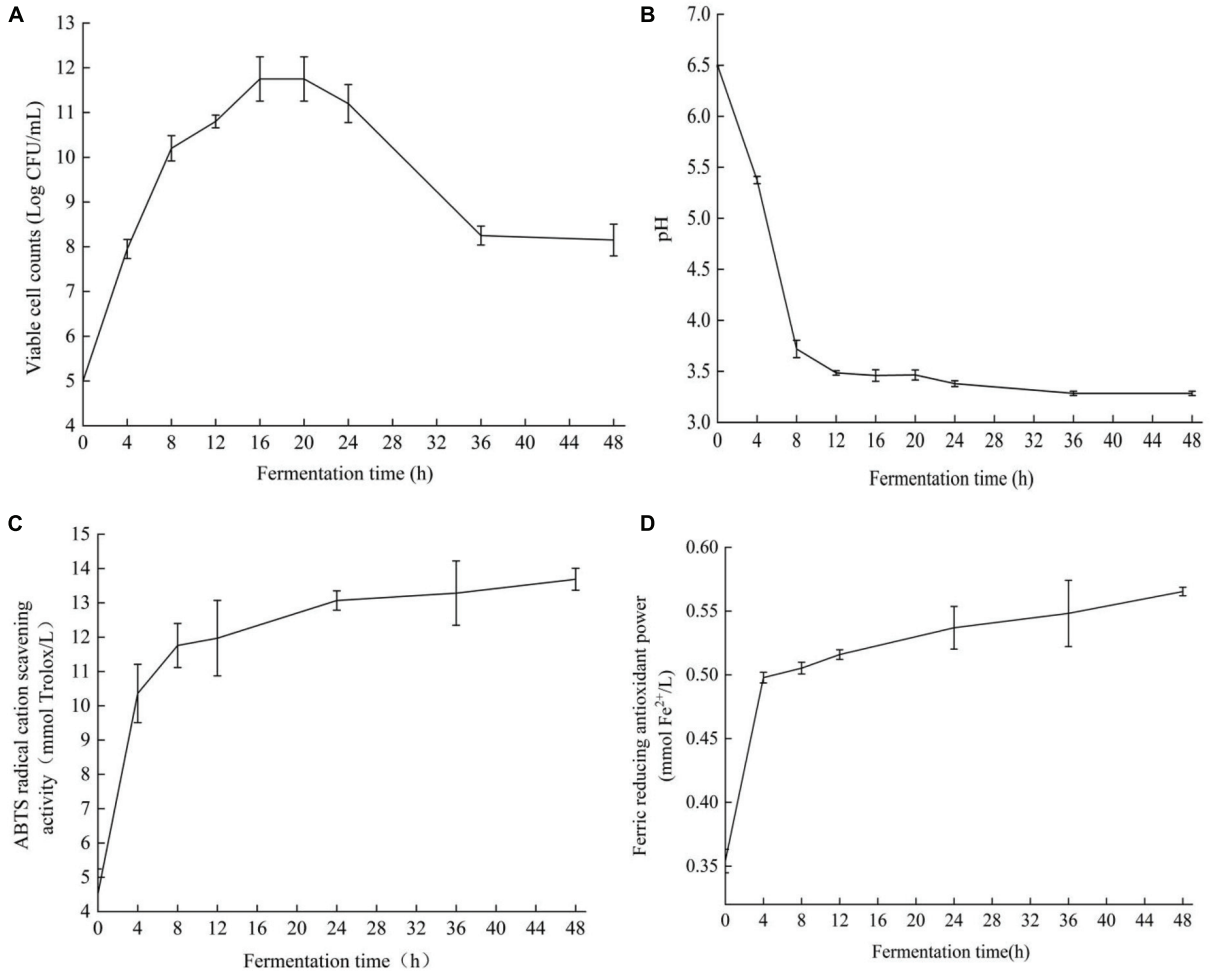

FIGURE 2
Viable cell count **(A)**, changes of pH **(B)**, $ABTS^{+}$ free radical scavenging ability **(C)**, FRAP reducing antioxidant capacity **(D)** of Ginkgo biloba kernel juice fermented by strain Y2.

standard, and the results were expressed in mmol/LTrolox equivalents. The Iron Reducing Antioxidant Ability (FRAP) of the fermented samples was evaluated by the method of Yan et al. (22).

Determination of volatile flavor compounds and 4′-*O*-methylpyridoxine content of fermented ginkgo biloba kernel juice

The volatile components were separated, collected, and analyzed using a triple quadrupole GC-MS (Trace 1310/TSQ 9000, Thermo Scientific) (23). The headspace vial was filled with nitrogen to expel the air in the vial, and 5 mL tested sample was taken into the Thermo RSH autosampler for extraction. The extraction head was placed in the gas chromatography injection port, the injection port temperature was 250°C, the aging was 30 min, the oven temperature was set to 80°C, the water bath was set for 20 min, the adsorption extraction was 30 min, and the extraction head was inserted into the injection port for analysis for 5 min. The MPN content was determined reference to the method described by Yoshimura using the Agilent 1260 fluorescence detector (detection wavelength was 291 nm) (24).

Statistical analysis

All experiments were performed three times in the same way, and all samples were analyzed in triplicate. The significance analysis was performed using SPSS Statistics 20 (IBM Corp., NY, USA), and the significance was assessed at $p < 0.05$ value. The principal component

analysis (PCA) was performed using Origin 2018 (Origin Lab Corp., UK), and all data results were expressed as mean ± standard deviation.

Results and discussion

Evaluation of acid-producing capacity and antibacterial activity of ginkgo biloba kernel juice fermented by lactic acid bacteria strains from the surface of ginkgo fruit

In this study, nine LAB strains were isolated from the surface of ginkgo fruit. The developmental tree established by the BLAST program and the results of the physiology and biochemistry of the strains confirmed that all the selected strains were all *Lactobacillus plantarum* (Table 1 and Figure 1). Next, the acid-producing and antibacterial activities of the nine strains were evaluated. The pH of ginkgo biloba kernel juice, fermented by different strains, decreased, indicating that these strains had good acid production capacity. Among them, the pH of ginkgo biloba kernel juice fermented by the strain Y2 had a lower pH than the other strains, indicating that Y2 has a stronger growth and metabolism in ginkgo biloba kernel juice (25). In addition, the pH of ginkgo biloba kernel juice fermented by the strain Y2 had the best antibacterial effect on pathogenic bacteria (*E. coli*, *S. aureus,* and *B. cereus*), with inhibition zone diameters of 13.77 ± 0.32, 21.54 ± 0.58, and 15.57 ± 0.53 mm, respectively. When the acidity of fermented ginkgo biloba kernel juice is high, the pH value of the medium decreases, reducing conductivity for pathogenic bacterial growth (26). Lactic acid and compounds such as bacteriocins and synthetic hydrogen peroxide produced by the fermentation of lactic acid bacteria inhibit microbial growth (27). In conclusion, the strain Y2 had a good growth and metabolic status in ginkgo biloba kernel juice, and was selected as an effective fermentation strain for further experiments.

Changes of viable cell count, pH value and antioxidant ability during strain Y2 fermentation

Cell viability is a functional feature used to evaluate bacterial growth (28). The strain Y2 grew well in ginkgo biloba kernel juice without any nutritional supplements according to the number of viable cells of strain Y2 in the fermenting process, showing that ginkgo biloba kernel juice could be used as a fermentation substrate (Figure 2A). The strain Y2 grew rapidly in the logarithmic phase from 4 to 8 h, and the number of viable bacteria increased significantly, indicating that Y2 was suitable for growth in ginkgo biloba kernel juice. The number of viable cells started at 5.0 ± 0.02 log CFU/mL and grew rapidly to 10.0 ± 0.03 log CFU/mL after 8 h of fermentation. After 24 h of fermentation, the number of viable cells stabilized at 12.1 ± 0.08 log CFU/mL. After 48 h of fermentation, the number of viable cells of LAB Y2 remained at 8.4 ± 0.03 log CFU/mL. The initial pH of ginkgo biloba kernel juice was 6.2 ± 0.04 (Figure 2B). In the early stage of fermentation, a large amount of lactic acid was produced, and the pH value of the fermentation broth decreased rapidly. After 12 h of fermentation, the rate of pH continued to gradually slow down reaching a final pH of 3.27 ± 0.07 at 48 h. According to the characteristics of lactic acid bacteria fermentation and acid production, Y2 was a LAB with strong acid production ability and good fermentation effect. The changes in antioxidant activity during the fermentation of ginkgo biloba kernel juice were shown in Figures 2C,D. The $ABTS^+$ radical scavenging capacity and FRAP reducing capacity increased with time. After 48 h of fermentation, the free radical scavenging rate of $ABTS^+$ increased from 4.52 ± 0.72 to 13.69 ± 0.32 mM, and the reducing capacity of FRAP increased from 0.35 ± 0.01 to 0.62 ± 0.02 mM. After 0–4 h of fermentation, the $ABTS^+$ free radical scavenging rate and FRAP reducing ability increased significantly, and the antioxidant activity of the fermentation broth improved significantly. After 24 h of fermentation, the lifting speed approached slowly, and the antioxidant activity was basically stable at the end of fermentation.

TABLE 4 Changes in the content of different free amino acids in fermented and unfermented (μ g/mL).

Fermentation time (h)	0	48
Asp	4.61 ± 0.06^a	2.71 ± 0.01^b
Thr	5.37 ± 0.04^a	3.39 ± 0.01^b
Ser	6.10 ± 0.01^a	2.32 ± 0.01^b
Glu	74.22 ± 0.01^a	67.51 ± 0.02^b
Gly	1.72 ± 0.02^b	7.62 ± 0.02^a
Ala	20.83 ± 0.05^a	7.58 ± 0.03^b
Cys	1.09 ± 0.01^c	2.34 ± 0.04^a
Val	3.81 ± 0.05^b	5.88 ± 0.02^a
Met	0.43 ± 0.01^b	1.58 ± 0.03^a
Ile	3.68 ± 0.03^a	1.82 ± 0.02^b
Leu	6.40 ± 0.01^a	3.43 ± 0.06^b
Tyr	10.72 ± 0.04^b	11.79 ± 0.03^a
Phe	3.63 ± 0.06^a	3.42 ± 0.03^b
Lys	5.18 ± 0.03^b	6.92 ± 0.06^a
NH_3	0.48 ± 0.01^b	0.58 ± 0.03^a
His	42.45 ± 0.01^a	28.40 ± 0.01^b
Arg	55.68 ± 0.01^b	72.28 ± 0.02^a

Results are expressed as the mean ± standard deviation of three replicates. The mass concentrations of substances in different time periods are represented by different letters, indicating significant differences ($p < 0.05$).

TABLE 2 Total sugar, total protein and total phenolic content of Ginkgo biloba kernel juice fermented by strain Y2.

Fermentation time (h)	Total sugar content (μ g/mL)	Total protein content (mg/mL)	Total phenolic content (mg/L)
0	190.78 ± 2.04^{a}	12.77 ± 1.14^{a}	116.51 ± 0.51^{b}
4	187.40 ± 0.63^{a}	10.72 ± 1.04^{b}	92.51 ± 2.51^{d}
8	185.90 ± 0.13^{a}	8.02 ± 1.45^{c}	104.17 ± 3.33^{c}
12	185.03 ± 0.25^{b}	7.61 ± 0.04^{c}	104.67 ± 0.58^{c}
24	132.90 ± 4.08^{c}	7.34 ± 0.13^{c}	105.01 ± 1.01^{c}
36	108.90 ± 0.25^{d}	7.29 ± 0.27^{c}	126.17 ± 0.77^{a}
48	105.25 ± 3.24^{d}	4.15 ± 0.19^{d}	127.83 ± 0.28^{a}

Results are expressed as the mean ± standard deviation of three replicates. The mass concentrations of substances in different time periods are represented by different letters, indicating significant differences ($p < 0.05$).

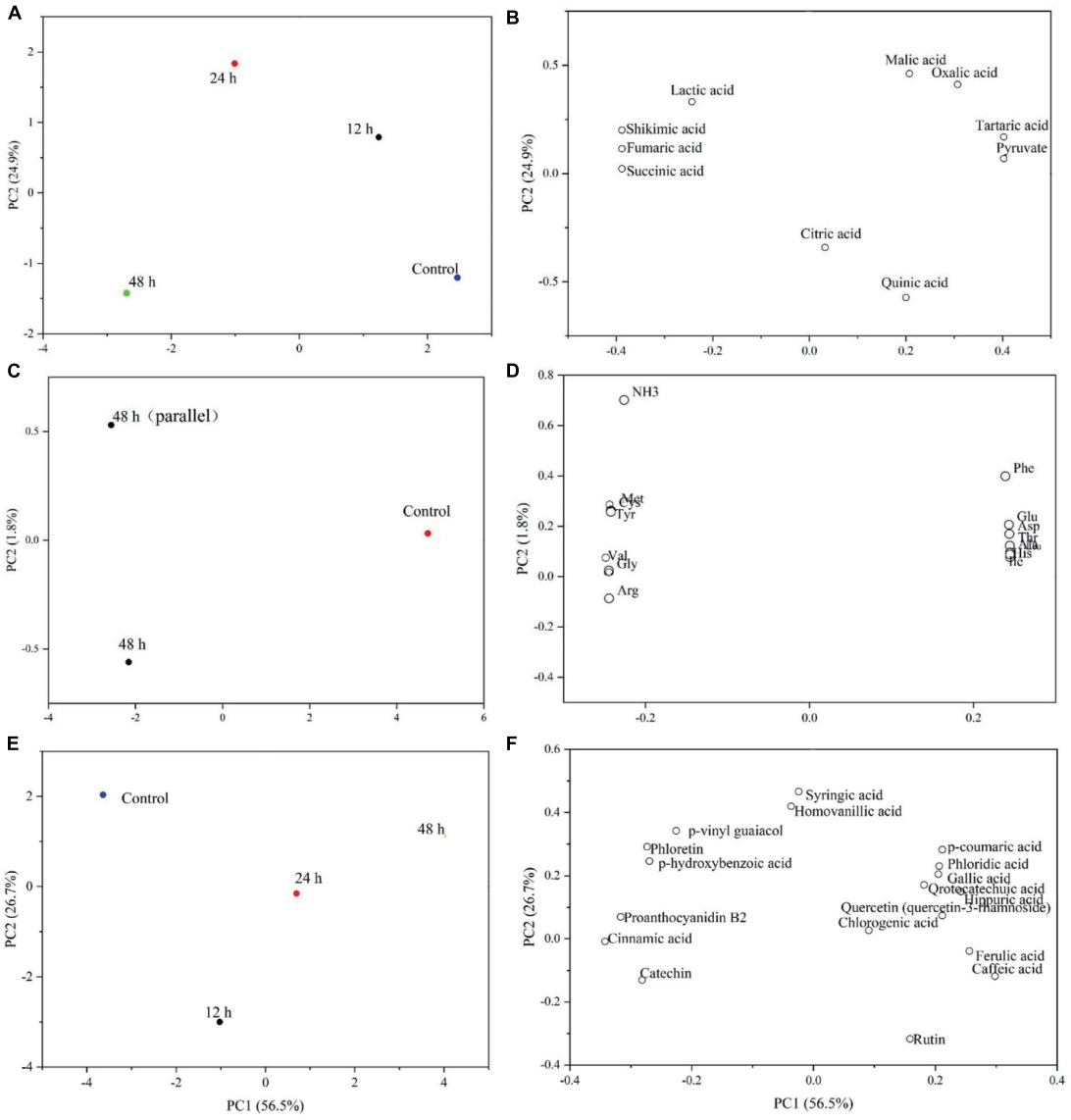

FIGURE 3
Principal component analysis of changes in organic acids **(A,B)**, free amino acids **(C,D)** and phenolic acids **(E,F)** during fermentation of Ginkgo biloba kernel juice by Y2 for 48 h.

TABLE 3 Changes in the content of different organic acids during fermentation (μ g/mL).

Fermentation time (h)	0	4	12	24	48
Oxalic acid	43.01 ± 0.67^{a}	37.64 ± 0.12^{b}	44.64 ± 1.69^{a}	43.65 ± 0.68^{a}	37.63 ± 1.59^{b}
Tartaric acid	632.34 ± 19.98^{a}	536.93 ± 4.41^{b}	545.08 ± 32.27^{b}	514.06 ± 9.97^{b}	395.72 ± 2.61^{c}
Quinic acid	584.52 ± 0.68^{a}	448.64 ± 22.36^{c}	440.38 ± 13.16^{c}	229.27 ± 15.61^{d}	497.96 ± 1.6^{b}
Pyruvate	80.27 ± 0.27^{b}	83.12 ± 2.07^{a}	84.51 ± 1.45^{a}	61.39 ± 1.02^{c}	56.68 ± 1.56^{d}
Malic acid	926.91 ± 5.35^{b}	711.77 ± 10.41^{d}	866.05 ± 14.87^{c}	1019.7 ± 14.75^{a}	692.95 ± 3.51^{d}
Shikimic acid	13 ± 0.7^{e}	26.73 ± 1.36^{d}	73.78 ± 1.45^{c}	90.49 ± 0.48^{b}	114.15 ± 7.22^{a}
Lactic acid	403.33 ± 17.77^{c}	530.72 ± 25.16^{b}	731.24 ± 18.87^{a}	695.37 ± 3.88^{a}	722.58 ± 29.76^{a}
Citric acid	43.77 ± 0.55^{a}	37.28 ± 1.96^{b}	12.32 ± 0.25^{d}	35.37 ± 3.95^{b}	32.19 ± 0.83^{c}
Fumaric acid	0.04 ± 0.01^{c}	0.01 ± 0.01^{d}	0.01 ± 0.01^{d}	0.26 ± 0.01^{a}	0.23 ± 0.01^{b}
Succinic acid	163.04 ± 1.67^{b}	39.21 ± 0.96^{c}	57.12 ± 1.74^{c}	551.28 ± 31.12^{a}	565.83 ± 19.21^{a}

Results are expressed as the mean ± standard deviation of three replicates. The mass concentrations of substances in different time periods are represented by different letters, indicating significant differences ($p < 0.05$).

The consumption of total sugar content by Y2 fermentation and its influence on the bioactive components of organic acids

Carbon source catabolism could provide energy for the growth of *Lactobacillus* and indirectly promote an increase in organic acid content (29). The total sugar content decreased significantly from 12 to 36 h of fermentation, indicating that the lactic acid bacteria in the stable growth period consumed large amounts of carbon sources (**Table 2**). As fermentation entered the decay period (36–48 h of fermentation), lower substrate pH and reduced nutrients limited the growth of Y2 and indirectly affected its sugar metabolism, resulting in a stabilization of the total sugar contents (30). The consumption rate exceeded 44.85% after the fermentation ended.

During the fermentation, the organic acids were transformed into each other over time, and the total organic acid content increased by about approximately 5.86% after 48 h of fermentation. The components of all fermentation time periods were well separated from the control samples according to the component map (**Figure 3A**), showing that the fermentation of Y2 significantly changed the organic acid composition in ginkgo biloba kernel juice. According to the loading diagram (**Figure 3B**), malic acid, tartaric acid, citric acid, pyruvic acid and quinic acid all had high positive values for PCI, indicating that the content of these substances decreased during the fermentation process. While the decrease in malic acid was particularly obvious, levels of oxalic acid did not observe any changes during fermentation. Lactic acid, shikimic acid, fumaric acid, and succinic acid had high negative values for PCI, reflecting a general increase in content after fermentation.

Ginkgo kernel was rich in a variety of natural organic acids, of which malic acid had the highest content (926.91 ± 5.35 μg/mL), followed by pyruvic acid (80.27 ± 0.27 μg/mL), citric acid (43.77 ± 0.55 μg/mL) and tartaric acid (632.34 ± 19.98 μg/mL) (**Table 3**). Lactic acid was the main organic acid produced by the consumption of sugars by lactic acid bacteria in ginkgo biloba kernel juice, and the lactic acid content continued to increase throughout the fermentation process. The initial lactic acid content was 403.33 ± 17.77 μg/mL and increased to 722.58 ± 29.76 μg/mL after 48 h of fermentation. The production of abundant lactic acid reduced the pH value of the fermentation substrate. Pyruvate and citric acid could be decompose into various products such as lactic acid and acetic acid during fermentation (31). Malic acid, which was a good carbon source, observed the highest proportion of total organic acids. The content of malic acid decreased by about 25.25% during the fermentation process, while the content of lactic acid and succinic acid increased. Tartaric acid could be decomposed into various products, such as gluconic acid, which was then oxidized to 2-keto-D-gluconic acid (2-KGA) and 5-keto-D-gluconic acid (5-KGA) (32). During fermentation, the tartaric acid content gradually decreased, and the reduction rate was about 37.42%. In conclusion, lactic acid bacteria fermented ginkgo biloba kernel juice could transform and generate a variety of organic acids. Organic acid was the base of taste substance of ginkgo biloba kernel juice, and was the precursor of many flavor substances. Volatile flavor substances such as acids, alcohols, and aldehydes will be produced in the process of microbial metabolism. Therefore, we evaluated the changes of flavor substances before and after fermentation (**Table 5**).

Study on the change of total protein content and free amino acid profile of Y2 fermentation

Lactic acid bacteria could degrade macromolecular proteins into small peptide chains, amino acid proteases and peptidases through their own reproductive metabolism and

10.3389/fnut.2022.1025080

TABLE 5 Changes in the content of different phenolic acids during fermentation (μ g/mL).

Fermentation time (h)	0	4	12	24	48
Catechin	7.32 ± 0.06^{c}	9.55 ± 0.18^{a}	7.52 ± 0.12^{b}	6.70 ± 0.01^{d}	6.73 ± 0.06^{d}
Hippuric acid	5.48 ± 0.06^{d}	16.47 ± 0.03^{b}	4.71 ± 0.04^{e}	15.52 ± 0.34^{c}	17.8 ± 0.71^{a}
Homovanillic acid	2.60 ± 0.03^{b}	3.36 ± 0.01^{a}	2.31 ± 0.06^{d}	2.51 ± 0.01^{c}	2.53 ± 0.04^{c}
p-coumaric acid	0.16 ± 0.01^{c}	0.10 ± 0.01^{e}	0.14 ± 0.01^{d}	0.18 ± 0.01^{b}	0.25 ± 0.01^{a}
Phloretin	0.48 ± 0.02^{a}	0.37 ± 0.01^{b}	0.34 ± 0.01^{b}	0.35 ± 0.01^{b}	0.33 ± 0.01^{c}
p-vinyl guaiacol	1.58 ± 0.01^{a}	0.05 ± 0.46^{d}	0.40 ± 0.01^{c}	1.16 ± 0.01^{b}	0.59 ± 0.01^{c}
Proanthocyanidin B2	125.92 ± 0.56^{b}	152.28 ± 0.92^{a}	111.86 ± 1.5^{c}	98.79 ± 0.17^{d}	97.76 ± 0.40^{d}
Chlorogenic acid	2.38 ± 0.01^{d}	3.64 ± 0.08^{a}	2.43 ± 0.07^{d}	3.35 ± 0.05^{b}	2.86 ± 0.24^{c}
p-hydroxybenzoic acid	9.64 ± 0.09^{b}	12.35 ± 0.18^{a}	8.04 ± 0.02^{c}	7.65 ± 0.09^{d}	7.91 ± 0.04^{c}
Syringic acid	0.50 ± 0.01^{a}	0.71 ± 0.02^{a}	0.40 ± 0.01^{b}	0.48 ± 0.01^{a}	0.50 ± 0.01^{b}
Phloridic acid (para-hydroxypropionic acid)	0.73 ± 0.03^{b}	0.77 ± 0.02^{b}	0.58 ± 0.01^{d}	0.68 ± 0.01^{c}	1.09 ± 0.05^{a}
Ferulic acid	0.22 ± 0.01^{e}	0.32 ± 0.01^{d}	0.37 ± 0.01^{c}	0.46 ± 0.01^{b}	0.61 ± 0.04^{a}
Cinnamic aldehyde	0.11 ± 0.01^{a}	0.12 ± 0.01^{a}	0.11 ± 0.01^{a}	0.10 ± 0.01^{b}	0.10 ± 0.01^{c}
Gallic acid	1.16 ± 0.01^{c}	1.51 ± 0.01^{b}	1.11 ± 0.01^{c}	1.10 ± 0.03^{c}	1.87 ± 0.10^{a}
Protocatechuic acid	1.88 ± 0.02^{c}	2.75 ± 0.04^{b}	1.81 ± 0.01^{d}	1.67 ± 0.04^{e}	3.62 ± 0.05^{a}
Caffeic acid	0.45 ± 0.02^{d}	0.58 ± 0.05^{b}	0.52 ± 0.03^{c}	0.61 ± 0.02^{b}	0.73 ± 0.06^{a}
Rutin	0.11 ± 0.11^{b}	0.09 ± 0.73^{c}	0.24 ± 0.01^{a}	0.11 ± 0.01^{b}	0.21 ± 0.01^{a}
Quercitrin (quercetin-3-rhamnoside)	0.01 ± 0.01^{d}	0.03 ± 0.01^{a}	0.01 ± 0.01^{c}	0.01 ± 0.01^{e}	0.02 ± 0.01^{b}

Results are expressed as the mean ľ standard deviation of three replicates. The mass concentrations of substances in different time periods are represented by different letters, indicating significant differences ($p < 0.05$).

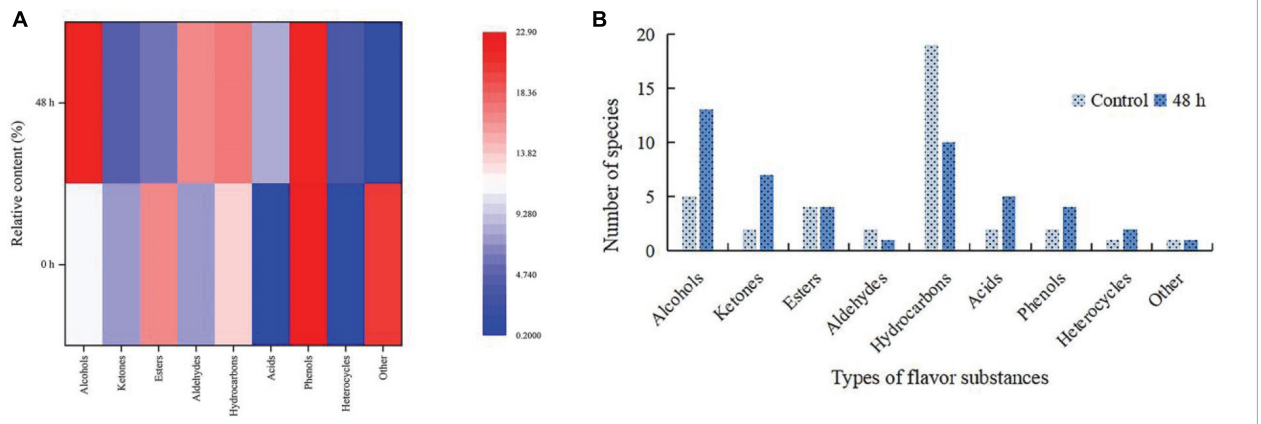

FIGURE 4
Changes in relative content **(A)** and number of species **(B)** of volatile flavor compounds in Ginkgo biloba kernel juice fermented by Y2 for 48 h.

hydrolysis during fermentation (33). Under the catalytic reaction, the proteases could degrade the protein into smaller peptides that are degraded into the small-molecule free amino acids by the action of the peptidase (34). The total protein content of ginkgo biloba kernel juice decreased continuously during the fermentation process, and approximately 67.51% of the metabolism was consumed at the end of fermentation (Table 2).

Among all free amino acids, glutamic acid had the highest content (74.22 ± 0.01 μg/mL), followed by arginine (55.68 ± 0.01 μg/mL) and alanine (20.83 ± 0.05 μg/mL) (Table 4). Glutamate, free histidine and alanine levels decreased significantly after fermentation. During the fermentation process, under the action of lactic acid bacteria decarboxylase, Glu is converted into γ-aminobutyric acid, and Asp is converted into Ala (35). The combination of aspartic acid, glutamic acid and Na^{+} makes the sample umami, which would give ginkgo biloba juice rich flavor substances. In addition, the content of aromatic amino acids (Phe) decreased significantly after fermentation, while the content of another aromatic tyrosine (Tyr) increased, owing to the effect of amino acid invertase on the fermentation process (36). The content of branched-chain amino acids (Leu, Ile) also decreased significantly after fermentation, then were

TABLE 6 Relative content change of fermented and unfermented flavor substances (%).

Component name	CAS no.	Retention time (min.)	Relative content (%)	
			0 h	48 h
Alcohols				
Ethanol	64-17-5	1.456	2.46	3.01
2-ethyl-1-Hexanol,	104-76-7	11.792	7.18	3.1
1-Octanol	111-87-5	13.224	0.68	1.58
1-Dodecanol	112-53-8	24.529	0.13	–
3-methyl-3-Buten-1-ol,	763-32-6	2.885	–	0.85
1-Pentanol	71-41-0	2.905	–	0.46
1-Hexanol	111-27-3	6.292	–	2.39
1-Heptanol	111-70-6	9.807	–	3.24
1-Octen-3-ol	3391-86-4	10.139	–	2.65
2-Octen-1-ol	22104-78-5	13.147	–	0.36
1-Nonanol	143-08-8	16.353	–	1.40
Geraniol	106-24-1	18.764	–	1.80
2,4-Decadien-1-ol	14507-02-9	20.672	–	0.27
1,3,4,5,6,8a-hexahydro-4,7-dimethyl-1-(1-methylethyl)-, (1S,4R,4aS,8aR)-4a(2H)-Naphthalenol,	19912-67-5	28.218	–	0.28
Ketones				
Acetone	67-64-1	1.52	7.16	1.78
7-methyl-2-Oxepanone,	2549-59-9	10.924	0.25	–
trans-.beta.-Ionone	79-77-6	18.875	–	0.62
3,4,4a,5,6,7-hexahydro-1,1,4a-trimethyl-2(1H)-Naphthalenone,	4668-61-5	19.475	–	1.13
dihydro-5-pentyl-2(3H)-Furanone,	104-61-0	21.699	–	0.40
2-Tridecanone	593-08-8	25.056	–	0.41
2-Pentadecanone	2345-28-0	29.68	–	0.11
7,9-Di-tert-butyl-1-oxaspiro(4,5)deca-6,9-diene-2,8-dione	82304-66-3	34.224	–	0.08
Esters				
Ethyl Acetate	141-78-6	1.889	4.54	–
Methyl anthranilate	134-20-3	21.155	8.63	3.97
Acetic acid, decyl ester	112-17-4	22.936	2.80	1.94
2-Undecanol, acetate	14936-67-5	23.513	0.22	0.13
Decanoic acid, 3- hydroxy-, methyl ester	56618-58-7	24.241	–	0.09
Aldehydes				
Hexanal	66-25-1	4.082	3.88	–
Nonanal	124-19-6	14.25	3.25	–
2,5-dimethyl-Benzaldehyde	5779-94-2	17.594	–	16.15
Hydrocarbons				
n-Hexane	110-54-3	1.812	0.61	–
Trichloromethane	67-66-3	1.906	0.47	0.17
3-methyl-Butanal	590-86-3	2.12	0.47	–
2,3,4-trimethyl-Hexane	921-47-1	6.014	0.82	–
Undecane	1120-21-4	12.748	2.45	–
2,4-dimethyl-Decane	2801-84-5	12.926	1.22	–
Dodecane	112-40-3	17.198	0.83	0.58
Longifolene	475-20-7	22.886	0.40	0.15
(1S,4S,4aS)-1-Isopropyl-4,7-dimethyl-1,2,3,4,4a,5-hexahydronaphthalene	267665-20-3	24.009	0.29	–
1-Isopropyl-4,7-dimethyl-1,2,3,4,5,6-hexahydronaphthalene	16729-00-3	24.579	0.33	–
cis-Muurola-4(15),5-diene	157477-72-0	25.046	0.41	–

(Continued)

TABLE 6 (Continued)

Component name	CAS no.	Retention time (min.)	Relative content (%)	
			0 h	48 h
Pentadecane	629-62-9	25.139	0.25	–
1-Isopropyl-4,7-dimethyl-1,2,3,5,6,8a-hexahydronaphthalene	16729-01-4	25.777	1.72	–
Trans-Calamenene	73209-42-4	25.783	1.95	–
Cubenene	29837-12-5	25.998	0.35	–
Alpha-calacorene	21391-99-1	26.256	0.52	8.79
4-Isopropyl-6-methyl-1-methylene-1,2,3,4-tetrahydronaphthalene	50277-34-4	26.736	0.09	–
Alpha-corocalene	20129-39-9	28.091	0.05	2.2
1,3,4,5,6,8a-hexahydro-4,7-dimethyl-1-(1-methylethyl)-, (1S,4R,4aS,8aR)-4a(2H)-Naphthalenol	19912-67-5	28.221	0.75	–
1,5-dimethyl-Cyclopentene	16491-15-9	18.59	–	0.55
Tridecane	629-50-5	20.018	–	1.62
Cis-Calamenene	72937-55-4	25.78	–	0.73
2-Acetoxytridecane		28.158	–	0.15
1,6-dimethyl-4-(1-methylethyl)-Naphthalene	483-78-3	29.254	–	2.18
Acids				
L-Lactic acid	79-33-4	3.797	0.20	–
Propanoic acid, anhydride	123-62-6	10.142	0.69	–
Methoxy-acetic acid	625-45-6	2.271	–	2.16
Acetic anhydride	108-24-7	2.285	–	4.18
2-methyl-Butanoic acid	116-53-0	5.866	–	0.29
2-ethyl-Hexanoic acid	149-57-5	14.837	–	0.24
Dodecanoic acid	143-07-7	26.628	–	1.02
Phenols				
Alpha-cubebene	17699-14-8	21.397	2.27	–
2,4-Di-tert-butylphenol	96-76-4	25.445	20.53	13.47
3-ethyl-Phenol	620-17-7	16.273	–	0.29
Eugenol	97-53-0	21.568	–	7.48
Trans-Isoeugenol	5932-68-3	23.966	–	0.37
Heterocycles				
Decane-rel-(1R,2S,6S,7S,8S)-8-Isopropyl-1-methyl-3-methylenetricyclo[4.4.0.02,7]	18252-44-3	22.47	0.27	–
2,3-dihydro-1,1,5,6-tetramethyl-1H-Indene,	942-43-8	16.313	–	0.11
3,5,6,8a-tetrahydro-2,5,5,8a- tetramethyl-,trans-2H-1-Benzopyran,	41678-29-9	20.434	–	3.41
Other				
Oxime-, methoxy-phenyl		7.614	20.49	1.65

"–" is not detected.

metabolized into keto acids, alcohols and fatty acids through amino acid converting enzymes. Phe and Thr could be converted into benzyl alcohol, phenylethanol and acetaldehyde with certain flavor under the action of an amino acid converting enzyme. Arginine is converted to citrulline by the enzyme arginine deiminase during lactic acid fermentation, which is further broken down into ornithine and free ammonia (37).

The total free amino acid content increased by approximately 6.88% after 48 h of fermentation. The effects of lactic acid fermentation on free amino acid profiles were studied using principal component analysis (PCA). In principal component analysis, PC1 and PC2 accounted for 98.2 and 1.8% of the data variance, respectively. As shown in the composition diagram (**Figure 3C**), the samples of unfermented ginkgo biloba kernel juice were located on the positive side of PC1, and the samples fermented for 48 h were distributed on the negative side. This indicated that lactic acid bacteria had a significant effect on the change in free amino acid content during the fermentation of ginkgo biloba kernel juice. Specific changes in the free amino acids were observed through in the loading diagram (**Figure 3D**). Phe, Thr, Leu, Ile, Asp, Ser, Ala, and free histidines were all positively correlated with PC1, indicating that these amino acids would be affected

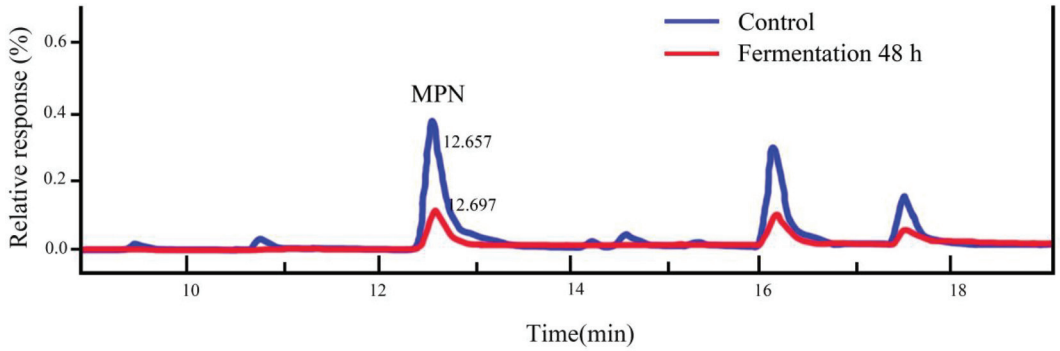

FIGURE 5
Changes between fermented and unfermented MPN content.

by the fermentation process. Whereas, Lys, Val, Met, Gly, Cys, Tyr, and Arg were all negatively correlated with PC2, indicating that their content increased with the fermentation time.

Effect of Y2 fermentation on the structure of phenolic substances

Ginkgo kernels were also rich in a variety of phenolic substances, which led to the production of many secondary metabolites during fermentation, including phenolic acids, stilbenes, lignins, and aromatic compounds (38). Therefore, it is necessary to study the effect of LAB fermentation on the phenolic components in ginkgo biloba kernel juice.

As shown in **Table 1**, the total phenolic content of ginkgo biloba kernel juice at the beginning of fermentation was 116.51 ± 0.51 mg/L. It decreased significantly within 4 h of fermentation, and then increased slowly. After 48 h of fermentation, the total phenolic content of the samples was approximately 9.72% higher than that of the unfermented samples. Procyanidin B2 is an oligomer, dimer and polymer of catechin (39). The highest content of flavonoids in ginkgo kernel was about 7.32 ± 0.06 μg/mL of catechin and about 125.92 ± 0.56 μg/mL of procyanidin B2 (**Table 5**). Procyanidin B2 increased by approximately 20.93%, and catechin increased by approximately 30.46% after 4 h of fermentation. The increase in the total flavonoid content could result in an increase in the antioxidant activity of the fermented samples. In the process of fermenting ginkgo biloba kernel juice, the improvement in antioxidant activity was highly correlated with the transformation of phenolic substances (40). Previous studies have reported that phenolic compounds could be used as reducing agents as well as free radical scavengers and singlet oxygen quenchers (41). Phenols could be converted into each other, and the antioxidant activity of the fermentation broth can be improved (42). It was also shown that the antioxidant capacity of phenolic substances in ginkgo biloba kernel juice was significantly improved after Y2 fermentation (**Figures 2C,D**). There is also a certain relationship between FRAP and phenolic content, and the presence of phenolic substances can effectively reduce Fe^{3+} to Fe^{2+} form (43). Therefore, the increase in phenolic substances was an important factor affecting the antioxidant activity of fermentation.

As shown in **Figures 3E,F**, principal component analysis (PCA) was used to analyze the effect of Y2 fermentation on phenolic components in ginkgo biloba kernel juice. After 48 h of fermentation, phloridzin, epicatechin and gallate in the samples were metabolized to form gallic acid and phloretin with a strong antioxidant quality (44). *L. plantarum* fermentation could produce some phenolic acid decarboxylases, such as ferulic acid. These extracellular enzymes act on phenolic components, and from a chemical point of view, glycosylation, methylation and other types of substitutions are carried out, resulting in structural changes. This lead to the mutual conversion of phenolic substances in the sample, thereby changing their oxidative activity (45). The p-hydroxybenzoic acid content decreased by approximately 17.95% after fermentation. Further, the content of chlorogenic acid was the highest at 4 h of fermentation (3.64 ± 0.08 μg/mL), and it increased by about 20.17% at the end of fermentation. The increase in chlorogenic acid content leads to an increase in pharmacological functions, such as antioxidant, antiviral, anti-cancer and antibacterial capacities (46). During the fermentation period of 4–8 h, the content of chlorogenic acid gradually decreased, potentially under the action of extracellular enzyme hydrolysis, which indirectly led to an increase in caffeic acid, p-coumaric acid and ferulic acid. Phenolic acids not only have various pharmacological effects such as anti-inflammatory, antioxidant, anti-mutation, and anti-cardiovascular disease, but also have co-color effects (such as ferulic acid), which can enhance the stability of their own colors after fermentation (47). There are few studies on

the volatile flavor compounds after fermentation, and further research is needed.

Study on volatile flavor compounds by fermentation of Y2

A total of 64 volatile flavor compounds were identified in ginkgo biloba kernel juice before and after fermentation, including three kinds of aldehydes, 18 kinds of alcohols, 9 kinds of ketones, 8 kinds of esters, 29 kinds of hydrocarbons, 6 kinds of phenols, 3 kinds of heterocycles, 7 kinds of acids, and two other types. From the analysis results, the fermented samples and the unfermented samples were quite different, and the similarities of volatile flavor substances were low. The relative content and species of ginkgo biloba kernel juice in alcohols, acids, and heterocyclic compounds were significantly increased after 48 h of fermentation (**Figure 4**).

The main aroma substances in unfermented ginkgo biloba kernel juice were 2-ethyl-1-hexanol, 1-octanol, and n-octanol (**Table 6**). The total relative content of volatile flavor compounds increased by 125.48% after fermention. Among them, the total relative content of alcohol increased by about 104.69%, potentially due to the emergence of new generation of various volatile flavor substances. After 48 h of fermentation, the contents of 1-octanol and n-octanol increased significantly, the contents of 2-ethyl-1-hexanol and 1-octanol decreased, and 1-heptanol, 1-octen-3-ol and 2-octen-1-ol newly formed. The relatively high contents of newly generated alcohols were geraniol (1.81%), 1-octen-3-ol (2.65%) and 1-heptanol (3.24%). These alcohols were mainly produced by metabolism during microbial processes, degradation of unsaturated fatty acids, and reduction of carbon-based compounds during fermentation. Aldehydes are unstable compounds, and the relative content of aldehydes increased by about 126.5%, among which the highest content was 16.15% 2,5-dimethylbenzaldehyde. The relative content of hydrocarbons increased by about 32.92%, while the types of hydrocarbons decreased after fermentation. Meanwhile, the relative content of newly generated aromatic compounds was higher, of which 1,6-dimethyl-4-(1-methylethyl)-naphthalene accounted for about 2.18% of the total relative content after fermentation. The increase of total content of alcohols and esters in ginkgo biloba kernel juice could mpart stronger fruity and floral aromas (48). Under the metabolic activity of lactic acid bacteria, more aldehydes are reduced to alcohols and acids, and the increase of alcohols will increase the corresponding esters, which is also the reduction of aldehydes in fermented ginkgo biloba kernel juice, while alcohol, the reasons for the increase in esters (49). The content of acids increased by about 786.01%, and the relative content of acids increased significantly. The strain Y2 produced a large amount of acids during the fermentation process, among which the new acids were 2.16% methoxy-acetic acid, 1.02% dodecanoic acid, 0.29% 2-methylbutyric acid, 0.24% 2-ethylhexanoic acid. Among them, the relative contents of L-lactic acid and propionic anhydride decreased after the fermentation, while the relative content of acetic anhydride was high (4.18%). Meanwhile, the relative content of phenols changed scarcely, and eugenol (7.48%) and 3-ethylphenol (0.29%) were newly formed at the end of fermentation. The former was produced by the reaction of guaiacol and allyl alcohol, and had strong antibacterial activity. The latter had an aromatic odor and was widely used in organic synthesis and as a solvent (50). Future research will focus on the transformation mechanism between these molecules and their effect on the flavor of ginkgo biloba kernel juice.

Effect of Y2 fermentation on the content of 4′-*O*-methylpyridoxine

4′-O-methylpyridoxine (MPN), also known as ginkgo toxin, is an anti-vitamin B6 compound, and one of the toxic components in ginkgo kernels. If ingested in large amounts, adverse symptoms, such as vomiting, clonic seizures, and loss of consciousness could occur (51). Relevant studies had shown that MPN could be effectively converted into 4′-*O*-methylpyridoxine-5-glycoside (MPNG) after heating, microwave irradiation and boiling (52). In this study, the MPN content in ginkgo biloba kernel juice was identified, by comparison with standard chemicals determined by high performance liquid phase (HPLC) analysis (**Figure 5**). The content of MPN was reduced by roughly 82.25% after fermentation for 48 h, indicating that strain Y2 could effectively gradate MPN. Relevant studies have shown that lactic acid bacteria have the function of adsorbing toxins during the fermentation process. During the growth of lactic acid bacteria, a large number of polysaccharides and peptidoglycan were produced on the cell wall, which played a key role in adsorbing the toxic substance 4′-O-methylpyridoxine in ginkgo biloba kernel juice (53). It also had been reported that MPN could be phosphorylated to form 4′-*O*-methylpyridoxine-5′-phosphate (MPNP) under the action of phosphoric acid produced during LAB fermentation (54). However, there are few studies on the degradation mechanism of 4′-*O*-methylpyridoxine content by LAB fermentation, and we will further investigate how strain Y2 bio-transformed MPN.

Conclusion

This work showed that LAB fermentation was a potential way to improve the beneficial value and safety of ginkgo biloba kernel juice. The total relative content of volatile flavor substances increased by about 125.48%, and 24 new substances were added. The biotransformation and biosynthesis content of

the phenols was increased, and the total phenolic concentration increased by about 9.72%, which indirectly led to the enhance of antioxidant capacity of the fermentation. The increase of the aromatic amino acids and volatile flavor substances reflected the metabolism of lactic acid bacteria in fruit juice. In addition, 4′-*O*-methylpyridoxine, as one of the toxic substances in ginkgo biloba kernel, showed a degradation rate above 82.25%, and the total ginkgo acid content in the final product was less than 41.53 mg/L. As few reports about the degradation of 4′-*O*-methylpyridoxine by fermentation, further studied will focus on the degradation mechanism. Our results showed that the LAB fermented ginkgo biloba kernel juice had broad application prospects.

Data availability statement

The original contributions presented in this study are included in the article/supplementary material, further inquiries can be directed to the corresponding author/s.

Author contributions

JY and YS performed the experiments and analyzed the data. JC, YC, HZ, and TG drafted the manuscript. FX and SP analyzed and discussed the data. YT and JL contributed to the writing—review, editing, and funding acquisition. All authors have read and agreed to the published version of the manuscript.

Funding

This research was funded by the Natural Science Research General Project of Jiangsu Higher Education Institutions (Nos. 20KJB550008 and 21KJB550003), the National Natural Science Foundation of China (Nos. 32100037 and 32201964), Science and Technology Projects of Jiangsu (No. BE2021353), Jiangsu Planned Projects for Postdoctoral Research Funds (No. 2021K364C), Postdoctoral Research Funds of Lianyungang city (No. ZKK2021006), and the Innovative Project of the Priority Academic Program Development of Jiangsu Higher Education Institutions (No. 2021JSPAPD20).

Conflict of interest

The authors declare that the research was conducted in the absence of any commercial or financial relationships that could be construed as a potential conflict of interest.

Publisher's note

All claims expressed in this article are solely those of the authors and do not necessarily represent those of their affiliated organizations, or those of the publisher, the editors and the reviewers. Any product that may be evaluated in this article, or claim that may be made by its manufacturer, is not guaranteed or endorsed by the publisher.

References

1. Dubber MJ, Kanfer I. Determination of terpene trilactones in *Ginkgo biloba* solid oral dosage forms using HPLC with evaporative light scattering detection. *J Pharm Biomed Anal.* (2006) 41:135–40. doi: 10.1016/j.jpba.2005.11.010

2. Lim HB, Kim DH. Correction to: effects of roasting conditions on physicochemical properties and antioxidant activities in *Ginkgo biloba* seeds. *Food Sci Biotechnol.* (2018) 27:1549. doi: 10.1007/s10068-018-0454-6

3. Hosoda S, Kawazoe Y, Shiba T, Numazawa S, Manabe A. Anti-obesity effect of *Ginkgo* vinegar, a fermented product of *Ginkgo* seed coat, in mice fed a high-fat diet and 3T3-L1 preadipocyte cells. *Nutrients.* (2020) 12:230. doi: 10.1186/s12906-019-2756-5

4. Ahlemeyer B, Krieglstein J. Pharmacological studies supporting the therapeutic use of *Ginkgo biloba* extract for Alzheimer's disease. *Pharmacopsychiatry.* (2003) 36:8–14. doi: 10.1055/s-2003-40454

5. Ademiluyi AO, Oyeniran OH, Jimoh TO, Oboh G, Boligon AA. Fluted pumpkin (*Telfairia occidentalis*) seed modulates some markers of erectile function in isolated rat's corpus cavernosum: influence of polyphenol and amino acid constituents. *J Food Biochem.* (2019) 43:e13037. doi: 10.1111/jfbc.13037

6. Arenz A, Klein M, Fiehe K. Occurrence of neurotoxic 4′-O-methylpyridoxine in *Ginkgo biloba* leaves, *Ginkgo* medications and Japanese *Ginkgo* food. *Planta Med.* (1996) 62:548–51. doi: 10.1055/s-2006-957967

7. Lu Y, Sun L, Li C, Wang X, Li W, Zhao T, et al. Comparative mass spectrometry analysis of N-glycans from the glycoproteins of eight allergy-inducing plants. *Food Chem.* (2022) 384:132440. doi: 10.26914/c.cnkihy.2020.022032

8. Prete R. Lactic acid bacteria exopolysaccharides producers: a sustainable tool for functional foods. *Foods.* (2021) 10:1653. doi: 10.3390/FOODS10071653

9. Verón HE, Gauffin Cano P, Fabersani E, Sanz Y, Isla MI, Fernández Espinar MT, et al. Cactus pear juice fermented with autochthonous *Lactobacillus plantarum* S-811. *Food Funct.* (2019) 10:1085–97. doi: 10.1039/C8FO01591K

10. Wang J, Ren S, Fang XX. Data comparison of the effects of feeding *Ginkgo* leaf fermentation and Chinese herbal medicine on meat ducks. *J Phys.* (2019) 1423:012018. doi: 10.1088/1742-6596/1423/1/012018

11. Hu P, Song W, Shan YJ. *Lactobacillus paracasei* sub sp. paracasei M5L induces cell cycle arrest and calreticulin translocation via the generation of reactive oxygen species in HT-29 cell apoptosis. *Food Funct.* (2015) 6:2257–65. doi: 10.1039/c5fo00248f

12. Yi L, Qi T, Hong Y, Deng L, Zeng K. Screening of bacteriocin-producing lactic acid bacteria in Chinese homemade pickle and dry-cured meat, and bacteriocin identification by genome sequencing. *LWT.* (2020) 125:109177. doi: 10.1016/j.lwt.2020.109177

13. Binte Abu Bakar SY, Salim M, Clulow AJ, Hawley A, Pelle J, Geddes DT, et al. Impact of pasteurization on the self-assembly of human milk lipids during digestion. *J Lipid Res.* (2022) 63:100183. doi: 10.1016/J.JLR.2022.100183

14. Kaprasob R, Kerdchoechuen O, Laohakunjit N, Sarkar D, Shetty K. Fermentation-based biotransformation of biaoctive phenolics and volatile compounds from cashew apple juice by screening lactic acid bacteria. *Process Biochem.* (2017) 59:141–9. doi: 10.1016/j.procbio.2017.05.019

15. Bungenstock L, Abdulmawjood A, Reich F. Evaluation of antibacterial properties of lactic acid bacteria from traditionally and industrially produced fermented sausages from Germany. *PLoS One.* (2020) 15:e0230345. doi: 10.1371/journal.pone.0230345

16. Cai H, Tian Z. Determination of total sugar content in strawberries by phenol-sulfuric acid method. *Jilin Agric.* (2019) 4:46. doi: 10.14025/j.cnki.jlny.2019.04.011

17. Lü X, Li D, Huang Y, Zhang Y. Application of a modified Coomassie Brilliant Blue protein assay in the study of protein adsorption on carbon thin films. *Surf Coat Technol.* (2007) 201:6843–6. doi: 10.1016/j.surfcoat.2006.09.019

18. Luo K. Effect of organic acids on the morphology and particle size of titanium dioxide (E171) in processed food. *J Hazard Mater.* (2022) 432:128666. doi: 10.1016/J.JHAZMAT.2022.128666

19. Kwaw E, Ma Y, Tchabo W. Effect of fermentation parameters and their optimization on the phytochemical properties of lactic-acid-fermented mulberry juice. *J Food Meas Charact.* (2017) 11:1462–73. doi: 10.1007/s11694-017-9525-2

20. Chiang ELC, Lee S, Medriano CA. Assessment of physiological responses of bacteria to chlorine and UV disinfection using a plate count method, flow cytometry, and viability PCR. *J Appl Microbiol.* (2021) 132:1788–801. doi: 10.1111/JAM.15325

21. Shi HT, Wang BY, Bian CZ, Han YQ, Qiao HX. Fermented *Astragalus* in diet improved laying performance, egg quality, antioxidant and immunological status and intestinal microbiota in laying hens. *AMB Express.* (2020) 10:159. doi: 10.21203/rs.3.rs-30575/v2

22. Yan Z, Xie L, Li M. Phytochemical components and bioactivities of novel medicinal food – Peony roots. *Food Res Int.* (2020) 140:109902. doi: 10.1016/j.foodres.2020.109902

23. Matsubara H, Imamura Y. GC-MS analysis of volatile sulfuric compounds in sweet potato shochu and the identification of off-flavor substances. *J JA Soc Brew Chem.* (2011) 106:493–501. doi: 10.6013/jbrewsocjapan.106.493

24. Yoshimura T, Udaka N. High performance liquid chromatographic determination of ginkgotoxin and ginkgotoxin−5'−glucoside in *Ginkgo biloba* seeds. *J Liq Chromatogr R T.* (2007) 29:605–16. doi: 10.1080/10826070500531466

25. Piao M, Liu J, Liu Q, Kim D, Dhungana SK, Kim J, et al. Development of antioxidative soy sauce fermented with enzymatic hydrolysates of *Eupolyphaga sinensis*. *J Pure Appl Micro.* (2016) 10:2511–9.

26. Pereira A, Maciel TC, Rodrigues S. Probiotic beverage from cashew apple juice fermented with *Lactobacillus casei*. *Food Res Int.* (2011) 44:1276–83. doi: 10.1016/j.foodres.2010.11.035

27. Tang HW, Phapugrangkul P, Fauzi HM. Lactic acid bacteria bacteriocin, an antimicrobial peptide effective against multidrug resistance: a comprehensive review. *Int J Pept Res Ther.* (2022) 28:1–14. doi: 10.1007/s10989-021-10317-6

28. Kamatani T, Fukunaga K, Miyata K. Construction of a system using a deep learning algorithm to count cell numbers in nanoliter wells for viable single-cell experiments. *Sci Rep.* (2017) 7:16831. doi: 10.1038/s41598-017-17012-x

29. Deutscher J. The mechanisms of carbon catabolite repression in bacteria. *Curr Opin Microbiol.* (2008) 11:87–93. doi: 10.1016/j.mib.2008.02.007

30. Tang H, Qian B, Xia B, Zhuan Y, Yao Y, Gan R, et al. Screening of lactic acid bacteria isolated from fermented *Cornus officinalis* fruits for probiotic potential. *J Food Saf.* (2018) 38:e12565. doi: 10.1111/jfs.12565

31. Dudley EG, Steele JL. Succinate production and citrate catabolism by cheddar cheese nonstarter lactobacilli. *J Appl Microbiol.* (2005) 98:14–23. doi: 10.1111/j.1365-2672.2004.02440.x

32. Kotera U, Umehara K, Kodama T, Yamada K. Isolation method of highly tartaric acid producing mutants of gluconobacter suboxydans. *Agric Biol Chem.* (2014) 36:1307–13. doi: 10.1080/00021369.1972.10860418

33. Farrell K, Musaus M, Navabpour S, Martin K, Ray WK, Helm RF, et al. Proteomic analysis reveals sex-specific protein degradation targets in the amygdala during fear memory formation. *Front Mol Neurosci.* (2021) 14:716284. doi: 10.3389/FNMOL.2021.716284

34. Diana M, Rafecas M, Quílez J. Free amino acids, acrylamide and biogenic amines in gamma-aminobutyric acid enriched sourdough and commercial breads. *J Cereal Sci.* (2014) 60:639–44. doi: 10.1016/j.jcs.2014.06.009

35. Nishimura K, Ijiri D, Shimamoto S, Takaya M, Ohtsuka A, Goto T. Genetic effect on free amino acid contents of egg yolk and albumen using five different chicken genotypes under floor rearing system. *PLoS One.* (2021) 16:e0258506. doi: 10.1371/JOURNAL.PONE.0258506

36. Yvon M, Rijnen L. Flavour formation by amino acid catabolism. *Biotechnol Adv.* (2006) 24:238–42. doi: 10.1016/j.biotechadv.2005.11.005

37. Mira de Orduña R, Liu SQ, Patchett ML, Pilone GJ. Kinetics of the arginine metabolism of malolactic wine lactic acid bacteria *Lactobacillus buchneri* CUC-3 and *Oenococcus oeni* Lo111. *J Appl Microbiol.* (2000) 89:547–52. doi: 10.1046/j.1365-2672.2000.01135.x

38. Manach C, Scalbert A, Morand C, Rémésy C, Jiménez L. Polyphenols: food sources and bioavailability. *Am J Clin Nutr.* (2004) 79:727–47. doi: 10.1093/ajcn/79.5.727

39. Crozier A, Jaganath IB, Clifford MN. Chem inform abstract: dietary phenolics: chemistry, bioavailability and effects on health. *Nat Prod Rep.* (2009) 26:1001–43. doi: 10.1002/chin.200946244

40. Chen Y, Wang Y, Chen J, Tang H, Wang C, Li Z, et al. Bioprocessing of soybeans (*Glycine max* L.) by solid-state fermentation with *Eurotium cristatum* YL-1 improves total phenolic content, isoflavone aglycones, and antioxidant activity. *RSC Adv.* (2020) 10:16928–41. doi: 10.1039/C9RA10344A

41. Emmanuel K, Yongkun M, William T. Effect of *Lactobacillus* strains on phenolic profile, color attributes and antioxidant activities of lactic-acid-fermented mulberry juice. *Food Chem.* (2018) 250:148–54. doi: 10.1016/j.foodchem.2018.01.009

42. Xiao Y, Wu X, Yao X, Chen Y, Ho CT, He C, et al. Metabolite profiling, antioxidant and α-glucosidase inhibitory activities of buckwheat processed by solid-state fermentation with *Eurotium cristatum* YL-1. *Food Res Int.* (2021) 143:110262. doi: 10.1016/j.foodres.2021.110262

43. Vadivel V, Stuetz W, Scherbaum V, Biesalski HK. Total free phenolic content and health relevant functionality of Indian wild legume grains: effect of indigenous processing methods. *J Food Compos Anal.* (2011) 24:935–43. doi: 10.1016/j.jfca.2011.04.001

44. Tao Y, Wu P, Dai Y, Luo X, Manickam S, Li D, et al. Bridge between mass transfer behavior and properties of bubbles under two-stage ultrasound-assisted physisorption of polyphenols using macroporous resin. *Chem Eng J.* (2022) 436:135158. doi: 10.1016/J.CEJ.2022.135158

45. Amrane-Abider M, Nerín C, Tamendjari A, Serralheiro MLM. Phenolic composition, antioxidant and antiacetylcholinesterase activities of *Opuntia ficus-indica* peel and flower teas after in vitro gastrointestinal digestion. *J Sci Food Agric.* (2022) 102:4401–9. doi: 10.1002/JSFA.11793

46. Matsuda R, Sakagami H, Amano S, Iijima Y, Sano M, Uesawa Y, et al. Inhibition of neurotoxicity/anticancer activity of bortezomib by caffeic acid and ahlorogenic acid. *Anticancer Res.* (2022) 42:781–90. doi: 10.21873/anticanres.15536

47. Cao YX, Wu ZF, Weng PF. Effect of phenolic acids on color and volatile flavor substances during storage of bayberry fermented wine. *Food Sci.* (2021) 42:78–85. doi: 10.7506/spkx1002-6630-20200712-161

48. Zhen S, Dong H, Chun-hui Z, Hai L, Xia L, Zhi-bin L, et al. Profile analysis of the volatile flavor compounds of quantitative marinated chicken during processing. *Sci Agric Sin.* (2016) 49:3030–45. doi: 10.3864/j.issn.0578-1752.2016.15.017

49. Le Y, Yang H. Xanthan gum modified fish gelatin and binary culture modulates the metabolism of probiotics in fermented milk mainly via amino acid metabolism pathways. *Food Res Int.* (2022) 161:111844. doi: 10.1016/J.FOODRES.2022.111844

50. Chen Y, Li P, Liao L, Qin Y, Jiang L, Liu Y. Characteristic fingerprints and volatile flavor compound variations in Liuyang Douchi during fermentation via HS-GC-IMS and HS-SPME-GC-MS. *Food Chem.* (2021) 361:130055. doi: 10.1016/j.foodchem.2021.130055

51. Lim HB, Kim DH. Effect of heat treatment on 4′-O-methylpyridoxine (MPN) content in *Ginkgo biloba* seed extract solution. *J Sci Food Agric.* (2018) 98:5153–6. doi: 10.1002/jsfa.9017

52. Hao G. Determination of native contents of 4′- O -methylpyridoxine and its glucoside in raw and heated *Ginkgo biloba* seeds by high-performance liquid chromatography. *J Food Meas Charact.* (2020) 14:917–24. doi: 10.1007/s11694-019-00341-y

53. Haskard CA, El-Nezami HS, Kankaanpaa PE. Surface binding of aflatoxin B1 by lactic acid bacteria. *Appl Environ Microbiol.* (2001) 67:3086–91. doi: 10.3969/j.issn.1004-8456.2003.03.005

54. Kästner U, Hallmen C, Wiese M. The human pyridoxal kinase, a plausible target for ginkgotoxin from *Ginkgo biloba*. *FEBS J.* (2007) 274:1036–45. doi: 10.1111/j.1742-4658.2007.05654.x

frontiers | Frontiers in Nutrition

TYPE Review
PUBLISHED 28 October 2022
DOI 10.3389/fnut.2022.1044871

OPEN ACCESS

EDITED BY
Runqiang Yang,
Nanjing Agricultural University, China

REVIEWED BY
Jiaojiao Zhang,
Zhejiang Agriculture and Forestry University, China
Shangde Sun,
Henan University of Technology, China

*CORRESPONDENCE
Fang Wei
willasa@163.com

SPECIALTY SECTION
This article was submitted to Nutrition and Food Science Technology, a section of the journal Frontiers in Nutrition

RECEIVED 15 September 2022
ACCEPTED 12 October 2022
PUBLISHED 28 October 2022

CITATION
Zhang Y, Xiao H, Lv X, Wang D, Chen H and Wei F (2022) Comprehensive review of composition distribution and advances in profiling of phenolic compounds in oilseeds. *Front. Nutr.* 9:1044871. doi: 10.3389/fnut.2022.1044871

Comprehensive review of composition distribution and advances in profiling of phenolic compounds in oilseeds

Yao Zhang, Huaming Xiao, Xin Lv, Dan Wang, Hong Chen and Fang Wei*

Key Laboratory of Oilseeds Processing of Ministry of Agriculture, Hubei Key Laboratory of Lipid Chemistry and Nutrition, Oil Crops Research Institute, Chinese Academy of Agricultural Sciences, Wuhan, China

A wide range of phenolic compounds participate in oilseed growth, regulate oxidative stability of corresponding vegetable oil, and serve as important minor food components with health-promoting effects. Composition distribution of phenolic compounds varied in oilseeds. Isoflavones, sinapic acid derivatives, catechin and epicatechin, phenolic alcohols, chlorogenic acid, and lignans were the main phenolic compounds in soybean, rapeseed, peanut skin, olive, sunflower seed, sesame and flaxseed, respectively. Among which, the total isoflavones content in soybean seeds reached from 1,431 to 2,130 mg/100 g; the main phenolic compound in rapeseed was sinapine, representing 70–90%; chlorogenic acid as the predominant phenolic compound in sunflower kernels, represented around 77% of the total phenolic content. With the rapid development of analytical techniques, it is becoming possible for the comprehensive profiling of these phenolic compounds from oilseeds. This review aims to provide recently developments about the composition distribution of phenolic compounds in common oilseeds, advanced technologies for profiling of phenolic compounds by the metabolomics approaches based on mass spectrometry. As there is still limited research focused on the comprehensive extraction and determination of phenolics with different bound-forms, future efforts should take into account the non-targeted, pseudo-targeted, and spatial metabolomic profiling of phenolic compounds, and the construction of phenolic compound database for identifying and quantifying new types of phenolic compounds in oilseeds and their derived products.

KEYWORDS

oilseeds, phenolic compounds, composition distribution, analytical methods, metabolomics

Abbreviations: DESI, desorption electrospray ionization; GC, gas chromatography; HPLC, high-performance liquid chromatography; HRMS, high resolution mass spectrometry; LC, liquid chromatography; MALDI, matrix-assisted laser desorption ionization; MRM, multiple reaction monitoring; MS, mass spectrometry; MS/MS, tandem mass spectrometry; MSI, mass spectrometry imaging; NADES, natural deep eutectic solvent; OPLS-DA, orthogonal partial least square discriminant analysis; PCA, principal component analysis; QqQ, triple quadrupole; QTOF, quadrupole time of flight.

Introduction

Oilseeds normally possess high economic value, thereby the oilseed cultivation area has expanded over 82% and approximately 240% for total world production of oilseeds in the past 30 years (1). Oilseeds are widely used for producing edible oil (2). Edible oil accounts for more than 75% of total lipids consumed and has become an indispensable component in human diet (3, 4). Oilseeds and the derived edible oil are also rich in protein, dietary fiber, phenolic compounds, phytosterols or other functional components (5). Among them, phenolic compounds are one of the most abundant components in oilseeds, and they are also the important material basis for various biological activities of oilseeds (4). Some phenolic compounds as minor food components also have significant effects on human nutrition and health (6).

According to the chemical structures, phenolic compounds are characterized by having at least one benzene ring bearing one or more hydroxyl groups (7). Numerous groups of phenolic compounds have been isolated and identified in oilseeds from small molecules to macromolecules (8, 9). The unique chemical structures endow them with irreplaceable functional activity, such as antioxidant activity, anti-inflammatory, anti-cancer, anti-viral, antimicrobial, hypoglycemic and hypolipidemic effects (2, 4, 9–11). As naturally-occurring antioxidants, phenolic compounds are more acceptable to consumers than synthetic antioxidants for safety concerns (11, 12). Thus, discovery and identification of natural phenolic compounds from oilseeds may provide a new class of nutrients.

Composition of phenolic compounds in different oilseeds is different, resulting in the difference of physiological characters and nutritional value of oilseeds (2). Composition of phenolic compound in oilseeds is influenced by many factors, including crop cultivar, genotype, location, soil type, climate condition, maturity, harvest time, and so on (13–15). Therefore, the study of phenolic compounds in oilseeds can not only provide theoretical support for their potential application as natural antioxidants or material basis of functional foods and nutritional supplements, but also improve the comprehensive utilization value of oilseed products and by-products. To better study the phenolic compounds in oilseeds, it is necessary to summarize the composition distribution and profiling methods of phenolic compounds in oilseeds. However, there are few reviews on the composition distribution of phenolic compounds in different oilseeds. New analytical methods for the profiling of phenolic compounds will help us to understand more comprehensively the distribution of phenolic compounds in oilseeds and the modification and transformation rules of these phytochemicals during various processing and storage, which can provide conclusive evidence for the assessment of maturity of oilseeds, targeted cultivation of nutrient-rich oilseeds, selection of more suitable raw materials for oil industry, and adulteration identification of edible vegetable oil. Therefore, it has attracted our research interest on characterizing the composition distribution of phenolic compounds present in oilseeds. Current review aims to bring new insights into the possible researches for exploring nutritional characteristics of phenolic compounds in oilseeds. To this end, we summarized the composition distribution of phenolic compounds in common oilseeds. It has been also reviewed the recent analytical methods of phenolic compounds, including extraction, identification and quantification methods.

Composition distribution of phenolic compounds in oilseeds

Oilseeds are a group of seeds used to extract oil, including soybean, rapeseed, peanut, olive, sesame, sunflower seed, flaxseed and so on. A full scope of the type and structure of phenolic compounds in oilseeds is of great significance for the evaluation of the nutritional and functional properties of oilseeds. According to the existent form, phenolic compounds can be classified into free, soluble conjugated, and insoluble-bonded forms. As shown in **Figure 1**, free phenolics were presented in red background, while conjugated phenolics in blue background. Insoluble-bonded phenolics are often bound to cell wall substances through covalent linkages (8). Among them, free phenolics can be directly extracted and determined, while conjugated or insoluble-bonded phenolics would be measured as free forms after acidic, alkali or enzymatic hydrolysis (16). These kinds of indirect measurement of the conjugated or bound phenolic compounds may give inaccurate or wrongly levels of them in oilseeds, and thereby lead to the underestimate of their health benefits. However, there are relatively few researches on conjugated or bound phenolic compounds, especially their direct determination method and investigation of their health functions. According to chemical structures, phenolic compounds can also be classified into flavonoids, phenolic acids, phenolic alcohols, stilbenes, lignans, and tannins (**Figure 1**) (4, 11). Herein, composition distribution of phenolic compounds in common oilseeds were reviewed as follows and detail summarized data were shown in **Table 1**.

Soybean

Soybean is a widely consumed food material and one of the largest oilseeds with annual production of around 333.67 million tons in the world (1). Phenolic compounds identified in soybeans are mainly isoflavones (mainly daidzein, glycitein, genistein and their glucosides), phenolic acids (ferulic acid, *p*-coumaric acid, chlorogenic acid, caffeic acid, syringic acid, vanillic acid, salicylic acid, protocatechuic acid, etc.) and anthocyanins (9). These phenolic compounds have been reported with numerous biological activities related to their

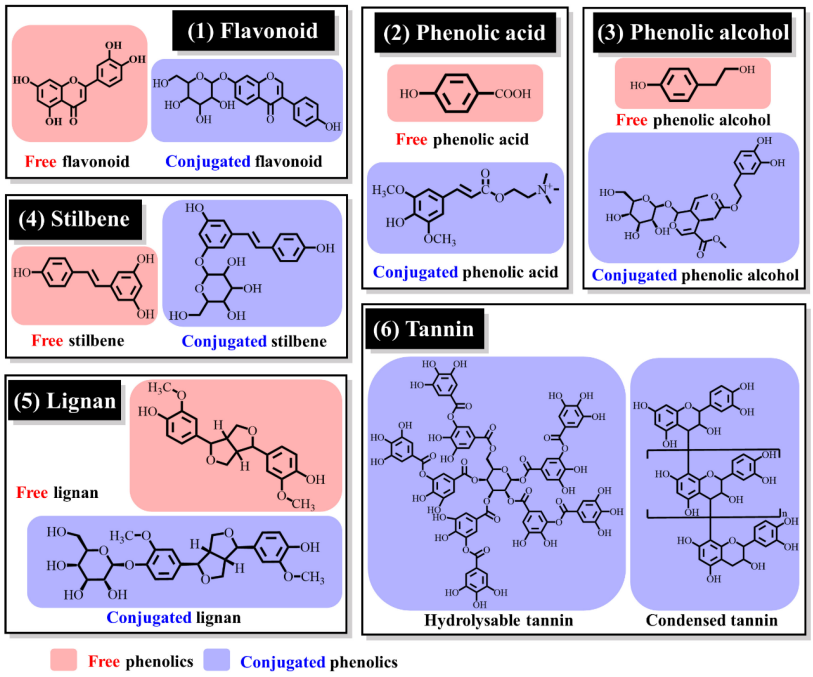

FIGURE 1
Classification and structures of representative phenolic compounds.

antioxidant properties (10). Isoflavones are major phenolic compounds formed during soybean growth with amount in the range of 1,431–2,130 mg/100 g and they are mainly distributed in the cotyledon and hypocotyl of soybean seeds (9). Soybean isoflavone aglycones, including genistein, daidzein, and glycitein, enhance the bioavailability, bioactivity, and nutrient values in comparison with glucosides since the lipid soluble isoflavone aglycones can be better absorbed by the intestinal villi of human body (17). Soybean seed coats and hulls are the primary byproducts during the production of soybean oil or protein. Although the isoflavones contents in seed coats and hulls are very low, studies have shown that they are a potential source of phytochemicals, such as polyphenolics, anthocyanins and proanthocyanidins (18).

Rapeseed

Rapeseed is a major oilseed crop and cash crop in the world with its production increasing faster than that of other oilseeds over the past two decades with approximately 34 million hectares planting area of oilseed rape and over 70 million tons rapeseed yield worldwide (1). Concentrations of free, esterified, and insoluble bound phenolic acids in rapeseed were reported to be in the range of 60–262, 570–1,520, and 0–105 mg/100 g, respectively (2). Sinapine, sinapic acid, and sinapoly glucoside are the most important phenolic compounds in rapeseed. Sinapic acid is a free phenolic acid accounting for 9–16% of the total phenolic acids and more than 70% of the free phenolic acids, which can act as an antioxidant, anticancer, and anti-inflammatory agent (19). Sinapine, the choline ester of sinapic acid, is the predominant esterified phenolic acid in rapeseed produced through phenylalanine or hydroxycinnamate pathway, which contributes to the bitter taste, astringency, and dark color of rapeseed derived products (20). Sinapoyl glucoside was reported to be the second most abundant phenolic compound in rapeseed with the content of 89.7 ± 5.0 mg/100 g (21). Canolol, assumed to be formed by the decarboxylation of sinapic acid, was first identified in rapeseed oil. Canolol showed strong antioxidant properties and involved in many physiological activities, including anti-mutagenic properties and gastric tumor inhibition (19, 22). Moreover, canolol exerts 15% higher antioxidant activity than sinapic acid (23). Other sinapic acid derivatives such as disinapoyl gentiobioside, quercetin-sinapoyl-di-hexosepentose, sinapoyl malate and disinapoyl glucoside were also observed in rapeseed (22). Phenolic acids, such as gallic acid, syringic acid, chlorogenic acid, ferulic acid, vanillic acid, protocatechuic acid, caffeic acid, cinnamic acid, *p*-coumaric acid and *p*-hydroxybenzoic acid also have been found from rapeseed (24). Rapeseed meal, as a low economic value by-product of rapeseed oil production, is unsuitable for human consumption due to the presence of anti-nutritional compounds, including phytic acid, glucosinolates and condensed tannins. These compounds contributed to the

TABLE 1 Composition distribution of phenolic compounds in common oilseeds and their products.

Oilseeds	Distribution	Phenolic compounds	Content (mg/100 g)	References
Soybean	Seed	Stilbene	Resveratrol (49.20 ± 2.74)	(9, 48, 68, 69)
		Free phenolic acid	Gallic acid (1.33 ± 0.08), *p*-hydroxybenzoic acid (1.00 ± 0.06), protocatechuic acid (18.36 ± 1.03), syringic acid (1.77 ± 0.10), *p*-coumaric acid (1.24 ± 0.07), caffeic acid (1.87 ± 0.18), salicylic acid (2.09 ± 0.12), sinapic acid (5.39 ± 0.28), ferulic acids (7.33 ± 0.34), cinnamic acid (1.93 ± 0.21)	
		Conjugated phenolic acid	Chlorogenic acid (6.97 ± 0.39)	
		Free flavonoid	Quercetin (0.51 ± 0.04), kaempferol (0.30 ± 0.04), glycitein (nd–63.82), genistein (268–448), daidzein (173–305), L-epicatechin (3.77 ± 0.26), baicalein (0.08 ± 0.01), morin (5.50 ± 0.44), myricetin (0.83 ± 0.08)	
		Conjugated flavonoid	Rutin (1.40 ± 0.12), genistin (11–26), daidzin (16–30), malonylgenistein (581–796), malonyldaidzein (383–633)	
	Sprout	Free flavonoid	Daidzein (0.45), genistein (0.23)	(70)
		Conjugated flavonoid	Daidzin (0.50), genistin (0.14), malonyldaidzin (1.80), malonylgenistin (0.86 ± 0.01)	
	Embryo	Free phenolic acid	Gallic acid (0.00–0.13), vanillic acid (0.08–0.79), caffeic acid (0.22–4.26), syringic acid (0.00–1.13), ferulic acid (0.05–2.13), *p*–coumaric acid (0.14–1.77), *o*-coumaric acid (0.08–1.67), *t*-cinnamic acid (0.00–0.07)	(71)
		Conjugated phenolic acid	Chlorogenic acid (0.22–9.58)	
		Free flavonoid	Catechin (0.05–1.42), myricetin (0.16–4.14), quercetin (0.04–0.50), naringenin (0.00–2.69), kaempferol (0.00–0.13), hesperetin (0.00–0.15)	
		Conjugated flavonoid	Rutin (0.29–9.25), naringin (0.02–0.93), hesperidin (0.06–1.45)	
	Cotyledon	Free phenolic acid	Gallic acid (0.00–0.09), vanillic acid (0.01–0.22), caffeic acid (0.01–0.18), syringic acid (0.00–0.29), *p*-coumaric acid (0.01–0.26), *o*-coumaric acid (0.01–0.44), *t*-cinnamic acid (0.01–0.14), ferulic acid (0.06–0.71)	(71)
		Conjugated phenolic acid	Chlorogenic acid (0.00–2.10)	
		Free flavonoid	Catechin (0.04–0.55), myricetin (0.04–3.33), quercetin (0.03–1.76), naringenin (0.06–0.65), kaempferol (0.00–0.44), hesperetin (0.01–0.06)	
		Conjugated flavonoid	Rutin (0.04–0.56), naringin (0.07–0.76), hesperidin (0.06–0.57)	
	Coat	Free phenolic acid	Gallic acid (0.05–0.70), vanillic acid (0.01–5.34), caffeic acid (0.05–5.92), syringic acid (0.01–79.11), *p*-coumaric acid (0.01–2.91), *o*-coumaric acid (0.01–3.13), *t*-cinnamic acid (0.00–0.59), ferulic acid (0.02–22.21)	(71)
		Conjugated phenolic acid	Chlorogenic acid (0.29–51.62)	
		Free flavonoid	Catechin (0.72–25.75), myricetin (0.09–4.52), quercetin (0.00–8.65), naringenin (0.02–0.76), kaempferol (0.01–0.62), hesperetin (0.00–0.24)	
		Conjugated flavonoid	Rutin (0.01–27.13), naringin (0.09–9.10), hesperidin (0.02–7.04)	
Rapeseed	Seed	Simple phenol	Canolol (1.82 ± 0.16)	(21, 24, 72)
		Free phenolic acid	Caffeic acid (10.26 ± 0.59), ferulic acid (2.17 ± 0.09), sinapic acid (26.2 ± 1.1)	
		Conjugated phenolic acid	Sinapine (757 ± 24), sinapoyl glucose (89.7 ± 5.0), quercetin-sinapoyl-di-hexosepentose (32.0 ± 1.4), sinapoyl malate (86.9 ± 2.0), disinapoyl gentiobioside (74.6 ± 1.6), sinapoylcholine thiocyanate-glucoside (42.1 ± 0.7)	
	Hull	Free phenolic acid	Sinapic acid (4.32 ± 0.43)	(21)
		Conjugated phenolic acid	Sinapine (38.1 ± 0.1), sinapoyl glucose (9.32 ± 0.38), quercetin-sinapoyl-di-hexosepentose (7.92 ± 0.42), sinapoyl malate (52.3 ± 0.3), disinapoyl gentiobioside (14.6 ± 0.3), sinapoylcholine thiocyanate-glucoside (8.36 ± 0.23)	
	Cotyledon	Free phenolic acid	Sinapic acid (42.9 ± 1.3)	(21)
		Conjugated phenolic acid	Sinapine (839 ± 29), sinapoyl glucose (105 ± 0), quercetin-sinapoyl-di-hexosepentose (35.1 ± 0.3), sinapoyl malate (89.1 ± 0.9), disinapoyl gentiobioside (68.5 ± 1.5), sinapoylcholine thiocyanate-glucoside (34.3 ± 0.2)	

(Continued)

TABLE 1 (Continued)

Oilseeds	Distribution	Phenolic compounds	Content (mg/100 g)	References
	Endosperm	Free phenolic acid	Sinapic acid (25.5 ± 0.1)	(21)
		Conjugated phenolic acid	Sinapine (919 ± 3), sinapoyl glucose (12.7 ± 0.5), sinapoyl malate (38.2 ± 2.1), disinapoyl gentiobioside (114 ± 1), sinapoylcholine thiocyanate-glucoside (84.2 ± 0.4)	
	Meal	Simple phenol	Canolol (1.22 ± 0.11)	(72, 73)
		Free phenolic acid	Sinapic acid (35.09–174.59), *p*-coumaric acid (nd–2.08), syringic acid (0.12–4.64), gallic acid (4.38–7.12), caffeic acid (nd–10.21), ferulic acid (nd–6.51)	
		Conjugated phenolic acid	Sinapine (2066.30–3213.62), sinapoyl glucoside (105.16–598.75), disinapoyl gentiobiose (34.49–261.71)	
	Oil	Simple phenol	Canolol (2.59–35.03)	(74)
		Free phenolic acid	Sinapic acid (0.31–0.82), *p*-hydroxybenzoic acid (nd–0.01), syringic acid (0.02–0.04), *p*-coumaric acid (0.01), ferulic acid (0.05–0.10), cinnamic acid (0.01–0.02)	
		Conjugated phenolic acid	Sinapine (0.00–0.12)	
Peanut	Seed	Free phenolic acid	Gallic acid (nd–0.05), 2,5–dihydroxybenzoic acid (0.05–0.10), 2,6-dihydroxybenzoic acid (0.05–0.11), caffeic acid (0.06–0.18), ferulic acid (0.09–0.20), sinapic acid (0.05–0.07), vanillic acid (0.08–0.14), protocatechuic acid (nd–0.06), *p*-coumaric acid (0.23–1.88), *m*-coumaric acid (0.61–1.77), *o*-coumaric acid (0.12–0.32)	(75)
		Free flavonoid	Isorhamnetin (0.04–0.08), rhamnazin (nd–0.05), quercetin (0.05–0.12), catechin (0.08–1.53)	
		Conjugated flavonoid	Eriocitrin (nd–0.17), rutin (0.16–1.67), astragalin (0.05–0.08), manniflavanone (0.05–0.07), isoquercetin (nd–0.21)	
	Skin	Stilbene	Resveratrol (0.36 ± 0.05)	(8, 76)
		Free phenolic acid	Protocatechuic acid (10.21 ± 0.01), *p*-hydroxybenzoic acid (1.03 ± 0.06), caftaric acid (1.51 ± 0.12), *c*-coutaric acid (2.37 ± 0.02), *t*-coutaric acid (4.96 ± 0.35), *p*-coumaric acid (0.53 ± 0.06), chicoric acid (3.44 ± 0.12), chicoric acid (3.12 ± 0.13)	
		Free flavonoid	Quercetin (2.11 ± 0.27), isorhamnetin (1.51 ± 0.02), diosmetin (0.40 ± 0.01), catechin (45.47 ± 0.04), epicatechin (33.66 ± 0.76)	
	Kernel	Stilbene	Resveratrol (0.07 ± 0.01)	(77)
		Free phenolic acid	Gallic acid (0.12 ± 0.01), protocatechuic acid (1.36 ± 0.07), *p*-hydroxybenzoic acid (4.80 ± 0.12), vanillic acid (6.92 ± 0.26), *p*-coumaric acid (3.15 ± 0.10), caffeic acid (0.09 ± 0.02), syringic acid (0.14 ± 0.01), ferulic acid (4.79 ± 0.12), *p*-coumaric acid (0.04 ± 0.01), cinnamic acid (5.77 ± 0.14)	
		Free flavonoid	Quercetin (1.57 ± 0.06)	
		Conjugated phenolic acid	Chlorogenic acid (0.32 ± 0.05)	
	Sprout	Stilbene	Resveratrol (0.03 ± 0.01)	(77)
		Free phenolic acid	Gallic acid (0.08 ± 0.01), protocatechuic acid (0.76 ± 0.12), *p*-hydroxybenzoic acid (3.18 ± 0.13), vanillic acid (4.28 ± 0.16), *p*-coumaric acid (1.96 ± 0.13), caffeic acid (0.04 ± 0.00), syringic acid (0.04 ± 0.01), ferulic acid (3.16 ± 0.13), *p*-coumaric acid (0.02 ± 0.00), cinnamic acid (4.39 ± 0.10)	
		Free flavonoid	Quercetin (0.79 ± 0.04)	
		Conjugated phenolic acid	Chlorogenic acid (0.11 ± 0.01)	
	Meal	Free phenolic acid	Ferulic acid (1.14 ± 0.05), *p*-coumaric acid (1.19 ± 0.01), *c*-coutaric acid (5.37 ± 0.04), *t*-coutaric acid (2.44 ± 0.14), ellagic acid (1.96 ± 0.15)	(76)
Olive	Fruit	Free phenolic acid	*p*-Coumaric acid (0.04–1.30), gallic acid (2.09–35.85), ferulic acid (0.13–13.18), caffeic acid (0.43–14.03), syringic acid (0.47–20.74), *t*-cinnamic acid (0.04–4.44), 3,4–dihydroxybenzoic acid (1.58–33.11), 1,2-dihydroxybenzene acid (1.87–75.47)	(78, 79)
		Free phenolic alcohol	Tyrosol (1.16–15.20), hydroxytyrosol (0.99–37.40)	
		Free flavonoid	Kaempherol (0.64–18.11), isorhamnetin (1.02–9.48), quercetin (0.40–11.74), catechin (3.08–52.45)	

(Continued)

TABLE 1 (Continued)

Oilseeds	Distribution	Phenolic compounds	Content (mg/100 g)	References
		Conjugated phenolic alcohol	Oleuropein (nd–379), verbascoside (4.35–253.10)	
		Conjugated flavonoid	Naringenin (0.30–7.14), apigenin 7 glycoside (0.32–9.30)	
	Virgin olive oil	Simple phenol	Vanillin (0.08–0.10)	(80)
		Lignan	Pinoresinol (0.34–0.42), acetoxypinoresinol (1.79–1.97)	
		Free phenolic acid	Vanillic acid (0.02–0.03), *p*-coumaric acid (0.24–0.27)	
		Free phenolic alcohol	Tyrosol (0.91–1.94), hydroxytyrosol (0.82–1.39)	
		Free flavonoid	Luteolin (0.19–0.25), apigenin (0.04–0.10)	
		Conjugated phenolic alcohol	Hydroxytyrosol acetate (0.14–0.50)	
	Extra virgin olive oil	Lignan	Pinoresinol (0.01–0.02), acetoxypinoresinol (0.43–1.15)	(81)
		Free phenolic acid	*p*-Hydroxybenzoic acid (0.05–0.09), 3-hydroxybenzoic acid (0.03–0.12), vanillic acid (0.27–1.32), *p*-coumaric acid (0.14–0.46), cinnamic acid (0.03–0.05), ferulic acid (0.01–0.02)	
		Free phenolic alcohol	Tyrosol (10.59–45.06), hydroxytyrosol (15.27–59.51)	
		Free flavonoid	Luteolin (0.32–1.02), apigenin (0.02–0.03)	
	Pomace	Simple phenol	Vanillin (nd–7.40)	(82)
		Free phenolic acid	Caffeic acid (nd–9.70)	
		Free phenolic alcohol	Tyrosol (nd–13.30)	
		Free flavonoid	Apigenin (nd–2.00)	
		Conjugated flavonoid	Rutin (1.60–20.40), ligstroside (nd–16.20)	
Sesame	Seed	Stilbene	Resveratrol (0.07 ± 0.01)	(35–37, 42)
		Lignan	Sesamin (111–941), sesamolin (20–335), sesamol (nd–15), sesaminol (2.67 ± 0.09), sesamolinol (1.48 ± 0.06), syringaresinol (0.47 ± 0.18), pinoresinol (1.75 ± 0.01), secoisolariciresinol (0.02 ± 0.01), medioresinol (0.76 ± 0.09)	
		Free phenolic acid	*p*-Hydroxybenzoic acid (0.61–8.53), syringic acid (8.40 ± 0.29), caffeic acid (0.42–1.56), *p*-coumaric acid (nd–3.60), ferulic acid (nd–18.79), gallic acid (102.20 ± 4.37), 3,4-dihydroxybenzoic acid (23.27 ± 1.05), 1,2-dihydroxybenzene acid (98.09 ± 3.63), *t*-cinnamic acid (0.05 ± 0.01), protocatechuic acid (0.17–19.91)	
		Free flavonoid	Quercetin (1.78–18.15), kaempferol (0.96 ± 0.19), isorhamnetin (2.88 ± 0.45), catechin (61.96 ± 1.28)	
		Conjugated phenolic acid	Chlorogenic acid (nd–7.77)	
	Oil	Lignan	Sesamol (nd–31), sesamin (207–751), sesamolin (29–398)	(37, 83)
		Free phenolic acid	Hydroxybenzoic acid (0.77 ± 0.01), quinic acid (0.18 ± 0.01), protocatechuic acid (0.36 ± 0.02), syringic acid (0.43 ± 0.02)	
Sunflower seed	Seed	Lignan	Sesamin (0.84 ± 0.02), sesaminol (0.04 ± 0.02), sesamol (3.85 ± 0.63), sesamolinol (0.38 ± 0.09), syringaresinol (0.58 ± 0.07), conidendrin (0.02), dimethylmatairesinol (0.15), lariciresinol (0.16 ± 0.01), medioresinol (0.05 ± 0.01), pinoresinol (0.01), secoisolariciresinol (0.03 ± 0.01)	(42)
	Kernel	Free phenolic acid	Caffeic acid (19.20–26.70), ferulic acid (7.20–91.50)	(40)
		Conjugated phenolic acid	Chlorogenic acid (1945.70–3050.50), caffeoylquinic acid (36.50–51.40)	
	Shell	Free phenolic acid	Caffeic acid (0.50–1.00), ferulic acid (0.30–1.00)	(40)
		Conjugated phenolic acid	Chlorogenic acid (26.60–59.10), caffeoylquinic acid (1.50–4.80)	
	Oil	Conjugated phenolic acid	Chlorogenic acid (20–320)	(84)
Flaxseed	Seed	Lignan	Sesamin (0.59 ± 0.01), sesaminol (0.17 ± 0.01), sesamol (4.73 ± 1.04), sesamolinol (0.12), syringaresinol (0.22 ± 0.01), conidendrin (0.01), dimethylmatairesinol (0.06 ± 0.02), lariciresinol (0.34 ± 0.13), medioresinol (0.01), pinoresinol (0.05 ± 0.01), secoisolariciresinol (0.02)	(42)
	Capsule	Lignan	Secoisolarisiresinol diglucoside (22.61–758.90), secoisolarisiresinol glucoside (4.29–33.60)	(43)

(Continued)

TABLE 1 (Continued)

Oilseeds	Distribution	Phenolic compounds	Content (mg/100 g)	References
		Free phenolic acid	Caffeic acid (10.50–81.53), *p*-coumaric acid (17.48–74.11), ferulic acid (18.00–47.91)	
		Free phenolic alcohol	Coniferyl alcohol (7.51–39.89)	
		Conjugated phenolic acid	Chlorogenic acid (2.23–24.82)	
	Oil	Lignan	Diphyllin (0.003–0.004), pinoresinol (0.004–0.005), matairesinol (0.003), secoisolariciresinol (0.003)	(45)
		Simple phenol	Vanillin (0.01–0.02)	
		Free phenolic acid	Vanillic acid (0.002–0.004), ferulic acid (0.001), *p*-Hydroxybenzoic acid (0.002–0.003)	

nd, not detected.

low bioavailability, low digestibility, and unpleasant flavor of rapeseeds. While phytic acid, glucosinolates and condensed tannins were reported with good pharmacological activity in anti-cancer and anti-oxidation (25–27). Moreover, rapeseed meal is a good source of phenolic compounds since a large proportion of phenolics were remained in meal after oil extracting (20). We noticed that thousands of metric tons of rapeseed by-products were produced every year in oil industry. These rapeseed by-products could be recycled as invaluable sources of potential nutraceuticals and natural antioxidants.

Peanut

Peanut is a critical oilseed crop widely cultivated in many countries and it is an important food material consumed worldwide (28). The content of soluble phenolic compounds, insoluble phenolic compounds, soluble flavonoids, and total anthocyanin in peanuts ranged from 706 to 1,458, from 1,071 to 1,262, from 58 to 133, and from 3.36 to 11.49 mg/100 g, respectively (29). Although peanut skin accounts for only a small portion of peanut fruit, it was discarded 7.5×10^5 tons a year as a by-product (28). Peanut skin has high antioxidant activity for its abundant phenolic compounds, such as phenolic acids, stilbenes, flavonoids, anthocyanins and procyanidins, thereby it can be used as natural antioxidant with a wide range of clinical applications (8, 28). Furthermore, peanut shells, as the by-product of peanut industry, contain polyphenols, flavonoids, luteolin and functional compounds for human consumption (30). The abundance of luteolin in peanut shells has attracted the attention of some researchers and it has been reported with a variety of biological functions such as antioxidant, anti-inflammatory, anti-depression, anti-convulsion, anti-anxiety, anti-allergy, antimicrobial, immunity improvement and anticancer effects (31). However, the byproducts of peanut industry, including peanut skin and shell, have not been well utilized. It still requires more researches on the profiling of bioactive phenolic compounds in peanut. Thereby we can better explore their economic values as food additives, medical and health products, and other industrial supplies for the prosperity and stable development of peanut industry.

Olive

Olive has long been considered as important health foods in both the West and the East. Various kinds of phenolic compounds can be observed in olives, including phenolic acids, phenolic alcohols, flavonoids, and lignans. Among them, oleuropein, ligstroside, demethyloleuropein, verbascoside, tyrosol and hydroxytyrosol are the major phenolic components in olive fruits (32). They are responsible for several biological properties, including antioxidant, anti-inflammatory, antimicrobial, antiviral, anti-carcinogenic, and cardiovascular protection effects (33). Among them, oleuropein is the most representative polyphenolic constituent in olive, responsible for the bitterness of both olive fruits and olive oil. The predominant phenolic compounds found in olive oil are oleuropein and its hydrolytic products, hydroxytyrosol, and tyrosol. Hydroxytyrosol has a strong antioxidant effect and the addition of hydroxytyrosol to olive oil can decrease oxidation progress of the oil (33). Olive pomace, the solid waste of olive oil industry, is an interesting source of phenolic compounds, since only 1–2% of the total content of phenolic compounds of olives went into olive oil through its extraction process, while 98% of them remained in the olive pomace, making it a valuable candidate for bio-functional and value-added applications (12).

Sesame

Sesame (*Sesamum indicum* L.) is a member of the Pedaliaceae plant family (14). It is an oilseed widely distributed in the world with around 6.55 million tons production all over the world, with approximately 96% of its production occurs in Africa and Asia, the remaining 4% occurs in the Americas and Europe (34). In recent years, sesame has

received increasing attention due to its high content of phenolic compounds including phenolic acids (ferulic acid, *p*-hydroxybenzoic acid and *p*-coumaric acid, among others), flavonoids, and lignans (35, 36). These phenolic compounds are momentous natural antioxidants and radical scavengers in various physiological activities, such as antihypertensive, hepatoprotective, and antimutagenic effects (14). Lignan is one of the largest groups of phenolics in sesame, with contents in sesame seed and oil range from 252 to 1,276 and 338 to 1,153 mg/100 g, respectively. Common sesame lignans consist of sesamin, sesamolin, sesamol, pinoresinol, and other lignan glycosides (35, 37). Shi et al. found that black sesame seeds showed higher sesamin (198–941 mg/100 g) and sesamolin content (106–335 mg/100 g) than other sesame cultivars (37). Consumption of sesame is beneficial to human health due to the protective effects of theses phenolic compounds against numerous chronic diseases (38). In addition, sesame seed cake also possess amounts of phenolic compounds, among which phenolic acids and lignans are the most concerned components associated with antioxidant properties.

Sunflower seed

Sunflower is a globally important oilseed crop and ornamental crop with its seed oil accounts for approximately 10% of the world's edible plant-derived oil (39). World production of sunflower seeds was around 56.07 million tons in recent years with Russian as main producer followed by Ukraine, Argentina, Romania, and China (1). Sunflower seeds are an important source of vegetable oil and high-quality protein, but also contain considerable amounts of phenolic constituents. The total phenolic content of sunflower kernels and shells are reported to be in the range of 2,938.8 to 4,175.9 and 40.8 to 86.0 mg/100 g, respectively. And chlorogenic acid was reported to be the predominant phenolic acid in sunflower kernels, along with much lower levels of caffeic acid and quinic acid, varying with the location of seed on sunflower head, storage temperature and variety (40). After oil extraction, sunflower seed meal is a major source of protein used for animal nutrition. However, high amounts of phenolic compounds, particularly chlorogenic acids, remained in sunflower seed meal, causing a great waste of resources (41). Therefore, sunflower seed by-products also are a good source of phenolic compounds and require further exploration and utilization.

Flaxseed

Flaxseed has been cultivated over 5,000 years as an oilseed crop with around 3.07 million tons production worldwide for the past few years (1). Flaxseed is a good source of lignans with content of 386.0–593.5 mg/100 g. The most abundant lignan is secoisolariciresinol diglucoside, while other lignans, such as the isomer of secoisolariciresinol diglucoside, secosisolariciresinol, matairesinol, pinoresinol, pinoresinol diglucoside, lariciresinol, and isolariciresinol, present in relatively low level in flaxseed (42, 43). As the precursors of enterodiol and enterolactone, secoisolariciresinol diglucoside and matairesinol are considered to have phyto-estrogenic effects. In dehulled and defatted flaxseed, ferulic acid and *t*-cinnamic acid were reported to be the major phenolic acids, while relative trace level of *p*-coumaric acid, caffeic acid, chlorogenic acid, gallic acid, protocatechuic acid, sinapic acid and *p*-hydroxybenzoic acid were also observed (44). In flaxseed oil, Herchi et al. reported the detection of secoisolariciresnol, coumaric acid methyl ester, ferulic acid and its methyl ester, pinoresinol, matairesinol, diphyllin, *p*-hydroxybenzoic acid, vanillic acid and vanillin (45). In flaxseed capsules, abundant phenolic compounds, including coniferyl alcohol, glucoside of secoisolarisiresinol, chlorogenic acid, *p*-coumaric acid, caffeic acid, and ferulic acid were also found (43). However, the functional characteristic of phenolic compounds in flaxseed is still unclear and needs to be further explored.

Others

Other oilseeds such as castor seed, perilla seed, camellia seed, oil palm, walnut, and cottonseed all contain various phenolic compounds. Phytochemical analysis by Shafiq et al. confirmed the presence of phenolic compounds making the castor (*Ricinus communis*) a pharmaceutical source (46). Hong et al. profiled polyphenols in different varieties of *Camellia oleifera* seed cakes. A total of 73 unequivocal or tentative phenolic compounds were identified from methanol extracts of camellia seed cake (47). For the phenolic compounds in walnut, Wu et al. found that the majority of walnut phenolics were presented in the free form (51.1–68.1%), followed by bound form (21.0–38.0%), and esterified form (9.7–18.7%) (16). It differed the composition of phenolic compounds in different oilseeds, and distinctive phenolic compounds presented in individual tissues of the same oilseeds. Therefore, profiling of phenolic compounds in oilseeds is of great significance to the breeding of high-quality oilseeds and the comprehensive utilization of phenolic compounds.

Profiling of phenolic compounds in oilseeds

Extraction methods for phenolic compounds

Extraction methods have significant impacts on the extraction efficiency of free, soluble conjugated, and insoluble-bonded phenolic compounds from complex matrices of

oilseeds. In previous reported publications, various kinds of organic solvents (such as methanol, ethanol, ethyl acetate, and acetone) and extraction methods, including Soxhlet extraction, liquid-liquid extraction, solid-liquid extraction, ultrasound or microwave or enzyme-assisted extraction, solid phase extraction, dispersive solid-phase extraction, magnetic solid-phase extraction, subcritical fluid extraction, pulsed electric fields extraction, pressurized solvent extraction, homogenate assisted extraction, and high hydrostatic pressure assisted extraction have been utilized (4, 48, 49). Although most of these methodologies have high extraction performance, it should be noted that several factors in these techniques may limit their application in the extraction of phenolic compounds from oilseeds, including the solvent toxicity, thermal instability, polarity range, solubility, selectivity, and the use of high-cost equipment (4, 11, 12). Nowadays, a new generation of solvent called natural deep eutectic solvent (NADES) has been proposed for the extraction of phenolic compounds from plant sources, which is a eutectic mixture mixed by hydrogen bond acceptor and hydrogen bond donor (12). NADES has a set of advantageous properties, such as low volatility, non-flammability, chemical and thermal stability, adjustable ability, low toxicity, and high solubility (49). NADES was demonstrated to be a desirable extraction medium for phenolic compounds from three aspects: (1) it can replace organic solvent and dissolve a wide range of compounds; (2) it can form hydrogen bonds with phenolic compounds, improving their dissolution and extraction ability; (3) it offers enhanced extraction efficiency under the premise of environmentally friendly and green extraction (49). In addition, the combining of NADES and assisted extraction method can also result in increased extraction efficiency. Chanioti et al. compared extraction with various types of solvents and different innovative assisted extraction methods such as ultrasound, microwave, homogenization, and high hydrostatic. Results showed that the best extraction efficiency of phenolic compounds from olive pomace was achieved by using NADES as extraction solvent, and homogenization assisted extraction as extraction method (12).

TABLE 2 Extraction and analytical methods of phenolic compounds in oilseeds and their products.

Source	Phenolic compounds	Extraction method	Determination method	References
Sesame, peanut, rapeseed meal	TPC, TFC, TTC	UAE, SLE (acetone, ethanol, methanol)	Spectrophotometer	(35, 73, 85)
Sesame, sunflower meal, flaxseed capsule, rapeseed, rapeseed meal and rapeseed oil	Phenolic compounds, lignans	UAE, SLE, LLE (acetone distilled water, methanol)	HPLC-PDA, UPLC	(19, 35, 43, 86)
Virgin olive oil, rapeseed, walnut kernel, rapeseed oil	Phenolic compounds	LLME, LLE, SLE, SPE, QuEChERS (methanol, ethyl acetate)	UHPLC-ESI-MS/MS, LC-MS/MS, UPLC-MS/MS	(4, 6, 16, 53, 56, 74)
Sesame	Phenolic compounds	SLE (methanol)	HPLC-QqQ-MS/MS	(57)
Rapeseed and rapeseed oil, soybean, peanut, olive mill pomace and wastewater	Phenolic compounds, isoflavone aglycones	SLE, LLE, Microwave-assisted acid hydrolysis (methanol, ethanol, ethyl acetate)	UPLC-ESI-QTOF-MS/MS, UHPLC-ESI-QTOF-MS/MS, UPLC-QTOF-MS, HPLC-ESI-QTOF-MS	(22, 48, 82, 85)
Soybean seed coat, peanut	Phenolic compounds	Soxhlet extraction, UAE (ethanol, acetone)	HPLC-Q-Orbitrap-MS/MS, LC-ESI-Orbitrap-MS	(18, 75)
Peanut by-product	Phenolic acids and flavonoids	SLE (acetone)	HPLC-ESI-MS^n	(76)
Peanut shell	Luteolin	d-$Ti_3C_2T_x$/MWCNTs	Electrochemical sensing platform	(31)

TPC, total phenolic content; TFC, total flavonoid content; TTC, total tannin content; UAE, Ultrasound-assisted extraction; SLE, solid-liquid extraction; LLE, liquid-liquid extraction; LLME, liquid-liquid micro extraction; SPE, solid-phase extraction; QuEChERS, Quick-Easy-Cheap-Effective-Rugged-Safe method; d-$Ti_3C_2T_x$/MWCNTs, titanium carbide/multi-walled carbon nanotubes; HPLC-PDA, high-performance liquid chromatography-photodiode array; UPLC, ultra-performance liquid chromatography; UHPLC-ESI-MS/MS, ultrahigh pressure liquid chromatography-electrospray ionization-tandem mass spectrometry; LC-MS/MS, liquid chromatography-tandem mass spectrometry; UPLC-MS/MS, ultra-performance liquid chromatography-tandem mass spectrometry; HPLC-QqQ-MS/MS, high-performance liquid chromatography-triple quadrupole-tandem mass spectrometry; UPLC-ESI-QTOF-MS/MS, ultra-performance liquid chromatography-electrospray ionization-quadrupole time of flight-tandem mass spectrometry; UHPLC-ESI-QTOF-MS/MS, ultrahigh pressure liquid chromatography-electrospray ionization-quadrupole time of flight-tandem mass spectrometry; UPLC-QTOF-MS, ultra-performance liquid chromatography-quadrupole time of flight-mass spectrometry; HPLC-ESI-QTOF-MS, high-performance liquid chromatography-electrospray ionization-quadrupole time of flight-mass spectrometry; HPLC-Q-Orbitrap-MS/MS, high-performance liquid chromatography-quadrupole-orbitrap-tandem mass spectrometry; LC-ESI-Orbitrap-MS, liquid chromatography-electrospray ionization-orbitrap-mass spectrometry; HPLC-ESI-MS^n, high-performance liquid chromatography-electrospray ionization-multistage mass spectrometry.

In addition, free phenolic compounds can be directly extracted by organic solvents such as methanol and acetone, while conjugated or bound phenolic compounds would be extracted after acidic, alkali or enzymatic hydrolysis (16). There is little research on the direct extraction method of bound phenolic compounds. Thus, the method of simultaneous extraction of free, conjugated and bound phenolic compounds needs to be further studied. The recent reported extraction and analytical methods of phenolic compounds in oilseeds were summarized in **Table 2**.

Metabolomic methods for phenolic compounds

Various analytical methods have been reported for the profiling of phenolic compounds. The total phenolic, flavonoid, tannin and lignan content were often measured by spectroscopic analysis (35). Although these spectroscopic methods are simple and convenient, they cannot separate the phenolic compounds individually (11). Chromatographic methods including gas chromatography (GC) and liquid chromatography (LC) have the advantages of high sensitivity and separation effects. GC based method is rarely used for the determination of phenolic compounds, since the phenolic compounds are of low volatility, and the high temperature during derivatization lead to oxidation of phenolic compounds (50). LC method can realize qualitative and quantitative analysis of phenolic compounds without derivatization step. The limited number of chemical standards restricted LC method to identify unknown phenolic compounds in oilseeds (51). Nuclear magnetic resonance can do non-invasive analysis and enables better metabolite annotation. However, its application was limited by the sensitivity (52). For the past few years, mass spectrometry (MS) with the merits of high sensitivity, high selectivity, and high throughput has developed rapidly for the determination and identification of metabolites from complex matrices in metabolomics. MS based metabolomics has gradually stood out in the profiling of phenolic compounds from oilseeds (53, 54). Metabolomic methods for phenolic compounds profiling can be further divided into untargeted, targeted, pseudo-targeted and spatial metabolomics.

Untargeted metabolomics for phenolic compounds

Untargeted metabolomic analysis can provide global analysis of phenolic compounds in oilseeds, which allows the profiling of hundreds of phenolic related compounds in a single run. Nowadays, high-resolution mass spectrometers (HRMS), including quadrupole time of flight (QTOF) MS, Orbitrap MS, Fourier transform ion cyclotron resonance MS, have gained wide acceptance in untargeted metabolomics for better performance in collection of full-scan spectra with high resolution mass to charge ratios (51, 54). Full scan acquisition mode of HRMS can provide abundant information and retrospective analysis. Tandem mass spectrometry (MS/MS) mode, such as parallel reaction monitoring, data-dependent acquisition, data-independent acquisition, and data-independent all ion fragmentation modes, is applied for structure elucidation and quantification of phenolic compounds (54). For example, Ma et al. reported the application of high-performance liquid chromatography (HPLC)-electrospray ionization-MS^n to separate and identify the phenolic constituents in peanut skins. By this method, phenolic compounds, including proanthocyanidins, phenolic acids, stilbenes, and flavonoids, could be found from peanut skins (8). Negro et al. reported a HPLC-QTOF-MS based untargeted metabolomic method for profiling of phenolic compounds from eight different extra virgin olive oils (55). Król-Grzymała and Amarowicz compared the phenolic compounds composition of six soybean cultivars from two European countries by HPLC-QTOF-MS. They found that the established method can be employed in the selection of soybean cultivars with higher levels of phenolics (9). Despite the high coverage of untargeted metabolomic methods, they still need some developments in the following aspects, including (a) unsatisfactory reproducibility and low selectivity; (b) compound identification for the huge structural diversity of phenolic compounds; (c) quantitative accuracy for the wide content variation of phenolic compounds in oilseeds (54).

Targeted metabolomics for phenolic compounds

Targeted metabolomic methods are usually used for identification and absolute quantitation of phenolic compounds of interest. Normally, multiple reaction monitoring (MRM) mode in triple quadrupole (QqQ) MS is the most frequently used strategy in targeted metabolomic profiling with high sensitivity, high specificity, and excellent quantification ability (54). MRM mode selectively monitor compounds using the MRM transitions with both precursor ion and product ion from their MS/MS analysis. Becerra-Herrera et al. developed an efficient method to determinate 28 phenolic compounds from olive oil by dynamic MRM mode in QqQ-MS (56). Wang et al. developed a simultaneous quantification method for 13 trace and micro phenolic compounds from rapeseed (6). Miho et al. performed targeted metabolomic profiling of phenolics from virgin olive oils of 44 olive cultivars, and the results indicated that the method supports the phenolic profile as a criterion to be considered in olive breeding programs (53). In addition, Yu et al. developed a rapid and accurate method for the simultaneous analysis of phenolic compounds in rapeseed oils by mixed-mode solid-phase extraction coupled with chemical labeling assisted LC-MS (4). Nonetheless, the targets are still limited to the known metabolites and are powerless for the unknown metabolites (51). Therefore, other

methods should be re-developed for those unknown and commercial unavailable phenolic compounds. Besides, it is often economically impractical to obtain all of standards to achieve global profiling of phenolic compounds in oilseeds by targeted metabolomic method.

Pseudo-targeted metabolomics for phenolic compounds

To establish a high-coverage, high-throughput, sensitive, selective method for quantification of phenolics in oilseeds, a new strategy named pseudo-targeted or widely targeted metabolomics has been proposed. This strategy can simultaneously monitor hundreds to thousands of metabolites by dynamic MRM mode. Pseudo-targeted method merged the advantages of untargeted and targeted metabolomics and can provide high-quality and rich-information data for the analysis of large-scale samples (57). During pseudo-targeted metabolomic analysis, exact mass, and MS/MS information of compound can be obtained from untargeted profiling at the first step, ensuring high coverage of the compounds. Then targeted method in MRM mode is used to perform high specific analysis and guarantee high quality data collection. Pseudo-targeted methods have a far-ranging application in phenolic compound discovery and determination studies. For instance, Peng et al. identified or tentatively characterized a total of 112 extractable phenolic compounds and 78 non-extractable bound phenolic compounds from black soybeans by pseudo-targeted LC-MS method (58). Wang et al. used widely targeted metabolomics for determination of different metabolites including phenolic compounds from black and white sesame seeds, which can give directions for the genomic breeding of sesame and provides important insight for the innovation of high-quality black sesame varieties (57). In summary, pseudo-targeted metabolomics can realize both qualitative and quantitative analysis with high coverage and high performance. It was the most useful semiquantitative method for discovery new phenolic compounds. However, it also has some drawbacks: (a) the MRM transitions were obtained from biological samples rather than standards; (b) structural identification and data processing procedure should be more automated and convenient.

Spatial metabolomics for phenolic compounds

Imaging the spatial distributions and dynamics of phenolic compounds in oilseeds is significant for our understanding of oilseed metabolism. Mass spectrometry imaging (MSI) is a sensitive and label-free approach for the localization of the metabolites in biological samples (59, 60). MSI can provide qualitative, quantitative and positioning information of the analytes in a single experiment (59). According to the desorption/ionization techniques, MSI can be divided into matrix-assisted laser desorption/ionization (MALDI)-MSI, desorption electrospray ionization (DESI)-MSI, and secondary ion (SI)-MSI (60). Among which, MALDI-MSI, as one of the main platforms for metabolite analysis, can offer a decent spatial resolution of imaging and a wide detectable mass range with the soft ionization type (60). Up to date, MALDI-MSI has been successfully applied to plant biology exploration, including (a) imaging the spatial distributions of plant secondary metabolites; (b) unraveling the complex defense mechanisms of plants; (c) visualizing the biosynthetic and metabolic pathways of plant metabolites. For example, Enomoto and Nirasawa reported the application of MALDI-MSI to investigate the localization of flavan-3-ols in peanut testa. Results showed that flavan-3-ols were primary localized in the outer epidermis of peanut testa, which may contribute to the improvement of the extraction and purification efficiencies of flavan-3-ols from peanut testa (61). DESI-MSI showed potential in discovering and guiding investigations into new metabolic routes in plant tissue. Bhandari et al. investigated the changes of metabolite patterns during development of oilseed rape by MSI experiments. Results showed that the method could be used to establish the metabolite atlas serving as a reference for investigating systemic and local effects of pathogen infection or environmental stress (59). In a word, MSI is a powerful tool for direct mapping of tissue sections and simultaneous monitoring the spatial distribution of various compounds. While its application in plant tissues is limited as the hard cell walls of plant tissues may cause barriers in cryosectioning of the samples, resulting difficults for MSI of phenolic compounds in oilseeds. Therefore, efficient and excellent sectioning techniques of plant tissues need to be further developed.

Other emerging technique such as boronic acid-functionalized magnetic multi-walled carbon nanotubes coupled with flexible branched polymer nanocomposites applied as matrix for MALDI-TOF-MS analysis were developed by Li et al. and the method demonstrated to be efficient for the analysis of flavonoids in foods (62). An electrochemical sensor constructed with d-$Ti_3C_2T_x$/MWCNTs composite material was reported by Liu et al. for the detection of luteolin, and the method showed advantages of low detection limit, good selectivity and high sensitivity (31). Researchers are increasingly developing modern techniques to improve the separation ability, detection sensitivity, and accuracy of analytical method for phenolic compounds in complex matrices.

Data processing and statistical analysis

As rapid development of high-resolution techniques, it has become the most important issue for dealing with massive amount of metabolomics data. To solve this problem, several data mining strategies have been developed, including (a) compound discoverer software for automatically performing peak alignment, MS and MS/MS spectra extraction; (b) available database with the retention time, accurate mass, precursor and

product ion spectrum, fragmentation patterns, etc. information; (c) new powerful software package for data mining; (d) new data mining method, such as machine learning based method (54). Up to date, different instrument manufacturers have designed their own data processing software, including MassHunter (Agilent), Xcalibur (Thermo Fisher), Labsolutions (Shimadzu), Compass Hystar (Bruker) and XCMS/Analyst (AB Sciex). Tsugawa et al. developed the MS-Dial software for data processing of raw files from different instrument manufactures with an enriched LipidBlast library identified 1,023 lipid compounds (63). For metabolite database, there are already some self-built or public metabolite databases, such as MassBank, KNAPSAcK, MetaCyc, ChemSpider, HMDB, METLIN, PubChem and mzCloud library (54). For the new self-packaged software and data mining method, a number of research groups have begun to intervene in this area. For instance, Luo et al. developed a systematic and automated software named MRM-Ion Pair Finder for acquiring characteristic MRM ion pairs by precursor ions alignment, MS/MS spectrum extraction and reduction, characteristic product ion selection and ion fusion (51). SWATHtoMRM strategy was developed by Zha et al. to extract MRM transitions for targeted analysis with coverage as high as 1,000–2,000 metabolites (64). In addition, MRMPROBS, MRM-DIFF, MRMAnalyzer, and Skyline are also used to design MRM method and extract target peaks (52). Lyu et al. developed a high-throughput method based on MS/MS molecular networking to characterize, discover, and predict unknown phenolic compounds with the aid of global natural products social molecular networking library (65).

Besides, chemometric tools are increasingly being used to analysis metabolomics data. In metabolomic analysis, univariate statistical approaches such as *t*-tests and analysis of variance are often used to identify the significant changes of metabolites between different groups. For multivariate analysis, principal component analysis (PCA) and hierarchical clustering analysis are the frequently used explorative multivariate methods. Miho et al. used PCA of phenolic concentrations to distinguish between virgin olive oils and found that virgin olive oils obtained in three consecutive crop seasons could be effectively distinguished by PCA (28). In addition, linear discriminant analysis, such as partial least squares discriminant analysis, orthogonal partial least square discriminant analysis (OPLS-DA), and multiple linear regression, partial least squares, orthogonal partial least squares etc., are the widely used statistical analysis approaches for classification and regression analysis. Zhang et al. used partial least square discriminant analysis to screen for differential metabolites and found that significantly differential phenolic compounds between rapeseeds including syringin, kaempferol, isorhamnetin, and

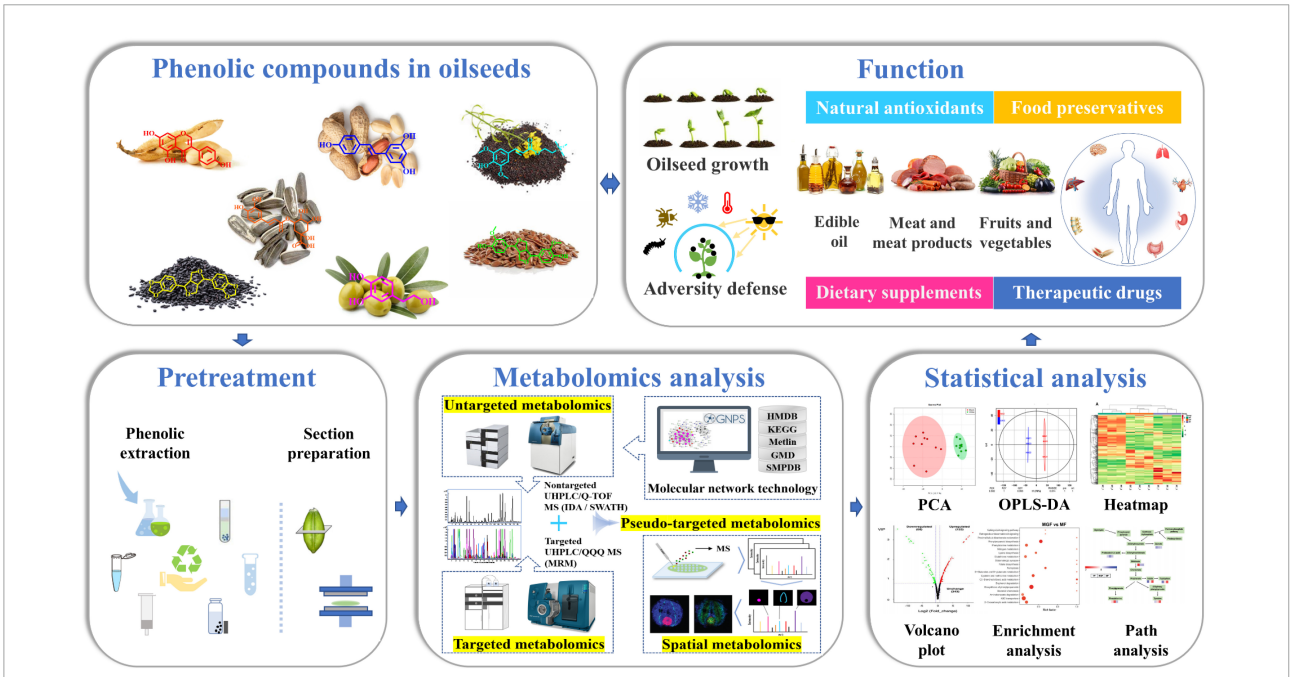

FIGURE 2
Flow chart of phenolic compound analysis. Phenolic compounds in oilseeds play an important role in oilseed growth and adversity defense. The profiling of phenolic compounds includes pretreatment, metabolomics analysis and statistical analysis. Pretreatment includes phenolic compounds extraction and section preparation. Metabolomics analysis can be further divided as untargeted, targeted, pseudo-targeted and spatial metabolomics. Statistical analysis commonly includes PCA, OPLS-DA, Heatmap analysis, Volcano plot analysis, enrichment analysis, and path analysis. The analysis results can provide reliable data support for the applications of phenolic compounds in foods, health care products and medicines.

sinapic acid (66). These statistical analyses can be performed on MetaboAnalyst platform,[1] SIMCA software, or R package (43). Recently, machine learning methods such as random forest and support vector machines have presented new strategies in multivariate analysis (67). And the identified metabolites can be further used to generate metabolic pathways on the small molecule pathway database[2] or KEGG pathway database[3] (54). Wang et al. performed pathway analysis based on KEGG pathway database between white and black sesame and found that metabolic pathways differentially altered between white and black sesame seeds mainly included phenylpropanoid biosynthesis, tyrosine metabolism, and riboflavin metabolism (31). Pathway enrichment analysis can be performed on the web-based sever Metabolite Sets Enrichment Analysis.[4] The flow chart of phenolic compound analysis was shown in **Figure 2**. Phenolic compounds in oilseeds play an important role in oilseed growth and adversity defense (9). The profiling of phenolic compounds includes pretreatment, metabolomics analysis, and statistical analysis. Pretreatment includes phenolic compounds extraction and tissue section preparation. Metabolomics analysis can be further divided as untargeted, targeted, pseudo-targeted and spatial metabolomics. Statistical analysis commonly includes PCA, OPLS-DA, heatmap analysis, volcano plot analysis, enrichment analysis, and path analysis. The analysis results can provide reliable data support for the applications of phenolic compounds in foods, health care products and medicines.

Conclusion and expectation

Phenolic compounds, a class of green renewable resources with rich reserves, are of great importance in the fields of food, medicine, agriculture, and chemical industry, which are closely related to human health. Phenolic compounds have been studied extensively for their antioxidant and therapeutic properties. Their nutritional and health effects have been demonstrated in multiple scientific studies, and claims for health effects are officially recognized. Variations in the organoleptic, nutraceutical and functional properties of oilseeds are mainly due to variations in the types, contents, and metabolic properties of phenolic compounds. Besides, the concentration and type of phenolics in oilseed products greatly depend on production processes used. Accordingly, it has become an important topic for how to fully, reasonable, and scientific exploiting and utilization of this green resources.

Although phenolic compounds have been widely studied in plant-based matrices for their wide and potent biological properties, there are no standardized procedures for sample preparation and analysis of these compounds. Future trends in the analysis of phenolic compounds could include: (a) Phenolic database can be established according to the characteristics of the inherent phenolic composition in oilseeds. (b) More sophisticated extraction techniques, especially techniques with low-solvent and low-time consuming, high efficiency, high coverage, and automated analytical techniques should be developed. (c) Information about the modification and fate of phenolic compounds in oilseeds during various processing and storage progress needs further exploration. (d) The knowledge gap between traditional applications and scientific evidence of phenolic compounds should be bridged. (e) The physiological effects of phenolic compounds on human body is still an urgently subject to be detailed investigated.

Author contributions

YZ: methodology, investigation, and writing. HX: original draft preparation. XL: methodology and investigation. DW: reviewing. HC: supervision. FW: supervision, reviewing, and editing. All authors contributed to the article and approved the submitted version.

Funding

This work was supported by the National Key R&D Program Key Special Project (Grant No. 2021YFD1600103). We also gratefully acknowledge the support of National Natural Science Foundation of China (Grant No. U21A20274), Key Research Projects of Hubei Province (Grant No. 2020BBA045), Agricultural Science and Technology Innovation Project of Chinese Academy of Agricultural Sciences (CAAS-ASTIP-2013-OCRI), and Collaborative innovation task of Chinese Academy of Agricultural Sciences (CAAS-XTCX2016005).

Conflict of interest

The authors declare that the research was conducted in the absence of any commercial or financial relationships that could be construed as a potential conflict of interest.

Publisher's note

1 http://www.metaboanalyst.ca
2 http://smpdb.ca/
3 https://www.genome.jp/kegg
4 http://www.msea.ca

References

1. FAO. *Food and agriculture organization of the united nations*. (2021). Available online at: http://faostat.fao.org (accessed on august 8, 2021)

2. Alu'datt MH, Rababah T, Alhamad MN, Al-Mahasneh MA, Alli I. A review of phenolic compounds in oil-bearing plants: Distribution, identification and occurrence of phenolic compounds. *Food Chem.* (2017) 218:99–106. doi: 10.1016/j.foodchem.2016.09.057

3. Yang R, Zhang L, Li P, Yu L, Mao J, Wang X, et al. A review of chemical composition and nutritional properties of minor vegetable oils in China. *Trends Food Sci Technol.* (2018) 74:26–32. doi: 10.1016/j.tifs.2018.01.013

4. Yu X, Yu L, Ma F, Li P. Quantification of phenolic compounds in vegetable oils by mixed-mode solid-phase extraction isotope chemical labeling coupled with UHPLC-MS/MS. *Food Chem.* (2021) 334: 127572–127580. doi: 10.1016/j.foodchem.2020.127572

5. Li X, Zhang L, Zhang Y, Wang D, Wang X, Yu L, et al. Review of NIR spectroscopy methods for nondestructive quality analysis of oilseeds and edible oils. *Trends Food Sci Technol.* (2020) 101:172–81. doi: 10.1016/j.tifs.2020.05.002

6. Wang D, Zhang L, Yu L, Ma F, Li P. Simultaneous quantification of trace and micro phenolic compounds by liquid chromatography tandem-mass spectrometry. *Metabolites.* (2021) 11:589–602. doi: 10.3390/metabo11090589

7. Lund MN. Reactions of plant polyphenols in foods: Impact of molecular structure. *Trends Food Sci Technol.* (2021) 112:241–51. doi: 10.1016/j.tifs.2021.03.056

8. Ma Y, Kosińska-Cagnazzo A, Kerr WL, Amarowicz R, Swanson RB, Pegg RB. Separation and characterization of soluble esterified and glycoside-bound phenolic compounds in dry-blanched peanut skins by liquid chromatography-electrospray ionization mass spectrometry. *J Agric Food Chem.* (2014) 62: 11488–11504. doi: 10.1021/jf503836n

9. Król-Grzymała A, Amarowicz R. Phenolic compounds of soybean seeds from two European countries and their antioxidant properties. *Molecules.* (2020) 25: 2075–2085. doi: 10.3390/molecules25092075

10. Alu'datt MH, Rababah T, Ereifej K, Alli I. Distribution, antioxidant and characterisation of phenolic compounds in soybeans, flaxseed and olives. *Food Chem.* (2013) 139:93–9. doi: 10.1016/j.foodchem.2012.12.061

11. López-Fernández O, Domínguez R, Pateiro M, Munekata PE, Rocchetti G, Lorenzo JM. Determination of polyphenols using liquid chromatography-tandem mass spectrometry technique (LC-MS/MS): A review. *Antioxidants.* (2020) 9:479–505. doi: 10.3390/antiox9060479

12. Chanioti S, Katsouli M, Tzia C. Novel processes for the extraction of phenolic compounds from olive pomace and their protection by encapsulation. *Molecules.* (2021) 26: 1781–1798. doi: 10.3390/molecules26061781

13. Castillo-Luna A, Criado-Navarro I, Ledesma-Escobar CA, López-Bascóna MA, Priego-Capotea F. The decrease in the health benefits of extra virgin olive oil during storage is conditioned by the initial phenolic profile. *Food Chem.* (2021) 336: 127730–127736. doi: 10.1016/j.foodchem.2020.127730

14. Tenyang N, Ponka R, Tiencheu B, Djikeng FT, Azmeera T, Karuna MSL, et al. Effects of boiling and roasting on proximate composition, lipid oxidation, fatty acid profile and mineral content of two sesame varieties commercialized and consumed in far-north region of Cameroon. *Food Chem.* (2017) 221: 1308–1316. doi: 10.1016/j.foodchem.2016.11.025

15. Zeb A. A comprehensive review on different classes of polyphenolic compounds present in edible oils. *Food Res Int.* (2021) 143: 110312–110331. doi: 10.1016/j.foodres.2021.110312

16. Wu S, Shen D, Wang R, Li Q, Mo R, Zheng Y, et al. Phenolic profiles and antioxidant activities of free, esterified and bound phenolic compounds in walnut kernel. *Food Chem.* (2021) 350: 129217–129225. doi: 10.1016/j.foodchem.2021.129217

17. Fiechter G, Opacak I, Raba B, Mayer HK. A new ultrahigh pressure liquid chromatography method for the determination of total isoflavone aglycones after enzymatic hydrolysis: Application to analyze isoflavone levels in soybean cultivars. *Food Res Int.* (2013) 50:586–92. doi: 10.1016/j.foodres.2011.03.038

18. Chen Y, Shan S, Cao D, Tang D. Steam flash explosion pretreatment enhances soybean seed coat phenolic profiles and antioxidant activity. *Food Chem.* (2020) 319: 126552–126559. doi: 10.1016/j.foodchem.2020.126552

19. Wang W, Yang B, Li W, Zhou Q, Liu C, Zheng C. Effects of steam explosion pretreatment on the bioactive components and characteristics of rapeseed and rapeseed products. *LWT Food Sci Technol.* (2021) 143: 111172–111181. doi: 10.1016/j.lwt.2021.111172

20. Li J, Guo Z. Identification and quantification of phenolic compounds in rapeseed originated lecithin and antioxidant activity evaluation. *LWT- Food Sci Technol.* (2016) 73:397–405. doi: 10.1016/j.lwt.2016.06.039

21. Cong Y, Cheong LZ, Huang F, Zheng C, Wan C, Zheng M. Effects of microwave irradiation on the distribution of sinapic acid and its derivatives in rapeseed and the antioxidant evaluation. *LWT-Food Sci Technol.* (2019) 108:310–8. doi: 10.1016/j.lwt.2019.03.048

22. Cong Y, Zheng M, Huang F, Liu C, Zheng C. Sinapic acid derivatives in microwave-pretreated rapeseeds and minor components in oils. *J Food Compos Anal.* (2020) 87: 103394–103402. doi: 10.1016/j.jfca.2019.103394

23. Chew SC. Cold-pressed rapeseed (*Brassica napus*) oil: Chemistry and functionality. *Food Res Int.* (2020) 131: 108997–109009. doi: 10.1016/j.foodres.2020.108997

24. Yang M, Zheng C, Zhou Q, Liu CS, Li WL, Huang FH. Influence of microwaves treatment of rapeseed on phenolic compounds and canolol content. *J Agric Food Chem.* (2014) 62:1956–63. doi: 10.1021/jf4054287

25. Chai WM, Wei QM, Deng WL, Zheng YL, Chen XY, Huang Q, et al. Anti-melanogenesis properties of condensed tannins from *Vigna angularis* seeds with potent antioxidant and DNA damage protection activities. *Food Funct.* (2019) 10:99–111. doi: 10.1039/C8FO01979G

26. Masunaga T, Murao N, Tateishi H, Koga R, Ohsugi T, Otsuka M, et al. Anti-cancer activity of the cell membrane-permeable phytic acid prodrug. *Bioorg Chem.* (2019) 92: 103240–103247. doi: 10.1016/j.bioorg.2019.103240

27. Merinas-Amo T, Lozano-Baena M, Obregón-Cano S, Alonso-Moraga Á, Haro-Bailón A. Role of glucosinolates in the nutraceutical potential of selected cultivars of *Brassica rapa*. *Foods.* (2021) 10: 2720–2739. doi: 10.3390/foods10112720

28. Kim MY, Kim HJ, Lee YY, Kim MH, Lee JY, Kang MS, et al. Antioxidant and anti-inflammatory effects of Peanut (*Arachishypogaea* L.) skin extracts of various cultivars in oxidative-damaged HepG2 cells and LPS-induced raw 264.7 macrophages. *Food Sci Nutr.* (2020) 9:973–84. doi: 10.1002/fsn3.2064

29. Ferreira CD, Ziegler V, Bubolz VK, Silva JD, Cardozo MMC, Elias MC, et al. Effects of the roasting process over the content of secondary metabolites from peanut grains (*Arachis hypogaea*. L) with different colorations of testa. *J Food Qual.* (2016) 39:685–94. doi: 10.1111/jfq.12235

30. Hassan AB, Maiman SAA, Alshammari GM, Mohammed MA, Alhuthayli HF, Ahmed IAM, et al. Effects of boiling and roasting treatments on the content of total phenolics and flavonoids and the antioxidant activity of peanut (*Arachis hypogaea* L.) pod shells. *Processes.* (2021) 9: 1542–1552. doi: 10.3390/pr9091542

31. Liu W, Yang X, Li M, Gui QW, Jiang H, Li Y, et al. Sensitive detection of luteolin in peanut shell based on titanium carbide/carbon nanotube composite modified screen-printed electrode. *Microchem J.* (2022) 175: 107135–107141. doi: 10.1016/j.microc.2021.107135

32. Shahidi F, Ambigaipalan P. Phenolics and polyphenolics in foods, beverages and spices: Antioxidant activity and health effects - A review. *J Funct Foods.* (2015) 18:820–97. doi: 10.1016/j.jff.2015.06.018

33. Mancebo-Campos V, Salvador MD, Fregapane G. Antioxidant capacity of individual and combined virgin olive oil minor compounds evaluated at mild temperature (25 and 40°C) as compared to accelerated and antiradical assays. *Food Chem.* (2014) 150:374–81. doi: 10.1016/j.foodchem.2013.10.162

34. Choi J, Moon K. Non-destructive discrimination of sesame oils via hyperspectral image analysis. *J Food Compos Anal.* (2020) 90: 103505–103511. doi: 10.1016/j.jfca.2020.103505

35. Chen Y, Lin H, Lin M, Zheng Y, Chen J. Effect of roasting and in vitro digestion on phenolic profiles and antioxidant activity of water-soluble extracts from sesame. *Food Chem Toxicol.* (2020) 139: 111239–111248. doi: 10.1016/j.fct.2020.111239

36. Salamatullah AM, Alkaltham MS, Uslu N, Özcan MM, Hayat K. The effects of different roasting temperatures and times on some physicochemical properties and phenolic compounds in sesame seeds. *J Food Process Preserv.* (2021) 45: 15222–15234. doi: 10.1111/jfpp.15222

37. Shi LK, Liu RJ, Jin QZ, Wang XG. The contents of lignans in sesame seeds and commercial sesame oils of China. *J Am Oil Chem Soc.* (2017) 94: 1035–1044. doi: 10.1007/s11746-017-3018-7

38. Sohouli MH, Haghshenas N, Hernández-Ruiz Á, Shidfar F. Consumption of sesame seeds and sesame products has favorable effects on blood glucose levels but not on insulin resistance: A systematic review and meta-analysis of controlled clinical trials. *Phytother Res.* (2022) 36: 1126–1134. doi: 10.1002/ptr.7379

39. Filho JGO, Egea MB. Sunflower seed byproduct and its fractions for food application: An attempt to improve the sustainability of the oil process. *J Food Sci.* (2021) 86: 1497–1510. doi: 10.1111/1750-3841.15719

40. Weisz GM, Kammerer DR, Carle R. Identification and quantification of phenolic compounds from sunflower (*Helianthus annuus* L.) kernels and shells by

HPLC-DAD/ESI-MSn. *Food Chem.* (2009) 115:758–65. doi: 10.1016/j.foodchem.2008.12.074

41. Wildermuth SR, Young EE, Were LM. Chlorogenic acid oxidation and its reaction with sunflower proteins to form green-colored complexes. *Compr Rev Food Sci Food Saf.* (2016) 15:829–43. doi: 10.1111/1541-4337.12213

42. Ghisoni S, Chiodelli G, Rocchetti G, Kane D, Lucini L. UHPLC-ESI-QTOF-MS screening of lignans and other phenolics in dry seeds for human consumption. *J Funct Foods.* (2017) 34:229–36. doi: 10.1016/j.jff.2017.04.037

43. Wang H, Guo X, Wu Y, Wang Y, Liu RH, Chen L, et al. Dynamic changes of phytochemical profiles identified key points of flaxseed capsule maturation for lignan accumulation. *Ind Crops Prod.* (2020) 147: 112219–112225. doi: 10.1016/j.indcrop.2020.112219

44. Herchi W, Arraez-Roman D, Trabelsi H, Bouali I, Boukhchina S, Kallel H, et al. Phenolic compounds in flaxseed: A review of their properties and analytical methods. an overview of the last decade. *J Oleo Sci.* (2014) 63:7–14. doi: 10.5650/jos.ess13135

45. Herchi W, Sawalha S, Arraez-Roman D, Boukhchina S, Segura-Carretero A, Kallel H, et al. Determination of phenolic and other polar compounds in flaxseed oil using liquid chromatography coupled with time-of-flight mass spectrometry. *Food Chem.* (2011) 126:332–8. doi: 10.1016/j.foodchem.2010.10.070

46. Shafiq N, Arshad U, Yaqoob N, Khan J, Bilal M. Structure-based experimental and theoretical analysis of *Ricinus communis* for their HepG2 human carcinoma cell line inhibitors. *Process Biochem.* (2021) 104:152–60. doi: 10.1016/j.procbio.2021.03.012

47. Hong C, Chang C, Zhang H, Jin Q, Wu G, Wang X. Identification and characterization of polyphenols in different varieties of *Camellia oleifera* seed cakes by UPLC-QTOF-MS. *Food Res Int.* (2019) 126: 108614–108631. doi: 10.1016/j.foodres.2019.108614

48. Kim DH, Yang WT, Cho KM, Lee JH. Comparative analysis of isoflavone aglycones using microwave-assisted acid hydrolysis from soybean organs at different growth times and screening for their digestive enzyme inhibition and antioxidant properties. *Food Chem.* (2020) 305: 125462–125474. doi: 10.1016/j.foodchem.2019.125462

49. Rente D, Paiva A, Duarte AR. The role of hydrogen bond donor on the extraction of phenolic compounds from natural matrices using deep eutectic systems. *Molecules.* (2021) 26: 2336–2367. doi: 10.3390/molecules26082336

50. Beale DJ, Pinu FR, Kouremenos KA, Poojary MM, Dias DA. Review of recent developments in GC-MS approaches to metabolomics-based research. *Metabolomics.* (2018) 14:152–82. doi: 10.1007/s11306-018-1449-2

51. Luo P, Dai W, Yin P, Zeng Z, Kong H, Zhou L, et al. MRM-Ion Pair Finder: A systematic approach to transform non-targeted mode to pseudo-targeted mode for metabolomics study based on liquid chromatography-mass spectrometry. *Anal Chem.* (2015) 87: 5050–5055. doi: 10.1021/acs.analchem.5b00615

52. Zheng F, Zhao X, Zeng Z, Wang L, Lv W, Wang Q, et al. Development of a plasma pseudotargeted metabolomics method based on ultra-high-performance liquid chromatography-mass spectrometry. *Nat Protoc.* (2020) 15: 2519–2537. doi: 10.1038/s41596-020-0341-5

53. Miho H, Moral J, Barranco D, Ledesma-Escobar CA, Priego-Capote F, Díez CM. Influence of genetic and interannual factors on the phenolic profiles of virgin olive oils. *Food Chem.* (2021) 342: 128357–128365. doi: 10.1016/j.foodchem.2020.128357

54. Cao G, Song Z, Hong Y, Yang Z, Song Y, Chen Z, et al. Large-scale targeted metabolomics method for metabolite profiling of human samples. *Anal Chim Acta.* (2020) 1125:144–51. doi: 10.1016/j.aca.2020.05.053

55. Negro C, Aprile A, Luvisi A, Nicolì F, Nutricati E, Vergine M, et al. Phenolic profile and antioxidant activity of Italian monovarietal extra virgin olive oils. *Antioxidants.* (2019) 8:161–74. doi: 10.3390/antiox8060161

56. Becerra-Herrera M, Sanchez-Astudillo M, Beltran R, Sayago A. Determination of phenolic compounds in olive oil: New method based on liquid-liquid micro extraction and ultrahigh performance liquid chromatography-triple-quadrupole mass spectrometry. *LWT Food Sci Technol.* (2014) 57:49–57. doi: 10.1016/j.lwt.2014.01.016

57. Wang D, Zhang L, Huang X, Wang X, Yang R, Mao J, et al. Identification of nutritional components in black sesame determined by widely targeted metabolomics and traditional Chinese medicines. *Molecules.* (2018) 23: 1180–1191. doi: 10.3390/molecules23051180

58. Peng H, Li W, Li H, Deng Z, Zhang B. Extractable and non-extractable bound phenolic compositions and their antioxidant properties in seed coat and cotyledon of black soybean (*Glycinemax* (L.) merr). *J Funct Foods.* (2017) 32:296–312. doi: 10.1016/j.jff.2017.03.003

59. Bhandari DR, Wang Q, Friedt W, Spengler B, Gottwald S, Rompp A. High resolution mass spectrometry imaging of plant tissues: Towards a plant metabolite atlas. *Analyst.* (2015) 140: 7696–7709. doi: 10.1039/C5AN01065A

60. Liu B, Meng X, Li K, Guo J, Cai Z. Visualization of lipids in cottonseeds by matrix-assisted laser desorption/ionization mass spectrometry imaging. *Talanta.* (2021) 221:9. doi: 10.1016/j.talanta.2020.121614

61. Enomoto H, Nirasawa T. Localization of flavan-3-ol species in peanut testa by mass spectrometry imaging. *Molecules.* (2020) 25:2373–84. doi: 10.3390/molecules25102373

62. Li FK, Wang M, Zhou J, Yang M, Wang T. Nanocomposites of boronic acid-functionalized magnetic multi-walled carbon nanotubes with flexible branched polymers as a novel desorption/ionization matrix for the capture and direct detection of cis-diol-flavonoid compounds coupled with MALDI-TOF-MS. *J Hazard Mater.* (2022) 429:7. doi: 10.1016/j.jhazmat.2021.128055

63. Tsugawa H, Cajka T, Kind T, Ma Y, Higgins B, Ikeda K, et al. MS-DIAL: Data-independent MS/MS deconvolution for comprehensive metabolome analysis. *Nat Methods.* (2015) 12:523–6. doi: 10.1038/nmeth.3393

64. Zha H, Cai Y, Yin Y, Wang Z, Li K, Zhu ZJ. SWATHtoMRM: Development of high-coverage targeted metabolomics method using SWATH technology for biomarker discovery. *Anal Chem.* (2018) 90: 4062–4070. doi: 10.1021/acs.analchem.7b05318

65. Lyu Q, Wen X, Liu Y, Sun C, Chen K, Hsu CC, et al. Comprehensive profiling of phenolic compounds in white and red Chinese bayberries (Morella rubra Sieb. et Zucc.) and their developmental variations using tandem mass spectral molecular networking. *J Agric Food Chem.* (2021) 69:741–9. doi: 10.1021/acs.jafc.0c04117

66. Zhang Y, Xiao H, Lv X, Zheng C, Wu Z, Wang N. Profiling and spatial distribution of phenolic compounds in rapeseed by two-step extraction strategy and targeted metabolomics combined with chemometrics. *Food Chem.* (2023) 401:5. doi: 10.1016/j.foodchem.2022.134151

67. Wu B, Wei F, Xu S, Xie Y, Lv X, Chen H, et al. Mass spectrometry-based lipidomics as a powerful platform in foodomics research. *Trends Food Sci Technol.* (2020) 107:358–76. doi: 10.1016/j.tifs.2020.10.045

68. Cui M, Wu D, Bao K, Wen Z, Hao Y, Luo L. Dynamic changes of phenolic compounds during artificial aging of soybean seeds identified by high-performance liquid chromatography coupled with transcript analysis. *Anal Bioanal Chem.* (2019) 411: 3091–3101. doi: 10.1007/s00216-019-01767-5

69. Yuan M, Jia X, Ding C, Zeng H, Du L, Yuan S, et al. Effect of fluorescence light on phenolic compounds and antioxidant activities of soybeans (*Glycine max* L. Merrill) during germination. *Food Sci Biotechnol.* (2015) 24: 1859–1865. doi: 10.1007/s10068-015-0243-4

70. Lee JH, Jeong SW, Cho YA, Park S, Kim YH, Bae DW, et al. Determination of the variations in levels of phenolic compounds in soybean (*Glycine max* Merr.) sprouts infected by anthracnose (*Colletotrichum gloeosporioides*). *J Sci Food Agric.* (2013) 93: 3081–3086. doi: 10.1002/jsfa.6142

71. Kim JA, Jung WS, Chun SC, Yu CY, Ma KH, Gwag JG, et al. A correlation between the level of phenolic compounds and the antioxidant capacity in cooked-with-rice and vegetable soybean (*Glycine max* L.) varieties. *Eur Food Res Technol.* (2006) 224:259–70. doi: 10.1007/s00217-006-0377-y

72. Yu G, Guo T, Huang Q. Preparation of rapeseed oil with superhigh canolol content and superior quality characteristics by steam explosion pretreatment technology. *Food Sci Nutr.* (2020) 8: 2271–2278. doi: 10.1002/fsn3.1502

73. Zhang M, Zheng C, Yang M, Zhou Q, Li W, Liu C, et al. Primary metabolites and polyphenols in rapeseed (*Brassica napus* L.) cultivars in China. *J Am Oil Chem Soc.* (2019) 96:303–17. doi: 10.1002/aocs.12179

74. Song JG, Cao C, Li J, Xu YJ, Liu YF. Development and validation of a QuEChERS-LC-MS/MS method for the analysis of phenolic compounds in rapeseed oil. *J Agric Food Chem.* (2019) 67: 4105–4112. doi: 10.1021/acs.jafc.9b00029

75. Juliano FF, Alvarenga JFR, Lamuela-Raventos RM, Massarioli AP, Lima LM, Santos RC, et al. Polyphenol analysis using high-resolution mass spectrometry allows differentiation of drought tolerant peanut genotypes. *J Sci Food Agric.* (2020) 100:721–31. doi: 10.1002/jsfa.10075

76. Camargo AC, Regitano-d'Arce MAB, Rasera GB, Canniatti-Brazaca SG, Prado-Silva L, Alvarenga VO, et al. Phenolic acids and flavonoids of peanut by-products: Antioxidant capacity and antimicrobial effects. *Food Chem.* (2017) 237:538–44. doi: 10.1016/j.foodchem.2017.05.046

77. Aljuhaimi F, Özcan MM. Influence of oven and microwave roasting on bioproperties, phenolic compounds, fatty acid composition, and mineral contents of nongerminated peanut and germinated peanut kernel and oils. *J Food Process Preserv.* (2018) 42: 13462–13469. doi: 10.1111/jfpp.13462

78. Medjkouh L, Tamendjari A, Alves RC, Laribi R, Oliveira MBPP. Phenolic profiles of eight olive cultivars from Algeria: Effect of Bactrocera oleae attack. *Food Funct.* (2018) 9:890–7. doi: 10.1039/C7FO01654A

79. Özcan MM, Fındık S, Aljuhaimi F, Ghafoor K, Babiker EE, Adiamo OQ. The effect of harvest time and varieties on total phenolics, antioxidant activity

and phenolic compounds of olive fruit and leaves. *J Food Sci Technol.* (2019) 56:5. doi: 10.1007/s13197-019-03650-8

80. Lukiæ I, Krapac M, Horvat I, Godena S, Kosic U, Bubola KB. Three-factor approach for balancing the concentrations of phenols and volatiles in virgin olive oil from a late-ripening olive cultivar. *LWT Food Sci Technol.* (2018) 87:194–202. doi: 10.1016/j.lwt.2017.08.082

81. Dini I, Graziani G, Fedele FL, Sicari A, Vinale F, Castaldo L, et al. Effects of trichoderma biostimulation on the phenolic profile of extra-virgin olive oil and olive oil by-products. *Antioxidants.* (2020) 9:284–95. doi: 10.3390/antiox9040284

82. Višnjevec AM, Baker P, Charlton A, Preskett D, Peeters K, Tavzes È, et al. Developing an olive biorefinery in Slovenia: Analysis of phenolic compounds found in olive mill pomace and wastewater. *Molecules.* (2021) 26:7–20. doi: 10.3390/molecules26010007

83. Zeb A, Muhammad B, Ullah F. Characterization of sesame (*Sesamum indicum* L.) seed oil from Pakistan for phenolic composition, quality characteristics and potential beneficial properties. *J Food Meas Charact.* (2017) 11: 1362–1369. doi: 10.1007/s11694-017-9514-5

84. Scharlack NK, Aracava KK, Rodrigues C. Effect of the type and level of hydration of alcoholic solvents on the simultaneous extraction of oil and chlorogenic acids from sunflower seed press cake. *J Sci Food Agric.* (2017) 97:4612–20. doi: 10.1002/jsfa.8331

85. Yang QQ, Kim G, Farha AK, Luo Q, Corke H. Phenolic profile, antioxidant and antiproliferative activities of diverse peanut cultivars. *J Food Meas Charact.* (2020) 14: 2336–2367. doi: 10.1007/s11694-020-00483-4

86. Slabi SA, Mathé C, Framboisier X, Defaix C, Mesieres O, Galet O, et al. A new SE-HPLC method for simultaneous quantification of proteins and main phenolic compounds from sunflower meal aqueous extracts. *Anal Bioanal Chem.* (2019) 411: 2089–2099. doi: 10.1007/s00216-019-01635-2

frontiers | Frontiers in Nutrition

TYPE Original Research
PUBLISHED 03 November 2022
DOI 10.3389/fnut.2022.1006440

OPEN ACCESS

EDITED BY
Yu Xiao,
Hunan Agricultural University, China

REVIEWED BY
Xiaoan Li,
Shandong University of Technology, China
Asgar Ali,
University of Nottingham Malaysia, Malaysia
Jianwei Gao,
Institute of Vegetables and Flowers, Shandong Academy of Agricultural Sciences, China

*CORRESPONDENCE
Haile Ma
mhl@ujs.edu.cn
Yi-Ming Zhao
zhaoyiming1129@126.com

SPECIALTY SECTION
This article was submitted to Nutrition and Food Science Technology, a section of the journal Frontiers in Nutrition

RECEIVED 29 July 2022
ACCEPTED 17 October 2022
PUBLISHED 03 November 2022

CITATION
Hong C, Zhou H-C, Zhao Y-M and Ma H (2022) Ultrasonic washing as an abiotic elicitor to induce the accumulation of phenolics of fresh-cut red cabbages: Effects on storage quality and microbial safety. *Front. Nutr.* 9:1006440. doi: 10.3389/fnut.2022.1006440

Ultrasonic washing as an abiotic elicitor to induce the accumulation of phenolics of fresh-cut red cabbages: Effects on storage quality and microbial safety

Chen Hong[1], Hong-Chang Zhou[1], Yi-Ming Zhao[1,2]* and Haile Ma[1,2]*

[1]School of Food and Biological Engineering, Jiangsu University, Zhenjiang, China, [2]Institute of Food Physical Processing, Jiangsu University, Zhenjiang, China

Ultrasonic washing has been proved to be an abiotic elicitor to induce the accumulation of phenolics in some fruit and vegetables. However, the feasibility of ultrasonic washing on the accumulation of phenolics in fresh-cut red cabbages has not yet been reported. Therefore, the effects of ultrasonic washing on the phenolics and related phenolic metabolism enzymes of fresh-cut red cabbages, as well as quality and microbial safety during cold storage, were investigated. Firstly, the single-factor tests were used to optimize the ultrasonic processing parameters, including frequency mode, frequency amplitude, power density, frequency cycle time, and ultrasonic washing. Then the activities of the enzymes related to phenolic metabolisms after optimal ultrasound treatment were investigated, including phenylalanine ammonia-lyase (PAL), polyphenol oxidase (PPO), and peroxidase (POD). Additionally, the quality and microbial safety of fresh-cut red cabbages stored at 4°C under the optimal ultrasound treatment were evaluated. The results showed that the content of soluble phenolics (SPs) in fresh-cut red cabbages increased significantly during storage under the optimal conditions (28 ± 2 kHz, 60 W/L, 400 ms, and 20 min) compared with the control ($P < 0.05$). The PAL activity was activated and the PPO and POD activities were inhibited after ultrasonic washing, which contributed to the increase in the content of SPs. Meanwhile, the storage quality and microbial safety of fresh-cut red cabbages were improved. Ultrasonic washing reduced the weight loss and respiration rate and improved the color and texture characteristics. Additionally, the fresh-cut red cabbages after ultrasonic washing showed more retention of ascorbic acid (AA), total soluble proteins (TSPs), total soluble sugars (TSSs), and total soluble solids (SSs) compared with the control. Finally, ultrasonic washing effectively

inhibited the growth of bacteria, molds and yeasts, which is beneficial to the extension of the shelf-life of fresh-cut red cabbages. Therefore, ultrasonic washing can be used as a tool to increase the content of SPs in fresh-cut red cabbages while retaining quality attributes and microbial safety.

KEYWORDS

ultrasonic washing, fresh-cut red cabbages, phenolic content, phenolic accumulation, storage quality, microbial safety

Introduction

Red cabbages (*Brassica oleracea var. capitata f. rubra*), which belong to the Cruciferous family, are rich in phenolics (1, 2). As the largest category of phytochemicals in plant-based foods, phenolics are highly associated with the antioxidant ability of fruit and vegetables (3, 4). They can protect the human body against damage from reactive oxygen species, reducing the risk of chronic diseases such as cancer and cardiovascular diseases (5). Thus, red cabbages are good sources of natural antioxidants. Studies have shown that cooking methods such as boiling, steaming, stir-frying, and microwave processing can reduce the total phenolic content of red cabbages (6). In order to minimize the losses of phenolics, red cabbages are often made into fresh-cut vegetables and eaten as salads (7).

Washing is an essential step to ensure food safety in the process of fresh-cut fruit and vegetables. This process can remove impurities, including residual soils, debris, insects, pesticides, and microorganisms. Meanwhile, it can clean the juice released from the shredded fruit and vegetables to decrease the food corruption rate, improve edible quality, and prolong the shelf-life (8, 9). Currently, chemical washing methods are commonly used in the fruit and vegetable industry, especially disinfectants based on chlorine and chlorinated compounds due to their convenience, low cost, and high antimicrobial activity (9, 10). Nevertheless, chlorine-based compounds are corrosive, damaging human health by causing skin and respiratory tract irritation. Moreover, water hyperchlorination caused by these chemicals can produce carcinogens that are harmful to the environment, such as high-concentration trihalomethane (11). Therefore, emerging technologies, such as high pressure, electrolyzed water, pulsed electric field, irradiation, ozone, and ultrasound, have been considered alternatives in the food industry in recent years (12–15).

As a residual-free, safe, and eco-friendly novel technology, ultrasonic washing has been widely used in the postharvest preservation and storage of fruit and vegetables, such as strawberries, lettuces, red bell peppers, and cherry tomatoes (16, 17). It is well known that cavitation effects are the unique physical phenomena caused by the propagation of ultrasonic waves in liquids, including physical effects (e.g., shock waves, micro-jets, shear force, and turbulence) and chemical effects (i.e., the production of a large number of free radicals) (18). Evidences have shown that the cavitation effects can enhance the elution of soil, elimination of microorganisms, and degradation of pesticide residues when ultrasonic washing is applied to fruit and vegetables (19–21). Additionally, it has been also reported that the quality of fruit and vegetables can be effectively maintained by the change in the activities of endogenous enzymes when subjected to ultrasonic washing (11). More interestingly, bioactive compounds in fruit and vegetables can be remarkably affected during the washing process, such as phenolics, carotenoids, and ascorbic acid (AA) (13, 21), especially phenolics. Ultrasound has been considered an abiotic elicitor that induces the accumulation of phenolics in fruit and vegetables, such as broccoli florets (22), mangoes (23), and kiwifruit (24), which is conducive to the obtainment of functional fruit and vegetables with increased levels and bioavailability of nutraceuticals (25, 26). The accumulation of phenolics may be related to the regulation of phenolic metabolism enzymes after ultrasonic washing, such as phenylalanine ammonia-lyase (PAL), polyphenol oxidase (PPO), and peroxidase (POD) (22, 27). However, not all fruit and vegetables are applicable to ultrasonic washing such as fresh-cut tomatoes and carrots, which showed lower phenolic content than water washing (28, 29). Currently, there are few studies on ultrasonic washing applied to red cabbages. Therefore, the feasibility of ultrasound as an abiotic elicitor to induce the accumulation of phenolics in fresh-cut red cabbages remains to be investigated.

In this study, the effects of ultrasonic frequency mode, frequency amplitude, ultrasonic power density, frequency cycle time, and ultrasonic time on the phenolics in fresh-cut red cabbages were studied by single-factor tests. The activities of phenolic metabolism enzymes after ultrasound treatment were explored, including PAL, PPO, and POD. Meanwhile, the effects of ultrasonic washing on other quality parameters [weight, respiration rate, color, firmness, AA, total soluble proteins (TSPs), total soluble sugars (TSSs), and total soluble solids (SSs)] and microbial safety (total number of bacteria, molds and yeasts) during 4°C storage were investigated under optimized conditions.

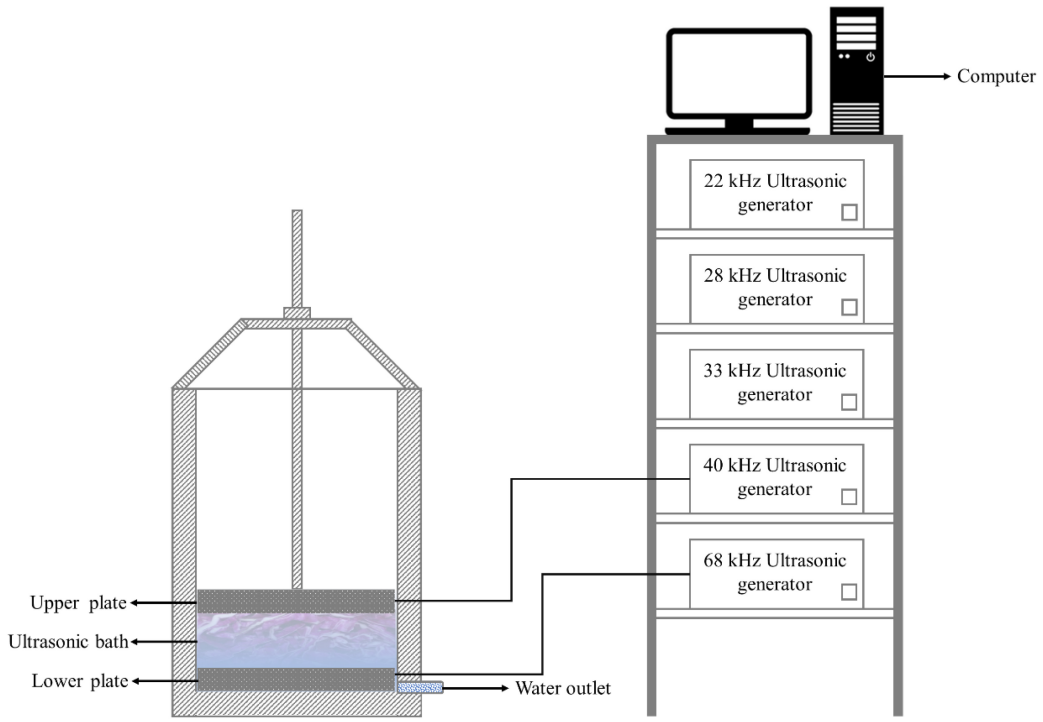

FIGURE 1
Schematic diagram of the flat-plate ultrasound equipment.

Materials and methods

Raw materials

Fresh red cabbages (*Brassica oleracea var. capitata f. rubra*) at the maturity stage (100–120 days after sowing, i.e., the red cabbages were sowed in February or March and harvested in June or July) were obtained from local markets in Zhenjiang (China) and pre-selected based on size, color, and visual quality to ensure initial consistency. The red cabbages were placed in a refrigerator at 4°C until the experiment. Before processing, the three outer leaves and any other leaves with visible damage were discarded. Then the red cabbages were manually cut into pieces of approximately 0.5 cm × 5 cm by a sterile knife. The fresh-cut red cabbages were used in the following sections.

Ultrasonic washing procedure

The fresh-cut red cabbages were washed with the flat-plate ultrasound equipment manufactured by Jiangsu University (as shown in **Figure 1**). The equipment can be operated by four frequency modes: single-fixed frequency, single-sweep frequency, double-fixed frequency, and double-sweep frequency. Single-frequency ultrasound is controlled by either the upper flat or lower flat. For dual-frequency ultrasound, both flats work at the same time. The maximum power of a single plate is 600 W. The sweep frequency model ($\alpha \pm \delta$ kHz) refers to the sweep frequency cycle of the increasing period from $\alpha - \delta$ to $\alpha + \delta$ kHz and the decreasing period from $\alpha + \delta$ to $\alpha - \delta$ kHz with the same linear speed in the form of an isosceles triangle. α is the central frequency of 22, 28, 33, 40, and 68 kHz. δ is the frequency amplitude, i.e., ± 1 and ± 2 kHz. An increasing period plus a decreasing period is defined as the cycle time of the sweep frequency. When the δ is set to zero, the operation is a fixed frequency model. The effects of ultrasound operating parameters on the phenolics of fresh-cut red cabbages were investigated by single-factor tests. The details, including ultrasonic frequency mode, frequency amplitude, ultrasonic power density, frequency cycle time, and ultrasonic time, are shown in **Table 1**. The operating parameters were selected based on the published reviews (14, 30) and previous studies in our research group (31, 32).

The same batch of red cabbages was used for the evaluation of the same factor with different levels to ensure the comparability of phenolic content, except for the factor of ultrasonic frequency mode. As there were 30 levels of frequency modes in the study, it was difficult to treat the same batch of fresh-cut red cabbages at one time. Therefore, different batches of red cabbages were used to study the effects of single-frequency and dual-frequency modes.

Fresh-cut red cabbages (500 g) were placed in an ultrasonic bath (36 cm × 29 cm × 100 cm) containing sterile distilled water for ultrasonic washing. The water temperature was kept

TABLE 1 Levels of ultrasonic frequency mode, ultrasonic power density, frequency amplitude, frequency cycle time, and ultrasonic time in the single-factor tests.

Factors	Levels
Ultrasonic frequency mode	Single-fixed frequency: 22, 28, 33, 40, and 68 kHz Single-sweep frequency: 22 ± 2, 28 ± 2, 33 ± 2, 40 ± 2, and 68 ± 2 kHz Dual-fixed frequency: 22/28, 22/33, 22/40, 22/68, 28/33, 28/40, 28/68, 33/40, 33/68, and 40/68 kHz Dual-sweep frequency: (22 ± 2)/(28 ± 2), (22 ± 2)/(33 ± 2), (22 ± 2)/(40 ± 2), (22 ± 2)/(68 ± 2), (28 ± 2)/(33 ± 2), (28 ± 2)/(40 ± 2), (28 ± 2)/(68 ± 2), (33 ± 2)/(40 ± 2), (33 ± 2)/(68 ± 2), and (40 ± 2)/(68 ± 2) kHz
Frequency amplitude	±1 and ±2 kHz
Ultrasonic power density	20, 40, 60, 80, and 100 W/L
Frequency cycle time	100, 200, 300, 400, and 500 ms
Ultrasonic time	10, 15, 20, 25, and 30 min

at 20°C to avoid thermal effects. After treatment, excess water was removed with sterile filter paper from the surface of the samples and air-dried on a clean bench (OptiClean 1300, Heal Force Bio-Meditech Co., Shanghai, China). Then samples were placed in polystyrene containers and refrigerated at 4°C. They were taken every 2 days (0, 2, 4, 6, and 8 days) during storage for experimental analysis. Each experiment was repeated in triplicates. The results were expressed as means of three triplicates ± standard deviations. Fresh-cut red cabbages washed with sterile distilled water were used as the control.

Determination of phenolic content

Extraction of soluble phenolics

The soluble phenolics (SPs) of the fresh-cut red cabbages were extracted by the method of Abdel-Aal et al. (33) with some modifications. Briefly, samples (30 g) were mixed with 300 mL of 80% chilled methanol. Then the mixtures were homogenized using a JYL-350S homogenizer (Joyoung Co., Ltd., Zhejiang, China) for 2 min. The supernatants were obtained by centrifugation at 10,000 rpm for 10 min for further analysis of SPs. Meanwhile, the sediments were used for the extraction of insoluble-bound phenolics (IPs).

Extraction of insoluble-bound phenolics

The IPs were extracted according to the method of Viacava et al. (34) with some modifications. Briefly, the sediments from the above extraction of SPs were hydrolyzed with 20 mL of 4 M NaOH at room temperature for 1 h with continuous shaking under nitrogen gas by a ZQZY-78CN shaker (Zhichu Biotechnology Co., Ltd., Shanghai, China). Then samples were acidified to pH 2 with 6 M HCl and centrifuged at 10,000 rpm for 10 min to obtain the supernatants. The supernatants were extracted with 20 mL ethyl acetate for 10 min, then centrifuged, and eventually dried under a nitrogen stream until dryness. The extracted sediments were redissolved in 5 ml of 80% methanol for the analysis of IPs.

Determination of the contents of soluble phenolics and insoluble-bound phenolics

The contents of SPs and IPs were quantified by the Folin-Ciocalteu method. The admixtures of 1 mL sample solution, 0.5 mL Folin-Ciocalteu reagent, 2 mL of 7.5% Na_2CO_3, and 6 mL distilled water were incubated at 70°C for 30 min. Then the absorbance of the solution was measured at 750 nm using a T6 UV/VIS spectrophotometer (Purkinje General Instrument Co., Ltd., Shanghai, China). The phenolic content was expressed as mg GAE/100 g FW fresh weight (note: GAE-gallic acid equivalents; FW-fresh weight).

Due to the differences in the initial contents of SPs in different batches of fresh-cut red cabbages used for frequency modes, it is difficult to directly compare the frequency modes by the content of SPs. Therefore, the phenolic retention rate under different frequency modes were used for the comparison. The retention rate of SPs was calculated as the following equation:

$$\text{Phenolic retention rate} = \frac{\text{Contentof SPs after storage}}{\text{Content of SPs in the control group on Day 0}} \quad (1)$$

Determination of the activities of phenylalanine ammonia-lyase, polyphenol oxidase, and peroxidase

For PAL activity measurement, fresh-cut red cabbages (30 g) were homogenized with 150 mL of chilled 0.05 M phosphate buffer solution (pH 7.8) for 2 min. Then the mixtures were centrifuged at 10,000 rpm for 10 min at 4°C, and the supernatant was collected to measure the PAL activity with an ELISA kit (Tongwei Reagent Co., Ltd., Shanghai, China) according to the manufacturer's instructions. One unit of PAL activity was defined as the amount of enzyme that produced 1 μg cinnamic acid per hour.

For PPO and POD activity measurement, fresh-cut red cabbages (30 g) were homogenized with 150 mL of chilled 0.05 M phosphate buffer solution (pH 7.8) containing 1% polyvinylpyrrolidone for 2 min, and then centrifuged at 10,000 rpm for 10 min at 4°C. The supernatant was used for the following analysis of PPO and POD activities. The activities of PPO and POD were measured according to the method of Yeoh and Ali (27) with slight modifications. The assay of PPO activity was conducted by mixing 145 μL of 0.1 M catechol and 5 μL of supernatant. Absorbance was taken every 15 s for 4 min at 420 nm using an automatic microplate reader (Infinite

200 PRO, Tecan Trading AG, Switzerland). One unit of PPO activity was defined as the amount of enzyme that resulted in an increase of 0.01 absorbance unit per second. POD activity was measured by adding 1 μL of supernatant and 145 μL of 0.1 M sodium phosphate buffer (pH 6.0) blended with 20 mM guaiacol and 4 mM H_2O_2. The absorbance of the mixtures was recorded at 470 nm every 15 s for 4 min using the same automatic microplate reader as mentioned before. One unit of POD activity was defined as the amount of enzyme that resulted in an increase of 0.01 absorbance unit per second.

Determination of weight retention rate and respiration rate

The weight retention rate of the samples was calculated as follows:

$$\text{Weight retention rate} = \frac{\text{Weight after storage}}{\text{Weight in the control group on Day 0}} \quad (2)$$

The respiration rate was measured by the F-900 Portable Analyzer (Felix instruments Co., Ltd., WA, United States). For each group, fresh-cut red cabbages (90 g) were placed in a 2-L sealed vessel in a well-ventilated environment at 25°C and kept sealed for 1 h. The respiration rate was measured by the changes in the concentration of CO_2 and expressed as mg $CO_2 \cdot kg^{-1} \cdot h^{-1}$ (35).

Determination of browning degree and cut surface color

The determination of the browning degree was based on the method of Li et al. (36) with some modifications. Fresh-cut samples (30 g) were homogenized with 300 mL of 80% ethanol. Then the mixtures were centrifuged at 10,000 rpm for 10 min to obtain the supernatant. The browning degree was expressed as the absorbance of the supernatant measured at 420 nm by a T6 UV/VIS spectrophotometer.

The color of the cut surface was measured by a CR-400 colorimeter (Konica Minolta, Japan) calibrated with a standard white plate. The CIELAB color coordinates L^* (lightness), a^* (green to red), and b^* (blue to yellow) were collected at ten different spots from the cut surface, and the average values were reported. The total color difference (ΔE) was calculated according to the following equation:

$$\Delta E = \sqrt{(L^* - L_0^*)^2 + (a^* - a_0^*)^2 + (b^* - b_0^*)^2} \quad (3)$$

Where L_0^*, a_0^*, and b_0^* are the values of the standard white plate.

Determination of firmness

Firmness was determined by an XT2i Texture analyzer (Stable Micro Systems, Godalming, United Kingdom) equipped with a P/2N probe with a diameter of 2 mm. Parameters referred to the method of Xu et al. (37) with some modifications and were set as follows: pretest speed, 1 mm/s; test speed, 1 mm/s; post-test speed, 10 mm/s; auto-trigger force, 5 g; and travel distance of the probe, 9 mm. The firmness was recorded with the maximum force (g) during penetration.

Determination of the contents of ascorbic acid, total soluble proteins, total soluble sugars, and total soluble solids

Fresh-cut samples (30 g) were homogenized with 300 mL of 0.05 M oxalic acid containing 0.0002 M ethylene diamine tetraacetic acid, 0.05 M phosphate buffer solution (pH 7.8), 80% ethanol, and distilled water, respectively. The supernatant after centrifugation at 10,000 rpm for 10 min was used to measure the contents of AA, TSPs, TSSs, and SSs. The AA content was evaluated using phosphomolybdate-blue spectrophotometry (38). The contents of TSPs and TSSs were measured with the Bradford method and anthrone method using bovine serum albumin and glucose as a standard, respectively. The content of SSs was determined using a hand-held refractometer (ATAGO Tokyo, Japan).

Microbiological analysis

The total number of bacteria, molds and yeasts in fresh-cut red cabbages were measured according to the method of Yildiz et al. (39) with some modifications. Samples (30 g) were immersed in a sterile saline solution of 300 mL, then homogenized using an LC-PJ-400M sterile homogenizer (Lichen-Bx Instrument Technology Co., Ltd., China) for 2 min. The homogenate was decimally diluted using sterile saline. Then the dilution solution (0.1 mL) was taken and surface plated onto plate count agar (Sinopharm Chemical Reagent Co., Ltd., Shanghai, China) at 37°C for 48 h and Bangladeshi-red culture medium (Sinopharm Chemical Reagent Co., Ltd., Shanghai, China) at 28°C for 96 h to count the total number of bacteria, molds and yeasts, respectively.

Scanning electron microscopy of fresh-cut red cabbage leaves

In order to observe the anatomical characteristics (i.e., cross section and abaxial epidermis) of fresh-cut red cabbage

leaves by a field emission scanning electron microscopy (Model Regulus8100, Hitachi, Japan), leaf samples were prepared according to the method of Marasek-Ciolakowska et al. (40) with some modifications. Fresh sample sections were fixed in 2.5% glutaraldehyde and then dehydrated in an ethanol series. Then the tissues were desiccated with critical point drying CO_2 and sputter-coated with gold for observation.

Statistical analysis

SPSS 19 (SPSS Inc., Chicago, IL, United States) and excel 2016 software were applied to perform the analysis of variance (ANOVA). Significant difference was determined among the treatments using Duncan's test with a 95% level of confidence ($P < 0.05$). Origin 2018 and excel 2016 software were used in the graphical report.

Results and discussion

Analysis of ultrasound operating parameters

Effects of ultrasonic frequency mode on the contents of soluble phenolics and insoluble-bound phenolics

The effects of single-fixed and single-sweep frequency on the contents of SPs and IPs are shown in **Supplementary Figure 1**, and the effects of dual-fixed and dual-sweep frequency on the contents of SPs and IPs are displayed in **Supplementary Figure 2**. As can be seen from **Supplementary Figures 1**, **2**, the content of SPs in the red cabbage extracts varied with different ultrasonic frequency treatments. An appropriate frequency model could increase the content of SPs. Similar results were observed in the study of Alenyorege et al. (31), in which treatment with 28 ± 2 kHz increased the content of SPs in the Chinese cabbages while treatment with 28/68 kHz could decrease the content of SPs. Additionally, the content of IPs (approximately 3–5 mg GAE/100 g FW) in fresh-cut red cabbages was much lower than the content of SPs. Moreover, there was no significant difference in the content of IPs after ultrasonic washing during storage compared with control ($P > 0.05$), whatever the frequency mode was. These results showed that the increase in the content of SPs in fresh-cut red cabbages was irrelevant to the IPs, although some researchers found that the increase in the content of SPs in extracts after ultrasound treatment could be due to the breakage of cross-links in IPs (41). Therefore, the subsequent analysis of the effects of ultrasonic washing on phenolics in fresh-cut red cabbages will be conducted from the perspective of SPs.

In order to compare the effects of various frequency treatments on the content of SPs, the retention rate of SPs under the treatments of single-fixed, single-sweep, dual-fixed, and dual-sweep frequency are summarized in **Supplementary Figure 3**. As observed from **Supplementary Figures 3A,B**, on the whole, the phenolic retention rate after single-sweep frequency treatments was higher than that treated by single-fixed frequency. Although fresh-cut red cabbages treated by 33 ± 2 kHz showed the highest phenolic retention rate on Day 2, the phenolics were unstable during the following storage and markedly degraded. Meanwhile, the phenolic retention rate in fresh-cut red cabbages treated by 28 ± 2 kHz remained high level among the whole storage and increased to the maximum on Day 6. For the dual-sweep frequency treatment (as seen in **Supplementary Figures 3C,D**), the 40/68 kHz treatment was more conducive to the retention of phenolics than the other combined treatments.

The effects of the optimal single-frequency (28 ± 2 kHz) and dual-frequency (40/68 kHz) mode on the content of SPs in fresh-cut red cabbages are shown in **Figure 2**. The content of SPs in fresh-cut red cabbages washed with 28 ± 2 kHz was significantly increased compared with the control ($P < 0.05$), and the samples treated with 28 ± 2 kHz (113.64 ± 3.14 mg GAE/100 g FW) showed higher content of SPs than that washed with 40/68 kHz (105.73 ± 3.71 mg GAE/100 g FW) on Day 2. Therefore, the 28 ± 2 kHz treatment was more suitable for fresh-cut red cabbages.

Effects of frequency amplitude on the content of soluble phenolics

The effects of frequency amplitude on the content of SPs in fresh-cut red cabbages are shown in **Figure 3A**. The 28 ± 2 kHz treatment (139.68 ± 1.06 mg GAE/100 g FW) significantly increased the content of SPs compared with the 28 ± 1 kHz treatment (134.65 ± 1.08 mg GAE/100 g FW) and control (134.22 ± 1.71 mg GAE/100 g FW) on Day 0 ($P < 0.05$), while there was no significant difference between the 28 ± 1 kHz treatment and control. Moreover, the content of SPs treated at 28 ± 2 kHz and 28 ± 1 kHz was significantly higher than the control during the following storage ($P < 0.05$), except for a decrease under the 28 ± 1 kHz treatment on Day 8. These results suggested that ±2 kHz was more conducive to the accumulation of phenolics in fresh-cut red cabbages. Frequency amplitude is one of the important factors that affect the quality of fruit and vegetables during the ultrasonic washing process (32). Wang et al. (42) also found that frequency amplitude could affect the stability of caffeic acid and erucic acid.

Effects of ultrasonic power density on the content of soluble phenolics

The effects of ultrasonic power density on the content of SPs in fresh-cut red cabbages are displayed in **Figure 3B**. The 60-W/L treatment showed the highest content of SPs (120.93 ± 3.34 mg GAE/100 g FW) compared with other treatments during the whole storage. Meanwhile, it can be found

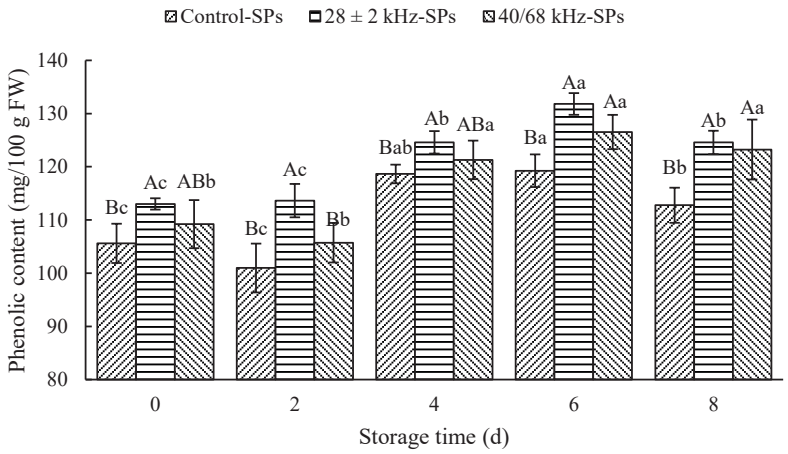

FIGURE 2
Effects of the optimal single-frequency and dual-frequency mode on the content of soluble phenolics (SPs) in fresh-cut red cabbages. The results represent the means of three triplicates ± standard deviations. Different capital letters mean that the effects of different treatments for the same day are significantly different ($P < 0.05$); different lowercase letters mean that the effects of storage times for the same treatment are significantly different ($P < 0.05$). Control: fresh-cut red cabbages were washed with sterile distilled water; treatment: ultrasonic power density of 60 W/L, frequency cycle time of 500 ms, and ultrasonic time of 15 min.

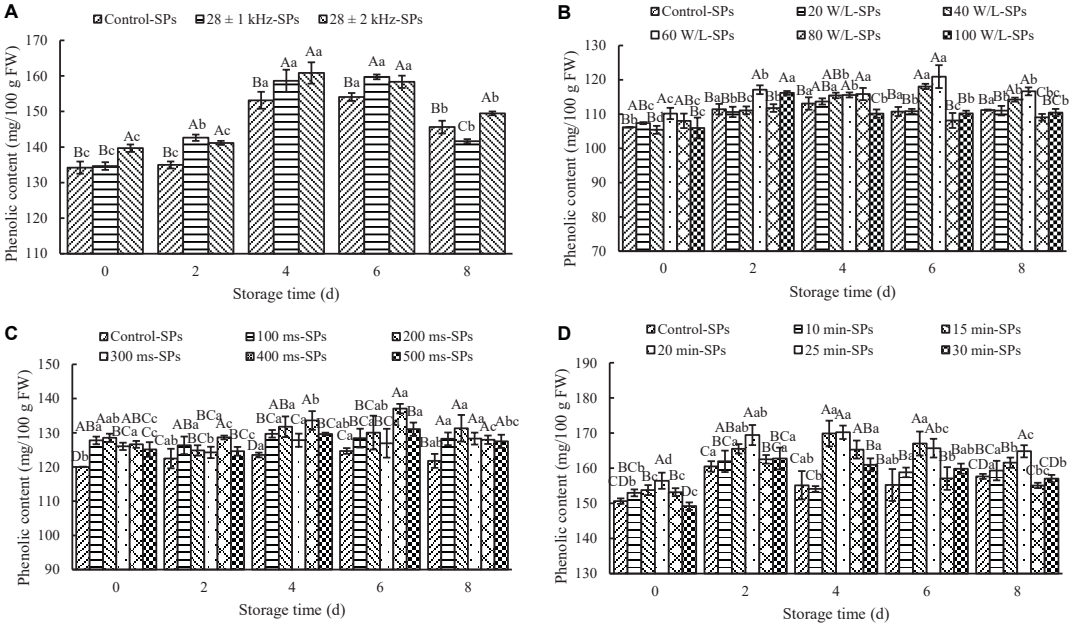

FIGURE 3
Effects of ultrasonic power density, frequency amplitude, frequency cycle time, and ultrasonic time on the content of soluble phenolics (SPs). The results represent the means of three triplicates ± standard deviations. Different capital letters mean that the effects of different treatments for the same day are significantly different ($P < 0.05$); different lowercase letters mean that the effects of storage times for the same treatment are significantly different ($P < 0.05$). **(A)** Frequency amplitude; treatment: ultrasonic power density of 60 W/L, frequency cycle time of 500 ms, and ultrasonic time of 15 min. **(B)** Ultrasonic power density; treatment: ultrasonic frequency mode of 28 ± 2 kHz, frequency cycle time of 500 ms, and ultrasonic time of 15 min. **(C)** Frequency cycle time; treatment: ultrasonic frequency mode of 28 ± 2 kHz, ultrasonic power density of 60 W/L, and ultrasonic time of 15 min. **(D)** Ultrasonic time; treatment: ultrasonic frequency mode of 28 ± 2 kHz, ultrasonic power density of 60 W/L, and frequency cycle time of 400 ms. Control: fresh-cut red cabbages were washed with sterile distilled water.

that excessively low or high power density was harmful to the accumulation of SPs in fresh-cut red cabbage. The content of SPs in fresh-cut red cabbages treated with a low power density (e.g., 20 W/L) showed no significant difference compared with the control during storage ($P > 0.05$). Meanwhile, high power density (e.g., 80 and 100 W/L) was not conducive to the

retention of phenolics during the later storage. Similar results were also found in Pinheiro et al. (43), Wang et al. (44), and Wu et al. (45). For example, Wang et al. (44) found that there was no significant difference in the content of SPs in cherry tomatoes between the 66.4 W/L treatment and control during storage ($P > 0.05$). Tomatoes treated with 145.79 W/L had lower content of SPs than the control during the later storage, while the content of SPs under the treatment of 106.19 W/L showed an increase during the later storage, and it was significantly higher than that in the control group on Day 20 ($P < 0.05$). Wu et al. (45) also found that the content of SPs in bok choy under the 150-W treatment and 180-W treatment significantly increased compared with the control ($P < 0.05$), while the 120-W treatment and 210-W treatment had no significant difference compared with the control ($P > 0.05$). Based on the results above, the ultrasonic power density of 60 W/L was selected as the optimal for further study.

Effects of frequency cycle time on the content of soluble phenolics

The frequency cycle time is one of the unique ultrasonic parameters in the sweep-frequency mode (32). The effects of frequency cycle time on the content of SPs in fresh-cut red cabbages are shown in **Figure 3C**. As can be seen from the figure, the frequency cycle time could affect the content of SPs, and an increase in the content of SPs can be observed for samples treated with different frequency cycle times compared to the control during the whole storage. The content of SPs at a short frequency cycle time (e.g., 100 and 200 ms) was remarkably higher than that at a long one (e.g., 500 ms) on Day 0. It may be due to the fact that a shorter sweep cycle means a faster change of sweep frequency, which produces a bigger vibration and strengthens the cavitation effects (42). Thus, the degree of hydroxylation in food materials was enhanced. However, the content of SPs at 400 ms markedly increased during the following storage. It reached the maximum value (137.06 ± 1.38 mg GAE/100 g FW) on Day 6, which was significantly higher than other treatments ($P < 0.05$). Based on the results above, the frequency cycle time of 400 ms was selected as the optimal for further study.

Effects of ultrasonic time on the content of soluble phenolics

The effects of ultrasonic time on the content of SPs in fresh-cut red cabbages are shown in **Figure 3D**. The content of SPs in ultrasound-treated samples increased with ultrasonic time until reaching the maximum at 20 min (156.42 ± 2.30 mg GAE/100 g FW) and then decreased with longer ultrasonic time on Day 0. The content of SPs under 30 min treatment was even lower than that of the control. On the one hand, the decrease in the content of SPs might result from the greater disruption of cell wall material and more inordinateness of inner structure caused by longer ultrasound treatment (46), leading to SPs draining away with the water during the process of ultrasonic washing. On the other hand, oxidation reactions promoted by the interaction with free radicals formed during sonication may be another reason for the degradation of phenolics (43). Additionally, the content of SPs in fresh-cut red cabbages treated for 20 min was the highest compared with other treatments throughout the storage. It firstly increased to the maximum on Day 4 and then decreased afterward. Moreover, it can be found that excessively short or long ultrasonic time was not conducive to the retention of the content of SPs in fresh-cut red cabbages. The content of SPs treated for 10 min had no significant difference compared with the control ($P > 0.05$), while the content of SPs after 30 min treatment was significantly lower than that of the 20 min treatment during storage ($P < 0.05$). Similar results were observed in the study of Lu et al. (47) and Gani et al. (48). For example, Gani et al. (48) found a significant increase in the content of SPs in strawberries as the ultrasonic time increased from 0 to 40 min during storage, followed by a decrease when the treatment time was increased to 60 min. Based on the results above, the optimal ultrasound treatment time was selected as 20 min for further study.

Effects of ultrasonic washing on the content of soluble phenolics

Based on the above results, it was found that appropriate ultrasonic washing could increase the content of SPs in fresh-cut red cabbages immediately or during storage. These results were consistent with the study of Yildiz et al. (24), Mustapha et al. (49), and Tovar-Pérez et al. (50). For example, Mustapha et al. (49) found that the SPs in ultrasound-treated cherry tomatoes increased with the prolongation of the storage period and was significantly higher than that in water-washed samples on Day 0 and Day 21 ($P < 0.05$). The immediate increase in the content of SPs after treatment mainly might be due to the increased extractability of phenolics, which may result from the hydroxylation of food materials caused by cavitation effects, especially flavonoids (31, 51, 52). Ashokkumar et al. (53) also reported that the hydroxylation of phenol and cyanidin 3-glucoside was initiated when treated by ultrasound. Meanwhile, as shown in **Supplementary Figures 4**, **5**A,B, the scanning electron micrograph of cross sections in the leaves showed that the fresh-cut red cabbages treated by optimized ultrasonic conditions showed no damage to the structural anatomy of the leaves compared to the control on Day 0. The undamaged leaf structure contributes to the retention of phenolics (46). The accumulation of phenolics in fresh-cut red cabbages during storage may be attributed to the fact that the biosynthesis rate of phenolics is higher than the consumption rate (22, 54, 55). On the one hand, the biosynthetic pathway of phenolics can be activated. It is widely acknowledged that plants subjected to postharvest abiotic stresses can undergo a series of events, resulting in the accumulation of molecules with health-promoting properties, such as phenolics, carotenoids, AA, and

glucosinolates (13, 14, 25, 56). When fruit and vegetables suffer from appropriate ultrasound treatment, wounded cells release adenosine triphosphate from the cytoplasm, which binds to unwounded cell receptors. The binding can elicit the production of secondary signaling molecules, such as reactive oxygen species (ROS), ethylene, and jasmonic acid. These secondary signals can activate the expression of primary and secondary metabolic genes, thus triggering the biosynthesis of phenolics (14, 56, 57). Additionally, the balance of ROS in fruit and vegetables can also be broken due to a large number of free radicals caused by acoustic cavitation (58). Therefore, the ROS scavenging systems in fruit and vegetables can be activated after ultrasonic washing. Phenolics, as one of the main components of non-enzymatic antioxidant systems, can be biosynthesized to eliminate excess ROS. It is because phenolics have dynamic antioxidant properties which neutralize the consequences produced by oxidative stress (59, 60). On the other hand, the consumption rate of phenolics after ultrasonic washing may be inhibited. Firstly, fewer phenolics can be used for lignin biosynthesis after ultrasonic washing. Phenolics are considered the precursors for lignin biosynthesis (22). Hence, the reduction of lignin content means less loss of phenolics (54). For example, Wang and Fan (61) reported that the biosynthesis of lignin in green asparagus subjected to ultrasonic washing was effectively retarded compared to the untreated ones. The delay of lignin biosynthesis was conducive to the retention of phenolics. Secondly, the activities of enzymes involved in the oxidative degradation of phenolics subjected to ultrasound treatment can be inhibited, such as polyphenol oxidase (PPO) and peroxidase (POD) (62). However, it was also found that inappropriate ultrasonic washing after fresh-cutting could decrease the content of SPs of red cabbages immediately and even reduce the cutting-induced accumulation of phenolics during storage. Similar results were found in the study of Cuéllar-Villarreal et al. (28), in which the level of total phenolics in ultrasound-treated carrots (300 s) was significantly lower than that in the control ones. It is likely that phenolics are released from the food matrix into the water due to ultrasound-induced damage to tissues (63). Additionally, the cutting-stress signals that induce the biosynthesis of phenolics may be removed by ultrasonic washing, causing the reduction of the cutting-induced accumulation of phenolics (64).

Analysis of the activities of phenylalanine ammonia-lyase, polyphenol oxidase, and peroxidase

The changes in the activities of PAL, PPO, and POD in fresh-cut red cabbages treated by ultrasonic washing are shown in **Figure 4**. As shown in **Figure 4A**, the PAL activity of fresh-cut red cabbages with or without ultrasonic washing showed the tendency to first rise and then decline with the extension of the shelf-life, reaching the maximums on Day 2. In addition, the PAL activity of fresh-cut red cabbages after ultrasound treatment increased significantly compared with the control ($P < 0.05$). PAL plays a critical role in the phenylpropanoid cycle, which contributes to the conversion of *L*-phenylalanine to trans-cinnamic acid with ammonia elimination and induces the biosynthesis of various phenylpropanoid-derived secondary products, such as SPs (65). Therefore, the increase in PAL activity is conducive to the biosynthesis of phenolics. The results shown in **Figure 4A** and **Figure 3D** indicated that the change trends of PAL and SPs were similar. However, the changes in the content of SPs performed a more noticeable lag effect than PAL changes. Similar lag effects were also observed in the study of Zhu et al. (66), in which they found that the changes in the SPs of fresh-cut potato slices at different ultrasound treatments were similar to the changes in the PAL activity and were delayed to a certain extent. PAL has been considered an inducible enzyme under biotic and abiotic stress (65). Therefore, cutting may be responsible for the increase of PAL activity of fresh-cut red cabbages in early storage. For example, Heredia and Cisneros-Zevallos (67) found that cutting could induce the activity of PAL in carrots and the PAL activity increased with wounding intensity. Whereas the decrease in PAL activity during the later storage may be due to aging and browning consumption till the end (68). Additionally, PAL activity has also been proposed to play a significant role in the plant defense against ultrasound stress, such as fresh-cut pineapples, Roman lettuces, carrots, Lentinula edodes, and cherry tomatoes (27, 28, 69–71). It might be because the formation of free radicals due to the sonolysis of water may impose oxidative stress on the plant cell systems and induce higher PAL activity to protect the cells from oxidative damage (27). Therefore, the PAL activity and the content of SPs in ultrasound-treated fresh-cut red cabbages were induced at higher levels under the combined mechanical and oxidative stress injury during storage.

According to **Figure 4B**, the PPO activity after ultrasonic washing was significantly lower than that in control samples during the whole storage ($P < 0.05$), except on Day 2. Similarly, the POD activity in control samples was also relatively higher than that in ultrasound-treated ones throughout the cold storage (as shown in **Figure 4C**). The POD activity in fresh-cut red cabbages with or without ultrasonic washing increased firstly and then remained stable with the extension of storage time. The POD activity during the later stage (e.g., on Day 6 and Day 8) significantly increased compared with that on Day 0, which may be related to tissue senescence (44, 72). Based on the results above, it was found that both the PPO and POD activities in fresh-cut red cabbages subjected to ultrasonic washing could be inhibited throughout the cold storage. Similar results were found in the study of Yeoh and Ali (27) and Pan et al. (68). For example, Yeoh and Ali (27) demonstrated that PPO and POD activities in fresh-cut pineapples were suppressed by ultrasound treatments, which supported our results. Thus, the browning

10.3389/fnut.2022.1006440

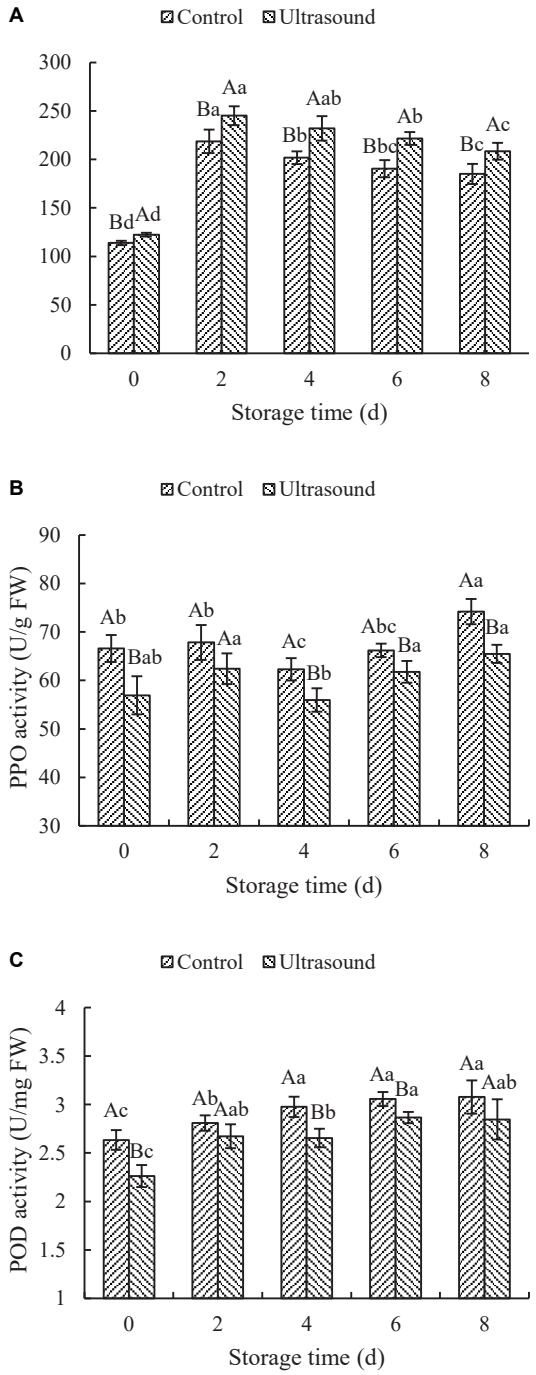

FIGURE 4
Effects of ultrasonic washing on the activities of phenylalanine ammonia-lyase (PAL) **(A)**, polyphenol oxidase (PPO) **(B)**, and peroxidase (POD) **(C)**. The results represent the means of three triplicates ± standard deviations. Different capital letters mean that the effects of different treatments for the same day are significantly different ($P < 0.05$); different lowercase letters mean that the effects of storage times for the same treatment are significantly different ($P < 0.05$). Control: fresh-cut red cabbages were washed with sterile distilled water; ultrasound treatment: ultrasonic frequency mode of 28 ± 2 kHz, ultrasonic power density of 60 W/L, frequency cycle time of 400 ms, and ultrasonic time of 20 min.

inhibition of fresh-cut red cabbages after ultrasound treatment was exerted by reducing the activity of PPO and POD, which were typical enzymes involved in browning. It is universally acknowledged that phenolics can act as hydrogen donors to participate in the decomposition reaction of hydrogen peroxide catalyzed by POD, and PPO can convert phenolics into quinones (65). The phenolic content in fruit and vegetables correlates with the PPO and POD activities, and the higher levels of PPO and POD activities can cause more consumption of phenolic content. Therefore, the decrease in the content of SPs in fresh-cut red cabbages during the later storage may result from high levels of PPO and POD activities. Meanwhile, the consumption of SPs of fresh-cut red cabbages after ultrasonic washing was inhibited due to the inhibition of PPO and POD activities, which consequently resulted in higher content of SPs in ultrasound-treated fresh-cut red cabbages in comparison to control. The physiological enzyme activity can be activated and passivated by ultrasound treatment. The enzyme inhibition effect of ultrasound treatment depends on the chemical structure of proteins and the tolerance of enzymes to ultrasound (73). The inhibition of PPO and POD activities after ultrasound treatment may result from the physical and chemical effects of cavitation, which produce shear forces to break down the Van der Waals forces and hydrogen bonding of polypeptide chains, leading to the modification of enzyme structures (74).

Analysis of quality parameters

Effects of ultrasonic washing on weight retention rate and respiration rate

The changes in the weight of ultrasound-treated fresh-cut red cabbages during storage are shown in **Figure 5A**. Weight is considered an important indicator in evaluating the quality of postharvest fruit and vegetables, and its reduction reflects water loss during storage (75). As seen in **Figure 5A**, the weight of fresh-cut red cabbages increased significantly after ultrasonic washing ($P < 0.05$). It is probably because the mass transfer of water from the liquid medium to the samples can be promoted by ultrasound. Similar results were also observed in the study of Wang et al. (76), in which carrot slices immersed in distilled water gained more water after processing with low-frequency ultrasound treatment than untreated samples. Moreover, as shown in **Figure 5A**, the weight retention rate of fresh-cut red cabbages after ultrasonic washing was significantly higher than that of control during the whole storage, although the weight of fresh-cut red cabbage decreased with the increase of storage time ($P < 0.05$). Lower weight loss was observed in the ultrasound-treated samples. The epidermal cells in the leaves of fresh-cut red cabbages had higher water content compared with that in control ones (as shown in **Supplementary Figure 5**). It might be because the water molecules were confined by hydrogen bonds, which decreased the loss of water (36). Similarly, Fan et al.

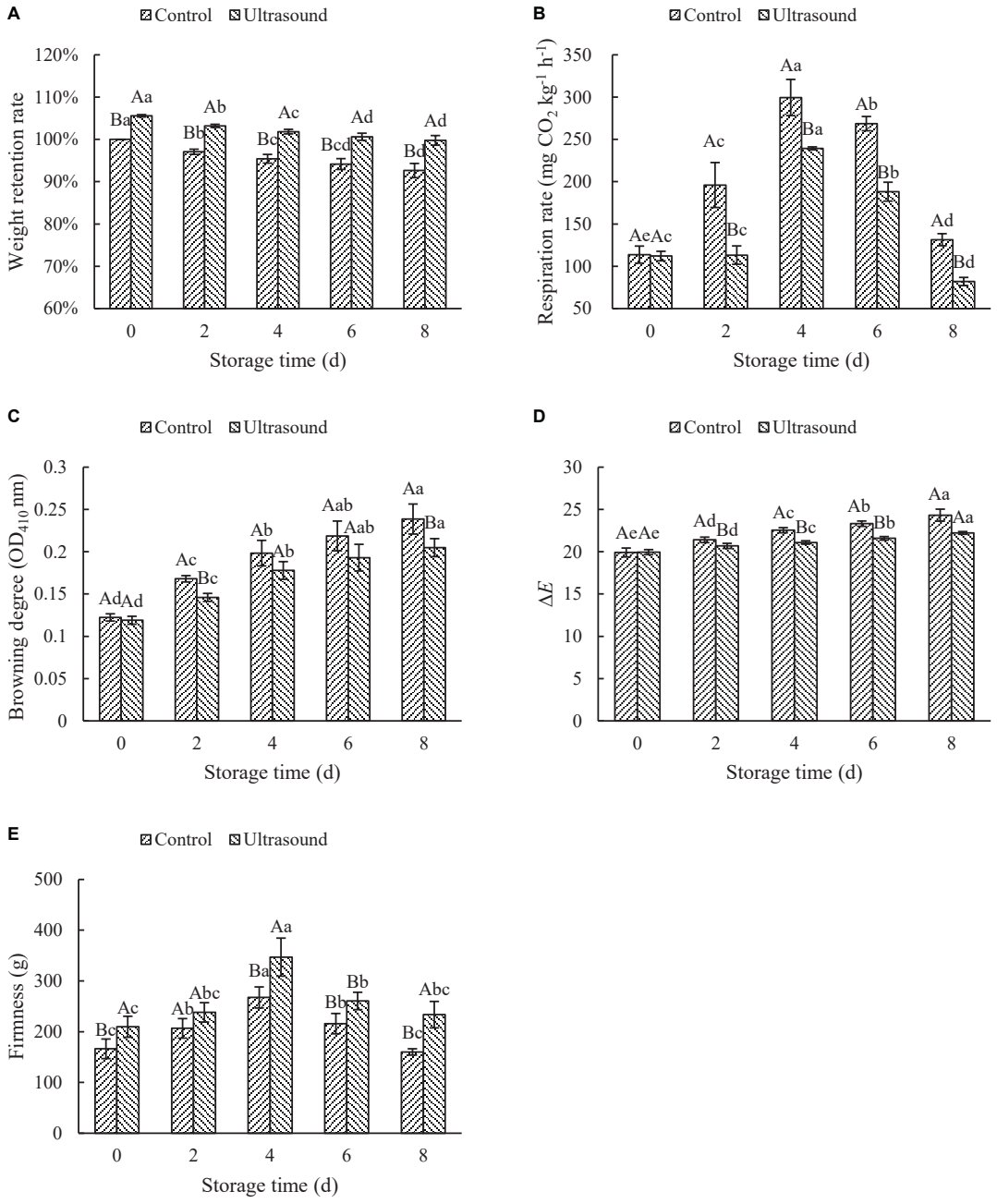

FIGURE 5
Effects of ultrasonic washing on the weight retention rate **(A)**, respiration rate **(B)**, color **(C,D)**, and firmness **(E)**. The results represent the means of three triplicates ± standard deviations. Different capital letters mean that the effects of different treatments for the same day are significantly different ($P < 0.05$); different lowercase letters mean that the effects of storage times for the same treatment are significantly different ($P < 0.05$). Control: fresh-cut red cabbages were washed with sterile distilled water; ultrasound treatment: ultrasonic frequency mode of 28 ± 2 kHz, ultrasonic power density of 60 W/L, frequency cycle time of 400 ms, and ultrasonic time of 20 min.

(77) also found that the water loss of fresh-cut lettuces after ultrasonic washing was reduced compared with the control.

Respiration rate is an important parameter in determining deterioration rate and the onset of senescence, which is proportional to product deterioration rate and inversely proportional to its shelf-life. As shown in **Figure 5B**, the respiratory rate of fresh-cut red cabbages with or without ultrasonic washing increased firstly and then decreased during storage, reaching the maximum on Day 4. The increase in the respiratory rate at the initial storage stage might be due to the cutting (mechanical damages), which boosted the respiratory rate (78). Whereas the decrease of it during

the later storage may result from the large consumption of materials in the early storage (e.g., sugars and O_2), which inhibited the respiration rate. Li et al. (36) also found that the activities of enzymes involved in respiration (e.g., succinic dehydrogenase, glucose-6-phosphate dehydrogenase, and 6-phosphogluconate dehydrogenase) increased firstly and then decreased with the extension of storage time, which may be another other reason for the changes in the respiration rate. Additionally, the respiration rate after ultrasonic washing was significantly lower than that of the control ($P < 0.05$). Similar results were also found in other vegetables subjected to ultrasonic washing, such as lettuces, white mushrooms, straw mushrooms, and asparaguses (36, 74, 79, 80). On the one hand, the lower respiration rate can be attributed to the hydrogen peroxide formation in distilled water during sonication, which reduces the oxygen used for respiration (81). On the other hand, ultrasonic washing can decrease the activities of respiration enzymes, thus reducing the respiration rate (36). Li et al. (36) found that ultrasound treatment could inhibit respiratory rates *via* inactivating the activities of enzymes involved in respiratory pathways of straw mushrooms, including phosphohexoisomerase, succinic dehydrogenase, glucose-6-phosphate dehydrogenase, 6-phosphogluconate dehydrogenase, and cytochrome oxidase. Moreover, more stomata in the leaves of fresh-cut red cabbages after ultrasonic washing were closed since epidermal cells with high water content squeezed the guard cells (as shown in **Supplementary Figure 5**). The closure of stomata reduced the respiration rate of fresh-cut red cabbages, which may also contribute to the retention of water during storage. Therefore, ultrasound treatment could effectively inhibit the respiration rate of fruit and vegetables to improve storage quality. However, it was found that ultrasound could increase the respiration rate in previous literature (28). Inconsistent results could be explained by the differences in ultrasonic conditions (e.g., frequency, time, and power output) and types of fruit and vegetables (30, 44).

Effects of ultrasonic washing on color and firmness

Color is one of the most important factors that reflect the appearance quality of fresh-cut fruit and vegetables, which directly affects the purchase intention of the consumers. Browning is a particular problem for white-fleshed fresh-cut products including red cabbages due to the oxidations of phenolics triggered by polyphenol oxidase (39). The effects of ultrasonic washing on the browning degree and total color difference (ΔE) of fresh-cut red cabbages during storage are shown in **Figures 5C,D**. There was no significant difference in browning degree and ΔE between the ultrasound and control samples on Day 0. Then the browning degree and ΔE with or without ultrasonic washing showed an increasing trend with the extension of storage time, and the fresh-cut red cabbages treated by ultrasound showed a significantly lower browning degree and ΔE values compared with the control ($P < 0.05$). The results suggested that ultrasonic washing could effectively inhibit the browning of fresh-cut red cabbages during storage and maintain the appearance of the color (as shown in **Supplementary Figure 6**). These results were consistent with the conclusions of Li et al. (36), Yildiz et al. (39), and Wen et al. (82). For example, Wen et al. (82) observed a noticeable increase in whiteness index, a decrease in the browning index, and lower ΔE values in ultrasound-treated fresh-cut lotus roots compared to the control during storage. These phenomena might result from the changes in PPO and POD activity related to the browning (36). Qiao et al. (29) also found that the PPO and POD activity in fresh-cut potatoes were inhibited by ultrasound washing, thus alleviating the enzymatic browning during storage.

Firmness is an important determinant of textural quality that affects consumer preference and the acceptability of fresh-cut fruit and vegetables. The changes in firmness depend on the cell turgor pressure, the integrity of the cell wall, and intercellular adhesion (12). As shown in **Figure 5E**, the firmness of fresh-cut red cabbages with or without ultrasonic washing rose to the maximum on Day 4, followed by a decrease with the increase in storage time. Fresh-cut red cabbages treated by ultrasound exhibited higher firmness than the control during storage. Similarly, Gani et al. (48) also found that the firmness of strawberries treated by ultrasonic washing for 10–40 min rose firstly and then declined with the increasing storage time. Fruit firmness under ultrasound treatment was higher than untreated samples throughout all refrigerated storage. Likewise, Yu et al. (69) also observed that lettuces treated by ultrasound showed higher firmness than the water-washed ones during storage, and the firmness increased with the storage time. The optimized ultrasound treatment did not affect the structural anatomy of the leaves as mentioned before, which was beneficial to maintain the texture characteristics. The increase in firmness may be due to the fact that the self-recovery system of plants was initiated when treated with ultrasound and the production of phenolic compounds might help the plants regain tissue firmness (69). Additionally, another possible reason is that ultrasound treatment inhibits the activities of enzymes that are mainly responsible for fruit softening, such as pectin methylesterase and polygalacturonase (83). However, the loss of firmness at the later stage of storage is most often attributed to the enzymatic breakdown of the middle lamella and cell wall by pectin methylesterase, polygalacturonase, β-galactosidase, and cellulase (84). Moreover, the water of leaves also influences the firmness of fruit and vegetables. Softening of fruit and vegetables is relatively attributed to a considerable increase in water loss through respiration (85, 86). The loss of turgor of the cell (loss of water) can produce dehydration of the tissues, an increase in elasticity, and a decrease in firmness (87), especially at the end of the storage (as shown in **Supplementary Figures 5E,F**). However, further studies are needed to monitor the moisture loss of fruit and vegetables

TABLE 2 Effects of ultrasonic washing on the contents of ascorbic acid (AA), total soluble proteins (TSPs), total soluble sugars (TSSs), and total soluble solids (SSs) in fresh-cut red cabbages during 4°C storage.

Nutrient	Treatment	Storage time				
		Day 0	Day 2	Day 4	Day 6	Day 8
AA (mg/100 g FW)	Control	83.16 ± 2.29^{Ac}	85.97 ± 3.69^{Abc}	91.38 ± 3.19^{Ba}	89.62 ± 3.65^{Aab}	89.61 ± 2.37^{Aab}
	Ultrasound	85.99 ± 1.92^{Ad}	88.61 ± 2.74^{Acd}	99.46 ± 3.17^{Aa}	93.21 ± 3.28^{Ab}	92.58 ± 4.09^{Abc}
TSPs (mg/g FW)	Control	2.07 ± 0.21^{Ac}	2.45 ± 0.06^{Ab}	2.24 ± 0.25^{Bbc}	2.88 ± 0.12^{Ba}	2.78 ± 0.15^{Aa}
	Ultrasound	2.09 ± 0.16^{Ad}	2.44 ± 0.08^{Ac}	2.59 ± 0.12^{Ac}	3.41 ± 0.11^{Aa}	3.02 ± 0.21^{Ab}
TSSs (g/g FW)	Control	30.31 ± 1.05^{Aa}	27.49 ± 1.19^{Ab}	24.15 ± 1.16^{Ac}	22.70 ± 0.87^{Bc}	22.68 ± 1.59^{Bc}
	Ultrasound	30.85 ± 1.45^{Aa}	28.01 ± 1.14^{Ab}	25.75 ± 1.03^{Ac}	24.99 ± 1.15^{Ac}	25.08 ± 0.97^{Ac}
SSs (%)	Control	0.50 ± 0.02^{Aa}	0.48 ± 0.02^{Ba}	0.50 ± 0.01^{Aa}	0.34 ± 0.03^{Bc}	0.30 ± 0.01^{Bd}
	Ultrasound	0.49 ± 0.03^{Ab}	0.53 ± 0.02^{Aa}	0.52 ± 0.02^{Aab}	0.45 ± 0.03^{Ac}	0.40 ± 0.02^{Ad}

The results represent the means of three triplicates ± standard deviations. Different capital letters mean that the effects of different treatments for the same day are significantly different ($P < 0.05$); different lowercase letters mean that the effects of storage times for the same treatment are significantly different ($P < 0.05$). Control: fresh-cut red cabbages were washed with sterile distilled water; ultrasound: ultrasonic frequency mode of 28 ± 2 kHz, ultrasonic power density of 60 W/L, frequency cycle time of 400 ms, and ultrasonic time of 20 min. FW, fresh weight.

subjected to ultrasonic washing and its relation to texture characteristics during storage.

Effects of ultrasonic washing on the contents of ascorbic acid, total soluble proteins, total soluble sugars, and total soluble solids

The AA content is an important index to evaluate the nutritional value of fruit and vegetables (36). As shown in Table 2, although the AA content of fresh-cut red cabbages after ultrasonic washing was higher than that of the control ones, there was only a significant difference on Day 4 during storage ($P < 0.05$). Similarly, Wang et al. (44) also found that the AA content of cherry tomatoes treated with ultrasonic washing at 106.19 and 145.74 W/L was significantly higher than that of the control on Day 8 or Day 16 ($P < 0.05$), while there was no significant difference during other storage time. The higher retention rate of AA content in fruit and vegetables after ultrasonic washing can be attributed to the removal of dissolved oxygen caused by the cavitation effects of ultrasound, which inhibited the oxidation of AA (23, 61). Furthermore, the inactivation of fruit enzymes induced by ultrasound treatment, e.g., AA oxidase and lipoxygenase, maybe another reason to prevent the degradation of AA (11). However, it is also found that ultrasonic washing has no effects on AA content in some fruit and vegetables, and sometimes even has negative effects (88). Overall, current reports regarding the effects of ultrasound on AA content in fruit and vegetables have been controversial. These differences could be attributed to variations in species, treatments, and analytical methods.

Proteins are considered nutrient sources to support the physiological metabolisms of fruit and vegetables and are important to the evaluation of nutrition and quality. As shown in Table 2, the content of TSPs in fresh-cut red cabbages subjected to ultrasonic washing was higher than that of the control during the later storage, especially on Day 4 and Day 6. Similar results were also observed in the study of Li et al. (36), in which 10-min ultrasonic washing could effectively prevent the utilization of TSPs in straw mushrooms, thus retaining more TSPs compared with the control. Therefore, ultrasonic washing can contribute to the retention of proteins in fruit and vegetables. However, there are rare reports on the mechanisms that explain the effects of ultrasound on the proteins of fruit and vegetables. More retention of TSPs after ultrasound treatment can be explained by the inhibition of enzymes related to protein degradation, such as succinic dehydrogenase and lipoxygenase (11, 36). Consequently, the oxidation and catabolism of amino acids were suppressed, improving the retention.

Sugars are important energy sources of fruit and vegetables, mainly involved in the carbohydrate metabolisms in cells. Effects of ultrasonic washing on the content of TSSs are shown in Table 2. The content of TSSs in fresh-cut red cabbages with or without ultrasonic washing declined gradually with the prolonged storage time. At the end of the storage time, fresh-cut red cabbages treated with ultrasound showed higher content of TSSs compared with the control. Similarly, Li et al. (36) also found that ultrasound treatment could notably retain the content of TSSs in straw mushrooms and reduce their consumption. Therefore, the degradation of TSSs in fruit and vegetables can be alleviated after ultrasonic washing, which is beneficial to the maintenance of quality. The consumption of sugars is generally related to normal metabolic processes, especially respiratory rate (85, 89, 90). It can be found that more TSSs of fresh-cut red cabbages were consumed with the increase in the respiratory rate at the beginning of the storage time. The consumption of TSSs was reduced when the respiratory rate of samples was inhibited with ultrasound. Moreover, Fan et al. (75) thought that the activity of enzymes related to carbohydrate metabolisms could be inhibited by the cavitation effects of ultrasound, causing more reservations of sugars. Similarly, Li et al. (36) also found that the activities

TABLE 3 Effects of ultrasonic washing on the microorganisms of fresh-cut red cabbages during 4°C storage.

Microorganism	Treatment	The number of microorganisms during storage (log_{10} CFU/g)				
		Day 0	Day 2	Day 4	Day 6	Day 8
Bacteria	Control	2.57 ± 0.03^{Ae}	3.23 ± 0.01^{Ad}	4.01 ± 0.05^{Ac}	4.95 ± 0.03^{Ab}	5.53 ± 0.05^{Aa}
	Ultrasound	2.23 ± 0.07^{Be}	2.99 ± 0.01^{Bd}	3.66 ± 0.05^{Bc}	3.96 ± 0.03^{Bb}	4.67 ± 0.05^{Ba}
Molds and yeasts	Control	1.63 ± 0.05^{Ae}	2.19 ± 0.02^{Ad}	2.89 ± 0.05^{Ac}	3.16 ± 0.02^{Ab}	3.71 ± 0.03^{Aa}
	Ultrasound	1.19 ± 0.06^{Be}	1.94 ± 0.02^{Bd}	2.12 ± 0.02^{Bc}	2.64 ± 0.05^{Bb}	2.84 ± 0.03^{Ba}

The results represent the means of three triplicates ± standard deviations. Different capital letters mean that the effects of different treatments for the same day are significantly different ($P < 0.05$); different lowercase letters mean that the effects of storage times for the same treatment are significantly different ($P < 0.05$). Control: fresh-cut red cabbages were washed with sterile distilled water; ultrasound: ultrasonic frequency mode of 28 ± 2 kHz, ultrasonic power density of 60 W/L, frequency cycle time of 400 ms, and ultrasonic time of 20 min.

of enzymes involved in the glycolytic pathway and hexose monophosphate pathway of straw mushrooms were inhibited by ultrasound treatment, including phosphohexoisomerase, glucose-6-phosphate dehydrogenase, and 6-phosphogluconate dehydrogenase.

The changes in the content of SSs in fresh-cut red cabbages after ultrasonic washing are shown in Table 2. The content of SSs in ultrasound-treated samples increased firstly and then decreased with the prolonged storage time, and it was significantly higher than that in the control ones at the end of storage time. Similar results were also found in the study of Temizkan et al. (90), in which the content of SSs in white nectarines treated with ultrasound at 300 W increased firstly until reaching the maximum on Day 5 and then decreased, and the values were significantly higher than the control ones during the storage time from Day 10 to Day 45. Higher content of SSs may be associated with lower metabolisms, i.e., reduced respiration and delayed senescence (91). The decrease in the content of SSs during the later storage may result from the consumption of respiration (90). In addition, Wang and Fan (61) also thought that the high retention of SSs in green asparaguses subjected to ultrasonic washing was due to the inactivation of enzymes related to metabolisms caused by ultrasound treatment. The activities of enzymes mentioned above involved in respiration and carbohydrate metabolisms were suppressed, thus reducing the consumption of SSs.

Analysis of microbial safety

Cutting can increase the contact area between the microorganisms and fruit and vegetables. Meanwhile, the juice flowing from shredded tissues can provide favorable breeding conditions for microorganisms, increasing food corruption and quality deterioration (8, 9, 92). The effects of ultrasonic washing on the microorganisms in fresh-cut red cabbages during storage are shown in Table 3. At the initial storage stage, fresh-cut red cabbages with or without ultrasonic washing showed a low total number of bacteria, molds and yeasts, and then they presented a rapid growth with the increase in storage time. However, the microbial numbers after ultrasonic washing were significantly lower than the control during storage ($P < 0.05$). The total number of bacteria, molds and yeasts in ultrasound samples on Day 8 (4.57 ± 0.05 and 2.84 ± 0.05 log_{10} CFU/g, respectively) were even lower than the control ones on Day 6 (4.95 ± 0.03 and 3.16 ± 0.02 log_{10} CFU/g, respectively). The decrease in the number of microorganisms might be due to the bactericidal effects and shock effects of ultrasound (93). Microorganisms can be inactivated by cavitation effects to some extent due to high temperature, high pressure, and free radicals produced by bubble explosion (21). Meanwhile, powerful jets produced by the collapse of cavitation bubbles would dislodge microorganism cells on the fruit surface (83). All of these can reduce the number of microorganisms after ultrasonic washing. Similar phenomena have been observed in cucumbers, bok choy, lettuces, kiwifruit, and quince (24, 39, 45, 75, 77). Therefore, ultrasonic washing can slow down the growth of microorganisms and reduce the decay incidence of fresh-cut red cabbages.

Conclusion

In order to evaluate the feasibility of ultrasonic washing on the phenolic accumulation in fresh-cut red cabbages, the effects of ultrasound operating parameters on the phenolics were studied by single-factor tests. The optimal ultrasonic washing conditions, i.e., single-sweep frequency of 28 ± 2 kHz, power density of 60 W/L, frequency cycle time of 400 ms, and ultrasonic time of 20 min, were obtained, under which the content of soluble phenolics (SPs) was significantly increased compared with the control ($P < 0.05$). The activity of phenylalanine ammonia-lyase (PAL) related to phenolic biosynthesis after ultrasonic washing increased markedly during the whole storage, whereas the polyphenol oxidase (PPO) and peroxidase (POD) related to phenolic degradation decreased remarkably. Meanwhile, the storage quality of fresh-cut red cabbages under the optimized ultrasonic washing was improved, including reduced weight loss, decreased respiration rate, alleviated browning, and increased firmness. Besides, more AA,

TSPs, TSSs, and SSs of fresh-cut red cabbages were retained during storage. Moreover, the growth of microorganisms was inhibited by ultrasonic washing, thus improving the edible safety of fresh-cut red cabbages and prolonging their shelf-life. In conclusion, ultrasonic washing could be used as an abiotic elicitor to increase the phenolics of fresh-cut red cabbages during storage and improve the storage quality and microbial safety simultaneously. Therefore, ultrasonic washing is promising to represent as an alternative sanitization step for fruit and vegetables to develop high quality and extended shelf-life of ready-to-eat fresh fruit and vegetables. However, further studies are needed to elucidate the accumulation of phenolics in fruit and vegetables caused by ultrasound stress because phenolics can be affected by various factors, such as the types of fruit and vegetables and treatment conditions. Additionally, the mechanisms underlying the enhancement of phenolic content after ultrasonic washing also need to be further explored, which is useful to regulate the defense systems of fruit and vegetables to obtain improved nutritional quality.

Data availability statement

The original contributions presented in this study are included in the article/**Supplementary material**, further inquiries can be directed to the corresponding authors.

Author contributions

CH contributed to the conceptualization, methodology, formal analysis, and writing—original draft. Y-MZ and H-CZ contributed to the writing—review and editing. HM contributed to the conceptualization, resources, and supervision. All authors contributed to the article and approved the submitted version.

Funding

We acknowledge the financial support of the National Natural Science Foundation of China (No. 32072353) and the Senior Talent Program of Jiangsu University (No. 5501360012).

Conflict of interest

The authors declare that the research was conducted in the absence of any commercial or financial relationships that could be construed as a potential conflict of interest.

Publisher's note

All claims expressed in this article are solely those of the authors and do not necessarily represent those of their affiliated organizations, or those of the publisher, the editors and the reviewers. Any product that may be evaluated in this article, or claim that may be made by its manufacturer, is not guaranteed or endorsed by the publisher.

Supplementary material

The Supplementary Material for this article can be found online at: https://www.frontiersin.org/articles/10.3389/fnut.2022.1006440/full#supplementary-material

References

1. Podsêdek A, Sosnowska D, Redzynia M, Anders B. Antioxidant capacity and content of *Brassica oleracea* dietary antioxidants. *Int J Food Sci Technol.* (2006) 41:49–58. doi: 10.1111/j.1365-2621.2006.01260.x

2. Cartea ME, Francisco M, Soengas P, Velasco P. Phenolic compounds in *Brassica* vegetables. *Molecules.* (2010) 16:251–80. doi: 10.3390/molecules16010251

3. Gómez-Maqueo A, Escobedo-Avellaneda Z, Welti-Chanes J. Phenolic compounds in Mesoamerican fruits—characterization, health potential and processing with innovative technologies. *Int J Mol Sci.* (2020) 21:8357. doi: 10.3390/ijms21218357

4. Rashmi BH, Negi SP. Phenolic acids from vegetables: a review on processing stability and health benefits. *Food Res Int.* (2020) 136:109298. doi: 10.1016/j.foodres.2020.109298

5. Montenegro-Landívar MF, Tapia-Quirós P, Vecino X, Reig M, Valderrama C, Granados M, et al. Polyphenols and their potential role to fight viral diseases: an overview. *Sci Total Environ.* (2021) 801:149719. doi: 10.1016/j.scitotenv.2021.149719

6. Şengül M, Yildiz H, Kavaz A. The effect of cooking on total polyphenolic content and antioxidant activity of selected vegetables. *Int J Food Prop.* (2013) 17:481–90. doi: 10.1080/10942912.2011.619292

7. Podsêdek A. Natural antioxidants and antioxidant capacity of *Brassica* vegetables: a review. *LWT Food Sci Technol.* (2007) 40:1–11. doi: 10.1016/j.lwt.2005.07.023

8. Gil MI, Selma MV, López-Gálvez F, Allende A. Fresh-cut product sanitation and wash water disinfection: problems and solutions. *Int J Food Microbiol.* (2009) 134:37–45. doi: 10.1016/j.ijfoodmicro.2009.05.021

9. Ramos B, Miller FA, Brandão TRS, Teixeira P, Silva CLM. Fresh fruits and vegetables—an overview on applied methodologies to improve its quality and safety. *Innov Food Sci Emerg Technol.* (2013) 20:1–15. doi:10.1016/j.ifset.2013.07.002

10. São José JFBD, Vanetti MCD. Application of ultrasound and chemical sanitizers to watercress, parsley and strawberry: microbiological and physicochemical quality. *LWT Food Sci Technol.* (2015) 63:946–52. doi: 10.1016/j.lwt.2015.04.029

11. São José JFBD, Andrade NJD, Ramos AM, Vanetti MCD, Stringheta PC, Chaves JBP. Decontamination by ultrasound application in fresh fruits and vegetables. *Food Control.* (2014) 45:36–50. doi: 10.1016/j.foodcont.2014.04.015

12. Wu S, Nie Y, Zhao J, Fan B, Huang X, Li X, et al. The synergistic effects of low-concentration acidic electrolyzed water and ultrasound on the storage quality

of fresh-sliced button mushrooms. *Food Bioproc Tech.* (2017) 11:314–23. doi: 10.1007/s11947-017-2012-2

13. Denoya GI, Colletti AC, Vaudagna SR, Polenta GA. Application of non-thermal technologies as a stress factor to increase the content of health-promoting compounds of minimally processed fruits and vegetables. *Curr Opin Food Sci.* (2021) 42:224–36. doi: 10.1016/j.cofs.2021.06.008

14. Jacobo-Velázquez DA, Cuellar-Villarreal MD, Welti-Chanes J, Cisneros-Zevallos L, Ramos-Parra PA, Hernández-Brenes C. Nonthermal processing technologies as elicitors to induce the biosynthesis and accumulation of nutraceuticals in plant foods. *Trends Food Sci Technol.* (2017) 60:80–7. doi: 10.1016/j.tifs.2016.10.021

15. Sudheer S, Yeoh WK, Manickam S, Ali A. Effect of ozone gas as an elicitor to enhance the bioactive compounds in *Ganoderma lucidum*. *Postharvest Biol Technol.* (2016) 117:81–8. doi: 10.1016/j.postharvbio.2016.014

16. Bilek SE, TurantaŞ F. Decontamination efficiency of high power ultrasound in the fruit and vegetable industry, a review. *Int J Food Microbiol.* (2013) 166:155–62. doi: 10.1016/j.ijfoodmicro.2013.06.028

17. Chen F, Zhang M, Yang CH. Application of ultrasound technology in processing of ready-to-eat fresh food: a review. *Ultrason Sonochem.* (2020) 63:104853. doi: 10.1016/j.ultsonch.2019.104953

18. Yasui K. *Acoustic Cavitation and Bubble Dynamics*. Cham: Springer International Publishing (2018). doi: 10.1007/978-3-319-68237-2

19. Yuan S, Li C, Zhang Y, Yu H, Xie Y, Guo Y, et al. Ultrasound as an emerging technology for the elimination of chemical contaminants in food: a review. *Trends Food Sci Technol.* (2021) 109:374–85. doi: 10.1016/j.tifs.2021.01.048

20. Azam SMR, Ma H, Xu B, Devi S, Siddique MAB, Stanley SL, et al. Efficacy of ultrasound treatment in the removal of pesticide residues from fresh vegetables: a review. *Trends Food Sci Technol.* (2020) 97:417–32. doi: 10.1016/j.tifs.2020.01.028

21. Jiang Q, Zhang M, Xu B. Application of ultrasonic technology in postharvested fruits and vegetables storage: a review. *Ultrason Sonochem.* (2020) 69:105261. doi: 10.1016/j.ultsonch.2020.105261

22. Aguilar-Camacho M, Welti-Chanes J, Jacobo-Velázquez DA. Combined effect of ultrasound treatment and exogenous phytohormones on the accumulation of bioactive compounds in broccoli florets. *Ultrason Sonochem.* (2018) 50:289–301. doi: 10.1016/j.ultsonch.2018.09.031

23. Yildiz G, Aadil RM. Comparative analysis of antibrowning agents, hot water and high-intensity ultrasound treatments to maintain the quality of fresh-cut mangoes. *J Food Sci Technol.* (2021) 59:202–11. doi: 10.1007/s13197-021-05001-y

24. Yildiz G, Yildiz G, Khan MR, Aadil RM. High-intensity ultrasound treatment to produce and preserve the quality of fresh-cut kiwifruit. *J Food Process Preserv.* (2022) 46:16542. doi: 10.1111/jfpp.16542

25. López-Gámez G, Elez-Martínez P, Martín-Belloso O, Soliva-Fortuny R. Enhancing carotenoid and phenolic contents in plant food matrices by applying non-thermal technologies: bioproduction vs improved extractability. *Trends Food Sci Technol.* (2021) 112:622–30. doi: 10.1016/j.tifs.2021.04.022

26. Jacobo-Velázquez DA. Definition of biofortification revisited. *ACS Food Sci Technol.* (2022) 2:782–3. doi: 10.1021/acsfoodscitech.2c00110

27. Yeoh WK, Ali A. Ultrasound treatment on phenolic metabolism and antioxidant capacity of fresh-cut pineapple during cold storage. *Food Chem.* (2017) 216:247–53. doi: 10.1016/j.foodchem.2016.07.074

28. Cuéllar-Villarreal MDR, Ortega-Hernández E, Becerra-Moreno A, Welti-Chanes J, Cisneros-Zevallos L, Jacobo-Velázquez DA. Effects of ultrasound treatment and storage time on the extractability and biosynthesis of nutraceuticals in carrot (*Daucus carota*). *Postharvest Biol Technol.* (2016) 119:18–26. doi: 10.1016/j.postharvbio.2016.04.013

29. Qiao L, Gao M, Zheng J, Zhang J, Lu L, Liu X. Novel browning alleviation technology for fresh-cut products: preservation effect of the combination of *Sonchus oleraceus* L. extract and ultrasound in fresh-cut potatoes. *Food Chem.* (2021) 348:129132. doi: 10.1016/j.foodchem.2021.129132

30. Ali A, Yeoh WK, Forney C, Siddiqui MW. Advances in postharvest technologies to extend the storage life of minimally processed fruits and vegetables. *Crit Rev Food Sci Nutr.* (2018) 58:2632–49. doi: 10.1080/10408398.2017.1339180

31. Alenyorege EA, Ma H, Ayim I, Zhou C, Wu P, Hong C, et al. Effect of multi-frequency ultrasound surface washing treatments on *Escherichia coli* inactivation and some quality characteristics of non-heading Chinese cabbage. *J Food Process Preserv.* (2018) 42:13747. doi: 10.1111/jfpp.13747

32. Xu X, Zhang L, Feng Y, ElGasim A, Yagoub A, Sun Y, et al. Vacuum pulsation drying of okra (*Abelmoschus esculentus* L. Moench): better retention of the quality characteristics by flat sweep frequency and pulsed ultrasound pretreatment. *Food Chem.* (2020) 326:127026. doi: 10.1016/j.foodchem.2020.127026

33. Abdel-Aal ESM, Rabalsk I. Effect of baking on free and bound phenolic acids in wholegrain bakery products. *J Cereal Sci.* (2013) 57:312–8. doi: 10.1016/j.jcs.2012.12.001

34. Viacava F, Santana-Gálvez J, Heredia-Olea E, Pérez-Carrillo E, Nair V, Cisneros-Zevallos L, et al. Sequential application of postharvest wounding stress and extrusion as an innovative tool to increase the concentration of free and bound phenolics in carrots. *Food Chem.* (2020) 307:125551. doi: 10.1016/j.foodchem.2019.125551

35. Ni Z, Xu S, Ying T. The effect and mechanism of ultrasonic treatment on the postharvest texture of shiitake mushrooms (*Lentinula edodes*). *Int J Food Sci Technol.* (2018) 53:1847–54. doi: 10.1111/ijfs.13768

36. Li N, Chen F, Cui F, Sun W, Zhang J, Qian L, et al. Improved postharvest quality and respiratory activity of straw mushroom (*Volvariella volvacea*) with ultrasound treatment and controlled relative humidity. *Sci Hortic.* (2017) 225:56–64. doi: 10.1016/j.scienta.2017.06.057

37. Xu Y, Wang D, Zhao W, Zheng Y, Wang Y, Wang P, et al. Low frequency ultrasound treatment enhances antibrowning effect of ascorbic acid in fresh-cut potato slices. *Food Chem.* (2022) 380:132190. doi: 10.1016/j.foodchem.2022.132190

38. Tan ZW, Song CY, Zheng MX, Cui BH, Zong CW. Optimization and determination of the content of reduction-type Vc in ripe fruit of *Vaccinium μliginosum* with phosphomolybdate-blue spectrophotometry. *Hubei Agric Sci.* (2015) 54:1713–6. doi: 10.14088/j.cnki.issn0439-8114.2015.07.047

39. Yildiz G, Izli G, Aadil RM. Comparison of chemical, physical, and ultrasound treatments on the shelf life of fresh-cut quince fruit (*Cydonia oblonga* Mill.). *J Food Process Preserv.* (2019) 44:14366. doi: 10.1111/jfpp.14366

40. Marasek-Ciolakowska A, Soika G, Warabieda W, Kowalska U, Rybczyński D. Investigation on the relationship between morphological and anatomical characteristic of savoy cabbage and kale leaves and infestation by cabbage whitefly (*Aleyrodes proletella* L.). *Agronomy.* (2021) 11:275. doi: 10.3390/agronomy11020275

41. Gouda M, Bekhit AED, Tang Y, Huang Y, Huang L, He Y, et al. Recent innovations of ultrasound green technology in herbal phytochemistry: a review. *Ultrason Sonochem.* (2021) 73:105538. doi: 10.1016/j.ultsonch.2021.105538

42. Wang J, Ma H, Pan Z, Qu W. Sonochemical effect of flat sweep frequency and pulsed ultrasound (FSFP) treatment on stability of phenolic acids in a model system. *Ultrason Sonochem.* (2017) 39:707–15. doi: 10.1016/j.ultsonch.2017.05.034

43. Pinheiro J, Alegria C, Abreu M, Goncalves EM, Silva CLM. Influence of postharvest ultrasounds treatments on tomato (*Solanum lycopersicum*, cv. Zinac) quality and microbial load during storage. *Ultrason Sonochem.* (2015) 27:552–9. doi: 10.1016/j.ultsonch.2015.04.009

44. Wang W, Ma X, Zou M, Jiang P, Hu W, Li J, et al. Effects of ultrasound on spoilage microorganisms, quality, and antioxidant capacity of postharvest cherry tomatoes. *J Food Sci.* (2015) 80:C2117–26. doi: 10.1111/1750-3841.12955

45. Wu W, Gao H, Chen H, Fang X, Han Q, Zhong Q. Combined effects of aqueous chlorine dioxide and ultrasonic treatments on shelf-life and nutritional quality of bok choy (*Brassica chinensis*). *LWT Food Sci Technol.* (2018) 101:757–63. doi: 10.1016/j.lwt.2018.11.073

46. Traore MB, Sun A, Gan Z, Long WY, Senou H, Zhu Y, et al. Assessing the impact of the combined application of ultrasound and ozone on microbial quality and bioactive compounds with antioxidant attributes of cabbage (*Brassica Oleracea* L. Var. Capitata). *J Food Process Preserv.* (2020) 44:14779. doi: 10.1111/jfpp.14779

47. Lu C, Ding J, Park HK, Feng H. High intensity ultrasound as a physical elicitor affects secondary metabolites and antioxidant capacity of tomato fruits. *Food Control.* (2020) 113:107176. doi: 10.1016/j.foodcont.2020.107176

48. Gani A, Baba WN, Ahmad M, Shah U, Khan AA, Wani IA, et al. Effect of ultrasound treatment on physico-chemical, nutraceutical and microbial quality of strawberry. *LWT Food Sci Technol.* (2016) 66:496–502. doi:10.1016/j.lwt.2015.10.067

49. Mustapha AT, Zhou C, Amanor-Atiemoh R, Ali T, Sun Y. Efficacy of dual-frequency ultrasound and sanitizers washing treatments on quality retention of cherry tomato. *Innov Food Sci Emerg Technol.* (2020) 62:102348. doi: 10.1016/j.ifset.2020.102348

50. Tovar-Pérez EG, Aguilera-Aguirre S, López-García U, Valdez-Morales M, Ibarra-Zurita AK, Ortiz-Basurto RI, et al. Effect of ultrasound treatment on the quality and contents of polyphenols, lycopene and rutin in tomato fruits. *Czech J Food Sci.* (2020) 38:20–7. doi: 10.17221/189/2019-CJFS

51. Soria AC, Villamiel M. Effect of ultrasound on the technological properties and bioactivity of food: a review. *Trends Food Sci Technol.* (2010) 21:323–31. doi: 10.1016/j.tifs.2010.04.003

52. Tan Mei Chin B, Ali A, Kamal H, Mustafa MA, Khaliq G, Siddiqui Y. Optimizing parameters on antioxidant capacity of watermelon pulp using conventional orbital shaker and ultrasound assisted extraction methods. *J Food Process Preserv.* (2021) 45:15123. doi: 10.1111/jfpp.15123

53. Ashokkumar M, Sunartio D, Kentish SE, Mawson R, Simons L, Vilkhu K, et al. Modification of food ingredients by ultrasound to improve functionality. *Innov Food Sci Emerg Technol.* (2008) 9:155–60. doi: 10.1016/j.ifset.2007.05.005

54. Becerra-Moreno A, Redondo-Gil M, Benavides J, Nair V, Cisneros-Zevallos L, Jacobo-Velázquez DA. Combined effect of water loss and wounding stress on gene activation of metabolic pathways associated with phenolic biosynthesis in carrot. *Front Plant Sci.* (2015) 6:837. doi: 10.3389/fpls.2015.00837

55. Surjadinata BB, Jacobo-Velázquez DA, Cisneros-Zevallos L. UVA, UVB and UVC light enhances the biosynthesis of phenolic antioxidants in fresh-cut carrot through a synergistic effect with wounding. *Molecules.* (2017) 22:668. doi: 10.3390/molecules22040668

56. Jacobo-Velázquez DA, Santana-Gálvez J, Cisneros-Zevallos L. Designing next-generation functional food and beverages: combining nonthermal processing technologies and postharvest abiotic stresses. *Food Eng Rev.* (2021) 13:592–600. doi: 10.1007/s12393-020-09244-x

57. Cisneros-Zevallos L, Jacobo-Velázquez DA. Controlled abiotic stresses revisited: from homeostasis through hormesis to extreme stresses and the impact on nutraceuticals and quality during pre- and postharvest applications in horticultural crops. *J Agric Food Chem.* (2020) 68:11877–9. doi: 10.1021/acs.jafc.0c06029

58. Dobránszki J, Asbóth G, Homoki D, Bíró-Molnár P, Silva JATD, Remenyik J. Ultrasonication of in vitro potato explants: activation and recovery of antioxidant defence system and growth response. *Plant Physiol Biochem.* (2017) 121:153–60. doi: 10.1016/j.plaphy.2017.10.022

59. Hasan MM, Bashir T, Bae H. Use of ultrasonication technology for the increased production of plant secondary metabolites. *Molecules.* (2017) 22:1046. doi: 10.3390/molecules22071046

60. Fernandez-Jaramillo AA, Duarte-Galvan C, Garcia-Mier L, Jimenez-Garcia SN, Contreras-Medina LM. Effects of acoustic waves on plants: an agricultural, ecological, molecular and biochemical perspective. *Sci Hortic.* (2018) 235:340–8. doi: 10.1016/j.scienta.2018.02.060

61. Wang J, Fan L. Effect of ultrasound treatment on microbial inhibition and quality maintenance of green asparagus during cold storage. *Ultrason Sonochem.* (2019) 58:104631. doi: 10.1016/j.ultsonch.2019.104631

62. Nicolau-Lapeña I, Lafarga T, Viñas I, Abadias M, Bobo G, Aguiló-Aguayo I. Ultrasound processing alone or in combination with other chemical or physical treatments as a safety and quality preservation strategy of fresh and processed fruit and vegetables: a review. *Food Bioproc Tech.* (2019) 12:1452–71. doi: 10.1007/s11947-019-02313-y

63. Nowacka M, Wedzik M. Effect of ultrasound treatment on microstructure, colour and carotenoid content in fresh and dried carrot tissue. *Appl Acoust.* (2016) 103:163–71. doi: 10.1016/j.apacoust.2015.06.011

64. Gastélum-Estrada A, Hurtado-Romero A, Santacruz A, Cisneros-Zevallos L, Jacobo-Velázquez DA. Sanitizing after fresh-cutting carrots reduces the wound-induced accumulation of phenolic antioxidants compared to sanitizing before fresh-cutting. *J Sci Food Agric.* (2020) 100:4995–8. doi: 10.1002/jsfa.10555

65. Appu M, Ramalingam P, Sathiyanarayanan A, Huang J. An overview of plant defense-related enzymes responses to biotic stresses. *Plant Gene.* (2021) 27:100302. doi: 10.1016/j.plgene.2021.100302

66. Zhu Y, Du X, Zheng J, Wang T, You X, Liu H, et al. The effect of ultrasonic on reducing anti-browning minimum effective concentration of purslane extract on fresh-cut potato slices during storage. *Food Chem.* (2020) 343:128401. doi: 10.1016/j.foodchem.2020.128401

67. Heredia JB, Cisneros-Zevallos L. The effect of exogenous ethylene and methyl jasmonate on pal activity, phenolic profiles and antioxidant capacity of carrots (*Daucus carota*) under different wounding intensities. *Postharvest Biol Technol.* (2009) 51:242–9. doi: 10.1016/j.postharvbio.2008.07.001

68. Pan Y, Chen L, Pang L, Chen X, Jia X, Li X. Ultrasound treatment inhibits browning and improves antioxidant capacity of fresh-cut sweet potato during cold storage. *RSC Adv.* (2020) 10:9193–202. doi: 10.1039/c9ra06418d

69. Yu J, Engeseth NJ, Feng H. High intensity ultrasound as an abiotic elicitor—effects on antioxidant capacity and overall quality of Romaine lettuce. *Food Bioproc Tech.* (2015) 9:262–73. doi: 10.1007/s11947-015-1616-7

70. Shi D, Yin C, Fan X, Yao F, Qiao F, Xue S, et al. Effects of ultrasound and gamma irradiation on quality maintenance of fresh *Lentinula edodes* during cold storage. *Food Chem.* (2022) 373:131478. doi: 10.1016/j.foodchem.2021.131478

71. Wang J, Wu Z, Wang H. Combination of ultrasound-peracetic acid washing and ultrasound-assisted aerosolized ascorbic acid: a novel rinsing-free disinfection method that improves the antibacterial and antioxidant activities in cherry tomato. *Ultrason Sonochem.* (2022) 86:106001. doi: 10.1016/j.ultsonch.2022.106001

72. Zhang L, Yu X, Yagoub AEA, Owusu-Ansah P, Wahia H, Ma H, et al. Effects of low frequency multi-mode ultrasound and it's washing solution's interface properties on freshly cut cauliflower. *Food Chem.* (2022) 366:130683. doi: 10.1016/j.foodchem.2021.130683

73. Kentish S, Feng H. Applications of power ultrasound in food processing. *Annu Rev Food Sci Technol.* (2014) 5:263–84. doi: 10.1146/annurev-food-030212-182537

74. Mizrach A. Ultrasonic technology for quality evaluation of fresh fruit and vegetables in pre- and postharvest processes. *Postharvest Biol Technol.* (2008) 48:315–30. doi: 10.1016/j.postharvbio.2007.10.018

75. Fan K, Zhang M, Jiang F. Ultrasound treatment to modified atmospheric packaged fresh-cut cucumber: influence on microbial inhibition and storage quality. *Ultrason Sonochem.* (2019) 54:162–70. doi: 10.1016/j.ultsonch.2019.02.003

76. Wang L, Xu B, Wei B, Zeng R. Low frequency ultrasound pretreatment of carrot slices: effect on the moisture migration and quality attributes by intermediate-wave infrared radiation drying. *Ultrason Sonochem.* (2018) 40:619–28. doi: 10.1016/j.ultsonch.2017.08.005

77. Fan K, Zhang M, Bhandari B, Jiang F. A combination treatment of ultrasound and ε-polylysine to improve microorganisms and storage quality of fresh-cut lettuce. *LWT Food Sci Technol.* (2019) 113:108315. doi: 10.1016/j.lwt.2019.108315

78. Fugate KK, Suttle JC, Campbell LG. Ethylene production and ethylene effects on respiration rate of postharvest sugarbeet roots. *Postharvest Biol Technol.* (2010) 56:71–6. doi: 10.1016/j.postharvbio.2009.12.004

79. Lagnika C, Zhang M, Mothibe KJ. Effects of ultrasound and high pressure argon on physico-chemical properties of white mushrooms (*Agaricus bisporus*) during postharvest storage. *Postharvest Biol Technol.* (2013) 82:87–94. doi: 10.1016/j.postharvbio.2013.03.006

80. Wang M, Li J, Fan L. Quality changes in fresh-cut asparagus with ultrasonic-assisted washing combined with cinnamon essential oil fumigation. *Postharvest Biol Technol.* (2022) 187:111873. doi: 10.1016/j.postharvbio.2022.111873

81. Mead EL, Sutherland RG, Verrall RE. The effect of ultrasound on water in the presence of dissolved gases. *Can J Chem.* (1976) 54:1114–20. doi: 10.1139/v76-159

82. Wen B, Li D, Tang D, Huang Z, Kedbanglai P, Ge Z, et al. Effects of simultaneous ultrasonic and cysteine treatment on antibrowning and physicochemical quality of fresh-cut lotus roots during cold storage. *Postharvest Biol Technol.* (2020) 168:111294. doi: 10.1016/j.postharvbio.2020.111294

83. Xu YT, Zhang LF, Zhong JJ, Jie S, Ye XQ, Liu DH. Power ultrasound for the preservation of postharvest fruits and vegetables. *Int J Agric Biol.* (2013) 6:116–25. doi: 10.3965/j.ijabe.20130602.0013

84. Ketsa S, Daengkanit T. Firmness and activities of polygalacturonase, pectinesterase, β-galactosidase and cellulase in ripening durian harvested at different stages of maturity. *Sci Hortic.* (1999) 80:181–8. doi: 10.1016/S0304-4238(98)00242-8

85. Fagundes C, Carciofi BAM, Monteiro AR. Estimate of respiration rate and physicochemical changes of fresh-cut apples stored under different temperatures. *Food Sci Technol.* (2013) 33:60–7. doi: 10.1590/s0101-20612013005000023

86. Alenyorege EA, Ma H, Ayim I, Aheto JH, Hong C, Zhou C. Reduction of *Listeria innocua* in fresh-cut Chinese cabbage by a combined washing treatment of sweeping frequency ultrasound and sodium hypochlorite. *LWT Food Sci Technol.* (2019) 101:410–8. doi: 10.1016/j.lwt.2018.11.048

87. Martín-Diana AB, Rico D, Barry-Ryan C, Frías JM, Mulcahy J, Henehan GTM. Calcium lactate washing treatments for salad-cut iceberg lettuce: effect of temperature and concentration on quality retention parameters. *Food Res Int.* (2005) 38:729–40. doi: 10.1016/j.foodres.2005.02.005

88. Calderón-Martínez V, Delgado-Ospina J, Ramírez-Navas JS, Flórez-López E, Valdés-Restrepo MP, Grande-Tovar CD, et al. Effect of pretreatment with low-frequency ultrasound on quality parameters in gulupa (*Passiflora edulis* sims) pulp. *Appl Sci.* (2021) 11:1734. doi: 10.3390/app11041734

89. Santos J, Herrero M, Mendiola JA, Oliva-Teles MT, Ibáñez E, Delerue-Matos C, et al. Fresh-cut aromatic herbs: nutritional quality stability during shelf-life. *LWT Food Sci Technol.* (2014) 59:101–7. doi: 10.1016/j.lwt.2014.05.019

90. Temizkan R, Atan M, Büyükcan MB, Caner C. Efficacy evaluation of ultrasound treatment on the postharvest storability of white nectarine by both physicochemical and image processing analyses. *Postharvest Biol Technol.* (2019) 154:41–51. doi: 10.1016/j.postharvbio.2019.04.014

91. Glowacz M, Rees D. Using jasmonates and salicylates to reduce losses within the fruit supply chain. *Eur Food Res Technol.* (2015) 242:143–56. doi: 10.1007/s00217-015-2527-6

92. López-Gálvez F, Allende A, Gil MI. Recent progress on the management of the industrial washing of fresh produce with a focus on microbiological risks. *Curr Opin Food Sci.* (2021) 38:46–51. doi: 10.1016/j.cofs.2020.10.026

93. Dai J, Bai M, Li C, Cui H, Lin L. Advances in the mechanism of different antibacterial strategies based on ultrasound technique for controlling bacterial contamination in food industry. *Trends Food Sci Technol.* (2020) 105:211–22. doi: 10.1016/j.tifs.2020.09.016

frontiers | Frontiers in Nutrition

TYPE Original Research
PUBLISHED 14 November 2022
DOI 10.3389/fnut.2022.993475

OPEN ACCESS

EDITED BY
Yu Xiao,
Hunan Agricultural University, China

REVIEWED BY
Lijun Sun,
Northwest A&F University, China
Pau Loke Show,
University of Nottingham Malaysia Campus, Malaysia
Hao Hu,
Huazhong Agricultural University, China

*CORRESPONDENCE
Yongbin Han
hanyongbin@njau.edu.cn
Changnian Song
songchangnian@njau.edu.cn

SPECIALTY SECTION
This article was submitted to Nutrition and Food Science Technology, a section of the journal Frontiers in Nutrition

RECEIVED 13 July 2022
ACCEPTED 16 September 2022
PUBLISHED 14 November 2022

CITATION
Xie G, Shen J, Luo J, Li D, Tao Y, Song C and Han Y (2022) Simultaneous extraction and preliminary purification of polyphenols from grape pomace using an aqueous two-phase system exposed to ultrasound irradiation: Process characterization and simulation. *Front. Nutr.* 9:993475. doi: 10.3389/fnut.2022.993475

Simultaneous extraction and preliminary purification of polyphenols from grape pomace using an aqueous two-phase system exposed to ultrasound irradiation: Process characterization and simulation

Guangjie Xie[1], Juan Shen[1], Ji Luo[2], Dandan Li[1], Yang Tao[1], Changnian Song[3]* and Yongbin Han[1]*

[1]Whole Grain Food Engineering Research Center, College of Food Science and Technology, Nanjing Agricultural University, Nanjing, China, [2]Institute of Agricultural Products Processing, Jiangsu Academy of Agricultural Sciences, Nanjing, China, [3]College of Horticulture of Nanjing agricultural University, Nanjing, China

In this study, an ultrasound-assisted aqueous two-phase (ATP) extraction method was used for the extraction and purification of phenolic compounds from grape pomace. The effect of acoustic energy densities (AED, 41.1, 63.5, 96.1, 111.2 W/L) and temperatures (20, 30, 40°C) on the yield of phenolics was investigated. An artificial neural network (ANN) was successfully used to correlate the extraction parameters with phenolic yield. Then, a diffusion model based on Fick's second law was used to model the mass transfer process during ultrasound-assisted ATP extraction and evaluate the effective diffusion coefficient of phenolics. The results revealed the increase in AED, and the temperature increased the effective diffusivity of phenolics. The HPLC analysis of anthocyanins and flavonols showed that ultrasound significantly increased the extraction yield of anthocyanins compared with the traditional method. High amounts of rutin and myricetin were recovered using the ATPS systems. Sugars were mainly distributed in the bottom phase, whereas phenolics were located in the top phase. Conclusively, ultrasound-assisted aqueous two-phase (ATP) extraction can be used as an effective method to achieve the simultaneous separation and preliminary purification of phenolics from grape pomace.

KEYWORDS

ultrasound, aqueous two-phase, grape pomace, phenolic compounds, artificial neural network, diffusion model, purification

Introduction

Grape pomace is a major byproduct of the grape processing industry. It mainly comprises peel, stem, seed, and part of pulp (1). The amounts of waste and byproducts of grapes make up ∼20% of the total processed grapes (2). Currently, the utilization of grape pomace is low, and more studies are needed to explore the strategies for the utilization of grape pomace. Grape pomace is rich in bioactive phenolic compounds, which exert antiproliferative properties against colon cancer cells (3). Moreover, phenolics have antioxidant, antibacterial, cardioprotective, and skin anti-aging activities (4–8). Therefore, grape pomace can serve as raw materials for the recovery of phenolics for effective resource utilization and increment of economic value.

Several methods for the extraction of phenolic compounds have been explored, such as alkaline hydrolysis treatment (9), solvent extraction and pressurized liquid extraction (10), enzyme-assisted extraction (11), and microwave-assisted extraction (12). The methods mentioned earlier have certain problems, such as low extraction rate, environmentally unfriendly, and high energy consumption. However, ultrasound-assisted extraction (UAE) is a novel method for the extraction of phenolics. UAE improves the extraction rate and extraction yield of active ingredients (13). Meanwhile, aqueous two-phase extraction (ATPE) is widely applied in the separation of biomolecules (14). For example, ethanol coupled with ammonium sulfate is a common and economic aqueous two-phase system (ATPS) used for the extraction of anthocyanins from mulberry (15). ATPE method is used for the extraction and purification of active compounds, thus improving the purity of the extract. The combination of the two strategies results in efficient separation of bioactive substances from the material. Therefore, the combined ultrasound and ATPE approach can ensure simultaneous efficient extraction and purification (16). In the literature, ATPE was combined with the ultrasonic approach as an ultrasound-assisted aqueous two-phase method to extract polyphenols from the chaff (17). However, the research on the purification of bioactive compounds using this method is still limited. Thus, grape pomace can be used with high value, and it provides a new method for preliminary separation and purification for industrial production to study the recovery of polyphenols from grape pomace using the method of ultrasound-assisted aqueous two-phase extraction.

An artificial neural network (ANN) is a method of data analysis designed to simulate the function of the human brain. This method has been widely applied in the food-science discipline (18–20). ANN has been utilized to simulate and optimize complex food processes (21). For example, Tao et al. studied the influences of various operating parameters on the extraction yield of phenolics from wine lees (22). Tao et al. also studied the optimization of encapsulation of blueberry anthocyanin extracts by an artificial neural network and genetic algorithm (23). Furthermore, the construction of mathematical models with physical significance can be used to study mass transfer mechanisms during extraction. Such a numerical simulation method based on a diffusional model was employed to clarify the effect of ultrasound on the mass transfer mechanism during yeast biosorption (20). Besides, the physical simulation can be helpful to visualize and explore the mass transfer mechanism of extraction (24). However, few studies have used physical models to explore the effect of ultrasound-assisted ATP extraction of phenolics.

In the present study, ultrasound was combined with aqueous two-phase (ATP) for the simultaneous extraction and purification of phenolic substances from grape pomace. The aqueous two-phase system (ATPS) was established, and the effects of acoustic energy density, temperature, and ultrasound duration on the yield of total phenolics were explored. An artificial neural network model was used to explore the relationship between extraction parameters and the yield of phenolics. Moreover, the extraction mechanism was established using the diffusion model. The profiles of individual phenolics in the top and bottom phases were analyzed by HPLC. In addition, the change in sugar content in the system was evaluated, and the purity of phenolic extract was determined. This study aimed to establish an appropriate and easy extraction and purification strategy for phenolic substances from grape pomace, as well as to provide a theoretical basis and technological guidance for the extraction process.

Materials and methods

Materials and chemicals

Seedless grapes with similar maturity (Cultivar: Xiahei) were purchased from Nanjing Zhongcai Agricultural Product Market (Jiangning, Nanjing). After reaching the laboratory, grape samples were immediately stored at −20°C in darkness before use. Ammonium sulfate and anhydrous ethanol were purchased from Sinopharm Chemical Reagents Co., Ltd. (Shanghai, China). All other chemicals used were of analytical or chromatographic grades.

Preparation of grape pomace

Frozen grapes were thawed at room temperature, washed, and pressed using a domestic juice extractor purchased from Midea Household Appliance Manufacturing Co., Ltd (MJ-WBL2501A, China). Grape pomace was collected, dried at 50°C for 12 h, grounded, and sieved to

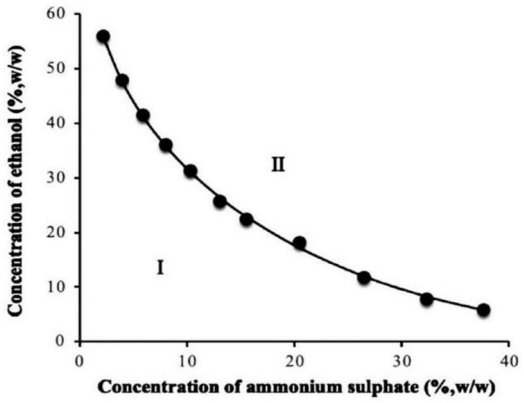

FIGURE 1
Phase diagram for ethanol-ammonium sulfate aqueous two-phase system.

obtain particles with the size between 425 and 125 μm. The grape pomace samples were stored at −20°C in darkness.

Establishment of an aqueous two-phase system

ATPS comprising ethanol and ammonium sulfate was selected as the solvent for the extraction of phenolics from grape pomace, according to previous studies (25, 26).

The formation of ethanol-ammonium sulfate ATP mainly involves the competition between alcohol and salt for water molecules. The system has divided the suspensions into two phases when the two sides compete for water to a certain extent due to the repulsion, namely the ethanol-rich phase and ammonium sulfate-rich phase (27). The phase diagram of ethanol-ammonium sulfate measured in this study is presented in Figure 1. The region above the curve is the two-phase region (II). The two phases are formed when alcohol and salt reach a certain proportion. In this region, the top phase is rich in alcohol and the bottom phase is rich in salt.

Two aqueous phase system was established based on the phase diagram. The operation steps of the two-phase system construction: dissolve a certain mass of ammonium sulfate in a certain volume of deionized water, and then add a certain volume of ethanol to make the total mass of the two-phase system (100 g). Stir until the solution is clarified. After standing for 1 min, the system is divided into two phases: the upper phase is the ethanol-rich phase and the lower phase is the salt-rich phase.

The two-node data were fitted using the empirical equation of binodal curves suitable for small molecular alcohol-salt ATPS (28). The equation for the binodal curve is expressed as follows:

$$w_1 = \exp(a + bw_2^{0.5} + cw_2 + dw_2^2) \quad (1)$$

where w_1 represents the mass fraction of ethanol, w_2 represents the mass fraction of ammonium sulfate; and a, b, c, and d represent the fitting parameters. The data were calculated and fitted using MATLAB R2016a. The values of the relevant parameters were then obtained. The following relationship was obtained after substituting the parameters:

$$w_1 = exp(-0.1408 - 2.882w_2^{0.5} - 0.3998w_2 - 5.608w_2^2) \quad (2)$$

The correlation coefficient R^2 obtained by fitting is 0.9992 and the absolute error AAD value is 2.02%. Notably, R^2 is close to 1 and the AAD value is <5% indicating a good fitting degree. The concentrations of ethanol and ammonium sulfate required for phase equilibria can be effectively obtained using this equation, thus facilitating the construction of ATPS. In addition, the phase diagram of ATPS provides a theoretical basis for the design of subsequent extraction experiments.

Xavier et al. (26) reported that phenolics were mainly distributed in the top phase and recovered in the top phase in the ATPS. Using the recovery and yield of phenolics as the index, the concentration of ethanol and ammonium sulfate was screened at 30°C and 96.1 W/L to determine the appropriate concentration of phase for phenolics extraction. According to the phase diagram, the ATP solvent consists of ethanol and ammonium sulfate.

ATP-assisted simultaneous extraction and preliminary purification under ultrasonic irradiation

First, 2.5 g of grape pomace particles were added into a 100 mL conical flask containing 50 mL aforementioned ATP solution. Then, this flask was fixed well in a thermostatic water bath system. The 20-kHz ultrasound probe was inserted into the solution at the same depth of 2 cm. The ultrasound probe was connected with an ultrasound generator (VCX130, Sonics and Materials Inc., Newtown, USA). The actual acoustic energy density (AED) distributed in the ATP solution corresponding to a certain ultrasonic power was measured by the calorimetry method (29). The detailed experimental setup is illustrated in Supplementary Figure 1. Ultrasonic treatment was performed in an intermittent mode of 5 s on and 5 s off. During sonication, the samples in both upper and lower phases were taken periodically.

Experimental design

A full-factorial design was employed to generate the experimental runs, to explore the effects of AED levels (41.1,

63.5, 96.1, 111.2 W/L), temperature (20, 30, 40°C), and time on the yield of phenolics. For comparison purpose, the ATP extraction test under reciprocating shaking at 30°C and 100 rpm was taken as a control. All the processes were performed in triplicates.

Chemical analysis

Determination of total phenolic content

Total phenolic content was determined by the well-known Folin-Ciocatteu method (26), which was expressed as gallic acid equivalent in mL. The detailed procedure was described in the study of Singleton et al. (25). The distribution coefficient and recovery of polyphenols are calculated using the following equations:

$$K = \frac{C_T}{C_B} \tag{3}$$

$$Y_T(\%) = \frac{C_T V_T}{(C_T V_T + C_B V_B)} \times 100\% \tag{4}$$

$$Y_B(\%) = \frac{C_B V_B}{(C_T V_T + C_B V_B)} \times 100\% \tag{5}$$

where Y_T represents the recovery of polyphenols in the top phase (%), Y_B indicates the recovery of polyphenols in the bottom phase (%), C_T represents the total phenolic concentration in the top phase (mg/L), and C_B indicates the total phenolic concentration in the bottom phase (mg /L). V_T and V_B indicate the volumes of the top phase solution and bottom phase solution, respectively.

Determination of total sugar content

The concentration of total sugar was determined by Anthrone sulphuric acid colorimetry (30). Specifically, 1 mL of the sample was mixed with 4 mL of sulfuric acid anthrone reagent (2 mg/mL). After shaking, the mixture was quickly placed in a boiling water bath for 10 min and then cooled in an ice water bath for 10 min. The absorbance at 620 nm was measured. Glucose was used as the standard to make the calibration curve and the content was expressed as mg glucose/mL.

Determination of purity of phenolic samples

The top phase solution (containing phenolics) after ATP extraction was collected and the involved phenolic amount was determined. Then, the samples were desalted by run water dialysis (15). The extract was concentrated by rotational evaporation. The samples were freeze-dried for 72 h and weighed. The purity of the samples was determined as the ratio of the total phenolic mass to the extracted mass.

Analysis of phenolic profile

HPLC (LC-2010A, Shimadzu, Japan) was used to explore the profile of individual phenolics obtained from ultrasonic-assisted ATP extraction, water bath oscillation ATP extraction, and crude extraction using 50% ethanol solution, as well as individual phenolics in grape pomace. Contents of individual anthocyanins were determined using HPLC as described previously (31). Chromatographic conditions and methods were slightly modified. The sample was analyzed by HPLC after passing through a 0.45 μm organic filtration membrane. An Agilent TC-C18 column (250 × 4.6 mm, 5 μm) was used for the separation of anthocyanins. The mobile phase comprised (A) trifluoroacetic acid (0.5%) and (B) pure acetonitrile solution. A gradient elution program was used as follows: 0 ∼ 5 min, 15 ∼ 18% B; 5 ∼ 11 min, 18 ∼ 21% B; 11 ∼ 13 min, 21 ∼ 22% B; 13 ∼ 15 min, 22 ∼ 23% B; 15 ∼ 19 min, 23 ∼ 24% B; 19 ∼ 22 min, 24 ∼ 25% B; 22 ∼ 35 min, 25 ∼ 30% B; 35 ∼ 45 min, 15% B. The column temperature and detection wavelength were 30°C and 520 nm, respectively. Injection volume and the flow rate were set at 10 μL and 0.6 mL/min, respectively.

Contents of flavonols were determined by HPLC following a method described previously (32). The chromatographic conditions and methods were slightly modified. Pretreatment was conducted before analysis (33). The pH value of the polyphenol extract was first adjusted to 7.0. Extraction was then performed with ethyl acetate at a volume ratio of 1:1. The extraction time was 20 min, and the extraction was conducted in triplicates. After each extraction, the organic phase was collected, and the extract was concentrated by rotational evaporation at 40°C. The extract was then dissolved in methanol. The sample was analyzed by HPLC after passing through a 0.45 μm organic filtration membrane. The chromatographic conditions included a mobile phase comprising (A) acetic acid aqueous solution (1%) and (B) methanol acetate solution (1%). A gradient elution program was used as follows: 0–10 min, 10–26% B; 10–25 min, 26–40% B; 25–45 min, 40–65% B; 45–55 min, 65–95% B; 55–58 min, 95–10% B; 58–65 min, 10% B. Column temperature and detection wavelength were set at 25°C and 350 nm, respectively. Injection volume and the flow rate were set at 20 μL and 0.6 mL/min, respectively. The content was expressed as mg/g.

Determination of particle size

The particle size of grape pomace before and after extraction was determined by a laser particle size analyzer [LS-C(III), OMEC, Zhuhai, China]. The obscuration rate, particle refraction

index, and particle absorption rate were set as 5–10%, 1.57, and 0.001, respectively.

Mathematical modeling

Artificial neural network model of extraction parameters

The correlation between ATPE parameters and the phenolic extraction yield was explored using a statistical model. For this purpose, a three-layer feedforward artificial neural network model was established in the present study. The model mainly comprised an input layer, hidden layer, and output layer, with several neurons. AED, temperature, and time represented three nodes of the input layer, and the total phenol yield was included in a neuron of the output layer. The number of neurons in the hidden layer was adjusted from 5 to 20, and the transfer function type was also tested (34).

Transfer functions used in neural network model construction mainly included logsig function, tansig function, and purelin function. The coefficient of determination R^2, root mean square error *RMSE,* and absolute error *AAD* were determined to evaluate the constructed model. These parameters were determined as follows (35):

$$R^2 = 1 - \frac{\sum_{i=1}^{n} (Y_{i,p} - Y_{i,e})^2}{\sum_{i=1}^{n} (Y_{i,e} - Y_m)^2} \quad (6)$$

$$RMSE = \sqrt{\frac{\sum_{i=1}^{n} (Y_{i,e} - Y_{i,p})^2}{n}} \quad (7)$$

$$AAD = \left[\frac{\sum_{i=1}^{n} \left(\left| Y_{i,p} - Y_{i,e} \right| / Y_{i,e} \right)}{\mathrm{n}} \right] \times 100 \quad (8)$$

where $Y_{i,p}$ indicates the predicted extraction yield of the test model (mg/g), $Y_{i,e}$ represents the experimental value (mg/g), *Ym* indicates the average experimental value (mg/g), and n represents the number of test groups.

The neural network toolbox in MATLAB r2016a was used for the construction of the artificial neural network model. The model can be expressed as follows:

$$Y_{ANN} = purelin(LW^{(2,1)} tansig(IW^{(1,1)} xn + b^{(1)}) + b^{(2)}) \quad (9)$$

where Y_{ANN} represents the extraction yield of phenolics under a certain condition predicted by the model, $LW^{(2,1)}$ indicates the layer weight matrix, $IW^{(1,1)}$ represents the input weight matrix, x_n represents the input test condition, $b^{(1)}$ indicates the target deviation of the hidden layer, and $b^{(2)}$ represents the target deviation of the output layer.

Mass transfer diffusion model

A diffusion model based on Fick's second law was used to simulate the intraparticle diffusion process of phenolic during the extraction process. This simulation was then used to explore the mechanism of ultrasonic-enhanced phenolics extraction in the entire aqueous two-phase system, to determine the effective diffusion coefficient, as well as to study the promotion effect of ultrasound. The following assumptions were considered:

(i) Grape pomace particles are spherical, and phenolic compounds were uniformly distributed in the particles before extraction, and the content only varied with time and space.
(ii) Chemical reactions and degradation of phenolic compounds did not occur during the entire extraction process.
(iii) Distribution of polyphenols in ATP solution during sonication was uniform.

The equation of the spherical diffusion model of phenolic compounds is shown below (36):

$$\frac{\partial C_s}{\partial t} = D_e \left(\frac{1}{x^2} \frac{\partial}{\partial x} \left(X^2 \frac{\partial C_s}{\partial x} \right) \right) \quad (10)$$

where Cs represents the distribution content of phenolics; *De* indicates the effective diffusion coefficient of phenolics; *x* represents the radial distance of phenolics diffusion direction; t indicates the diffusion time.

The initial and boundary conditions of the diffusion model were as follows:

$$C_s(x, 0) = C_S^0 \qquad 0 \le x \le \mathrm{r} \quad (11)$$

$$C_L(0) = 0 \quad (12)$$

The following equation can be obtained from Equations (10, 11):

$$-D_e A \left[\frac{\partial C_s(x,t)}{\partial x} \right] = V \frac{dC_L}{dt} \qquad x = r \quad (13)$$

where *r* represents the radius of the particle (m), C_L indicates the average concentration of phenolics in the ATP solution (g/m^3), *A* represents the surface area of the grape pomace particle (m^2), and *V* indicates the volume of the extraction solution (m^3).

Equation (10) was solved using the *pdepe* function in Matlab2016a, and the initial and boundary conditions were determined. The diffusion coefficient *De* was adjusted until the *RMSE* value between the predicted value and the experimental value of extraction yield was minimized. Then, R^2 and *AAD* values were used as model evaluation indexes.

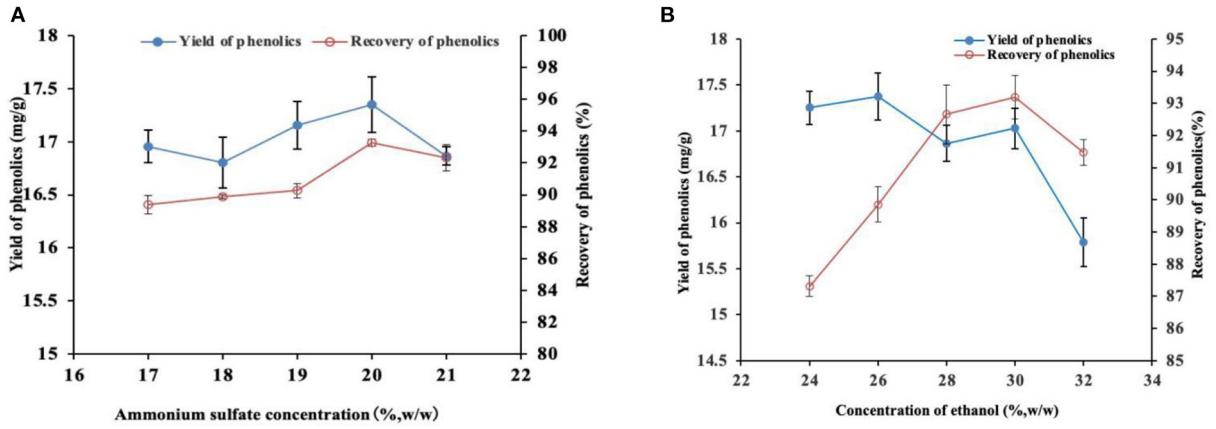

FIGURE 2
Effect of different ammonium sulfate **(A)** and ethanol **(B)** concentrations on the yield and recovery of phenolics.

Statistical analyses

All treatments and analyses were conducted in triplicate. Data were expressed as mean ± SD values. Statistical analysis was performed using Microsoft Office 2013 and SAS version 9.2 (SAS Institute, Cary, NC, USA). Duncan's multiple comparison method was used to compare mean values among groups. $P < 0.05$ represented statistical significance. MATLAB2016a was used to analyze and determined the correlation between the artificial neural network model and the mass transfer and diffusion model.

Results and discussion

Determination of the phase composition and concentration

Ultrasound-assisted ATPE was then performed at 40°C and 96.1 W/L for 60 min to determine the concentrations of ammonium sulfate and ethanol. The phase diagram and relevant literature (15) indicated that when the concentration of ethanol was 30% (w/w) and the concentration of ammonium sulfate was in a certain range, the ATPS was separated stably. Therefore, the concentration of ethanol was fixed at 30%(w/w) and the concentration of ammonium sulfate was then determined. The results for the determination of ammonium sulfate concentration are presented in Figure 2A. Recovery of phenolics was highest at 93.27% when the concentration of ammonium sulfate was 20% (Figure 2A). This yield was significantly higher relative to that under other concentrations ($P < 0.05$). Notably, the highest yield achieved at a 20% concentration was not significantly different compared with the extraction when the concentration of ammonium sulfate was 21% ($P > 0.05$). The extraction yield of the target product is another basic index to evaluate the performance of ATPS. The phenolic extraction yield at 20% ammonium sulfate was 17.35 mg/g, which was higher compared with that under other ammonium sulfate concentrations. However, the difference was not statistically significant ($P > 0.05$). Therefore, the 20% ammonium sulfate concentration was selected in the subsequent tests based on the results of the two evaluation indexes.

The concentration of ammonium sulfate was fixed at 20%, and the optimum concentration of ethanol was determined based on the recovery and yield of phenolics. The phenolic recovery was the highest (93.19%) at 30% ethanol concentration, which was significantly higher compared with other concentrations (Figure 2B). However, the optimum recovery was not significantly different compared with the recovery at the ethanol concentration of 28% ($P < 0.05$). The phenolic yield was highest (17.37 mg/g) at 26% ethanol concentration, which was significantly higher relative to that achieved at 32% ethanol concentration. However, the optimum yield was not significantly different relative to that achieved at other ethanol concentrations ($P > 0.05$). Therefore, the 30% ethanol concentration was selected in the subsequent experiments. In summary, the ethanol-ammonium sulfate ATPS has good distribution and extraction performance at 30% ethanol concentration and 20% ammonium sulfate concentration. Accordingly, ATPS was established based on these concentrations of the phase components for the following research.

Comparison of ultrasound-assisted and reciprocating shaking extraction

Variation of phenolic yield with extraction time under ultrasonic-assisted (30°C, 96.1 W/L) and reciprocating shaking

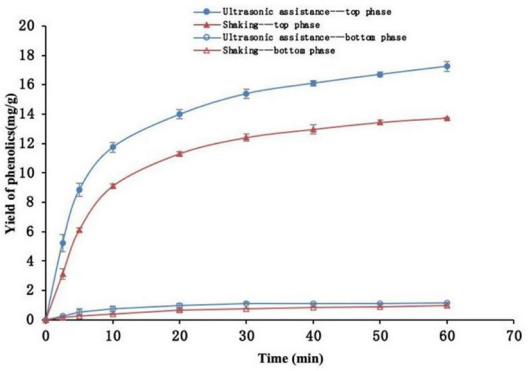

FIGURE 3
Phenolics yield after extraction with and without ultrasonic assistance.

(30°C, 100 rpm) conditions was compared as shown in Figure 3. The findings indicated that the yields of phenolics in the top and bottom phases rapidly increased at the first 10 min and then slowly increased after this point. The yield of phenolics in the top phase was higher compared with that in the bottom phase throughout the extraction period. The distribution coefficient of phenolics in the top phase at 60 min an extraction time was 12.23 and the recovery was 93.70% under ultrasonic conditions. The distribution coefficient at this extraction period was 12.12 and the recovery was 93.40% under the reciprocating shaker conditions. The results showed no significant difference in distribution coefficient and recovery between the two extraction methods ($P > 0.05$). The distribution coefficient of phenolics in ethanol solution was significantly higher relative to that in the salt solution, implying that they were mainly distributed in the top phase solution (37).

The results showed that the phenolic yield with ultrasound-assisted was significantly higher compared with that with reciprocating shaker ($P < 0.05$) throughout the extraction process. The phenolic yield with ultrasound-assisted increased by 25.12% when the extraction time was 60 min compared with the yield with reciprocating shaking. Notably, the ultrasonic wave had a significant effect on improving the extraction efficiency of phenolics. Ultrasonic wave significantly increases the extraction yield of phenolics compared with reciprocating shaking mainly by improving the diffusion of phenolics from grape pomace particles to the solvent (38).

Effects of AED and temperature on yield of phenolics during extraction

The yield of the phenolics in the top phase was used as an index to explore the effect of ATP extraction parameters. Effects of different AED on the yield of phenolics at 20, 30, and 40°C are shown in Figure 4. The findings showed that the yields of phenolics rapidly increased at the first 20 min and then slowly increased under the same temperature and different AEDs, and approached equilibrium at 60 min. The yield of phenolics increased with an increase in AED. AED had a significant effect on phenolic yield ($P < 0.05$). This implies that an increase in AED promotes surface washing of phenolics and unimpeded diffusion of the broken particle solute in the early stage, thus increasing extraction yield. Moreover, an increase in AED in the internal diffusion stage where the phenolics were impeded may promote breakage of the plant cell wall and accelerate the release of phenolics, thus increasing the extraction yield of phenolics. The findings from the preliminary experiment showed that the acoustic energy density within the scope of this study did not cause significant degradation of phenolics. However, previous studies report that a significantly high AED can promote the degradation of extracted components (39). In addition, the energy resulting from the bursting of cavitation bubbles is reduced when the AED reaches a certain level, ultimately reducing the promotion effect on extraction (40). Therefore, a reasonable ultrasonic intensity should be selected for practical application.

Effects of different temperatures on the yield of phenolics at 41.1, 63.5, 96.1, and 111.2 W/L are presented in Figure 5. The yield of phenolics increased with an increase in extraction time at different temperatures. A higher temperature was associated with a higher yield of phenolics compared with lower temperatures ($P < 0.05$) at the same extraction time. An increase in temperature increased solubility and diffusion coefficient of phenolics and promoted softening and swelling of particles, as well as reduced the viscosity of the solvent. These factors promote the mass transfer of phenolic substances in the system (41). Notably, the excessive temperature had a negative effect on extraction yield. Phenolics are heat-sensitive compounds, which are easily degraded at extremely high temperatures. In addition, extremely high temperatures reduce the energy generated when ultrasonic cavitation bubbles burst (24). Therefore, a suitable temperature should be selected for the extraction of phenolics.

Establishment of artificial neural network model

The topology of the model was optimized by adjusting the number of neurons in the hidden layer. The number of neurons in the hidden layer in the present study was eight. Components of the neural network used in this study are presented in Supplementary Figure 2. Regression of predicted values obtained after data training, verification, and testing is presented in Supplementary Figure 3. The correlation coefficient R-value was above 0.997. These findings and the dispersion

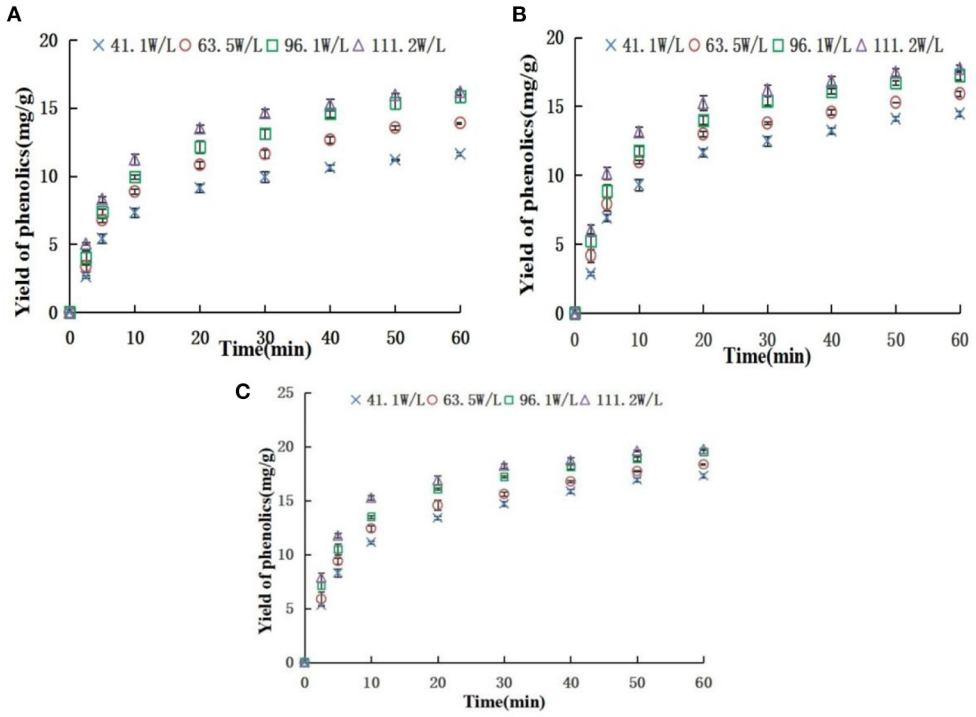

FIGURE 4
Effect of acoustic energy density on yield of phenolics [**(A)** 20°C; **(B)** 30°C; **(C)** 40°C].

degree of data distribution showed that the regression of the model obtained after training was satisfactory (22).

Optimal parameters and fitting performance evaluation results of the artificial neural network model are presented in Table 1. The findings showed that the correlation coefficient R^2 of this model was high (0.998), whereas the *RMSE* and *AAD* values were low (0.211 mg/g and 1.846%, respectively). This implies that the model fitting and prediction values were satisfactory. Theoretically, this algorithm can predict the yield of phenolics under any conditions within the range of the experimental conditions. Therefore, it can be used for effective visualization and intelligent extraction of phenolics.

An extraction diffusion model was successfully established

The extraction process was numerically simulated using the diffusion model to further study the extraction of phenolics in grape pomace by ATPS under ultrasound as well as evaluate the promoting effect of ultrasound. The particle size of grape pomace was determined using a laser particle size analyzer after ultrasonic-assisted extraction with different AED, before simulation. The results are presented in Figure 6. The median particle size (*Dv*50) of grape pomace particles after ultrasound-assisted extraction with different AED at 41.1, 63.5, 96.1, and 111.2 W/L was 671.67, 674.00, 667.00, and 669.00 um, respectively. The findings showed no significant difference in particle size under different ultrasonic conditions ($P > 0.05$). Therefore, particle size change of grape pomace was not considered when constructing the mass transfer diffusion model.

The values of effective diffusion coefficient *De* under different extraction conditions and results of the evaluation of model fitting degree are presented in Supplementary Table 1. *RMSE* values of all treatment groups were low, *AAD* values were below 10%, and R^2 was above 0.99. This indicates that the diffusion model can effectively fit the mass transfer process of phenolic extraction. A comparison of simulated and experimental values under all extraction conditions is presented in Figure 7. The simulated values were slightly different from the experimental values in some ranges; however, the fit degree was high and the correlation was good.

Effective diffusion coefficient *De* is an important parameter for evaluating mass transfer and diffusion process of phenolics. It indicates the speed of diffusion of the target substance in the medium. The effective diffusion coefficient *De* ranged between 1.67×10^{-10} and 5.83×10^{-10} m^2/s under the extraction conditions of this study (Supplementary Table 1). Tao et al. (18) reported that the *De* value ranged from 5.0×10^{-11} to 1.58

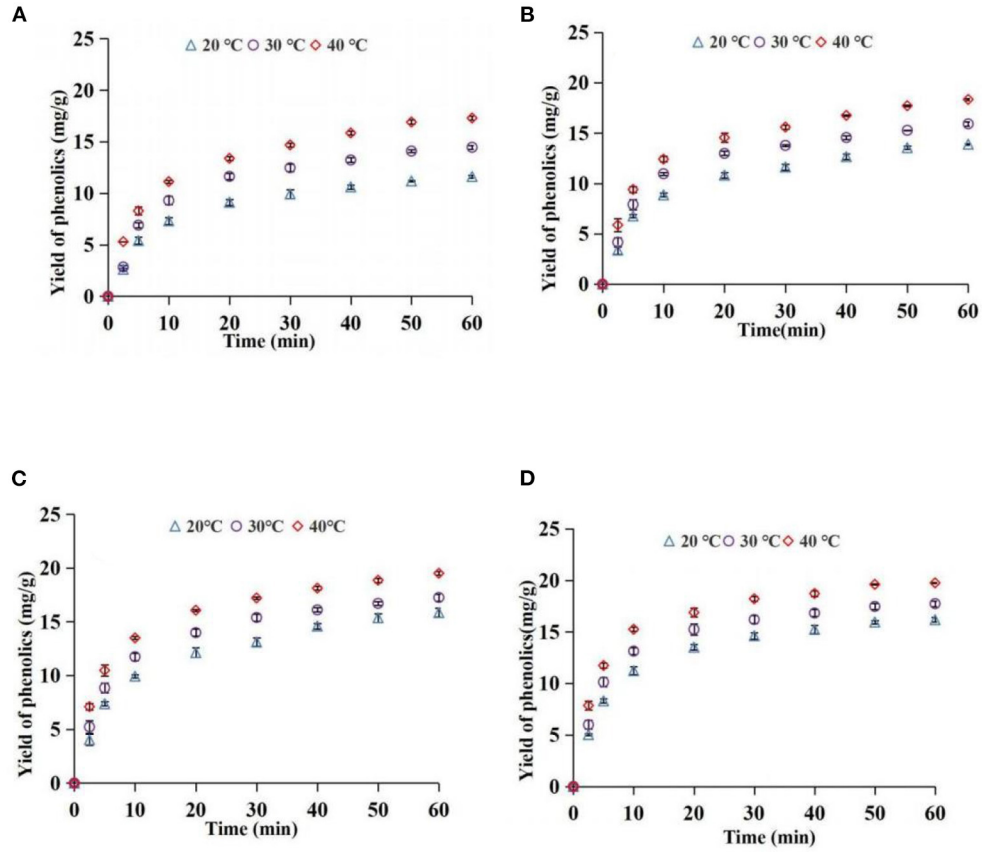

FIGURE 5
Effect of temperature on yield of phenolics [**(A)** 41.1 W/L; **(B)** 63.5 W/L; **(C)** 96.1 W/L; **(D)** 111.2 W/L].

TABLE 1 Model-related parameters and fitting performance evaluation results.

Input weight matrix (destination: hidden layer; source: inputs)			Bias vector (destination: hidden layer)	Layer weight matrix (destination: output layer; source: hidden layer)		Bias (destination: output layer)	R^2	RMSE	ADD
−0.0208	−1.8692	0.4737	3.657	−0.8835	T				
−0.5234	−0.232	−0.3317	1.9563	−1.2199					
−0.0265	−0.0456	4.5969	5.4388	2.3043					
0.1863	0.2145	0.7919	0.4626	0.6161		−1.0773	0.998	0.211	1.846
0.3811	0.4395	−0.2017	1.4884	1.1					
−0.9496	−4.0299	−7.4196	4.7981	0.0043					
1.0147	−1.9058	−1.1701	−0.5057	0.0354					
4.7435	2.6728	−0.2655	4.7459	−0.0408					

$\times 10^{-10}$ using distilled water as extraction solvent. The *De* value ranged from 1.62×10^{-10} to 4.67×10^{-10} when the solvent was 50% ethanol-aqueous solution, which is close to the *De* value range obtained in the current study. This indicates that the range of *De* values obtained in the present study is reliable.

De value is correlated with material structure, solvent type, and extraction conditions (such as temperature and acoustic energy density). A high temperature is correlated with a high *De* value ($P < 0.05$) under the same AED condition (Supplementary Table 1). This observation may be because the thermal activation energy of atoms is higher and the

migration rate increases at a higher temperature, thus increasing the diffusion coefficient (42). This result was consistent with findings from previous research (43). A high AED was correlated with a high *De* value ($P < 0.05$) at the same temperature (Supplementary Table 1). The findings of the present study showed that the particle size of grape pomace did not change significantly under different acoustic energy densities. This indicates that ultrasonic waves to grape pomace mainly damaged the outer tissue of the particles. An increase in AED promotes damage to ultrasonic cavitation effect and mechanical effect on the complete surface of grape pomace particles. In addition, high AED promotes the internal diffusion of polyphenol, thus increasing the *De* value (18).

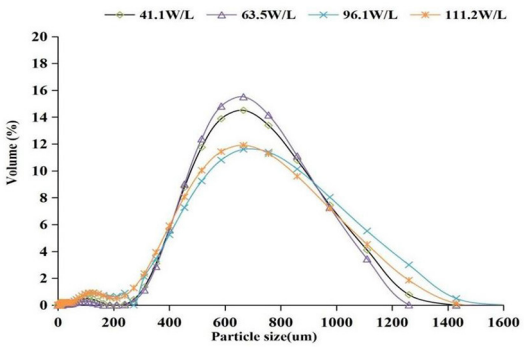

FIGURE 6
Particle size distribution of grape pomace at different acoustic energy densities.

The quadratic polynomial function was used in this study to explore the relationship between *De* value and temperature and AED. The results were as shown below:

$$De \times 10^{10} = -1.599 + 0.02055 \cdot AED + 0.1213 \cdot T - 6.285 \cdot 10^{-5} \cdot AED^2 - 6.25 \cdot 10^{-5} \cdot T^2 - 7.966 \cdot 10^{-5} \cdot AED \cdot T \quad \left(R^2 = 0.991\right) \quad (14)$$

R^2 of this equation was 0.991, indicating a high fit degree. The function shows that the effect of temperature on the *De* value

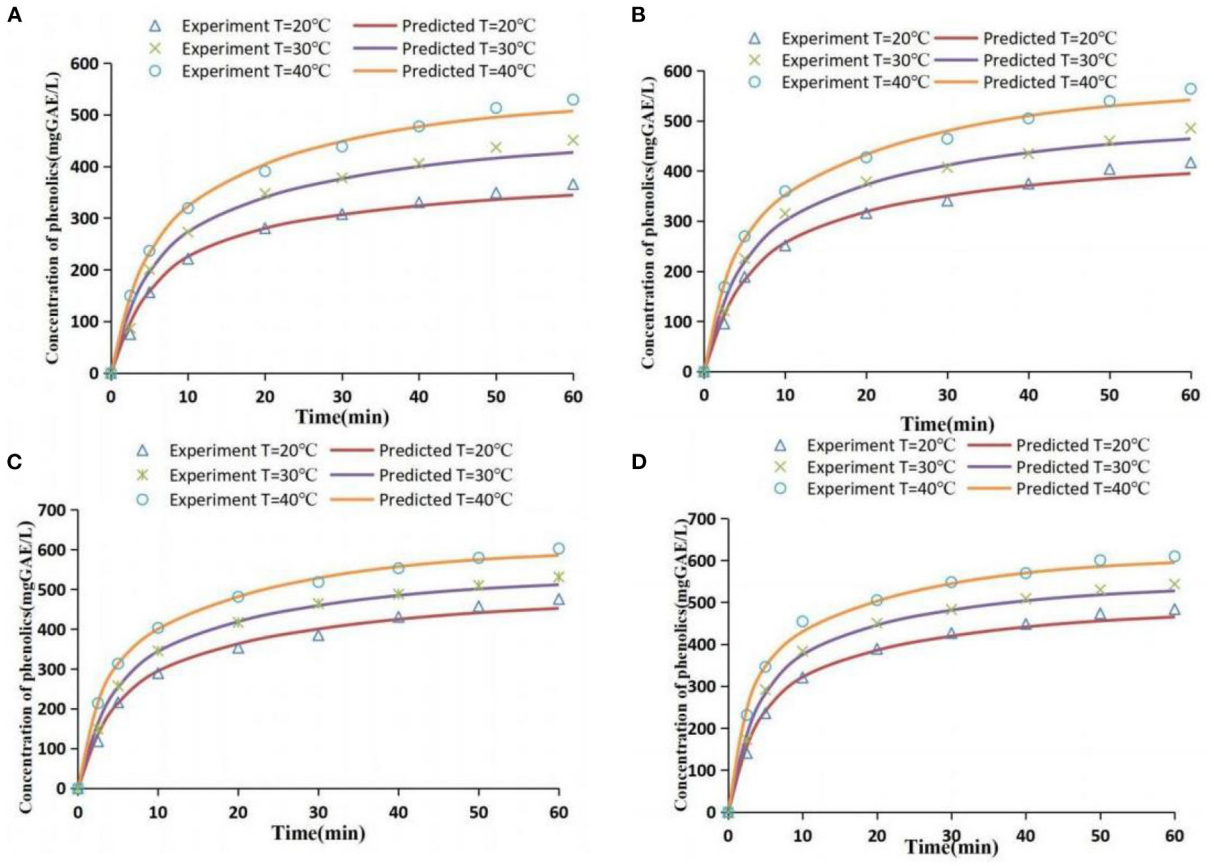

FIGURE 7
Comparison of experimental values and simulated values [extraction conditions: **(A)** 41.1 W/L; **(B)** 63.5 W/L; **(C)** 96.1 W/L; **(D)** 111.2 W/L].

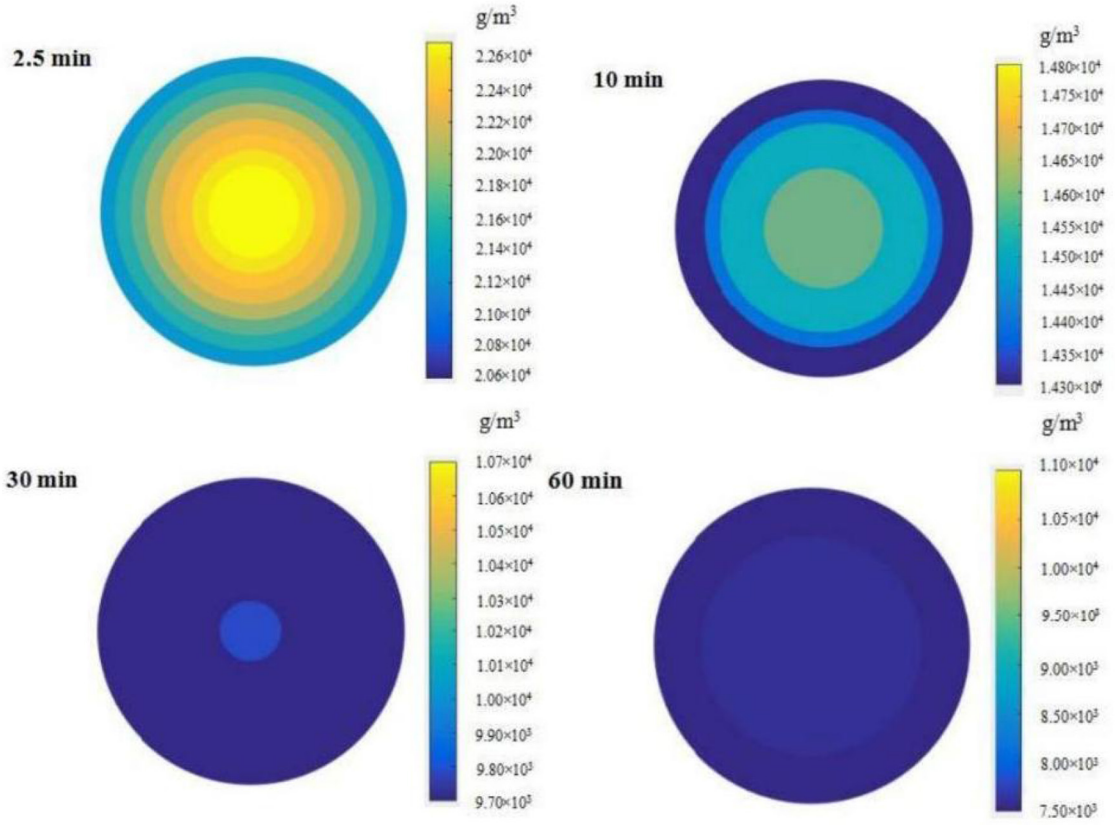

FIGURE 8
Distribution of phenolics content within grape pomace at different extraction time points (Extraction conditions: 30°C and 96.1 W/L).

is higher compared with that of sound energy density, which is consistent with previous results (44).

The distribution of phenolics in grape pomace was simulated by a programming method based on the diffusion model when the extraction time was 2.5, 10, 30, and 60 min, to explore the change in the distribution of phenolics in grape pomace during extraction. The simulation results at 30°C and 96.1 W/L are presented in Figure 8. The findings showed that between 2.5 and 60 min, the occurrence of particle interior near the surface was associated with lower phenolic content. The phenolic content distribution became more uniform with an increase in extraction time, and the difference between the phenolic content in the core part and the surface became smaller.

Analysis of individual phenolic content

The yields and the content of individual phenolics in grape pomace (extracted three times) were obtained by ultrasound-assisted ATP extraction (30°C and 96.1 W/L) and reciprocating shaking ATP extraction (30°C and 100 rpm) with 50% ethanol solution crude extraction (30°C and reciprocating shaking) are presented in Table 2. The purpose of analyzing the content of individual phenolics was to analyze the extraction from the perspective of individual phenolics; therefore, only anthocyanins and flavonols were analyzed. The findings showed that the yield of anthocyanins extracted by ultrasound with exception of paeoniflorin pigm-3-glucoside was significantly higher relative to the yield obtained by non-ultrasonic extraction ($P < 0.05$). The findings showed that the ultrasonic method effectively promoted the extraction of anthocyanins. The extraction yield under ultrasonic conditions of the three individual anthocyanins was more than 75% of the total content. The extraction yield of the three individual anthocyanins under non-ultrasonic extraction using 50% ethanol solution was higher compared with that under reciprocating shaking ATP. This is mainly attributed to the different solubilities of anthocyanins due to the different polarities of the two systems and solutions. Yilmaz and Toledo (45) reported that the solvent type significantly affects the extraction rate of phenolics. The extraction rates for rutin using 50% ethanol solution were lower than the rates achieved using ATPS ($P < 0.05$). However, a higher yield of myricetin was obtained using ATPS compared with 50%

10.3389/fnut.2022.993475

TABLE 2 Extraction yield of individual anthocyanins and flavonols.

Species	Monomer phenols	Ultrasound-assisted ATP extraction (μg/g)	Reciprocating shaking ATP extraction (μg/g)	50% ethanol solution crude extraction (μg/g)	Raw materials (μg/g)
Anthocyanins	Centrinin-3-glucoside	46.47 ± 1.74b	29.76 ± 2.93d	42.12 ± 2.92c	61.28 ± 0.27a
	Paeoniflorin pigm-3-glucoside	27.01 ± 3.79b	16.35 ± 1.48c	27.02 ± 1.42b	31.86 ± 1.80a
	Mallet pigment−3-glucoside	35.97 ± 2.32b	22.74 ± 2.64d	28.90 ± 2.17c	42.43 ± 2.98a
Flavonols	Rutin	30.80 ± 3.54a	27.78 ± 2.94b	19.40 ± 1.75c	35.04 ± 7.60a
	Myricetin	23.89 ± 1.37c	19.96 ± 1.57c	30.40 ± 0.82b	69.97 ± 3.37a

Values followed by different letters in each line indicate significant differences ($p < 0.05$) among pre-treatments.

ethanol solution. This difference in rates can be attributed to different solubilities of rutin and myricetin under different solvent systems.

Distribution of sugars at the top and bottom phases during extraction

The separation effect of ATP on sugar is an important reference index for the purification of phenolics. The concentration evolution of total sugars in the top and bottom phases during the extraction process was determined to evaluate the separation properties of phenolics and sugars (Figure 9). The findings showed that total sugar content increased gradually with an increase in time during the extraction process, and the increasing trend was significant in the bottom phase compared with the top phase. The concentration of sugar in the top and bottom phases under ultrasound exhibited a significant difference at 2.5 min, whereas the difference was not significant under reciprocating shaking. The distribution speed of sugar in ATPS under the ultrasound method was significantly higher than that of the water bath oscillation. In addition, the distribution coefficient under the ultrasound-assisted condition was significantly higher compared with that under the reciprocating shaking condition ($P < 0.05$) at 60 min. The partition coefficients of the top phase sugar contents were 4.80 (ultrasound) and 3.29 (reciprocating shaking), respectively, at 60 min, and the recovery rates were 79.86% (ultrasound) and 72.96% (reciprocating shaking), respectively. This implies that sugars were mainly distributed in the salt-rich phase during ATP extraction of phenolics. Wu et al. (15) separated anthocyanins and sugars using an aqueous two-phase system of ethanol-ammonium sulfate. The results showed that 89.5% of the sugars were distributed in the bottom phase. In the present study, phenolics were mainly distributed in the top alcohol-rich phase; thus the system can effectively separate phenolics and sugars in different phases, aiding the purification of phenolics.

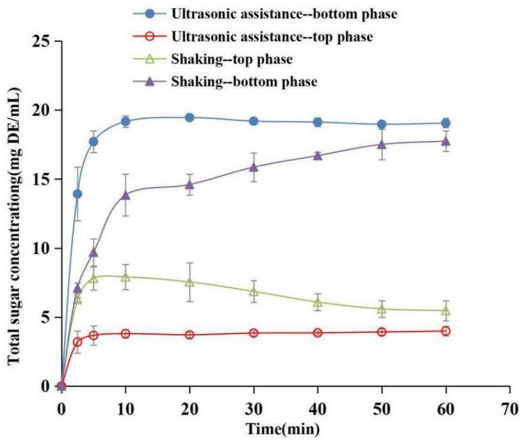

FIGURE 9
Concentration evolution of total sugars as a function of time in top phase and bottom phase (Extraction conditions: sonication: 30°C and 96.1 W/L; shaking: 30°C and 100 rpm).

Comparison of phenolics purity under different extraction conditions

The purity of phenolics obtained by ultrasonic-assisted ATP extraction (30°C and 96.1 W/L), reciprocating shaking ATP extraction (30°C and 100 rpm), 50% ethanol solution crude extraction (30°C and 100 rpm), and the purity of phenolics in raw materials were compared (Figure 10). The findings showed that the purity of phenolics was 6.98% after ultrasonic-assisted ATP extraction, which was 181.15 and 58.3% higher compared with 2.48% of raw materials and 4.41% of conventional 50% ethanol crude extraction. The purification effect was significantly different among the three methods ($P < 0.05$). In addition to polyphenols, grape pomace contains sugars, organic acids, pectin, oligosaccharides, protein, minerals, vitamins, and other substances (46, 47). The polarity of the top and bottom phases of ATPS is quite different; thus the molecular forces and dissolution properties of these substances in the top and bottom phases are also different. In addition,

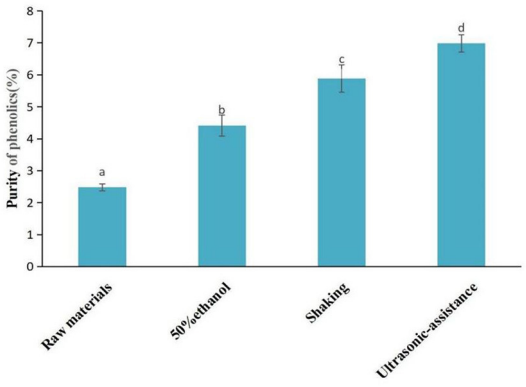

FIGURE 10
Comparison of purity of phenolics in extracts using different extraction methods.

the compounds are distributed in different phases during the extraction process, which helps to improve the purity of target extraction components.

Conclusion

The findings of the present study show that ultrasound-assisted ATP is an effective technology for the extraction and purification of phenolics from grape pomace. The appropriate phase composition concentration of ATPS for extraction of phenolics from grape pomace was 30% ethanol (w/w) and 20% ammonium sulfate. The yield of phenolics increased with an increase in AED and temperature. ANN showed high efficacy in correlating extraction parameters with phenolic yield with a correlation coefficient above 0.98. The model showed high efficacy in the visualization and intelligent extraction of phenolics. Moreover, Fick's second law diffusion model revealed the mechanism of ultrasound-assisted ATP in the mass transfer process. Notably, *De* value increased with an increase in AED and temperature. Three anthocyanins and two flavonols were analyzed by HPLC, and the results indicated that the ultrasound method improved the extraction yield of anthocyanins. Higher yields of rutin and myricetin were achieved using ATPS and a 50% ethanol aqueous system, respectively. Sugars were mainly distributed in the bottom phase, whereas phenolics were mainly distributed in the bottom phase. This partition characteristic effectively alleviates the influence of impurities such as sugars on the quality of phenolics. The phenolic purity of the final extract was 6.98%, which was 58.3% higher compared with that of the traditional solid-liquid extraction, indicating effective preliminary purification of phenolics using the method. In summary, enhanced extraction of phenolics and preliminary purification of phenolics was achieved using ultrasound-assisted ATP extraction technology. This strategy has broad application prospects in phenolic extraction from grape pomace and promoting resource utilization of grape pomace.

However, one of the major trends is that there is gaining interest in using new raw materials with benign, eco-friendly, low cost, and recyclable characteristics to form ATPS. Salts such as phosphates and sulfates would pose wastewater treatment problems if the salts are not subjected to recycling. Hence, efforts have been put into the replacement of these salts with biodegradable salt, such as citrate.

Data availability statement

The original contributions presented in the study are included in the article/Supplementary material, further inquiries can be directed to the corresponding author/s.

Author contributions

GX: conceptualization, methodology, validation, formal analysis, writing—original draft preparation, and writing—review and editing. JS: software. JL: methodology and writing—review and editing. DL: formal analysis. YT: software, formal analysis, writing—original draft preparation, and supervision. CS: supervision. YH: conceptualization, writing—review and editing, and supervision. All authors have read and agreed to the published version of the manuscript.

Funding

This work was supported by the Fundamental Research Funds for the Central Universities, China (Grant No. KJQN201824) and the National Natural Science Foundation of China (Grant No. 31701616).

Conflict of interest

The authors declare that the research was conducted in the absence of any commercial or financial relationships that could be construed as a potential conflict of interest.

Publisher's note

All claims expressed in this article are solely those of the authors and do not necessarily represent those

of their affiliated organizations, or those of the publisher, the editors and the reviewers. Any product that may be evaluated in this article, or claim that may be made by its manufacturer, is not guaranteed or endorsed by the publisher.

Supplementary material

The Supplementary Material for this article can be found online at: https://www.frontiersin.org/articles/10.3389/fnut.2022.993475/full#supplementary-material

References

1. Demirkol M, Tarakci Z. Effect of grape (*Vitis labrusca* L.) pomace dried by different methods on physicochemical, microbiological and bioactive properties of yoghurt. *LWT.* (2018) 97:770–7. doi: 10.1016/j.lwt.2018.07.058

2. de Souza VB, Thomazini M, Balieiro JCC, Fávaro-Trindade CS. Effect of spray drying on the physicochemical properties and color stability of the powdered pigment obtained from vinification byproducts of the Bordo grape (*Vitis labrusca*). *Food Bioprod Process.* (2015) 93:39–50. doi: 10.1016/j.fbp.2013.11.001

3. Jara-Palacios MJ, Hernanz D, Cifuentes-Gomez T, Escudero-Gilete ML, Heredia FJ, Spencer JP. Assessment of white grape pomace from winemaking as source of bioactive compounds, and its antiproliferative activity. *Food Chem.* (2015) 183:78–82. doi: 10.1016/j.foodchem.2015.03.022

4. Farhadi K, Esmaeilzadeh F, Hatami M, Forough M, Molaie R. Determination of phenolic compounds content and antioxidant activity in skin, pulp, seed, cane and leaf of five native grape cultivars in West Azerbaijan province, Iran. *Food Chem.* (2016) 199:847–55. doi: 10.1016/j.foodchem.2015.12.083

5. Rodriguez-Rodriguez R, Justo ML, Claro CM, Vila E, Parrado J, Herrera M.D, et al. Endothelium-dependent vasodilator and antioxidant properties of a novel enzymatic extract of grape pomace from wine industrial waste. *Food Chem.* (2012) 135:1044–51. doi: 10.1016/j.foodchem.2012.05.089

6. Peixoto CM, Dias MI, Alves MJ, Calhelha RC, Barros L, Pinho SP, et al. Grape pomace as a source of phenolic compounds and diverse bioactive properties. *Food Chem.* (2018) 253:132–8. doi: 10.1016/j.foodchem.2018.01.163

7. Wittenauer J, Mackle S, Sussmann D, Schweiggert-Weisz U, Carle R. Inhibitory effects of polyphenols from grape pomace extract on collagenase and elastase activity. *Fitoterapia.* (2015) 101:179–87. doi: 10.1016/j.fitote.2015.01.005

8. Xu Y, Burton S, Kim C, Sismour E. Phenolic compounds, antioxidant, and antibacterial properties of pomace extracts from four Virginia-grown grape varieties. *Food Sci Nutr.* (2016) 4:125–33. doi: 10.1002/fsn3.264

9. Cabezudo I, Meini MR, Di Ponte CC, Melnichuk N, Boschetti CE, Romanini D. Soybean (Glycine max) hull valorization through the extraction of polyphenols by green alternative methods. *Food Chem.* (2021) 338:128131. doi: 10.1016/j.foodchem.2020.128131

10. Croxatto Vega G, Sohn J, Voogt J, Birkved M, Olsen SI, Nilsson AE. Insights from combining techno-economic and life cycle assessment – a case study of polyphenol extraction from red wine pomace. *Resour Conserv Recycl.* (2021) 167:105318. doi: 10.1016/j.resconrec.2020.105318

11. Dominguez-Rodriguez G, Marina ML, Plaza M. Enzyme-assisted extraction of bioactive non-extractable polyphenols from sweet cherry (*Prunus avium* L.) pomace. *Food Chem.* (2021) 339:128086. doi: 10.1016/j.foodchem.2020.128086

12. Gonzalez-Rivera J, Duce C, Campanella B, Bernazzani L, Ferrari C, Tanzini E, et al. *In situ* microwave assisted extraction of clove buds to isolate essential oil, polyphenols, and lignocellulosic compounds. *Ind Crops Prod.* (2021) 161:113203. doi: 10.1016/j.indcrop.2020.113203

13. Ninčević Grassino A, Ostojić J, Miletić V, Djaković S, Bosiljkov T, Zorić Z, et al. Application of high hydrostatic pressure and ultrasound-assisted extractions as a novel approach for pectin and polyphenols recovery from tomato peel waste. *Innov Food Sci Emerg Technol.* (2020) 64:102424. doi: 10.1016/j.ifset.2020.102424

14. Chethana S, Nayak CA, Madhusudhan MC, Raghavarao KS. Single step aqueous two-phase extraction for downstream processing of C-phycocyanin from spirulina platensis. *J Food Sci Technol.* (2015) 52:2415–21. doi: 10.1007/s13197-014-1287-9

15. Wu X, Liang L, Zou Y, Zhao T, Zhao J, Li F, et al. Aqueous two-phase extraction, identification and antioxidant activity of anthocyanins from mulberry (*Morus atropurpurea* Roxb.). *Food Chem.* (2011) 129:443–53. doi: 10.1016/j.foodchem.2011.04.097

16. Qin B, Liu X, Cui H, Ma Y, Wang Z, Han J. Aqueous two-phase assisted by ultrasound for the extraction of anthocyanins from *Lycium ruthenicum* Murr. *Prep Biochem Biotechnol.* (2017) 47:881–8. doi: 10.1080/10826068.2017.1350980

17. Đordević T, Antov M. Ultrasound assisted extraction in aqueous two-phase system for the integrated extraction and separation of antioxidants from wheat chaff. *Sep Purif Technol.* (2017) 182:52–8. doi: 10.1016/j.seppur.2017.03.025

18. Tao Y, Wang Y, Pan M, Zhong S, Wu Y, Yang R, et al. Combined ANFIS and numerical methods to simulate ultrasound-assisted extraction of phenolics from chokeberry cultivated in China and analysis of phenolic composition. *Sep Purif Technol.* (2017) 178:178–88. doi: 10.1016/j.seppur.2017.01.012

19. Buciński A, Karamać M, Amarowicz R, Pegg RB. Modeling the tryptic hydrolysis of pea proteins using an artificial neural network. *LWT Food Sci Technol.* (2008) 41:942–5. doi: 10.1016/j.lwt.2007.06.021

20. Tao Y, Han Y, Liu W, Peng L, Wang Y, Kadam S, et al. Parametric and phenomenological studies about ultrasound-enhanced biosorption of phenolics from fruit pomace extract by waste yeast. *Ultrason Sonochem.* (2017) 52:193–204. doi: 10.1016/j.ultsonch.2018.11.018

21. Silva S.F, Anjos CA, Cavalcanti RN, Celeghini RM. Evaluation of extra virgin olive oil stability by artificial neural network. *Food Chem.* (2015) 179:35–43. doi: 10.1016/j.foodchem.2015.01.100

22. Tao Y, Wu D, Zhang Q, Sun D. Ultrasound-assisted extraction of phenolics from wine lees: modeling, optimization and stability of extracts during storage. *Ultrason Sonochem.* (2014) 21:706–15. doi: 10.1016/j.ultsonch.2013.09.005

23. Tao Y, Wang P, Wang J, Wu Y, Han Y, Zhou J. Combining various wall materials for encapsulation of blueberry anthocyanin extracts: optimization by artificial neural network and genetic algorithm and a comprehensive analysis of anthocyanin powder properties. *Powder Technol.* (2017) 311:77–87. doi: 10.1016/j.powtec.2017.01.078

24. Tao Y, Wu Y, Han Y, Chemat F, Li D, Show P. Insight into mass transfer during ultrasound-enhanced adsorption/desorption of blueberry anthocyanins on macroporous resins by numerical simulation considering ultrasonic influence on resin properties. *Chem Eng J.* (2020) 380:122530. doi: 10.1016/j.cej.2019.122530

25. Aydogan Ö, Bayraktar E, Mehmetoglu Ü. Aqueous two-phase extraction of lactic acid: optimization by response surface methodology. *Sep Sci Technol.* (2011) 46:1164–71. doi: 10.1080/01496395.2010.550270

26. Xavier L, Freire MS, Vidal-Tato I, González-Álvarez J. Recovery of phenolic compounds from eucalyptus wood wastes using ethanol-salt-based aqueous two-phase systems. *Ciencia Tecnol.* (2017) 19:3–14. doi: 10.4067/S0718-221X2017005000001

27. Wang Y, Yan Y, Hu S, Han J, Xu X. Phase diagrams of ammonium sulfate +ethanol/1-propanol/2-propanol + water aqueous two-phase systems at 298.15 K and correlation. *J Chem Eng Data.* (2010) 55:876–81. doi: 10.1021/je900504e

28. Wang Y, Mao Y, Han J, Liu Y, Yan Y. Liquid–Liquid equilibrium of potassium phosphate/potassium citrate/sodium citrate + ethanol aqueous two-phase systems at (298.15 and 313.15) K and correlation. *J Chem Eng Data.* (2010) 55:5621–6. doi: 10.1021/je100501f

29. Tao Y, Wang P, Wang Y, Kadam SU, Han Y, Wang J, et al. Power ultrasound as a pretreatment to convective drying of mulberry (*Morus alba* L.) leaves: impact on drying kinetics and selected quality properties. *Ultrason Sonochem.* (2017) 31:310–8. doi: 10.1016/j.ultsonch.2016.01.012

30. Wu GH, Hu T, Huang ZL, Jiang JG. Characterization of water and alkali-soluble polysaccharides from *Pleurotus tuber-regium* sclerotia. *Carbohydr Polym.* (2013) 96:284–90. doi: 10.1016/j.carbpol.2013.03.036

31. Cui C, Zhang S, You L, Ren J, Luo W, Chen W, et al. Antioxidant capacity of anthocyanins from *Rhodomyrtus tomentosa* (Ait.) and identification of the major anthocyanins. *Food Chem.* (2013) 139:1–8. doi: 10.1016/j.foodchem.2013.01.107

32. Zhang W, Han F, He J, Duan C. HPLC-DAD-ESI-MS/MS analysis and antioxidant activities of nonanthocyanin phenolics in mulberry (*Morus alba* L.). *J Food Sci.* (2013) 73:C512–8. doi: 10.1111/j.1750-3841.2008.00854.x

33. Juan C, Jianquan K, Junni T, Zijian C, Ji L. The profile in polyphenols and volatile compounds in alcoholic beverages from different cultivars of mulberry. *J Food Sci.* (2012) 77:C430–6. doi: 10.1111/j.1750-3841.2011.02593.x

34. Bhatti MS, Kapoor D, Kalia RK, Reddy AS, Thukral AK. RSM and ANN modeling for electrocoagulation of copper from simulated wastewater: multi objective optimization using genetic algorithm approach. *Desalination.* (2011) 274:74–80. doi: 10.1016/j.desal.2011.01.083

35. Klein M, Aserin A, Ben Ishai P, Garti N. Interactions between whey protein isolate and gum Arabic. *Colloids Surf B Biointerfaces.* (2010) 79:377–83. doi: 10.1016/j.colsurfb.2010.04.021

36. Gong W, Li D, Wu Y, Manickam S, Sun X, Han Y, et al. Sequential phenolic acid co-pigmentation pretreatment and contact ultrasound-assisted air drying to intensify blackberry drying and enhance anthocyanin retention: a study on mass transfer and phenolic distribution. *Ultrason Sonochem.* (2021) 80:105788. doi: 10.1016/j.ultsonch.2021.105788

37. Guerrero MS, Torres JS, Nunez MJ. Extraction of polyphenols from white distilled grape pomace: optimization and modelling. *Bioresour Technol.* (2008) 99:1311–8. doi: 10.1016/j.biortech.2007.02.009

38. Tao Y, Zhang Z, Sun DW. Kinetic modeling of ultrasound-assisted extraction of phenolic compounds from grape marc: influence of acoustic energy density and temperature. *Ultrason Sonochem.* (2014) 21:1461–9. doi: 10.1016/j.ultsonch.2014.01.029

39. Zhang WN, Zhang HL, Lu CQ, Luo JP, Zha XQ. A new kinetic model of ultrasound-assisted extraction of polysaccharides from Chinese chive. *Food Chem.* (2016) 212:274–81. doi: 10.1016/j.foodchem.2016.05.144

40. Wang M, Yuan W. Modeling bubble dynamics and radical kinetics in ultrasound induced microalgal cell disruption. *Ultrason Sonochem.* (2016) 28:7–14. doi: 10.1016/j.ultsonch.2015.06.025

41. Tao Y, Sun DW. Enhancement of food processes by ultrasound: a review. *Crit Rev Food Sci Nutr.* (2015) 55:570–94. doi: 10.1080/10408398.2012.667849

42. Cacace JE, Mazza G. Mass transfer process during extraction of phenolic compounds from milled berries. *J Food Eng.* (2003) 59:379–89. doi: 10.1016/S0260-8774(02)00497-1

43. Milic PS, Rajkovic KM, Stamenkovic OS, Veljkovic VB. Kinetic modeling and optimization of maceration and ultrasound-extraction of resinoid from the aerial parts of white lady's bedstraw (*Galium mollugo* L.). *Ultrason Sonochem.* (2013) 20:525–34. doi: 10.1016/j.ultsonch.2012.07.017

44. Tao Y, Zhang Z, Sun DW. Experimental and modeling studies of ultrasound-assisted release of phenolics from oak chips into model wine. *Ultrason Sonochem.* (2013) 21:1839–48. doi: 10.1016/j.ultsonch.2014.03.016

45. Yilmaz Y, Toledo RT. Oxygen radical absorbance capacities of grape/wine industry byproducts and effect of solvent type on extraction of grape seed polyphenols. *J Food Composit Anal.* (2006) 19:41–8. doi: 10.1016/j.jfca.2004.10.009

46. Saura C, Fulgencio. Antioxidant dietary fiber product: a new concept and a potential food ingredient. *J Agric Food Chem.* (1998) *46*: 4303–6. doi: 10.1021/jf9803841

47. Llobera A, Cañellas J. Dietary fibre content and antioxidant activity of Manto Negro red grape (*Vitis vinifera*): pomace and stem. *Food Chem.* (2007) 101:659–66. doi: 10.1016/j.foodchem.2006.02.025

frontiers | Frontiers in Nutrition

TYPE Original Research
PUBLISHED 07 December 2022
DOI 10.3389/fnut.2022.1080147

OPEN ACCESS

EDITED BY
Runqiang Yang,
Nanjing Agricultural University, China

REVIEWED BY
Peiyou Qin,
Institute of Crop Sciences (CAAS), China
Hong-Yan Liu,
Institute of Urban Agriculture (CAAS), China

*CORRESPONDENCE
Daniel A. Jacobo-Velázquez
djacobov@tec.mx

SPECIALTY SECTION
This article was submitted to Nutrition and Food Science Technology, a section of the journal Frontiers in Nutrition

RECEIVED 25 October 2022
ACCEPTED 18 November 2022
PUBLISHED 07 December 2022

CITATION
Villamil-Galindo E, Antunes-Ricardo M, Piagentini AM and Jacobo-Velázquez DA (2022) Adding value to strawberry agro-industrial by-products through ultraviolet A-induced biofortification of antioxidant and anti-inflammatory phenolic compounds. *Front. Nutr.* 9:1080147. doi: 10.3389/fnut.2022.1080147

Adding value to strawberry agro-industrial by-products through ultraviolet A-induced biofortification of antioxidant and anti-inflammatory phenolic compounds

Esteban Villamil-Galindo[1,2], Marilena Antunes-Ricardo[3,4], Andrea Marcela Piagentini[1] and Daniel A. Jacobo-Velázquez[5,6]*

[1]Instituto de Tecnología de Alimentos, Facultad de Ingeniería Química, Universidad Nacional del Litoral, Santa Fe, Argentina, [2]Consejo Nacional de Investigaciones Científicas y Técnicas (CONICET), Santa Fe, Argentina, [3]Tecnológico de Monterrey, The Institute for Obesity Research, Monterrey, Mexico, [4]Tecnológico de Monterrey, Escuela de Ingeniería y Ciencias, Monterrey, Mexico, [5]Tecnológico de Monterrey, The Institute for Obesity Research, Zapopan, Mexico, [6]Tecnológico de Monterrey, Escuela de Ingeniería y Ciencias, Zapopan, Mexico

Background: The revalorization of agro-industrial by-products by applying ultraviolet A (UVA) radiation to biofortify with phenolic compounds has been studied in recent times, showing improvements in the individual and total phenolic content and their bioactivity. Therefore, the main aim of this work was to optimize the biofortification process of phenolic compounds by UVA radiation to strawberry agro-industrial by-products (RF). Moreover, the effect of UVA radiation on the potential biological activity of the phenolics accumulated in RF due to the treatment was also determined.

Methods: The assays followed a factorial design with three variables at three levels: UVA dose (LOW, MEDIUM, and HIGH), storage temperature (5, 10, and 15°C), and storage time (0, 24, 48, and 72 h). At each experimental condition, phenylalanine ammonia-lyase (PAL) and polyphenol oxidase (PPO) enzymatic activities, total phenolic compound content (TPC), phenolics profile (TPC_{HPLC}), and agrimoniin content (AGN) were evaluated; and the optimal UVA dose, storage time, and temperature were determined. *In vitro* bioaccessibility of the accumulated phenolic compound was studied on RF tissue treated with UVA at optimal process conditions. The digested extracts were tested for antiproliferative activity in colorectal cancer cells, cellular antioxidant capacity, and anti-inflammatory activity.

Results: The results showed that applying UVA-HIGH (86.4 KJ/m^2) treatment and storing the tissue for 46 h at 15°C increased PAL activity (260%), phenolic content (240%), and AGN (300%). The biofortification process improves the bioaccessibility of the main phenolic compound of RF by 9.8 to 25%. The digested optimum extract showed an IC50 for HT29 and Caco-2 cells of 2.73

and 5.43 μg/mL, respectively, and presented 60% cellular antioxidant capacity and 30% inhibition of NOX production.

Conclusion: The RF treated with UVA is an excellent source of phenolic compounds; specifically, ellagitannins and the UVA radiation proved to be efficient in biofortify RF, significantly improving the phenolic compounds content and their bioactive properties with adequate bioaccessibility, adding value to the strawberry agro-industrial by-products.

KEYWORDS

biofortification, revalorization, UV radiation, circular economy, ellagitannins, postharvest abiotic stresses

Introduction

Post-harvest processing of fruit and vegetables generates two types of agro-industrial by-products: avoidable and non-avoidable. Avoidable by-products are generated due to poor post-harvest handling during storage, processing, and transportation. On the other hand, non-avoidable by-products are derived from the conditioning of fruits and vegetables where the non-usable or non-edible parts of the product are eliminated (peels, seeds, leaves, stalks, or products in bad condition) (1). Agro-industrial by-products represent a significant challenge in their management and disposal in developed and developing countries (1). In the case of strawberry agro-industrial packaging, non-avoidable by-products can represent 7–20% of production (2). Different studies have been performed to describe the composition and the use of agro-industrial by-products in food and nutraceutical industries due to the composition rich in bioactive compounds such as vitamins, amino acids, dietary fiber, and secondary metabolites, in particular phenolic compounds (3, 4). The different strategies for the use of agro-industrial by-products allow the transformation from linear to circular processes, reducing the carbon footprint, maximizing the use of resources, offering environmental and economic benefits, and improving efficiency in developing countries' agro-industries (4).

The polyphenolic distribution in strawberries depends on the crop's tissue, variety, and environmental factors. Nevertheless, the major phenolic compounds in the strawberry plant have been reported as ellagitannins, phenolic acids, and flavonoids such as anthocyanins and quercetin glycosides (5). These metabolites offer different physiological functions to plants and are synthesized in response to different exogenous stimuli, one of the most common is UV radiation (6). The high energy rate of ultraviolet radiation can generate damage at the cellular level. However, the response of plants is generated depending on the dose and type of radiation they receive. The electromagnetic spectrum of UV radiation is between 100 and 400 nm, usually subdivided into 3 regions UVA (315–400 nm), UVB (280–315 nm), and UVC (100–280) (7), having different elicitor effects on plants. It has been reported that UV radiation activates enzymes related to the biosynthesis and utilization of phenolic compounds and depending on the biosynthesis rate and utilization rate, accumulation of phenolics can be observed in the tissue (8).

Obtaining health-promoting compounds from agro-industrial by-products is one strategy used to revalue agro-industrial by-products (2). Likewise, agro-industrial by-products can also be used as biofactories of phenolic compounds by applying different abiotic stresses that modulate their secondary metabolism, obtaining significant increases in the concentration of phenolic compounds (9). UV radiation may trigger phenylpropanoid metabolism in plant tissues. For instance, increases of up to 500% in total phenolic content have been reported in carrots (8), and a 700% increase in quercetin in red prickly pears (10). However, there are no specific UV radiation conditions to induce the accumulation of phenolics since each plant tissue responds differently to abiotic stresses.

To incorporate phenolic compounds extracted from agro-industrial by-products in different food or dietary supplement formulations, it is necessary to study their behavior in human metabolism. The cytotoxicity of phenolic compounds has been studied in healthy cell lines with different metabolic functions (11) and in cell cultures of different types of cancer and their antioxidant and anti-inflammatory activity (12). Various bioactivities of phenolic compounds obtained from strawberries and other plant parts have been reported in experimental *in vitro* studies, showing their potential to be a source of nutraceutical compounds (13). However, there is no report on the bioactivity of these compounds after the digestion process, as their content and stability are significantly affected by the type of matrix in which they are found and the gastrointestinal process. There is no report in the literature regarding the application of UV radiation to improve phenolic content from strawberry agro-industrial by-products and evaluate their bioaccessibility and

bioactivity. Therefore, the main objective of this work was to add value to strawberry by-products by determining the optimal conditions of UVA radiation, storage temperature, and time to increase phenolic compounds' content and assess their stability during digestion, cytotoxicity, and potential biological activity.

Materials and methods

Plant material and reagents

The by-products of strawberry (RF) (*Fragaria* × *ananassa* Duch) were obtained during postharvest industrial conditioning of strawberries from a field at Coronda, Argentina (31°58′00″S 60°55′00″W). The by-products of RF consist of sepals, peduncles, and fruit remains. The RF was packed in 40 μm polypropylene bags and stored at −80°C. Before assays, the samples were freeze-dried (5.2 % moisture content) and ground to a particle size <1 mm.

Polyvinylpolypyrrolidone (PVPP), Folin-Ciocalteu reagent, 2′,7′-dichlorodihydrofluorescein diacetate (DCFH-DA), pepsin from porcine gastric mucose (E.C.3.4.23.1 800–2500 units/mg protein), pancreatin from porcine pancreas (8XUSP), fluorescein, 2,2′-azobis(2-amidinopropane) dihydrochloride (AAPH), dichlorofluorescein diacetate and lipopolysaccharides (LPS), acetonitrile (HPLC grade), methanol (HPLC grade), ferulic acid, gallic acid, ellagic acid, procyanidin, quercetin, kaempferol, and albumin standards were obtained from Sigma Chemical Co. (St. Louis, MO, USA). DL-dithiothreitol (DTT) was purchased from Merck KGaA (Darmstadt, Germany). Sodium acetate trihydrate and potassium phosphate dibasic were acquired from Cicarelli Reagents S.A. (Santa Fe, Argentina). Fetal bovine serum and antibiotics for cell culture were from GIBCO (Grand Island, NY). Celltiter 96 aqueous one solution cell proliferation assay and Griess reagent were obtained from Promega (Madison, WI).

Ultraviolet a radiation and storage conditions

Ultraviolet A (UVA) radiation treatment was carried out in a climate chamber (Memmert, Germany) equipped with two 8 W UVA lamps with a 320–400 nm spectrum range. The irradiation doses tested were 28.8 KJ/m^2 (UVA-LOW), 57.6 KJ/m^2 (UVA-MEDIUM), and 86.4 KJ/m^2 (UVA-HIGH), determined with a UVA dosimeter (model 501, Solar Light Co., PA, USA). The sample was inverted in the middle of the process to ensure a homogeneous UVA radiation dose. The RF was exposed to UVA radiation for 1, 2, and 3 h at 20°C. After each treatment, the UVA-treated RF (RF-E) samples were packed in polypropylene boxes covered with PVC film (20 g). The UVA-treated samples (RF-E) and the control samples (RF-N, untreated RF tissue), equally packed, were stored at 5, 10, and 15°C, 90% RH, for 24, 48, and 72 h, to compare the effect of temperature storage stress.

Enzymatic activity determinations

Phenylalanine ammonia-lyase activity

The phenylalanine ammonia-lyase (PAL) activity was measured according to Van de Velde et al. (14) with some modifications. Five grams (5 g) of strawberry by-product with 10 mL of extractant solution (phosphate buffer 100 mmol L^{-1} pH 8, EDTA 2 mmol L^{-1}, PVPP 30 g L^{-1}, DTT 7 mmol L^{-1}, Triton X-100 0.1% v/v) were homogenized for 30 s and stirred for 45 min at 4°C. The mixture was centrifuged at 12,000 × *g* for 20 min at 4°C, and the supernatant was used to assess PAL activity. The reaction mixture was 1060 μL of Tris–HCl 100 mmol L^{-1} pH = 8.8, 530 μL phenylalanine 50 mmol L^{-1}, and 150 μL of enzymatic extract. The reaction mixture was incubated at 37°C for 1 h, the reaction was stopped with 260 μL of TCA 10 g L^{-1}, and centrifuged at 12,000×*g* for 10 min. Cinnamic acid production was measured by the absorbance change at 290 nm (Genesis 10S UV–Vis spectrophotometer, Thermo Scientific, Germany). The results were expressed as the change of absorbance by an hour and milligram of protein (ΔA mg protein^{-1} h^{-1}).

Polyphenol oxidase activity

The technique adapted from Rodríguez-Arzuaga et al. (15) was used to determine the polyphenol oxidase (PPO) activity. Strawberry by-product (5 g) were homogenized and stirred (1 h at 4°C) with 10 mL of extraction solution (phosphate buffer 100 mmol L^{-1} pH = 6, PVPP 30 g L^{-1}, Triton X-100 0.1% v/v, NaCl 1 mol L^{-1}). The mixture was centrifuged at 12,000 × *g* for 15 min at 4°C, and the supernatant was used to assess PPO activity. The reaction mixture (900 μL of distilled water, 200 μL of pyrocatechol 200 mmol L^{-1}, 150 μL of phosphate buffer 1 mol L^{-1} pH = 6, and 250 μL of extract) was incubated for 1 h at 37°C. Absorbance variation was measured at 410 nm, and the results were expressed as (ΔA mg protein^{-1} h^{-1}).

Protein determination in enzyme extracts

The Lowry et al. (16) method was applied to determine the protein content in the PAL and PPO extracts. Enzymatic extract (200 μL) in adequate dilution was added to 2 mL of reagent C (100 parts of 3.0% Na_2CO_3, 0.4% NaOH, 4% sodium tartrate, and 1 part of reagent B: 2% $CuSO_4$·5 H2O), and incubated at room temperature for 10 min. Then, 200 μL of Folin-Ciocalteu reagent was added (1 N), the mixture was vigorously shaken, incubated at 20°C for 30 min, and the absorbance was determined at 660 nm. A calibration curve was generated using 1 mg L^{-1} of albumin. The results were expressed as mg of protein per g of sample (mg g^{-1}).

Phenolic compound characterization

Phenolic compounds extraction

Phenolic compounds from RF were extracted as previously described by Villamil-Galindo et al. (17). Briefly, 1 g of RF was sonicated for 15 min (T40, Teslab, Buenos Aires, Argentina) with 5 mL of 80% methanol with 0.5% formic acid and centrifuged at 12000×*g* for 20 min (Neofuge 18R Heal Force refrigerated centrifuge, Shanghai, China). The supernatant was collected, and the pellet was reextracted under the same conditions. The supernatants were mixed and brought up to 10 mL. The extracts were stored at –20°C until analyses.

Determination of phenolic compound profiles

The phenolic compounds profile was determined in each RF sample using an LC-20AT high-performance liquid chromatograph with a diode array detector and Lab Solutions for data processing and control software (Shimadzu Co., Kyoto, Japan). Separation was performed on a Gemini 5 μ C18 110 Å 250 × 4.6 mm hybrid reverse phase column attached to a guard column (Phenomenex Inc, CA, USA). Determinations were performed according to Villamil-Galindo et al. (2).

Identification of phenolic compounds was performed by retention times and UV-Vis absorption spectra compared with commercial phenolic compounds standards. The integrated areas of the obtained peaks (mAU * min) of the standard phenolic compounds were plotted as a function of their concentrations. The equations for calculating the extracts' content were obtained from each linear regression. The results were expressed as g of phenolic compound kg^{-1} by-product.

Total phenolic content

The total phenolic content (TPC) determination of the RF samples was performed according to Villamil-Galindo et al. (2) with some modifications using the Folin-Ciocalteu method. Twenty microliters (20 uL) of the extracts, 100 uL Folin-Ciocalteu reagent (0.66 N), 100 uL of sodium carbonate solution (10%), and 780 uL of distilled water were mixed and allowed to react at 20°C for 30 min in triplicate. Then, the mixture was put into a 96-well plate, and the absorbance was measured at 765 nm in the microplate reader (Synergy HT, Bio-Tek, Winooski, VT, USA). The results were expressed as g of gallic acid equivalents (GAE) per kilogram of strawberry by-product (g GAE kg^{-1}).

In vitro gastrointestinal digestion assay

The assay was performed according to the methodology proposed by Flores et al. (18). It consists of three distinct stages: oral phase (Simulated Saliva Fluid, SF), gastric phase (Simulated Gastric Fluid, GF), and intestinal phase (Simulated Duodenal Fluid, DF, and bile solution, BF) (IF). The composition of the different phases was prepared according to **Supplementary Table 1**.

Samples (RF-N and RF-E) were weighted into a stoppered 125 mL Erlenmeyer flask at a ratio of 1:3 w/v with SF. The SF fluid containing human a-amylase (Sigma-Aldrich Inc., St. Louis, MO, USA) was added, and the sample was incubated at pH 6.8 ± 0.2 for 2 min. Then, 6 mL of GF containing porcine gastric pepsin Sigma-Aldrich Inc. (St. Louis, MO, USA) was added, pH adjusted to 1.3 ± 0.2, and the sample was re-incubated for 1 h. The final step in the digestion procedure included the addition of 6 mL DF and 3 mL BF containing porcine pancreatin (Sigma-Aldrich Inc., St. Louis, MO, USA). The pH was adjusted to 7.0 ± 0.2, and samples were incubated for another 1 h at 37°C in a shaker (New Brunswick Scientific, Eppendorf). Aliquots (0.5 mL) were collected after each phase, and the samples were immediately placed into a water bath at 90°C for 3 min to inactive the enzymes. Then, they were centrifuged at 4°C for 15 min at 9000 × *g* (Eppendorf Centrifuge 5804R, Germany), and the supernatant was collected. Each digestion was performed in triplicate. Each phase obtained was analyzed by HPLC-DAD, and the final phase (intestinal phase) was used to perform the cell culture assays. The results were expressed as a percentage (%) of bioaccessibility according to the ratio between the phenolic compound concentration in the intestinal fraction and their initial concentration in the raw material or dried extract (Equation 1).

$$\textit{Bioacessibility}\ (\%) = \frac{\textit{Phenolic compounds intestinal phase}}{\textit{Phenolic compound in raw material (Dried extract)}} \times 100 \quad (1)$$

Cell culture

Cell lines, human colorectal adenocarcinoma cells (Caco-2 and HT29), mouse macrophage (RAW 264.7), and adult primary dermal fibroblast; (HDFa) were purchased from the American Type Culture Collection (Manassas, VA, USA). The cells were maintained in modified eagle medium (DMEM) supplemented with 5% fetal bovine serum (FBS) and 1% antibiotic, streptomycin (10,000 μg/mL), at 37°C and under 5% CO_2 in a humidified incubator.

Anti-inflammatory potential

The potential anti-inflammatory activity of the resuspended digestion of freeze-dried raw material was tested at a previously determined concentration of 1.75 μg/mL of digested RF. RAW 264.7 cell line was used to measure nitric oxide (NO) production induced by Lipopolysaccharides (LPS) from *Salmonella enterica* serotype typhimurium (L7261, Sigma-Aldrich, St Louis, MO; USA). This macrophage cell line is a cell type that responds quickly to stimuli, thus facilitating the screening of the immune

response to the presence of phenolic compounds present in RF digests, which is vital as it is a source of bioactives that is not usually edible. The assay was performed according to Moreno-García et al. (19)., with some modifications. Prior, 100 μL with 5×10^5 cells were seeded in each well of a 96-well cell culture plate. After 24 h, 50 μL of each sample was placed in triplicate and incubated for 4 h at 37°C, followed by the addition of 50 μL LPS (10 μg/mL) to half of the wells to stimulate the inflammatory process. Half of the wells were used as a control with 50 μL DMEM medium and incubated for 18 h at 37°C.

The NO production was determined by Griess Reagent System (Promega, Madison, WI, USA) following the manufacturer's instructions. Briefly, 100 μL of each sample and the controls were taken and placed in a new 96-well plate, and 10 μL of component A (10 mg/mL) (Sulfanilic acid) was added to each well, shaking the plates for 10 min, followed by the addition of 10 μL of component B(1 mg/mL) [N-(1-naphthyl) ethylenediamine dihydrochloride]. The quantification was done using a nitrites standard curve (0.78–50 μM, R^2 0.99) measuring the absorbance at 550 nm, considering cells without LPS stimuli and cell viability. The initial plate was used to determine the RAW 264.7 viability using CellTiter 96 Aqueous One Solution Cell Proliferation Assay (Promega, Madison, WI, USA). The absorbance was measured at 490 nm to determine cell viability. The data were expressed as a percentage of inhibition compared to the positive control plate and cell viability.

Antioxidant cellular activity

During the digestive process of RF as a source of phenolic compounds, their residence time in the colon is long, so it is important to study the anti-radical capacity of these phenolic compounds in colon cells. To measure the level of reactive oxygen species (ROS) produced by the cells in the presence of different digested extracts (from RF-N and RF-E samples) at 2.2 μg/mL, Caco-2 cells suspension was seeded at a density of 5×10^5 cells/mL on a black 96-well microplate in 100 μL growth medium per plate 24 h before the assay. To determine the antioxidant cellular activity of different extracts, the methodology proposed by Moreno-García et al. (19) was used with some modifications. After 24 h, the medium was removed, and each well was carefully washed with PBS pH 7.4 (1×). Samples were diluted in DMEM medium to 2× concentration, then 2′,7′-dichlorodihydrofluorescein diacetate (DCFH-DA, 120 μM) fluorescent agent was added in a final concentration of 60 μM. The mixture was added at a volume of 100 uL in each well. For negative and positive control, 100 μL of DMEM medium with 60 μM DCFH was placed. For the reaction blank, 100 μL of DMEM was added. The plate was incubated at 37°C for 20 min. Subsequently, the reaction solutions were removed from each well, and the cells were washed twice with PBS. To induce the pro-oxidant stimuli in the cells, 100 μL/well of APPH [2,2′-Azobis(2-methylpropionamidine) dihydrochloride] at 500 μM was added, except for blank (100 μL of DMEM) and negative control wells (100 μL of PBS). Fluorescence emitted at 538 nm with excitation at 485 nm was measured every 2 min for 120 min at 37°C. The results were expressed following (Equation 2)

$$\%\,(CAA) \;=\; 1 - \left(\int SA \Big/ \int CA\right) \qquad (2)$$

where, $\int SA$ is the integrated area under sample fluorescence versus time curve and, $\int$CA is the integrated area from the control curve.

Antiproliferative activity

The digested fraction of RF-N and RF-E having a long residence time in the colon, its antiproliferative activity was evaluated in colon cancer cells (Caco-2 and HT29), and healthy control (HDFa) cells were used. The ratio of live and dead cells was determined by the methodology proposed by Pacheco-Ordaz et al. (20). Different extract concentrations were tested (0.0094-122 mg/mL). Caco-2, HT29, and HDFa were seeded in a 96-well plate in a suspension of 100 μL at 5×10^5 cells/mL. After 24 h of incubation at 37°C, 100 μL of each extract was placed at the final concentrations, and the plates were incubated for 48 h at 37°C. Subsequently, 10 μL of CellTiter 96 Aqueous One Solution Cell Proliferation Assay (Promega, Madison, WI) was added in each well, and then, absorbance was measured at 490 nm in a microplate reader (Synergy HT, Bio-Tek, Winooski, VT, USA). The IC_{50} values (half maximal inhibitory concentration) for each sample were determined from the percentage viability versus concentration data; these were fitted to an asymmetric sigmoidal equation, and the appropriate concentration to inhibit 50% viability in the cells studied was calculated.

Statistical analysis

The effect of UVA dose (UVA), storage time (ST), and temperature (TM) on PPO and PAL activities, TPC, TPC_{HPLC}, and agrimoniin content (AGN) were determined by analysis of variance (ANOVA). Significant differences among treatment means were determined by Tukey's test ($p < 0.05$). The response surface methodology (RSM) allowed modeling and optimizing (simultaneous optimization of several response variables) the biofortification process in phenolic compounds, using a second-order polynomial equation to model and obtain the coefficients of each response as a function of UVA, ST, and TM. The linear stepwise regression procedure was used to reduce the non-significant terms in the model, which was determined by the R^2 and the lack of fit. Analyses were performed with

STATGRAPHICS Centurion XV (StatPoint Technologies Inc., Warrenton. VA, USA).

Results and discussion

Effect of ultraviolet a dose, storage time, and temperature on the strawberry by-product biofortification process

The RSM allowed studying and modeling the effect of the UVA radiation dose, storage temperature (ST), and storage time (TM) on the enzymatic activity of PAL, PPO, total phenolic (TPC and TPC_{HPLC}), and the agrimoniin content (AGN) of strawberry agro-industrial by-products (RF) (**Supplementary Table 2** and **Supplementary Equations 2–5**).

According to the coefficients of determination (R^2 0.62–0.89) and the lack of fit test (p-value 0.10–0.52), the quadratic model best described the behavior of the different response variables studied (**Supplementary Table 2**).

Phenylalanine ammonia-lyase activity

Phenylalanine ammonia-lyase is a ubiquitous enzyme in plants; it catalyzes the first step in phenylpropanoid metabolism, accumulating antioxidant phenolic compounds. Using elicitors such as UVA radiation to increase ROS production in strawberry agro-industrial by-products plays a major role in activating the PAL enzyme (21). PAL activity was mainly affected by UVA ($p < 0.001$), ST ($p < 0.01$), and TM ($p < 0.001$), and the quadratic factors UVA^2 ($p < 0.05$) and TM^2 ($p < 0.01$) (**Supplementary Table 2**). Initially, the RF tissue showed an average PAL activity of 0.04 ΔA mg $protein^{-1}$ h^{-1} (**Figure 1**), which is 57% higher than reported for the whole strawberry fruit with 0.017 ΔA mg $protein^{-1}$ h^{-1} (14).

Immediately after UVA radiation treatments, PAL activity presented the highest increase (304%) for UVA-HIGH treatment, followed by UVA-MEDIUM (236%). Otherwise, there were no differences ($p > 0.05$) in the PAL initial activity with UVA-LOW. The physiological response of plants to UVA radiation varies significantly, and the mechanisms of response are not completely clear. What is known is that the absorption of different doses of UVA is mediated through photoreceptors present in different parts of the strawberry plant, cytochrome receptors (CRY), and phototropin receptors (PHOT) (22, 23). When the UVA photoreceptors are saturated, ROS are generated as the first signal, inducing the transcription of regulatory genes, leading to the expression of enzymes from the phenylpropanoid pathway such as PAL, triggering an increase in mitochondrial respiration, accelerating the metabolism of the plant tissue (22). These physiological events are likely occurring in the strawberry agro-industrial residue, which initially responds according to the intensity of the UVA dose.

During the different storage times and temperatures, the PAL activity varied significantly (**Figure 1**). There was a slight decrease in PAL for UVA-MEDIUM and UVA-HIGH samples after 24 h at 5°C ($p < 0.05$). However, after 48 h, the highest increases in PAL were determined at 5°C, for the control (RF-N, 290%), UVA-MEDIUM (297%), UVA-LOW (373%), and UVA-HIGH (427%), compared to the initial PAL activity of the RF control sample (RF-N, ST = 0). These results agreed with those previously reported for lettuce treated with UVA intensity of 19 μmol m^{-2} s^{-1}, where storage at 16°C induced a 300% increase in PAL activity (24). RF samples stored at 10°C showed less PAL activity than those at 5°C. However, the highest PAL increases were obtained between 24 to 48 h of storage, with the RF-N and UVA-LOW samples showing similar ($p > 0.05$) increases of 200% and 117%, respectively, followed by UVA-MEDIUM (260%). Nevertheless, the highest increase was 322% with 0.12 ΔA mg $protein^{-1}$ h^{-1} at 10°C with UVA-HIGH. The RF-E with UVA-HIGH at 15°C showed PAL increments between 192 and 285% at 72 h of storage (0.08–0.11 ΔA mg $protein^{-1}$ h^{-1}). These results disagree with the expected increase of enzyme activity with temperature. The optimal temperature for PAL activity is 37°C, and its temperature-dependence enzymatic activity has already been reported (25). However, the PAL enzyme is encoded by a multigene family that generates several isoforms of the enzyme, which may result in variability in each plant tissue. These results agree with those reported by Formica-Oliveira et al. (26) where the most significant PAL increases in stressed tissues are generated after 24–48 h of storage, followed by the accumulation of phenolic compounds in 48–72 h with a moderate rise in PAL activity.

Polyphenol oxidase

Ultraviolet A (UVA) ($p < 0.01$), ST ($p < 0.05$), and TM ($p < 0.001$) significantly affected PPO activity. Additionally, the interaction of the factors UVAxTM was significant ($p < 0.001$) on PPO (**Supplementary Table 2**), meaning the effect of UVA dose depends on TM value. The influence of different doses of UVA radiation on PPO is shown in **Figure 2**. UVA-LOW treatment did not exert significant changes in PPO activity compared with the control (0.18 ΔA mg $protein^{-1}$ h^{-1}). Initially, UVA-MEDIUM treatment increased PPO activity by 236%, whereas the UVA-HIGH sample showed a PPO increase of 181%. The lower increase in PPO activity observed in UVA-HIGH samples could be explained in terms of a potential denaturation of the protein since excess energy from longer radiation times could generate a partial denaturation of the enzyme.

Moreover, after 24 h of storage (5°C), the PPO activity of RF-N increased by 57%, which remained relatively constant until 72 h. UVA-LOW samples maintained their PPO activity constant for up to 72 h. For RF-E UVA-MEDIUM and HIGH after 72 h, a decrease in PPO was observed, reaching up to 33% lower than the PPO of the initial RF-N. At 10°C and

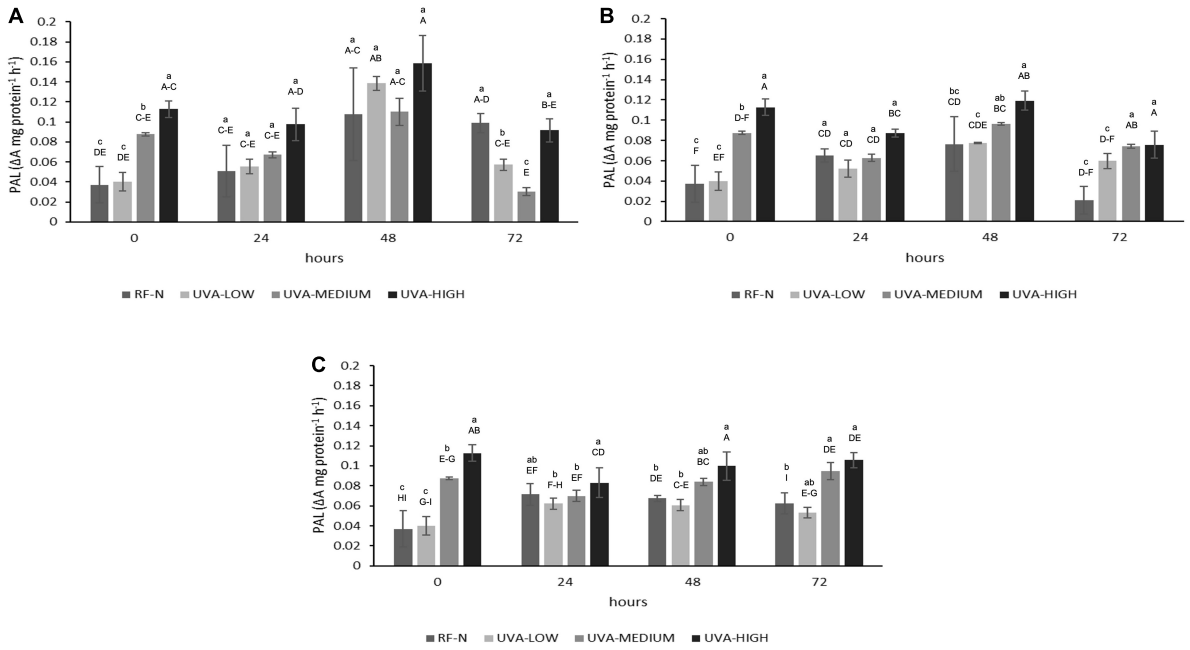

FIGURE 1
Phenylalanine ammonia-lyase (PAL) activity of UVA-treated strawberry by-products during storage at **(A)** 5°C, **(B)** 10°C, and **(C)** 15°C. RF-N: Strawberry agro-industrial by-product control. UVA-LOW: RF irradiated with 28.8 KJ/m^2. UVA-MEDIUM: RF irradiated with 57.6 KJ/m^2. UVA-HIGH: RF irradiated with 86.4 KJ/m^2 Different lower-case letters mean significant differences ($p \leq 0.05$) among treatments at the same storage time. Different capital letters mean significant differences ($p \leq 0.05$) among different storage times.

24 h, RF-N and UVA-LOW showed increases in PPO activity between 66 and 48%, respectively. In contrast, the trend was toward a decrease in PPO compared to the initial treatment time for UVA-MEDIUM and UV-HIGH at 10°C and 24 h (Figure 2B). For the samples stored at 15°C, a reduction in PPO activity was determined for all treatments, especially in the UVA-HIGH treatment, which had an initial activity of 0.32 ΔA mg protein^{-1} h^{-1}, and it dropped to 0.12 ΔA mg protein^{-1} h^{-1} after 48 h of storage. This behavior can be explained by the fact that the strawberry PPO enzyme has an average optimum pH and temperature of 6.2 and 35°C (27). In the case of strawberries, the average pH is between 3.4 and 3.5, which may have a synergistic effect with the different storage temperatures and radiation doses, controlling PPO activity by reducing the oxidation of *de novo* phenolic compounds synthesized (14). Similarly, Teoh et al. (28) showed a synergistic effect of low pH with high doses of UVC radiation in controlling the PPO activity of potato slices. Otherwise, Ding and Ling (29) reports that UVC doses of 0.04 KJ/m^2 applied on banana peel induced enzymatic browning. On the other hand, plant tissues maintain a balance between *de novo* synthesis and utilization of phenolic compounds, which correlates with an increase in PPO activity (30). PPO had very slight increases for RF-E even after 72 h at 15°C for all UVA doses; the PPO activity of RF-E samples was lower than RF control samples (RF-N). However, Chen et al. (31) have already reported this behavior in plant tissues, where the PPO activity of irradiated lettuce at low doses (10 μmol m^{-2} s^{-1}) decreased by almost 40%.

Total phenolic content

The effect of UV radiation on different plants vary widely, depending on factors such as the stage of maturity of the plant or fruit, cultivar, type of crop, availability of carbon source in the plant (sugars and amino acids), and type and dose of radiation (17). For RF, the TPC was significantly affected ($p < 0.01$) by TM and TM^2. The interaction term UVAxTM^2 also affected TPC ($p < 0.05$) (Supplementary Table 2). The initial content of total soluble phenolic compounds of RF-N was 5.8 mg AGE/g RF. At ST = 0, the UVA-LOW treatment did not change TPC (Figure 3). However, the elicitor effect can be evidenced with the UVA-MEDIUM treatment with TPC 6.8 mg AGE/g. Likewise, following a dose-dependent behavior with UVA-HIGH, an increase of 46% in TPC (8.4 mg AGE/g) was achieved, correlating with that shown in the PAL (Figure 1), indicating that UVA stress generates the modulation of secondary metabolism in RF tissue through the synthesis of new phenolic compounds.

According to the TPC obtained at 5°C, the metabolism of phenylpropanoids remained active in the biosynthesis of phenolic compounds, with the most significant increases being observed after 48 h, achieving up to 158% more phenolic compounds for RF with UVA-HIGH (14.9 mg

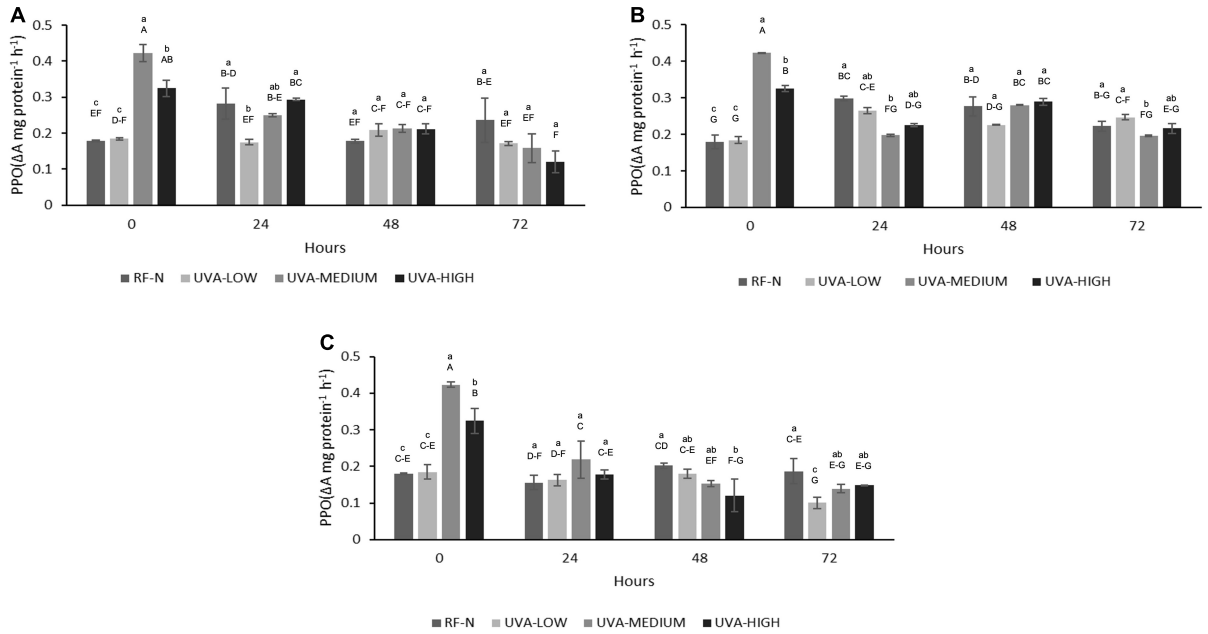

FIGURE 2
Polyphenol Oxidase (PPO) activity of UVA-treated strawberry by-products during storage at **(A)** 5°C, **(B)** 10°C, **(C)** 15°C. RF-N: Strawberry agro-industrial by-product control. UVA-LOW: RF irradiated with 28.8 KJ/m^2. UVA-MEDIUM: RF irradiated with 57.6 KJ/m^2. UVA-HIGH: RF irradiated with 86.4 KJ/m^2. Different lower-case letters mean significant differences ($p \leq 0.05$) among treatments at the same storage time. Different capital letters mean significant differences ($p \leq 0.05$) among different storage times.

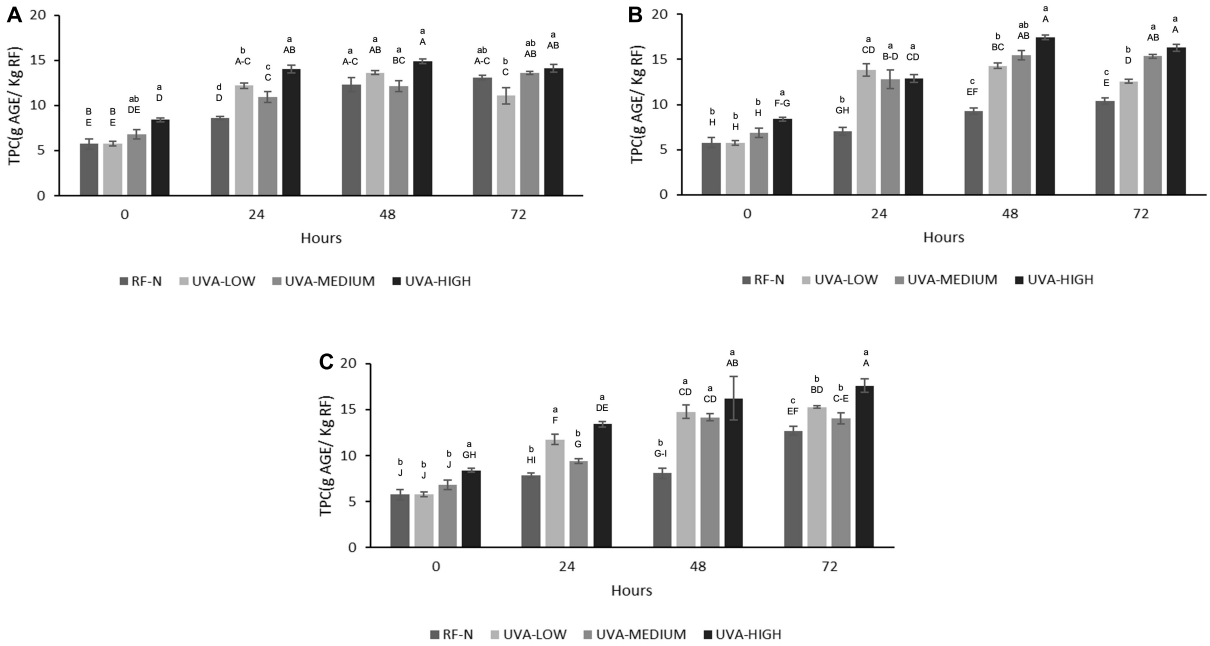

FIGURE 3
Total phenolic content (TPC) of UVA-treated strawberry by-products during storage at **(A)** 5°C, **(B)** 10°C, **(C)** 15°C. RF-N: Strawberry agro-industrial by-product control. UVA-LOW: RF irradiated with 28.8 KJ/m^2. UVA-MEDIUM: RF irradiated with 57.6 KJ/m^2. UVA-HIGH: RF irradiated with 86.4 KJ/m^2. Different lower-case letter, means significant differences ($p \leq 0.05$) between the different treatments at the same storage time. Different capital letter means significant differences ($p \leq 0.05$) between different storage times.

AGE/g) as compared to the initial control value. However, the most significant increase was determined after storing the UVA-HIGH samples at 10°C for 48 h, obtaining a TPC of 17.4 mg AGE/g, 142% higher than the control (9.3 mg AGE/g) after 48 h of storage, positively correlating with the 322% increase in PAL for the same period. A similar increase was achieved with UVA-HIGH treatment after 72 h at 15°C (17.6 mg AGE/G), showing that the increase in TPC was not affected by the storage temperature ($p > 0.05$). UVA is the major component of the solar UV spectrum, 95% UVA (315–380nm) and UVB (280–315 nm), despite being less harmful than UVB and UVC radiation. UVA radiation can penetrate plant tissue, generating physiological responses to control the stress condition, as observed in RF tissue at different doses and subsequent storage (32).

Phenolic compounds profile

The use of UVA radiation as an elicitor has been little studied. The phenolic biofortification with UVA radiation has been reported in a few plant tissues such as *Rosa hybrida* and *Fuchsia hybrida* (33), *Betula pendula* (32), *Daucus carota* (8), *Brassica oleracea* (34), *Vaccinium sect. Cyanococcus* cv "*Duke*" (35) and *Glycine max* sprout (36).

It has been reported that UVA radiation can affect the photosynthesis process in plant tissues and modulate the synthesis of specific phenolic compounds (37), and regarding by-products, Formica-Oliveira et al. (38) studied the effect of UVB and UVC radiation on broccoli by-products; and Sánchez-Rangel et al. (39) studied the effect of UVC on the biosynthesis of phenolics in carrot bagasse. The profile of phenolic compounds obtained by HPLC-DAD allowed the quantification and identification of 8 individual phenolic compounds (**Tables 1A**,**B**), with hydrolyzable tannins such as tetragalloyl glucose isomer (TGI) and agrimoniin (AGN) as the main compounds, ellagic acid derivatives such as ellagic acid pentoside (EAP) and free ellagic acid (EA) and flavonoids such as procyanidin tetramer (PACT), quercetin 3-O-glucuronide (Q3G) and Kaempferol 3-o-glucuronide (K3G). The effects of UVA, ST, and TM on the individual phenolic compounds are shown in **Tables 1A**,**B**. Moreover, the total sum of the identified phenolic compounds (TPC_{HPLC}) was fitted to a second-order model with UVA ($p < 0.001$), ST ($p < 0.001$), and TM ($p < 0.01$) as the independent variables (**Supplementary Equation 4**). The TPC_{HPLC} variation was affected by the 3 studied factors, UVA, ST, and TM, and the interaction of the factors STxTM (<0.01) (**Supplementary Table 2**). The major compound, AGN, is of great interest because several authors have reported the multiple bioactivities with applications in the nutraceutical industry (40, 41). For this reason, it was also modeled and included in the multiple response optimization (**Supplementary Equation 5**). According to the results obtained, the UVA and TM affected ($p < 0.01$) the AGN content.

After exposure of RF to the different UVA doses, the TPC_{HPLC} changed similarly to the TPC determined by the Folin-Ciocalteu method, with no significant differences between the control and UVA-LOW samples (1.7–1.8 g/Kg). However, for UVA-MEDIUM, the phenolic compounds increased by 29%, and the most significant increase was observed in the UVA-HIGH treatment (2.9 g/Kg), which was 70% higher than the RF control. For storage at 5°C, the highest increases occurred after 24–48 h with an average content of 2.5 g/kg (**Figure 4**). There were no significant differences among TPC_{HPLC} of RF-E samples after 24–48 h at 5°C, being up to 54% higher than the control for the same period, and similar to that reported by Surjadinata et al. (8), who applied UVA 12.7 Wm^{-2} for 6 h on wounded carrots, achieving a 100% increase in total phenols and up to 300% increase in chlorogenic acid. At 10°C, the highest increases were determined after 24–48 h with an average content of 2.5 g/kg. However, the highest accumulation of phenolic compounds was obtained after 48 h at 15°C (3.3 g/Kg RF), 104% higher than the control (**Figure 4**). Similar to the results obtained for broccoli by-products using UVB-C 10 KJ/m^2, after 48 h at 15°C showed an increase of 88% of phenolic compounds (38).

The results in **Figure 5** indicate the positive effect of UVA on the biofortification of strawberry agro-industrial by-products with AGN. The initial accumulation of AGN was proportional to the UVA dose being UVA-LOW < UVA-MEDIUM < UVA-HIGH reaching an increase of 184% (1.7 g/Kg) compared to the control (0.6 g/Kg). A maximum accumulation of AGN (2.0 g/kg) was achieved during storage at 10°C for 48 h, obtaining a higher increase than that obtained by Moreira-Rodríguez et al. (34) in broccoli sprouts applying UVA radiation (3.16 W/m^2 for 120 min), achieving a maximum increase in the compound 5-sinapoyl-quinic acid (121%). As earlier described, although the mechanism of how UVA modulates the biosynthesis of phenolic compounds is not fully elucidated, these results show AGN as the compound with the highest accumulation in RF, which is in contrast with previous reports for fruit subjected to pre-harvest UVB radiation, where anthocyanins and flavonols are mainly increased (42). In addition, UVA radiation is shown to be an efficient non-thermal alternative technology to biofortify with phenolic compounds and strawberry agro-industrial conditioning by-products.

Determination of the optimum biofortification process conditions to increase phenolics accumulation in the strawberry by-product

Based on Derringer's desirability function, the multiple response optimization procedure was applied to determine the optimal experimental conditions of the biofortification in RF phenolic compounds. The objective was to obtain the optimum UVA dose, storage time (ST), and temperature

10.3389/fnut.2022.1080147

TABLE 1A Changes in the individual phenolic compound concentration of strawberry by-products as affected by UVA dose, storage time, and temperature.

UVA	Storage temp (°C)	Storage time (h)	TGI (g/Kg)	EAP (g/Kg)	AGN (g/Kg)	EA (g/Kg)
RF-N	5	0	0.26 ± 0.04a	0.21 ± 0.01m-p	0.60 ± 0.01q	0.05 ± 0.003m
		24	0.14 ± 0.01d–g	0.20 ± 0.001n–p	0.90 ± 0.19n–p	0.09 ± 0.03 e-l
		48	0.13 ± 0.02e–h	0.24 ± 0.01i–n	0.93 ± 0.25 n–p	0.07 ± 0.01i–m
		72	0.13 ± 0.001e–i	0.25 ± 0.05i–n	0.77 ± 0.18pq	0.07 ± 0.003i–m
	10	0	0.26 ± 0.01a	0.21 ± 0.01m–p	0.60 ± 0.01q	0.05 ± 0.003 m
		24	0.10 ± 0.01h–k	0.23 ± 0.03k–p	1.25 ± 0.26 i–l	0.09 ± 0.02 e–j
		48	0.11 ± 0.01f–j	0.21 ± 0.01m–p	1.08 ± 0.02l–n	0.11 ± 0.003 b–f
		72	0.11 ± 0.02f–j	0.14 ± 0.02 q	0.79 ± 0.03pq	0.06 ± 0.002k–m
	15	0	0.26 ± 0.04a	0.21 ± 0.04m–p	0.60 ± 0.01q	0.05 ± 0.003m
		24	0.13 ± 0.001e–i	0.82 ± 0.01j–o	0.82 ± 0.19p	0.07 ± 0.01i–m
		48	0.14 ± 0.001d–f	0.21 ± 0.01m–p	1.33 ± 0.18 g–k	0.06 ± 0.01j–m
		72	0.13 ± 0.02d–h	0.23 ± 0.06 k–p	1.32 ± 0.07g–k	0.07 ± 0.04i–m
Low	5	0	0.15 ± 0.01c–e	0.23 ± 0.02k–p	0.84 ± 0.05op	0.08 ± 0.02f–l
		24	0.15 ± 0.02c–e	0.30 ± 0.01c–i	1.25 ± 0.03i–m	0.10 ± 0.03 b–h
		48	0.16 ± 0.02c–e	0.31 ± 0.04c–h	1.62 ± 0.05c–f	0.11 ± 0.01b–e
		72	0.09 ± 0.02jk	0.24 ± 0.02k–p	1.04 ± 0.07m–o	0.06 ± 0,02lm
	10	0	0.15 ± 0.01c–e	0.23 ± 0.02k–p	0.84 ± 0.05op	0.08 ± 0.02f–l
		24	0.08 ± 0.002k	0.23 ± 0.04k–p	1.08 ± 0.06l–n	0.07 ± 0.01h–m
		48	0.10 ± 0.001i–k	0.24 ± 0.01i–n	1.39 ± 0.01f–k	0.08 ± 0.01f–l
		72	0.11 ± 0.003f–j	0.31 ± 0.01c–g	1.51 ± 0.08c–h	0.10 ± 0.01b–g
	15	0	0.15 ± 0.01c–e	0.23 ± 0.02k–p	0.84 ± 0.05op	0.08 ± 0.02f–l
		24	0.13 ± 0.001d–h	0.23 ± 0.01k–p	0.94 ± 0.03n–p	0.07 ± 0.01i–m
		48	0.11 ± 0.0003g–k	0.34 ± 0.01a–c	1.41 ± 0.07f–j	0.11 ± 0.01a–e
		72	0.11 ± 0.01f–j	0.38 ± 0.003ab	1.25 ± 0.28i–m	0.12 ± 0.01a—-d
Medium	5	0	0.15 ± 0.01c–e	0.28 ± 0.01d–k	1.11 ± 0.04l–n	0.09 ± 0.01c–i
		24	0.13 ± 0.01d–h	0.22 ± 0.005l–p	1.24 ± 0.12j–m	0.07 ± 0.01i–m
		48	0.16 ± 0.005b–d	0.25 ± 0.005h–n	1.46 ± 0.07e–h	0.11 ± 0.0001b–f
		72	0.15 ± 0.003c–e	0.26 ± 0.01g–n	0.91 ± 0.01n–p	0.08 ± 0.01g–l
	10	0	0.15 ± 0.01c–e	0.28 ± 0.01d–k	1.11 ± 0.04l–n	0.09 ± 0.01c–i
		24	0.09 ± 0.004jk	0.25 ± 0.001i–n	1.18 ± 0.05k–m	0.10 ± 0.001b–g
		48	0.11 ± 0.004f–j	0.32 ± 0.02c–f	1.42 ± 0.07 e–j	0.10 ± 0.01b–g
		72	0.12 ± 0.01f–j	0.18 ± 0.02pq	0.96 ± 0.07n–p	0.08 ± 0.02f–l
	15	0	0.15 ± 0.01c–e	0.28 ± 0.01d–k	1.11 ± 0.04l–n	0.09 ± 0.01c–i
		24	0.09 ± 0.004jk	0.27 ± 0.002f–l	1.37 ± 0.04f–k	0.09 ± 0.005e–j
		48	0.12 ± 0.007f–j	0.19 ± 0.01o–q	1.92 ± 0.04ab	0.07 ± 0.002j–m
		72	0.10 ± 0.01jk	0.23 ± 0.01k–p	1.40 ± 0.11f–j	0.09 ± 0.01d–j
High	5	0	0.18 ± 0.01bc	0.33 ± 0.02b–d	1.70 ± 0.11c–e	0.11 ± 0.02a–e
		24	0.12 ± 0.004f–j	0.26 ± 0.01g–m	1.46 ± 0.16e–i	0.07 ± 0.003i–m
		48	0.15 ± 0.01de	0.27 ± 0.005f–l	1.58 ± 0.07c–g	0.11 ± 0.01a–e
		72	0.11 ± 0.02f–j	0.30 ± 0.01c–j	1.25 ± 0.10h–l	0.09 ± 0.01e–k
	10	0	0.18 ± 0.04bc	0.33 ± 0.02b–d	1.70 ± 0.11c–e	0.11 ± 0.023a–e
		24	0.15 ± 0.01de	0.28 ± 0.005e–k	1.71 ± 0.10b–d	0.10 ± 0.01b–f
		48	0.10 ± 0.0004jk	0.28 ± 0.07d–k	2.05 ± 0.07a	0.16 ± 0.003a
		72	0.12 ± 0.02f–j	0.26 ± 0.02g–n	1.63 ± 0.03c–f	0.13 ± 0.001ab
	15	0	0.18 ± 0.01bc	0.33 ± 0.01b–d	1.70 ± 0.11c–e	0.11 ± 0.02a–e
		24	0.13 ± 0.003d–h	0.33 ± 0.005b–e	1.49 ± 0.08d–h	0.09 ± 0.01e–j
		48	0.16 ± 0.01b–e	0.38 ± 0.01ab	1.99 ± 0.04a	0.12 ± 0.01abc
		72	0.19 ± 0.001b	0.40 ± 0.004a	1. 77 ± 0.06 bc	0.14 ± 0.001ab

Mean g/Kg ± standard deviation (n = 3). TGI, tetragalloyl glucose isomer; EAP, ellagic acid pentoside; AGN, agrimoniin; EA, free ellagic acid. Different letter in a column indicates significantly differences among all treatments.

10.3389/fnut.2022.1080147

TABLE 1B Changes in the individual phenolic compound concentration of strawberry by−products as affected by UVA dose, storage time, and temperature.

UVA	Storage temp (°C)	Storage time (h)	PACT (g/Kg)	Q3G (g/Kg)	K3G (g/Kg)	KP (g/Kg)	TPC_{HPLC} (g/Kg)
RF-N	5	0	0.19 ± 0.01a	0.18 ± 0.01j–n	0.10 ± 0.01f–h	0.01 ± 0.003h–l	1.71 ± 0.10o–q
		24	0.10 ± 0.0001i–q	0.18 ± 0.03k–o	0.11 ± 0.02d–f	0.01 ± 0.003 j–l	1.76 ± 0.32o–q
		48	0.12 ± 0.05 f–p	0.20 ± 0.005e–k	0.11 ± 0.004c–f	0.01 ± 0.001e–j	1.88 ± 32m–p
		72	0.10 ± 0.001j–q	0.19 ± 0.04 h–m	0.10 ± 0.02f–j	0.01 ± 0.004h–l	1.66 ± 0.06pq
	10	0	0.19 ± 0.01a	0.18 ± 0.01j–n	0.10 ± 0.01f–h	0.01 ± 0.004i–l	1.71 ± 0.10o–q
		24	0.12 ± 0.01f–o	0.19 ± 0.03 h–m	0.11 ± 0.02d–f	0.01 ± 0.002kl	2.16 ± 0.38j–m
		48	0.11 ± 0.003 h–p	0.17 ± 0.002 k–o	0.11 ± 0.004c–f	0.01 ± 0.002j–l	1.97 ± 0.04k–o
		72	0.12 ± 0.004 f–o	0.16 ± 0.0002m–o	0.08 ± 0.01ij	0.002 ± 0.0001m	1.53 ± 0.21q
	15	0	0.19 ± 0.01a	0.18 ± 0.01j–n	0.10 ± 0.01f–h	0.01 ± 0.0004h–l	1.71 ± 0.10o–q
		24	0.12 ± 0.003f–n	0.16 ± 0.005 l–o	0.08 ± 0.01 h–j	0.01 ± 0.0001l	1.69 ± 0.18o–q
		48	0.14 ± 0.02d–i	0.19 ± 0.001h–n	0.10 ± 0.002 f–h	0.01 ± 0.0004h–l	2.26 ± 0.17g–k
		72	0.09 ± 0.03k–q	0.18 ± 0.05j–n	0.10 ± 0.03f–i	0.01 ± 0.004i–l	2.21 ± 0.31h–k
Low	5	0	0.13 ± 0.03e–k	0.18 ± 0.01i–n	0.10 ± 0.01f–h	0.01 ± 0.001g–l	1.80 ± 0.10o–q
		24	0.12 ± 0.04f–n	0.21 ± 0.004d–j	0.11 ± 0.004d–f	0.02 ± 0.001d–i	2.33 ± 0.05f–j
		48	0.06 ± 0.001qr	0.20 ± 0.02e–k	0.11 ± 0.01d–f	0.02 ± 0.002c–g	2.65 ± 0.13c–e
		72	0.09 ± 0.04m–r	0.09 ± 0.020g–m	0.10 ± 0.01f–h	0.01 ± 0.001i–l	1.86 ± 0.16 n–p
	10	0	0.13 ± 0.03e–k	0.18 ± 0.01i–n	0.10 ± 0.01f–h	0.01 ± 0.001g–l	1.80 ± 0.10o–q
		24	0.08 ± 0.03o–r	0.14 ± 0.06o	0.07 ± 0.03j	0.01 ± 0.004l	1.81 ± 0.25 o–q
		48	0.14 ± 0.003c–g	0.16 ± 0.001m–o	0.07 ± 0.02j	0.01 ± 0.0002i–l	2.25 ± 0.03g–k
		72	0.05 ± 0.003r	0.14 ± 0.0004o	0.09 ± 0.001g–j	0.01 ± 0.001l	2.37 ± 0.07e–j
	15	0	0.13 ± 0.03e–k	0.18 ± 0.01i–n	0.10 ± 0.01f–h	0.01 ± 0.001g–l	1.80 ± 0.10o–q
		24	0.13 ± 0.01e–k	0.18 ± 0.02h–n	0.09 ± 0.01f–j	0.01 ± 0.002l	1.84 ± 0.02n–p
		48	0.11 ± 0.05g–p	0.26 ± 0.005a–c	0.13 ± 0.001b–e	0.02 ± 0.003a–c	2.53 ± 0.14d–g
		72	0.12 ± 0.01f–m	0.29 ± 0.001a	0.15 ± 0.003ab	0.02 ± 0.0002ab	2.53 ± 0.31d–g
Medium	5	0	0.17 ± 0.0001a–d	0.20 ± 0.01f–k	0.11 ± 0.01e–g	0.01 ± 0.004d–i	2.21 ± 0.05h–k
		24	0.13 ± 0.01f–l	0.18 ± 0.001j–n	0.09 ± 0.002 f–j	0.01 ± 0.0003l	2.14 ± 0.14 j–n
		48	0.13 ± 0.0001e–k	0.22 ± 0.01d–h	0.13 ± 0.02a–d	0.01 ± 0.0002h–l	2.53 ± 0.09d–g
		72	0.13 ± 0.03f–k	0.19 ± 0.01g–l	0.10 ± 0.0001f–i	0.01 ± 0.002g–l	1.90 ± 0.07l–p
	10	0	0.17 ± 0.0001a–d	0.20 ± 0.01f–k	0.11 ± 0.01e–g	0.02 ± 0.004d–i	2.21 ± 0.05h–k
		24	0.18 ± 0.002a–c	0.18 ± 0.02h–n	0.10 ± 0.001f–i	0.01 ± 0.006l	2.18 ± 0.05i–l
		48	0.11 ± 0.03h–p	0.22 ± 0.012c–g	0.13 ± 0.01b–e	0.02 ± 0.006 b–f	2.49 ± 0.15 d–h
		72	0.09 ± 0.01n–r	0.21 ± 0.02d–j	0.10 ± 0.01f–i	0.01 ± 0.001kl	1.80 ± 0.12o–q
	15	0	0.17 ± 0.0001a–d	0.20 ± 0.01f–k	0.11 ± 0.01e–g	0.02 ± 0.005d–i	2.21 ± 0.05h–k
		24	0.08 ± 0.002p–r	0.17 ± 0.01k–o	0.10 ± 0.004f–j	0.01 ± 0.0001f–k	2.24 ± 0.06g–k
		48	0.12 ± 0.001g–p	0.15 ± 0.01no	0.08 ± 0.02g–j	0.01 ± 0.005j–l	2.71 ± 0.09cd
		72	0.13 ± 0.01d–j	0.18 ± 0.01j–n	0.14 ± 0.005ab	0.01 ± 0.001j–l	2.33 ± 0.04f–j
High	5	0	0.14 ± 0.02c–h	0.24 ± 0.001b–d	0.13 ± 0.01a–c	0.01 ± 0.003 a–d	2.91 ± 0.17bc
		24	0.17 ± 0.0004a–d	0.19 ± 0.003 h–m	0.10 ± 0.004f–i	0.01 ± 0.001f–k	2.47 ± 0.16d–i
		48	0.19 ± 0.01ab	0.20 ± 0.14 f–k	0.14 ± 0.0003ab	0.002 ± 0.001a–d	2.74 ± 0.09cd
		72	0.17 ± 0.01a–e	0.24 ± 0.14 b–e	0.14 ± 0.005 a–c	0.02 ± 0.0015c–g	2.37 ± 0.08e–j
	10	0	0.14 ± 0.01c–h	0.24 ± 0.001b–d	0.13 ± 0.01a–c	0.02 ± 0.003 a–d	2.91 ± 0.17bc
		24	0.13 ± 0.003c–h	0.18 ± 0.01k–o	0.15 ± 0.01a	0.01 ± 0.0003f–k	2.76 ± 0.09cd
		48	0.19 ± 0.003ab	0.22 ± 0.01c–g	0.11 ± 0.02e–g	0.02 ± 0.001a–d	3.21 ± 0.01a
		72	0.12 ± 0.02l–r	0.22 ± 0.01d–i	0.11 ± 0.02e–g	0.02 ± 0.0001a–e	2.62 ± 0.06 c–f
	15	0	0.14 ± 0.02c–h	0.24 ± 0.001b–d	0.13 ± 0.01a–c	0.02 ± 0.0003 a–d	2.91 ± 0.2bc
		24	0.10 ± 0.003i–q	0.23 ± 0.005c–f	0.14 ± 0.01ab	0.02 ± 0.0001c–h	2.57 ± 0.08d–f
		48	0.16 ± 0.003b–f	0.24 ± 0.005b–d	0.15 ± 0.01ab	0.02 ± 0.001a	3.30 ± 0.06a
		72	0.15 ± 0.01c–g	0.27 ± 0.002ab	0.13 ± 0.01a–e	0.02 ± 0.001ab	3.10 ± 0.07ab

Mean g/Kg ± standard deviation (n = 3). PACT, procyanidin tetramer; Q3, quercetin 3-o-glucuronide; K3G, Kaempferol 3-o-glucuronide; TPC_{HPLC}, Total phenolic content by HPLC. Different letter in a column indicates significantly differences ($p < 0.05$) between all treatments studied.

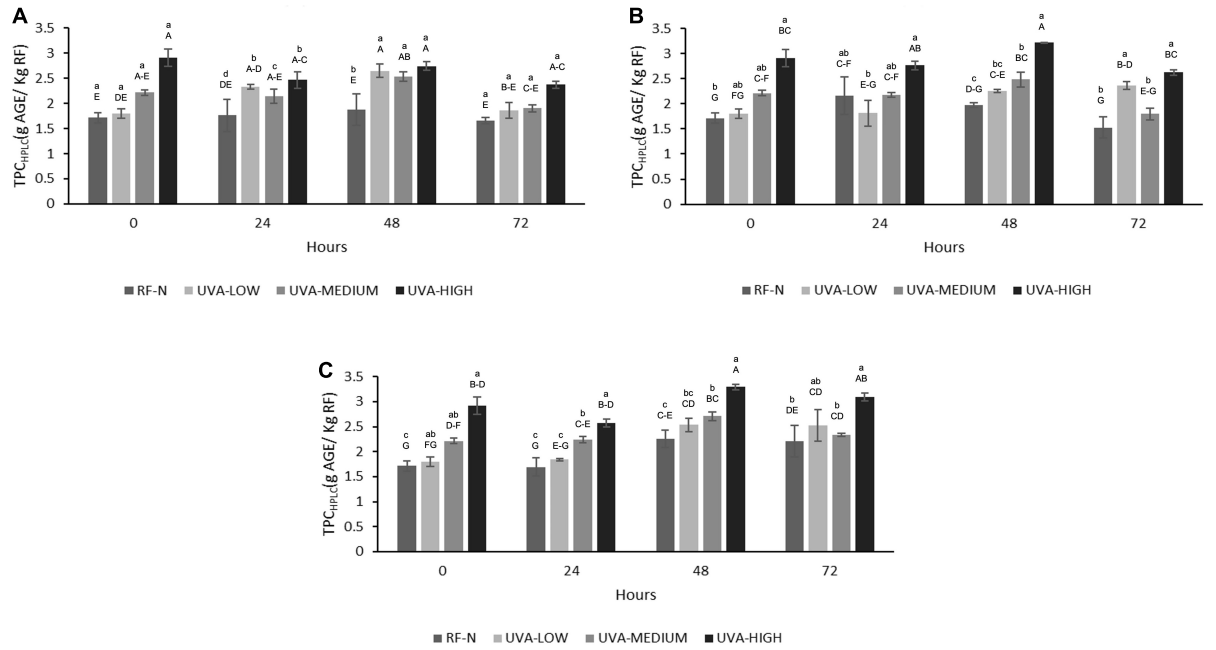

FIGURE 4
Total phenolic content determined by HPLC (TPC$_{HPLC}$) of UVA-treated strawberry by-products during storage at **(A)** 5°C, **(B)** 10°C, **(C)** 15°C. RF-N: Strawberry agro-industrial by-product control. UVA-LOW: RF irradiated with 28.8 KJ/m^2. UVA-MEDIUM: RF irradiated with 57.6 KJ/m^2. UVA-HIGH: RF irradiated with 86.4 KJ/m^2. Different lower-case letters, mean significant differences ($p \leq 0.05$) among different treatments at the same storage time. Different capital letters mean significant differences ($p \leq 0.05$) among different storage times.

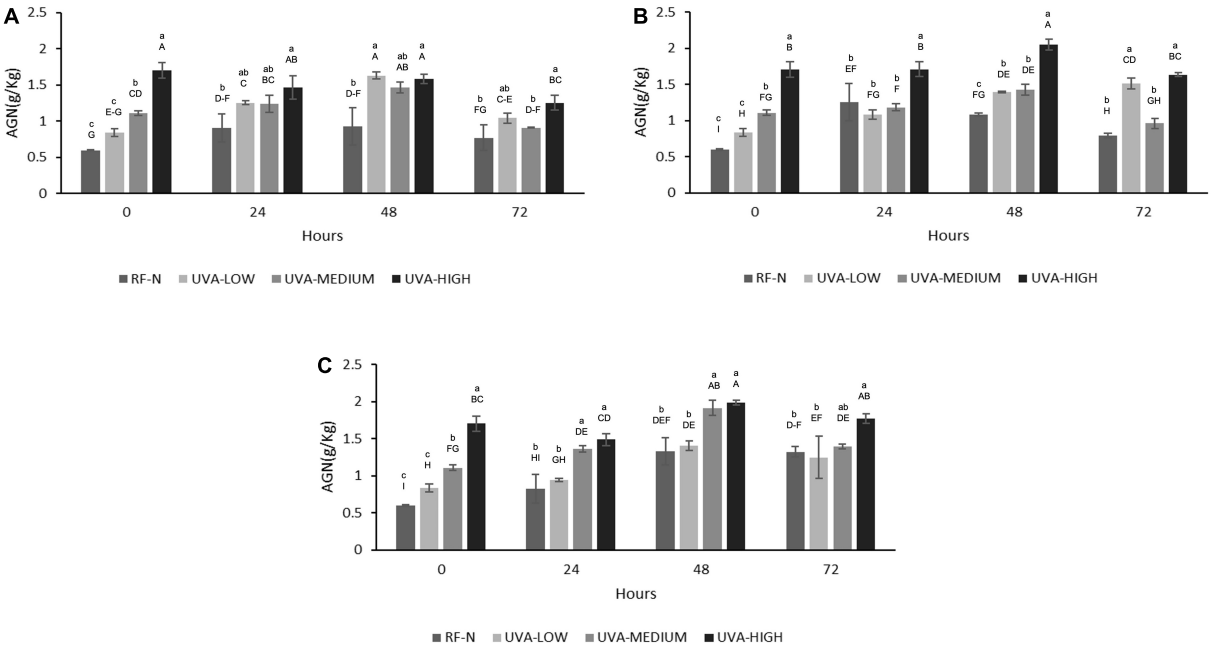

FIGURE 5
Agrimoniin concentration (AGN) of UVA-treated strawberry by-products during storage at **(A)** 5°C, **(B)** 10°C, **(C)** 15°C. RF-N: Strawberry agro-industrial by-product control. UVA-LOW: RF irradiated with 28.8 KJ/m^2. UVA-MEDIUM: RF irradiated with 57.6 KJ/m^2. UVA-HIGH: RF irradiated with 86.4 KJ/m^2. Different lower-case letters mean significant ($p \leq 0.05$) differences among treatments at the same storage time. Different capital letters mean significant differences ($p \leq 0.05$) among different storage times.

(TM) that maximize the content of phenolic compounds (TPC and TPC_{HPLC}), agrimoniin content (AGN), and PAL activity, minimizing PPO activity in the strawberry by-products.

Table 2 shows the results from the simultaneous optimization. The optimum biofortification process conditions to increase phenolics accumulation in the strawberry by-products were a UVA dose of 86.4 KJ/m^2 (UVA-HIGH), ST = 15°C, and TM = 46 h. Under these conditions, the predicted values of the different responses were: PAL = 0.13 ΔA mg $protein^{-1}$ h^{-1}, PPO = 0.16 ΔA mg $protein^{-1}$ h^{-1}, TPC, 16.7 g AGE/Kg RF, TPC_{HPLC} = 3.1 g/Kg RF and, AGN = 1.9 g/Kg RF (Table 3). Finally, the biofortification process was carried out at the optimal conditions to validate the predicted results and to determine the antioxidant and anti-inflammatory properties of UVA-induced biofortification phenolic compounds. The experimental results obtained are shown in Table 2. The experimental values obtained for TPC, TPC_{HPLC}, and AGN were similar ($p > 0.05$) to the predicted values, indicating the models' adequacy. However, the experimental PAL values were higher (23%) than the predicted values, while the experimental PPO values were lower (25%) than the predicted values.

In vitro gastrointestinal digestion assay

The beneficial health effects of phenolic compounds depend not only on the profile or amount of compounds but also on the release and transformation during the physiological processes of digestion. However, the low bioaccessibility of phenolic compounds has been widely reported due to

TABLE 2 Optimal biofortification treatment of strawberry by-products (RF) and their experimental and predicted response values.

Optimized treatment variables			Responses	PAL (ΔA mg $protein^{-1}$ h^{-1})	PPO (ΔA mg $protein^{-1}$ h^{-1})	TPC (g AGE/Kg)	TPC_{HPLC} (g AGE/Kg)	AGN (g /Kg)
UVA	ST (°C)	TM (h)						
High	15	46	*Predicted*	0.13b	0.16a	16.7a	3.1a	1.9a
High	15	46	*Experimental*	0.16a	0.12b	15.9a	2.9a	1.7a

UVA, UVA radiation dose; ST, storage temperature; TM, storage time; PAL, Phenylalanine Ammonia Lyase activity; PPO, Polyphenol Oxidase activity; TPC, Total phenolic content; TPC_{HPLC}, Total phenolic content by HPLC; AGN, Agrimoniin. Different letter indicates significant differences between Predicted and Experimental values $p < 0.05$ by *t*-test.

TABLE 3 Bioaccessibility of strawberry by-products (RF) phenolic compounds.

Sample	Compound	Salival fluid	Gastric phase	Intestinal phase	Bioaccessibility (%)	
		g/Kg			Gastric phase	Instestinal phase
RF-N	TGI	0.10 ± 0.003a	0.05 ± 0.001b	0.07 ± 0.001ab*	49.8	71.8*
	EAP	0.34 ± 0.005a	0.04 ± 0.001b	0.02 ± 0.001c	11.8	7.1
	AGN	1.35 ± 0.06a	0.15 ± 0.01b	0.13 ± 0.004b	10.9	9.80
	EA	0.13 ± 0.003a	0.03 ± 0.005b	0.01 ± 0.0001c	19.9	9.1
	PACT	0.14 ± 0.01a	0.11 ± 0.002b	0.11 ± 0.01b	79.2	79.2
	Q3G	0.23 ± 0.01a	0.05 ± 0.001b	0.02 ± 0.001c	19.9	10.0
	K3G	0.23 ± 0,01a	0.04 ± 0.002b	0.02 ± 0.001c	16.2	6.8
	KP	0.02 ± 0.001	n.d	n.d	n.d	n.d
	TPC_{HPLC}	2.55 ± 0.07a	0.46 ± 0.02b	0.39 ± 0.003b	18.0	15.3
RF-E	TGI	0.15 ± 0.004a*	0.08 ± 0.03b	0.05 ± 0.003b	51.4	36.1
	EAP	0.36 ± 0.002a*	0.10 ± 0.02b*	0.04 ± 0.004c*	27.2*	11.1*
	AGN	1.79 ± 0.03a*	0.51 ± 0.01b*	0.45 ± 0.01c*	28.4*	25.1*
	EA	0.15 ± 0.004a*	0.04 ± 0.002b*	0.03 ± 0.002c*	28.1*	17.9*
	PACT	0.17 ± 0.01a*	0.12 ± 0.003b*	0.10 ± 0.01b	71.7*	59.7
	Q3G	0.26 ± 0.01a*	0.07 ± 0.004b*	0.03 ± 0.001c*	27.2*	11.9*
	K3G	0.28 ± 0.01a*	0.05 ± 0,002b*	0.02 ± 0.005c	19.0*	5.7
	KP	0.04 ± 0.001*	n.d	n.d	n.d	n.d
	TPC_{HPLC}	3.20 ± 0.01a*	0.97 ± 0.04b*	0.71 ± 0.001c*	30.3*	22.2*

RF-N, Strawberry by-product control; RF-E, Strawberry by-product under optimal biofortification conditions TGI, tetragalloyl glucose isomer (TGI); EAP, ellagic acid pentoside; AGN, agrimoniin; EA, free ellagic acid. procyanidin tetramer; Q3, quercetin 3-o-glucuronide; K3G, Kaempferol 3-o-glucuronide; TPC_{HPLC}, Total phenolic content by HPLC. n.d, Not detected. Different lower-case letters in the same row indicate significant differences by Tukey's test ($p < 0.05$). *: Means differences ($p < 0.05$) between the same compound of RF-N and RF-E samples.

the biotransformations they undergo during the digestive process (43). As RFs are an important source of phenolic compounds, it is important to know their behavior and stability during the gastric process, as these by-products can be revalued by obtaining dietary supplements, and it is necessary to guarantee an adequate and safe bioaccessibility of the bioactive compounds. The individual phenolic compounds were quantified at the different stages of the *in vitro* digestion test. The results are shown in **Table 3**, where the RF-N and RF-E phenolic bioaccessibility was compared. The different phases showed a significant effect ($p < 0.05$) on the concentration of individual phenolic compounds (EAP, EA, Q3G, and K3G) for RF-N and RF-E (EAP, AGN, EA, Q3G, K3G, TPC_{HPLC}). AGN ellagitannin was the major compound in all intestinal phases for both RF-N and RF-E, showing a decrease in initial concentration from 1.35 g/kg in RF-N to 0.13 g/kg in the IF, having a bioaccessibility of 9.8%. RF-E started with 1.79 g/kg, and the digestive process reduced it to 0.45 g/kg in IF (25.1%). These results agree with other reports regarding the digestive stability of phenolic compounds from different plant matrices (43–45).

Concerning the bioaccessibility of phenolics from strawberries, it has been reported that anthocyanins, their primary group of phenolic compounds, present low bioaccessibility (1% on average) (43, 46). Ariza et al. (47) reported the bioaccessibility of strawberry achenes which were the majority and the most bioaccessible, with 0.0297 g/Kg of hydrolyzable tannins in the intestinal phase. On the other hand, the PACT compound had the highest bioaccessibility in the intestinal phase, with 79.2% for RF-N and 59.7% for RF-E. These results align with those reported for epicatechin bioaccessibility in sweet cherry with 40% and those reported for cocoa procyanidins with a range of 68.5–70.9% (48, 49). Thus, showing the importance of procyanidins as a source of bioactive compounds with high bioaccessibility. This was followed by the TGI with 71.8 and 36.1%, respectively, indicating that the biofortification process with UVA reduced the bioaccessibility of this compound. K3G was the compound with the lowest bioaccessibility in RF-N (6.8%) and RF-E (5.7%). The phenolic compounds of the different parts of strawberries are not very stable at the basic pH typical of the gastric phase. However, compounds such as ellagic acid in RF-E showed a bioaccessibility of 24% in the gastric phase and 17.9% in the intestinal phase, similar to that reported for blackberry with 14 % (43). Quercetin and kaempferol glycosides were the compounds most affected by the digestive process, as gastric pH generates the biotransformation of these compounds into aglycones which are more unstable. These observations have already been reported on the bioaccessibility of whole strawberries (45).

Regarding TPC_{HPLC}, the trend of decreasing content in the different stages of digestion continues, initially with a content of 2.5 and 3.2 g/Kg for RF-N and RF-E, respectively; they reached the intestinal phase with 0.39 and 0.71 g/Kg, respectively. According to Olivero-David et al. (50), about 95% of phenolic compounds that reach the intestinal phase pass directly to the large intestine without being absorbed, interacting with the microbiota, and through their enzyme complexes, new metabolites with different bioactivities are obtained. It was also observed that the biofortification process using UVA radiation and subsequent storage at 15°C for 46 h significantly improved the content of phenolic compounds that reached the intestinal phase (EAP, AGN, PACT, Q3G, and TPC_{HPLC}).

Antiproliferative activity of radiation to strawberry agro-industrial by-products digested fraction on healthy control and cancer cells

There is little information on the anticancer potential of strawberry agro-industrial residues. In addition, RF, being a rich source of phenolic compounds, during the digestive process when consuming these compounds from RF, have a contact time in the colon, thus in this work, we evaluated the antiproliferative capacity in colon cancer lines (Caco-2 and HT29) compared to a control with healthy HDFA cell lines (20). **Figure 6** shows the IC_{50} determined for the digested extract biofortified with phenolic compounds under optimal conditions (RF-E) compared to the digested control extract (RF-N) in colon cancer cells, and as healthy control cells, the HDFa cell line (Fib) was used. A dose-dependence against the proliferation of cell viability was evident in all 3 cell lines. For Caco-2, both extracts showed an IC_{50} of 5.53 and 5.43 μg/mL for RF-N and RF-E, respectively. However, for HT29, the IC_{50} of the RF-E extract (2.73 μg/mL) was significantly lower than RF-N (3.37 μg/mL). Compared to the control with healthy cells (Fib) with 11.97–10.47 μg/mL for RF-N and RF-E, respectively, a significantly higher IC_{50} was observed compared to the IC_{50} of the cancer lines studied, being lower than the IC_{50} reported for blueberry phenolic compounds in Caco-2 and HT29 cells (15–50 μg/mL) (51).

According to the results in **Table 3**, in the RF-E extracts, the main phenolic compound in the digested fraction was agrimoniin, a dimer composed of two α-1-O-galloyl-2,3:4,6-bis-hexahydroxydiphenoylD-glucose units linked by a C-O-C bond between two gallic acid residues. In some berries, the digestive process enhances the antiproliferative activity of quercetin and kaempferol glycosides (52); however, for RF, the release of flavonol aglycones negatively affected the stability of these compounds. Several authors have validated the antiproliferative effect of strawberry phenolic compounds (52–54) with an average IC_{50} for HT29 of 114 μg/mL; however, there is no known report on the antiproliferative activity of phenolic compounds from strawberry agro-industrial

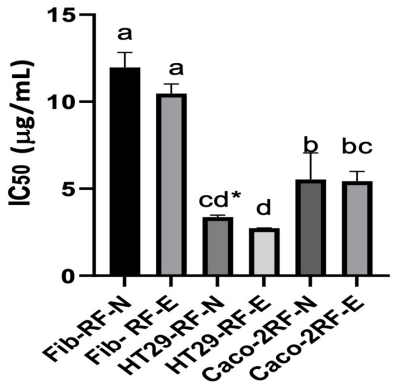

FIGURE 6
IC_{50} determination on HDFa and Cancer cell lines. Fib: Adult primary dermal fibroblast cell line. HT29: Human Colorectal Adenocarcinoma cell line. Caco-2: Human colorectal adenocarcinoma cell line. Different letter indicates significant differences between IC_{50} of different cell lines $p < 0.05$ by Tukey's test. * Means significantly differences ($p < 0.05$) between strawberry by-product control (RF-N) and: Strawberry by-product biofortified (RF-E) according to *t*-test $p < 0.05$.

residues, which showed better activity than whole fruit compounds with a lower IC_{50}. These results show the antiproliferative potential of the strawberry agro-industrial by-product on colon cancer cells to be more significant in the biofortified extract with UVA application and safe in healthy cells. Since colorectal cancer is the primary type of cancer and has one of the highest mortality rates in society, it is important to revalue strawberry agro-industrial by-products through biofortification with phenolic compounds, to extract the compounds and use the extract to prevent this disease.

Cellular antioxidant activity

The by-products of strawberry processing have ellagitannins as the main compounds, which, depending on their degree of polymerization, have better bioactivity, as their amphiphilic character allows them to diffuse passively into the cell membrane and then pass into the aqueous cell medium (55). Imbalances between pro-oxidant and antioxidant species at the physiological level trigger several conditions that facilitate the development of chronic non-communicable diseases (6). Figure 7A shows the antioxidant cellular capacity of digested RF extracts (2.2 mg/mL) to inhibit the APPH radical on the Caco-2 cell line. The RF-E showed a significantly higher antioxidant capacity (69%) than the digested extract of RF-N (58 %), being 11% higher, thanks to the content of phenolic compounds that reach bioaccessibility in the biofortified tissue, being higher than that reported by Lang (56) for the blueberry extract with 25% CAA.

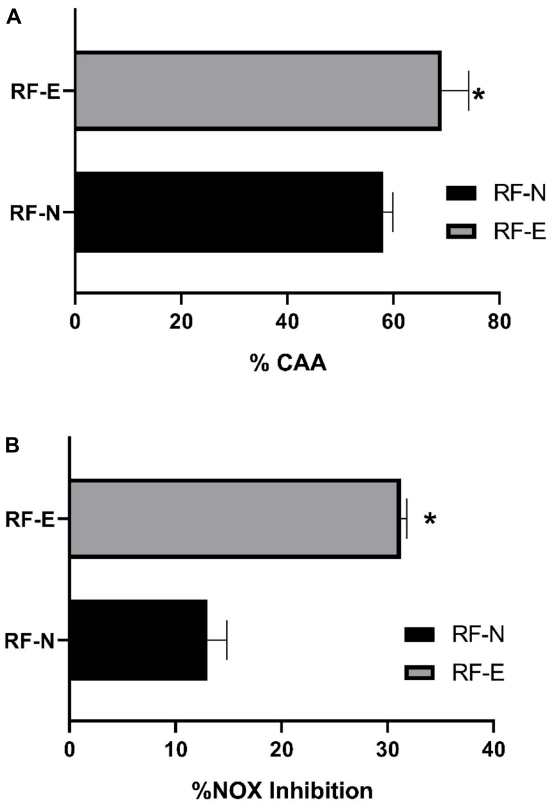

FIGURE 7
(A) Cellular antioxidant capacity inhibition (%CAA) by APPH radical. **(B)** Nitric Oxide (NOX) cell production inhibition (%). Bar indicates standard deviation. *: Means significantly differences between strawberry by-product control (RF-N) and strawberry by-product biofortified (RF-E) samples, according to *t*-test $p < 0.05$.

According to the phenolic profile identified in the digested fraction of the RF-E, ellagitannins were the major compounds that have been widely reported in the different parts of the strawberry plant, where, in addition, the *in vitro* free radical inhibitory capacity has been demonstrated (2). Oxidases are one of the primary sources of ROS in the cell. The enzymes nitric oxide synthase and nitric oxide synthase produce nitric oxide from L-arginine and molecular oxygen. Triggering an overproduction of ROS, ellagitannins of RF-digested extracts with their hydroxyl groups can neutralize free radicals, especially agrimoniin, which has been reported as a potent free radical scavenger (57). Regular strawberry consumption has recently been reported to reduce ROS production and oxidative biomarker levels (58, 59). However, little information is available on the cellular antioxidant potential of the various parts of the strawberry plant, such as the sepal, stalk, and leaves that constitute the residue of agro-industrial strawberry conditioning. This work demonstrated the CAA potential of these by-products, allowing them to be used in the search for sustainable alternatives for obtaining bioactive compounds.

Anti-inflammatory potential

The process of chronic inflammation is correlated with the development of metabolic syndrome, which has become one of the major causes of death in the Western world due to poor lifestyle habits (60). Therefore, compounds with an effective anti-inflammatory activity that prevents the development of a pre-disease state into a chronic disease are currently being sought. The anti-inflammatory potential of phenolic compounds in the RAW cell line exhibits a dose-dependent behavior. In this study, the concentration at which the viability of RAW cells was not significantly affected (>80%) was determined at a concentration of 1.1 mg/mL **Figure 7B** shows the nitric oxide inhibition capacity in RAW 264.7 cells. The RF-N digested tissue with a concentration of 1.1 mg/mL achieved 13% inhibition of NOX production, while RF-E was significantly higher ($p < 0.05$) with 31% inhibition. Fang et al. (61) reported for purified oxyresveratrol extracts with a concentration of 6 μg/mL a 50% reduction in NOX production, compared to the digested crude extract of RF-E, which achieved 31%, is promising as the unpurified extract has good anti-inflammatory activity. Fumagalli et al. (62) studied digested strawberry extract (10 μg/mL), which had tannins as major compounds, and found a potent inhibition of IL-8 secretion, and procyanidins showed prevention of TNF-α induction. Ellagitannins and their metabolites can control inflammatory mediators such as TNF-α, IL-1β, IL-6, and IL-8 by inhibiting oxidase enzymes (NOS) (63). According to **Table 3**, agrimoniin was the main compound after the RF digestion process and is probably the compound with the highest bioactivity in RF extracts. Moreover, Hoffmann et al. (64) reported that agrimoniin-rich fractions of *Potentilla erecta* showed high anti-inflammatory effects in *in vitro* and *in vivo* assays. Biofortified agro-industrial by-products have a relevant bioactive potential that allows a greater revalorization of these by-products by obtaining extracts rich in high-value hydrolyzable tannins such as agrimoniin.

Conclusion

Agro-industrial strawberry residues responded to the elicitor effect of UVA radiation and storage at different temperatures activating PAL activity, PPO, and *de novo* synthesis of phenolic compounds. In addition, the biofortification process was successfully optimized. The optimum biofortification point was applying a UVA-HIGH (86 KJ/m^2) and then storing at 15°C for 46 h. The use of UVA radiation and storage as a tool for biofortification with phenolic compounds for the revalorization of strawberry agro-industrial by-products proved to be an alternative technology that effectively induced the secondary metabolism of these waste tissues, obtaining increases of 184% concerning the control. Agrimoniin (AGN) was the compound mainly generated by applying UVA radiation (1.9 g/Kg RF) with 25% of bioaccessibility. Procyanidin was the compound with the highest bioaccessibility with 59.7%. The biofortification process applied significantly improved the bioaccessibility of the total phenolic compounds and their bioactivities, such as antiproliferative capacity in Caco-2 and HT29 colorectal cancer cells, and the safety of RF extract demonstrated on the HDFa (Fib) cell line, as the IC_{50s} for Fib were significantly higher (10 μg/mL) than those shown for Caco2 and HT29 (5.43–2.73 μg/mL, respectively) and cellular antioxidant capacity, and anti-inflammatory activity, where RF-E (69 and 31%, respectively) showed superiority over RF-N (58 and 13%, respectively). Thus, applying UVA radiation in strawberry by-products allowed a greater revalorization of RF through increasing phenolic compound content and bioactivity, turning this by-product into a sustainable, low-cost source of valuable bioactive compounds with preventive applications in chronic degenerative diseases.

Data availability statement

The raw data supporting the conclusions of this article will be made available by the authors, without undue reservation.

Author contributions

EV-G: conceptualization, data curation, validation, investigation, writing – original draft, and formal analysis. MA-R: validation, investigation, methodology, and writing. AP: conceptualization, reviewing and editing, supervision, project administration, and funding acquisition. DJ-V: conceptualization, methodology, writing – reviewing and editing, supervision, project administration, and funding acquisition. All authors contributed to the article and approved the submitted version.

Funding

This research was performed with research funds from the Agencia Nacional de Promoción Científica y Tecnológica (ANPCyT, Argentina; PICT 2017-406), the Universidad Nacional del Litoral (UNL), and The Institute for Obesity – Research Challenge-Based Research Funding Program 2022 (I018 - IOR001 - C5-T1 – E) from Tecnológico de Monterrey. EV-G received a scholarship and doctoral grant from CONICET (Argentina).

Conflict of interest

The authors declare that the research was conducted in the absence of any commercial or financial relationships that could be construed as a potential conflict of interest.

Publisher's note

All claims expressed in this article are solely those of the authors and do not necessarily represent those of their affiliated organizations, or those of the publisher, the editors and the reviewers. Any product that may be evaluated in this article, or claim that may be made by its manufacturer, is not guaranteed or endorsed by the publisher.

Supplementary material

The Supplementary Material for this article can be found online at: https://www.frontiersin.org/articles/10.3389/fnut.2022.1080147/full#supplementary-material

References

1. Priefer C, Jörissen J, Bräutigam KR. Food waste prevention in Europe - A cause-driven approach to identify the most relevant leverage points for action. *Resour Conserv Recycl.* (2016) 109:155–65. doi: 10.1016/j.resconrec.2016.03.004

2. Villamil-Galindo E, Van de Velde F, Piagentini AM. Extracts from strawberry by-products rich in phenolic compounds reduce the activity of apple polyphenol oxidase. *LWT.* (2020) 133:110097. doi: 10.1016/j.lwt.2020.110097

3. Cano-Lamadrid M, Artés-Hernández F. By-products revalorization with non-thermal treatments to enhance phytochemical compounds of fruit and vegetables derived products: a review. *Foods.* (2022) 11:59. doi: 10.3390/foods11010059

4. Campos DA, Gómez-García R, Vilas-Boas AA, Madureira AR, Pintado MM. Management of fruit industrial by-products—a case study on circular economy approach. *Molecules.* (2020) 25:320. doi: 10.3390/molecules25020320

5. Nowicka A, Kucharska AZ, Sokół-Łętowska A, Fecka I. Comparison of polyphenol content and antioxidant capacity of strawberry fruit from 90 cultivars of Fragaria × ananassa Duch. *Food Chem.* (2019) 270:32–46. doi: 10.1016/j.foodchem.2018.07.015

6. Jacobo-Velázquez DA. Definition of biofortification revisited. *ACS Food Sci Technol.* (2022) 2:782–3. doi: 10.1021/acsfoodscitech.2c00110

7. Darré M, Vicente AR, Cisneros-Zevallos L, Artés-Hernández F. Postharvest ultraviolet radiation in fruit and vegetables: applications and factors modulating its efficacy on bioactive compounds and microbial growth. *Foods.* (2022) 11:653. doi: 10.3390/foods11050653

8. Surjadinata BB, Jacobo-Velázquez DA, Cisneros-Zevallos L. UVA, UVB and UVC light enhances the biosynthesis of phenolic antioxidants in fresh-cut carrot through a synergistic effect with wounding. *Molecules.* (2017) 22:668. doi: 10.3390/molecules22040668

9. Jacobo-Velázquez DA, Martínez-Hernández GB, del C, Rodríguez S, Cao C-M, Cisneros-Zevallos L. Plants as biofactories: physiological role of reactive oxygen species on the accumulation of phenolic antioxidants in carrot tissue under wounding and hyperoxia stress. *J Agric Food Chem.* (2011) 59:6583–93. doi: 10.1021/jf2006529

10. Ortega-Hernández E, Nair V, Welti-Chanes J, Cisneros-Zevallos L, Jacobo-Velázquez DA. Wounding and UVB light synergistically induce the biosynthesis of phenolic compounds and ascorbic acid in red prickly pears (*Opuntia ficus-indica* cv. Rojo Vigor). *Int J Mol Sci.* (2019) 20:5327. doi: 10.3390/ijms20215327

11. González-Sarrías A, Núñez-Sánchez MÁ, Tomás-Barberán FA, Espín JC. Neuroprotective effects of bioavailable polyphenol-derived metabolites against oxidative stress-induced cytotoxicity in human neuroblastoma SH-SY5Y cells. *J Agric Food Chem.* (2017) 65:752–8. doi: 10.1021/acs.jafc.6b04538

12. Gutiérrez-Grijalva EP, Antunes-Ricardo M, Acosta-Estrada BA, Gutiérrez-Uribe JA, Basilio Heredia J. Cellular antioxidant activity and in vitro inhibition of α-glucosidase, α-amylase and pancreatic lipase of oregano polyphenols under simulated gastrointestinal digestion. *Food Res Int.* (2019) 116:676–86. doi: 10.1016/j.foodres.2018.08.096

13. Zhu Q, Nakagawa T, Kishikawa A, Ohnuki K, Shimizu K. In vitro bioactivities and phytochemical profile of various parts of the strawberry (Fragaria × ananassa var. Amaou). *J Funct Foods.* (2015) 13:38–49. doi: 10.1016/j.jff.2014.12.026

14. Van de Velde F, Fenoglio C, Piagentini AM, Pirovani ME. Modeling the impact of the type of cutting and storage temperature on the bioactive compound content, phenylpropanoid metabolism enzymes and quality attributes of fresh-cut strawberries. *Food Bioprocess Technol.* (2018) 11:96–109. doi: 10.1007/s11947-017-1996-y

15. Rodríguez-Arzuaga M, Salsi MS, Piagentini AM. Storage quality of fresh-cut apples treated with yerba mate (*Ilex paraguariensis*). *J Food Sci Technol.* (2021) 58:186–96. doi: 10.1007/s13197-020-04528-w

16. Lowry OH, Rosenbrough NJ, Farr AL, Randall RJ. Protein measurements by Folin-phenol reagent. *J Biol Chem.* (1951) 193:266–75.

17. Villamil-Galindo E, Van de Velde F, Piagentini AM. Strawberry agro-industrial by-products as a source of bioactive compounds: effect of cultivar on the phenolic profile and the antioxidant capacity. *Bioresour Bioprocess.* (2021) 8:61. doi: 10.1186/s40643-021-00416-z

18. Flores FP, Singh RK, Kerr WL, Pegg RB, Kong F. Total phenolics content and antioxidant capacities of microencapsulated blueberry anthocyanins during in vitro digestion. *Food Chem.* (2014) 153:272–8. doi: 10.1016/j.foodchem.2013.12.063

19. Moreno-García KL, Antunes-Ricardo M, Martínez-Ávila M, Milán-Carrillo J, Guajardo-Flores D. Evaluation of the antioxidant, anti-inflammatory and antihyperglycemic activities of black bean (Phaseolus vulgaris L.) by-product extracts obtained by supercritical CO2. *J Supercrit Fluids.* (2022) 183:105560. doi: 10.1016/j.supflu.2022.105560

20. Pacheco-Ordaz R, Antunes-Ricardo M, Gutiérrez-Uribe J, González-Aguilar G. Intestinal permeability and cellular antioxidant activity of phenolic compounds from mango (*Mangifera indica* cv. Ataulfo) peels. *Int J Mol Sci.* (2018) 19:514. doi: 10.3390/ijms19020514

21. Gyula P, Schäfer E, Nagy F. Light perception and signalling in higher plants. *Curr Opin Plant Biol.* (2003) 6:446–52. doi: 10.1016/S1369-5266(03)00082-7

22. Verdaguer D, Jansen MAK, Llorens L, Morales LO, Neugart S. UV-A radiation effects on higher plants: exploring the known unknown. *Plant Sci.* (2017) 255:72–81. doi: 10.1016/j.plantsci.2016.11.014

23. Rabelo MC, Bang WY, Nair V, Alves RE, Jacobo-Velázquez DA, Sreedharan S. UVC light modulates vitamin C and phenolic biosynthesis in acerola fruit: role of increased mitochondria activity and ROS production. *Sci Rep.* (2020) 10:21972. doi: 10.1038/s41598-020-78948-1

24. Chen Y, Fanourakis D, Tsaniklidis G, Aliniaeifard S, Yang Q, Li T. Low UVA intensity during cultivation improves the lettuce shelf-life, an effect that is not sustained at higher intensity. *Postharvest Biol Technol.* (2021) 172:111376. doi: 10.1016/j.postharvbio.2020.111376

25. Kong JQ. Phenylalanine ammonia-lyase, a key component used for phenylpropanoids production by metabolic engineering. *RSC Adv.* (2015) 5:62587–603. doi: 10.1039/c5ra08196c

26. Formica-Oliveira AC, Martínez-Hernández GB, Aguayo E, Gómez PA, Artés F, Artés-Hernández F. UV-C and hyperoxia abiotic stresses to improve healthiness of carrots: study of combined effects. *J Food Sci Technol.* (2016) 53:3465–76. doi: 10.1007/s13197-016-2321-x

27. Panadare D, Rathod VK. Extraction and purification of polyphenol oxidase: a review. *Biocatal Agric Biotechnol.* (2018) 14:431–7. doi: 10.1016/j.bcab.2018.03.010

28. Teoh LS, Lasekan O, Adzahan NM, Hashim N. The effect of ultraviolet treatment on enzymatic activity and total phenolic content of minimally processed potato slices. *J Food Sci Technol.* (2016) 53:3035–42. doi: 10.1007/s13197-016-2275-z

29. Ding P, Ling YS. Browning assessment methods and polyphenol oxidase in UV-C irradiated Berangan banana fruit. *Int Food Res J.* (2014) 21:1667–74.

30. Torres-Contreras AM, Nair V, Cisneros-Zevallos L, Jacobo-Velázquez DA. Plants as biofactories: stress-induced production of chlorogenic acid isomers in potato tubers as affected by wounding intensity and storage time. *Ind Crops Prod.* (2014) 62:61–6. doi: 10.1016/j.indcrop.2014.08.018

31. Chen Y, Li T, Yang Q, Zhang Y, Zou J, Bian Z, et al. Radiation is beneficial for yield and quality of indoor cultivated lettuce. *Front Plant Sci.* (2019) 10:1563. doi: 10.3389/fpls.2019.01563

32. Morales LO, Tegelberg R, Brosché M, Keinänen M, Lindfors A, Aphalo PJ. Effects of solar UV-A and UV-B radiation on gene expression and phenolic accumulation in *Betula pendula* leaves. *Tree Physiol.* (2010) 30:923–34. doi: 10.1093/treephys/tpq051

33. Helsper JPFG, De Vos CHR, Maas FM, Jonker HH, Van Den Broeck HC, Jordi W, et al. Response of selected antioxidants and pigments in tissues of Rosa hybrida and Fuchsia hybrida to supplemental UV-A exposure. *Physiol Plant.* (2003) 117:171–8. doi: 10.1034/j.1399-3054.2003.00037.x

34. Moreira-Rodríguez M, Nair V, Benavides J, Cisneros-Zevallos L, Jacobo-Velázquez DAUVA. UVB light doses and harvesting time differentially tailor glucosinolate and phenolic profiles in broccoli sprouts. *Molecules.* (2017) 22:1065. doi: 10.3390/molecules22071065

35. Nguyen CTT, Kim J, Yoo KS, Lim S, Lee EJ. Effect of prestorage UV-A, -B, and -C radiation on fruit quality and anthocyanin of "Duke" blueberries during cold storage. *J Agric Food Chem.* (2014) 62:12144–51. doi: 10.1021/jf504366x

36. Lim YJ, Lyu JI, Kwon SJ, Eom SH. Effects of UV-A radiation on organ-specific accumulation and gene expression of isoflavones and flavonols in soybean sprout. *Food Chem.* (2021) 339:128080. doi: 10.1016/j.foodchem.2020.128080

37. Jacobo-Velázquez DA, Moreira-Rodríguez M, Benavides J. UVA and UVB radiation as innovative tools to biofortify horticultural crops with nutraceuticals. *Horticulturae.* (2022) 8:387. doi: 10.3390/horticulturae8050387

38. Formica-Oliveira AC, Martínez-Hernández GB, Díaz-López V, Artés F, Artés-Hernández F. Use of postharvest UV-B and UV-C radiation treatments to revalorize broccoli byproducts and edible florets. *Innov Food Sci Emerg Technol.* (2017) 43:77–83. doi: 10.1016/j.ifset.2017.07.036

39. Carlos Sánchez-Rangel J, Benavides J, Jacobo-Velázquez DA. Valorization of carrot pomace: UVC induced accumulation of antioxidant phenolic compounds. *Appl Sci.* (2021) 11:10951. doi: 10.3390/app112210951

40. Wang BQ, Jin ZX. Agrimoniin induced SGC7901 cell apoptosis associated mitochondrial transmembrane potential and intracellular calcium concentration. *J Med Plants Res.* (2011) 5:3513–9.

41. Grochowski DM, Skalicka-Woźniak K, Orhan IE, Xiao J, Locatelli M, Piwowarski JP, et al. A comprehensive review of agrimoniin. *Ann N Y Acad Sci.* (2017) 1401:166–80. doi: 10.1111/nyas.13421

42. Warner R, Wu BS, MacPherson S, Lefsrud M. A review of strawberry photobiology and fruit flavonoids in controlled environments. *Front Plant Sci.* (2021) 12:611893. doi: 10.3389/fpls.2021.611893

43. Van de Velde F, Pirovani ME, Drago SR. Bioaccessibility analysis of anthocyanins and ellagitannins from blackberry at simulated gastrointestinal and colonic levels. *J Food Compos Anal.* (2018) 72:22–31. doi: 10.1016/j.jfca.2018.05.007

44. Antunes-Ricardo M, Rodríguez-Rodríguez C, Gutiérrez-Uribe JA, Cepeda-Cañedo E, Serna-Saldívar SO. Bioaccessibility, intestinal permeability and plasma stability of isorhamnetin glycosides from *Opuntia ficus-indica* (L.). *Int J Mol Sci.* (2017) 18:1816. doi: 10.3390/ijms18081816

45. Azzini E, Intorre F, Vitaglione P, Napolitano A, Foddai MS, Durazzo A, et al. Absorption of strawberry phytochemicals and antioxidant status changes in humans. *J Berry Res.* (2010) 1:81–9. doi: 10.3233/BR-2010-009

46. Sandhu AK, Huang Y, Xiao D, Park E, Edirisinghe I, Burton-Freeman B. Pharmacokinetic characterization and bioavailability of strawberry anthocyanins relative to meal intake. *J Agric Food Chem.* (2016) 64:4891–9. doi: 10.1021/acs.jafc.6b00805

47. Ariza M, Forbes-Hernández T, Reboredo-Rodríguez P, Afrin S, Gasparrini M, Cervantes L, et al. Strawberry and achenes hydroalcoholic extracts and their digested fractions efficiently counteract the AAPH-induced oxidative damage in HepG2 cells. *Int J Mol Sci.* (2018) 19:2180. doi: 10.3390/ijms19082180

48. Gonçalves J, Ramos R, Luís Â, Rocha S, Rosado T, Gallardo E. Assessment of the bioaccessibility and bioavailability of the phenolic compounds of *Prunus avium* L. by in Vitro digestion and cell model. *ACS Omega.* (2019) 4:7605–13. doi: 10.1021/acsomega.8b03499

49. Gìltekin-Özgiven M, Berktaş I, Özçelik B. Change in stability of procyanidins, antioxidant capacity and in-vitro bioaccessibility during processing of cocoa powder from cocoa beans. *LWT Food Sci Technol.* (2016) 72:559–65. doi: 10.1016/j.lwt.2016.04.065

50. Olivero-David R, Ruiz-Roso MB, Caporaso N, Perez-Olleros L, De Las Heras N, Lahera V, et al. In vivo bioavailability of polyphenols from grape by-product extracts, and effect on lipemia of normocholesterolemic Wistar rats. *J Sci Food Agric.* (2018) 98:5581–90. doi: 10.1002/jsfa.9100

51. Yi W, Fischer J, Krewer G, Akoh C. Phenolic compounds from blueberries can inhibit colon cancer cell proliferation and induce apoptosis. *J Agric Food Chem.* (2005) 53:7320–9. doi: 10.1021/jf051333o

52. Seeram NP, Adams LS, Zhang Y, Lee R, Sand D, Scheuller HS, et al. Blackberry, black raspberry, blueberry, cranberry, red raspberry, and strawberry extracts inhibit growth and stimulate apoptosis of human cancer cells in vitro. *J Agric Food Chem.* (2006) 54:9329–39. doi: 10.1021/jf061750g

53. Shi N, Clinton SK, Liu Z, Wang Y, Riedl KM, Schwartz SJ, et al. Strawberry phytochemicals inhibit azoxymethane/dextran sodium sulfate-induced colorectal carcinogenesis in Crj: CD-1 mice. *Nutrients.* (2015) 7:1696–715. doi: 10.3390/nu7031696

54. Zhang Y, Seeram NP, Lee R, Feng L, Heber D. Isolation and identification of strawberry phenolics with antioxidant and human cancer cell antiproliferative properties. *J Agric Food Chem.* (2008) 56:670–5. doi: 10.1021/jf071989c

55. Ky I, Le Floch A, Zeng L, Pechamat L, Jourdes M, Teissedre PL. Tannins. *Encycl Food Health.* (2015) 7:247–55. doi: 10.1016/B978-0-12-384947-2.00683-8

56. Lang Y, Li B, Gong E, Shu C, Si X, Gao N, et al. Effects of α-casein and β-casein on the stability, antioxidant activity and bioaccessibility of blueberry anthocyanins with an in vitro simulated digestion. *Food Chem.* (2021) 334:127526. doi: 10.1016/j.foodchem.2020.127526

57. Giampieri F, Tulipani S, Alvarez-Suarez J, Quiles J, Mezzetti B, Battino M. The strawberry: composition, nutritional quality, and impact on human health. *Nutrition.* (2012) 28:9–19. doi: 10.1016/j.nut.2011.08.009

58. Battino M, Beekwilder J, Denoyes-Rothan B, Laimer M, McDougall GJ, Mezzetti B. Bioactive compounds in berries relevant to human health. *Nutr Rev.* (2009) 67:S145–50. doi: 10.1111/j.1753-4887.2009.00178.x

59. Giampieri F, Alvarez-Suarez JM, Gasparrini M, Forbes-Hernandez TY, Afrin S, Bompadre S, et al. Strawberry consumption alleviates doxorubicin-induced toxicity by suppressing oxidative stress. *Food Chem Toxicol.* (2016) 94:128–37. doi: 10.1016/j.fct.2016.06.003

60. Battino M, Giampieri F, Cianciosi D, Ansary J, Chen X, Zhang D, et al. The roles of strawberry and honey phytochemicals on human health: a possible clue on the molecular mechanisms involved in the prevention of oxidative stress and inflammation. *Phytomedicine.* (2021) 86:153170. doi: 10.1016/j.phymed.2020.153170

61. Fang SC, Hsu CL, Yen GC. Anti-inflammatory effects of phenolic compounds isolated from the fruits of *Artocarpus heterophyllus*. *J Agric Food Chem.* (2008) 56:4463–8. doi: 10.1021/jf800444g

62. Fumagalli M, Sangiovanni E, Vrhovsek U, Piazza S, Colombo E, Gasperotti M, et al. Strawberry tannins inhibit IL-8 secretion in a cell model of gastric inflammation. *Pharmacol Res.* (2016) 111:703–12. doi: 10.1016/j.phrs.2016.07.028

63. Pap N, Fidelis M, Azevedo L, do Carmo MAV, Wang D, Mocan A, et al. Berry polyphenols and human health: evidence of antioxidant, anti-inflammatory, microbiota modulation, and cell-protecting effects. *Curr Opin Food Sci.* (2021) 42:167–86. doi: 10.1016/J.COFS.2021.06.003

64. Hoffmann J, Casetti F, Bullerkotte U, Haarhaus B, Vagedes J, Schempp CM, et al. Anti-inflammatory effects of agrimoniin-enriched fractions of *Potentilla erecta*. *Molecules.* (2016) 21:792. doi: 10.3390/molecules21060792

frontiers | Frontiers in Nutrition

TYPE Original Research
PUBLISHED 14 December 2022
DOI 10.3389/fnut.2022.1067597

OPEN ACCESS

EDITED BY
Runqiang Yang,
Nanjing Agricultural University, China

REVIEWED BY
Viduranga Y. Waisundara,
Australian College of Business and Technology, Sri Lanka
Apollinaire Tsopmo,
Carleton University, Canada

*CORRESPONDENCE
Ren-You Gan
✉ ganrenyou@163.com;
✉ ganry@sifbi.a-star.edu.sg
Bo-Li Guo
✉ guoboli2007@126.com

†PRESENT ADDRESS
Ren-You Gan,
Singapore Institute of Food and Biotechnology Innovation (SIFBI), Agency for Science, Technology and Research (A*STAR), Singapore, Singapore

SPECIALTY SECTION
This article was submitted to Nutrition and Food Science Technology, a section of the journal Frontiers in Nutrition

RECEIVED 12 October 2022
ACCEPTED 30 November 2022
PUBLISHED 14 December 2022

CITATION
Liu H-Y, Liu Y, Li M-Y, Ge Y-Y, Geng F, He X-Q, Xia Y, Guo B-L and Gan R-Y (2022) Antioxidant capacity, phytochemical profiles, and phenolic metabolomics of selected edible seeds and their sprouts. *Front. Nutr.* 9:1067597. doi: 10.3389/fnut.2022.1067597

Antioxidant capacity, phytochemical profiles, and phenolic metabolomics of selected edible seeds and their sprouts

Hong-Yan Liu[1], Yi Liu[1], Ming-Yue Li[2], Ying-Ying Ge[3], Fang Geng[2], Xiao-Qin He[1], Yu Xia[1], Bo-Li Guo[4]* and Ren-You Gan[1]*†

[1]Chengdu National Agricultural Science and Technology Center, Research Center for Plants and Human Health, Institute of Urban Agriculture, Chinese Academy of Agricultural Sciences, Chengdu, China, [2]Key Laboratory of Coarse Cereal Processing (Ministry of Agriculture and Rural Affairs), Sichuan Engineering and Technology Research Center of Coarse Cereal Industrialization, College of Food and Biological Engineering, Chengdu University, Chengdu, China, [3]Department of Food Science and Technology, School of Agriculture and Biology, Shanghai Jiao Tong University, Shanghai, China, [4]Institute of Food Science and Technology, Chinese Academy of Agricultural Sciences, Beijing, China

Sprouts are recognized as nutritional and functional vegetables. In this study, 17 selected seeds were germinated simultaneously. The antioxidant capacity and total phenolic content (TPC) were determined for seeds and sprouts of all species. Both seed and sprout of white radish, with the highest antioxidant capacity, and TPC among all the 17 species, were further determined for phenolic metabolomics. Four phenolic classes with 316 phenolic metabolites were identified. 198 significantly different metabolites with 146 up-regulated and 52 down-regulated were confirmed, and high amounts of phenolic acids and flavonoids were found to be accumulated in the sprout. Several metabolism and biosynthesis, including phenylpropanoid, favone and flavonol, phenylalanine, and various secondary metabolites, were significantly activated. Significant correlations were found among FRAP, DPPH, ABTS, TPC, and phenolic profiles. Therefore, white radish sprout could be served as antioxidant and could be a good source of dietary polyphenols.

KEYWORDS

germination, phenolic, antioxidant activity, sprouts, metabolomics

1 Introduction

Phenolic compounds are secondary metabolites in plants (1). In recent years, phenolic compounds have attracted increasing attention based on their nutrition and health benefit. It is reported that phenolic compounds have protective effect against oxidative reactions, which was connected with diminishing the dangers of cancer, coronary illness and diabetes, restraint of bacterial, inflammation and allergies (2–4).

The edible seeds have been widely reported to show various health effects (5, 6). Germination is a kind of processing method, the germinated sprouts generally accumulated more phenolic compounds which could prevent lipids from oxidation (7, 8), making them as valuable sources of food ingredients. In comparison with seed, germination has many advantages for improving the nutritional and functional qualities, such as the accumulation of many biologically active compounds, including γ-aminobutyric acid, minerals, phenolic acids, flavonoids, vitamins, etc. (9, 10).

At present, the phenolic content as well as the antioxidant activities of many edible seeds and sprouts (e.g., legumes, Brassica, and Gramineae) has been studied. However, the germination condition, and applied antioxidants assay in most previous reports were not uniform, and the differences in growth conditions (light sources and time, different treatment of seeds, and environmental shocks) might lead to dramatic differences in the chemical compounds, metabolomics and antioxidant activity (11–14), making it difficult to compare the results and achieve consistent conclusion directly. In addition, little information was available about the main phenolic compounds in sprout that responsible for these antioxidant properties. As a result, it is necessary to study on phenolic compounds and antioxidant capacity of both seed and sprout in the same germinating condition. Meanwhile, the main metabolites that contribute to the antioxidant activity in seed and sprout must be excavated.

It is not clear how the phenolic compounds and their antioxidant activities change throughout seed germination, and it is necessary to identify the optimum plant species with optimum physiological stages in order to accumulate the maximum phenolic accumulation. As a result, we hypothesized that the phenolic metabolites and their antioxidant activities of sprouts would change with germination days. With the improvement of analytical methods and instrument sensitivity, phenolic metabolomics analysis covering more than 2,000 metabolites could be determined simultaneously. In this study, the total phenolic contents (TPCs) as well as the antioxidant activities of 17 types of seeds and their 6-day sprouts were analyzed. Furthermore, the white radish (with the highest antioxidant capacity and TPC values) was selected for another germination trial in order to investigate the dynamic changes of antioxidant capacity and TPC at different germination stages (1, 2, 3, 4, 5, 6 days, respectively). In addition, the phenolic metabolomics in the white radish seed and sprout extract were analyzed qualitatively and quantitatively by ultra-performance liquid chromatography-electrospray ionization mass spectrometry/mass spectrometry (UPLC-ESI-MS/MS), in order to confirm the main different phenolic compounds after germination. Finally, the relationships between the antioxidant capacity and phenolic profiles were analyzed. The obtained results may provide references for the selection of edible seeds and sprouts with high antioxidant capacity as raw materials for functional foods.

2 Materials and methods

2.1 Chemicals and reagents

The chemicals of 6-hydroxy-2,5,7,8-tetramethylchromane-2-carboxylic acid (Trolox), 2,2'-azino-bis (3-ethylbenz-thiazoline-6-sulfonic acid) (ABTS), 1,1-diphenyl-2-picryl-hydrazyl (DPPH), 2,4,6-tri(2-pyridyl)-S-triazine (TPTZ), Folin–Ciocalteu's phenol reagent, and gallic acid and catechin were purchased from Sigma-Aldrich (St. Louis, MO, USA). The sodium acetate, ferric chloride, and Na_2CO_3 (> 99%) were purchased from Beijing Solarbio Technology Co., Ltd. (Beijing, China). The methanol (chromatographic grade grade) was obtained from Beijing Yishan Huitong Technology Co., Ltd. (Beijing, China). Milli-Q ultra-pure water was used for all experiments.

2.2 Sprout growth and pretreatments

Based on the common grains and vegetables, totally 17 crop seeds of broccoli (*Brassica oleracea* L. var. italic), pakchoi (*Brassica campestris* L. ssp. *chinesis* var. communis), pakchoi seedlings (*Brassica campestris* L. ssp. *chinensis* var. communis), purple radish (*Raphanus sativus* L.), white radish (*Raphanus sativus* L.), sunflower (*Helianthus annuus* L.), water spinach (*Ipomoea aquatica* Forssk.), barley (*Hordeum vulgare* L.), triticale (*X Triticosecale* Wittm.), wheat (*Triticum aestivum* L.), perilla (*Perilla frutesches* L. Britt), alfalfa (*Medicago sativa* L.), lentil (*Lens culinaris* Medik.), pea (*Pisum sativum* L.), pine willow (*Lathyrus quinquenervius* (Miq.) Litv), okra (*Abelmoschus esculentus* L. Moench), and vanilla (*Vanilla planifolia* L.) were purchased from Weifang Shuishengtian Agriculture Technology Co., Ltd. (Weifang, China). All the seeds were collected at the same region in the year of 2021.

After cleaning and picking out bad seeds, the seeds were soaking for 5–24 h, and germinated for 6 days with 12 h daylight and 12 h darkness each day. The germination temperature was 25°C and the humidity was kept at 90%. The de-ionized water was used as substrate to germinate, and all the sprouts were sampled after 6 days germination. Furthermore, the white radish sprouts (with the highest antioxidant capacity and TPC) were sampled after 24, 48, 72, 96, and 120 h of germination with the same seeds. After harvest, the sprout samples were frozen with liquid nitrogen treatment immediately, and then freeze-dried for 24 h. Finally, seeds and sprouts were further milled in a miller (Tube Mill 100 control, IKA, Germany) to obtain powder samples. The growth status of sprouts was shown in **Supplementary Figure 1**.

2.3 Analysis of the total phenolic content

About 0.5 g of seed or sprout powder by adding 10 mL of 80% (v/v) ethanol was shaken for 24 h at 22°C, the solution was then centrifuged with 3,000 × g for 30 min at 4°C, the supernatant was collected and diluted by 80% of ethanol before determination the measurement. All the contents were finally corrected with the dilution fold finally. The TPC was detected by Folin–Ciocalteu method described previously with a little modification (15), and the absorbance at 760 nm was determined. Finally, the TPC of seed or sprout was expressed as mg gallic acid equivalent (GAE)/100 g DW. Each sample was determined in triplicate.

2.4 Analysis of the antioxidant activities

The sample extraction and dilution methods were the same as the methods for analysis of TPC, all the values were finally corrected with the dilution fold, and each sample was determined in triplicate.

The DPPH working solution was prepared by adjusting the DPPH solution (100 μM) with 80% methanol to an absorbance of 0.70 ± 0.05 at 515 nm. 100 μL of the properly diluted supernatant with 3.9 mL working solution was mixed to react for 60 min in dark at room temperature, and the solution was then detected at 515 nm. Finally, μmol of Trolox/g of seeds and sprouts were used to express DPPH values.

A total of 100 μL of the properly diluted supernatant was mixed with 3 mL FRAP working solution (300 mmol/L of sodium acetate buffer, 10 mmol/L of TPTZ solution, and 20 mmol/L of ferric chloride solution, 10:1:1 [v/v/v)] for 4 min at room temperature, and the absorbance at 593 nm was tested further. Finally, the FRAP value of seed and sprout was shown as μmol Fe(II)/g DW.

The 7 mmol/L ABTS solution and 2.45 mmol/L potassium persulfate solution were mixed at a volume ratio of 1:1 to obtain the ABTS stock solution. The ABTS stock solution was diluted with ultra-pure water to ensure its absorbance was 0.710 ± 0.05 at 734 nm as ABTS working solution. When determination, 100 μL of the properly diluted supernatant mixed with 3.9 mL working solution was reacted at room temperature for 6 min in darkness. The absorbance of the solution at 734 nm was then detected. Finally, the ABTS value of seed or sprout was expressed as μmol Trolox/g dry weight (DW).

2.5 Metabolomics analysis

White radish seed and sprout samples were freeze-dried by a vacuum freeze-dryer (SJIA-5S, Ningbo Shuangjia Instrument Co., Ltd., Ningbo, China), and crushed by a mixer mill (MM 400, Retsch) as fine powder. The prepared powder sample (50 mg) was then dissolved by 1.2 mL 70% methanol solution, and vortex for 30 s every 30 min with six times in total. Finally, the extracts were centrifuged for 3 min at 12,000 rpm, and then filtrated with 0.22 μ m filter.

The extracts were determined by UPLC-ESI-MS/MS system (UPLC, SHIMADZU Nexera X2HPLC-MS/MS system; MS, Applied Biosystems 4500 Q TRAP). The HPLC column was SB-C18 (2.1 mm × 100 mm, 1.8 μm). The solvent system was composed with water containing 0.1% formic acid (solvent A) and 0.1% (v/v) formic acid in acetonitrile (solvent B). The program conditions were set as follows: 5–95% B from 0 to 9 min and kept for 1 min, and 95–5% B from 10 to 11 min and kept for 3 min. The temperature, low velocity, and injection volume were 40°C, 0.35 mL/min, and 4 μL, respectively.

The effluent was alternatively connected to an ESI-triple quadrupole-linear ion trap (QTRAP)-MS, equipped with an ESI Turbo Ion-Spray interface, operating in positive and negative ion modes and controlled by the Analyst 1.6.3 software (AB Sciex, Framingham, MA, USA). In triple quadrupole (QqQ) and Linear ion trap (LIT) modes, 10 and 100 μmol/L polypropylene glycol solutions were used for instrument tuning and quality calibration, respectively, QqQ scans were acquired as multiple reaction monitoring mode (MRM) experiments with collision gas (nitrogen) set to medium, declustering potential (DP) and collision energy (CE) for individual MRM transitions were done with further DP and CE optimization. The ESI source was operated as follows: temperature 550°C. The ion spray voltage in positive and negative mode, respectively, was 5.5 and 4.5 kV. Set at 50, 60, and 25 psi for the ion source gases I, II, and curtain gas, respectively. A pooled sample was run after every two samples to serve as quality control (QC) to estimate the variables.

Phenolic compounds were tentatively identified according to a previous study (16). Both primary and secondary MS information was compared with the database self-builted by Metware Biotechnology Co., Ltd. (Wuhan, China) as well as the publicly available databases covering metabolites. In order to identify the molecules qualitatively, metabolite primary and secondary mass spectrometry data, including the accurate precursor ion (Q1), and product ion (Q3) value, retention times (RT), declustering potential (DP), and collision energy (CE) were subjected to qualitative analysis by referencing self-built database MWDB (Metware Biotechnology Co., Ltd., Wuhan, China) and public mass spectrometry databases such as MassBank,[1] KNAPSAcK,[2] HMDB,[3] and METLIN,[4] these information in the samples were intelligently matched with the

1 http://www.massbank.jp
2 http://kanaya.naist.jp/KNApSAcK
3 http://www.hmdb.ca
4 http://metlin.scripps.edu/index.php

database one by one, and the mass tolerance of MS and MS/MS were set as ± 10 ppm.

Triple quadrupole mass spectrometry was responsible for the quantification of metabolites. Based on MRM scanning, the quadrupole first searched for precursor ions (parent ions) of target substances while screening any ions derived from substances of different molecular weights to eliminate their interference preliminarily. The precursor ions were fragmented *via* induced ionization in the collision chamber to form many fragment ions, which were then filtered through QqQs to select single-fragment ions with the desired characteristics. MultiQuant quantitative software was used to integrate and to obtain quantitative data. After the metabolite mass spectrometry data were obtained for each sample, all the mass spectrum peaks were subjected to area integration. In order to qualitative and quantitative analyze of each metabolite in different samples more accurately, each mass spectrum peak was corrected according to the RT and peak shape of each metabolite. The relative content of each metabolite was represented with chromatographic peak area integrals.

2.6 Statistical analysis

The results were presented as mean ± standard deviation (SD). The ANOVA and Pearson correlation analysis were analyzed by SPSS statistical software (IBM SPSS Statistics 20.0, SPSS Inc., Chicago, IL). PCA (principal component analysis) and OPLS-DA (orthogonal partial least squares-discrimination analysis) were conducted by R.[5] The metabolism data was normalized by unit variance scaling and zero-centered

5 http://www.r-project.org/

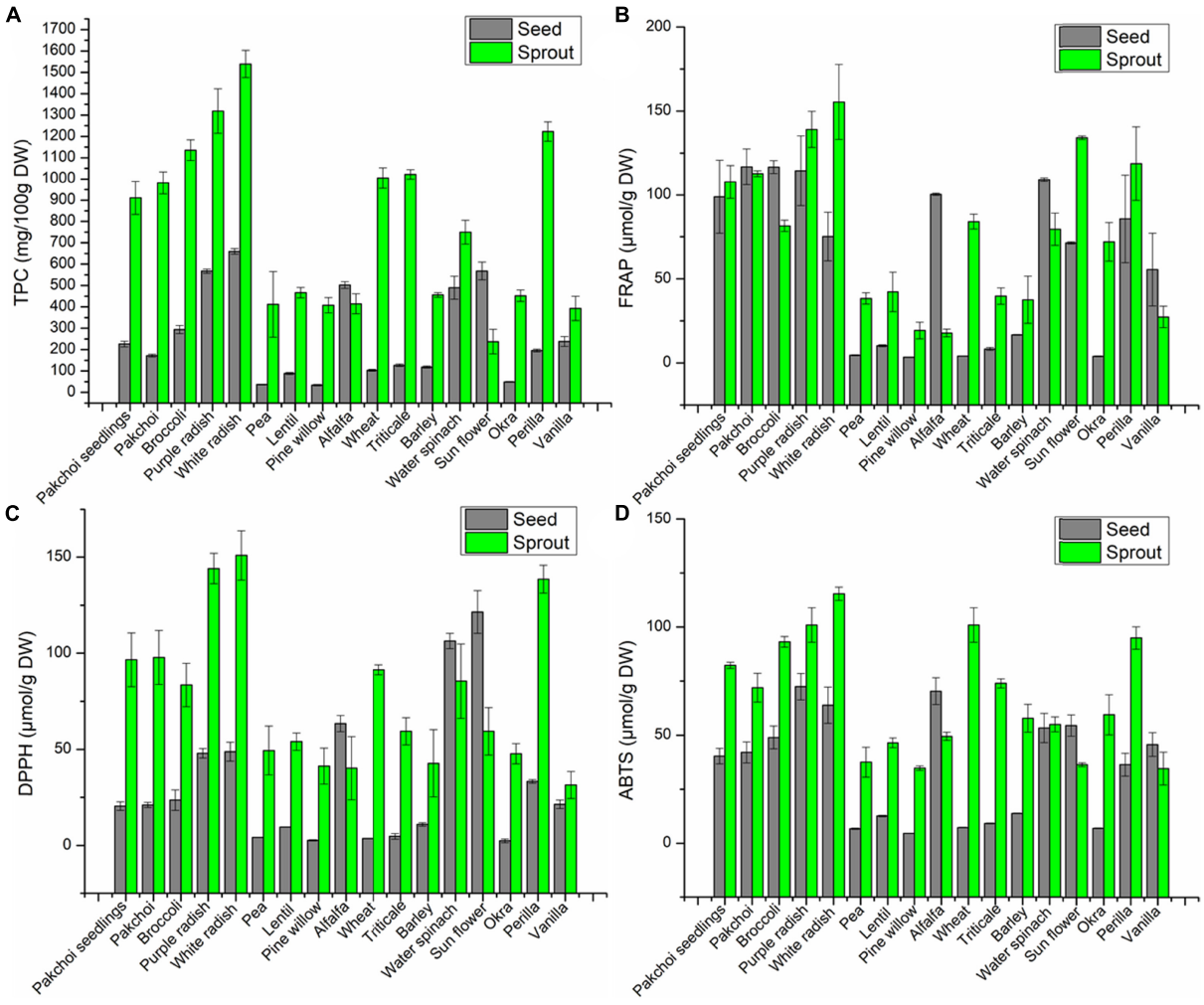

FIGURE 1
The TPC **(A)**, FRAP **(B)**, DPPH **(C),** and ABTS **(D)** values of 17 seeds and their sprouts.

to ensure that the processed data conformed to standard normal distribution.

3 Results

3.1 The TPC and antioxidant activity of seeds and sprouts

The TPC of all sprouts were higher than corresponding seeds, except for alfalfa and oil sunflower (Figure 1A). What's more, the TPC of white radish sprout and its seed were highest among all the sprouts or seeds, respectively, reaching 15.39 and 6.60 mg GAE/g DW, followed by purple radish with 13.19 and 5.67 mg GAE/g DW for sprout and seed, respectively. The TPC accumulated within 6 days of germination accounted for 4.03-fold (pakchoi seedings), 5.71-fold (pakchoi), 3.86-fold (broccoli), 2.32-fold (purple radish), 2.33-fold (white radish), 11.20-fold (pine willow), 0.82-fold (alfalfa), 9.73-fold (wheat), 8.05-fold (Triticale), 3.84-fold (barely), 1.53-fold (water spinach), 0.42-fold (sunflower), 9.23-fold (okra), 6.23-fold (Perilla), and 1.65-fold (vanilla) compared with their seeds.

The results of antioxidant activity based on the FRAP assay showed that among 17 edible seeds and sprouts, the antioxidant activities in most of the sprouts were higher than those of their seeds, which was inconsistent or contrary to the TPC results among these nine seeds (Figure 1B). The results of antioxidant activity measured based on DPPH assay showed that except for spinach, alfalfa and oil sunflower, the antioxidant activities of the remaining 14 sprouts were higher than those of their seeds (Figure 1C). The results of antioxidant activity based on the ABTS assay showed that except for alfalfa and oil sunflower, the antioxidant activities of the remaining 15 sprouts were higher than those of their seeds (Figure 1D).

In addition, the highest antioxidant activity in all sprout was found in white radish, the FRAP, DPPH, and ABTS values, respectively, were 155.4 μmol Fe(II)/g DW, 150.9 μmol Trolox/g DW, and 115.4 μmol Trolox/g DW. Followed by purple radish, respectively were 139.0 μmol Fe (II)/g DW, 144.1 μmol Trolox/g DW, and 101.0 μmol Trolox/g DW.

3.2 The dynamic changes of TPC and antioxidant activity during germination

According to the above experimental results, white radish sprouts showed the highest antioxidant capacities. As a result, they were selected for subsequent research. The dynamic changes of TPC, FRAP, DPPH, and ABTS in white radish during germination were analyzed (Figure 2). TPC generally showed an increasing trend in the first 4 days, and then decreased afterward. The FRAP value increased rapidly in the first 3 days and kept stable in the following germination days. The DPPH value increased with the germination time during the first 5 days and decreased slightly on the sixth day. The ABTS value generally increased during the first 4 days, this was consistent with the TPC result.

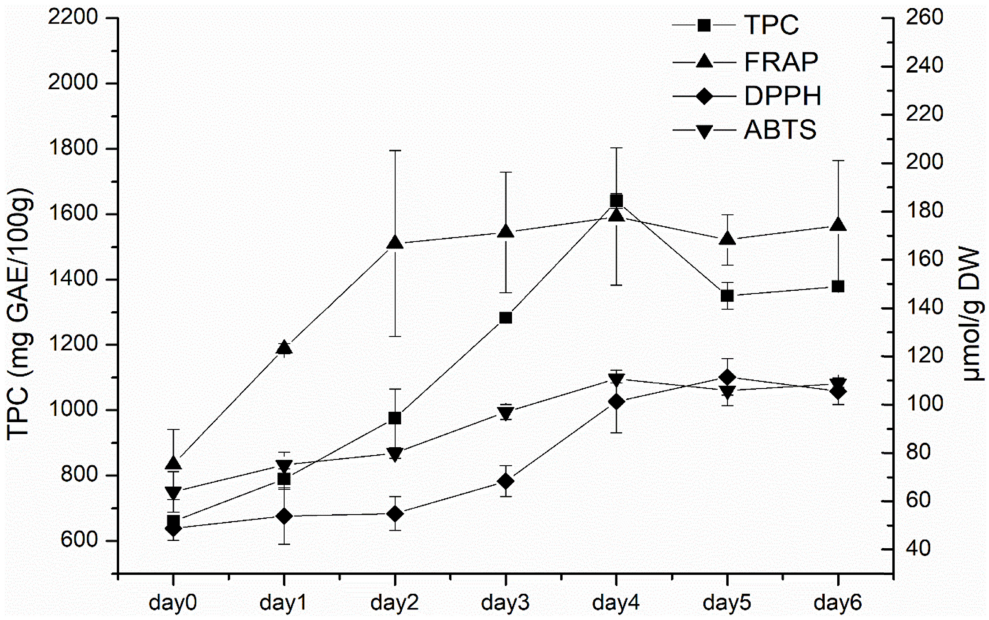

FIGURE 2
The TPC and antioxidant capacities (ABTS, DPPH, and FRAP) of white radish during germination.

3.3 Metabolomics analysis of white radish seed and its sprouts

3.3.1 The differences in phenolic classes between seed and sprout

In total, 316 phenolic metabolites were identified, including 155 phenolic acids, 129 flavanols, 29 lignans, and coumarins, and 3 tannins. After comparing the sum of each phenolic class between seed and sprout (**Supplementary Table 1**), the abundance of each phenolic class in radish sprout was significantly higher than those in seed by *t*-test ($P < 0.05$) (**Figure 3**).

The proportion of QC samples with CV values less than 0.3 exceeds 75%, indicating that the stability of this experimental data (**Supplementary Figure 2A**). The TIC plots for three QC samples were overlapped both in positive and negative mode (**Supplementary Figures 2B,C**), indicating this method was extremely stable and reliable.

3.3.2 The differences in phenolic compounds between seed and sprout

According to the PCA result, the first three principal components were extracted to be 84.47, 5.08, and 4.04%, respectively (**Supplementary Figure 3**). These plots showed that the seed and sprout of white radish could be clearly separated by phenolic compounds. These results suggested significant differences in the phenolic profiles of white radish during germination.

Orthogonal partial least squares-discrimination analysis was employed to investigate the different compounds between radish seed and sprout (**Figure 4A**). Differential metabolites were determined by VIP (VIP $\geq$ 1) and absolute Log_2FC ($|Log_2FC| \geq 1.0$). VIP values were extracted from OPLS-DA result, which also contain score plots and permutation plots, was generated using R package MetaboAnalyst R. The data was log transform (log_2) and mean centering before OPLS-DA. In order to avoid overfitting, a permutation test (200 permutations) was performed. The validation result of the OPLS-DA model was $R^2X = 0.881$, $R^2Y = 1$, $Q^2 = 0.998$. The R^2Y and Q^2-values exceed 0.9, indicating that the model was excellent, with good predictability and high fit accuracy (**Supplementary Figure 4**). There were 251 phenolic compounds whose VIP scores were higher than 1. Based on $P < 0.05$ and VIP $\geq$ 1, totally 198 significantly different metabolites were observed between white radish seed and sprout, with 52 down-regulated and 146 up-regulated (**Figure 4B**). In particular, there were 34 down-regulated and 72 up-regulated in phenolic acids, 14 down-regulated and 58 up-regulated in flavonoids, 3 down-regulated and 19 up-regulated in lignans and coumarins, 2 down-regulated and 1 up-regulated in tannins. The screening of differentially abundant phenolic metabolites between white radish seed and sprout was based on FC > 2 (or < 0.5) and $P < 0.05$, compounds with top 20 fold change were listed in **Figure 4B**. There were 17 compounds (including sinapoylsinapoyltartaric acid, procyanidin A6, syringaresinol-4'-O-glucoside, etc.) were up-regulated (red) and 3 compounds (vanillic acid, 2, 4-dihydroxybenzoic acid, and 2, 5-dihydroxybenzoic acid) were down-regulated (green) (**Figure 4C**).

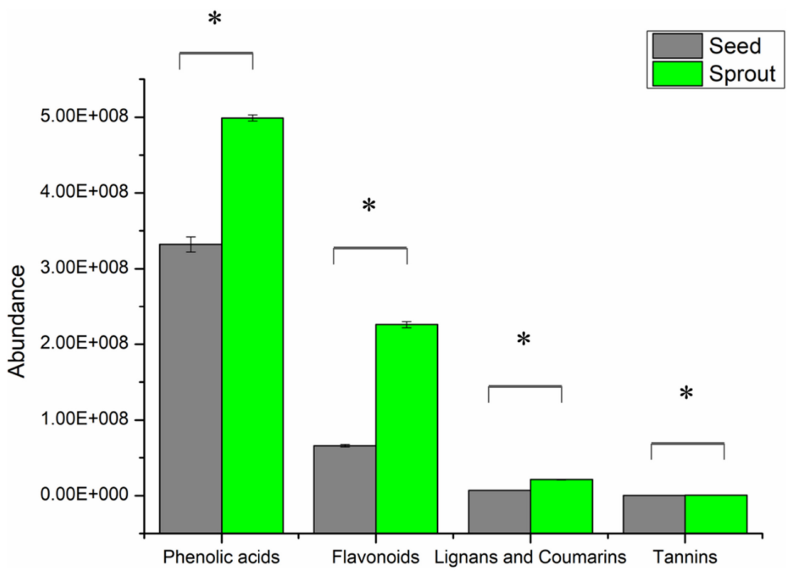

FIGURE 3
The abundance of phenolic classes between white radish seed and sprout. *Indicated significantly different ($P < 0.05$).

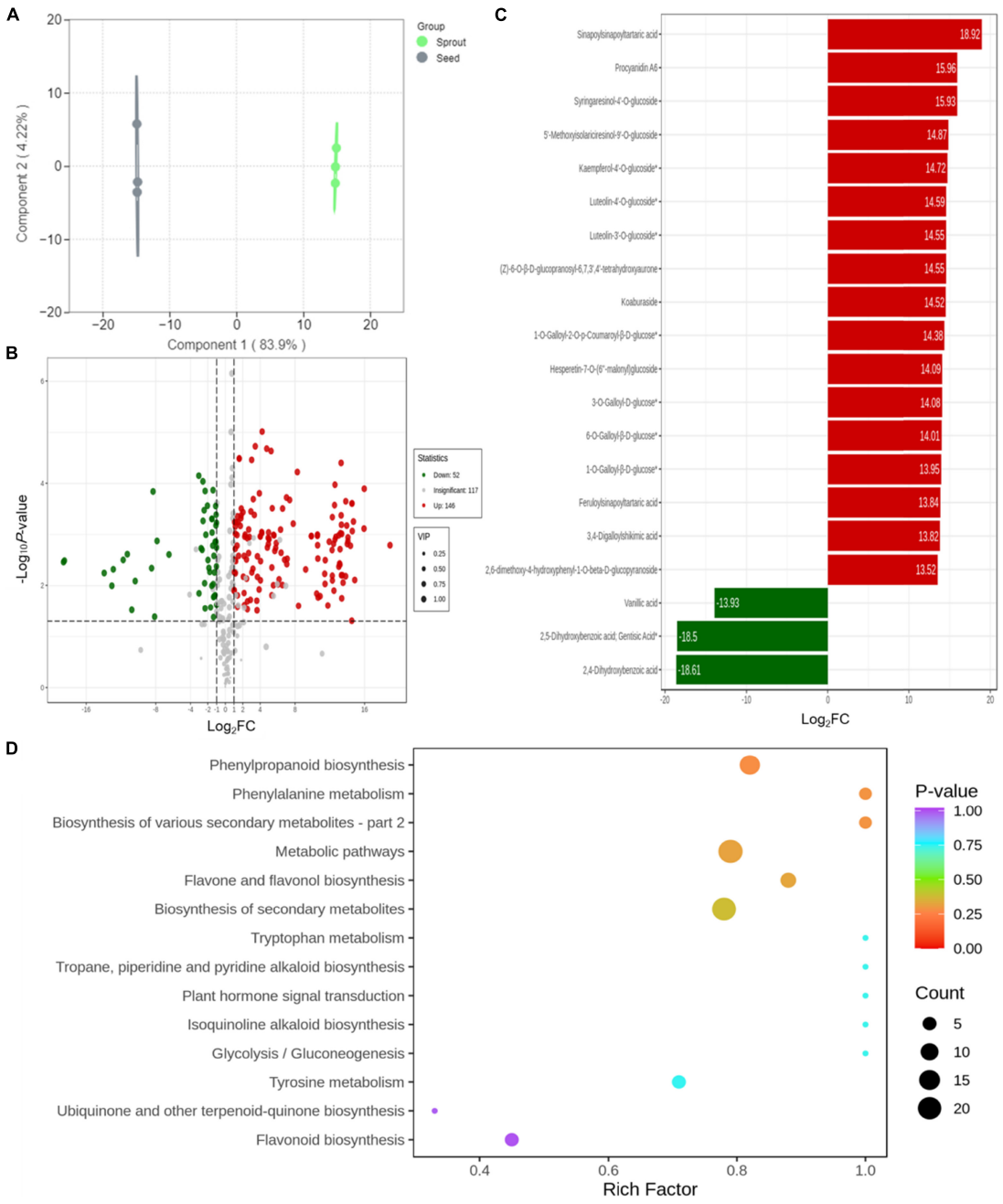

FIGURE 4
(A) Orthogonal partial least squares-discrimination analysis result for discriminating of white radish seed and sprout; **(B)** volcano plots of the up- and down-accumulated metabolites for comparison groups of seed and sprout; **(C)** bar chart of the top 20 differentially abundant phenolic compounds with the largest fold change (FC) value; **(D)** KEGG enrichment of differential metabolites in the comparison of seed and sprout.

The metabolite accumulation information was studied by the public databases of Kyoto Encyclopedia of Genes and Genomes (KEGG) in this work. The differential metabolites for white radish seed vs. sprout were involved in 14 pathways presented in bubble plots. Several metabolic pathways including "phenylpropanoid biosynthesis," "phenylalanine metabolism," "biosynthesis of various secondary metabolites," "biosynthesis of secondary metabolites," "metabolic pathways," and "flavone and flavonol biosynthesis" were significantly enriched ($P < 0.05$) (Figure 4D).

The top 10 differentially abundant phenolic compounds with the largest fold change (FC) value between white radish seed and sprout were listed in Figure 5. Among them, 2,5-dihydroxybenzoic acid (gentisic acid) and 2,4-dihydroxybenzoic

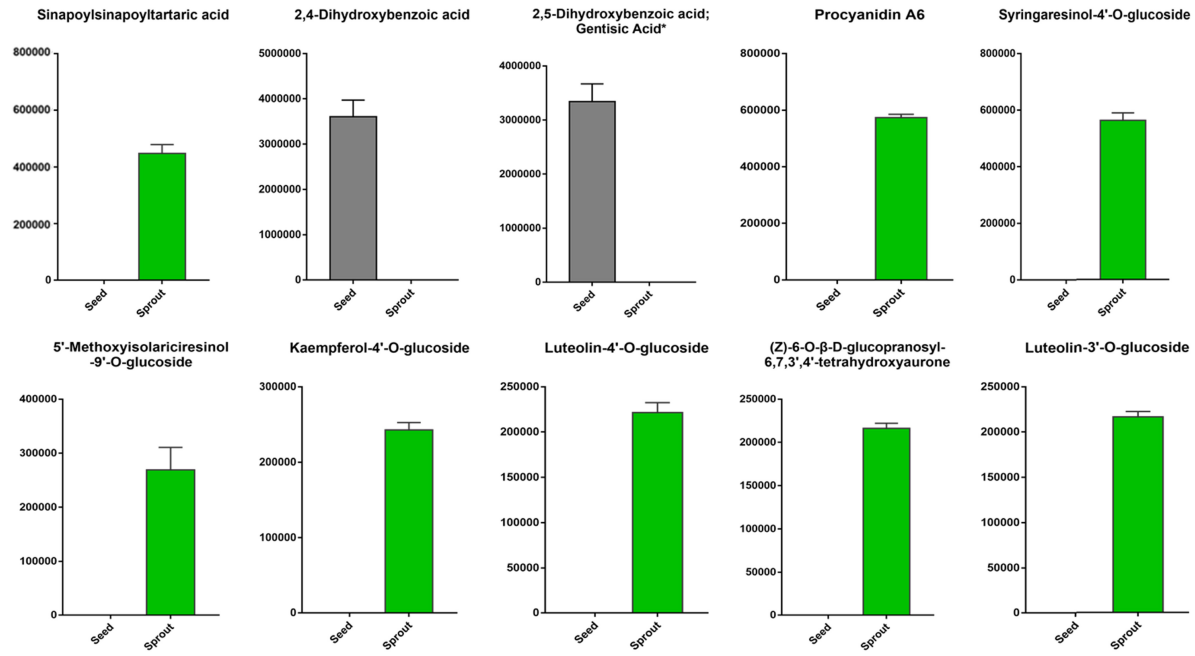

FIGURE 5
The top 10 differentially abundant phenolic compounds with the largest fold change (FC) value in the pairwise comparison of white radish seed and sprout.

acid were not identified in white radish sprout, but were identified in seeds. The other six phenolic compounds, including sinapoylsinapoyltartaric acid, procyanidin A6, syringaresinol-4′-O-glucoside, 5′-methoxyisolariciresinol-9′-O-glucoside, kaempferol-4′-O-glucoside, luteolin-4′-O-glucoside, (Z)-6-O-β-D-glucopranosyl-6,7,3′,4′-tetrahydroxyaurone, and luteolin-3′-O-glucoside were only found in white radish sprouts.

3.3.3 Correlation analysis between antioxidant activity and main phenolic profiles

Furthermore, Pearson correlation analysis was conducted between FRAP, DPPH, ABTS, TPC, and each phenolic class of all white radish seeds and sprouts (**Figure 6**). Significantly positive correlations were obtained among FRAP, DPPH, ABTS, TPC, phenolic acids, flavonoids, lignans, and coumarins, and tannins ($P < 0.05$). The Pearson correlation coefficients ranged from 0.84 to 0.99, indicating very strong correlation among these parameters.

4 Discussion

The enhancement in phenolic content and antioxidant activity after germination has been broadly reported in wheat (17–19), barley (20), and radish (21). The TPC (DW) and DPPH values of wheat, radish, broccoli, lentil, and alfalfa sprouts are significantly higher than the dormant seed and imbibed seed (22). Also, some studies showed that TPC and antioxidant activities significantly increased during germination in lentil (4, 23) and legumes (24). The TPC, DPPH values, and ABTS values of radish and broccoli sprouts after 5-day growth were higher than those in their seeds (25). These results were consistent with ours. Significant changes in phenolic composition and antioxidant activity were found in the 17 edible seeds and sprouts, the reason might be associated with the initiation of endogenous enzymes and complicated biochemical metabolism (17). However, some samples with higher TPC have lower antioxidant capacity, this could be explained by the fact that some other compounds in extracts influence the responses of the FRAP, ABTS, and DPPH reagents, and this similar results was observed in previous studies (15, 25).

The TPC and DPPH values of 6-day-old alfalfa sprouts were lower than their seeds (26), we also found a similar result in the study. However, the TPC, DPPH, and ABTS values of alfalfa and sunflower seeds were higher than those in their sprouts, indicating that germination might cause a slight reduction of phenolics in some cases. Phenolic compounds are easily to lose while soaking of seeds since they are slightly soluble in water. In addition, they may also be utilized as precursors of cell walls, hormones, and other control substances during growing (19, 27).

In a previous study, the TPC and ABTS of radish both in 5-day old sprouts were higher than those in broccoli and sunflower

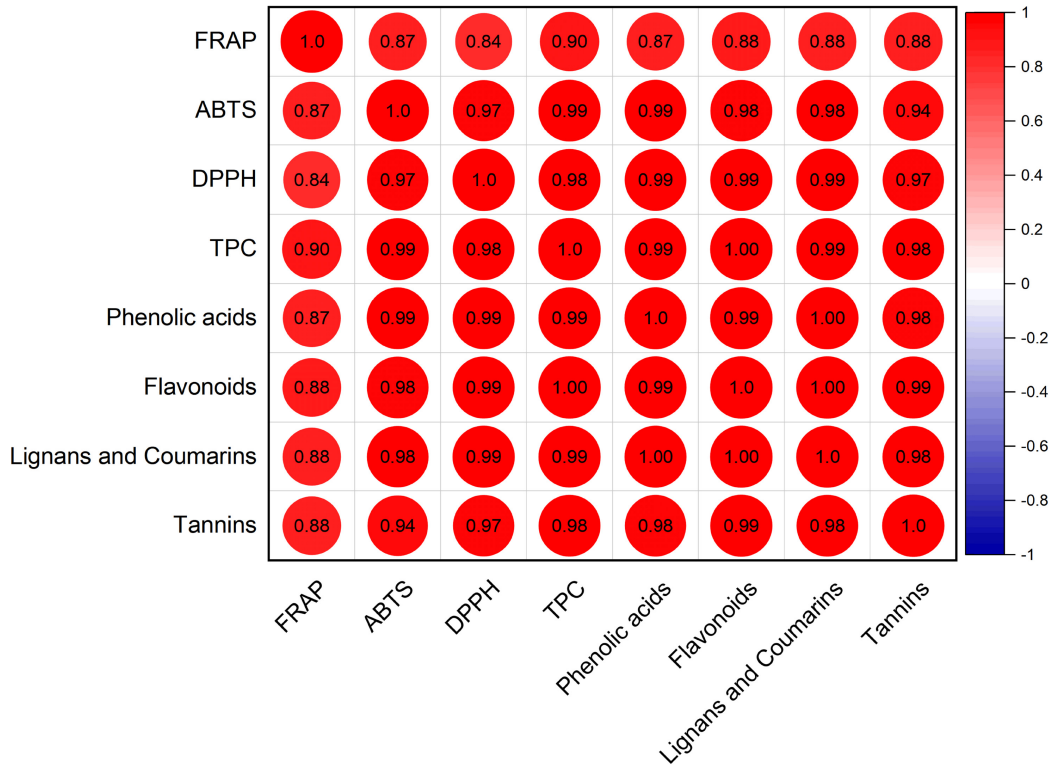

FIGURE 6
Correlation analysis among antioxidant capacity, TPC, and phenolic profiles.

sprouts (25), The TPC (dry mass) in radish seed was higher than those in broccoli, followed by sunflower, sunflower, alfalfa, and wheat (22, 25). The DPPH, FRAP, and ABTS of lentil seed were higher than those in pea (white) (28). Meanwhile, the TPC and antioxidant capacity of barely were reported to be higher than those in wheat or rye (29), these results were consistent with ours. We also found that the TPC and antioxidant capacity of radish were highest among all the samples, this indicated that the white radish accumulated more phenolic contents than other kinds of seeds during germination, probably due to the higher activity of enzymes for phenolic synthesis in the radish sprout (3).

According to the result of phenolic metabolomics, all four classes of phenolic profiles were significant differences between seed and sprout, and most phenolic compounds were significantly enhanced after germination. Phenolic acids (both free and bound) and flavonoids were the main phenolic profiles in radish seed and sprout, which was consistent with previous results (25). By comparing the top 20 compounds with the largest VIP values in the OPLS-DA model, and the top 20 phenolic compounds with the largest FC, the procyanidin A6 (belong to tannins), glucose (belong to phenolic acids), luteolin (belong to flavonoids) and glucoside (belong to flavonoids) were the most different compounds. According to a previous study, the phenolics, ascorbic acid, flavonoids, and glucosinolates were the major compounds in *Brassicaceae* sprouts such as radish (25, 30, 31). Meanwhile, many pathways were significantly activated, including phenylpropanoid, favone, and flavonol, phenylalanine, and various secondary metabolites. Among them, the phenylpropanoid biosynthesis pathway was reported as a key pathway associated with the production of phenolic acids, lignins, tannins, etc. (32).

The correlation coefficient between antioxidant activity (FRAP, ABTS, and DPPH) and TPC were 0.90, 0.99, and 0.98 for extracts originated from seeds and sprouts. A previous study showed that the antioxidant activity evaluated by FRAP assays was significantly correlated with the TPC ($r = 0.773$) and bound phenolic acids ($r = 0.874$) (25). Our study also showed that significant correlations were found between antioxidant activity and phenolic classes (phenolic acids, flavonoids, lignans and coumarins, and tannins ($P < 0.05$). The TPC, phenolic acids, flavonoids, lignans and coumarins, and tannins also showed significant positive correlations with antioxidant activity in DPPH and ABTS assays ($P < 0.05$). It was previously known that flavonoids were potent antioxidants. Therefore, increased relative amounts of flavonoids and their aglycon may be associated with increased total antioxidant activity (16, 33). Additionally, phenolic acids, which are commonly present in plant cell walls as an integrated component

with polysaccharides, also shown antioxidant activity (34, 35). The glycoside compounds in phenolic acids also could protect the oxidative damage and antioxidant effects (36). The findings above imply that phenolic compounds might be a reliable predictor of *in vitro* antioxidant activity in edible seeds and spouts.

Data availability statement

The original contributions presented in this study are included in the article/**Supplementary material**, further inquiries can be directed to the corresponding authors.

Author contributions

H-YL: conceptualization, methodology, and writing—original draft. YL: data curation. M-YL and X-QH: visualization and resources. Y-YG, FG, and YX: visualization and investigation. B-LG: conceptualization and data curation. R-YG: writing—review and editing, supervision, and funding acquisition. All authors contributed to the article and approved the submitted version.

Funding

This work was supported by the Agricultural Science and Technology Innovation Program (ASTIP- IUA-2022007), the Local Financial Funds of National Agricultural Science and Technology Center, Chengdu (NASC2020KR02 and NASC2021KR08), the Sichuan Science and Technology Program (2021JDRC0141), and the Key Laboratory of Agro-Products Processing and Storage Open Project (S2022KFKT-02).

Conflict of interest

The authors declare that the research was conducted in the absence of any commercial or financial relationships that could be construed as a potential conflict of interest.

Publisher's note

All claims expressed in this article are solely those of the authors and do not necessarily represent those of their affiliated organizations, or those of the publisher, the editors and the reviewers. Any product that may be evaluated in this article, or claim that may be made by its manufacturer, is not guaranteed or endorsed by the publisher.

Supplementary material

The Supplementary Material for this article can be found online at: https://www.frontiersin.org/articles/10.3389/fnut.2022.1067597/full#supplementary-material

References

1. Koeduka T, Sugimoto K, Watanabe B, Someya N, Kawanishi D, Gotoh T, et al. Bioactivity of natural O-prenylated phenylpropenes from *Illicium Anisatum* leaves and their derivatives against spider mites and fungal pathogens. *Plant Biol.* (2014) 16:451–6. doi: 10.1111/plb.12054

2. Gan RY, Chan CL, Yang QQ, Li HB, Zhang D, Ge YY, et al. Bioactive compounds and beneficial functions of sprouted grains. *Sprouted Grains.* (2019) 10:191–246. doi: 10.1016/B978-0-12-811525-1.00009-9

3. Gan RY, Wang MF, Lui WY, Wu K, Corke H. Dynamic changes in phytochemical composition and antioxidant capacity in green and black mung bean (*Vigna radiata*) sprouts. *Int J Food Sci Technol.* (2016) 51:2090–8. doi: 10.1111/ijfs.13185

4. Gharachorloo M, Tarzi BG, Baharinia M. The effect of germination on phenolic compounds and antioxidant activity of pulses. *J Am Oil Chem Soc.* (2013) 90:407–11. doi: 10.1007/s11746-012-2170-3

5. Li H, Xia Y, Liu HY, Guo H, He XQ, Liu Y, et al. Nutritional values, beneficial effects, and food applications of broccoli (*Brassica oleracea* var. Italica Plenck). *Trends Food Sci Technol.* (2022) 119:288–308. doi: 10.1016/j.tifs.2021.12.015

6. Li H, Zou L, Li XY, Wu DT, Liu HY, Li HB, et al. Adzuki bean (*Vigna angularis*): chemical compositions, physicochemical properties, health benefits, and food applications. *Compr Rev Food Sci Food Saf.* (2022) 21:2335–62. doi: 10.1111/1541-4337.12945

7. Finnie S, Brovelli V, Nelson D. *Sprouted Grains as a Food Ingredient Sprouted Grains*. Amsterdam: Elsevier (2019). doi: 10.1016/B978-0-12-811525-1.00006-3

8. Gawlik-Dziki U, Dziki D, Pietrzak W, Nowak R. Phenolic acids prolife and antioxidant properties of bread enriched with sprouted wheat flour. *J Food Biochem.* (2017) 41:e12386. doi: 10.1111/jfbc.12386

9. Gan RY, Lui WY, Wu K, Chan CL, Dai SH, Sui ZQ, et al. Bioactive compounds and bioactivities of germinated edible seeds and sprouts: an updated review. *Trends Food Sci Technol.* (2017) 59:1–14. doi: 10.1016/j.tifs.2016.11.010

10. Le TN, Luong HQ, Li HP, Chiu CH, Hsieh PC. Broccoli (*Brassica oleracea* L. var. italica) sprouts as the potential food source for bioactive properties: a comprehensive study on *in vitro* disease models. *Foods.* (2019) 8:532. doi: 10.3390/foods8110532

11. Ampofo JO, Ngadi M. Ultrasonic assisted phenolic elicitation and antioxidant potential of common bean (*Phaseolus vulgaris*) sprouts. *Ultrason Sonochem.* (2020) 64:104974. doi: 10.1016/j.ultsonch.2020.104974

12. Michalczyk M, Fiutak G, Tarko T. Effect of hot water treatment of seeds on quality indicators of alfalfa sprouts. *Lwt-Food Sci Technol.* (2019) 113:108270. doi: 10.1016/j.lwt.2019.108270

13. Oh MM, Rajashekar CB. Antioxidant content of edible sprouts: effects of environmental shocks. *J Sci Food Agric.* (2009) 89:2221–7. doi: 10.1002/jsfa.3711

14. Zhang XY, Bian ZH, Yuan XX, Chen X, Lu CG. A review on the effects of light-emitting diode (LED) light on the nutrients of sprouts and microgreens. *Trends Food Sci Technol.* (2020) 99:203–16. doi: 10.1016/j.tifs.2020.02.031

15. Liu HY, Liu Y, Mai YH, Guo H, He XQ, Xia Y, et al. Phenolic content, main flavonoids, and antioxidant capacity of instant sweet tea (*Lithocarpus litseifolius*

[Hance] Chun) prepared with different raw materials and drying methods. *Foods.* (2021) 10:1930. doi: 10.3390/foods10081930

16. Li W, Wen LC, Chen ZT, Zhang ZL, Pang XL, Deng ZC, et al. Study on metabolic variation in whole grains of four proso millet varieties reveals metabolites important for antioxidant properties and quality traits. *Food Chem.* (2021) 357:129791. doi: 10.1016/j.foodchem.2021.129791

17. Alvarez-Jubete L, Wijngaard H, Arendt EK, Gallagher E. Polyphenol composition and *in vitro* antioxidant activity of amaranth, quinoa buckwheat and wheat as affected by sprouting and baking. *Food Chem.* (2010) 119:770–8. doi: 10.1016/j.foodchem.2009.07.032

18. Pham VH, Hatcher DW, Barker W. Phenolic acid composition of sprouted wheats by ultra-performance liquid chromatography (UPLC) and their antioxidant activities. *Food Chem.* (2011) 126:1896–901. doi: 10.1016/j.foodchem.2010.12.015

19. Žilić S, Basić Z, Hadži-Tašković Šukalović V, Maksimović V, Janković M, Filipović M. Can the sprouting process applied to wheat improve the contents of vitamins and phenolic compounds and antioxidant capacity of the flour? *Int J Food Sci Technol.* (2014) 49:1040–7. doi: 10.1111/ijfs.12397

20. Ha KS, Jo SH, Mannam V, Kwon YI, Apostolidis E. Stimulation of phenolics, antioxidant and alpha-glucosidase inhibitory activities during barley (*Hordeum vulgare* L.) seed germination. *Plant Foods Hum Nutr.* (2016) 71:211–7. doi: 10.1007/s11130-016-0549-2

21. Hanlon PR, Barnes DM. Phytochemical composition and biological activity of 8 varieties of radish (*Raphanus sativus* L.) sprouts and mature taproots. *J Food Sci.* (2011) 76:C185–92. doi: 10.1111/j.1750-3841.2010.01972.x

22. Cevallos-Casals BA, Cisneros-Zevallos L. Impact of germination on phenolic content and antioxidant activity of 13 edible seed species. *Food Chem.* (2010) 119:1485–90. doi: 10.1016/j.foodchem.2009.09.030

23. Świeca M, Gawlik-Dziki U, Kowalczyk D, Złotek U. Impact of germination time and type of illumination on the antioxidant compounds and antioxidant capacity of *Lens culinaris* sprouts. *Sci Hortic-Amsterdam.* (2012) 140:87–95. doi: 10.1016/j.scienta.2012.04.005

24. Khang DT, Dung TN, Elzaawely AA, Xuan TD. Phenolic profiles and antioxidant activity of germinated legumes. *Foods.* (2016) 5:27. doi: 10.3390/foods5020027

25. Pajak P, Socha R, Galkowska D, Roznowski J, Fortuna T. Phenolic profile and antioxidant activity in selected seeds and sprouts. *Food Chem.* (2014) 143:300–6. doi: 10.1016/j.foodchem.2013.07.064

26. Ibrahim RS, Khairy A, Zaatout HH, Hammoda HM, Metwally AM, Salman AM. Chemometric evaluation of alfalfa sprouting impact on its metabolic profile using HPTLC fingerprint-efficacy relationship analysis modelled with partial least squares regression. *J Pharm Biomed Anal.* (2020) 179:112990. doi: 10.1016/j.jpba.2019.112990

27. Khandelwal S, Udipi SA, Ghugre P. Polyphenols and tannins in Indian pulses: effect of soaking, germination and pressure cooking. *Food Res Int.* (2010) 43:526–30. doi: 10.1016/j.foodres.2009.09.036

28. Marathe SA, Rajalakshmi V, Jamdar SN, Sharma A. Comparative study on antioxidant activity of different varieties of commonly consumed legumes in India. *Food Chem Toxicol.* (2011) 49:2005–12. doi: 10.1016/j.fct.2011.04.039

29. Zielinski H, Kozlowska H. Antioxidant Activity and Total Phenolics in Selected Cereal Grains and Their Different Morphological Fractions. *J Agric Food Chem.* (2000) 48:2008–16. doi: 10.1021/jf990619o

30. Lv XG, Meng GL, Li WN, Fan DD, Wang X, Espinoza-Pinochet CA, et al. Sulforaphane and its antioxidative effects in broccoli seeds and sprouts of different cultivars. *Food Chem.* (2020) 316:126216. doi: 10.1016/j.foodchem.2020.126216

31. Samec D, Pavlovic I, Redovnikovic IR, Salopek-Sondi B. Comparative analysis of phytochemicals and activity of endogenous enzymes associated with their stability, bioavailability and food quality in five Brassicaceae sprouts. *Food Chem.* (2018) 269:96–102. doi: 10.1016/j.foodchem.2018.06.133

32. Ramakrishna R, Sarkar D, Manduri A, Iyer SG, Shetty K. Improving phenolic bioactive-linked anti-hyperglycemic functions of dark germinated barley sprouts (*Hordeum vulgare* L.) using seed elicitation strategy. *J Food Sci Technol.* (2017) 54:3666–78. doi: 10.1007/s13197-017-2828-9

33. Ravishankar D, Rajora AK, Greco F, Osborn HMI. Flavonoids as prospective compounds for anti-cancer therapy. *Int J Biochem Cell Biol.* (2013) 45:2821–31. doi: 10.1016/j.biocel.2013.10.004

34. Guo H, Fu MX, Wu DT, Zhao YX, Li H, Li HB, et al. Structural characteristics of crude polysaccharides from 12 selected Chinese teas, and their antioxidant and anti-diabetic activities. *Antioxidants.* (2021) 10:1562. doi: 10.3390/antiox10101562

35. Rao RSP, Muralikrishna G. Non-Starch polysaccharide-phenolic acid complexes from native and germinated cereals and millet. *Food Chem.* (2004) 84:527–31. doi: 10.1016/S0308-8146(03)00274-7

36. Falcioni G, Fedeli D, Tiano L, Calzuola I, Mancinelli L, Marsili V, et al. Antioxidant activity of wheat sprouts extract *in vitro*: inhibition of DNA oxidative damage. *J Food Sci.* (2002) 67:2918–22. doi: 10.1111/j.1365-2621.2002.tb08838.x

frontiers | Frontiers in Nutrition

TYPE Original Research
PUBLISHED 10 January 2023
DOI 10.3389/fnut.2022.1081351

OPEN ACCESS

EDITED BY
Baoru Yang,
University of Turku, Finland

REVIEWED BY
Ding-Tao Wu,
Chengdu University, China
Min Wang,
Northwest A&F University, China

*CORRESPONDENCE
Lidong Wang
✉ wanglidong-521@163.com
Changyuan Wang
✉ byndwcy@163.com

SPECIALTY SECTION
This article was submitted to Nutrition and Food Science Technology, a section of the journal Frontiers in Nutrition

RECEIVED 27 October 2022
ACCEPTED 28 December 2022
PUBLISHED 10 January 2023

CITATION
Wang L, Li X, Gao F, Liu Y, Lang S and Wang C (2023) Effects of pretreatment with a combination of ultrasound and γ-aminobutyric acid on polyphenol metabolites and metabolic pathways in mung bean sprouts.
Front. Nutr. 9:1081351.
doi: 10.3389/fnut.2022.1081351

Effects of pretreatment with a combination of ultrasound and γ-aminobutyric acid on polyphenol metabolites and metabolic pathways in mung bean sprouts

Lidong Wang[1,2,3]*, Xiaoqiang Li[1], Fei Gao[1], Ying Liu[1], Shuangjing Lang[1] and Changyuan Wang[1]*

[1]College of Food Science, Heilongjiang Bayi Agricultural University, Daqing, China, [2]Daqing Center of Inspection and Testing for Agricultural Products and Processed Products Ministry of Agriculture and Rural Affairs, Heilongjiang Bayi Agricultural University, Daqing, China, [3]Department of National Coarse Cereals Engineering Research Center, Heilongjiang Bayi Agricultural University, Daqing, China

Background: Polyphenols play an important role in human nutrition, therefore, how to improve its content with innovative approach is important, and understanding the metabolic pathys is necessary. Mung beans are rich in polyphenols, which made them have physiological functions such as hypoglycemia, antioxidant, and hypotension. However, the content of polyphenols in natural mung bean is relatively low, and it needs to be increased. The methods of increasing polyphenol content in grains and beans by enrichment include physical stress, such as ultrasonic stress, hypoxia stress and ultraviolet radiation, and single exogenous substance stress, such as exogenous amino acids, exogenous sugars. But, the enrichment of polyphenols using exogenous substances in combination with physical stress is less applied. Therefore, this study innovated the use of exogenous γ-aminobutyric acid (GABA) combined with ultrasonic stress to enrich mung bean sprouts polyphenols and enhance their content. The metabolic pathways of the enrichment process were also analyzed to provide a reference for studies related to the enrichment of polyphenols.

Methods: Mung bean seeds were pretreated with a combination of ultrasound and GABA under different conditions. Single-factor test and response surface methodology were used for optimizing pretreatment conditions of mung bean. Effects of combined pretreatments on the polyphenols content and antioxidant activity of sprouted mung beans were investigated. Additionally, metabolites were identified, and metabolic pathways were analyzed using non-targeted metabolomics techniques.

Results: Optimal conditions of mung bean pretreatment were found to be 370 W for ultrasound power, 40 min for ultrasonication time, 10 mmol/L for GABA concentration, and 8 h for the soaking duration. Under these conditions, the predicted polyphenol content was found to be 4.52 mg GAE/g DW. The pretreatment of mung beans with a combination of ultrasound and exogenous GABA resulted in mung bean sprouts with enhanced polyphenol content and antioxidant activity compared to mung beans germinated without pretreatment. A significant increase in the content of six polyphenols [Genistein, (-)-Epigallocatechin, Epicatechin, Nobiletin, Naringenin, Biochanin A] in the pretreated and germinated mung beans was found, and six metabolic pathways (flavonoid biosynthesis, isoflavones biosynthesis, biosynthesis of phenylpropanoids, anthocyanin biosynthesis, biosynthesis of secondary metabolites, and metabolic pathways) were significantly activated.

Conclusion: The obtained results suggest that a combination of ultrasound and exogenous GABA treatment can be used to produce mung bean sprouts with enriched polyphenols content and enhanced antioxidant activity.

KEYWORDS

polyphenols, antioxidant capacity, untargeted metabolomics, differential metabolites, metabolic pathways

1. Introduction

Mung beans (*Vigna radiata*) are small and green seeds belong to the legume family with a wide range of food applications (1). According to Chinese medicine, mung beans are thought to help in the body's detoxification, reduction of skin irritation, and clearing of body heat (2). Mung beans are rich in essential nutrients such as protein and starch (3). Also, mung beans contain bioactive substances such as phenolic acids and flavonoids with potential health benefits (4).

People are being pushed toward a healthy diet by the rise in health problems. Mung beans and their sprouts have received increasing attention for their high nutritional value. Sprouting can significantly reduce antinutrients content of mung beans while the content of beneficial substances such as polyphenols and dietary fiber can be enhanced (5). Treatments with magnetic field (6), ultrasound (7), UV irradiation (8), vacuum stress (9), and exogenous amino acids (10) were found to enhance the content of bioactive compounds such as polyphenols of grain and seed sprouts. For example, the cavitation and thixotropic effects of low-intensity ultrasound can enhance the penetration of cell wall and cell membrane, enzymes activity, the rate of material exchange and metabolism inside and outside the cell, and the growth and development of plants (11). Besides, there is a relationship between γ-aminobutyric acid (GABA) and the antioxidant system of plants. The GABA has an important role in growth and stress tolerance, signaling activation, regulation of protein degradation, and hormone synthesis in plants, as well as phenolic enrichment (12). Many studies have reported. Effect of treatment with exogenous sucrose (13), plasma-activated water (14), UV-B treatment (15), NaCl and glucose (16), sodium citrate, sodium acetate and sodium tartrate (17), Ca^{2+} (18), polyamines (19), spermidineon (20) germination quality, and active substances of mung bean sprouts. Although effects of germination on the phenolics content of legumes have been extensively studied, research performed to investigate effect of a combination of pretreatments on the polyphenols content of legumes during germination and to understand underlying mechanisms are limited. To the best of our knowledge, no scholars have studied the combination of ultrasound and exogenous GABA treatment of mung beans or other grain beans on the content of active substances and metabolic pathways. This study aimed to investigate effects of treatment with a combination of ultrasound and GABA pretreatment on the polyphenols content of mung beans sprouts. Differential polyphenol metabolites and metabolic pathways were also analyzed and identified. Treatment conditions were optimized to produce mung bean sprouts with enriched polyphenols content and higher antioxidant activity.

Abbreviations: M, mung bean; CM48, mung bean control germinated for 48 h; M48, mung bean ultrasonic and GABA treatment germinated for 48 h; T-AOC, total antioxidant capacity; ABTS, 2,2-Azino-bis-3-etilbenzotiazolin-6-sulfonic acid; DPPH, 2,2-diphenyl-1-picrylhydrazyl; FF, free flavonoids; FP, free polyphenols; RSC, radical scavenging capacity; GABA, γ-aminobutyric acid.

2. Materials and methods

2.1. Materials

Total Antioxidant Kit, ABTS, 2,2-diphenyl-1-picrylhydrazyl (DPPH), potassium persulfate, ethanol, formic acid, ammonium formate, and acetonitrile (Sigma-Aldrich, Shanghai, China). Folin-ciocalteu reagent, rutin, sodium carbonate, aluminum chloride, sodium nitrite, γ-aminobutyric acid, gallic acid, and sodium hypochlorite (Shanghai Macklin Biochemical Technology Co., Ltd., Shanghai, China). Other chemicals and reagents were of analytical grade.

2.2. Germination of mung beans

Mung bean seeds were obtained from Beidahuang Grain Group Co., Ltd. Seeds (50.00 g) with granular shapes and uniform sizes were chosen for the study. Surface of the mung bean seeds was disinfected by immersion in 0.5% (v/v) sodium hypochlorite solution for 15 min, and then rinsed three times with distilled water and drained. The treated mung bean seeds were placed in a 250 mL beaker, and GABA solution was added at a seed/liquid ratio of 1:3 (w/v). The samples were placed in an ultrasonic generator (KH-500GDV, Hechuang Ultrasonic Instrument Co., Ltd., Kunshan, China) at 20°C with a specific power for 40 min, and then transferred to a 30°C water bath. The soaked mung beans were placed in the germination tray and 500 mL of GABA solution was placed at the bottom of the germination tray, and the seeds were covered with two layers of gauze. The samples were placed in an incubator (ZXMP-R1230, Zhicheng Inc., Shanghai, China) at 30°C and a humidity of 75% for 48 h, and the GABA medium was replaced every 12 h. The mung bean sprouts were washed with distilled water to remove mucus, freeze-dried to constant weight, crushed three times, packaged in vacuum bags, and stored in a freezer at −80°C until use.

2.3. Single-factor experiment

A single-factor experiment was carried out to investigate the effects of ultrasound and GABA parameters on extraction efficiency and to determine a narrow range of different parameters. Four extraction parameters were studied, including GABA concentration (0, 5, 10, 15, and 20 mmol/L), GABA soaking time (2, 4, 6, 8 and 10 h), ultrasonic power (240, 280, 320, 360, and 400 W) and ultrasonic time (10, 20, 30, 40, and 50 min).

TABLE 1 Coded levels of independent variables.

Independent variables	Coded units	Coded levels		
		−1	0	1
GABA concentration (mmol/L)	X_1	5	10	15
Ultrasonic power (W)	X_2	320	360	400
Ultrasonic time (min)	X_3	10	30	50

2.4. Response surface optimization experiment

According to results of the single-factor experiment, three main variables (GABA concentration, ultrasonic power, and ultrasonic time) were chosen for the response surface optimization. Design Expert Software (version 8.0.6.1, Stat-Ease, Inc., Minneapolis, USA) was used to generate a Box-Behnken design and analyze the data. A 3-level, 3-factor Box-Behnken design was generated by the software, consisting of 17 experimental runs (21). Each variable was coded at three levels (−1, 0, 1). The experimental factors and levels are listed in **Table 1**.

2.5. SEM analysis

Ultrasonic treatment can effectively activate various enzymatic activities and accelerate the germination process. It promotes the decomposition of large molecules such as starch and protein into small molecule compounds. Scanning electron microscopy (SEM) was used to observe the changes of the apparent morphology after pretreatment germination. SEM analysis carried out as described by Wang (22). Powder particles morphology was analyzed using a SEM (S-3400N, Hitachi Limited, Tokyo, Japan) at magnification of ×5000.

2.6. Extraction of mung bean sprouts

Optimal conditions for extraction of sprouts using ethanol were chosen based on a preliminary study. A sample of 20.00 g mung bean sprout powder was weighed into a 1,000 mL conical flask with a stopper and connected with a water-cooling device. Aqueous ethanol solution (60%, v/v) was added at a solid-to-liquid ratio of 1:35 (w/v) and mixed well. The mixture was stirred at a temperature of 40°C for 2 h using a magnetic stirrer. The extract was obtained by vacuum filtration. Each sample was extracted three times in parallel and stored in a refrigerator at 4°C for determination of free polyphenols,

free flavonoids content, antioxidant activity, and untargeted metabolomics assays.

2.7. Determination of free polyphenols and free flavonoids

The free polyphenols content was determined by the Folin-ciocalteu method (23). A sample of 1.0 mL extract was pipetted into a test tube, 3.0 mL of Folin-ciocalteu reagent was added, shaken well, and allowed to stand for 30 s. Then, 6.0 mL of 12% Na_2CO_3 solution was added, the mixture shaken well, and diluted to 25 mL. The mixture was stored in the dark at 25°C for 2 h, and the absorbance was measured at a wavelength of 765 nm using a spectrophotometer (TU-1800 UV, Beijing general analytical instrument, Beijing, China). The standard curve equation of gallic acid was as follows: y = 0.15x + 0.059 (R^2 = 0.9997). The results were recorded as mg of gallic acid equivalents per g dry weight (mg GAE/g DW) of mung bean sprouts.

The content of free flavonoids was determined with rutin as a standard (24). A sample of 3.0 mL extract was put into a 10 mL graduated test tube, and 0.3 mL of 5% $NaNO_2$ was added. The mixture was shaken well and allowed to react in the dark for 6 min, and 0.3 mL of 10% Al $(NO_3)_3$ was added, mixed well, and allowed to react in the dark again for 6 min. Finally, 4 mL of 4% NaOH solution was added, and the mixture was diluted to 10 mL using 70% ethanol solution, mixed well, and allowed to react in the dark for 15 min. The absorbance was then measured at a wavelength of 510 nm. The standard curve equation of rutin was as follows: y = 11.817x + 0.0362 (R^2 = 0.9992) of mung bean Sprouts. The data were expressed as mg rutin equivalents per g dry weight (mg RE/g DW) of mung bean sprouts.

2.8. Antioxidant activity assays

2.8.1. Total antioxidant capacity

The total antioxidant capacity of mung bean sprouts extract was determined using a T-AOC kit. The absorbance was measured at 520 nm (TU-1800 UV, Beijing general analyical instrument, Beijing, China). The total antioxidant capacity was calculated as follows:

$$T - AOC = 0.01 \times \frac{OD_1 - OD_2}{30} \times \frac{V_1}{V_2} \quad (1)$$

Where OD_1 is the absorbance value of the sample to be tested. OD_2 is the absorbance value of the control sample. V_1 is the volume of the reaction solution. V_2 is the sampling amount.

2.8.2. DPPH radical scavenging capacity

A sample of 0.40 mL extract was mixed with 2.6 mL of DPPH in ethanol solution (0.1 mmol/L, w/v) and placed in the dark for 30 min. Then, the absorbance was measured at 517 nm using absolute ethanol as a blank (25). The DPPH radical scavenging capacity was calculated as follows:

$$RSC = \left(1 - \frac{A_1 - A_2}{A_0}\right) \times 100\% \quad (2)$$

Where A_1 is the absorbance of 400 μL sample extract and 2.6 mL DPPH solution. A_2 is the absorbance of 400 μL extract and 2.6 mL absolute ethanol. A_0 is the absorbance of 400 μL absolute ethanol and 2.6 mL DPPH solution Control absorbance value of the solution.

2.8.3. ABTS radical scavenging capacity

A sample of 0.1 g ABTS and 0.029 g potassium persulfate powder was dissolved in deionized water to make 100 mL of ABTS free radical stock solution. The prepared solution was stored in a refrigerator at 4°C for 12 h and then was diluted until the absorbance at 734 nm was 0.700 ± 0.020. A sample of 0.2 mL extract was put in a test tube and 5.8 mL of ABTS solution was added, mixed well, and the mixture was allowed to react in the dark for 6 min. Then, the absorbance was measured at 734 nm (26). The ABTS radical scavenging activity was calculated as follows:

$$RSC = \left(\frac{A_1 - A_2}{A_1}\right) \times 100\% \quad (3)$$

Where A_1 is the absorbance value of the blank control group. A_2 is the absorbance value of the sample solution measurement group.

2.9. Untargeted metabolomic analysis

Untargeted metabolomics was performed with reference to Gabriele's method (27). The extract was centrifuged at 12,000 rpm for 10 min at 4°C, and the supernatant was filtered through a 0.22 μm membrane. The LC analysis was performed on a Vanquish UHPLC System (Thermo Fisher Scientific, Waltham, USA). Chromatography was carried out with an ACQUITY UPLC® HSS T3 column (150 × 2.1 mm, 1.8 μm) (Waters, Milford, MA, USA). Chromatographic conditions were chromatographic column, a flow rate of 0.25 mL/min, column temperature of 40°C, and injection volume of 2 μL. In the positive ion mode, the mobile phases were 0.1% formic acid acetonitrile (C) and 0.1% formic acid water (D), and in negative ion mode, the mobile phases were acetonitrile (A) and 5 mM ammonium formate water (B) (28). Mass spectrometry conditions were as follows: Thermo Orbitrap Exploris 120 mass detector (Thermo Fisher Scientific, Waltham, USA), electrospray ionization source (ESI), and data were collected in positive and negative ion modes. The first-level full scan was performed with a resolution of 60,000, the first-level ion scanning range was m/z 100–1000, and the second-level fragmentation was performed by HCD. The collision voltage

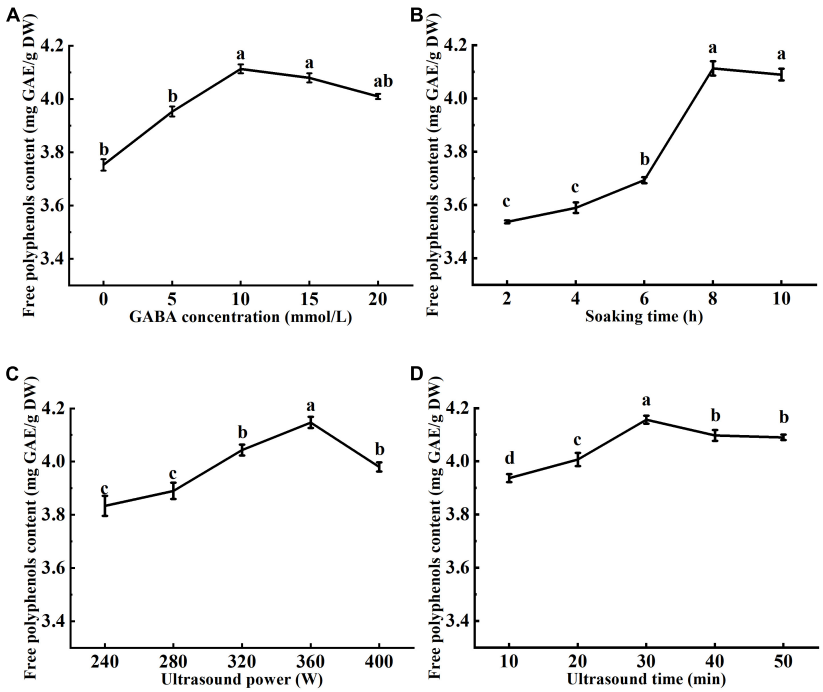

FIGURE 1
Effects of γ-aminobutyric acid (GABA) concentration **(A)**, soaking time **(B)**, ultrasonic power **(C)**, and ultrasonic time **(D)** on the free polyphenol content of mung bean. The GABA concentration, soaking time, ultrasonic power, and ultrasonic time were 10 mmol/L, 8 h, 360 W, and 30 min, respectively. Data are mean ± SD (n = 3). Different subscript letters indicate significant differences at $p < 0.05$.

was 30%, and the second-level resolution was 15,000. The first four ions were fragmented. At the same time, dynamic exclusion was used to remove unnecessary MS/MS information (29).

2.10. Statistical analysis

All experiments were carried out at least in triplicate, and the data were statistically analyzed and expressed as mean ± SD. Analysis of variance (ANOVA) and Duncan's multiple range test with a confidence interval of 95% was performed using SPSS 26 software (SPSS 26, International Business Machines Corporation, Armonk, New York, USA).

Data processing and multivariate analysis: The raw data were firstly converted to mzXML format by MSConvert in ProteoWizard software package (v3.0.8789) and processed using XCMS for feature detection, retention time correction, and alignment. The metabolites were identified by accuracy mass (<30 ppm) and MS/MS data which were matched with HMDB[1], massbank[2], LipidMaps[3], mzcloud[4], and KEGG[5]. Data were mean-centered using scaling. Models were built on principal component analysis (PCA), orthogonal partial least-square discriminant analysis (PLS-DA), and partial least-square discriminant analysis (OPLS-DA). P value < 0.05 and VIP values > 1 were considered to be statistically significant metabolites.

Pathway analysis: Differential metabolites were subjected to pathway analysis by MetaboAnalyst. The metabolites and corresponding pathways were visualized using KEGG Mapper tool.

3. Results

3.1. Single-factor analysis

Effects of ultrasound and GABA conditions, including GABA concentration, GABA soaking time, ultrasound power, and ultrasound treatment time on the free polyphenols content are shown in Figure 1. The free polyphenols content increased with the increase of GABA concentration up to 10 mmol/L (Figure 1A). At GABA concentration of 10 mmol/L, the highest free polyphenol content was 4.11 mg GAE/g DW. However, as the GABA concentration increased to 15 and 20 mmol/L, the free polyphenols content tended to decrease. It was reported that GABA as a signaling molecule binds

1 http://www.hmdb.ca
2 http://www.massbank.jp/
3 http://www.lipidmaps.org
4 https://www.mzcloud.org
5 http://www.genome.jp/kegg/

TABLE 2 Response surface design and free polyphenols content of the mung bean extracts.

Run	X_1 (mmol/L)	X_2 (W)	X_3 (min)	FP content (mg GAE/g DW)
1	0 (10)	0 (360)	0 (30)	4.59 ± 0.04
2	0 (10)	0 (360)	0 (30)	4.44 ± 0.06
3	−1 (5)	0 (360)	1 (50)	4.25 ± 0.03
4	−1 (5)	0 (360)	−1 (10)	4.15 ± 0.02
5	0 (10)	1 (400)	−1 (10)	4.23 ± 0.04
6	1 (15)	0 (360)	−1 (10)	4.19 ± 0.01
7	0 (10)	0 (360)	0 (30)	4.43 ± 0.06
8	0 (10)	0 (360)	0 (30)	4.54 ± 0.03
9	1 (15)	−1 (320)	0 (30)	4.22 ± 0.05
10	0 (10)	−1 (320)	−1 (10)	3.97 ± 0.02
11	0 (10)	1 (400)	1 (50)	4.36 ± 0.01
12	0 (10)	0 (360)	0 (30)	4.39 ± 0.06
13	1 (15)	0 (360)	1 (50)	4.48 ± 0.03
14	−1 (5)	−1 (320)	0 (30)	3.84 ± 0.01
15	−1 (5)	1 (400)	0 (30)	4.31 ± 0.05
16	1 (15)	1 (400)	0 (30)	4.13 ± 0.04
17	0 (10)	−1 (320)	1 (50)	4.13 ± 0.05

Box-Behnken design was used to optimize the conditions for enrichment of mung bean with polyphenols (Table 2), and a regression model was established as follows: three independent variables, including GABA concentration (X_1), ultrasonic power (X_2), and ultrasonic time (X_3), on the free polyphenol contents, are represented.

to glutamate receptors in plant cells (30). In this study, with the increase of GABA concentration, GABA bonded to the receptor to saturation, increasing the free polyphenols content. From Figure 1B, it can be seen the highest free polyphenol content was achieved when mung beans were soaked in GABA solution for 8 h. This may be attributed to that ultrasonic pretreatment caused changes in the structure of cell membranes, increasing GABA solution absorption capacity of the mung bean seeds, which reflected in increased free polyphenols content (31). When mung beans are soaked at appropriate temperature for enough time, the cell wall is soften, enhancing seed coat permeability, and releasing seed dormancy (32). GABA in solution penetrated the seeds and involved in the anabolism of polyphenols by activating related enzymes. However, the free polyphenol content decreased as soking prolonged to 10 h, which may be attributed to the loss of polyphenols and reduction of enzymes activity as soaking prolonged. A shorter soaking time is not enough to soften the seed coat and the embryonic axis is difficult to grow through the seed coat. Therefore, the soaking time of 8 h was chosen as optimal.

The cavitation of ultrasound produces tiny bubbles, which collapse at the mung bean seed coat, damaging the surface of the seed coat, and creating tiny holes. The seed coat is a physical barrier that prevents the seed from absorbing water and oxygen, which are necessary for seed germination. Therefore, increasing seed coat porosity may increase water and oxygen uptake and promote germination (33). It can be seen from Figure 1C that the free phenol content firstly increased then decreased with the increase of ultrasonic power. This may be explained by that the low ultrasonic power promoted hydration of the mung bean seeds and enhanced activity of polyphenol metabolic pathway enzymes (34, 35), accelerating synthesis of polyphenols and the release of bound phenolic compounds. Ultrasonication at 400 W resulted in a decrease in the polyphenol content. It may be attributed to mechanical damage and cavitation of high ultrasonic power, which resulted in structural breakage of mung bean seeds and loss of polyphenols. From Figure 1D, with the increase of sonication time, the free polyphenol content firstly increased reaching a maximum value at 30 min of ultrasonication, then tended to decrease. This may be explained by that ultrasonication for shorter time can effectively activate enzymes of polyphenol metabolic pathway and promotes the release of bound phenolics from the seed coat. However, the prolonged sonication produces damage to seed cells, reduces polyphenol synthesis, and enhance the loss of polyphenols in the soaking solution.

3.2. Response surface optimization

3.2.1. Effects of ultrasonic and GABA on the free polyphenols content

The response surface optimization design factor levels and results are shown in Tables 1, 2. Response surface results were analyzed with Design Expert 8 software, and the ANOVA results are shown in Table 3. The total model was highly significant ($p < 0.01$), the lack of fit was not significant ($p > 0.05$). The results showed that the polynomial has acceptable accuracy, it was possible to predict effects of GABA concentration, ultrasonic power, and ultrasonic time on the free polyphenol content of mung beans after germination. A significance test of the regression model showed that X_1, X_1^2, and X_2^2 had a significant effect on polyphenols content ($p < 0.05$), and X_2, X_3, X_1X_2, and X_3^2 had a highly significant effect on the polyphenols content ($p < 0.01$). However, effect of other factors was not significant. According the F value, effect of factors on the polyphenol content of mung bean sprouts was in the order ultrasound power > ultrasound time > GABA concentration.

$$Y = 4.48 + 0.059X_1 + 0.11X_2 + 0.085X_3 - 0.14X_1X_2 - 0.048X_1X_3 - 0.0075X_2X_3 - 0.13X_1^2 - 0.22X_2^2 - 0.081X_3^2.$$

TABLE 3 Analysis of variance (ANOVA) of response surface regression model.

Source	Sum of square	df	Mean square	*F*-value	Prob > *F*	Significance
Model	0.61	9	0.067	15.08	0.0009	**
X_1	0.028	1	0.028	6.18	0.0418	*
X_2	0.095	1	0.095	21.19	0.0025	**
X_3	0.058	1	0.058	12.95	0.0088	**
X_1X_2	0.08	1	0.078	17.56	0.0041	**
X_1X_3	0.009025	1	0.009025	2.02	0.1981	
X_2X_3	0.000225	1	0.0002250	0.050	0.8288	
X_1^2	0.070	1	0.070	15.69	0.0055	**
X_2^2	0.21	1	0.21	47.32	0.0002	**
X_3^2	0.028	1	0.028	6.26	0.0408	*
Residual	0.031	7	0.004465			
Lack of fit	0.00375	3	0.001125	0.16	0.9170	
Pure error	0.028	4	0.006970			
Corrected total	0.64	16				

*Significant ($p < 0.05$), **extremely significant ($p < 0.01$).

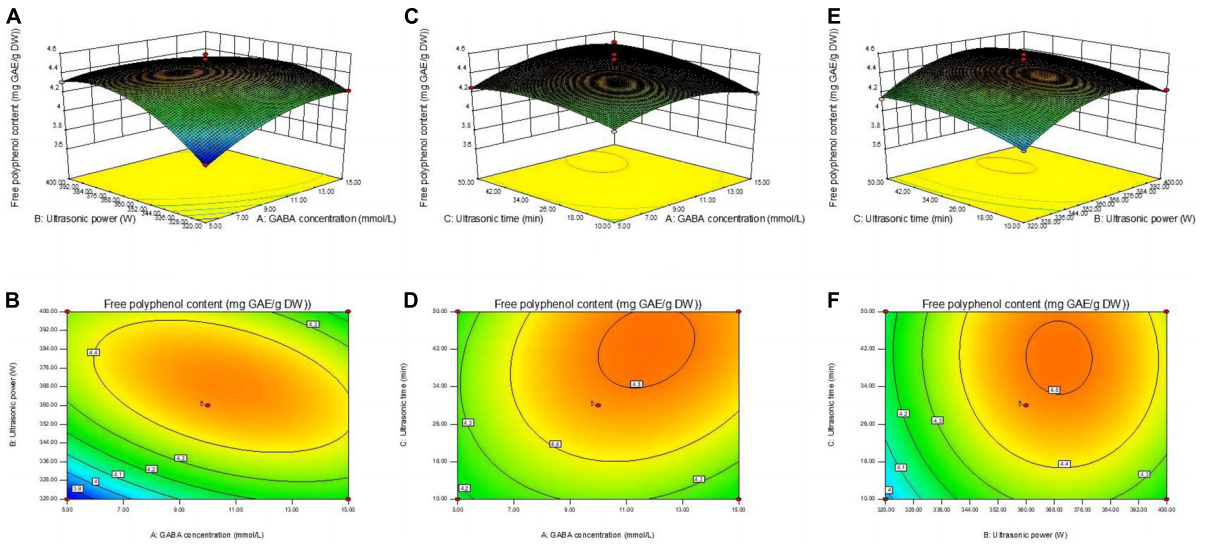

FIGURE 2
Contour lines and response surface diagrams of the interaction between X_1X_2 **(A,B)**, X_1X_3 **(C,D)**, and X_2X_3 **(E,F)**. (X_1) GABA concentration, (X_2) ultrasonic power, and (X_3) ultrasonic time.

3.2.2. Response surface interaction analysis

Analysis of the response surface map is based on a rational experimental design. Using the variability of the response surface and the sparsity of the contours, optimal process conditions can be determined while allowing visual evaluation of the interactions between factors. Changes in the response surface and contours in Figure 2 reflect the effect of interaction between GABA concentration (A) ultrasound power (B) and ultrasound time (C) on the free polyphenols content of germinated mung beans. The shape of the contour map reflects the interaction between various factors (13). When the contour is circular, this means that the interaction of the two factors is not significant, while elliptical or saddle-shaped contour indicates significant interaction between the two factors.

Figure 2 shows the response surface and contour plots for the interaction of AB (GABA concentration and ultrasound power), AC (GABA concentration and ultrasound time), and BC (ultrasound power and ultrasound time), where the AB

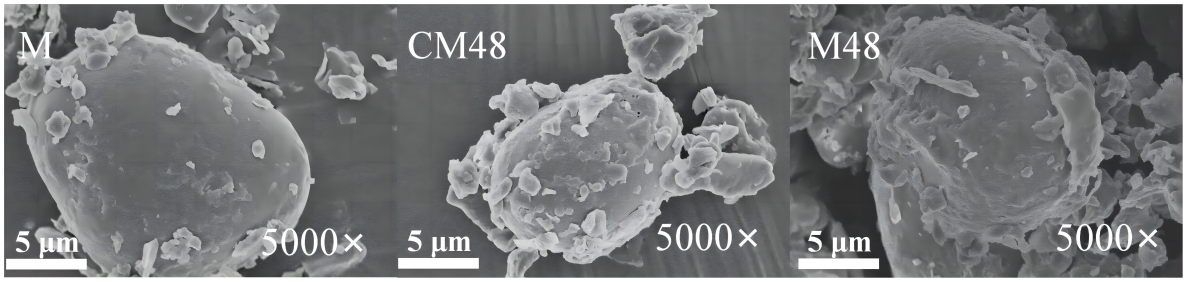

FIGURE 3
Scanning electron microscopy (SEM) images of the ungerminated and germinated mung beans. M, ungerminated mung bean; CM48, mung bean germinated for 48 h; M48, mung bean pretreated with a combination of ultrasonic and γ-aminobutyric acid (GABA) and germinated for 48 h.

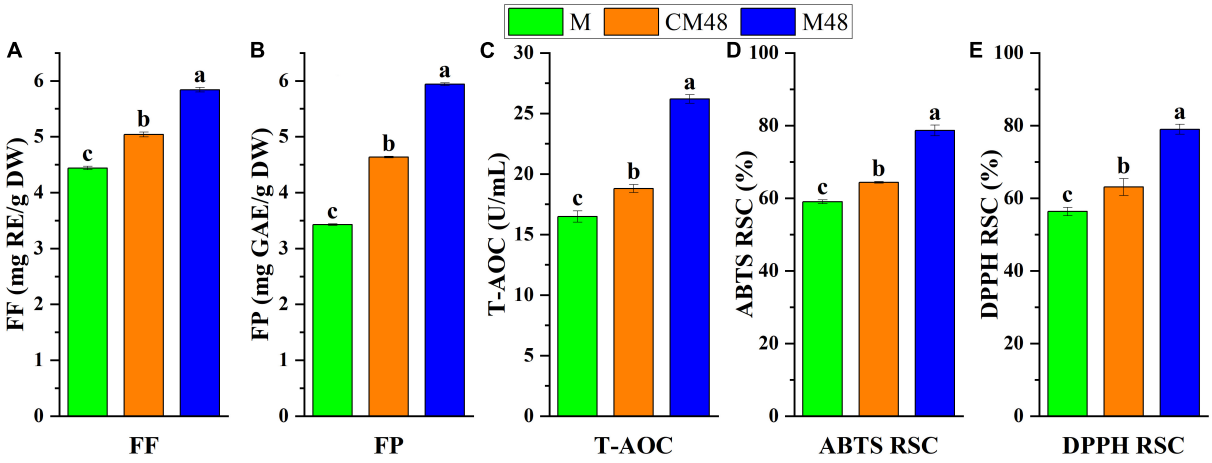

FIGURE 4
The free flavonoids content **(A)**, free polyphenols content **(B)**, and total antioxidant capacity **(C)**, ABTS radical scavenging activity **(D)**, and DPPH radical scavenging activity **(E)** of sprouted mung bean. M, mung bean; CM48, mung bean germinated for 48 h; M48, mung bean pretreated with a combination of ultrasonic and γ-aminobutyric acid (GABA) germinated for 48 h; FF, free flavonoids; FP, free polyphenols; T-AOC, total antioxidant capacity; ABTS, 2,2-Azino-bis-3-etilbenzotiazolin-6-sulfonic acid; DPPH, 2,2-diphenyl-1-picrylhydrazyl; RSC, radical scavenging capacity.

TABLE 4 Correlation analysis of free polyphenols (FP) and flavonoids (FF) content and antioxidant activity of mung bean sprouts.

Indicators	Flavonoid	Polyphenol	*T*-AOC	DPPH RSC	ABTS RSC
Flavonoid	1				
Polyphenol	0.998**	1			
T-AOC	0.993*	0.984*	1		
DPPH RSC	0.988*	0.978	0.999**	1	
ABTS RSC	0.962	0.946	0.988*	0.993*	1

*Significant ($p < 0.05$), **extremely significant ($p < 0.01$). *T*-AOC, total antioxidant capacity; ABTS, 2,2-Azino-bis-3-etilbenzotiazolin-6-sulfonic acid; DPPH, 2,2-diphenyl-1-picrylhydrazyl; RSC, radical scavenging capacity.

interaction was significant ($p < 0.05$, Table 2). The contour plots of AB are elliptical (Figures 2A, B), indicating a strong interaction between the relevant factors, while the contour plots of AC and BC are circular, indicating a relatively weak interaction between factors.

3.2.2. Determination and verification of optimal conditions

Process parameters were optimized using Design Expert 8 software. The optimal conditions for enrichment of mung bean sprout with polyphenols was obtained as follows: ultrasound power of 366.13 W, ultrasound time of 41.77 min, and GABA concentration of 11.27 mmol/L. The predicted polyphenols content was 4.52 mg GAE/g DW. As these parameters were not conducive to operation, parameters were adjusted to be ultrasound power 370 W, ultrasound time 40 min, and GABA concentration of 10 mmol/L. Validation tests were performed under these conditions (three times in parallel). Polyphenols content of 4.49 mg GAE/g was obtained for the mung bean sprouts, which was similar to the predicted value.

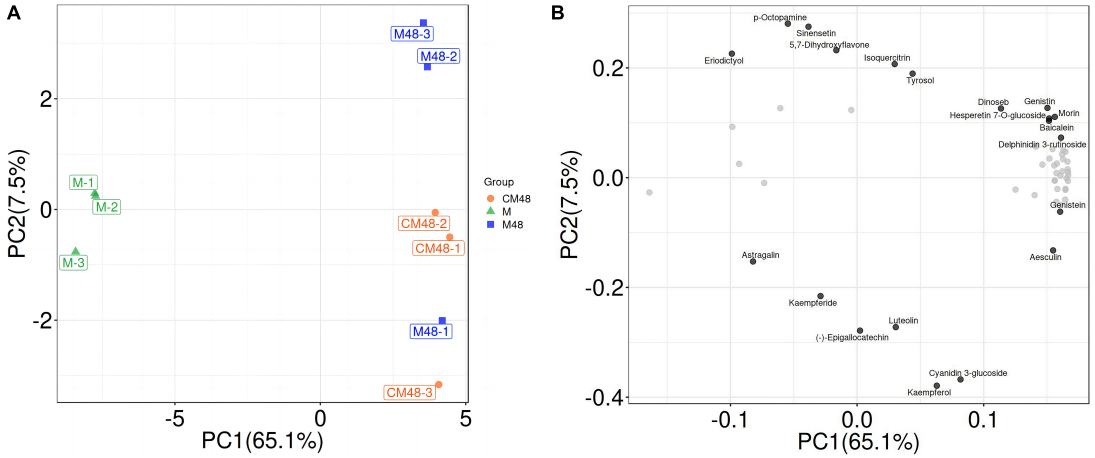

FIGURE 5
Untargeted metabolomics PCA score plot **(A)** and PCA-Loading plot **(B)**. M, ungerminated mung bean; CM48, mung bean germinated for 48 h; M48, mung bean pretreated with a combination of ultrasonic and γ-aminobutyric acid (GABA) and germinated for 48 h.

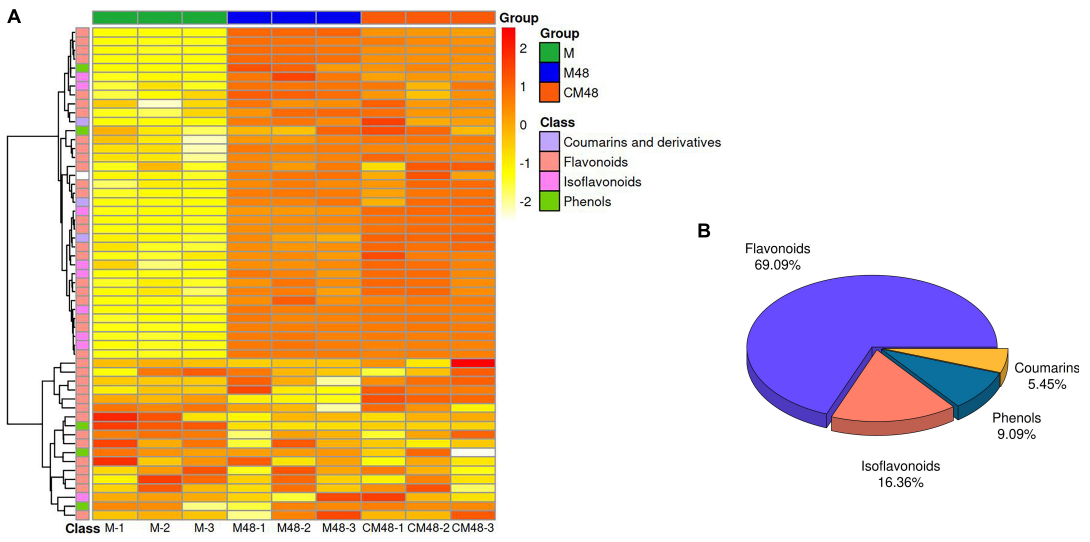

FIGURE 6
Polyphenol metabolites heat map **(A)** and component ratio chart **(B)** of mung bean sprouts. M, untreated mung bean; CM48, mung bean germinated for 48 h; M48, mung bean pretreated with ultrasonic and γ-aminobutyric acid (GABA) and germinated for 48 h.

This indicates that the optimized conditions for enrichment of mung bean sprout with polyphenols using response surface analysis are reliable.

3.3. Morphological structure of mung bean sprout powder

Surface morphology of mung bean sprouts powder is shown in Figure 3. It can be seen that surface of the untreated mung bean powder is smooth with a small number of attached fine particles. However, surface of the germinated mung bean powder is disrupted with scaly and lamellar structure. This may be attributed to damage and breakdown in surface of starch granules and protein during germination (36). Besides, the cavitation and mechanical effects of ultrasound treatment might contribute to changes in morphological structure of mung bean sprouts particles (37).

3.4. Free polyphenols, flavonoids content, and antioxidant activity

The free polyphenols and flavonoids content, total antioxidant capacity, ABTS free radical scavenging, and DPPH free radical scavenging activities of the ungerminated and

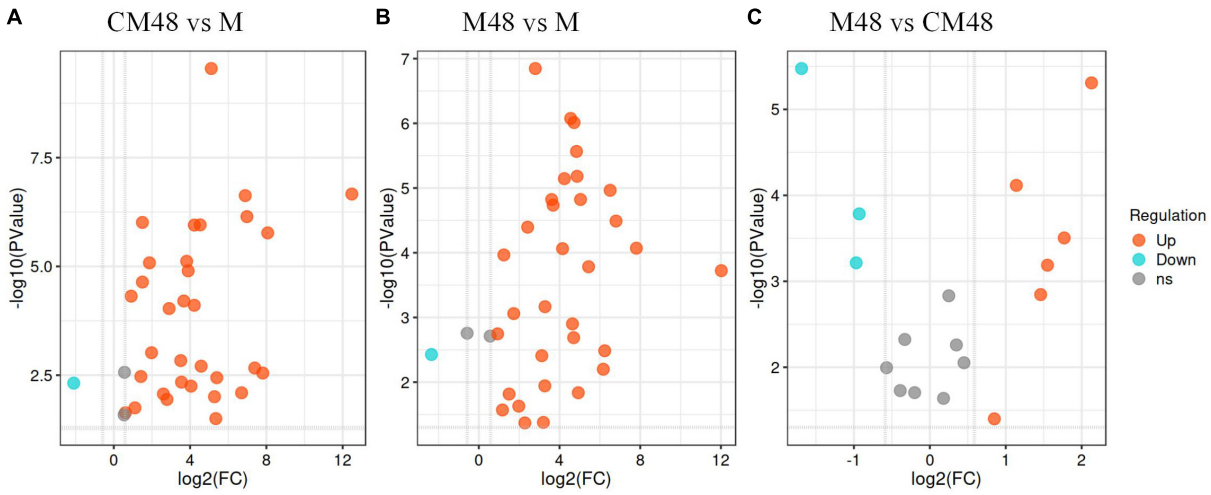

FIGURE 7
Volcano plot depicting up- and down- accumulated metabolites for each pairwise comparison. M, ungerminated mung bean; CM48 vs. M **(A)**, M48 vs. M **(B)**, and M48 vs. CM48 **(C)**; CM48, mung bean germinated for 48 h; M48, mung bean pretreated with a combination of ultrasonic and γ-aminobutyric acid (GABA) and germinated for 48 h.

germinated mung bean seeds are shown in Figures 4A–E. A combination treatment with ultrasound and GABA resulted in mung bean sprouts with enhanced free polyphenols and flavonoids contents compared to both the untreated mung bean seeds and seeds germinated without ultrasonic and GABA treatments.

Ultrasonic makes the seed shell fragment and accelerates the hydration process, leading to changes in the molecular structure and catalysis of enzymes, triggering the defense response system and enhancing the production of secondary metabolites such as polyphenols (38). Also, the cavitation and mechanical effects of ultrasonics enhance the permeability of cell membranes, promoting the diffusion and membrane transport of ions and metabolites (39). The exogenous GABA can pass through the cell membrane and enter the cell. Effect of GABA can be attributed to that it regulates the key enzyme genes of polyphenols synthesis, increasing protein expression and enzyme activity (40), stimulate hormone production, regulate growth and development, and further cause intracellular physiological and biochemical changes, regulating polyphenols metabolism pathway gene expression to achieve the enrichment effect. Therefore, the increase in polyphenols content of mung beans can be attributed to the combined effect of GABA, ultrasonic, and germination treatments.

The highest total antioxidant capacity, ABTS radical scavenging activity, and DPPH radical scavenging activity were found for mung bean subjected to a combination of GABA and ultrasound treatments and germinated for 48 h (Figures 3C–E). Polyphenolic compounds are natural antioxidants, therefore, the correlation between the free polyphenols and flavonoids content and antioxidant activities of the mung bean sprout extracts was analyzed. From Table 4, it can be seen that all correlation coefficients were above 0.946. The correlation between flavonoids and antioxidant capacity was higher. This is because the synthesis of flavonoids is downstream of the phenolic acid synthesis pathway and accumulates in larger quantities. These results indicate that the antioxidant activity is generally consistent with the polyphenols content, and the enhancement in antioxidant activity can be mainly attributed to the increase in antioxidants content such as polyphenols after GABA, ultrasound, and germination treatments of mung bean. Additionally, the antioxidant capabilities of mung beans may be influenced by the presence of vitamins such as vitamins E and C as well as other antioxidants (41). The contents of these substances increased by germination, enhancing the antioxidant capacity (42).

3.5. Differences in metabolites of mung bean sprouts

On the PCA score graph, the QC samples were clustered together, indicating that the results are highly reliable and reproducible, and the systematic error is within the controllable range (Figure 5). Different germination treatments were separated, and there was a clustering trend within the group. The analysis showed differences in metabolites of mung beans for different germination treatments. The untargeted metabolomics results also showed differences in the content and composition of polyphenols during the germination of mung beans treated by a combination of ultrasound with GABA. These differences are resulted from accumulation and metabolism of polyphenols metabolites during processing.

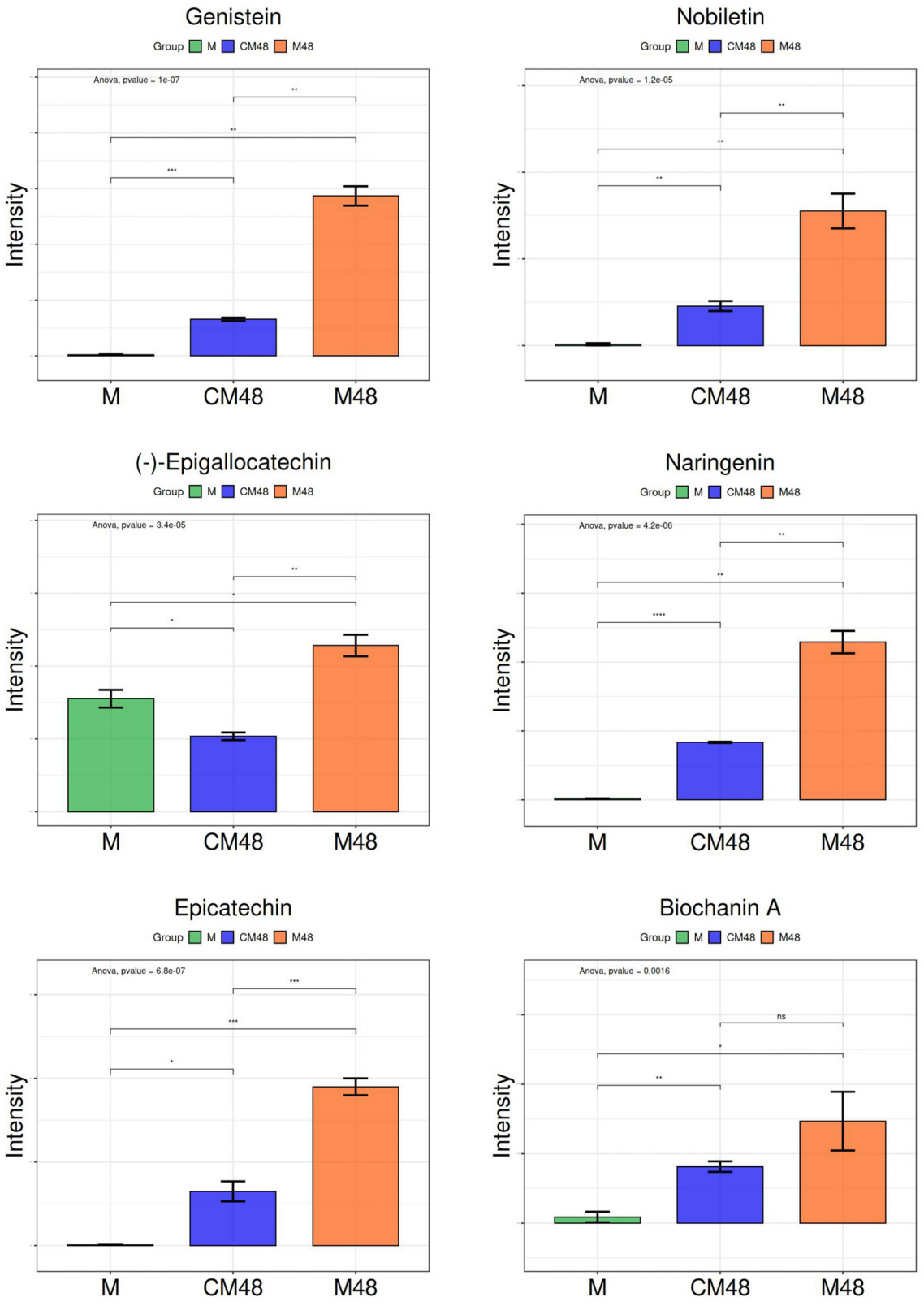

FIGURE 8
Changes in polyphenols of germinated mung beans. M, untreated mung bean; CM48, mung bean germinated for 48 h; M48, mung bean pretreated with a combination of ultrasonic and γ-aminobutyric acid (GABA) and germinated for 48 h.

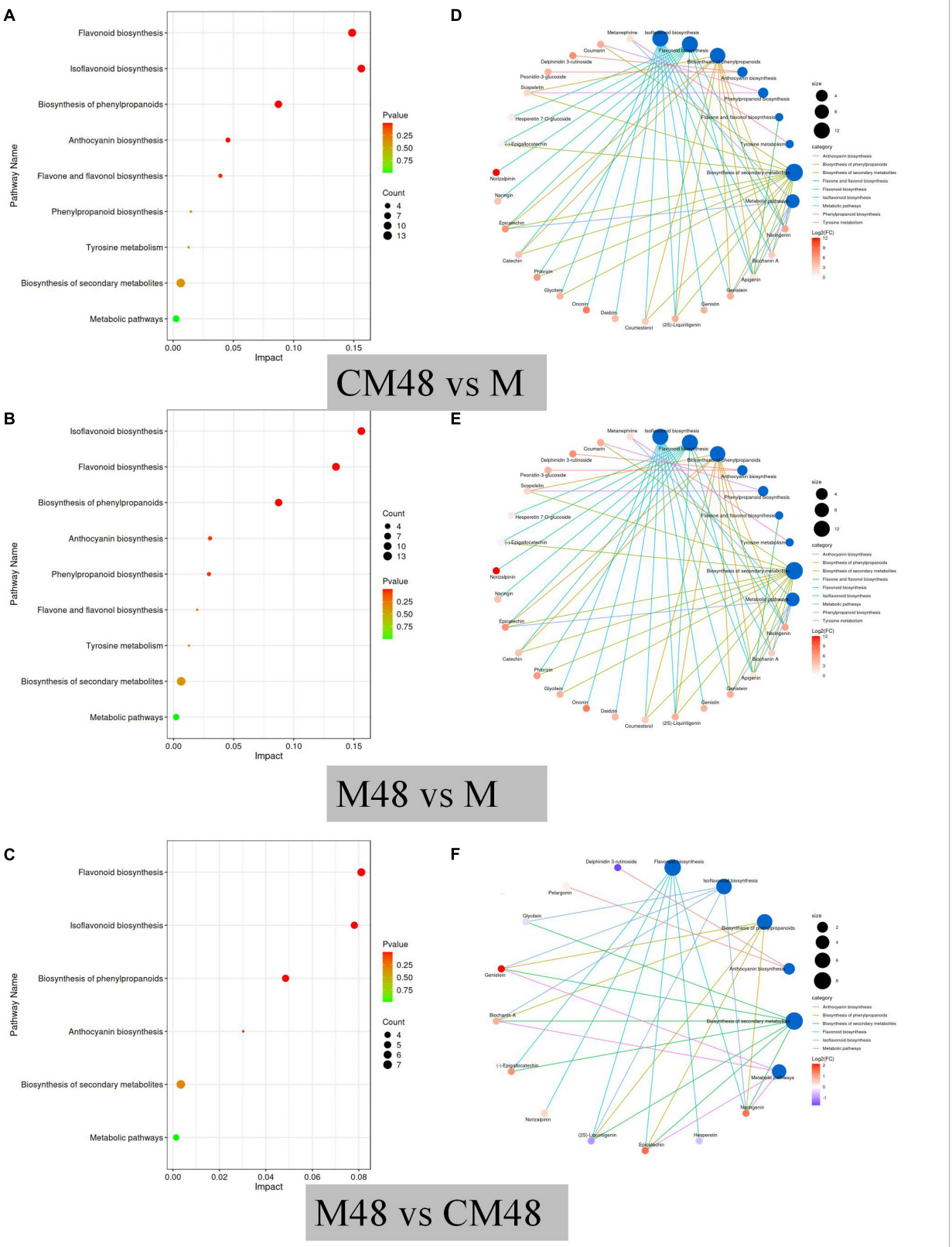

FIGURE 9
KEGG pathway enrichment of differential metabolites **(A–C)**, and network diagram of the distribution of differential metabolites in metabolic pathways **(D–F)**. M, ungerminated mung bean; CM48, mung bean germinated for 48 h; M48, mung bean pretreated with a combination of ultrasonic and γ-aminobutyric acid (GABA) and germinated for 48 h.

The ultrasonic pretreatment resulted in differences in the composition of metabolites in mung bean sprouts of different germination stages with exogenous GABA as a nutrient solution (**Figure 6**). About 55 polyphenolic metabolites were identified using non-targeted metabolomics techniques (**Figure 6A**). The identified polyphenol compounds can be divided into four categories, flavonoids, isoflavonoids, phenols, coumarins, and derivatives (**Figure 6B**).

Differential accumulation of polyphenolic compounds in mung beans treated with a combination of ultrasonic and GABA and germinated for 48 h (M48), mung bean germinated for 48 h without ultrasonic and GABA treatment (CM48), and untreated mung bean seeds (M), and the results are shown on a volcano plot (**Figure 7**). CM48 had 31 upregulated and 1 downregulated polyphenolic compound compared to M (**Figure 7A**). However, M48 showed 32 upregulated and 1 downregulated polyphenolic compound compared to M (**Figure 7B**). Additionally, M48 showed 6 upregulated [Genistein, (-)-Epigallocatechin, Epicatechin, Nobiletin, Naringenin, Biochanin A] and 3 downregulated [Delphinidin 3-rutinoside, Morin, (2S)-Liquiritigenin] polyphenolic compounds compared to CM48 (**Figure 7C**).

Figure 8 shows the relative content of six metabolites found in mung bean treated by a combination of ultrasound with GABA and germinated for 48 h. Genistein has been found to possess beneficial effects by inhibiting the migration of tongue cancer cells, preventing women's diseases and regulating intestinal health (43–45). (-)-Epigallocatechin and Epicatechin can be used as adjuvants in the treatment of hemostatic disorders caused by snake venom, and also have retinal and cardiovascular health effects (46–48). Nobiletin improves diabetic nephropathy, regulates platelet function, and reduces non-alcoholic fatty liver disease (49–51). Naringenin is an effective anti-cancer agent that reduces inflammation and allergic reactions (52, 53). Biochanin A can effectively lower blood lipids (54).

3.6. Metabolic pathway analysis

To explore the main metabolic pathways, differential polyphenol metabolites were annotated based on the KEGG database. The results showed that the main metabolic pathways of polyphenol metabolites in mung beans at different germination modes were isoflavones biosynthesis, flavonoid biosynthesis, biosynthesis of phenylpropanoids, anthocyanin biosynthesis, phenylpropanoid biosynthesis, flavone and flavonol biosynthesis, tyrosine metabolism, biosynthesis of secondary metabolites, and metabolic pathways (**Figures 9A, B**). The most important metabolic pathways were flavonoid biosynthesis, isoflavones biosynthesis, and biosynthesis of phenylpropanoids. Analysis of the differences in metabolic pathways between mung bean treated by a combination of ultrasound with GABA and germinated for 48 h and mung bean germinated without ultrasonic and GABA treatments (**Figure 9C**) revealed that six metabolic pathways were activated, including flavonoid biosynthesis, isoflavones biosynthesis, biosynthesis of phenylpropanoids, anthocyanin biosynthesis, biosynthesis of secondary metabolites, and metabolic pathways. **Figures 9D–F** shows distribution of the differential metabolites along the metabolic pathway between the different contrasts. From **Figures 9D, E**, it can be seen that both control germination and germination combined with ultrasound and GABA treatments were effective in activating polyphenol metabolic pathways. **Figure 9F** shows the differences in metabolic pathways between germination combined with ultrasound and GABA treatments and control germination groups, six metabolic pathways were enhanced after pretreatment. These findings suggest that pretreatment with a combination of ultrasound and exogenous GABA enhance the accumulation of polyphenols during mung bean germination.

4. Conclusion

Mung bean sprouts enriched with polyphenols were produced using a combination of ultrasound and exogenous GABA pretreatment. Ultrasound power of 370 W, ultrasound time of 40 min, and GABA concentration of 10 mmol/L were found to be optimal for pretreatment of mung bean seeds. The combined ultrasound and GABA pretreatment enhanced the content of free polyphenols and flavonoids and antioxidant capacity of the germinated mung beans compared to germination without pretreatment. Results of the untargeted metabolomic analysis indicated that a combination of ultrasound and exogenous GABA pretreatment significantly enhanced the content of six polyphenols in the germinated mung beans. The ultrasonic treatment at optimal power and time softened coat of mung bean seeds and enhanced the absorption of GABA solution. Besides, the cavitation effect of ultrasound produced tiny pores in the seed cell wall, which facilitated membrane transport of GABA. The GABA was involved in the flavonoids, isoflavones, and phenylpropanoids synthesis, and metabolic pathways. The appropriate intensity of ultrasound treatment enhanced the permeability of the cell wall and accelerated the transmembrane transport of GABA. GABA acted as an enzyme activator and promoted the metabolism of polyphenols. Further research is needed to investigate potential health benefits of the mung bean sprouts in animal models and human subjects.

Data availability statement

The original contributions presented in this study are publicly available. This data can be found here: https://figshare.com/articles/dataset/Untargeted_metabolic_data_xlsx/21431454/1.

Author contributions

LW and XL: conceptualization. SL and FG: methodology. XL: software and formal analysis. LW, XL, and FG: validation. XL, SL, and YL: investigation. CW and LW: resources and funding acquisition. SL and YL: data curation and visualization. XL and FG: writing—original draft preparation. LW and FG: writing—review and editing. LW: supervision and project administration. All authors read and agreed to the published version of the manuscript.

Funding

The authors gratefully acknowledged the financial support provided by the Natural Science Foundation of Heilongjiang Province (LH2020C087), the National Key Research and Development Program of China (2021YFD2100902), and the Major Science and Technology Projects of Heilongjiang Province (2021ZX12B0203 and 2021ZX12B06).

Conflict of interest

The authors declare that the research was conducted in the absence of any commercial or financial relationships that could be construed as a potential conflict of interest.

Publisher's note

All claims expressed in this article are solely those of the authors and do not necessarily represent those of their affiliated organizations, or those of the publisher, the editors and the reviewers. Any product that may be evaluated in this article, or claim that may be made by its manufacturer, is not guaranteed or endorsed by the publisher.

References

1. Qin L, Chen S, Xie L, Yu Q, Chen Y, Xie J. Recent advances in mung bean polysaccha-rides: extraction, physicochemical properties and biological activities. *Process Biochem.* (2022) 121:248–56. doi: 10.1016/j.procbio.2022.07.014

2. Li G, Wu Z, Bai W. Processing technology of compounded beverage by jujube and mung bean. *Food Sci.* (2007) 12:569–73. doi: 10.3321/j.issn:1002-6630.2007.12.136

3. Zhang L, Yu Y, Zhao Z, Yu R, Li Z, Zhang D. Separation and identification of metabolic mechanism in two cultivars of mung bean. *Food Sci.* (2021) 42:169–75. doi: 10.7506/spkx1002-6630-20200303-044

4. Chen R, Zhao J, Fan Z. Color and antioxidant activity of mung bean clear soup as affect-ed by boiling conditions. *Food Sci.* (2012) 33:115–20.

5. Qiu Y, Li L, Qian L, Li D, Fu L. Effecta of mung germination on its antioxidant ac-tivity. *Sci Technol Cereals Oils Foods.* (2021) 29:180–5. doi: 10.16210/j.cnki.1007-7561.2021.02.025

6. Shu L. *Effects of Magnetic Field Stree on Quality of Germinated Quinoa*. Jiangsu: Jiangnan University (2021). p. 36–9. doi: 10.27169/d.cnki.gwqgu.2021.000635

7. Hui X. *Study on the Mechanism of Mung Bean Seed Germination Promotion by Ultrasonic Radiation*. Shaanxi: Shaanxi Normal University (2017). p. 25–9.

8. Zhang D, Wang J, Zhang Y, Zhang H. Responses of ultraviolet radiation on seed ger-mination and physiological characteristics for seedlings of picea pungens englenan. *J Northwest Norm Univ.* (2021) 57:90–5. doi: 10.16783/j.cnki.nwnuz.2021.03.01510.16783/j.cnki.nwnuz.2021.03.015

9. Jiang X, Zhang G, Zhang D. Optimization of vacuum and germination treatment on γ-aminobutyric acid accumulation in pea. *Food Sci Technol.* (2020) 45:58–63. doi: 10.13684/j.cnki.spkj.2020.05.013

10. Yang H. Effects of exogenous amio acid on seeds germination and seedling growth of buckwheat under high temperature stress. *J Henan Agric Sci.* (2014) 43:20–3. doi: 10.15933/j.cnki.1004-3268.2014.11.006

11. Bai J. *Study on the Permeability of Plant Seed cell Membrane by Ultrasonic Radiation*. Shaanxi: Shaanxi Normal University (2014). p. 27–31.

12. Ding Y, Wang Y, Yao Y, Li W, Wang M, Wang P, et al. Effect of exog-enous γ-aminobutyric acid on the accumulation of phenolics and antioxidant capacity in germinated soybean. *Food Sci.* (2021) 42:72–8. doi: 10.7506/spkx1002-6630-20200614-189

13. Jaeeun Y, Hana L, Huijin H, Heon S, Jeehye S, Junsoo L. Sucrose-induced abiotic stress improves the phytochemical profiles and bioactivities of mung bean sprouts. *Food Chem.* (2023) 400:134069. doi: 10.1016/j.foodchem.2022.134069

14. Xiang Q, Liu X, Liu S, Ma Y, Xu C, Bai Y. Effect of plasma-activated water on microbial quality and physicochemical characteristics of mung bean sprouts. *Innov Food Sci Emerg Technol.* (2019) 52:49–56. doi: 10.1016/j.ifset.2018.11.012

15. Gui M, He H, Li Y, Chen X, Wang H, Wang T, et al. Effect of UV-B treatment during the growth process on the postharvest quality of mung bean sprouts (*Vigna radiata*). *Int J Food Sci Technol.* (2018) 53:2166–72. doi: 10.1111/ijfs.13804

16. Intira K. NaCl and glucose improve health-promoting properties in mung bean sprouts. *Sci Hortic.* (2019) 247:235–41. doi: 10.1016/j.scienta.2018.12.022

17. Jin X, Yang R, Guo L, Wang X, Yan X, Gu Z. iTRAQ analysis of low-phytate mung bean sprouts treated with sodium citrate, sodium acetate and sodium tartrate. *Food Chem.* (2017) 218:285–93. doi: 10.1016/j.foodchem.2016.09.029

18. Zhou T, Wang P, Yang R, Wang X, Gu Z. Ca2+ influxes and transmembrane transport are essential for phytic acid degradation in mung bean sprouts. *J Sci Food Agric.* (2018) 98:1968–76. doi: 10.1002/jsfa.8680

19. Zhou T, Wang P, Yang R, Gu Z. Polyamines regulating phytic acid degradation in mung bean sprouts. *J Sci Food Agric.* (2018) 98:3299–308. doi: 10.1002/jsfa.8833

20. Zhou T, Wang P, Gu Z, Ma M, Yang R. Spermidine improves antioxidant activity and energy metabolism in mung bean sprouts. *Food Chem.* (2020) 309:125759. doi: 10.1016/j.foodchem.2019.125759

21. Mai Y, Zhuang Q, Li Q, Du K, Wu D, Li H, et al. Ultra-sound-assisted extraction, identification, and quantification of antioxidants from 'Jinfeng' Kiwifruit. *Foods.* (2022) 11:827. doi: 10.3390/foods11060827

22. Wang L, Li X, Yu S, Liu S, Lang S. Understanding the changes in particle size, structure, and functional properties of waxy maize starch after jet-milling treatments. *J Food Process Eng.* (2021) 44:e13670. doi: 10.1111/jfpe.13670

23. Li J, Wang B. Folin-ciocalteu colorimetric determination of total polyphenols in mulberry fruits. *Food Sci.* (2009) 30:292–5.

24. Gao L, Li X. Study on microwave-assisted extraction and anti-oxidation activity of fla-vonoids from purple sweet potato. *J Zhe Jiang Univ.* (2009) 36:571–4. doi: 10.3785/j.issn.1008-9497.2009.05.02

25. Chen C, Chi-Tang H. Antioxidant properties of polyphenols extracted from green and black teas. *J Food Lipids.* (2010) 2:35–46.

26. Adom K, Liu R. Antioxidant activity of grains. *J Agric Food Chem.* (2002) 50:6182. doi: 10.1021/jf0205099

27. Gabriele R, Gianluca G, Matteo B, Adriano M, Marco T, Luigi L. Pigmented sorghum pol-yphenols as potential inhibitors of starch digestibility: an in vitro study combining starch digestion and untargeted metabolomics. *Food Chem.* (2020) 312:126077. doi: 10.1016/j.foodchem.2019.126077

28. Zelena E, Dunn W, Broadhurst D, Francis-Mcintyre S, Carroll K, Begley P. Develop-ment of a robust and repeatable uplc?ms method for the long-term metabolomic study of human serum. *Anal Chem.* (2009) 81:1357–64. doi: 10.1021/ac8019366

29. Want E, Masson P, Michopoulos F, Wilson I, Theodoridis G, Plumb R. Global metabolic profiling of animal and human tissues via uplc-ms. *Nat Protoc.* (2013) 8:17–32. doi: 10.1038/nprot.2012.135

30. Lacombe B, Becker D, Hedrich R. The identity of plant glutamate receptors. *Science.* (2001) 292:1486–7. doi: 10.1126/science.292.5521.1486b

31. Wang D, Dong X, Zhang X, Reb H. Effects of different soaking methods on water ab-sorption characteristics of mung bean. *Food Sci.* (2017) 38:83–9. doi: 10.7506/spkx1002-6630-201713014

32. Wang K, Yang S, Lin R, Liu B, Gao Y, Li X, et al. Optimization of processing technology and analysis of nutritional and functional components of mung bean sprouts. *Food Res Dev.* (2022) 13:155–63. doi: 10.12161/j.issn.1005-6521.2022.12.021

33. Ignacio L, Carlos M. Use of ultrasonication to increase germination rates of *Arabidopsis* seeds. *Plant Methods.* (2017) 13:31. doi: 10.1186/s13007-017-0182-6

34. Wen C, Zhang J, Zhang H, Duan Y, Ma H. Effects of divergent ultrasound pre-treatment on the structure of watermelon seed protein and the antioxidant activity of its hy-drolysates. *Food Chem.* (2019) 299:125165. doi: 10.1016/j.foodchem.2019.125165

35. Chiu K. Changes in microstructure, germination, sprout growth, phytochemical and mi-crobial quality of ultrasonication treated adzuki bean seeds. *Agronomy.* (2021) 11:1093. doi: 10.3390/agronomy1106 1093

36. Liu Y. *Effects of Sprouting on Structural and Physicochemical Properties of Macro Compo-nents From Mung Bean and Highland Barley and its Effects on Quality of Wheat Flour Noodie*. Shaanxi: Northwest A&F University (2019). p. 19–26. doi: 10.1007/s13197-018-3460-z

37. Ding J. *Effects of Hypoxic Stress and Ultrasonic Stimul on the γ-aminobutyric acid (GABA) Accumulation in Germinating Dehulled Rice and Metabolomic Mechanism*. Hubei: Huazhong Agricultural University (2016). p. 16–22. doi: 10.27158/d.cnki.ghznu.2016.000100

38. Miano A, Pereira J, Costa C, Augusto P. Enhancing mung bean hydration using the ultrasound technology: description of mechanisms and impact on its germination and main components. *Sci Rep.* (2016) 6:38996. doi: 10.1038/srep38996

39. Nobuki K, Kengo O, Katsuyuki Y. Sonoporation by single-shot pulsed ultrasound with microbubbles adjacent to cells. *Biophys J.* (2009) 96:4866–76. doi: 10.1016/j.bpj.2009.02.072

40. Zhao Y, Xie C, Wang P, Gu Z, Yang R. GABA regulates phenolics accumulation in soybean sprouts under NaCl stress. *Antioxidants.* (2021) 10:990. doi: 10.3390/antiox10060990

41. Dahiya P, Linnemann A, Boekel M, Khetarpaul N, Grewal R, Nout M. Mung bean: technological and nutritional potential. *Crit Rev Food Sci Nutr.* (2015) 55:670–88. doi: 10.1080/10408398.2012.671202

42. Małgorzata S, Michał Ş. Effect of ascorbic acid postharvest treatment on enzymatic brown-ing, phenolics and antioxidant capacity of stored mung bean sprouts. *Food Chem.* (2018) 239:1160. doi: 10.1016/j.foodchem.2017.07.067

43. Ardito F, Pellegrino M, Perrone D, Troiano G, Cocco A, Lo M. In vitro study on an-ti-cancer properties of genistein in tongue cancer. *Onco Targets Ther.* (2017) 10:5405–15. doi: 10.2147/ott.s133632

44. Yu L, Rios E, Castro L, Liu J, Yan Y, Dixon D. Genistein: dual role in women's health. *Nutrients.* (2021) 13:3048. doi: 10.3390/nu13093048

45. Kim B. Biological synthesis of genistein in *Escherichia coli*. *J Microbiol Biotechnol.* (2020) 30:770–6. doi: 10.4014/jmb.1911.11009

46. Pedro H, Marcus V, Isaac F, Silvana M. Catechin and epicatechin as an adjuvant in the therapy of hemostasis disorders induced by snake venoms. *J Biochem Mol Toxicol.* (2020) 34:e22604. doi: 10.1002/jbt.22604

47. Radina K, Ivan T. Effects of catechine and epicatechine on visual function and retinal perfu-sion. *Acta Ophthamol.* (2022) 100. doi: 10.1111/j.1755-3768.2022.231

48. Iveta B. Biological activities of (-)-epicatechin and (-)-epicatechin-containing foods: focus on cardiovascular and neuropsychological health. *Biotechnol Adv.* (2018) 36:666–81. doi: 10.1016/j.biotechadv.2018.01.009

49. Xu M, Wang R, Fan H, Ni Z. Nobiletin ameliorates streptozotocin-cadmium-induced diabetic nephropathy via NF-κB signalling pathway in rats. *Arch Physiol Biochem.* (2021):1–9. doi: 10.1080/13813455.2021.1959617

50. Sakthivel V, Harvey R, Marfoua S, Amanda J, Alexander R, Gagan D, et al. Pharma-cological actions of nobiletin in the modulation of platelet function. *Br Pharmacol Soc.* (2015) 172:4133–45. doi: 10.1111/bph.13191

51. Sarawoot B, Poungrat P, Putcharawipa M, Patoomporn P. Nobiletin alleviates high-fat di-et-induced nonalcoholic fatty liver disease by modulating AdipoR1 and gp91phox expres-sion in rats. *J Nutr Biochem.* (2021) 87:108526. doi: 10.1016/j.jnutbio.2020.108526

52. Abdur R, Mohammad A, Muhammad I, Kashif B, Gokhan Z. Comprehensive review on naringenin and naringin polyphenols as a potent anticancer agent. *Environ Sci Pollut Res.* (2022) 29:31025–41. doi: 10.1007/s11356-022-18754-6

53. Elvira E, Josep Q, Xavier G, Antoni B, Rosa M. In Vivo anti-inflammatory and antiallergic activity of pure naringenin, naringenin chalcone, and quercetin in mice. *J Nat Prod.* (2019) 82:177–82. doi: 10.1021/acs.jnatprod.8b00366

54. Xue Z, Zhang Q, Yu W, Wen H, Hou X, Li D, et al. Potential lipid-lowering mechanisms of biochanin A. *J Agric Food Chem.* (2017) 65:3842–50. doi: 10.1021/acs.jafc.7b00967

frontiers | Frontiers in Nutrition

TYPE Original Research
PUBLISHED 23 February 2023
DOI 10.3389/fnut.2023.1064662

OPEN ACCESS

EDITED BY
Yu Xiao,
Hunan Agricultural University, China

REVIEWED BY
Chong Xie,
Nanjing Agricultural University, China
Jie Yang,
Jiangsu Ocean Universiity, China
Donglu Fang,
Nanjing Forestry University, China

*CORRESPONDENCE
Yong Yang
✉ yangyong@hnucm.edu.cn
Kai He
✉ hekai69@126.com

SPECIALTY SECTION
This article was submitted to Nutrition and Food Science Technology, a section of the journal Frontiers in Nutrition

RECEIVED 08 October 2022
ACCEPTED 06 February 2023
PUBLISHED 23 February 2023

CITATION
Zheng H, Sun Y, Zheng T, Zeng Y, Fu L, Zhou T, Jia F, Xu Y, He K and Yang Y (2023) Effects of shear emulsifying/ball milling/autoclave modification on structure, physicochemical properties, phenolic compounds, and antioxidant capacity of lotus (*Nelumbo*) leaves dietary fiber. *Front. Nutr.* 10:1064662. doi: 10.3389/fnut.2023.1064662

Effects of shear emulsifying/ball milling/autoclave modification on structure, physicochemical properties, phenolic compounds, and antioxidant capacity of lotus (*Nelumbo*) leaves dietary fiber

Hui Zheng[1], Yan Sun[1], Tao Zheng[1], Yiqiong Zeng[1], Liping Fu[1], Tingting Zhou[1], Fan Jia[1], Yao Xu[1], Kai He[2]* and Yong Yang[1]*

[1]College of Pharmacy, Hunan University of Chinese Medicine, Changsha, China, [2]School of Pharmaceutical Science, Hunan University of Medicine, Huaihua, China

Lotus *(Nelumbo)* leaves are rich in polyphenols and dietary fiber, which have the potential as a high-quality fiber material in functional food. However, lotus leaves exhibit dense structure and poor taste, it is vital to develop appropriate modification methods to improve the properties of lotus leaves dietary fiber. In this study, the effects of three modification methods with shear emulsifying (SE), ball milling (BM), and autoclave treatment (AT) on structure, physicochemical properties, phenolic compounds, and antioxidant capacity of lotus leave dietary fiber (LDF) were evaluated. SEM indicated that there were significant differences in the microstructure of modified LDFs. FT-IR spectra and X-ray diffraction pattern of modified LDFs revealed similar shapes, while the peak intensity and crystalline region changed by modification. SE showed the greatest effect on crystallization index. SE-LDF had the highest water holding capacity, water swelling capacity, and bound phenolic content in LDFs, which increased by 15.69, 12.02, and 31.81%, respectively, compared with the unmodified LDF. BM exhibited the most dramatic effect on particle size. BM-LDF had the highest free phenolic and total phenolic contents in LDFs, which increased by 32.20 and 29.05% respectively, compared with the unmodified LDF. Phenolic compounds in LDFs were mainly free phenolic, and modifications altered the concents of flavonoids. The BM-LDF and SE-LDF exhibited higher antioxidant capacity than that of AT-LDF. Overall, SE-LDF showed better physical properties, and BM-LDF showed better bioactive components. SE and BM were considered to be appropriate modification methods to enhance the properties of LDF with their own advantages.

KEYWORDS

lotus (*Nelumbo*) leaves, dietary fiber, shear emulsifying, ball milling, physicochemical properties, phenolic compounds

1. Introduction

Dietary fibers mean carbohydrate polymers with 3 or more monomeric units, which are resistant to the endogenous digestive enzymes and thus neither hydrolyzed nor absorbed in the small intestine of humans (1). They have shown a positive impact on human health, such as reducing blood sugar and blood lipids, preventing obesity, and regulating intestinal flora (1, 2), therefore they have become a functional food raw material favored broadly by the consumer in recent years. Dietary fibers extracted from plants are often combined with natural plant polyphenols which show antioxidant activity (3), and which exhibit better functional characteristics for to human health than pure dietary fibers (4). These dietary fibers can be obtained from agricultural residue, and reasonable exploitation can greatly improve the added value of agricultural products, which has attracted the attention of researchers (5). However many dietary fibers in plant sources show disadvantages such as compact structure and poor taste, which lead to their low exploitation and utilization, it is necessary to modify dietary fibers in plant sources. Many studies have found that appropriate modifications, such as high pressure, high heat, shearing, extrusion and cellulase hydrolysis, can improve the positive impact of dietary fibers on human health by changing the structure, chemical components, physicochemical and functional properties (3, 6–8). Therefore, it is of great importance to select appropriate modification methods of dietary fibers, which is directly related to their exploitation value.

Shear emulsifying (SE) is based on the high-speed rotation rotor that creates a strong fluid shear force between the inner rotor and external stator, meanwhile the high rotational speed also produces intense laminar, turbulent and cavitation effects(9). These comprehensive effects change the structure, conformation and several properties of samples (6). SE has been widely used in the food industry for emulsification, dispersion, chemical reactions, cell disruption, deagglomeration, etc (9). Many studies have shown that SE can improve the extraction rate of soluble dietary fiber in raw materials, such as bamboo shoot fiber (10), defatted walnut flour (11) and akebia trifoliata koidz. seeds (12), while there are few studies on the application of shear emulsifying on insoluble dietary fiber. Our previous studies preliminarily showed that SE significantly enhanced the water-holding capacity and expansibility of insoluble dietary fiber compared with other fiber modification treatments, so SE may have its unique advantages in the modification of insoluble dietary fiber. Ball milling (BM) is a technique that uses mechanical as well as thermal effects to change the physical and chemical properties of raw materials (7), which has become a common fiber modification method in the food industry. The samples of planetary ball milling are mainly ground by the pressure, collision, and absorption between the grinding balls and the inner wall of the jar(s). The temperature may rise at the same time in this process, resulting in thermal effects (13). Due to these effects, BM can rapidly reduce the particle size of dietary fibers and modify the various properties of the material, such as asparagus leaf (3), grape pomace (13), soybean insoluble dietary fiber (14) and sea buckthorn insoluble dietary fiber (15). Autoclave treatment (AT) is a frequent method of food processing and sterilization. The combination of pressure treatment and thermal treatment can destroy the structure of macromolecules and lead to changes in functional properties, such as affecting the physical and chemical functions of fiber materials, affecting the dissolution rate of free polyphenols and antioxidant performance, which have been reported in many research reports, such as brewers' spent grain (8), whole grain oats (16), black bean (17), and waste orange peels (18).

Lotus (*Nelumbo*) originates in Asia and has seen cultivation for more than 3000 years as a food-stuff and a medicinal crop (19). The ancient literature of traditional Chinese medicine recorded lotus leaves can remove heart-fire and heart-heat, cool blood and arrest bleeding (20), and modern medical research has highlighted the promising health activities of lotus leaves including antioxidant activity, anti-diabetes, anti-obesity, anti-neurotic, anti-inflammation, anti-cancer, liver protection, etc (21, 22). Lotus *(Nelumbo)* leaves are rich in polyphenols compounds and dietary fiber (21), which meet the conditions as a source of high-quality dietary fibers. Therefore, lotus (*Nelumbo*) leaves dietary fiber (LDF) have a good exploitation potential which can be used as a high-fiber supplement in food processing. In recent years, there have been many studies on lotus *(Nelumbo)* leaves polyphenols (20, 22, 23), while the fiber components with large content in lotus *(Nelumbo)* leaves have hardly been reported. Due to the dense structure and poor taste of lotus *(Nelumbo)* leaves, it is vital to choose appropriate fiber modification methods to improve the exploitation value of lotus *(Nelumbo)* leaves. In this study, the effects of three modification methods with SE, BM, and AT on structure, physicochemical properties, phenolic compounds and antioxidant capacity of LDF were evaluated. The results of this research could providing an appropriate basis for further exploitation of LDF as a new high-quality fiber supplement in functional food.

2. Materials and methods

2.1. Materials

Dry lotus *(Nelumbo)* leaves was provided by Hunan Zhenxing Traditional Chinese Medicine Co., Ltd. (Changsha, Hunan, China). Cellulase (CAS 9012-54-8, S10041) was bought from Shanghai Yuanye Biotechnology Co., Ltd (Shanghai, China). Total dietary fiber assay kit (TDF-200A) was bought from Megazyme International Ireland Ltd (Bray, Ireland). Rutin, hyperoside, isoquercitrin, astragalin and quercetin were bought from Chengdu Aifa Biotechnology Co., Ltd (Chengdu, Sichuan, China). Catechin, myricetin and kaempferol were bought from Hefei Bome Biotechnology Co. Ltd (Hefei, Anhui, China). DPPH and ABTS were brought from Shanghai Maclean Biochemical Technology Co. Ltd (Shanghai, China). The rest of reagents were brought from Sinopharm Chemical Reagent Co., Ltd (Shanghai, China) and were analytical pure.

2.2. Modification treatment of lotus leaves powder

Dry lotus leaves, 4–7 cm long and 1–2 cm wide, were crushed with a pulverizer (FW-200, Beijing Zhongxing Weiye Instrument Co., Ltd, Beijing, China), and then passed through a 50-mesh sieve to obtain lotus leaves powder.

2.2.1. SE modification

Lotus leafes powder (30 g) was mixed with 750 mL distilled water, and was sheared at 8000 rpm for 30 min with a shear emulsifying (FM20-D, Shanghai Fluko Technology Development Co., Ltd., Shanghai, China). The mixture was centrifuged at 5000 rpm for 15 min to remove the supernatant. The SE modified lotus leaves powder was obtained by freeze-drying and sealed until use.

2.2.2. BM modification

Lotus leaves powder (50 g) was processed with a planetary ball mill (XQM-4, Changsha Tianchuang Powder Technology Co., Ltd, Changsha, Hunan, China), and mixed with 0.9 kilograms of zirconia balls in a 1-L vessel at 500 rpm for 30 min. The BM modified lotus leaves powder was obtained and sealed until use.

2.2.3. AT modification

Lotus leaves powder (250 g) was spread over a stainless steel dish, added 50 mL of distilled water and stirred well, and placed in a 4°C refrigerator for 3 h. Then the stainless steel dish was placed in an autoclave (LDZX-5DKBS, Shanghai Shen an Medical Instrument Factory, Shanghai, China) for 30 min at 121°C (0.10 MPa). The AT modified lotus leaves powder was obtained by freeze-drying and sealed until use.

2.3. Lotus leaves dietary fiber preparation

Lotus leaves powder (100 g) was mixed with 1500 mL of hydrochloric acid at the pH 4.0 with 2.50 g cellulase addition. The mixture was incubated at 50°C, 250 rpm for 2 h with vibration, and was centrifugated at 5000 rpm for 20 min to remove the supernatant. The precipitate was then gathered and dried by freeze-drying to obtain LDF. The lotus leaves powder, SE modified lotus leaves powder, BM modified lotus leaves powder and AT modified lotus leaves powder were extracted to obtain control (unmodified LDF), SE-LDF, BM-LDF and AT-LDF, respectively.

2.4. Structure

2.4.1. Scanning electron microscopy

The method was slightly modified according to Zhu et al. (15). The electron microscopy observation and photographing of sample was carried out using an SEM (EVO18, Carl Zeiss AG., Germany). Sample was loaded on a sample holder with double-sided conducting adhesive tapes, and coated with a gold layer. Subsequently, sample was observed at 10k × and 2k× magnification at 30.0 kv.

2.4.2. Fourier transform infrared spectroscopy

The method was slightly modified according to Jiang et al. (12). FTIR spectra of samples were analyzed with an FTIR spectroscopy instrument (Nicolet 380, Thermo Fisher Scientific Inc, USA). Sample (2 mg) was mixed with 200 mg of KBr and then pressed into one slice. FITR spectra was recorded in the full wavelength of 4000–400 cm^{-1}. The mixture was scanned for 32 times at a resolution of 4 cm^{-1}.

2.4.3. X-ray diffraction

XRD analysis of sample was carried out as described by Zheng et al. (24) and measured by an X-ray diffractometer (D8 Advance, Brooke AXS Co., Ltd., Germany). The determination was done at room temperature using Cu-Kα radiation source with a step size of 0.02°. The diffraction angle (2θ) was performed from 5 to 50° with a speed of 1°/min. The crystallinity index (CrI) of sample was calculated following equation.

$$CrI = \frac{I_{002} - I_{am}}{I_{002}} \times 100 \quad (1)$$

where I_{002} is the intensity of the 002 lattice diffraction at $2\theta = 22°$, and I_{am} is the intensity of diffraction at $2\theta = 18°$. I_{am} represents the amorphous region (amorphous cellulose, hemicellulose and lignin).

2.5. Physical and chemical analysis

2.5.1. Dietary fiber content determination

Soluble dietary fiber (SDF), insoluble dietary fiber (IDF) and total dietary fiber (TDF) of sample were measured according to AOAC 991.43 using a total dietary fiber assay kit.

2.5.2. Particle size determination

The method was slightly modified according to Chitrakar et al. (3). Particle size of sample was measured by a laser particle size analyzer (Bettersize2600E, Dandong Better Instrument Co., Ltd., Dandong, Liaoning, China). Distilled water was selected as the dispersant. D_{10}, D_{50}, and D_{90} are equivalent volume diameters determined at 10, 50, and 90% cumulative volume, respectively. A_{sf} represents specific surface areas of powder.

2.5.3. Water-holding capacity

The method was slightly modified according to Luo et al. (25). Sample (0.5 g) was well mixed with 10 mL of distilled water in a centrifuge tube at room temperature for 18 h. The supernatant was removed by centrifugation at 4000 rpm for 15 min, and the residue was immediately collected and weighted. WHC was calculated according to the following equation.

$$\mathbf{WHC(g/g)} = \frac{\mathbf{w_1 - w}}{\mathbf{w}} \quad (2)$$

Where w is the weight of dried sample (g), and w_1 is the weight of the residue (g) containing water.

2.5.4. Oil-holding capacity

The method was slightly modified according to Luo et al. (25). Sample (0.5 g) was well mixed with 10 mL of peanut oil in a centrifuge tube at room temperature for 18 h. The supernatant was

removed by centrifugation at 4000 rpm for 15 min, and the residue was immediately collected and weighted. OHC was calculated according to the following equation.

$$\mathbf{OHC(g/g)} = \frac{\mathbf{m_1 - m}}{\mathbf{m}} \quad (3)$$

Where m is the weight of dried sample (g), and m_1 is the weight of the residue (g) containing oil.

2.5.5. Water swelling capacity

The method was slightly modified according to Wang et al. (26). Sample (0.5 g) was placed in a test tube, 5 mL of water was added and it was hydrated for 18 h at 4°C. WSC was calculated according to the following equation.

$$\mathbf{WSC(mL/g)} = \frac{\mathbf{V_1 - V}}{\mathbf{m}} \quad (4)$$

Where V is the volume of dried sample (mL), V_1 is the volume of the hydrated sample (mL), and m is the weight of dried sample (g).

2.5.6. Color

The method was slightly modified according to Chen et al. (14). The color of sample was measured by a colorimeter analyzer (CS-820N, Hangzhou Caipu technology co., ltd., Hangzhou, Zhejiang, China). The color value was represented by the CEL L*, a*, b* values, where L* represents the brightness (0 is black, 100 is white); a* represents the redness and greenness (a* > 0, represents the degree of red; a* < 0 means green degree); b* means yellow and blue degree (b* > 0 means yellow degree, b* < 0 means blue degree). Color difference (ΔE) was calculated using the following equation. L_0, a_0, and b_0 represent the colors of control, which used for comparison.

$$\Delta\mathbf{E} = \sqrt{(\mathbf{L^* - L_0^*})^2 + (\mathbf{a^* - a_0^*})^2 + (\mathbf{b^* - b_0^*})^2} \quad (5)$$

2.6. Polyphenol extraction and determination

2.6.1. Extraction of phenolic compounds

Extraction of free phenolic (FP) was slightly modified according to Sameera et al. (27). Sample (1 g) was mixed with 25 mL of acetone/methanol/water (40:40:20, *v/v/v*). The mixture was placed in a shaking incubator at 40°C, at 250 rpm for 1 h and centrifuged at 5 000 rpm for 10 min. After three repeat extractions, the supernatants were pooled and the solvent was rotary evaporated in vacuo at 40°C to obtain FP extract. The solids remaining after the extraction was used for the extraction of bound phenolic (BP).

Extraction of BP was slightly modified according to Dong et al. (28). The solids remaining after the extraction of FP was mixed with 10 mL of 2 M sodium hydroxide. The mixture was placed in a shaking incubator at 250 rpm for 3 h at room temperature, then acidified with 6 M hydrochloric acid to pH 2 and centrifuged at 5000 rpm for 10 min. The supernatant was extracted with ethyl acetate, and the extraction was repeated three times. The ethyl acetate phase was collected, and the solvent was rotary evaporated in vacuo at 40°C to obtain BP extract.

2.6.2. Polyphenol content determination

Polyphenol contents of FP and BP extracts were determined using the Folin-Ciocalteu method according Tian et al. (29), with slight modifications. Extract solution (100 μL) was mixed with 7.9 mL of distilled water and 500 μL of Folin-Ciocalteu reagent, then after 5 min, 1.5 mL of sodium carbonate solution (20%, *w/v*) was added. After resting for 2 h at room temperature, in the dark, the absorbance at 765 nm was measured using a spectrophotometer (UV-1780, Suzhou Shimadzu Instrument Co., Ltd., Suzhou, Jiangsu, China). The result was expressed as mg of gallic acid (GA) equivalent in 1 g dry weight of sample (mg GA eq/g DW).

2.6.3. Flavonoids composition determination by HPLC

The method was slightly modified according to Chen et al. (19). The flavonoids composition in different samples was determined by HPLC (1260, Agilent Technologies Co. Ltd., USA) with a reversal phase column (XB-C18, Agilent Technologies Co. Ltd., USA). FP and BP extract solution were filtered through a 0.45 μm microporous membrane before injection. HPLC conditions: column temperature 30°C, detection wavelength 360 nm, injection volume 5 μL, flow rate 0.8 mL/min. The mobile phases were acetonitrile (A) and formic acid/water (0.1:99.9, *v/v*). The program of gradient elution: 0–10 min, 15% A; 10–25 min, 15–20% A; 25–40 min, 20–25% A; 40–55 min, 25–30% A; 55–60 min, 30–25% A; 60–70 min, 25–15% A.

2.7. Antioxidant capacity

2.7.1. DPPH free radical scavenging capacity

The method was slightly modified according to Ye et al. (30). FP and BP extract solution (100 μL) was mixed with 3.5 mL of DPPH solution (0.1 mmol/L in methanol) and left to stand for 20 min in the dark, then the absorbance was measured at 517 nm by a UV Visible Spectrophotometer (UV-1780, Suzhou Shimadzu Instrument Co., Ltd., Suzhou, Jiangsu, China). The result was expressed in micromoles of Trolox equivalent to 1 g dry weight of sample (μmol Trolox eq/g DW).

2.7.2. ABTS free radical scavening capacity

The method was slightly modified according to Wootton-Beard et al. (31). 7.0 mmol/L ABTS solution (400 mL) was mixed with 200 mL of 2.45 mmol/L potassium persulfate, and let stand for 12–16 h in the dark to form stable stock $ABTS^{+}\cdot$ solution. The $ABTS^{+}\cdot$ stock solution was diluted with deionized water to an absorbance of 0.70 ± 0.02 at 734 nm wavelength for later using. 50 μL of FP and BP extract solution was mixed with 4.9 mL of $ABTS^{+}\cdot$ solution and left to stand for 10 min in a dark environment at room temperature, then measured the absorbance at a wavelength of 734 nm by a UV Visible Spectrophotometer (UV-1780, Suzhou

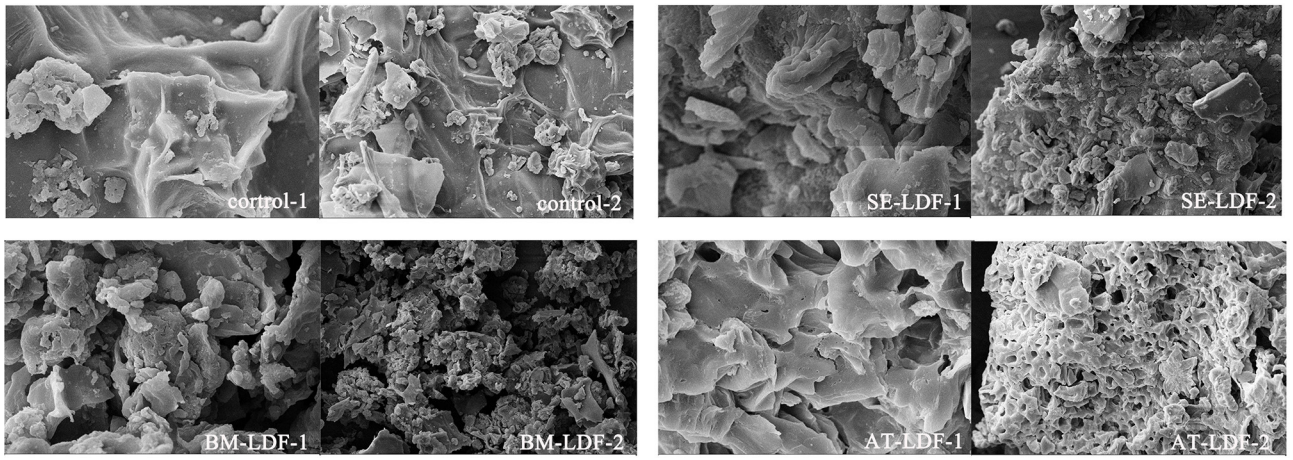

FIGURE 1
SEM images of control, SE-LDF, BM-LDF, and AT-LDF. Magnification: 1 (10 k ×), 2 (2 k ×). Control: lotus leaves dietary fiber. SE-LDF, shear emulsifying modified lotus leaves dietary fiber; BM-LDF, ball milling modified lotus leaves dietary fiber; AT-LDF, autoclave modified lotus leaves dietary fiber.

Shimadzu Instrument Co., Ltd., Suzhou, Jiangsu, China). The result was expressed in micromoles of Trolox equivalent to 1 g dry weight of sample (μmol Trolox eq/g DW).

2.8. Statistics analysis

All samples were prepared and analyzed in triplicate, and the experimental results are expressed as the mean ± standard deviation (Mean ± SD). The statiscal analyses were performed with IBM SPSS Statistics 23.0. One-way ANOVA was applied, followed by Duncan's multiple range test for mean comparisons and difference significance analysis ($p < 0.05$).

3. Results and discussion

3.1. Structural characterization

3.1.1. Scanning electron microscopy

The differences in many physicochemical properties of dietary fibers can be explained by the microstructure, such as dissolving out the capacity of functional components, adsorption capacity, water swelling capacity and powder fluidity, which can affect their applications in food (10). SEM images of the control, SE-LDF, BM-LDF and AT-LDF were shown in Figure 1. SEM images of all samples showed significantly different, except that there were some irregular clusters and spherical substances on the surface of samples, which were most likely the results of adsorbed small particle size fibers or residual bioactive compounds such as proteins and flavonoids (12).

The SEM of control showed that the fiber texture was clear and complete, and the surface was relatively flat and smooth without obvious holes and crakes. The surface of SE-LDF had a pronounced dendritic fibrous structure and few holes. This might be due to fluid shear stress and liquid layer friction forces of SE promoting particle breakage (9) and large porosity (10, 12), leading to more loose binding between components. With the removal of other components around the fiber bundle under fluid turbulence, the main structure of the fiber was preserved (32). In combination with the subsequent cellulase hydrolysis treatment, this pronounced dendritic fibrous structure and holes appeared on the surface of SE-LDF. According to the SEM of BM-LDF, the fiber texture and particle size of LDF were significantly changed by BM. Compared with other samples, the particle size was the smallest and more particles were aggregated with each other. This result might be attributed to the strong high collision, shear force and friction force caused by BM, which may severely destroy the glycosidic bond of the fiber and the hydrogen bond force between the molecules, resulting in particle breakage (7). Meanwhile, low particle size and high specific surface area leaded to an increase in the adsorption capacity of particles, making the irregular clusters and spherical substances on the surface of BM-LDF more than other samples (33). The SEM of AT-LDF exhibited a honeycomb type structure with relatively large regular holes, and relatively few irregular clusters and spherical substances on the surface. It has been reported that high heat treatment and high pressure treatment in AT can make the cellulose structure loose and expand, increase the holes, and destroy peptide bonds and glycosidic bonds, leading to transform insoluble components such as protein and polysaccharides into soluble forms (8, 18). In combination with the subsequent cellulase hydrolysis treatment, these soluble materials were removed (34) to form a honeycomb type structure with large relatively regular holes.

3.1.2. Fourier transform infrared spectroscopy

FT-IR spectra of control, SE-LDF, BM-LDF and AT-LDF were shown in Figure 2. All samples had similar characteristic spectra and typical functional groups of insoluble cellulose, which were similar to defatted walnut flour (11), grape pomace (13), okara (soybean residue) (14) and ginseng IDF (35). The broad absorption at 3287 cm^{-1} was mostly attributed to O-H stretching vibration in hydroxyl groups, which might be related to free hydroxyl

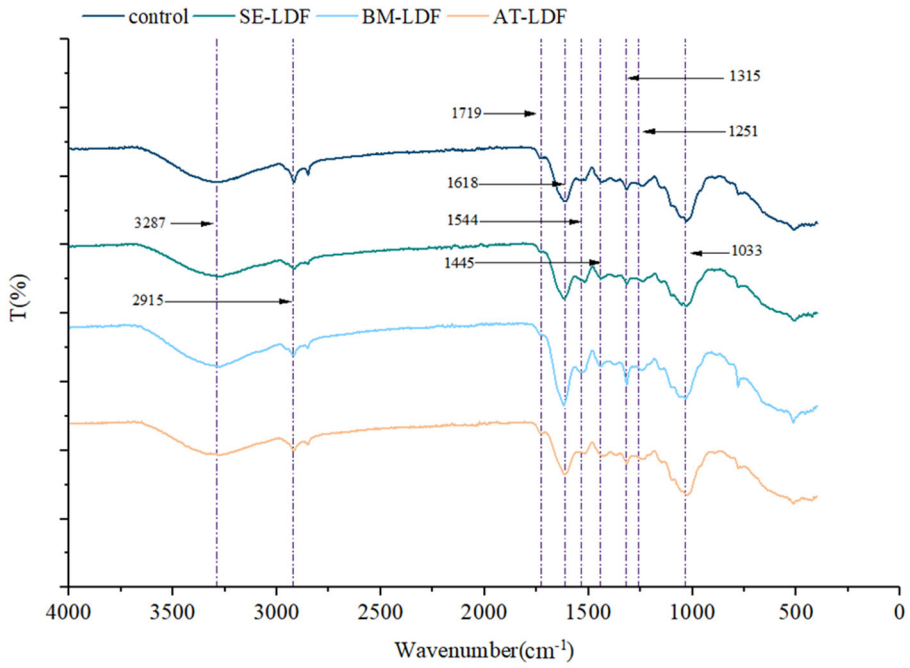

FIGURE 2
FT-IR spectra of control, SE-LDF, BM-LDF, and AT-LDF. Control: lotus leaves dietary fiber. SE-LDF, shear emulsifying modified lotus leaves dietary fiber; BM-LDF, ball milling modified lotus leaves dietary fiber; AT-LDF, autoclave modified lotus leaves dietary fiber.

groups exposure in cellulose, hemicellulose, lignin and phenols (36, 37). The weak peak at 2915 cm^{-1} was a result of the C-H stretching vibrations from methyl and methylene groups, representing the typical structure of cellulose and hemicellulose polysaccharides compounds (36, 38). The minor peak at 1719 cm^{-1} was assigned to the stretching vibration of C=O in hemicellulose (35). The notable peak at 1618 cm^{-1} indicated the presence of a benzene ring in lignin, which may be related to phenolic structures (13). The weak peak at 1544 cm^{-1}, along with the minor peak at 1445 cm^{-1}, was the aliphatic or aromatic C-H group vibration of lignin (35). The weak peak at 1315 cm^{-1} and 1251 cm^{-1} was mainly from the typical cellulose and hemicellulose structures (35, 37). The notable absorption at 1033 cm^{-1} originated from the C-O stretching vibration of C-O-C in the pyranose ring (38).

In our study, samples had similar FT-IR spectra in general, suggesting that three modification methods did not alter the main functional groups of LDF, which were similar to those of okara (soybean residue) (14) and sea buckthorn seed meal modified by BM (15), akebia trifoliata (Thunb.) koidz. Seeds modified by SE (12) and whole grain oats modified by AT (16). While the peak intensity of BM-LDF at some absorption peaks was stronger than other samples. The particle size of BM-LDF was the lowest in all samples, and previous studies have reported that BM promoted the exposure of functional groups and facilitated the access to the corresponding groups, which may be due to sharp reduction of particle size and breakage of fiber structure by mechanical effects of BM (14, 39). In addition, the major structure and content of polyphenols in BM-LDF may be also affected FT-IR spectra (37).

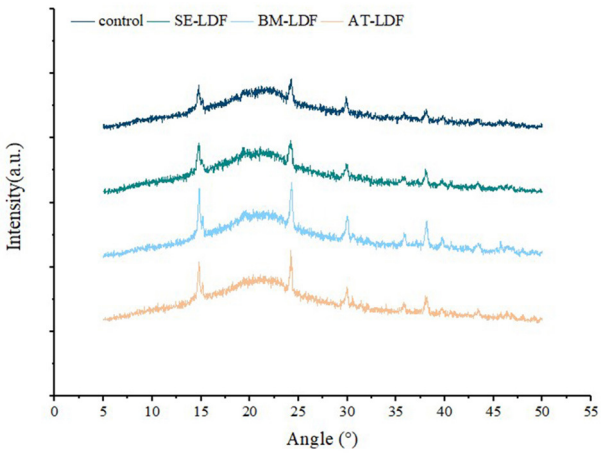

FIGURE 3
X-ray diffraction of control, SE-LDF, BM-LDF, and AT-LDF. Control: lotus leaves dietary fiber. SE-LDF, shear emulsifying modified lotus leaves dietary fiber; BM-LDF, ball milling modified lotus leaves dietary fiber; AT-LDF, autoclave modified lotus leaves dietary fiber.

3.1.3. X-ray diffraction

Insoluble dietary fibers extracted from plant cell wall mostly contains crystalline regions due to the presence of cellulose, and amorphous regions composed of non-crystalline cellulose, hemicellulose and lignin (35, 36). X-ray diffractometry has been widely used to determine the type of crystallization structure of dietary fibers. X-ray diffraction of control, SE-LDF, BM-LDF

10.3389/fnut.2023.1064662

TABLE 1 Effects of modification treatment on SDF, IDF, TDF, particle size distribution, WHC, OHC, WSC, and color of LDFs.

Characteristics	control	SE-LDF	BM-LDF	AT-LDF
SDF (g/100 g DW)	5.06 ± 0.43^{b}	4.12 ± 0.62^{b}	6.29 ± 0.49^{a}	7.30 ± 0.14^{a}
IDF (g/100 g DW)	72.32 ± 1.54^{a}	69.32 ± 0.41^{bc}	67.61 ± 1.46^{c}	71.19 ± 1.01^{ab}
TDF (g/100 g DW)	77.38 ± 1.49^{a}	73.45 ± 0.35^{b}	73.89 ± 1.68^{b}	78.49 ± 0.92^{a}
D_{10} (μm)	28.51 ± 0.40^{a}	12.87 ± 0.11^{c}	3.46 ± 0.05^{d}	21.59 ± 0.33^{b}
D_{50} (μm)	206.30 ± 0.95^{a}	171.20 ± 0.87^{b}	15.55 ± 0.35^{d}	161.00 ± 0.47^{c}
D_{90} (μm)	453.87 ± 4.64^{a}	399.40 ± 0.65^{c}	41.16 ± 0.55^{d}	411.00 ± 3.83^{b}
Asf(m^2/kg)	45.89 ± 0.83^{d}	74.47 ± 0.67^{b}	287.67 ± 4.67^{a}	61.17 ± 1.08^{c}
WHC (g/g DW)	5.80 ± 0.21^{b}	6.71 ± 0.21^{a}	3.46 ± 0.12^{d}	4.51 ± 0.12^{c}
OHC (g/g DW)	3.96 ± 0.28^{a}	3.73 ± 0.17^{a}	2.47 ± 0.32^{c}	3.18 ± 0.34^{b}
WSC (mL/g DW)	7.07 ± 0.16^{b}	7.92 ± 0.29^{a}	5.52 ± 0.41^{c}	4.84 ± 0.25^{d}
L*	53.69 ± 0.53^{b}	53.96 ± 0.56^{b}	56.45 ± 0.02^{a}	46.02 ± 0.76^{c}
a*	0.85 ± 0.04^{b}	0.47 ± 0.02^{c}	-0.21 ± 0.01^{d}	2.80 ± 0.08^{a}
b*	13.57 ± 0.30^{c}	14.41 ± 0.24^{b}	20.39 ± 0.04^{a}	9.48 ± 0.49^{d}
ΔE	-	0.96	7.43	8.91

All values were means ± sd, n = 3. Values with different letters were significantly different in the same row, $P < 0.05$. "-" represented not detected. Control, lotus leaves dietary fiber; SE-LDF, shear emulsifying modified lotus leaves dietary fiber; BM-LDF, ball milling modified lotus leaves dietary fiber; AT-LDF, autoclave modified lotus leaves dietary fiber; SDF, soluble dietary fiber; IDF, insoluble dietary fiber; TDF, total dietary fiber. D_{10}, D_{50} and D_{90} were equivalent volume diameters determined at 10, 50, and 90% cumulative volume, respectively. A_{SF} represented specific surface areas of powder. WHC, water holding capacity; OHC, oil holding capacity; WSC, water solubility capacity. L* represented the brightness (0 is black, 100 is white); a* represented the redness and greenness (a* > 0, represented the degree of red; a* < 0 means green degree); b* represented yellow and blue degree (b* > 0 means yellow degree, b* < 0 means blue degree), ΔE represented color difference.

and AT-LDF were shown in Figure 3. All samples had similar characteristic spectra, and there were characteristic diffraction peaks at a 2θ diffraction angle of 14.8° and 22.5° indicating that LDF had a crystalline cellulose I-type crystal structure (40). The three modification methods did not change the crystallization structure of LDF significantly, which was similar to those of waste orange peels modified by AT (18), deoiled cumin modified by SE (32) and okara (soybean residue) modified by BM (41). However, the intensity of some diffraction peaks changed after different modification treatments. The CrI of control, SE-LDF, BM-LDF and AT-LDF were 21.01, 15.71, 19.31 and 16.54% respectively, suggesting that the modifications leaded to the damage of the crystallization region of LDF. This result was might be attributed to modifications that reduced the CrI of LDF by destroying fiber structure, increasing fiber holes, reducing particle size and facilitating enzymatic hydrolysis (15, 32, 41). The peaks at a 2θ diffraction angle from 24° to 40° could be attributed to the denaturation of cellulose during SE, BM, AT or enzyme hydrolysis (35). Compared with other samples, SE-LDF showed the lowest CrI, suggesting SE-LDF was looser in structure and weaker at the intermolecular level. Studies have reported that low CrI was related to improving hydrophilic, lipophilic and swelling capacities of dietary fibers (15), which may be used to explain the better properties of SE-LDF in some aspects.

3.2. Physicochemical properties

3.2.1. Dietary fiber content

SDF, IDF and TDF contents of control, SE-LDF, BM-LDF and AT-LDF were shown in Table 1. The SDF, IDF and TDF contents of control were 5.06, 72.32 and 77.38 g/100 g DW, respectively. Compared with the control, BM and AT significantly increased SDF content in LDF by 24.31 and 44.27% ($P < 0.05$), and SE decreased SDF content in LDF by 18.58% although there was no significant difference between them ($P > 0.05$). The result was similar to those of waste orange peels (18) and brewers' spent grain (8) modified by AT, and those of waste orange peels (18), citrus fiber (38) and grape pomace (13) modified by BM. This might be because the effects of AT and BM on the structure of LDF as described above, degraded the high molecular weighted fiber of AT-LDF and BM-LDF into relatively small molecular weight polysaccharides and were conducive to dissolve in the water, resulting in higher SDF contents in AT-LDF and BM-LDF than that of control (14, 18). While the strong fluid shear by SE contributed to the release of water-soluble polysaccharides (10, 12), leading to a drop in residue of water-soluble polysaccharides and a lower SDF content in SE-LDF. Compared with the control, SE, BM and AT decreased IDF content in LDF by 4.15, 6.51 and 1.56% respectively, and IDF contents in SE-LDF and BM-LDF were significantly different from that in control ($P < 0.05$). A possible explanation may be that the effects of the three modifications on the fiber structure of lotus leaves were beneficial to the degradation of cellulose in the enzymatic hydrolysis process, which reduced the IDF contents in SE-LDF, BM-LDF and AT-LDF. In general, compared with the control, AT slightly increased TDF content in LDF by 1.43% ($P > 0.05$), and SE and BM significantly decreased TDF content in LDF by 5.08% and 4.51% ($P < 0.05$).

3.2.2. Particle size distribution

The food added with plant dietary fibers generally presents a rough texture and bad sensory acceptance (14). Reducing the particle size of dietary fibers can improve the rough texture and

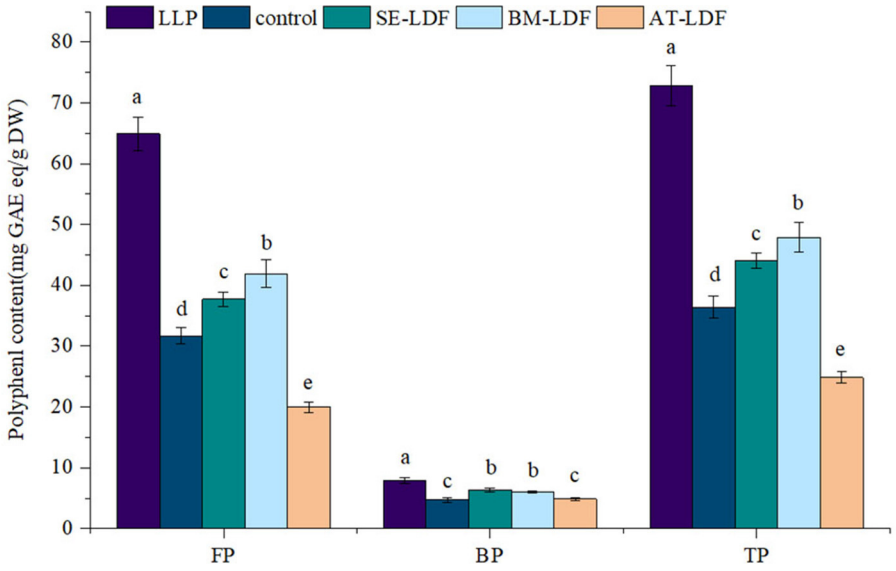

FIGURE 5
Polyphenol content of FP, BP, and TP in LLP and LDF. All values were means ± sd, $n = 3$. Values with different letters were significantly different in the same group; $P < 0.05$. FP, free phenolic; BP, bound phenolic; TP, total phenolic; LLP, lotus leaves powder; control, lotus leaves dietary fiber; SE-LDF, Shear emulsifying modified lotus leaves dietary fiber; BM-LDF, Ball milling modified lotus leaves dietary fiber; AT-LDF, Autoclave modified lotus leaves dietary fiber.

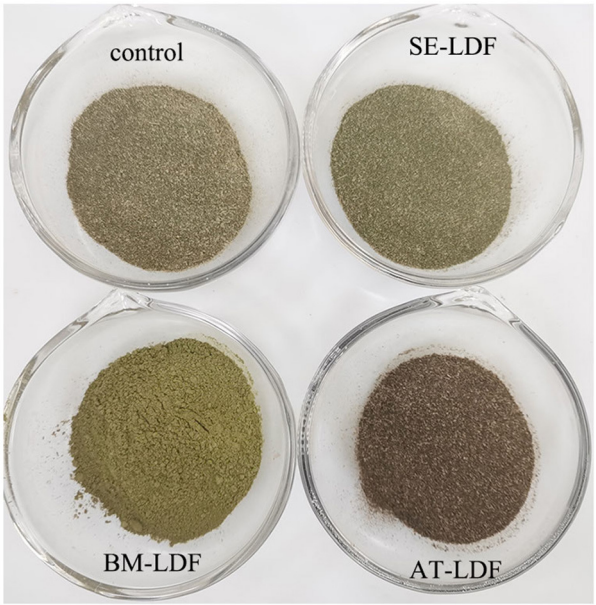

FIGURE 4
Real pictures of control, SE-LDF, BM-LDF, and AT-LDF. Control: lotus leaves dietary fiber. SE-LDF, shear emulsifying modified lotus leaves dietary fiber; BM-LDF, ball milling modified lotus leaves dietary fiber; AT-LDF, autoclave modified lotus leaves dietary fiber.

relates closely to enhancing its functionality (13, 42). D_{10}, D_{50} and D_{90} and specific surface areas (A_{sf}) of control, SE-LDF, BM-LDF and AT-LDF were shown in Table 1. Compared with the control, SE-LDF, BM-LDF and AT-LDF showed smaller D_{10}, D_{50}, and D_{90} and larger A_{sf}. It has been reported that high temperature, high pressure, extrusion, collision and fluid shear stress could break down glycosidic bonds and peptide bonds, which lead to particle breakage and destruction, the release of oligosaccharides and proteins, dissolution of soluble components, thus reduced particle size (16, 18). Additionally, D_{10}, D_{50}, and D_{90} of BM-LDF were the lowest, which were 3.46, 15.55, and 41.16 μm respectively, reaching the level of ultra-fine grinding, suggesting that the effect of BM on the particle size of LDF was stronger than that of AT and SE in our study. The BM-LDF exhibited relatively narrow particle size distribution and better particle uniformity. Many studies have also shown that BM could rapidly reduce the particle size of powder, even to the submicron level, therefore BM is commonly used in the processing of ultra-fine powder of fiber materials (3). The effects of SE and AT on the particle size of LDF were similar, and the D_{50} were 171.20 and 161.00 μm. A_{sf} of particles increases with the decrease of particle size (42), which indicated that BM-LDF may be more sufficient contact with the solution, leading to an increase in dissolving out capacity of functional components in sample and changing adsorption capacity of sample (13, 15).

3.2.3. Water-holding capacity, oil-holding capacity and water swelling capacity

WHC, OHC and WSC of dietary fibers have important significance for food quality, and are influenced by many factors, such as particle size, specific surface area, porosity, crystallinity and fiber spatial structure (33, 43). WHC can retain more water in food to reduce food dehydration and contraction (44), and promote gastrointestinal peristalsis in the human body (36). OHC can make the fat in food not easy to flow out and stabilize food quality, which helps to prolong the shelf life, and accelerate fat excretion

and reduce serum cholesterol levels in the human body (45). WHC affects food viscosity, and reduces intestinal transit time and delays gastric clearance speed in the human body (43). Previous studies have shown that the interaction of dietary fiber with water or oil can be summarized into two types: (i) physical forms through adsorption, encapsulation and interception of water or oil, and (ii) chemical bonds formed through the bonding of hydrophilic groups exposed to water or the bonding of lipophilic groups exposed to oil (32, 46).

WHC, OHC and WSC of control, SE-LDF, BM-LDF and AT-LDF were shown in Table 1. WHC, OHC and WSC of control were 5.80 g/g DW, 3.96 g/g DW, and 7.07 mL/g DW, respectively. WHC and WSC of SE-LDF were highest in all samples. OHC of SE-LDF was slightly lower than that of control but there was no significant difference between them ($P > 0.05$), and was significantly higher than those of BM-LDF and AT-LDF ($P < 0.05$). This result may be because fluid shear stress in SE was not excessively damaged the LDF fiber network structure and had little effect on the particle size. During the strong fluid shock, the polysaccharide, protein and other components encapsulated in LDF were more easily released so that the fiber structure of SE-LDF was looseer and the fiber gap increased, which were conducive to physical interception and the combination of chemical bonds. The result was similar to research on deoiled cumin (32), citrus peel (36) and bamboo shoot fiber (10) modified by SE. Compared with the control, BM reduced WHC, OHC, and WSC by 40.34, 37.63, and 21.92%, respectively. Ultra-fine particle size, wrinkled surface and porous structure by BM modification were beneficial to exposure of internal groups and combination of chemical bonds (15). However, some studies have shown that high-strength BM excessively damaged the network structure of dietary fiber, leading to the breakage of channels and pores, which reduced physical interception to water and oil (46). Under many factors, BM-LDF showed low WHC, OHC, and WSC. Similar observations have been reported in researches of asparagus leaf (3), grape pomace (13) and deoiled cumin (32). Compared with the control, AT reduced WHC, OHC, and WSC by 22.24, 19.70, and 31.54%, respectively. High pressure in AT destroyed integrity of fiber structure (46), and AT-LDF surface structure showed a similar honeycomb shape with large and relatively regular caves, as shown in Figure 1, which reduced steric hindrance between fiber, resulting in lower physical interception to water and oil. The result was similar to research on okara (soybean residue) (41). In general, SE was more beneficial to improve WHC, OHC, and WSC of LDF than BM and AT, which was consistent with the result of the crystallinity.

3.2.4. Color

The color of raw materials in the food industry is closely related to the sensory quality of food, and can also reflect the changes in the physical structure and chemical composition of raw materials during food processing (14). Color characteristics and real pictures of control, SE-LDF, BM-LDF, and AT-LDF were shown in Table 1 and Figure 4, suggesting that modification methods significantly affected the color characteristics of LDF. The influence of modification methods on color characteristics of dietary fiber was connected with particle size, Maillard reaction, phenolic compounds aggregation, chlorophyll release and roughness of particle surface (3, 14, 17, 41). The ΔE of SE-LDF was only 0.96 compared with the control, and the effect of SE on color difference of LDF was smaller than that of BM and AT. This may be because SE had little effect on the particle size. Meanwhile, the temperature was kept constant and oxygen was isolated during SE, which effectively reduced the occurrence of related chemical reactions. The ΔE of BM-LDF was 7.43 compared with the control, and BM significantly increased the value of L* and b* and decreased the value of a*. The result was similar to the effects of BM on okara (soybean residue) (14) and asparagus leaf (3). BM-LDF was ultra-fine powder that could facilitate powder mixing and powder surface smoothing, which increased the value of L*. Meanwhile, particle size reduction was conducive to the exposure and aggregation of polyphenolic compounds resulting in the increase of b*, and was beneficial to the release of chlorophyll leading to the decrease of a* (14, 41). AT-LDF had the highest ΔE of 8.91, indicating that AT showed the strongest effect on color difference. AT significantly decreased the value of L* and b*, and increased the value of a*. High temperature and high pressure in AT promoted the occurrence of Maillard reaction, oxidation reaction and chlorophyll degradation, resulting in dark brown products, which increased the value of a* and decreased the value of L* and b* (16, 41). The real pictures of samples also exhibited that BM-LDF and SE-LDF had better color quality than AT-LDF.

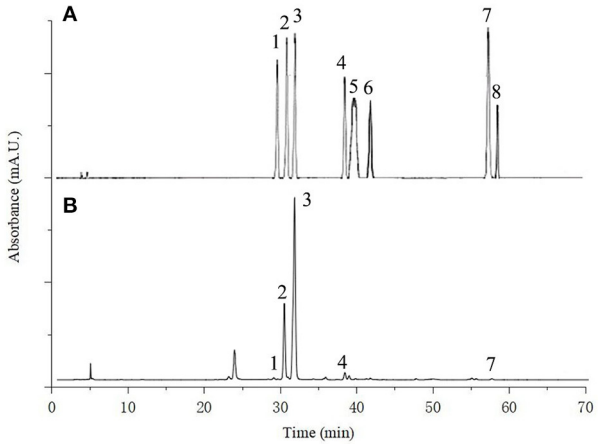

FIGURE 6
The HPLC chromatogram of **(A)** standard mixture solution of eight flavonoids [rutin (1) hyperoside (2) isoquercitrin (3) astragaline (4); catechin (5) myricetin (6) quercetin (7) and kaempferol (8)]; **(B)** free phenolic of lotus leaves powder.

3.3. Phenolic compounds and antioxidant capacity

3.3.1. Polyphenol content

According to the different binding strengths between phenolic compounds and cell wall matrix in plants (47), phenolic compounds in plants can be divided into FP and BP, and they play different health effects on the body. The combination of FP and plant cell wall matrix is relatively weak, which can be released in

10.3389/fnut.2023.1064662

TABLE 2 Flavonoids composition of FP and BP in LLP and LDFs (mg/100 g DW).

	Sample	Rutin	Hyperoside	Isoquercitrin	astragalin	Catechin	Myricetin	Quercetin	Kaempferol
FP									
	LLP	20.76 ± 3.81	710.76 ± 141.10	1998.14 ± 373.52	82.73 ± 17.98	-	-	10.91 ± 1.49	-
	Control	-	3.70 ± 0.45	724.85 ± 54.48	18.70 ± 2.11	-	-	-	-
	SE-LDF	-	-	176.35 ± 40.22	3.44 ± 0.44	-	-	-	-
	BM-LDF	-	119.03 ± 15.13	477.20 ± 45.34	9.98 ± 0.75	-	-	7.74 ± 1.78	-
	AT-LDF	4.50 ± 0.18	153.15 ± 27.52	701.51 ± 87.90	20.32 ± 3.82	-	-	-	-
BP									
	LLP	1.57 ± 0.31	62.03 ± 14.60	532.23 ± 90.48	6.10 ± 1.39	-	-	1.23 ± 0.13	-
	Control	0.41 ± 0.02	1.93 ± 0.34	148.03 ± 4.50	5.79 ± 0.08	-	-	0.77 ± 0.01	-
	SE-LDF	0.20 ± 0.06	3.00 ± 0.22	55.20 ± 6.84	1.67 ± 0.05	-	-	1.07 ± 0.10	-
	BM-LDF	-	8.28 ± 0.67	80.05 ± 5.29	1.16 ± 0.05	-	-	0.92 ± 0.03	-
	AT-LDF	0.43 ± 0.05	24.65 ± 5.36	116.27 ± 26.98	3.59 ± 0.31	-	-	-	-

All values are means ± sd, n = 3."-" means not detected. FP, free phenolic; BP, bound phenolic; LLP, lotus leaves powder; Control, lotus leaves dietary fiber; SE-LDF, shear emulsifying modified lotus leaves dietary fiber; BM-LDF, ball milling modified lotus leaves dietary fiber; AT-LDF, autoclave modified lotus leaves dietary fiber.

the human upper digestive tract to play a healthy role (48). BP has closely bound to the plant cell wall matrix, thus can resist the digestion of the stomach and small intestine to reach the human lower gastrointestinal tract, where is released from plant cell wall matrix by colonic fermentation, and play healthy effects by producing metabolites, such as vitamins and short-chain fatty acids, forming an antioxidant environment and regulating intestinal flora (49). Lotus leaves are rich in phenolic compounds and showed a stronger antioxidative effect which is related to many factors, such as varieties, growth climate, geographic location and culturing conditions of lotus leaves (21). The FP, BP and total phenolic (TP) contents of lotus leave powder, control, SE-LDF, BM-LDF and AT-LDF were shown in Figure 5. The FP, BP, and TP contents of lotus leave powder were 64.90, 7.90, and 72.81 mg GA eq/g DW, respectively. Some phenolic components of lotus leaves were still retained in LDF extracted, and the retention rates of FP, BP and TP of lotus leaves powder were 30.74–64.53, 61.65–80.25, and 34.09–65.77%. The FP content of samples was 4.09–8.21 times that of their BP content, showing the phenolic components in lotus leaves were mainly FP, which was similar to date (Phoenix dactylifera L.) seeds (27) and rosa roxburghii tratt leaves (50).

The FP, BP and TP contents of control were 31.68, 4.81, and 37.11 mg GA eq/g DW, respectively. Compared with the control, BM and SE significantly increased FP, BP, and TP contents ($P < 0.05$). The FP and TP contents in BM-LDF were the highest, increasing by 32.20 and 29.05% than that of the control, and were significantly higher than those in SE-LDF ($P < 0.05$). The BP content in SE-LDF was the highest with an increase of 31.81% than that of the control, which was slightly higher than that in BM-LDF, but there was no significant difference between them ($P > 0.05$). Compared with the control, AT significantly decreased FP and TP contents of LDF by 37.03 and 33.12% ($P < 0.05$), and slightly increased BP content of LDF by 3.33% while there was no significant difference between them ($P > 0.05$). Overall, AT seriously damaged phenolic compounds of LDF. Studies have shown that the higher temperature could degrade phenolic compounds by promoting enzymatic oxidation and non-enzymatic oxidation (51). Some fiber modification methods, such as BM (3, 13, 14), SE (12) and AT (17), were beneficial to the release of polyphenols during extraction by destroying fiber structure, increasing fiber pores and reducing particle size, resulting in reduce phenolic content remaining in extracted dietary fiber. AT modification decreased phenolic content in LDF, which was similar to the previous research (17). However, our study showed that BM and SE increased phenolic content in LDF compared with the control, which may be due to modified fiber structure and reduced particle size caused by BM and SE, especially the particle size of BM-LDF, which were conducive to the contact between LDF and solvent in the extraction of LDF polyphenols, improving the release of phenolic compounds from LDF. Overall, BM and SE increased the content of phenolic compounds in LDF compared with the control.

3.3.2. Flavonoids composition

In recent years, flavonoids compounds have been widely accepted as a category of the most important biologically active components of lotus leaves. Many previous studies have identified flavnoids of lotus leaves, mainly including rutin, hyperoside, catechin, quercetin, quercetin-3-O-glucopyranoside, isoquercitrin, astragalin, taxifolin, etc., and their type, content and properties related to varieties, growth climate, geographical location, culture conditions and other factors of lotus leaves (21). Figure 6 shows the chromatogram of a standard mixture solution and FP of lotus leaves powder. Five flavonoids were identified in lotus leaves powder: rutin, hyperoside, isoquercitrin, astragalin and quercetin, and catechin, myricetin and kaempferol were not detected in all samples. The result was similar to Liao et al. (52), which may be because the lotus leaves samples came from Hunan China, with similar geographical location and climatic conditions, agricultural and environmental factors. The flavonoids of FP and BP in lotus leaves powder, control, SE-LDF, BM-LDF, and AT-LDF were shown in Table 2. The result exhibited that the type of main flavonoids

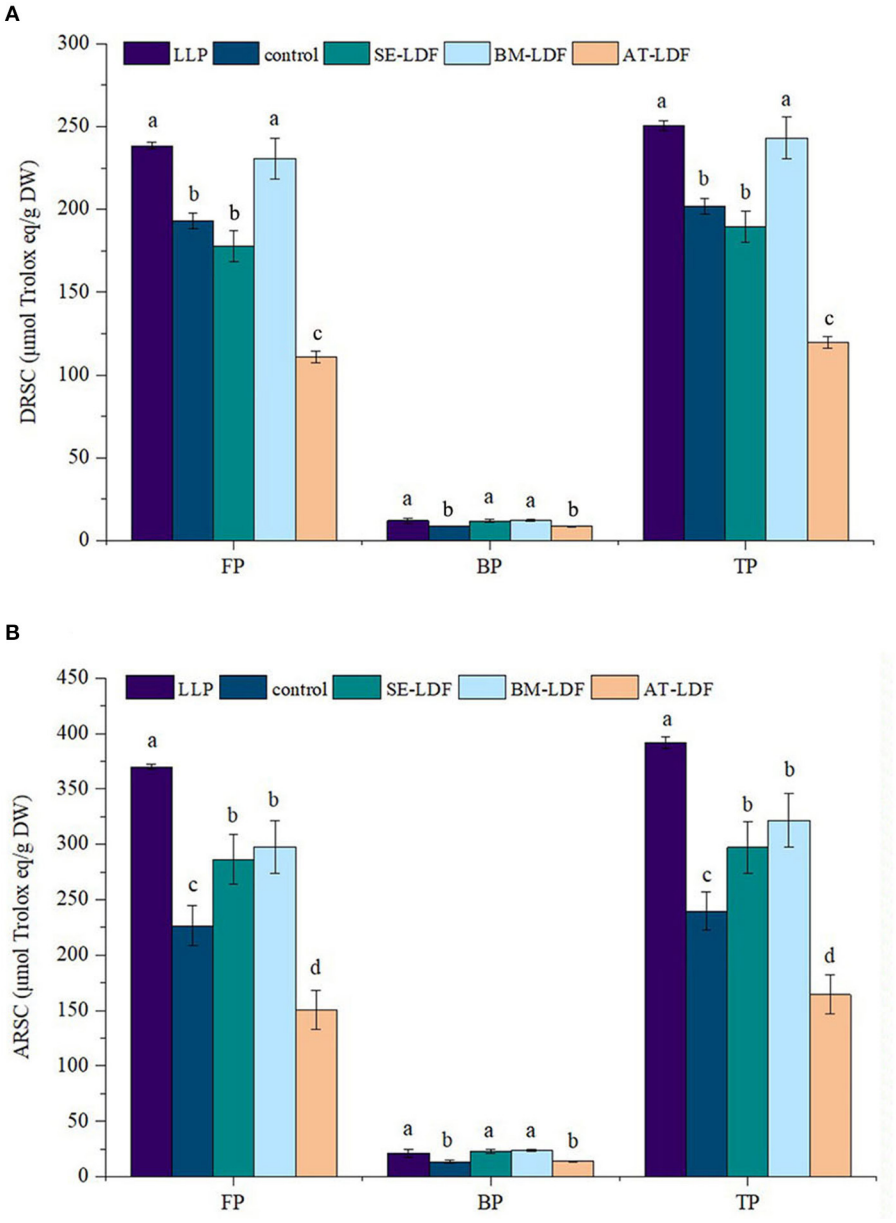

FIGURE 7
DRSC and ARSC of FP, BP, and TP in LLP and LDFs. **(A)** DRSC, DPPH free radical scavenging capacity; **(B)** ARSC, ABTS free radical scavenging capacity. All values were means ± sd, $n = 3$. Values with different letters were significantly different in the same group, $P < 0.05$. FP, free phenolic; BP, bound phenolic; TP, total phenolic. LLP, lotus leaves powder; control, lotus leaves dietary fiber; SE-LDF, shear emulsifying modified lotus leaves dietary fiber; BM-LDF, ball milling modified lotus leaves dietary fiber; AT-LDF, autoclave modified lotus leaves dietary fiber.

in FP and BP of lotus leaves powder were the same, including the above five flavonoids, and the flavonoids content of FP was higher than that of BP. Compared with lotus leaves powder, flavonoids composition of control, SE-LDF, BM-LDF, and AT-LDF decreased after enzymatic extraction.

Researchers have reported that the contents of isoquercitrin, hyperoside and astragalin in lotus leaves were relatively high (22, 23, 52). Modification decreased isoquercitrin content in LDF. Compared with the control, AT, BM, and SE reduced isoquercitrin of FP in LDF by 3.22, 34.17, and 75.67%, and reduced isoquercitrin of BP in LDF by 21.46, 45.92, and 62.71%. In general, modifications increased hyperoside content in LDF compared with the control. Hyperoside contents of FP and BP in AT-LDF were the highest, respectively 41.39 and 12.77 times of control. Compared with the control, AT increased astragalin of FP in LDF by 8.66%, and BM and SE reduced astragalin of FP in LDF by 46.63 and 81.60%. AT, BM and SE reduced astragalin of BP in LDF by 37.40, 79.97, and 71.16%. In addition, modification decreased rutin and quercetin content in LDF. Overall, AT-LDF showed higher flavonoids contents, and SE-LDF showed lower flavonoids contents among the three modified LDFs. This result was contrary to the polyphenol content of LDF. The phenolic compounds in lotus

leaves were mainly identified as phenolic acids and flavonoids in previous research (21). So this result may be because the polyphenol extract of LDF contained phenolic acids and other polyphenol components that were not concerned in our study.

3.3.3. Antioxidant capacity

The DRSC and ARSC are simple, economical and effective methods to evaluate the antioxidant properties of food, which have been widely used in the researches of functional foods. DRSC and ARSC of lotus leaves powder, control, SE-LDF, BM-LDF and AT-LDF were shown in Figure 7. The FP DRSC, BP DRSC and TP DRSC of lotus leaves powder were 238.48, 12.12 and 250.60 μmol Trolox eq /g DW, respectively. Compared with lotus leaves powder, DRSC of control, SE-LDF, BM-LDF and AT-LDF decreased after enzymatic extraction, while there was no significant difference in DRSC between lotus leaves powder and BM-LDF. The FP DRSC, BP DRSC and TP DRSC of control were 193.01, 8.84, and 201.85 μmol Trolox eq /g DW, respectively. BM-LDF showed the higher FP DRSC, BP DRSC and TP DRSC, increasing by 19.56, 38.80, and 20.40% than those of control, and there were significant differences with other samples ($P < 0.05$). SE showed significantly higher BP DRSC than that of control, increasing by 35.63% ($P < 0.05$), and slightly decreased FP DRSC and TP DRSC by 7.95 and 6.04% than those of the control. AT significantly decreased FP DRSC and TP DRSC by 42.47 and 40.66% than those of control ($P < 0.05$), and slightly decreased BP DRSC by 1.13% while there was no significant difference between them ($P > 0.05$).

The FP ARSC, BP ARSC and TP ARSC of lotus leaves powder were 369.95, 21.36, and 391.31 μmol Trolox eq/g DW, respectively. Compared with lotus leaves powder, FP ARSC and TP ARSC of control, SE-LDF, BM-LDF, and AT-LDF were significantly decreased after enzymatic extraction ($P < 0.05$). The FP ARSC, BP ARSC, and TP ARSC of control were 226.42.06, 13.39, and 239.81 μmol Trolox eq/g DW, respectively. The ARSC of SE-LDF and BM-LDF were significantly higher than those of control. The ARSC of BM-LDF was slightly higher than that of SE-LDF, and there was no significant difference between them ($P > 0.05$). Similar to the effect of AT on DRSC, AT significantly decreased FP ARSC and TP ARSC by 33.54 and 31.45% than those of the control ($P < 0.05$), and slightly increased BP ARSC by 3.88% while there was no significant difference between them ($P > 0.05$).

Those data showed a positive correlation between antioxidant activity and polyphenol content, which was similar to previous studies (39, 50). In general, DRSC and ARSC of FP were significantly higher than that of BP in LDF, and DRSC and ARSC of BM-LDF and SE-LDF were higher than those of the control and AT-LDF, suggesting BM and SE were contributed to the antioxidant activity of LDF.

4. Conclusion

Lotus (*Nelumbo*) leaves fiber exhibit a dense structure and poor taste. In this study, the three physical modifications of SE, BM, and AT were utilized to improve the properties of LDF. The results showed that the three modifications could change the microstructure of LDF and reduced the CrI of LDF to obtain a looser structure, and affected the physicochemical properties, polyphenol content, flavonoids composition and antioxidant capacity *in vitro* of LDF. In general, SE contributed to the looser structure and better physical characteristics of LDF, which may be more conducive to LDF promoting gastrointestinal peristalsis by water swelling, and reducing high-calorie components absorption by physical interception. SE-LDF may be more applicable as a functional food raw material with low caloric requirements. BM effectively reduced the particle size to improve the taste, facilitated the dissolution of bioactive components and increased the antioxidant capacity of LDF to play the functional characteristics. BM-LDF may be more applicable as a functional food raw material with better antioxidant function. Although AT improved the dense structure of LDF, it showed adverse effects on the physical properties, phenolic compounds and the antioxidant capacity of LDF. Overall, SE and BM are appropriate modifications to enhance the properties of LDF with their own advantages, and researchers should select appropriate modifications of LDF based on exploitation requirements.

Data availability statement

The original contributions presented in the study are included in the article/supplementary material, further inquiries can be directed to the corresponding authors.

Author contributions

HZ designed the research content, performed the experiments, analyzed the data, and wrote the manuscript. YS performed the experiments, analyzed the data, and wrote the manuscript. TZhe and YZ analyzed and discussed the data. LF and TZho performed the experiments and analyzed the data. FJ and YX wrote the manuscript. YY and KH designed the research content, analyzed the data, and modified the manuscript. All authors read and approved the final manuscript.

Funding

This work was financially supported by grants from Special project on modern agricultural industrial technology system construction of Hunan, China (No. 2022-67), the natural science funding project of Hunan, China (No. 2022JJ5410), Innovation and entrepreneurship training program for college students of China (No. 202110541060), and First-class discipline construction fund of Hunan University of Chinese Medicine of Changsha, Hunan, China (No. 4901020000200902).

Conflict of interest

The authors declare that the research was conducted in the absence of any commercial or financial relationships that could be construed as a potential conflict of interest.

Publisher's note

References

1. Makki K, Deehan E, Walter J, Bäckhed F. The impact of dietary fiber on gut microbiota in host health and disease. *Cell Host Microbe.* (2018) 23:705–15. doi: 10.1016/j.chom.2018.05.012

2. Fuller S, Beck E, Salman H, Tapsell L. New horizons for the study of dietary fiber and health: a review. *Plant Foods Hum Nutr.* (2016) 71:1–12. doi: 10.1007/s11130-016-0529-6

3. Chitrakar B, Zhang M, Zhang X, Devahastin S. Bioactive dietary fiber powder from asparagus leaf by-product: effect of low-temperature ball milling on physico-chemical, functional and microstructural characteristics. *Powder Technol.* (2020) 366:275–82. doi: 10.1016/j.powtec.2020.02.068

4. González-Aguilar G, Blancas-Benitez F, Sáyago-Ayerdi S. Polyphenols associated with dietary fibers in plant foods: molecular interactions and bioaccessibility. *Curr Opin Food Sci.* (2017) 13:848. doi: 10.1016/j.cofs.2017.03.004

5. Soleimanian Y, Sanou I, Turgeon S, Canizares D, Khalloufi S. Natural plant fibers obtained from agricultural residue used as an ingredient in food matrixes or packaging materials: a review. *Compr Rev Food Sci Food Saf.* (2022) 21:371–415. doi: 10.1111/1541-4337.12875

6. Ma M, Mu T, Sun H, Zhang M, Chen J. Yan Z. Optimization of extraction efficiency by shear emulsifying assisted enzymatic hydrolysis and functional properties of dietary fiber from deoiled cumin (*Cuminum cyminum* L). *Food Chem.* (2015) 179:270–7. doi: 10.1016/j.foodchem.2015.01.136

7. Gao W, Chen F, Wang X, Meng Q. Recent advances in processing food powders by using superfine grinding techniques: a review. *Compr Rev Food Sci Food Saf.* (2020) 19:2222–55. doi: 10.1111/1541-4337.12580

8. Naibaho J, Korzeniowska M, Wojdyo A, Figiel A, Viiard E. Fiber modification of brewers' spent grain by autoclave treatment to improve its properties as a functional food ingredient. *LWT-Food Sci Technol.* (2021) 149:111877. doi: 10.1016/j.lwt.2021.111877

9. Qin H, Xu Q, Li W, Dang X, Han Y, Lei K, et al. Effect of stator geometry on the emulsification and extraction in the inline single-row blade-screen high shear mixer. *Ind Eng Chem Res.* (2017) 56:9376–88. doi: 10.1021/acs.iecr.7b01362

10. Yang M, Wu L, Cao C, Wang S, Zhang D. Improved function of bamboo shoot fibre by high-speed shear dispersing combined with enzyme treatment. *Int J Food Sci Technol.* (2018) 54:844–53. doi: 10.1111/ijfs.14004

11. Khan G, Khan N, Khan Z, Ali F, Jan A, Muhammad N, et al. Effect of extraction methods on structural, physiochemical and functional properties of dietary fiber from defatted walnut flour. *Food Sci Biotechnol.* (2018) 27:1015–22. doi: 10.1007/s10068-018-0338-9

12. Jiang Y, Yin H, Zheng Y, Wang D, Liu Z, Deng Y. et al. Structure, physicochemical and bioactive properties of dietary fibers from Akebia trifoliata (Thunb) Koidz seeds using ultrasonication/shear emulsifying/microwave-assisted enzymatic extraction. *Food Res Int.* (2020) 136:109348. doi: 10.1016/j.foodres.2020.109348

13. Bender A, Speroni C, Moro K, Morisso F, Penna N. Effects of micronization on dietary fiber composition, physicochemical properties, phenolic compounds, and antioxidant capacity of grape pomace and its dietary fiber concentrate. *LWT-Food Sci Technol.* (2020) 117:108652. doi: 10.1016/j.lwt.2019.108652

14. Chen P, Lin C, Chen M, Chiang P. The micronization process for improving the dietary value of okara (soybean residue) by planetary ball milling. *LWT-Food Sci Technol.* (2020) 132:109848. doi: 10.1016/j.lwt.2020.109848

15. Zhu Y, Ji X, Yuen M, Yuen T, Yuen H, Wang M, et al. Effects of ball milling combined with cellulase treatment on physicochemical properties and in vitro hypoglycemic ability of sea buckthorn seed meal insoluble dietary fiber. *Front Nutr.* (2022) 8:820672. doi: 10.3389/fnut.2021.820672

16. Dong J, Yang M, Shen R, Zhai Y, Yu X, Wang Z. Effects of thermal processing on the structural and functional properties of soluble dietary fiber from whole grain oats. *Food Sci Technol Int.* (2019) 25:282–94. doi: 10.1177/1082013218817705

17. Escobedo A, Loarca-Piña G, Gaytan-Martínez M, Orozco-Avila I, Mojica L. Autoclaving and extrusion improve the functional properties and chemical composition of black bean carbohydrate extracts. *J Food Sci.* (2020) 85:2783–91. doi: 10.1111/1750-3841.15356

18. Khanpit V, Tajane S, Mandavgane S. Production of soluble dietary fiber concentrate from waste orange peels: study of nutritional and physicochemical properties and life cycle assessment. *Biomass Convers.* (2022) 185:90–8. doi: 10.1007/s13399-022-03007-w

19. Chen S, Yu Z, Fang J, Liu Y, Li S. Flavonoids in lotus (nelumbo) leaves evaluated by hplc–msn at the germplasm level. *Food Res Int.* (2013) 54:796–803. doi: 10.1016/j.foodres.2013.08.031

20. Wang Y, Li J, Dong L, Wu Q, Li L, Yang H, et al. Effects of thermal processing methods and simulated digestion on the phenolic content and antioxidant activity of lotus leaves. *J Food Process Preserv.* (2019) 43:e13869. doi: 10.1111/jfpp.13869

21. Zwa B, Yong C, Mza B, Zwa B, Fang Q, Yw C, et al. Lotus (*Nelumbo nucifera* gaertn) leaf: a narrative review of its phytoconstituents, health benefits and food industry applications – science direct. *Trends Food Sci Technol.* (2021) 112:631–50. doi: 10.1016/j.tifs.2021.04.033

22. Jia X, Zhang Q, Xu L, Yao W, Wei L. Lotus leaf flavonoids induce apoptosis of human lung cancer A549 cells through the ROS/p38 MAPK pathway. *Biol Res.* (2021) 54:7. doi: 10.1186/s40659-021-00330-w

23. Li C, Zhou Z, Long X, Pan Y, Wang R, Chen X, et al. Inhibitory effect of lotus leaf-enriched flavonoid extract on the growth of HT-29 colon cancer cells through the expression of PI3K-related molecules. *Biomed Res Int.* (2022) 2022:6770135. doi: 10.1155/2022/6770135

24. Zheng Y, Li Y. Physicochemical and functional properties of coconut (*Cocos nucifera* L) cake dietary fibres: effects of cellulase hydrolysis, acid treatment and particle size distribution. *Food Chem.* (2018) 257:135–42. doi: 10.1016/j.foodchem.2018.03.012

25. Luo X, Wang Q, Fang D, Zhuang W, Chen C, Jiang W, et al. Modification of insoluble dietary fibers from bamboo shoot shell: structural characterization and functional properties. *Int J Biol Macromol.* (2018) 120:1461–7. doi: 10.1016/j.ijbiomac.2018.09.149

26. Wang L, Xu H, Yuan F, Fan R, Gao Y. Preparation and physicochemical properties of soluble dietary fiber from orange peel assisted by steam explosion and dilute acid soaking. *Food Chem.* (2015) 185:90–8. 2015.03.112 doi: 10.1016/j.foodchem.2015.03.112

27. Sirisena S, Ng K. Ajlouni S. Antioxidant activities and inhibitory effects of free and bound polyphenols from date (*Phoenix dactylifera* L) seeds on starch digestive enzymes. *Int J Food Stud.* (2016) 5:212–23. doi: 10.7455/ijfs/5.2.2016.a9

28. Dong R, Yu Q, Liao W, Liu S, He Z, Hu X, et al. Composition of bound polyphenols from carrot dietary fiber and its *in vivo* and *in vitro* antioxidant activity. *Food Chem.* (2021) 339:127879. doi: 10.1016/j.foodchem.2020.127879

29. Tian W, Hu R, Chen G, Zhang Y, Wang W, Li Y. Potential bioaccessibility of phenolic acids in whole wheat products during in vitro gastrointestinal digestion and probiotic fermentation. *Food Chem.* (2021) 362:130135. doi: 10.1016/j.foodchem.2021.130135

30. Ye G, Wu Y, Liping W, Bin T, Shen W, Li X, et al. Comparison of six modification methods on the chemical composition, functional properties and antioxidant capacity of wheat bran. *LWT-Food Sci Technol.* (2021) 149:111996. doi: 10.1016/j.lwt.2021.111996

31. Wootton-Beard P, Moran A, Ryan L. Stability of the total antioxidant capacity and total polyphenol content of 23 commercially available vegetable juices before and after *in vitro* digestion measured by FRAP, DPPH, ABTS and Folin–Ciocalteu methods. *Food Res Int.* (2011) 44:217–24. doi: 10.1016/j.foodres.2010.10.033

32. Ma M, Mu T. Effects of extraction methods and particle size distribution on the structural, physicochemical, and functional properties of dietary fiber from deoiled cumin. *Food Chem.* (2016) 194:237–46. doi: 10.1016/j.foodchem.2015.07.095

33. Thielemans K, De Bondt Y, Van den Bosch S, Bautil A, Roye C. DeneyerA, et al. Decreasing the degree of polymerization of microcrystalline cellulose by mechanical impact and acid hydrolysis. *Carbohydr Polym.* (2022) 294:119764. doi: 10.1016/j.carbpol.2022.119764

34. Özkaya B, Turksoy S, Özkaya H, Duman B. Dephytinization of wheat and rice brans by hydrothermal autoclaving process and the evaluation of consequences for dietary fiber content, antioxidant activity and phenolics. *Innov Food Sc Emerg.* (2016) 39:209–15. doi: 10.1016/j.ifset.2016.11.012

35. Hua M, Lu J, Qu D, Liu C, Zhang L, Li S, et al. Structure, physicochemical properties and adsorption function of insoluble dietary fiber from ginseng residue: a potential functional ingredient. *Food Chem.* (2019) 286:522–9. 2019.01.114 doi: 10.1016/j.foodchem.2019.01.114

36. Huang J, Liao J, Qi J, Jiang W, Yang X. Structural and physicochemical properties of pectin-rich dietary fiber prepared from citrus peel. *Food Hydrocoll.* (2020) 110:106140. doi: 10.1016/j.foodhyd.2020.106140

37. Jiang G, Wu Z, Ameer K, Li S, Ramachandraiah K. Particle size of ginseng (*Panax ginseng* meyer) insoluble dietary fiber and its effect on physicochemical properties and antioxidant activities. *Appl Biol Chem.* (2020) 63:70. doi: 10.1186/s13765-020-00558-2

38. Song L, Qi J, Liao J, Yang X. Enzymatic and enzyme-physical modification of citrus fiber by xylanase and planetary ball milling treatment. *Food Hydrocoll.* (2021) 121:107015. doi: 10.1016/j.foodhyd.2021.107015

39. Speroni C, Bender A, Stiebe J, Ballus C, Emanuelli T. Granulometric fractionation and micronization: a process for increasing soluble dietary fiber content and improving technological and functional properties of olive pomace. *LWT-Food Sci Technol.* (2020) 130:109526. doi: 10.1016/j.lwt.2020.109526

40. Ago M, Endo T, Hirotsu T. Crystalline transformation of native cellulose from cellulose I to cellulose II polymorph by a ball-milling method with a specific amount of water. *Cellulose.* (2004) 11:163–7. doi: 10.1023/B:CELL.0000025423.32330.fa

41. Ullah I, Yin T, Xiong S, Huang Q, Din Z, Zhang J, et al. Effects of thermal pre-treatment on physicochemical properties of nano-sized okara (soybean residue) insoluble dietary fiber prepared by wet media milling. *J Food Eng.* (2018) 237:18–26. doi: 10.1016/j.jfoodeng.2018.05.017

42. Fu L, Geng S, Chen H, Yang Y, Zhang Y. Extraction of deoiled walnut dietary fibers and effects of particle sizes on the physiochemical properties. *Food Sci Technol.* (2018) 24:98190. doi: 10.3136/fstr.24.981

43. Jiang G, Bai X, Wu Z, Li S, Zhao C, Ramachandraiah K. Modification of ginseng insoluble dietary fiber through alkaline hydrogen peroxide treatment and its impact on structure, physicochemical and functional properties. *LWT-Food Sci Technol.* (2021) 150:11956. doi: 10.1016/j.lwt.2021.111956

44. Zhang Y, Qi J, Zeng W, Huang Y, Yang X. Properties of dietary fiber from citrus obtained through alkaline hydrogen peroxide treatment and homogenization treatment. *Food Chem.* (2020) 311:125873. doi: 10.1016/j.foodchem.2019.125873

45. Zheng Y, Wang X, Tian H, Li Y, Shi P, Guo W, et al. Effect of four modification methods on adsorption capacities and in vitro hypoglycemic properties of millet bran dietary fibre. *Food Res Int.* (2021) 147:110565. doi: 10.1016/j.foodres.2021.110565

46. Jiang Z, Mu S, Ma C, Liu Y, Ma Y, Zhang M, et al. Consequences of ball milling combined with high-pressure homogenization on structure, physicochemical and rheological properties of citrus fiber. *Food Hydrocoll.* (2022) 127:107515. doi: 10.1016/j.foodhyd.2022.107515

47. Li Q, Yang S, Li Y, Xue X, Huang Y, Luo H, et al. Comparative evaluation of soluble and insoluble-bound phenolics and antioxidant activity of two Chinese mistletoes. *Molecules.* (2018) 23:359. doi: 10.3390/molecules23020359

48. Nignpense B, Francis N, Blanchard C, Santhakumar A. Bioaccessibility and bioactivity of cereal polyphenols: a review. *Foods.* (2021) 10:1595. doi: 10.3390/foods10071595

49. Huang H, Chen J, Hu X, Chen Y, Xie J, Ao T, et al. Elucidation of the interaction effect between dietary fiber and bound polyphenol components on the anti-hyperglycemic activity of tea residue dietary fiber. *Food Funct.* (2022) 13:2710–28. doi: 10.1039/D1FO03682C

50. Yang Y, Li W, Xian W, Huang W, Yang R. Free and bound phenolic profiles of Rosa roxburghii tratt leaves and their antioxidant and inhibitory effects on α-glucosidase. *Front Nutr.* (2022) 9:922496. doi: 10.3389/fnut.2022.922496

51. Luo M, Hou F, Dong L, Huang F, Zhang R, Su D. Comparison of microwave and high-pressure processing on bound phenolic composition and antioxidant activities of sorghum hull. *Int J Food Sci Technol.* (2020) 55:3190–202. doi: 10.1111/ijfs.14583

52. Liao L, Chen J, Liu L, Xiao A. Screening and binding analysis of flavonoids with alpha-amylase inhibitory activity from lotus leaf. *J Brazil Chem Soc.* (2018) 29:587–93. doi: 10.21577/0103-5053.20170171

frontiers | Frontiers in Nutrition

TYPE Original Research
PUBLISHED 30 March 2023
DOI 10.3389/fnut.2023.1139698

OPEN ACCESS

EDITED BY
Khalid Gul,
University of Leeds, United Kingdom

REVIEWED BY
Manreet Singh Bhullar,
Kansas State University, United States
Viduranga Y. Waisundara,
Australian College of Business and Technology, Sri Lanka

*CORRESPONDENCE
Runqiang Yang
✉ yangrq@njau.edu.cn

SPECIALTY SECTION
This article was submitted to Nutrition and Food Science Technology, a section of the journal Frontiers in Nutrition

RECEIVED 07 January 2023
ACCEPTED 15 March 2023
PUBLISHED 30 March 2023

CITATION
Wang M, Liu G, Guo T, Xie C, Wang P and Yang R (2023) UV-B radiation enhances isoflavone accumulation and antioxidant capacity of soybean calluses.
Front. Nutr. 10:1139698.
doi: 10.3389/fnut.2023.1139698

UV-B radiation enhances isoflavone accumulation and antioxidant capacity of soybean calluses

Mian Wang, Guannan Liu, Tianwei Guo, Chong Xie, Pei Wang and Runqiang Yang*

College of Food Science and Technology, Nanjing Agricultural University, Nanjing, Jiangsu, China

Isoflavones are a class of flavonoids that belong to a large family of polyphenols and synthesized predominantly in legume, and they play important roles including acting as antioxidant, preventing osteoporosis, reducing the risk of atherosclerosis, and protecting against cardiovascular disease. This study focused on the accumulation and synthetic metabolism of isoflavone in soybean hypocotyl and cotyledon calluses under UV-B radiation. The results showed that UV-B radiation significantly up-regulated the gene expression of phenylalanine ammonia lyase (PAL), cinnamate-4-hydroxylase (C4H), 4-coumarate-CoA ligase (4CL), chalcone ketone synthase (CHS), chalcone isomerase (CHI), and isoflavone synthase (IFS), and enhanced their activity in soybean hypocotyl and cotyledon calluses. As a result, isoflavones content increased by 21.23 and 21.75% in soybean hypocotyl and cotyledon calluses, respectively. Among the isoflavones produced, malonyldaidzin was the dominant one in hypocotyl callus, while malonylglycitin and daidzein were the main isoflavones in cotyledon calluses. This study revealed that UV-B radiation induced isoflavone accumulation in soybean calluses, which could be an efficient strategy to improve the nutritional value of food and produce high levels of bioactive secondary metabolites.

KEYWORDS

UV-B radiation, isoflavone, soybean callus, antioxidant capacity, physiological metabolism

1. Introduction

Soybeans (*Glycine max* L.) are a major economic crop that provide high-quality protein and other bioactive metabolites. Isoflavones are the main secondary metabolites in soybean, and they are related to plant defense responses and health-related benefits for human (1). Isoflavones are synthesized from phenylalanine and can be divided into four groups (12 different monomers): aglycones (include daidzein, genistein and glycitein), glycosides (include daidzin, genistin, and glycitin), malonylglycosides (include malonyldaidzin, malonylgenistin, and malonylglycitin), and acetylglycosides (include acetyldaidzin, acetylgenistin, acetylglycitin) (2). Among them, glycosides and malonylglycosides account for 97–98% of total isoflavone in soybean (2), and

acetylglycosides are present in very low quantities. The content of isoflavone in soybean seeds is typically 0.2−1.6 mg/g dry weight (DW) (3).

Abiotic stress is usually used to enrich bioactive metabolites in plants. Ultraviolet B (UV-B, 280−315 nm) radiation can cause physiological and biochemical changes in plants by damaging photosynthesis tissues and altering DNA structure of cells. It up-regulates key genes expression involved in the phenylpropanoid metabolic pathway, leading to the increased enzymes activity and enhanced synthesis of isoflavone (4). Plant calluses grows rapidly, and has the ability to synthesize isoflavone. Calluses can be easily cultivated in controlled conditions and are not susceptible to external environment. Therefore the tissue culture technique is often used to promote the synthesis of secondary metabolites, such as isoflavone, paclitaxel, alkaloids, carotene, and glucosinolate (5). At present, the combination of tissue culture technique and UV-B radiation treatment has been extensively used to enrich biological metabolites to improve the nutritional value of food. Mohajer et al. (6) found that the survival rate of sainfoin (*Onobrychis viciifolia* Scop.) seeds decreased significantly under UV-B radiation, but flavonoids and phenolics content in their calluses increased. The effect of UV-B radiation on phenolic compounds, total flavonoids content and antioxidant capacity of *in vitro* grown *Echium orientale* L. shoots and calli was investigated (7). Phenolics and flavonoids content, especially rosmarinic acid and quercetin, increased in callus extracts of *Echium orientale* L. which were harvested after 1 week of UV-B treatment, resulting in the enhancement of their antioxidant activity (7). Besides, tempisque (*Sideroxylon capiri* Pittier) is classified as an endangered species and has a high level of phenolics and flavonoids in its leaves. Phenolics and flavonoids content increased in the fourth week with 4 h of UV-B exposure per day, and the highest concentrations of quercetin (230 μg/g DW), kaempferol (235 μg/g DW) and gallic acid (240 μg/g DW) were found in callus obtained from leaves explants (8). Mata-Ramírez et al. (9) evaluated the quantification and bioactivity of isoflavone in soybean callus submitted to UV-light stresses. It was found that UVC-light stress increased genistein-O-glucoside and genistein-O-glucosyl-malonate to 122 and 196% in soybean callus, respectively, resulting in the enhancement of anti-inflammatory and antioxidant activity in calluses. Therefore, the combination of tissue culture technique and UV-B radiation treatment is one of the effective ways to obtain bioactive compounds. This method is not affected by climate fluctuations, and reduce dependence on land and other natural resources. Besides, it ensures the consistency between production batch under controlled conditions.

Previous researches have explored the use of tissue culture technique combined with UV-B radiation to obtain biological metabolites. However, there are scarce reports about the effects of UV-B radiation on the accumulation of isoflavones in soybean calluses, as well as the composition and content of isoflavones in different soybeans calluses. The vitality of key enzymes in different soybean calluses is also unclear. Thus, the aim of this study was to investigate the formation of soybean hypocotyl and cotyledon calluses, assess the effects of UV-B radiation on the activity and gene expression of key enzymes in isoflavone synthesis, and analyze the composition and content of isoflavone, as well as their antioxidant activity. This study can help to improve the productivity of secondary metabolites with biological activity, and provide an efficient strategy for improving the nutrition quality of soybean-based processed food.

2. Materials and methods

2.1. Chemicals

Soybean seeds (*Glycine max* L., cultivar Dongnong, 2021) were provided by Jiangsu Academy of Agricultural Sciences, China, and stored at −20°C. This variety was selected from several soybeans according to the content of isoflavones. All reagents and solvents were analytical or higher grade and purchased from Sigma (Sigma-Aldrich GmbH, Shanghai, China), Sinopharm (Sinopharm Chemical Reagent GmbH, Shanghai, China) and Maclean (Maclean Biotechnology GmbH, Shanghai, China), including Murashige and Skoog (MS) basal medium, 1/2 MS medium (without sugar and agar), 2, 4-dichlorophenoxyacetic acid (2, 4-D), 6-Benzylaminopurine (6-BA), sucrose, agar, acetonitrile, 1,1-diphenyl-2-trinitrophenyl hydrazine (DPPH), 2,2-diazo-di (3-ethyl-benzothiazole-6-sulfonic acid) diammonium salt (ABTS) and 6-hydroxy-2,5,7,8-tetramethylchromone-2-carboxylic acid (Trolox), methanol (AR), ethyl acetate, cinnamic acid, coenzyme A (CoA), coumaric acid, L-phenylalanine, rutin, gallic acid, etc.

2.2. Plant material and surface sterilization

Soybeans were exposed to sodium hypochlorite (1%) for 15 min and manual oscillation, then rinsed in distilled water. Seeds were dipped into ethanol 75% (v/v) solution for 5 min, and washed with distilled water for 4−5 times. Finally, they were submerged in anhydrous ethanol for 30 s. After that, seeds were inoculated in the 1/2 Murashige and Skoog salt mixture (1/2 MS) media (with 3% sucrose + 0.7% agar, Ph 5.8) at 25°C for 2 days. Then, they were cultivated in the Murashige and Skoog salt mixture (MS) media (with 3% sucrose + 0.7% agar, pH 5.8) for 4 days (16 h/8 h light/dark). The 6-day-old sterile soybean sprouts were used to obtain hypocotyl and cotyledon.

2.3. Elicitation of soybean hypocotyl and cotyledon calluses

Optimization of hormone concentration in induced medium: Samples (hypocotyls or cotyledons) were separated from the 6-day-old sterile soybean sprouts, and cut into slices with a thickness of about 2 mm, flat side up, and then placed on Murashige and Skoog salt mixture (MS) media (with 3% sucrose + 0.7% agar, pH5.8). Explants were cultured at 25°C in light (16/8 h light/dark) and subcultured on the same medium every 7 days until the callus formation was observed (28 days). Five calluses were placed on per petri dish (90 × 20 mm). The hormones in the MS media were 2, 4-D (1 and 2 mg/L) and 6-BA (0.5 mg/L). The concentration and ratio of hormones were determined based on the growth state and total isoflavone content of callus (**Supplementary Table 2**).

Determination of UV-B radiation intensity: Calluses were cultivated for 28 days and then were treated with UV-B (Intensities: 20, 40 and 80 μW/cm^2, respectively) (Beijing Electric Power Source Research Institute, Beijing, China) at 25°C for 2 h, respectively. After that, calluses were kept in the same incubation conditions for 48 h in the dark. Isoflavone content was measured to determine the optimal UV-B radiation intensity (**Supplementary Table 3**). Soybean callus without UVB-light exposure was considered as the control.

Determination of re-incubation time: Soybean calluses were cultivated for 28 days and then irradiated by 40 μW/cm^2 UV-B for 2 h. Then, calluses were kept in the same incubation conditions for 0, 6, 12, 24, 36, 48 h in the dark. Isoflavone content was measured to determine the optimal re-incubation time (**Supplementary Table 4**).

2.3.1. Cultivation condition and treatments

Hypocotyls and cotyledons were separated from the 6-day-old sterile soybean sprouts, and cut into slices with a thickness of about 2 mm, flat side up, then cultured on MS media with 3% sucrose, 0.7% agar supplemented with 1 mg/L 2, 4-D and 0.5 mg/L 6-BA (pH 5.8) at 25°C in light (16 h/8 h light/dark) for 28 days. The medium was changed every 7 days. Calluses were irradiated by 40 μW/cm^2 UV-B for 2 h, then re-incubated for 12 h in the dark (T). Soybean calluses without UVB-light exposure were considered as the control (CK). Afterward, some of calluses were frozen-dried and milled to powder in an electric mill (A11 Basic Analytical Mill, IKA, Guangzhou, Guangdong, China), stored at −20°C for further measurements. The remaining calluses were frozen with liquid nitrogen and stored at −80°C until analysis.

2.4. Determination of malondialdehyde content and electrolyte leakage

Malondialdehyde (MDA) content of soybean calluses was determined as previously reported by Wang et al. (10) with some modifications. The absorbance values of samples were measured at 450 nm, 532 nm, and 600 nm, respectively. The MDA content was expressed as nmol/g fresh weight (FW).

To determine the electrolyte leakage of soybean calluses, 1.0 g of the samples were cut into small pieces (3 × 3 × 3 mm^3), and immersed in 30 mL of distilled water, then shaken at 25°C for 1 h. The conductivity was measured as EC_1. The reaction liquid was boiled for 10 min to inactivate the plant tissue. After cooling, the volume was adjusted to 30 mL, and the boiling conductivity was measured as EC_2. Electrolyte permeability (%) = (EC_1/EC_2) × 100%.

2.5. Growth parameters

The biomass of soybean calluses was determined by drying at 50°C until reaching a constant weight. The dry weight was measured every 3 days, and then the growth curve of hypocotyl and cotyledon calluses were plotted, respectively. There were three calluses in each dish.

2.6. Morphological observation

Sample materials and dehydration: Soybean calluses were cut into 3 × 3 × 3 mm^3 small pieces and immersed in FAA solution (70% ethanol: ice acetic acid: 38% formaldehyde = 18: 1: 1) for 48 h. Then, samples were dehydrated with 70% ethanol for 30 min, 85% ethanol for 30 min, 95% ethanol for 30 min, and ethanol for 20 min in order.

Waxing, embedding and producing: Samples were immersed in wax and kept at 42°C for 24 h, then heated at 58°C to remove dimethylbenzene. The wax was changed every 6 h. After that, samples were embedded and produced according to the method of paraffin slices (11). The thickness of each slice was 10 μ m.

Dewaxing and dyeing: The slices were dewaxed with dystershopine for 40 min, ethanol for 10 min, 75% alcohol for 5 min, and then washed with distilled water. The slices were dyed in the Safranin O solution for 2 h, washed with distilled water, and then immersed in 50, 70, and 80% of alcohol for 5 s in order. After that, the slices were immersed in fast green stain for 30 s, dehydrated with ethanol, and finally immersed in dimethylbenzene for 5 min, sealed and fixed with optics resin. The cell morphological structure of soybean calluses was observed in optical microscope (Eclipse Ci-L, Nikon, Chiyoda, Tokyo, Japan).

2.7. Quantification of total flavonoids content

The 0.05 g of frozen-dried sample was shaken at 25°C for 1 h with 80% methanol, centrifuged at 10,000 × *g* for 15 min at 4°C, and then the supernatant was collected. Three replicates were conducted and the supernatant was filtered. The filtrates were evaporated and concentrated at 40°C. The residue was dissolved with 50% methanol to 5 mL as free phenolic solution (FPS), and finally stored at −20°C until analysis.

After the extraction of FPS, the residue was shaken with 2 mol/L of NaOH at 25°C for 4 h, and pH was adjusted to 1.6−1.8. The sample was extracted with ethyl acetate for 15 min at room temperature, then centrifuged at 10,000 × *g* for 15 min at 4°C. The ethyl acetate layer was collected. Three replicates were conducted, and the combined supernatant was evaporated to dry at 40°C, and dissolved with 50% methanol to 5 mL, as bound phenolic solution (BPS), finally stored at −20°C until analysis.

Determination of total flavonoid content was based on the method described by Miliauskas et al. (12) using soybean calluses as experimental samples and rutin as the standard. Results were expressed as milligram (mg) of rutin equivalents (RE) per 100 g of DW.

2.8. Determination of antioxidant capacity

2,2-diazo-di (3-ethyl-benzothiazole-6-sulfonic acid) diammonium salt and 1,1-diphenyl-2-trinitrophenyl hydrazine radical scavenging activities of soybean calluses were measured as described by Chen et al. (13) using FPS and BPS as samples

and Trolox as the standard. They were expressed as micromole of Trolox equivalents per gram (g) of DW.

2.9. Identification and quantification of isoflavone by high-performance liquid chromatography

Soybean callus extract preparation: 100 mg of callus was weighed and mixed with 5 mL 80% (v/v) methanol, and then sonicated for 15 min at 40°C. After sonication, samples were centrifuged at 10,000 × *g* for 10 min at 4°C, and the supernatants were filtered with a 0.45 μm membrane filter for Agilent 1200 HPLC system (Agilent Technologies Co., Ltd., Santa Clara, CA, USA). Typical HPLC chromatograms of nine isoflavone monomers in soybean hypocotyl and cotyledon calluses were shown in **Supplementary Figure 2**. The mixed standard concentration selected in this study was 3.2, 6.4, 12.8, 25.6, and 51.2 μ g/mL.

A reversed phase column (Ultimate AQ-C18, 4.6 × 250 mm, 5 μm particle size) was used. Mobile phase A consisted of 0.1% acetic acid in water, and mobile phase B consisted of 0.1% acetic acid in acetonitrile. A 52 min gradient was programmed as follows: 0−50 min, 13−35% B; 50−51 min, 35−13% B; 51−52 min, 13% B. The column temperature maintained at 35°C. The injection volume was 20 μL and the flow rate was 1.0 mL/min. The measurement wavelength was 260 nm.

2.10. Determination of key enzymes activity in isoflavone synthesis

Determination of phenylalanine ammonia lyase (PAL), cinnamate-4-hydroxylase (C4H) and 4-coumarate-CoA ligase (4CL) activity was based on the method of Ma et al. (14) with slight modification. The activity was expressed as U/g FW.

The activity of chalcone ketone synthase (CHS), chalcone isomerase (CHI), and isoflavone synthase (IFS) was determined using CHS ELISA Kit (MBE21206), CHI ELISA Kit (MBE21201), and IFS ELISA Kit (MBE21199), respectively. The kits were all from Nanjing Jiancheng Institute of Biological Engineering (Nanjing, China). The 1.0 g of soybean calluses were full ground with 5 ml 9% physiological saline, centrifuged at 3,500 × *g* for 15 min at 4°C. The supernatant was collected, and analyzed according to the instructions. The activity was expressed as IU/g FW.

2.11. Quantitative RT-PCR

Total RNA isolation and real-time PCR were conducted according to Wang et al. (15) the reference gene was *En- longation Factor 1b* (*EF1b*). The primers for real-time PCR analysis of *PAL*, *C4H*, *4CL*, *CHS*, *CHI*, *IFS,* and *EF1b* were designed using Primer 5.0 primer design software according to primers published on NCBI, synthesized by GenScript Biotechnology Co., Ltd. (Nanjing, China). The detected genes and sequences of primers were listed in **Supplementary Table 1**.

2.12. Statistical analysis

Experimental data were expressed as mean ± standard deviation (SD) with three replications ($n \geq 3$). SPSS 18.0 (SPSS Inc., Chicago, IL, USA) was applied for significant difference tests. Data were analyzed by Duncan's multiple-range tests at $p < 0.05$.

3. Results

3.1. Physiological metabolism of soybean calluses under UV-B radiation

The soybean hypocotyl and cotyledon calluses were cultured for 28 days (**Supplementary Figures 1A, B**), and their biomass increased significantly from days 3−18 (**Supplementary Figures 1C, D**). When exposed to UV-B radiation, the cells were swollen and occasionally ruptured in soybean calluses (**Figure 1A**). Besides, MDA content in soybean cotyledon calluses significantly increased by 15.74% compared with the control (CK), and was higher than the content of hypocotyl callus (**Figures 1B, C**). However, there was no significant difference on the electrolyte permeability in soybean hypocotyl and cotyledon calluses.

3.2. Total flavonoids content and antioxidant capacity of soybean calluses

Total flavonoids content and the antioxidant activity of soybean calluses are shown in **Figure 2**. The content of free, bound and total flavonoids content increased by 12.81, 15.47, and 13.83% in soybean hypocotyl calluses under UV-B radiation, respectively, compared with the control (**Figure 2A**). And the content of free, bound and total flavonoids content significantly increased by 72.73, 81.25, and 76.54% in soybean cotyledon calluses under UV-B radiation, respectively. Results showed that total flavonoid content was higher in hypocotyl calluses, but cotyledon calluses were more sensitive to UV-B radiation to accumulate isoflavone.

The effects of UV-B on the *vitro* antioxidant properties of soybean calluses were represented by ABTS (B) and DPPH (C) radical scavenging ability (**Figures 2B, C**). The antioxidant capacity of phenolics increased significantly ($p < 0.05$) under UV-B radiation, especially free phenolics. As shown in **Figure 2B**, ABTS free radical scavenging ability of free phenolics increased by 18.85 and 18.32% in soybean hypocotyl and cotyledon calluses under UV-B radiation, respectively, compared with the control (**Figure 2B**). There was no significant difference on the ABTS free radical scavenging ability of bound phenolics in soybean calluses. The DPPH free radical scavenging capacity of free phenolics significantly increased by 106.16 and 14.49% in soybean hypocotyl and cotyledon calluses under UV-B radiation, respectively, compared with the control (**Figure 2C**). And the DPPH free radical scavenging capacity of bound phenolics improved only in soybean hypocotyl callus, increased by 83.33% compared with the control. Indicating that UV-B radiation could significantly promote the synthesis of total

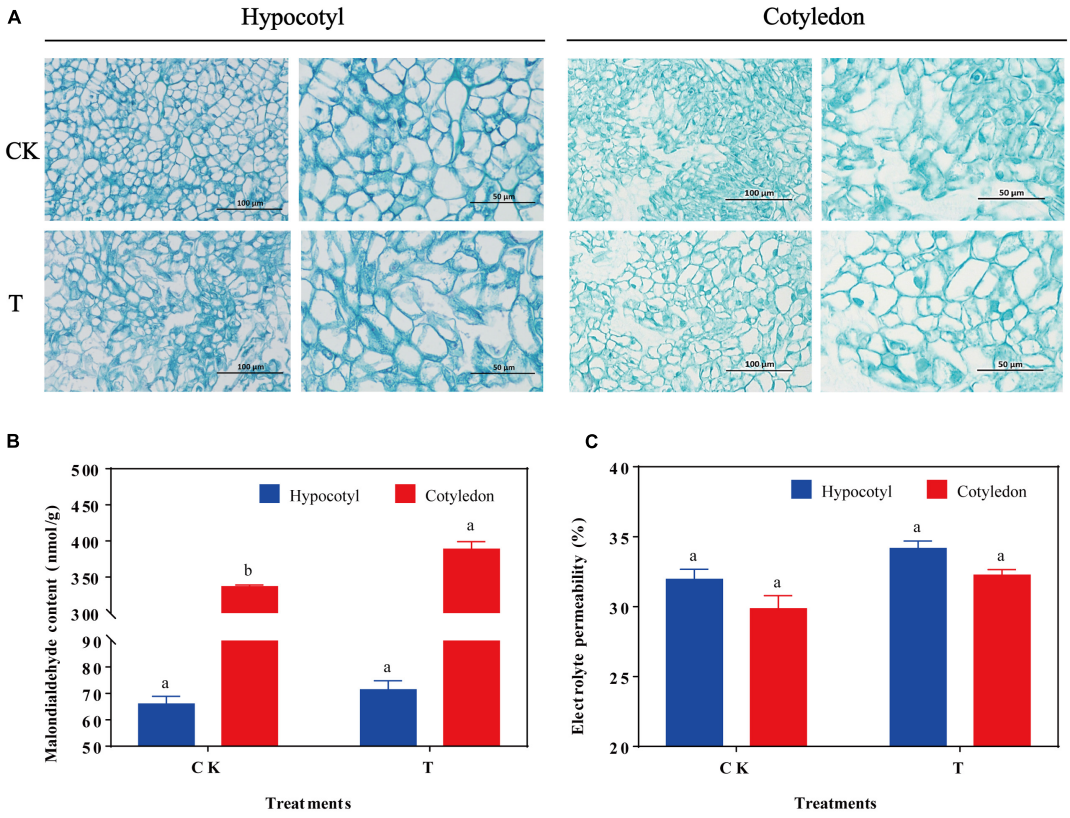

FIGURE 1
Effects of UV-B on cell structure **(A)**, MDA content **(B)**, and electrolyte leakage **(C)** of soybean hypocotyl and cotyledon calluses. The lower case letters indicated significant difference at $p < 0.05$ between treatments, *T*-test was used for data analysis. The data were presented as mean ± SD, $n = 3$.

flavonoids, and improve cellular antioxidant activity in soybean calluses.

3.3. Isoflavone composition and content in soybean calluses

The content of individual isoflavone in soybean hypocotyl and cotyledon calluses under UV-B radiation is shown in Table 1. Nine major isoflavones were detected, including three groups: aglycones (daidzein, genistein, and glycitein), glycosides (daidzin, genistin, and glycitin), and malonylglycosides (malonyldaidzin, malonylgenistin, and malonylglycitin). Compared with the control, isoflavone content increased by 21.23 and 21.75% in soybean hypocotyl and cotyledon calluses under UV-B radiation, respectively. The contents of individual isoflavone in different soybean calluses varied. In soybean hypocotyl callus, the content of daidzin, genistin, malonyldaidzin and malonylglycitin increased, but malonylgenistin content decreased compared with the control. Glycitin, daidzein, glycitein and genistein were not detected. In soybean cotyledon callus, four kinds of individual isoflavone including malonyldaidzin, malonylglycitin, daidzein and glycitein showed the relatively higher content compared with the control. And there was no significant difference in the content of glycitin and genistin. Daidzin, malonylgenistin and genistein were not detected.

3.4. The key enzyme activity

The synthesis of isoflavone is related to the key enzyme activity and its gene expression level in the synthetic metabolic pathway. The activity of PAL, C4H, 4CL, CHS, CHI, and IFS in soybean calluses was investigated (Figure 3). In soybean hypocotyl callus, the activity of PAL, C4H, 4CL, CHS, CHI, and IFS increased by 14.08, 38.07, 13.53, 38.75, 31.37, and 26.08% compared with the control, respectively. And the activity of PAL, C4H, CHS, CHI, and IFS significantly increased by 35.83, 33.13, 40.28, 101.14, and 47.42% in soybean cotyledon calluses under UV-B radiation, respectively, compared with the control. But there was no difference on the 4CL activity between the treatment and control group.

3.5. The gene expression of key enzymes

The relative expression of *PAL*, *C4H*, *4CL*, *CHS*, *CHI*, and *IFS* in soybean calluses was generally consistent with their activity (Figure 4). The relative expression of *PAL*, *C4H*, *C4H1*, *CHS*, *CHI1A*, *CHI4A*, *IFS1*, and *IFS2* increased by 67.33, 47.00, 55.00, 46.54, 53.39, 32.67, 52.38, and 50.50% in soybean hypocotyl callus under UV-B radiation, respectively. There was no significant difference on *4CL* expression in soybean hypocotyl callus (Figure 4C). Interestingly, *4CL3* and *CHI1B* expression significantly reduced by 38.61 and 69.00%, respectively, compared

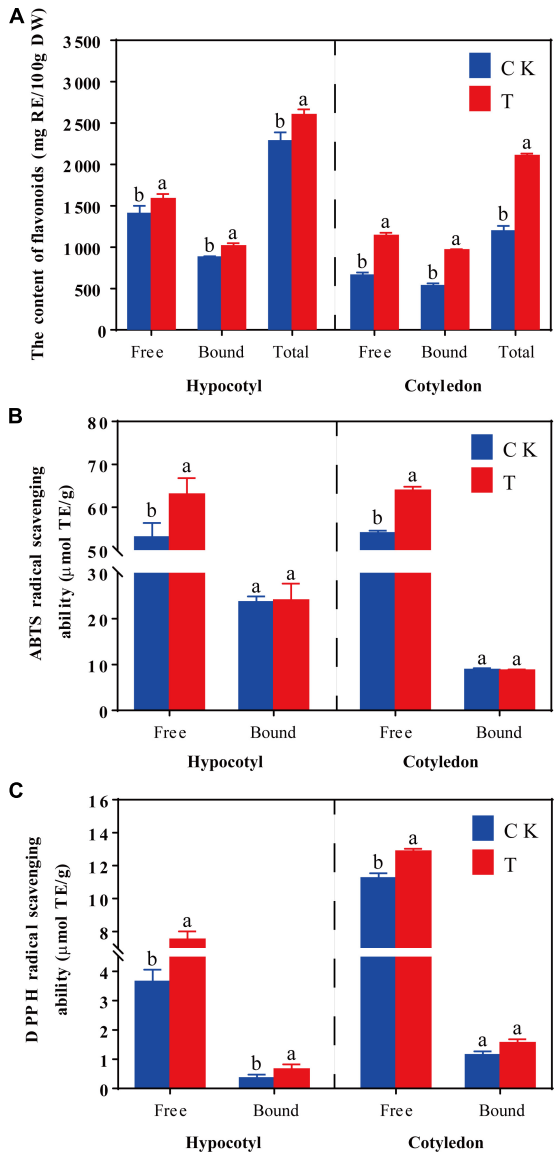

FIGURE 2
Effects of UV-B on the flavonoids content **(A)**, ABTS **(B)**, and DPPH **(C)** radical scavenging activity of soybean hypocotyl and cotyledon calluses. The lower case letters indicated significant difference at $p < 0.05$ between treatments, and *T*-test was used for data analysis. The data were presented as mean ± SD, $n = 3$.

with the control (Figures 4C, E). Besides, the relative expression of *C4H*, *C4H1*, *4CL3*, *CHS*, *CHI1A*, *CHI1B*, *CHI4A*, *IFS1*, and *IFS2* increased by 60.00, 59.41, 679.21, 66.34, 74.26, 36.45, 220.79, 113.86, and 101.98% in soybean cotyledon callus under UV-B radiation, respectively. And there was no significant difference on *PAL* and *4CL* expression.

4. Discussion

Ultraviolet B radiation caused oxidative damages of cells and affected the synthesis of various bioactive metabolites in soybean calluses (Figures 1, 2). Total flavonoids content increased by 13.84 and 76.54% in soybean hypocotyl and cotyledon calluses under UV-B radiation, respectively, as well as their antioxidant activity (Figure 2), indicating that the accumulation of flavonoids is the result of plant stress resistance (16). UV-B significant effects on some physiological indicators, antioxidant activity, and endogenous hormone levels during the growth and development of plants (17). Alvero-Bascos and Ungson (18) revealed that the level of three flavonoids (apigenin, vitexin, and isovitexin) was 20-fold higher than the control in callus cultures of jatropha (*Jatropha curcas* L.) exposed to UV-B (12.6 and 25.3 kJ/m^2). Besides, many phenolic compounds were synthesized *in vitro*-grown plant materials in *Echium orientale* L under UV-B radiation, especially rosmarinic acid and quercetin (7), and their concentrations were highly correlated with the antioxidant activity (19). Applying ultraviolet radiation has been a simple and effective technology to biofortify plant tissue with secondary metabolites (20). Hence, UV-B radiation was necessary for the synthesis of flavonoids and some other plant secondary metabolites in plant cells and tissues.

Ultraviolet B radiation (40 μW/cm^2) induced the synthesis of isoflavones, and their content increased significantly by 21.23 and 21.75% in soybean hypocotyl and cotyledon calluses, respectively, (Table 1). Previous study has shown that total isoflavone content is about 8,000 μg/g in 4-day-old soybean sprout under UV-B treatment (3), but it is up to half of the entire soybean sprout in each callus. It might due to the stress resistance capacity of plants varies between different development stages under UV-B radiation (21). Plants are more sensitive to UV-B during the early stage of development. Because the epidermal cell wall is thin and the stability of genes is low. Also, the effects are related to UV-B radiation intensity and radiation time (22). Therefore, the combination of tissue culture technique and UV-B radiation treatment is an effective way to enrich biological metabolites, such as isoflavone. In addition, callus culture technique cannot be affected by the external environment, with the advantages of conditional controlling, stable process, and resource consumption reduction.

The content of total isoflavone was basically same in soybean hypocotyl and cotyledon calluses under UV-B irradiation. However, the composition and content of individual isoflavone was different (Table 1; Supplementary Figure 2). Four individual isoflavones content was higher in soybean hypocotyl callus, including daidzin, genistin, malonyldaidzin and malonylglycitin. Malonylglycosides were the main isoflavone. Interestingly, glycitin, genistin, malonyldaidzin, malonylglycitin, and daidzein was detected in soybean cotyledon callus (Supplementary Figure 2). Compared with isoflavone in soybean hypocotyl callus, the types of isoflavone was more abundant in soybean cotyledon callus, and their content increased significantly under UV-B radiation (Table 1). The difference in isoflavone composition and content of soybean callus might be resulted from the specific sensitivity of different tissues to UV-B irradiation (23). The biosynthesis of isoflavone is also related to the degree of differentiation, soybean varieties and environmental conditions (24). In addition, soybean callus, with well growth and division ability, is a kind of undifferentiated parenchymatous cells. The function of individual isoflavone is different in soybean callus. Glycosidic isoflavone, which is mainly used to form cell parenchyma or organelle membrane to maintain the structural stability of cells, is abundant in callus (1). UV-B radiation can accelerate the conversion between malonyl-glycosidic and glycosidic isoflavone

TABLE 1 The content of individual isoflavone (μg/g) in soybean calluses under UV-B radiation.

Isoflavone	Hypocotyl		Cotyledon	
	CK	UV-B	CK	UV-B
Daidzin	74.81 ± 0.88[b]	161.89 ± 9.15[a]	ND	ND
Glycitin	ND	ND	201.86 ± 14.51[a]	188.45 ± 10.55[a]
Genistin	82.02 ± 1.87[b]	102.01 ± 1.42[a]	135.78 ± 4.42[a]	146.93 ± 4.80[a]
Malonyldaidzin	1,696.05 ± 33.72[b]	2,400.35 ± 107.78[a]	119.57 ± 3.56[b]	149.89 ± 8.30[a]
Malonylglycitin	ND	78.37 ± 3.77[a]	1,943.29 ± 6.38[b]	2,374.03 ± 9.24[a]
Malonylgenistin	1,141.39 ± 68.62[a]	887.43 ± 27.64[b]	ND	ND
Daidzein	ND	ND	747.73 ± 7.52[b]	908.80 ± 29.10[a]
Glycitein	ND	ND	ND	64.78 ± 2.77[a]
Genistein	ND	ND	ND	ND
Total	2,994.28 ± 35.89[b]	3,630.05 ± 131.46[a]	3,148.23 ± 0.25[b]	3,832.88 ± 64.77[a]

Effects of UV-B on the content of individual isoflavone in soybean hypocotyl and cotyledon calluses. ND meant not detected. The lower case letters in the same row indicated significant difference at $p < 0.05$ between CK and UV-B in the same callus. *T*-test was used. The data were presented as mean ± SD, $n = 4$.

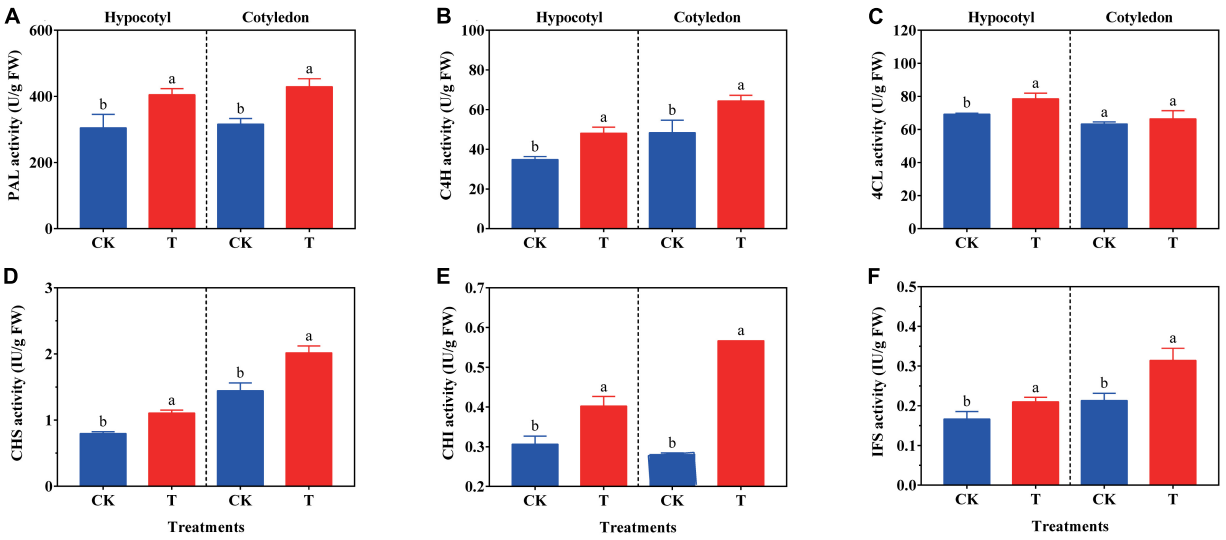

FIGURE 3
Effects of UV-B on PAL **(A)**, C4H **(B)**, 4CL **(C)**, CHS **(D)**, CHI **(E)**, and IFS **(F)** activity of soybean calluses. The lower case letters indicated significant difference at $p < 0.05$ between treatments, and *T*-test was used for data analysis. The data were presented as mean ± SD, $n = 3$.

(25). Daidzein and genistein, which could induce nod gene to activate nodulation process (26), were related to the regulation of bacterial communities in soybean root, so their contents were lower in soybean hypocotyl and cotyledon calluses (Table 1). Hence, the response of soybean hypocotyl and cotyledon calluses to UV-B radiation was different. According to their characteristics and specific sensitivity to UV-B, soybean callus can be used to enrich specific isoflavone as needed.

The composition and content of isoflavone was related to the regulation of activities and gene expression levels of PAL, C4H, 4CL, CHS, CHI, and IFS in isoflavone biosynthetic pathway (Figures 3, 4). Isoflavones could be accumulated by positively regulating the activity of key enzymes in soybean hypocotyl and cotyledon calluses exposed to UV-B compared with the control (Figure 3), especially CHS, CHI and IFS activity. The relative expression of key enzymes was basically consistent with their activity (Figure 4). PAL is the initial enzyme of phenylpropane metabolic pathway, including ten genes encoding for PAL found in the *L. japonicus* genome (27). All the genes encoding for enzymes of isoflavone pathway can be strongly induced under UV-B radiation, especially *LjPAL1*. Reports have shown that the transcription levels of *C4H*, *4CL*, and *IFS1* also increased significantly in soybean induced by UV-B stress, promoting the accumulation of polyphenols including *p*-coumaric acid, cinnamic acid and isoflavone (27). Besides, CHS, which connected phenylpropane metabolic pathway and isoflavone biosynthetic pathway, plays a vital role in the synthesis of isoflavone biosynthetic precursor molecules (naringenin chalcone and isoliquiritigenin) (28). UV-B radiation could stimulate the expression of *GmCHS1*, *GmCHS3*, *GmCHS4*, *GmCHS6*, and *GmCHS7* in soybean hypocotyl, improve the synthesis rate of naringenin chalcone and isoliquiritigenin, and promote the accumulation of daidzein, genistein and other

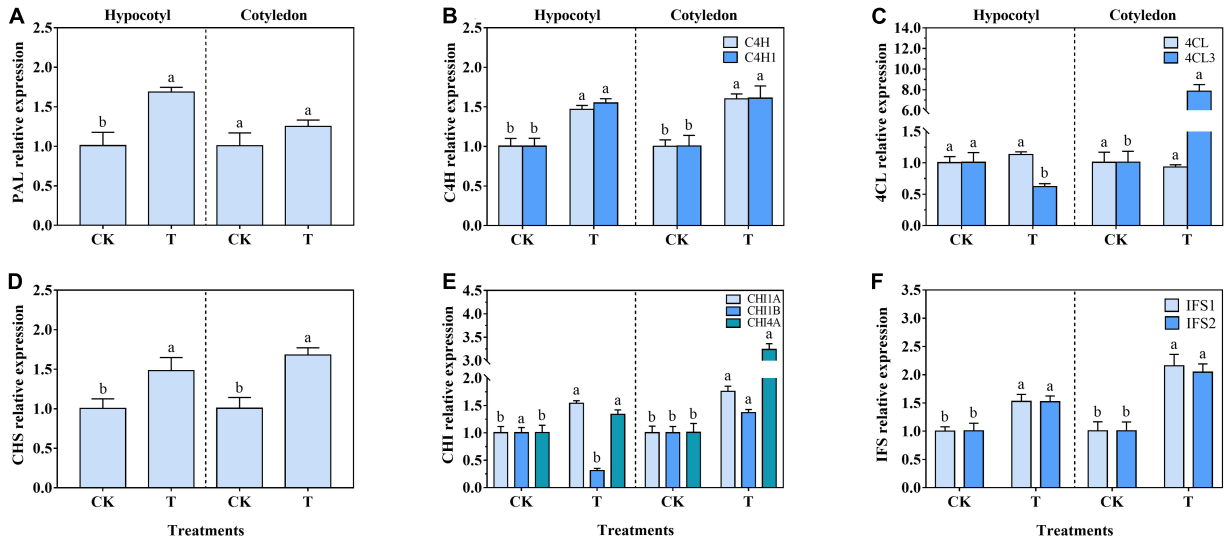

FIGURE 4
Effects of UV-B on PAL **(A)**, C4H **(B)**, 4CL **(C)**, CHS **(D)**, CHI **(E)**, and IFS **(F)** relative expression of soybean calluses. The lower case letters indicated significant difference at $p < 0.05$ between treatments, and *T*-test was used. The data were presented as mean ± SD, $n \geq 3$.

isoflavone monomers (29). The activity and expression of CHS was up-regulated in soybean hypocotyl and cotyledon calluses under UV-B radiation (**Figures 3D**, **4D**), promoting the transformation of 4-coumarinyl-CoA into isoflavone synthesis pathway. *IFS1* and *IFS2* plays a catalytic role in isoflavone synthesis, and *IFS2* is more likely to be adjusted by UV-B than *IFS1* (29). *IFS2* expression increased significantly in soybean under UV-B radiation, promoting the synthesis of genistein and daidzein, and improving the defense ability of soybean (30). The contents of daidzein and genistein in callus culture of *Pueraria lobata* were also closely related to the activity of IFS for isoflavone synthesis (31). Interestingly, results showed that *IF2* expression up-regulated in both hypocotyl and cotyledon calluses, but only daidzein was higher in content in soybean cotyledon callus, while genistein was not detected (**Figure 4F**; **Table 1**). It might due to the difference in the composition of endogenous isoflavones among soybean varieties (24). However, the expression of *4CL3* and *CHI1B* in soybean hypocotyl callus under UV-B radiation decreased significantly compared with the control (**Figures 4C, E**), because there might be a time lag between gene expression of key enzymes and isoflavone synthesis (32). The transcription and translation of key enzymes also affected the accumulation of bioactive metabolites. In addition, the sensitivity of this process to light stress was different. In sum, UV-B radiation was effective to enrich isoflavone in soybean calluses by up-regulating the gene expression and activity of key enzymes.

5. Conclusion

Isoflavones accumulated with specificity in soybean hypocotyl and cotyledon calluses under UV-B radiation. UV-B radiation promoted isoflavones synthesis with different effects on individual isoflavone, and enhanced antioxidant capacity of soybean calluses by regulating key enzyme (PAL, C4H, 4CL, CHS, CHI, and IFS) gene expression levels and their activity. The main isoflavones in hypocotyl callus were glycosides and malonylglycosides. The isoflavones in cotyledon calluses were mainly malonylglycosides and aglycones. These findings provide a new method for enriching specific individual isoflavone and improving the nutritional value of soybean processing products, and will help reduce resource occupation, improve the stability of products, and achieve sustainable development.

Data availability statement

The original contributions presented in this study are included in the article/**Supplementary material**, further inquiries can be directed to the corresponding author.

Author contributions

MW: validation, data curation, formal analysis, and writing—original draft. GL: methodology and data curation. TG: validation and formal analysis. CX: validation, software, and data curation. PW: software and data curation. RY: visualization and writing—review and editing. All authors contributed to the article and approved the submitted version.

Funding

This research was funded by the Priority Academic Program Development of Jiangsu Higher Education Institutions (PAPD).

Conflict of interest

The authors declare that the research was conducted in the absence of any commercial or financial relationships that could be construed as a potential conflict of interest.

Publisher's note

All claims expressed in this article are solely those of the authors and do not necessarily represent those of their affiliated organizations, or those of the publisher, the editors and the reviewers. Any product that may be evaluated in this article, or claim that may be made by its manufacturer, is not guaranteed or endorsed by the publisher.

Supplementary material

The Supplementary Material for this article can be found online at: https://www.frontiersin.org/articles/10.3389/fnut.2023.1139698/full#supplementary-material

References

1. Bi W, Zhao G, Zhou Y, Xia X, Wang J, Wang G, et al. Metabonomics analysis of flavonoids in seeds and sprouts of two Chinese soybean cultivars. *Sci. Rep.* (2022) 12:5541. doi: 10.1038/s41598-022-09408-1

2. Quinhone A, Ida E. Profile of the contents of different forms of soybean isoflavones and the effect of germination time on these compounds and the physical parameters in soybean sprouts. *Food Chem.* (2015) 166:173-178. doi: 10.1016/j.foodchem.2014.06.012

3. Ma M, Wang P, Yang R, Zhou T, Gu Z. UV-B mediates isoflavone accumulation and oxidative-antioxidant system responses in germinating soybean. *Food Chem.* (2019) 275:628-636. doi: 10.1016/j.foodchem.2018.09.158

4. Vanhaelewyn L, Straeten D, Coninck B, Vandenbussche F. Ultraviolet radiation from a plant perspective: The plant-microorganism context. *Front Plant Sci.* (2020) 11:597642. doi: 10.3389/fpls.2020.597642

5. Dymarska M, Janeczko T, Kostrzewa-Susłow E. The callus of *Phaseolus coccineus* and *Glycine max* biotransform flavanones into the corresponding flavones. *Molecules.* (2020) 25:5767. doi: 10.3390/molecules25235767

6. Mohajer S, Taha R, Mohajer M, Anuar N. UV-B irradiation effects on pigments and cytological behaviour of callus in sainfoin (*Onobrychis viciifolia* Scop.). *Pigm Resin Technol.* (2018) 47:496-501. doi: 10.1108/PRT-11-2016-0102

7. Yildirim A. Ultraviolet-B-induced changes on phenolic compounds, antioxidant capacity and HPLC profile of in vitro-grown plant materials in *Echium orientale* L. *Ind Crop Prod.* (2020) 153:112584. doi: 10.1016/j.indcrop.2020.112584

8. Martinez-Silvestre K, Santiz-Gomez J, Lujan-Hidalgo M, Ruiz-Lau N, Sanchez-Roque Y, Gutierrez-Miceli F. Effect of UV-B radiation on flavonoids and phenols accumulation in tempisque (*Sideroxylon capiri* Pittier) callus. *Plants Basel.* (2022) 11:473. doi: 10.3390/plants11040473

9. Mata-Ramírez D, Serna-Saldívar S, Antunes-Ricardo M. Enhancement of anti-inflammatory and antioxidant metabolites in soybean (*Glycine max*) calluses subjected to selenium or UV-light stresses. *Sci Hortic Amsterd.* (2019) 257:108669. doi: 10.1016/j.scienta.2019.108669

10. Wang M, Ding Y, Wang Q, Wang P, Han Y, Gu Z, et al. NaCl treatment on physio-biochemical metabolism and phenolics accumulation in barley seedlings. *Food Chem.* (2020) 331:127282-127313. doi: 10.1016/j.foodchem.2020.127282

11. Livingston D, Tuong T, Tisdale R, Zobel R. Visualising the effect of freezing on the vascular system of wheat in three dimensions by in-block imaging of dye-infiltrated plants. *J Microsc.* (2022) 286:252-262. doi: 10.1111/jmi.13101.

12. Miliauskas G, Venskutonis P, Beek T. Screening of radical scavenging activity of some medicinal and aromatic plant extracts. *Food Chem.* (2004) 85:231-237. doi: 10.1016/j.foodchem.2003.05.007

13. Chen Z, Ma Y, Weng Y, Yang R, Gu Z, Wang P. Effects of UV-B radiation on phenolic accumulation, antioxidant activity and physiological changes in wheat (*Triticum aestivum* L.) seedlings. *Food Biosci.* (2019) 30:100409-100417. doi: 10.1016/j.fbio.2019.04.010

14. Ma Y, Wang P, Zhou T, Chen Z, Yang R. Role of Ca^{2+} in phenolic compound metabolism of barley (*Hordeum vulgare* L.) sprouts under NaCl stress. *J Agric Food Chem.* (2019) 99:5176-5186. doi: 10.1002/jsfa.9764

15. Wang M, Zhu Y, Wang P, Gu Z, Yang R. Effect of γ-aminobutyric acid on phenolics metabolism in barley seedlings under low NaCl treatment. *Antioxidants.* (2021) 10:1421. doi: 10.3390/antiox10091421

16. Hao G, Du X, Zhao F, Shi R, Wang J. Role of nitric oxide in UV-B-induced activation of PAL and stimulation of flavonoid biosynthesis in Ginkgo biloba callus. *Plant Cell Tiss Org.* (2009) 97:175-185. doi: 10.1007/s11240-009-9513-2

17. Cisneros-Zevallos L and Jacobo-Velázquez D. Controlled abiotic stresses revisited: From homeostasis through hormesis to extreme stresses and the impact on nutraceuticals and quality during pre- and postharvest applications in horticultural crops. *J Agr Food Chem.* (2020) 68:11877-11879. doi: 10.1021/acs.jafc.0c06029

18. Alvero-Bascos E, Ungson L. Ultraviolet-B (UV-B) radiation as an elicitor of flavonoid production in callus cultures of Jatropha (*Jatropha curcas* L.). *Philipp Agric Sci.* (2012) 95:335-343.

19. Jacobo-Velázquez D and Cisneros-Zevallos L. Correlations of antioxidant activity against phenolic content revisited: A new approach in data analysis for food and medicinal plants. *Food Sci.* (2009) 74:107-113. doi: 10.1111/j.1750-3841.2009.01352.x

20. Jacobo-Velazquez D, Moreira-Rodriguez M and Benavides J. UVA and UVB radiation as innovative tools to biofortify horticultural crops with nutraceuticals. *Horticulturae.* (2022) 8:387. doi: 10.3390/horticulturae8050387

21. Xu R, Nan P, Yang Y, Pan H, Zhou T, Chen J. Ultraviolet irradiation induces accumulation of isoflavonoids and transcription of genes of enzymes involved in the calycosin-7-O-beta-D-glucoside pathway in Astragalus membranaceus Bge. var. mongholicus (Bge.) Hsiao. *Physiol Plantarum.* (2011) 142:265-273. doi: 10.1111/j.1399-3054.2011.01474

22. Frohnmeyer H, Staiger D. Ultraviolet-B radiation-mediated responses in plants: Balancing damage and protection. *Plant Physiol.* (2003) 133:1420-1428. doi: 10.1104/pp.103.030049

23. Nam T, Lim Y, Eom S. Flavonoid accumulation in common buckwheat (*Fagopyrum esculentum*) sprout tissues in response to light. *Hortic Environ Biote.* (2018) 59:19-27. doi: 10.1007/s13580-018-0003-5

24. Lee J, Kim H, Hwang T. Variation in protein and isoflavone contents of collected domestic and foreign soybean (*Glycine max* (L.) *Merrill*) germplasms in Korea. *Agric Basel.* (2021) 11:735. doi: 10.3390/agriculture11080735

25. Kudou S, Fleury Y, Welti D, Magnolato D, Uchida T, Kitamura K, et al. Malonyl isoflavone glycosides in soybean seeds (*Glycine-max Merrill*). *Agric Biol Chem.* (1991) 55:2227-2233. doi: 10.1080/00021369.1991

26. Toyofuku M, Okutani F, Nakayasu M, Hamamoto S, Takase H, Yazaki K, et al. Enhancement of developmentally regulated daidzein secretion from soybean roots in field conditions as compared with hydroponic culture. *Biosci Biotech Bioch.* (2021) 85:1165-1169. doi: 10.1093/bbb/zbab017

27. Kaducova M, Monje-Rueda M, Garcia-Calderon M, Perez-Delgado C, Eliasova A, Gajdosova S, et al. Induction of isoflavonoid biosynthesis in *Lotus japonicus* after UV-B irradiation. *J Plant Physiol.* (2019) 236:88-95. doi: 10.1016/j.jplph.2019.03.003

28. Garcia-Calderon M, Perez-Delgado C, Palove-Balang P, Betti M, Marquez A. Flavonoids and isoflavonoids biosynthesis in the model legume lotus japonicus: Connections to nitrogen metabolism and photorespiration. *Plants Basel.* (2020) 9:774-796. doi: 10.3390/plants9060774

29. Lim Y, Jeong H, Gil C, Kwon S, Eom S. Isoflavone accumulation and the metabolic gene expression in response to persistent UV-B irradiation in soybean sprouts. *Food Chem.* (2020) 303:1253-1276. doi: 10.1016/j.foodchem.2019.125376

30. Dillon F, Tejedor M, Ilina N, Chludil H, Mithofer A, Pagano E, et al. Solar UV-B radiation and ethylene play a key role in modulating effective defenses against Anticarsia gemmatalis larvae in field-grown soybean. *Plant Cell Environ.* (2018) 41:383-394. doi: 10.1111/pce.13104

31. Rani D, Kobtrakul K, Luckanagul J, Thaweesest W, Rojsitthisak P, De-Eknamkul W, et al. Differential gene expression levels, chemical profiles, and biological activities of *Pueraria candollei* var. mirifica callus cultures at different growth stages. *Plant Cell Tiss Org.* (2021) 147:61-72. doi: 10.1007/s11240-021-02105-3

32. Nakabayashi R, Mori T, Nishizawa T, Saito K. Temporal lag between gene expression and metabolite accumulation in flavonol biosynthesis of *Arabidopsis* roots. *Phytochem Lett.* (2017) 22:44-48. doi: 10.1016/j.phytol.2017.09.001

Frontiers in Nutrition

Explores what and how we eat in the context of health, sustainability and 21st century food science

A multidisciplinary journal that integrates research on dietary behavior, agronomy and 21st century food science with a focus on human health.

Discover the latest Research Topics

See more →

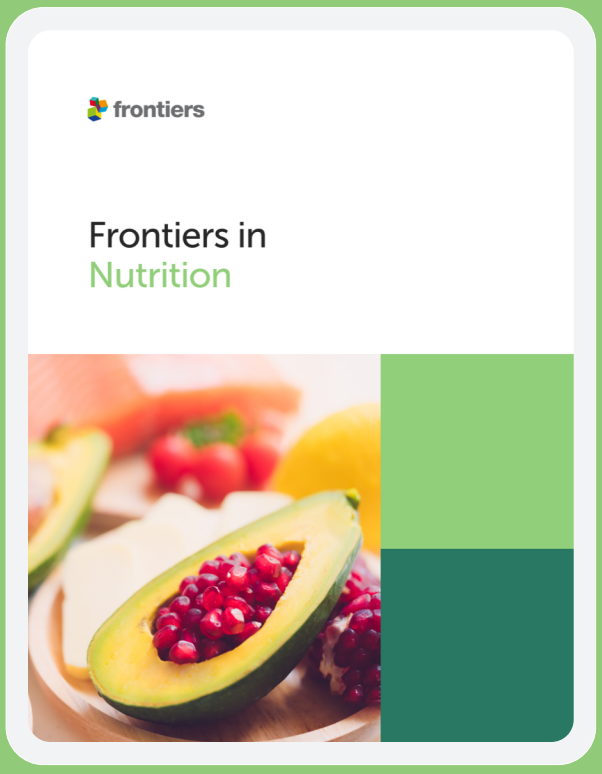

Frontiers

Avenue du Tribunal-Fédéral 34
1005 Lausanne, Switzerland
frontiersin.org

Contact us

+41 (0)21 510 17 00
frontiersin.org/about/contact